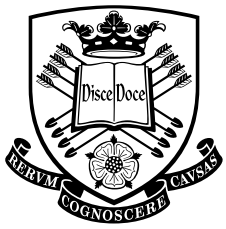

The University Of Sheffield.

FRAMEWORK FOR DEVELOPING LARGE-SCALE METAL ADDITIVE MANUFACTURING (MAM) SYSTEMS AND PROCEDURES

U Woy

Doctoral Thesis

2022

The University Of Sheffield.

FRAMEWORK FOR DEVELOPING LARGE-SCALE METAL ADDITIVE MANUFACTURING (MAM) SYSTEMS AND PROCEDURES

By:

Udisien Woy

A thesis submitted in partial fulfilment of the requirements for the degree of
Doctor of Philosophy

The University of Sheffield
Faculty of Engineering
Department of Advanced Manufacturing Research Centre (AMRC)

August 2022

Acknowledgements

The author gratefully acknowledges academic supervisors, Drs. Steven A. Jones, and Rosemary J. Gault, and industrial supervisor, Dr. Daniel Clark, for their valuable insights, notwithstanding the kindness, encouragement, patience, understanding and dedication, which facilitated the completion of this work.

The author sincerely thanks Prof. Keith Ridgway for his mentorship, and the Nuclear AMRC for funding this project. The entire management team, including 'Prof'. Keith Bridger, Mr Stuart Dawson, Mr Carl Hitchens, Dr. Will Kyffin, and Mr Jay Shaw, is recognised for their immense support, accommodation, and flexibility. The author thanks all BAM team members, especially Dr. Wei Guo, Miss Samantha Biddleston, and Mr. Jamie Todd for their unwavering support. The author also expresses gratitude to the numerous AMRC and Nuclear AMRC colleagues whose encouraging words and many supportive acts facilitated progress on this journey.

For providing essential industrial context and credence, the author is forever indebted to Rolls-Royce plc. and further acknowledges the expertise and support of key individuals, including Mr. Richard J. Harlow and Mrs. Victoria Scott.

The author is especially thankful to all development partners, particularly Mr. Dave Burns of KUKA Systems UK Ltd, and Mr. Trevor Towler and Mr. Keith Palmer of TPS WeldTech Ltd, for their commitment and enduring support.

Finally, the author is most grateful to Prof. Pete Osborne, Dr. Craig Buchanan, Prof. Supriyo Ganguly, and Prof. Adam T. Clare for their diligent efforts and valuable contributions to this work.

Abstract

Additive manufacturing (AM) is regarded as one of the most disruptive technologies of this era. However, the technology is still evolving, even as new applications continue to emerge, thus presenting an opportunity to manage disruptive changes more efficaciously, whilst strategically shaping critical innovation efforts. Accordingly, this study focusses on supplementary manufacturing requirements management (SMRM). Presently, maintenance challenges, such as the reworking of serviceable infrastructures and other similarly demanding industrial endeavours, contribute to higher costs, inefficiencies, and waste, with technical and other limitations, including disparate supply circumstances and demand patterns, further compounding issues.

Underpinned by SMRM applications, the grounded theory (GT) method was applied, to construct a framework for developing large-scale metal AM (MAM) systems and procedures. Case data was derived from the development and commissioning of a unique system and its embodied concepts, which were predominantly enabled by commercial off-the-shelf (COTS) solutions, and subsequent testing and validation of the resulting open architecture (OA) bulk AM (BAM) platform. Empirical and numerical investigations were facilitated by an industrial titanium (Ti-6Al-4V) aerospace component, which demonstrated the suitability and effectiveness of the BAM platform for specific SMRM operations. While the physical and mechanical properties of derived BAM materials were characteristic, and within range of referenced ASTM standards, disparities between the predicted and quantified effects of reprocessing operations on the component necessitate further investigation.

The main output of this study is a GT framework, which identifies six strategic developmental themes for more *adoptable*, *compliant*, *functional*, *operable*, *systemical*, and *adaptable* MAM solutions. Important priorities for improving interrelated system functions, procedures, and performance were also defined, alongside an original technical perspectives management concept, for navigating complex requirements in an evolving technology landscape, via the *documentation*, *clarification*, *validation*, and *prioritisation* of key elements that significantly impact planned innovations.

Contents

List of Figures

List of Tables

Nomenclature

2D	2-dimensional
3D	3-dimensional
AM	Additive manufacturing
AMR	Advanced manufacturing research
AMT	Advanced manufacturing technologies
AVC	Arc voltage control
BAM	Bulk additive manufacturing
BOM	Bill of materials
BSE	Backscatter electron
BTF	Buy-to-fly
CAD	Computer aided design
CAE	Computer aided engineering
CAM	Computer aided manufacturing
Capex	Capital expenses
CAx	Computer-aided technologies
CFD	Computational fluid dynamics
CMM	Coordinate measuring machine
CMT	Cold metal transfer
CNC	Computer numerical control
CO_2	Carbon dioxide
COTS	Commercial off the shelf
CT	Computed tomography
CTG	Cradle-to-grave
DAQ	Data acquisition
DED	Directed energy deposition
DED-EB	Directed energy deposition-electron beam
DED-LP	Directed energy deposition-laser powder
DED-LW	Directed energy deposition-laser wire
DED-WA	Directed energy deposition wire and arc
DLF	Directed light fabrication
DMD	Direct metal deposition
DMLS	Direct metal laser sintering
DoE	Design of experiments
DPI	Dye penetrant inspection
DTI	Dial test indicator
EBAM	Electron-beam additive manufacturing
EBF^3	E-beam free form fabrication
EBM	Electron-beam melting
EBSD	Electron backscattered diffraction
EDM	Electrical discharge machining
EOAT	End of arm tooling
FAT	Factory acceptance test
FDS	Functional design specification
FEA	Finite element analysis
FGM	Functionally graded materials
GMAW	Gas metal arc welding
GOM	Geometrical optical measuring
GT	Grounded theory
GTAW	Gas tungsten arc welding
GUI	Graphical user interface
HAZ	Heat affected zone
HIP	Hot isostatic pressing
HPA	High-priced artefacts
IFF	Ion Fusion Formation
IoT	Internet of things
IR	Infrared
KRC	Kuka Robot Controller
KRL	KUKA Robot Language
LCA	Life cycle analysis
LCL	Lower control limit
LENS	Laser engineered net shaping
LMD	Laser metal deposition
LMWD	Laser Metal Wire Deposition
LOF	Lack of fusion
MAM	Metal additive manufacturing
MITC	Maintenance, inspection, verification testing, and continuous improvement
MRL	Manufacturing readiness levels
MRO	Maintenance repair and overhaul
NDE	Non-destructive evaluation
NDT	Non-destructive testing
NNS	Near-net shaped
OA	Open architecture
OEM	Original equipment manufacturer
OES	Optical emission spectroscopy
OLB	Operators logbook
OLP	Offline programming
Opex	Operating expenses
PAW	Plasma arc welding
PBF	Powder bed fusion
PBF-EB	Powder bed fusion electron beam
PBF-LB	Powder bed fusion laser beam
PLB	Primary logbook
PoC	Proof-of-concept
PS	Planar substrates
PSD	Particle size distribution
RMS	Root mean square
RPD	Rapid plasma deposition
SAT	Site acceptance test
SEC	Specific energy consumption
SEM	Scanning electron microscope
SFFF	Solid free from fabrication
SG	Strain gauges
SLB	Secondary logbook
SLM	Selective laser melting
SMD	Shaped metal deposition
SMRM	Supplementary manufacturing requirements management
SPC	Statistical process control

SR	Supplementary requirements
TC	Thermocouples
TM	Thermo-mechanical
TMM	Thermo-mechanical metallurgical
UCL	Upper control limit
WAAM	Wire and arc additive manufacturing
WLAM	Wire and Laser additive manufacturing
XRD	X-ray diffraction
XRF	X-ray fluorescence spectrometry

Dedication

Dedicated to the late Chief Engr. Isaac Tobins Woy, whenever and wherever you may be. Eternally grateful for the enduring lessons on love and life.

Declaration

I, Udisien Woy, declare that the work presented in this Thesis is my own. I confirm that references made to material which is not of my own work are appropriately acknowledged.

I am aware of the University's Guidance on the Use of Unfair Means (www.sheffield.ac.uk/ssid/unfair-means). This work has not previously been presented for an award at this, or any other university.

Publications and conferences:

- **Woy U.,** Jones S., Gault R., Ridgway K., and McCluskey R., "*Evaluation of Shaped Metal Deposition (SMD) for applications in the energy industry",* High Value Manufacturing: Advanced Research in Virtual and Rapid Prototyping - Proceedings of the 6th International Conference on Advanced Research and Rapid Prototyping, VRAP 2013, pp. 619-622, Jan 2014.

- Tancogne-Dejean T., Roth C.C., **Woy U.,** and Mohr D., "*Probabilistic fracture of Ti–6Al–4V made through additive layer manufacturing"*, International Journal of Plasticity, 78:145-172, Mar 2016.

- **Woy U.,** Preston S., Patel V., Gault R., and Jones S., *"The Comparative Effects of the SMD Process on Type 316L Stainless Steel Powder Feedstock*" 40th International MATADOR Conference on Advanced Manufacturing, July 2019.

CHAPTER 1

1 Introduction

1.1 Background

The sustainability of high value large-scale metallic structures, which facilitate the efficient delivery of essential communal services, such as transportation and energy, remains an important technical, technological, and financial challenge. In the typical life cycle of these structures, unpredictable events [1–6], including manufacturing and service incidents, are encountered. However, there are often considerable differences between the perception and reality of managing the impact and uncertainties stemming from such events, anomalous or otherwise. Technically, specific requirements and necessary actions cannot be predetermined. Financially, decisions are influenced by the complexity of the problem and resources needed to achieve a satisfactory outcome [7]. Other factors, including the socio-economic impact of asset unavailability, and urgent environmental concerns [8,9], underscore the need for advanced manufacturing technologies (AMTs). For core industries, AMTs can enhance technical and commercial prospects for supplementary manufacturing requirements management (SMRM) by increasing the number of available options for the rapid and effective resolution of manufacturing and sustainability issues.

Additive manufacturing (AM) is an AMT that can potentially transform the management of principal and supplementary manufacturing requirements involving large metallic structures. Presently, the AM landscape is complex, owing to a variety of production capabilities and increasingly affordable but evolving entry level systems [10,11]. Industrialisation efforts are influenced by numerous technological components, different important technical perspectives, and the characteristics, benefits, and limitations of distinct technologies. Related considerations include the utility of commercial AM capabilities, relative to the criticality of requirements and other important factors driving development and/ or investment decisions [12,13]. Correspondingly, the growing need for industrial AM machines should be matched by demonstrably suitable capabilities that can fulfil specific manufacturing functions safely, efficiently, and satisfactorily.

In demonstrating that AM technologies, associated systems, and specific procedures, are suitable for large-scale manufacturing operations, the main industrial components and functions that are needed must be well defined. However, AM remains highly susceptible to further disruptions as the landscape continues to evolve [14], thus lacking the comparative technological stability presently associated with traditional manufacturing approaches. In relative terms, stability issues present differently in MAM, which is a more localised manufacturing process, as opposed to the generally encompassing nature of traditional forming processes. Therefore, a mechanism is needed for capturing the main features, configurations and procedures required for developing commercial capabilities for large-scale metal AM (MAM) applications. This mechanism can

minimise non-value adding reinventions, and/ or other similarly repetitive, and time-consuming activities, by supporting low-level development decisions, thus enabling developers to focus on more advanced technical features, functions and innovations that are more closely aligned to the industries and applications to which new large-scale MAM capabilities should add specific, quantifiable, and, preferably, greater value.

1.2 Study objectives

The objective of this study was to construct a grounded theory (GT) framework to support the development of large-scale MAM systems and procedures. Primarily informed by the need for managing supplementary manufacturing requirements, the aim was to establish a mechanism for describing interrelated technology and technical determinants influencing development decisions. The specific study objectives are stated below.

- Develop large-scale open architecture (OA) system, based on appropriate MAM technology, to determine pertinent developmental factors.
- Develop relevant industrial case study, to validate OA system, and elucidate factors in the deployment of suitable MAM technologies for SMRM.
- Develop numerical process models to explain the specific effects of MAM operations on system outputs and obtain data to supplement SMRM verification procedures.
- Consolidate and analyse data and insights derived from literature, distinct investigations, and development activities, to identify and explain the principal themes and ideas resulting from the study.
- Organise important emerging concepts across datasets or categories, to create a well-defined structure, and framework for developing large-scale MAM systems and procedures.

1.3 Research strategy

The main strategy for this study was formulated in response to the research question, '*what factors should be prioritised when developing large-scale MAM systems and procedures*, and importantly*, why?'*. A framework approach was preferred for organising developmental priorities for future industrial MAM systems and related procedures. The GT method [15] was applied to underpin investigations, which were initiated to establish the foundations of the framework. The GT approach combines both qualitative and quantitative techniques to obtain case data, which is systematically and comparatively analysed, to achieve "greater conceptual clarity or generate a conceptual framework" [16] about a complex and multi-disciplinary subject. Thus, it offered an ideal basis for navigating the current landscape to increase understanding of complex technology, technical, economic, business, and other important factors affecting the deployment of MAM for industrial applications, including SMRM. A schematic of the overall research strategy is depicted in Figure 1-1.

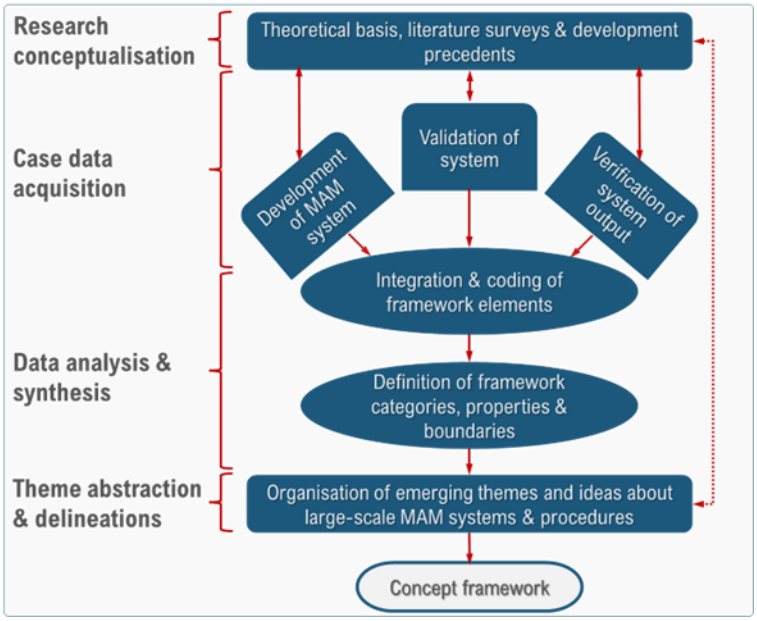

Figure 1-1. Overall research strategy for constructing a GT framework.

The overall strategy was premised on the idea that any generalisations or inferences about large-scale MAM systems requires direct knowledge and experience of such capabilities. Accordingly, formulating an approach for developing a large-scale OA MAM system concept, and implementing this unique and technologically representative instance, allows for the direct observation and analysis of interrelated developmental factors. However, establishing a representative capability neither guarantees conformance to specifications nor that the desired outcomes will be achieved. Instead, the utility of the system is determined by how well it fulfils designated functions. Here, a case study approach is particularly useful, as validation activities may be conducted under contextually appropriate (SMRM) conditions. Case studies also facilitate more in-depth analysis of specific application-level procedures and determinants associated with the utilisation of the resulting systems for industrial MAM operations. Post-validation, it is necessary to substantiate derived outputs via appropriate inspection procedures, before drawing conclusions about the suitability of OA MAM systems for both general and specific industrial applications. Furthermore, due to the criticality and potential implications of SMRM actions, there is a need to adopt other enabling technologies to support all developmental phases, particularly in relation to qualification and verification of manufacturing processes and outputs. Hence, numerical modelling and simulation techniques are ideal for exploring the effects of MAM processes and procedures to support the development and substantiation of empirical outputs. It was intended that through the development, validation, and substantiation of critical system and process outputs, relevant qualitative and quantitative data will accumulate, thus enabling the creation of a well-defined framework for organising key system and procedural themes influencing large-scale MAM operations.

1.4 Thesis structure

The thesis is organised into 9 chapters, including this chapter, which explores the rationale for the study. Chapter 2 provides further information on the research background, and how planned investigations were formulated. The main contributions of this work, embodied as a framework for developing large-scale MAM systems and procedures, was mainly derived from the core research activities in the intervening chapters, and supported by insights from applicable theories and techniques, literature surveys, and previous experience. The resulting case data was subsequently used for the analysis and abstraction of common ideas and themes for the framework, before critically reviewing the methodology and outcomes, in the concluding chapters of this study. The structure and outline of the thesis is presented hereafter.

Research scope and context

Chapter 1: Introduction to study motivation and background, including challenges with SMRM, and prospects for MAM technologies.

Chapter 2: Review of research precedents, including description of adopted theories and investigative strategy underpinning system development and validation activities.

MAM system development and related verification and validation studies

Chapter 3: Introduction of methodology and details of preliminary studies informing the formulation and refinement of the general investigative approach.

Chapter 4: Development and implementation of open architecture (OA) MAM system concepts, including analysis of development strategy and verification of system functions.

Chapter 5: Case study validation of OA MAM system for SMRM applications, involving development of reprocessing approach for specified operations on titanium Ti-6Al-4V alloy aerospace component.

Chapter 6: Implementation of numerical modelling and simulation techniques for verification of system outputs, including evaluation of selected reprocessing operations.

Establishment of concept GT framework

Chapter 7: Compilation of case data and organisation of ideas from preceding investigations, to inform deductive analysis and definition of framework elements.

Chapter 8: Critical review of study outcomes, limitations, and assumptions, including clarification of principal outputs, emerging concepts, and related definitions.

Research outcomes

Chapter 9: Summation of main findings and study implications, including recommended areas for future research.

1.5 Summary

The overall approach for systematically developing a GT framework was presented in this chapter. This approach is underpinned by the adoption of MAM technologies, to support typical and supplementary manufacturing life cycle requirements, for large-scale metallic structures. Due to relatively low adoption levels for critical engineering applications, the need to further substantiate the capability and industrial relevancy of this AMT was also highlighted. The reasons for supporting the development of new and improved future solutions, in a diverse AM landscape, were presented, in consideration of the significant potential for non-value adding innovations, which results in duplication of costs and efforts. The study objectives were also defined in this chapter, alongside the research strategy for closing the technology assimilation gap, and describing how the subject of relevancy will be explored, via the development of a concept framework.

In the following chapter, a literature survey of the main precedents for this study, including MAM technologies and other relevant topics, are presented.

CHAPTER 2

2 Literature Review

2.1 Introduction

In existing literature, additive manufacturing (AM) system concepts are not explicitly described or directly analysed, but typically embedded within the context of other primary investigations. Therefore, the purpose of this review is to establish an informed strategy for creating a framework to support the development of future large-scale metal AM (MAM) systems and procedures. Framed around the context of SMRM, and specific challenges involving large metallic structures, the survey also focuses on pertinent advances in MAM, and related development considerations, including applicable scientific philosophies, and other techniques underpinning foreseen investigations. While investigations were designed to facilitate the generation of case data for the proposed GT framework, this review establishes the main ideas and precedents influencing the core research activities implemented in this study.

2.2 Additive manufacturing (AM)

Additive manufacturing (AM) is well-defined as the process of joining distinct layers of material to create 3-dimensional (3D) objects [17,18]. This important distinguishing technological and commercial feature has influenced perceptions about AM, particularly 3D printing capabilities. Early 3D printers enabled greater design freedoms, but the initial focus on prototyping applications [11] or the product form, limited the perceived value and utility of these capabilities. Nevertheless, this important milestone marked the transition from early concept machines to commercialised AM systems that are now capable of fulfilling production requirements.

The advent of commercial 3D printers and propagation of 3D printing in mainstream media were crucial to establishing the disruptive nature of AM technologies, which was reinforced by the growth of the 3D printing cottage industry [10]. Perceived as a key driver in a new manufacturing revolution [10,11], the 3D printing movement has especially attracted significant investment from venture capitalist who are backing a growing number of privately funded AM companies [12,13]. Notwithstanding the hype, familiar trends and patterns are typical of the transition from cottage to contemporary industry, and contribute to persisting perceptions about the promising potential of AM technologies [14].

Presently, there are seven AM technology classifications, namely binder jetting, directed energy deposition (DED), material extrusion, material jetting, powder bed fusion (PBF), sheet lamination, and vat polymerisation [8, 9]. Binder jetting, DED, material jetting, and PBF are discretely capable of processing a range of materials,

including metals [17–20]. From the list of technologies suitable for MAM, only DED and PBF were prioritised for further in-depth reviews. DED was selected due to its relevance in the development of large-scale MAM applications [21–23], and PBF for its continuing commercial dominance in different industries [24–26], as well as the current significance of both DED and PBF technologies for SMRM and related applications [27–29]. Furthermore, this approach is consistent with the GT constant comparative method, which allows for increased understanding of pertinent cross-cutting themes affecting two important AM technology classes.

2.3 Adoption of MAM technologies

Factors influencing the adoption of MAM technologies are evaluated in this section. The capabilities, characteristics, limitations, and challenges associated with current developments are explored in relation to MAM system designs and applications, particularly for SMRM purposes. Due to the significance of predictability in product design, manufacturability, optimisation, performance, and safety studies, as well as the uncertainties surrounding SMRM, trends in AM simulation and modelling were also reviewed, to determine how specific approaches may support the implementation of the research strategy.

2.3.1 MAM systems and attributes

Due to the bourgeoning nature of AM, technologies with comparable traits are presently known by different proprietary and generic monikers. Likewise, there are several DED and PBF processes or techniques currently used within the MAM technology subclass. These technologies are typically categorised in relation to common system design and processing traits or capabilities. Focusing on DED and PBF capabilities, these common elements are presented in Figure 2-1, alongside well-known derivatives of the MAM technology subclass.

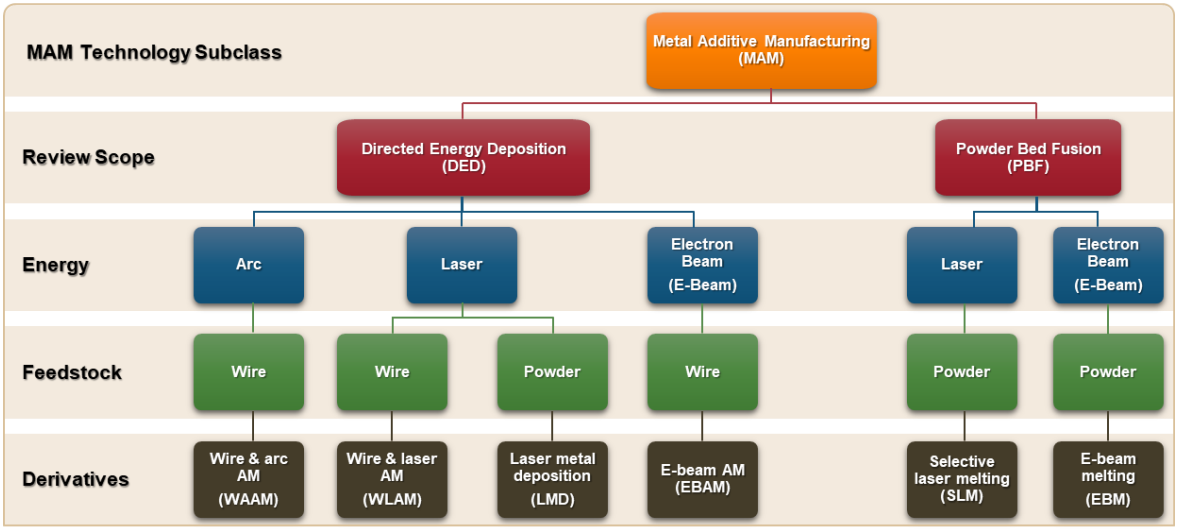

Figure 2-1. Common traits and derivatives of selected MAM technologies

In the design and development of MAM capabilities, DED system that are configured by combining the wire feedstock, with either an arc or laser energy source, are collectively referred to as wire and arc AM (WAAM) or wire and laser AM (WLAM) respectively. Laser metal deposition (LMD) is a common terminology for capabilities configured using a laser energy source and powder feedstock, while electron-beam AM (EBAM) is a proprietary term used for AM capabilities configured with the wire feedstock and electron beam energy source. Selective laser melting (SLM) and electron-beam melting (EBM) are the terminologies used for PBF capabilities configured using either a laser or electron beam respectively. PBF technologies exclusively utilise powder feedstock on a bed/ platform, while DED technologies are capable of directly depositing other feedstock material forms, including powder and wire. However, both PBF and DED technologies rely on a focussed beam of energy for heating the feedstock material during the layering process. For PBF technologies, this heat is generated from a power beam, which could be derived from a laser or an electron beam. The options for DED technologies include both power beam sources, and an electric arc or plasma source, which is used to generate sufficient heat to melt the feedstock material, thus ensuring adequate fusion between layers.

Before formulating a strategy for developing a suitably sized MAM capability, it was important to understand how different systems functioned, as well as the relative characteristics influencing the various commercial and non-commercial derivatives that exist. Therefore, the constituents, processing characteristics and procedures, governing both DED and PBF technologies, were evaluated.

2.3.1.1 Directed energy deposition (DED)

A typical DED system consists of a multi-axis deposition tool with a nozzle and a focussed thermal energy source for depositing material onto a fixed object [30–33]. This can occur within or without a build chamber, depending on the type of energy source used, and how it is configured. The configuration also enables multi-axis deposition capabilities, which enhances the flexibility of DED systems. The deposition tool can be manipulated around a fixed object, or vice-versa, using a movable build platform or positioner. It is also typical to manipulate the object and the tool synchronously, to suit more complex deposition operations. During the process, control of the tool is enabled by computer numerical control (CNC) or robotic controllers. Typical configurations of current DED system are depicted in Figure 2-2.

The DED process is initiated by depositing the feedstock material, in powder or wire form, via a nozzle or guide, onto an existing surface. Multiple feedstock materials can also be introduced via separate containers and/ or nozzles to either increase productivity or produce functionally graded materials (FGM) [34–36]. Next, the feedstock material is melted with a directed source of energy as it exits the nozzle to ensure adequate fusion of the deposited material before it solidifies. The typical layer thickness can range from about 0.25 mm to 0.5 mm for powder based processes, to more than 1 mm for wire depositions [37]. Presently, wire based DED processes (Figure 2-2(a) (c) and (d)) offer higher material efficiency or yield when compared to powder DED and PBF processes (Figure 2-2(b)), owing to the deposition of excess powder during the build. The method of

material melting and the atmosphere in which melting occurs also varies between power beam and arc technologies. A build chamber or enclosure is essential for power beam processes, but also offers the option of a more controlled processing environment for arc-based AM technologies.

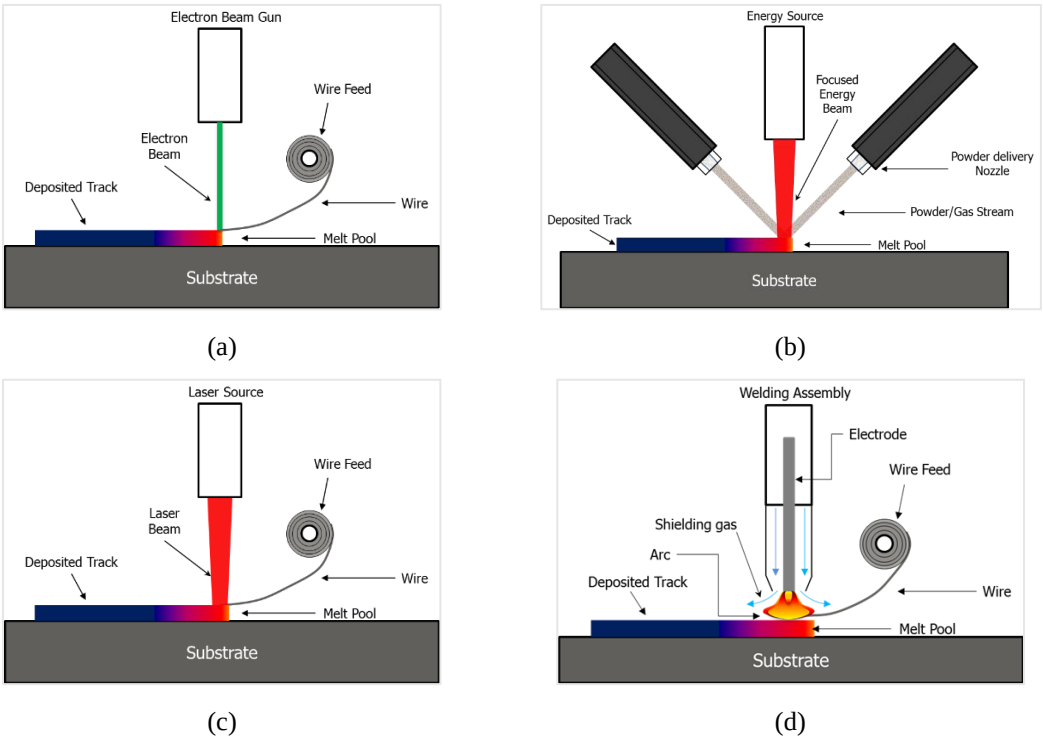

Figure 2-2. Typical setup for (a) EBAM (b) LMD (c) WLAM and (d) WAAM processes.

Different researchers evaluated the maturity of contemporary DED processes, for wider industry adoption, and found that there were variations in manufacturing readiness levels (MRL) [38–40]. MRL is used to gauge the maturity of a manufacturing process, relative to its commercialisation prospects. It is an important metric, due to the effects of variations on the development of reliable DED systems, stable processes, and related performance, validation, and qualification requirements, which are necessary for regulatory approval in relevant industry sectors [31]. Contemporary processes include the derivatives presented in Figure 2-1 (i.e. EBAM, LMD, WAAM, and WLAM), and other well-known DED technologies, such as directed light fabrication (DLF), direct metal deposition (DMD), e-beam free form fabrication (EBF^3), and laser engineered net shaping (LENS). However, due to the number of LMD variants with similar nomenclature, these processes will be collectively referred to, hereafter, as DED laser powder (DED-LP).

LENS® is a DED-LP process developed at Sandia National Laboratory, in the mid-to-late 1990s, and further developed and commercialised by Optomec, both based in the USA. LENS® systems consists of a deposition head, with a neodymium-doped yttrium aluminium Garnet (Nd:YAG) laser at its centre, typically surrounded by 2 or 4 nozzles. The deposition head is mounted on a 3-axis or 5-axis positioning system (CNC or robotic), along with a powder feed unit [41], resulting in a system that can process different metallic powders. Dissimilar powders can be used simultaneously through different nozzles, along with independent volumetric flow

control, which is suitable for FGM deposition. The process takes place in a controlled atmosphere or environment, with argon used as both a carrier and shielding gas. However, the LENS process is reportedly characterised by poor energy efficiency (~2-5%), with powder deposition rates of about 12×10^{-3} kg/min [42]. Direct metal deposition (DMD) is another DED-LP process, which was developed at the University of Michigan, USA [43]. In a DMD system, a carbon dioxide (CO_2) laser unit is used as the heat source, with helium, or a combination of helium and argon, used as both shielding and powder delivery gas. DMD capabilities also incorporate optical feedback systems that enable closed loop control of the build dimensions and deposition integrity, as well as the ability to run unattended [41,44]. The DMD process was subsequently adopted by TRUMPF GmbH, and has been used to manufacture parts from a variety of ferrous and non-ferrous metallic powders, and FGM amalgams [34,43,45–49]. Although the DMD and LENS® processes are similar, in terms of deposition rates and power efficiency, a commercial DMD variant reportedly offers significantly improved material consumption rates when compared to LENS® [42]. The DLF process is also similar to LENS, with powder efficiency of 10-15% and deposition rates of about 6 to 10×10^{-3} kg/min [42]. Developed at Los Alamos National Laboratory, USA [50], this DED-LP capability consists of a laser unit, a single nozzle metal powder delivery system and a multi-axis CNC laser beam positioner [51]. A characteristic DLF cooling rate of 10,000 K/s was demonstrated for AISI 316 stainless steel and enabled well-refined microstructures. However, scanning electron microscope (SEM) images showed extensive occurrence of non-melted powder within the surface of resulting parts [52].

EBF^3, also referred to as DED-EB in some literature sources [52], is a solid free form fabrication MAM process developed at NASA Langley Research Centre. Unlike DED-LP capabilities, an EBF^3 system consists of a vacuum chamber, operated at a pressure of 1.3×10^{-3} Pa, during the deposition of wire feedstock into the molten pool, which is created and sustained by a focussed electron beam [53]. The electron beam couples effectively with any electrically conductive material, inclusive of highly reflective metals, such as copper and aluminium. EBF^3 is characterised by high energy efficiency (>80%) and high volumetric deposition rates, particularly for aluminium, ranging from 0.33×10^{-3} to 0.6×10^{-3} m^3/h [54]. An identical setup can also be used for higher detailed depositions at lower deposition rates, restricted only by the wire feed mechanism and positioning accuracy, with the potential to introduce multiple wire feeders for fabricating FGMs. Hafley et al. [55] conducted deposition experiments in micro gravity (0-g), using the EBF^3 process, and produced deposits comparable to those produced in normal gravity (1-g).

WLAM, also known as laser metal wire deposition (LMWD) [56,57], utilises a laser beam as a heat source and metal wire as feedstock material. WLAM systems typically consist of an automated wire-feeding element, a laser unit, mounted on a CNC or robotic positioning system, and ancillary systems for pre-heating, cooling, and shielding gas delivery. In the presence of a shielding gas, metal wire is melted onto a substrate using the laser beam, with resulting 3D parts created from the relative motions of the welding unit and the substrate [32,58]. The diameter of the wire feedstock typically ranges from about 0.2 to 1.2 mm. WLAM has been used

to process a wide range of alloys, and is characterised by high feedstock consumption, and low energy efficiency, owing to the combination of wire feedstock and laser energy source respectively. The process exhibits high deposition rates presently associated with wire-feed systems, making it suitable for depositing larger volumes. However, the quality of the deposition is strongly dependent on the wire diameter and composition as well as other process variables, including the wire feed orientation, angle and feed rate [41]. Hence, an annular laser beam axially fed deposition head was developed, to solve performance related issues, such as process asymmetry and related directional dependence of the wire feedstock, in the WLAM process [59,60]. This coaxial arrangement enables the symmetrical and simultaneous heating of the work piece and wire-end surface over its circumference. It also enables greater control of the work piece illumination proportion, and energy density input.

A typical DED wire and arc (DED-WA) [61] or WAAM capability consists of an automated feedstock material delivery system and a manipulatable build platform in an enclosure or chamber. When fully sealed, the chamber can be flooded with argon gas to create an inert atmosphere during the deposition process [62–64]. The WAAM process utilises an electric arc as a heat source, and varying sizes of metal wire as feedstock material. Several research groups have investigated the suitability of different gas tungsten arc (GTA) based deposition processes, including GTA welding (GTAW), plasma arc welding (PAW) and gas metal arc welding (GMAW), for WAAM [32,62,63,65–68]. The WAAM technique has evolved from these traditional welding processes, thus different weldable materials have been investigated for MAM applications [32,61,69]. While PAW and GTAW processes utilise non-consumable electrodes for deposition, the GMAW process utilises the wire feedstock as a consumable electrode. The quality of GTAW and PAW based WAAM process outputs depend on key variables, including the wire feed orientation and shape of the arc, which is narrower in PAW, and affects resulting part dimensions. Compared to GTAW, the energy density is also higher in PAW-based WAAM, which enables higher processing speed with minimal distortion [32]. In general, processes configured using GTAW, PAW or GMAW as heat sources are characterised by relatively high feedstock, energy efficiency, and deposition rates. However, the higher energy efficiency results in higher specific heat input in WAAM, relative to other DED processes. Furthermore, the high temperature gradient, derived from a higher heat input, is linked to residual stress and distortions, with measurable effects on product form accuracy and performance. While it is possible to achieve satisfactory geometric quality with WAAM, there is a higher risk of relatively poor part accuracy, hence post deposition machining is typically required [70].

2.3.1.2 Power bed fusion (PBF)

The typical PBF build platform comprises a feedstock material reservoir, such as a hopper or feed cartridges, which delivers layers of powder that is subsequently spread across the build platform using a mechanical device, often a roller or blade. After a powder bed pre-heating procedure, a power beam selectively heats the areas of the deposited powder layer, which represents a cross-section or slice of the part being built. The build platform is subsequently lowered, allowing the material delivery, spreading, and melting sequence to be

successively repeated until the build process is complete. The final procedure involves the removal of the 3D part and unused or unmelted powder remnants from the build chamber, in preparation for a new build. The typical configurations of PBF build platforms are shown in Figure 2-3.

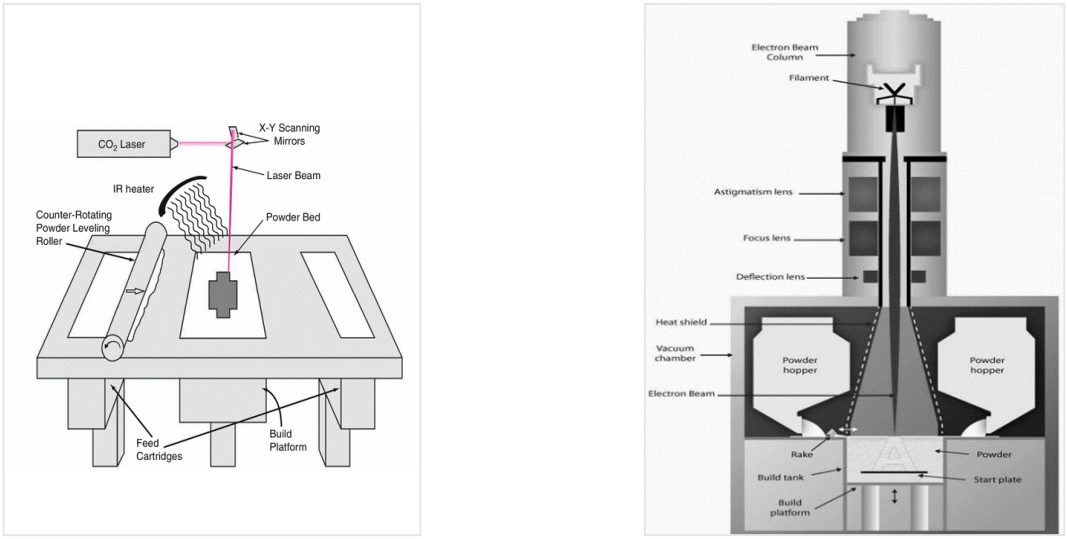

(a) (b)

Figure 2-3. Typical configurations for (a) laser [37] and (b) electron beam PBF platforms [71].

PBF processes are characterised by their ability to produce high resolution features, including intricate internal passages, whilst retaining dimensional control [30,31]. In commercial PBF systems, CNC significantly enables part accuracy, but can be limited by other control functions. The processing equipment and build platform are typically contained within a chamber to facilitate the monitoring and control of temperature, power and other critical system and process variables. The chamber may also be filled with inert or semi-inert shielding gases, such as argon or nitrogen, to minimise oxidation and material degradation during the build process. Afterwards, a cooling period is necessary for achieving a high tolerance and quality of fusion. Then, the deposited object and excess powder are removed, before cleaning the equipment, to minimise the risk of contamination between builds. It is due to the potential risk of contamination that PBF systems are often designated for the manufacture of components from specific alloys or materials. Deposited objects typically require post-processing to remove support structures, improve surface finish or enhance material properties. A heat treatment procedure may also be necessary for enhancing material homogenisation. Presently, the most commercialised PBF processes are direct metal laser sintering (DMLS), selective laser melting (SLM), and electron beam melting (EBM). Laser and electron beam systems, also known as PBF-EB and PBF-LB respectively, have different trademarked derivatives available on the market.

The EOS brand of 3D printers are archetypal DMLS systems, which deposit powder feedstock in layers that typically range from 20-60μm [26,72–74]. During the process, the powder is sintered, such that distinct layers are sufficiently bonded to create functional 3D objects. Additionally, material consolidation is considerably affected by the characteristics of the laser beam. Specifically, material laser absorptivity depends on the laser

wavelength, as well as the relationship between the laser energy, and power densification. Post-process treatments, such as an extra laser pass, hot isostatic pressing (HIP) and heat treatment, may be necessary to address processing , such as inadequate densification, and non-uniform microstructure and material properties, which are often evident in DMLS processed parts [26]. While the SLM process utilises similar procedures, the complete melting and solidification of material results in improved densification, microstructure and mechanical properties, when compared to DMLS outputs [75]. For both DMLS and SLM processes, a powder bed pre-heat temperature of about 200 ºC is typical [76], but the SLM system is reportedly characterised by poor energy efficiency of about 10 to 20 %, combined with high processing speeds [37]. Well-known SLM systems include the Renishaw 3D printer, and the patented LaserCUSING® technology from Concept Laser [74,77,78]. However, unlike DMLS and SLM processes, an electron beam is used for the EBM process, so a vacuum operational atmosphere is necessary, with beam control achieved by means of electromagnetic coils. Similar to laser beam technologies, there are commonalities between the EBM and EBF[3] processes, such as the required vacuum pressure of about 1×10^{-3} Pa [79,80]. Reportedly, the introduction of Helium at about 2×10^{-1} Pa, can help to maintain the chemical specification of deposited materials [79,81]. The build chamber may also be heated to specific temperatures of up to 900 ºC, for better control of deposition conditions [82]. Compared to other PBF processes, EBM processed parts have superior mechanical properties, low porosity, and low surface roughness. These current advantages are attributed to the combination of high temperature, low thermal gradient, and vacuum conditions within the build chamber, resulting in more uniform temperature distribution during the build process. The Arcam EBM machine is a leading commercial PBF brand [74,83].

2.3.1.3 Capabilities and typical applications

The capabilities of DED and PBF technologies, including the range of materials that can be processed, and other key markers of industrial relevance, were comparatively assessed to enhance understanding of common and specific attributes influencing current applications of available systems. The raw data obtained from different sources are summarised in Table 2-1. Specific capability data from the different categories identified in Table 2-1 were also compared for DED and PBF platforms, as graphically depicted in Figure 2-4.

The data supports perceptions about the superior accuracy and surface quality achievable with PBF capabilities. Although DED builds typically require post-processing operations, to achieve the desired surface quality, the deposition rates achievable, as well as the capacity to accommodate substantial build volumes, currently outperforms PBF capabilities. Within the DED technology subclass, capabilities configured with the wire feedstock generally exhibit high deposition rates, improved energy consumption, and higher material conversion and utilisation rates, when compared with DED capabilities configured for powder deposition. The feedstock parameters are also important in wire-DED, as the wire diameter can be sized to meet requirements for depositing bulk solids or adding finer details.

Table 2-1. Comparison of process capabilities for PBF and DED technologies

	Processing Technology								
Capability	DMLS [32,74,84,85]	SLM [32,74,84]	EBM [30,74,86,87]	LENS [42,88–90]	DMD [30,34,42,43,45–48,48]	DLF [40,51,91,92]	EBF[3] [53,54,93–95]	WLAM [32,96–99]	WAAM [32,42,65,67,100]
Material utilisation	10 – 15%	10 – 20%	10 – 20%	10 – 15%	10 - 90%.	10 - 20%	> 98%	> 98%	> 98%
Energy Efficiency	2 - 5%.	2 - 5%	15-20%	2 - 5%.	2 - 5%.	2 - 5%.	> 90%.	2 - 5%.	> 80%
Layer thickness (µm)	20 - 100	20 - 100	50 - 200	100 -1000	100 -1000	100 -1000	340 - 2000	500 – 2000	1000 - 2000
Build size (mm)	500×350×300	800×400×500	350×350×380	2000×1500×900	$2000\times10^3\times10^3$	2000×1000×750	5791×1219×1219	$> (10^3\times10^3\times10^3)$	$> (10^3\times10^3\times10^3)$
Build rate (kg/h)	0.12 - 0.6	0.12 - 0.6	0.25 – 0.35	0.36 - 0.75	0.36 - 0.6	0.36 - 0.6	0.4 - 9	0.65 - 8	0.72 - 48
Geometric accuracy (mm)	±0.05 - ±0.1	±0.025 - ±0.04	±0.025	±0.38 - ±0.50	±0.38 - ±0.50	±0.13 - ±0.51	±0.8	≥WD	±0.2
Surface finish (µm)	14 - 16	9 - 10	25 - 35	61 - 91	~40	~20	2 - 10	12±2	200
Porosity (%)	0.1 - 0.9	≤ 0.50	0.09 - 0.25	≤ 0.5	≤ 0.5	≤ 0.5	≤ 0.25	≤ 0.1	≤ 0.1
Detail	HR/CG/HC	HR/CG/HC	MR/CG/HC	LR/SG	LR/SG	LR/SG	LR/SG	LR/SG	LR/SG
Feature addition	N/A	N/A	N/A	✓	✓	✓	✓	✓	✓
Repair/ Remanufacture	N/A	N/A	N/A	✓	✓	✓	✓	✓	✓
Multi material	N/A	N/A	N/A	✓	✓	✓	✓	✓	✓
Residual stress	High	High	Low	High	High	High	Low	High	High
Heat Treatment	✓	✓	-	✓	✓	✓	-	✓	✓
Post processing	✓	✓	✓	✓	✓	✓	✓	✓	✓
Materials	Inconel, Al alloys, stainless steel, Titanium alloys	Inconel, Al alloys, stainless steel, Titanium alloys	Titanium alloys, cobalt chrome, Inconel, stainless steel, Al alloys	AISI 1018 steel, FeMn alloy, FeNi alloy, 316 SS, Ti-6Al-4V.	Inconel 625, Inconel 718, Cu–30Ni alloy, AISI 4340 steel, 316 SS, Ti-6Al-4V, Inconel-steel FGMs.	316L SS, Inconel 690, Inconel 718, Ti-6Al-4V	2219 Al, Ti-6Al-4V, Inconel 718, stainless steel 347, Copper – Steel FGM	Ti-6Al-4V, Inconel 718, H11 Steel, AISI 316L, 5356 Al, AW-5087	HS steels, 316L SS, Ti-6Al-4V, Inconel 718, 2024 Al, 2319 Al, 5087 Al) Bronze, Copper, Tungsten, Tantalum

Key: HR – High resolution, MR- Medium resolution, LR – Low resolution, CG – Complex Geometry, SG – Simple geometry, HC – Hollow channel, N/A – Not applicable, WD – Wire diameter.

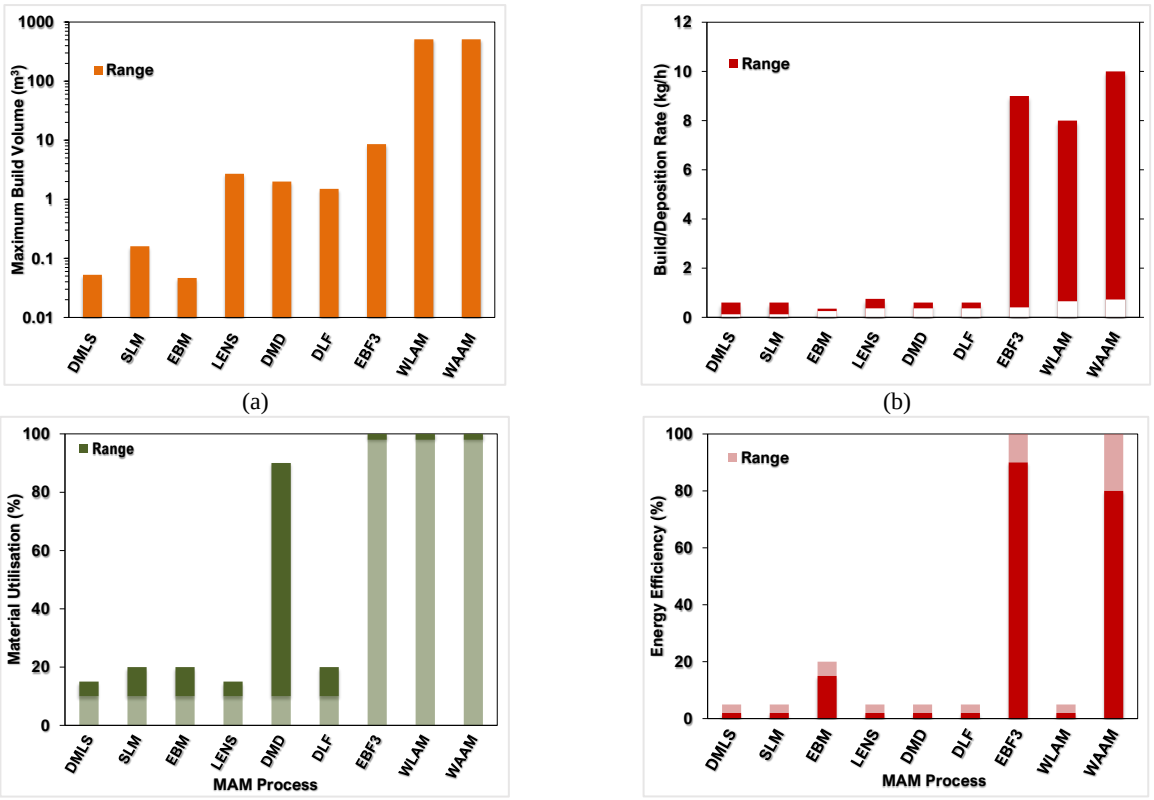

Figure 2-4. Comparison of (a) maximum build volume (b) build/deposition rate (c) material utilisation and (d) energy efficiency for metal additive manufacturing processes (ref: Table 2-1).

Williams et al. [101] reported compromised part fidelity at significantly higher deposition rates (e.g. >10kg/h), necessitating substantial machining operations to remove excess material, resulting in economically undesirable raw material conversion rates. Therefore, the study concluded that medium deposition rates, ranging from between 1 to 3 kg/h, improved material conversion, as well as the economic viability of WAAM processes. When considering potential applications for these capabilities, a wide range of engineering alloys used in high value manufacturing (as listed in Table 2-1) were found to be suitable for processing using both PBF and DED systems. Furthermore, other weldable materials can be deposited using the WAAM process, which facilitates the pre-selection of suitable applications based on relevant precedents. PBF and DED systems can also be developed to exploit the unique traits of MAM technology, via FGM deposition options, to create functionally graded components.

In general, PBF processes are typically associated with the production of small scale, high precision, and geometrically complex parts, with intricate features, hollow sections, and overhangs [36,74,87,102]. These advantages are attributed to the configuration of PBF systems, which allows for the selective and directed delivery of energy to melt small areas of the feedstock over the larger build platform, prioritising the unimpeded realisation of product forms. However, due to the prioritisation of the product form, reported challenges in the post-processing of parts, removal and reuse of excess material, and the need for designating equipment for specific alloys [26,30,31,72–74], are also directly attributable to PBF deposition procedures. Relative to PBF systems, flexibility is one of the main advantages of DED capabilities, which are reportedly

suited to and often associated with repair, remanufacturing, feature addition and large part fabrication [36,41,42,65,102,103]. DED systems are typically configured to maximise flexibility, whilst also fulfilling the need to create the desired 3D shapes or forms. This configuration also allows for higher deposition rates, with specific DED procedures contributing to higher material yield, particularly when comparing powder and wire feedstock requirements for similar products. However, the prioritisation of tooling flexibility, for focussed concurrent energy and material delivery, significantly restricts the relative complexity of resulting DED parts.

Todorov et al. [87] manufactured engine blades and vanes from Ti-6Al-4V and Inconel alloys to demonstrate the capabilities of PBF technologies for small scale production. When compared to conventional manufacturing approaches for similar products, the complex geometric design and internal cooling channels, introduced for cooling purposes, resulted in improved material utilisation. Dutta et al. [102] used EBM for the manufacture of an integrated hydraulic mount and manifold, which included internal channels, and resulted in an improved surface finish. Other parts fabricated with PBF machines include the fuel nozzle for the General Electric (GE)/ Safran LEAP® engine, manufactured using EOS' DMLS machines. Presented in Figure 2-5, the new nozzle had more sophisticated cooling channels and support structures, 5x reduction in the number of joints, and was 25% lighter when compared to the previous design manufactured via conventional methods, resulting in a five-fold increase in the component service life [36,74].

Figure 2-5. GE 3D-printed fuel nozzle tip for the LEAP engine [36,104]

Liu et al. [36] reported the successful use of DED processes for large part fabrication and repairs. Specifically, a LENS-based solution was adapted for the repair of aerospace components, and for repairing the erosion on an integrally bladed steel rotor. The LENS process was also used to build up a worn area on a Ti-6Al-4V gas turbine bearing housing. When compared to the cost of a new bearing, the LENS repair, including the post-repair machining operation required to achieve the final dimensions, resulted in a cost saving of about 50%. In another study, investigators at The Welding Institute (TWI) successfully built a thin-walled Inconel 718 combustion chamber for a helicopter engine, using a 5-axis LMD system. Featuring overhanging features, a powder efficiency of 70%, deposition rate of 0.9kg/h and build time of 7.5 hours were reported, alongside the overall component dimensions of Ø300 × 90 mm, which was achieved with an accuracy of 0.8 ± 0.9 mm, and average material porosity of 0.05% [36,105]. Dutta et al. [102] reported on the suitability of DED processes for feature addition on cast or forged parts, such as the addition of flanges and bosses on casings and housings.

The successful use of DMD for the repair and remanufacture of worn-out turbine blades and similar material overlay operations was also reported [106–109].

Williams et al. [70,100] reported several WAAM fabricated large-scale parts with medium complexity. Plasma arc based WAAM was used to produce a 1.2 m Ti–6Al–4V wing spar for an aerospace organisation. A multi-axis robotic system was used for automating the process, with a deposition rate of 0.8 kg/h, resulting in a buy-to-fly (BTF) ratio of 1.2. The BTF is often used in the aerospace industry to measure the difference between the starting and final mass of raw material retained in end products. An external Ti–6Al–4V landing gear assembly, weighing 24 kg and featuring a perpendicular and mildly tilted wall, T-junctions, and multiple crossings, was also manufactured by the researchers using WAAM, at a deposition rate of 0.8 kg/h. The resulting BTF ratio of 1.2 was equivalent to a 220 kg reduction in material yield, when compared to conventional manufacturing methods. Other large-scale parts reported include a 2.5 m aluminium wing rib (BTF = 12), a hollow section 0.8 m wing for a wind tunnel, and a truncated steel cone, with a wall thickness, base diameter, and BTF of 2.5 mm, 0.4 m, and 1.25, respectively.

Greer et al. [110] incorporated a GMAW-based WAAM variant called *metal big area AM* (mBAAM) into a case study involving the design and manufacture of a steel excavator arm with an overhang limit of 15º. The original design excavator arm, which was 2.1 m in length, with a mass of approximately 133 kg, was adapted for the WAAM process by applying topology optimisation techniques to optimise the structure, whilst maintaining product functionality. The WAAM part was subsequently manufactured using a modified Wolf Robotics welding cell with a Lincoln Electric R500 power source. A 25.4 mm thick build plate was bolted onto a thick steel table, which was secured to the floor of the welding cell before proceeding with a continuous deposition process. For stability, this continuous layering approach was maintained until the part was complete. Post-processing procedures involved the insertion of connecting holes, as well as the removal of sharp points and other areas of stress concentration. The details of this case study are depicted in Figure 2-6.

Figure 2-6. WAAM excavator arm manufactured by Greer et al. [110] showing (a) the build direction and overhang constraints, (b) fully fabricated part and (c) installed component after post-process machining.

2.3.2 Financial considerations

The business case is important when considering whether to adopt MAM technologies, as is the justification for the development of new MAM capabilities and features. Hence, some of the key financial considerations for large-scale MAM systems, and related SMRM concerns, were investigated.

2.3.2.1 Equipment acquisition

The cost of commercial and non-commercial PBF and DED systems were examined to support investment justifications. Available capital, operating and maintenance cost information were obtained from several studies, and the resulting cost data was further evaluated to elucidate decision factors. Focusing on the system and other related hardware costs were extracted to evaluate the technology versus cost implications. The collated data and resulting chart are presented in Table 2-2 and Figure 2-7 respectively.

Table 2-2. MAM hardware, operating and maintenance costs [82,111,112]

Process	Equipment	Hardware (£ '000)	Operating Cost/year (£ '000)	Maintenance Cost/year (£ '000)	Reference
Powder bed					
DMLS	EOS (M270)	350 - 534	5-10	25 - 30	[76,113–117]
DMLS	EOS (M280)				
SLM	MTT (SLM 250)	350 - 534	N/A	N/A	[118]
SLM	Renishaw (AM250)				
SLM	Realizer (SLM 250)				
SLM	Matsuura (Lumex Advanced)				
SLM	Concept Laser (XLine 1000R)	1345	N/A	N/A	[76,119]
EBM	Arcam (A2)	380 - 534	N/A	N/A	[76,115]
EBM	Arcam Q20	720	N/A	N/A	[76]
Powder feed					
LENS	Optomec (LENS MR-7)	600 - 800	N/A	N/A	[120]
	Optomec (LENS 850-R)	445 - 712	N/A	40	[121]
DMD	POM DMD (66R)				
DMD	Trumpf DMD505				
DLF	N/A	N/A	N/A	N/A	N/A
Wire feed					
EBF[3]	Sciaky (EBAM range)	>1600	N/A	N/A	[120]
WLAM	N/A	N/A	N/A	N/A	N/A
WAAM	MER (PTA SFFF)	N/A	N/A	N/A	[113]
WAAM	Honeywell (IFF)	N/A	N/A	N/A	[113,122]
WAAM	Norsk Titanium (RPD MERKE IV)	N/A	N/A	N/A	[123,124]
Wire Feed (OA)					
WAAM (CNC)		1,590 - 2500	N/A	N/A	[125,126]
WAAM (R)		250 - 325	N/A	N/A	[118,125,126]

Key: N/A – Not available in literature, OA – Open Architecture, R – Robotic.

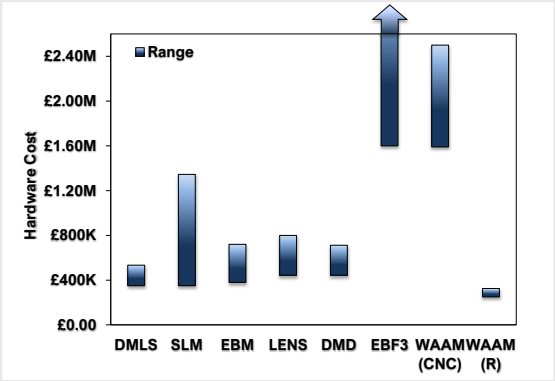

Figure 2-7. MAM system and related hardware costs.

Compared to a few DED processes, such as LENS, DMD and EBF[3], the PBF processes reviewed are already commercialised. Nevertheless, original equipment manufacturers (OEMs) are adapting and developing wire-based DED technologies for various applications. Some DED capabilities, including the Norsk Titanium's *rapid plasma deposition* (RPD) MERKE IV [127], and Honeywell's *ion fusion formation* (IFF) [128], were exclusively developed for internal use and thus not presently available for commercial purchase. However, these OEMs offer manufacturing capacity as a service, to meet a growing demand for these DED technologies.

In general, detailed information on commercial system costs, including MAM hardware ownership, are sparse in extant literature. Furthermore, procurement data on systems, such as the Sciaky EBAM 300, for instance, was only available via quotation requests from the manufacturer, which remains subject to supply conditions, including order quantities and related factors. Nonetheless, available data indicate that EBM systems are more expensive to procure and operate when compared to laser based PBF systems. Direct correlations have also been reported between the price of PBF machines, the build volume, and the beam power capacity [82].

In most cases, it was challenging to find maintenance and operating cost information, given the development stage and existing affiliations of developers responsible for most DED platforms in use today. For large-scale DED system, there were also wide variations in hardware costs. Bandari et al. [100] evaluated the cost and performance implications of systems configured with CNC vs robotic gantry systems, as well as the inclusion of ancillary units. It was reported that CNC system enabled higher accuracy than the robotic gantry system, but open architecture (OA) CNC configured DED systems were significantly more expensive. However, robotic gantry systems reportedly offered higher flexibility and part mobility, particularly when combined with a suitable manipulator, as well as the ability to use multiple robots or a robot mounted on linear drives to enlarge the build envelope.

2.3.2.2 Raw material

The choice and characteristics of the feedstock material form, used for the MAM process, can significantly affect the resulting material properties, and related system maintenance and operating costs [61,129]. Powder

feedstock characteristics include particle size distribution (PSD), surface morphology, shape, chemical composition, bulk packaging, and flow properties or flowability. Depending on the powder manufacturing process and specification, extra processing of the powder may be required, in addition to the reprocessing of unused powder to minimise waste, and the PSD requirements for discrete MAM technologies and systems. Other technical and operational considerations include the demanding storage and handling requirements associated with the powder feedstock, as well as the cost of compliance with health, safety, and environmental standards, due to the hazards associated with this material form. Conversely, the use of wire feedstock presents fewer procedural complications from an operational standpoint, particularly in relation to the handling and storage costs. Relative to the powder feedstock, the significantly smaller wire surface area to volume ratio diminishes the probability of contamination and oxidation during deposition, not to mention the higher raw material conversion rate. The specific metal feedstock cost comparison is shown in Table 2-3.

Table 2-3. Cost of different feedstock used for MAM applications.

Feedstock	**Specific costs (£/kg)**						
	316L SS [70,130]	17-4 PH SS [70,131,132]109, 190, 191]	Inconel® 718 [130]	Inconel® 625 [130,133]	Ti-6Al-4V [65,130,131,134–136]	Al 7075 [70,133]	Al 6061 [70,133]
Powder	40	78 -120	80	80	280 - 500	52	58
Wire	2 - 15	2 - 15	58	49	120	6 - 100	6 – 100

When comparing the cost of some of the most utilised industrial alloys today, available data indicates that the wire feedstock is generally more economical for the MAM process, with titanium alloy Ti-6Al-4V being the most expensive raw material to procure, in both wire and powder forms. However, the combination of relatively higher material costs and lower material conversion rates in powder-based MAM processes is an economical limitation. Dawes et al. [129] investigated supply chain options, for the procurement of powder feedstock materials, and concluded that there are currently three main options available; from MAM equipment providers, directly from powder atomisers, and third-party suppliers. Procuring powder from equipment vendors was found to be more expensive, but deviating from OEM material specifications or products reportedly affected the resulting build quality [137]. The higher specific cost of the powder feedstock is attributed to several factors, including the atomisation process, powder quality, supply conditions and demand. Furthermore, powder quality is directly dependent on the manufacturing process, which determines the resulting feedstock characteristics. Similarly, the wire quality and characteristics are influenced by the wire production process. For the MAM process, ensuring the quality of these important inputs is essential for achieving higher quality outputs. Nonetheless, the raw material cost is one of the many considerations influencing business decisions concerning DED and PBF processes.

2.3.2.3 Energy consumption

Energy consumption is a key industrial metric for assessing manufacturing efficiency and related cost implications, primarily at the process and system levels. At the process-level, MAM energy consumption

relates to the direct energy input during deposition, while system-level energy consumption represents the total energy expended. The system-level energy encompasses the process-level energy consumption, as well as the energy consumed by all sub systems and ancillary equipment directly linked to the process. A study by Baumers et al. [138] found direct correlations between the process-level energy consumption and the build or deposited mass, but no direct linkage between the complexity of deposited components and energy consumed at the system-level.

The specific energy consumption (SEC) is used as an indicator for energy efficiency, and was investigated by different researchers to provide a meaningful basis for comparing MAM and contemporary manufacturing methods [132,139,140]. While the SEC may include the specific deposition time or production rate, these studies mainly focused on the amount of energy used per specified product unit (i.e. MJ/kg), which is also an acceptable basis for measuring energy performance or SEC [141]. Accordingly, different DED and PBF process variants were evaluated, with typical SEC data directly obtained from surveyed literature, as summarised in Table 2-4.

Table 2-4. Specific energy consumption (SEC) data for different MAM processes.

Process		System	Material	SEC (MJ/kg)	Reference
Powder bed	DMLS	EOS M270	17-4 PH SS	251 - 462	[132]
	DMLS	EOS M270	17-4 PH SS	220	[131]
	SLM	MTT (SLM 250)	316L SS	83[a] – 106[b]	[142]
		Concept Laser M3 Linear	316L SS	423[a] – 588[b]	[142]
		Concept Laser M3 Linear	316L SS	96.8	[143]
		Renishaw AM250	413.2 Al	566[a] – 1160[b]	[144]
	EBM	Arcam (A1)	Ti-6Al-4V	61[a] – 177[b]	[138,142]
	EBM	Arcam (S12)	Ti-6Al-4V	113	[131]
Powder feed	LENS	Optomec LENS 750	H-13 tool steel	70	[139]
	LENS	Optomec LENS 750	Inconel 625	1469[c]	[145]
	DMD	POM DMD (66R)	N/A	N/A	N/A
		Trumpf DMD505	N/A	N/A	N/A
	DLF	-	-	-	N/A
	EBF[3]	Sciaky (EBAM 300)	N/A	N/A	N/A
Wire feed (commercial)	WLAM	N/A	N/A	N/A	N/A
	WAAM	MER PTAS	N/A	N/A	N/A
		Honeywell IFF	N/A	N/A	N/A
Wire Feed (OA)	WAAM (GMAW, CNC)	-	H-13 tool steel	32.3	[139]
	WAAM (GMAW, Robotic)	-	316L SS	18.65	[140]
	WAAM (GTAW, CNC)	-	N/A	N/A	N/A
	WAAM (GTAW, Robotic)	-	N/A	N/A	N/A

Key:
a – Full chamber utilisation; b – Partial chamber utilisation; c – Repair deposition and heat treatment for 16 hours. N/A – Not available in literature; OA – Open Architecture.

The reported SEC for PBF processes is dependent on the degree of utilisation of the build chamber, and the material being processed at similar deposition rates. Primarily, inefficient part orientation and under-utilisation of the build chamber adversely affects SEC, and for EBM, actual values varied between 61 and 177 MJ/kg,

corresponding to the full and partial utilisation of the build chamber [82]. Based on the reported values, the indicative SEC for EBM was typically lower than that of DMLS and SLM processes. The relatively higher deposition rates reported for the EBM process suggests that similar builds required less time to complete, when compared to DMLS and SLM processes, which consumed between 96 and 1160 MJ/kg. The higher values reported for SLM processes was attributed to the build chamber utilisation, as well as the SEC requirements during each phase of the process. Kellens et al. [143] observed the power levels for the subsystems of a Concept Laser M3 SLM machine during operation and noted that although the highest power peaks (~3.5 kW) were recorded during the powder raking or sweeping phase, the laser subsystem was the most energy intensive component, requiring 68% of the total machine power. However, experimental power monitoring studies by Baumers et al. [142] revealed that in some instances, differences between SEC can be independent of build chamber utilisation. For DED processes, available data indicate that the SEC is considerably lower than for most PBF processes, with consumption data for WAAM reportedly lower than LENS or DMD processes. Wilson et al. [145] indicated that the high SEC for LENS was due to the inclusion of energy data for a 16-hour heat treatment procedure, which was completed on the deposited component after a repair operation.

Due to the significance of energy usage on the environment, related energy considerations, such as the life cycle analysis (LCA) of PBF and DED processes were also investigated. This focus aligns with economic and regulatory trends concerning ecological and other manufacturing factors contributing to climate change. The or cradle-to-grave (CTG) energy consumption for wire DED, powder DED and post-process machining were estimated using a model developed by Jackson et al. [139]. Comparisons were made between WAAM (GMAW) and LENS for a steel component measuring 15 cm^3. The model predicted that the energy consumed during the WAAM process was 54% of the requirements for the LENS process. However, unlike the LENS components, which had a finer resolution, indicative of a higher surface quality, 30% more energy was consumed when machining the WAAM component. Overall, the LCA revealed similar total energy values for both DED processes, owing to higher energy requirements for wire production.

In consideration of SMRM requirements, relevant LCA studies relating to MAM applications were also reviewed. Huang et al. [146] studied the through life-cycle potential of MAM aircraft components to conserve energy and reduce greenhouse gas emissions. Significant energy savings were attributed to reduced feedstock requirements and fuel consumption of up to 6.4%. However, these potential savings were subject to the adoption of MAM components in the aerospace industry sector. Wilson et al. [145] carried out experimental studies on repairing components, typically classed as non-repairable, in an environmentally-friendly manner. The study objective was to repair stainless steel (316L) and Inconel® 625 turbine blades, using an Optomec LENS 750 system. The repaired blades matched the geometry of the original blade with an average accuracy of 0.03 mm. The reported strength and ductility of the repaired blade was comparable to conventionally manufactured Inconel® 625. The LCA studies also provided indications of the environmental and energy conservation benefits of repairing blades with small defects via DED. It was reported that for a repair volume

of 10%, when compared to a full blade replacement, energy consumption savings and greenhouse gas emissions reductions of up to 35% and 45%, respectively, were achievable.

Morrow et al. [147] carried out quantitative studies, to compare the energy consumption and emissions associated with the production of mould and die tooling, using DMD and CNC milling techniques. A detailed investigation of three case studies revealed the trade-offs necessary when selecting manufacturing methods and for end-of-life considerations in the tooling industry. In terms of energy consumption and emissions, tooling components with a high solid-to-cavity ratio (>7) tended to favour conventional manufacturing via CNC milling. For the simulated DMD manufacture of a fixture, with a low solid-to-volume ratio (0.33), they estimated a reduction of manufacturing time and energy consumption of 4% and 80% respectively. In another case study, the remanufacturing of a stamping tool via DMD for an American truck manufacturer was examined. It demonstrated significant economic and environmental savings, equivalent to $250,000 and 50% of the energy required for the tool steel production before CNC milling, for this DMD application. However, the processing parameters for the first two cases examined were sub-optimal, as the lowest possible deposition rate of 0.01 g/s was selected, and the energy required for post-DMD heat treatment was also included.

2.3.2.4 Attributable costs

Presently, it is difficult to estimate the complete economic benefits for MAM components, given that these processing techniques are still evolving. Nevertheless, and in addition to the cost of hardware, raw materials, and energy consumption, several researchers have studied the SEC of MAM relative to conventional manufacturing methods. Vayre et al.[148] evaluated the combined cost of the machine operation, raw material and consumables, and concluded that sintering-based processes were less expensive when compared to EBM and DED processes, where materials are completely melted. In addition, the high price of machines associated with these processes were balanced by the typically short pre-production phase required for small batches of products or parts.

Atzeni et al. [149] studied the adequacy of DMLS for small to medium batch production of a scaled model (1:5) of the main landing gear of the Italian aircraft P180 Avant II, relative to established manufacturing methods, including high pressure die casting and 5- axis machining. The analysis highlighted that 90% of the component cost was attributed to the cost of the MAM machine (EOS M270), with the remaining cost ascribed to the aluminium alloy AlSi10Mg raw material input. However, component redesign, which is a significant enabler for MAM production, particularly for small batch runs, was found to be negligible for medium to large batches. The MAM route was the least expensive option for this application, and matched the cost of machining operations, after producing 2 pieces, indicating correlations between MAM costs, and required product volumes. On the other hand, the cost of manufacture via high-pressure die-casting was highest for small volumes, achieving parity with MAM production costs after 42 pieces.

Piili et al. [150] analysed process induced expenses and related costs for DMLS manufactured stainless steel alloy PH1components. Build experiments were conducted using a benchmark component (A), and a 50% scaled down version (B), with similar wall thicknesses. Single piece and full chamber build experiments were carried out for components “A” and “B” and the build costs were analysed. Full chamber utilisation for “A” and “B” yielded 40 and 170 units respectively. The specific component cost structure is shown in Figure 2-8.

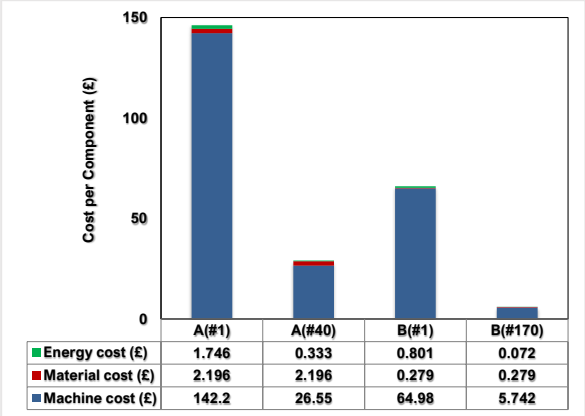

	A(#1)	A(#40)	B(#1)	B(#170)
Energy cost (£)	1.746	0.333	0.801	0.072
Material cost (£)	2.196	2.196	0.279	0.279
Machine cost (£)	142.2	26.55	64.98	5.742

Figure 2-8. Comparison of cost of single and full chamber build experiments for components A and B (Piili et al. [150]).

The data revealed that the cost of the machine was dominant for all experiments, which is consistent with previous observations [149]. However, utilisation of the full build chamber resulted in a cost saving of 79.6% and 91.6% for components A and B respectively, when compared to single unit builds for each component. Similar savings were also achieved when manufacturing times were considered, demonstrating the potential benefits of nesting parts, to optimise chamber utilisation and batch production runs.

Cunningham et al. [151] developed time-based activity cost models for assessing the cost effectiveness of WAAM. Selected data from the WAAM process chain, including substrate preparation, material deposition, heat treatment, machining, substrate removal and inspection, were incorporated into the cost model, which excluded other cost elements, such as the build scrap rates or defect generation data. Two Ti-6Al-4V case studies, including a propeller and an X-shaped part, were selected for comparisons. The cost of total production for WAAM, EBM and DMLS processes were also compared, as well as the cost of CNC milling for BTF ratios of 5, 10, 15 and 20. The model estimates showed that WAAM fabrication routes outperformed all other manufacturing processes and was highly cost effective, when compared to EBM and DMLS. In comparison to EBM, a potential cost reduction of 20-45% was predicted, while 69-79% costs reductions were predicted for the DMLS process. For CNC milling, predicted WAAM costs were comparable at a BTF ratio of 5, with 53% predicted cost reduction at a BTF ratio of 10. The cost comparisons are shown in Figure 2-9.

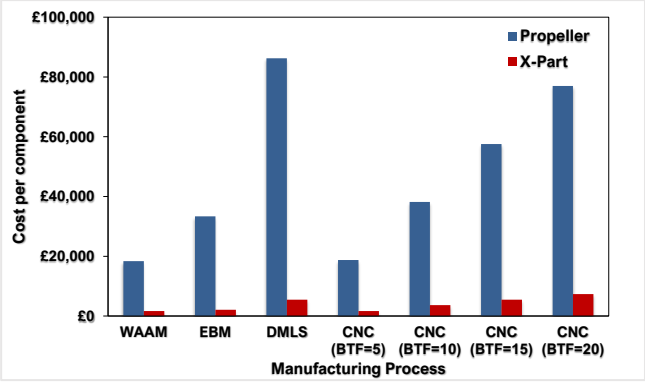

Figure 2-9. Comparison of AM and CNC production costs for two case study components by Cunningham et al. [151].

A model cost sensitivity analysis tool was used to identify key financial drivers for WAAM. It was reported that a ±20% variation in WAAM processing times resulted in cost increases of approximately ±11%, for the propeller, and ±5% for the X-part, with only ±1% change in machining time, indicating the potential for higher cost sensitivity in MAM processes. While the effects of product quality or defect rates on cost was not explicitly considered, the importance of cost effectiveness, relative to the lack of industrial standards for controlling MAM quality, was highlighted.

Stecker et al. [152] compared the cost and lead-time of Ti-6Al-4V components processed via EBF^3 and conventional manufacturing methods. Two representative aerospace components were selected for build experiments; a gimbal, which had a low solid-to-volume ratio, and was unavailable from the OEM, and a structural chord, which also had a low solid to volume ratio. These components were selected due to the large quantities of material waste generated when manufactured conventionally. Sciaky's EB VX300 system was used for deposition, at the rate of 2.3 kg/h for the gimbal, and 3.18 kg/h structural chord, with resulting masses of ~100 kg for the gimbal, and 9.1 kg for the structural chord. The EBF^3 components and related cost comparisons are depicted in Figure 2-10.

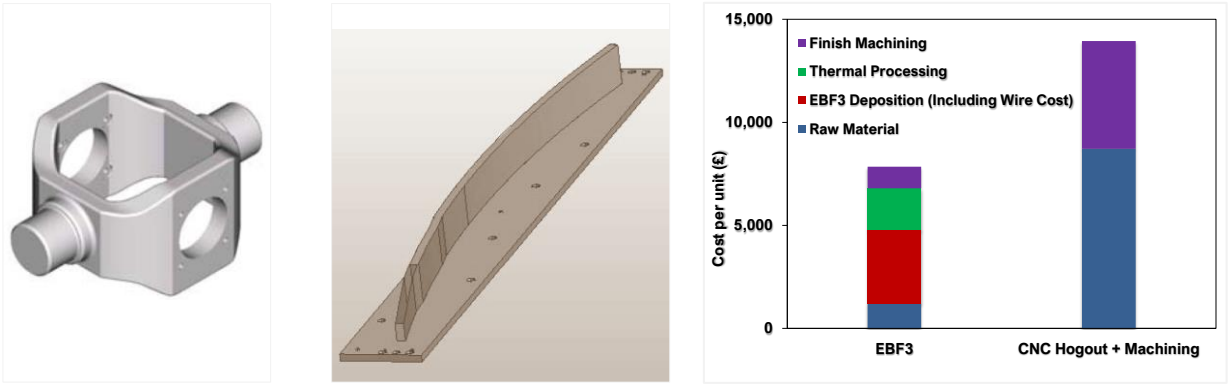

(a) (b) (c)

Figure 2-10. Illustrations of (a) gimbal and (b) structural chord manufactured via EBF^3 as reported by Stecker et al. [152] and (c) EBF^3 vs. CNC machining cost comparisons adapted from this study.

Material savings of over 50% were reported when the gimbal was fabricated using a combination EBF^3 and subsequent machining, in comparison to conventional CNC processing from a solid block of material. The cost for the EBF^{3}structural chord was compared with estimated costs for conventional CNC machining of this component, as shown in Figure 2-10(c). CNC machining resulted in a lower BTF, with an estimated 80% more raw material required, while the overall cost for the EBF^3 process was 43% lower than the estimate for conventional machining. The authors also noted that the cost of EBF^3 is dependent on two key interrelated variables, namely, the material feedstock, and deposition rates.

Bekker et al. [140] assessed the sustainability of WAAM manufacturing for large structures at Dutch robotics company, MX3D, in accordance with ISO standards. The EBM and DMLS cost and SEC benchmark studies carried out by Baumers et al. [131] were compared in this assessment, which excluded post-processing costs, energy for raw material production, and the impact on material properties. The cost and SEC comparison for all three MAM processes are shown in Figure 2-11.

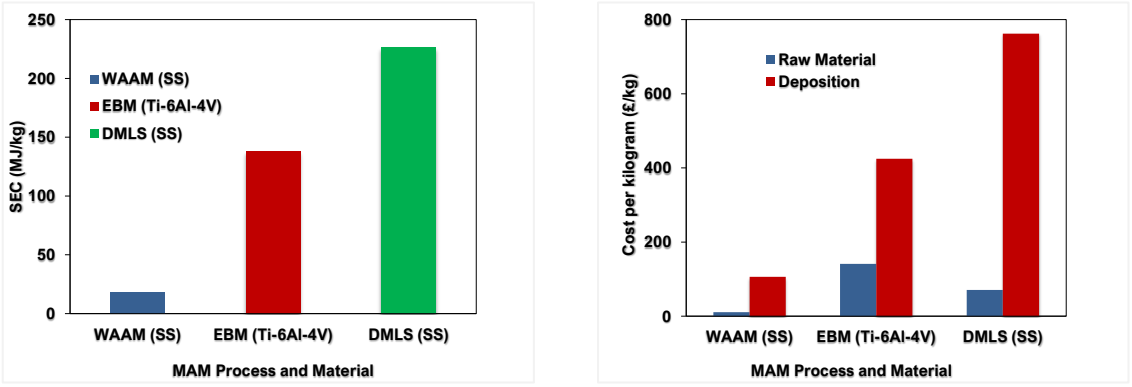

(a) (b)

Figure 2-11. Comparison of SEC and specific cost of MAM processes as documented by Bekker et al.[140].

The comparisons showed that the WAAM fabrication, with a deposition rate of 0.5 kg/h, the SEC (18.6 MJ/kg) and cost (£115/kg) for stainless steel, was significantly lower than the benchmarked values for EBM processed Ti-6Al-4V (138.2 MJ/kg and £566/kg), and DMLS processed stainless steel (226 MJ/kg and £833/kg).

2.3.3 MAM technology alignment for large-scale operations

So far, this review has been focussed on the analysis of different DED and PBF technologies, to determine the relative suitability for large-scale MAM operations, including SMRM. Correspondingly, an important consideration in the selection of manufacturing technologies is the suitability of a particular process for its intended applications. Compared to PBF technologies, which rely exclusively on the powder feedstock, DED technologies can be configured using the range of raw materials or feedstock forms and energy sources currently available for MAM. While DED and PBF systems both require mechanisms for delivering the feedstock and energy inputs onto designated surfaces or build platforms, these mechanisms are separately configured in PBF systems, which also require mechanical rollers or blades for spreading the powder feedstock

across the build platform. Conversely, DED system designs allow for the integration of both material and energy delivery mechanisms within a single compact unit or tool. This configuration offers significant flexibility because the compact unit can simultaneously and precisely dispense the material and energy inputs, which is highly desirable for SMRM activities. Flexibility also enables scalability, with distinctive benefits for large-scale MAM and SMRM operations, as evidenced by the relatively larger build volumes achievable using DED capabilities (Figure 2-6). However, it was previously identified that there are correlations between scaling factors (i.e. chamber size), energy requirements and MAM system costs.

The deposition atmosphere is also important when configuring MAM systems. Variations were noted between capabilities utilising different energy sources, with more stringent safety requirements governing the utilisation of power beams. While a controllable processing environment is highly advantageous for all MAM operations, operating without the constraints of a chamber, which is feasible for some DED processes, such as WAAM, can be beneficial under specific task circumstances and conditions, applicable to SMRM operations. When considering productivity and processing efficiency (Table 2-1), and compared to DED processes, where layers are relatively thicker (~0.25mm to >1mm), the typical layer thickness for PBF processes, ~20μm to 60μm, contributes to superior surface quality. Nevertheless, for large-scale MAM operations, DED systems configured with the wire feedstock option, offer higher deposition and material conversion rates, which are economically favourable. Evaluation of other cost factors revealed that irrespective of part complexity, specific MAM energy requirements at the system-level were largely determined by the deposition duration, and the build or deposited mass. Furthermore, the process input and output factors, such as the raw material, production, and finishing requirements, were more relevant when considering the CTG aspects of both DED and PBF technologies. However, without the appropriate industrial context or relevant application, these factors are more difficult to quantify. In general, and compared to the PBF commercial range, it was more challenging to estimate the specific costs of DED capabilities, due to the lack of pertinent data, which is somewhat indicative of the current developmental and/ or commercialisation state of this technology sub class.

A broad initial approach was necessary for enhancing understanding of PBF and DED system attributes and related procedures, and for shaping planned system development activities. When considering the different factors evaluated, including system configurations, capabilities, costs, and typical applications, DED was identified as the technology sub-class with a range of processes that were, at present, most suited to large-scale MAM and SMRM operations. In order to comprehend specific development challenges affecting DED technologies, while considering the requirements for a new MAM system, distinct processes were comparatively evaluated. The implications of utilising DED technologies for large-scale MAM and SMRM applications, was a key consideration for subsequent investigations, with a refined focus on correlations between systems, procedures, and the resultant materials or parts, including the required quality and properties.

2.4 DED quality and performance

The quality, consistency, and performance of manufactured products are reliable indicators of the true capabilities and evident suitability of distinct manufacturing processes. Hence, the quality and performance of materials and parts produced using identified DED technologies were reviewed in this section. Related substantiation requirements were also assessed, to support the formulation of an appropriate validation strategy, following the development of the MAM system and analysis of its specific outputs.

2.4.1 Geometric characteristics

Bi et al. [48] reported poor dimensional accuracy of SS 316 walls built using a DED-LP process, underscoring the need for tight process control, to improve the as-deposited build quality. Deposited walls were reportedly thicker at the beginning of the laser pass, due to the deposition sequence of feeding powder into the build vicinity before applying heat. Over subsequent layers, the build normalises, due to the sustained and synchronic application of material and heat. However, it is possible to improve the surface finish of DED components, using both in- and post-processing techniques. Taminger et al. [93] investigated different techniques for smoothing the ridged surfaces of EBF^3 processed 2219 Al pylons. High-speed milling, wire electrical discharge machining (EDM), bead blasting, and electron beam glazing were used for post-processing surfaces, which were examined using low and high magnification optical microscopy. The as-built and finished surfaces are shown in Figure 2-12, with related measurements presented in Table 2-5.

Table 2-5. Surface roughness and texture measurements for EBF^3 deposits [93].

Surface condition	RMS roughness (mm)	Waviness (mm)
As-built	2.337	0.762
High speed milling	(0.203 - 1.422)	0.010
Wire EDM	4.978	0.038
Bead blasting	5.918	0.305
Electron Beam glazing	0.452	0.102

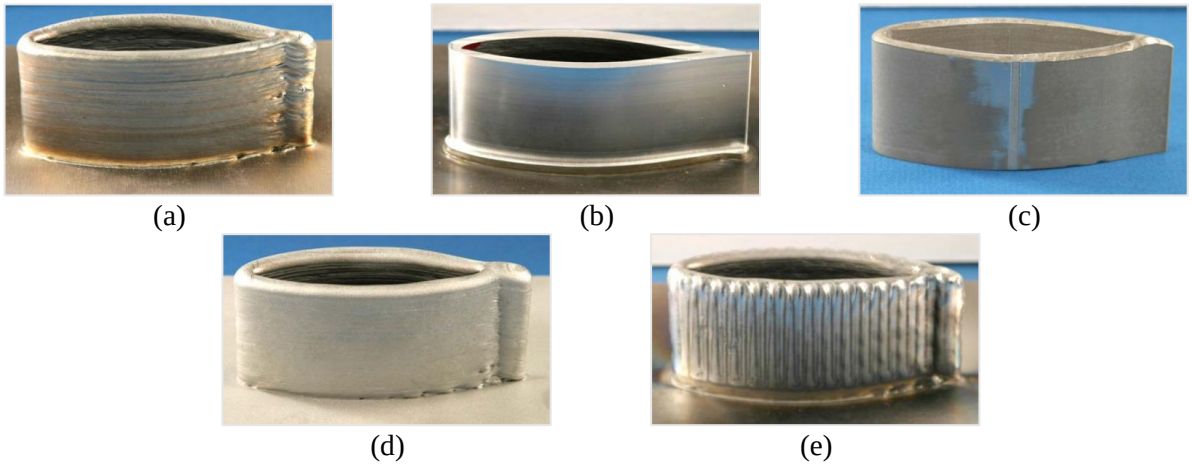

Figure 2-12. The effect of surface post processing on EBF^3 fabricated 2219 Al pylons: (a) as-built condition, (b) high speed milling, (c) wire EDM, (d) bead blasting and (e) electron beam glazing [93].

Although there were no discernible variations in surfaces finished using high-speed milling, reduced long-range waviness and a recast layer (< 5 μm thick) was observed on wire EDM surfaces, with fine asperities and increased localised surface roughness. The bead blasting process produced a combination of increased localised surface roughness and waviness comparable to the as-built sample. The electron beam glazing process produced a very smooth surface without long-range waviness. Overall, high-speed milling produced the optimal surface condition of low localised root mean square (RMS) finish and minimal long-range waviness.

Due to the relatively thicker build layers achievable with wire-based AM process, which can result in greater error margins, the accuracy of WAAM parts is up to 10 times lower than parts produced using powder-based or DED-LP technologies. Combined with a relatively higher deposition rate, WAAM is effective for low complexity or simpler geometries. Thus, a post-processing operation, such as milling, may be necessary for high accuracy parts [32]. Other studies have documented the issue of uneven surfaces, induced by non-uniform geometries within a single deposited layer or pass, particularly at the start and end of the build segment [153,154]. Nevertheless, substantial improvements in deposition rate and surface quality of WAAM components are achievable, as demonstrated for a large skin and core part, with consistent builds achieved at wire feed speeds of 24m/mins, for this tandem process [155].

2.4.2 Chemical composition

The chemical composition of a range of metals processed using different MAM technologies were investigated to elucidate the effects of these processes. Processed materials are susceptible to elemental depletion, which results in compositional variations, as demonstrated by different researchers. Wang et al. [156] used wavelength dispersive spectroscopy to analyse the chemical composition of pre-alloyed gas atomised Inconel 625 powder, deposited onto annealed Inconel 625 substrate plates. The analysis revealed variations in the concentration of alloy constituents in the horizontal direction, across the width of the build. A significant reduction of 4.5 at. % (atomic percentage) and 1.5 wt. % (weight percentage) of the element Chromium (Cr) was measured, from across the build height from the base plate. In this case, the depletion of Cr was attributed to the accumulation of heat in intermediate layers, higher melt pool temperatures in subsequent layers, and the vaporisation of volatile elements as the build progressed. Increased concentrations of Niobium (Nb) (1 at. %) and Molybdenum (Mo) (0.5 at. %) were also measured along the build height. In another study, Haden et al. [157] analysed the composition of 304 SS WAAM specimens via optical emission spectroscopy (OES) to quantify compositional variations between the deposited and feedstock materials. The analysis showed slight depletion of Nickel (Ni) content, from 10.31% in the wire, to 9.36% in the printed material. The latter conformed to the requirements of UNS-S-30400, for an AISI 304 chromium-nickel stainless steel, but did not conform to UNS-S-30800, due to the depletion of nickel content. The potential effects of the processing environment on material compositions were also reviewed. Bird and Hibberd [94] compared the chemical composition of the EBF^3 processed Inconel 718 samples to the wire feedstock and nominal composition for

Inconel 718 [158]. Direct current plasma emission spectroscopy was used to obtain measurements, which showed that the compositions of the EBF^3 parts matched the feedstock wires and nominal composition for Inconel 718. Thus, it was concluded that in this instance, none of the alloy elements were significantly volatilised during the EBF^3 process. In general, and irrespective of the MAM process, compositional changes are known to affect the lattice parameter or atomic arrangement of constituent alloys, thus offering an indirect but useful method for inferring material characteristics, such as the thermal properties, strain state, or defect structure [159,160].

2.4.3 Material characteristics

PBF and DED processed materials are significantly influenced by different factors, including the feedstock type, the processing mechanisms and environment, and alloy characteristics. In order to identify commonalities, a selection of alloys processed using both PBF and DED processes were investigated, beginning with different types and grades of steel. Other alloys, mainly nickel and titanium, were also explored, whilst maintaining focus on the reported effects of distinct processes on resulting materials and parts.

Bi et al. [48] built thin metal walls using stainless steel SS 316 powder, deposited onto C45 carbon steel plates, with resulting analysis revealing layers that were free of pores, micro cracks and other notable imperfections. Except for the last deposited layer, which had a relatively coarser microstructure, the typical fine-grained dendritic microstructure of the build was attributed to the tempering effects of newly deposited layers on pre-existing layers. DMD experiments were also carried out by Sun et al. [43], using gas atomised pre-alloyed AISI 4340 steel powder, deposited onto an AISI 4140 steel substrate. Material samples were subsequently extracted to evaluate the effect of post-process heat treatment, with differentiated martensite, and retained austenite evident in the as-deposited microstructure. After post-processing, the tempered martensite showed finely dispersed carbide precipitates, with fine granular cementite precipitation observed along the grain boundaries. Porosity in the DMD parts, and lack of fusion (LOF) defects between successive layers, were detected in the as-deposited AISI 4340 steel material. The calculated porosity ratio of ~3.3 %, derived from scanning electron microscope (SEM) images, was attributed to porosity in the powder feedstock, lack of powder in regions between deposited tracks, and micro-cracks in the resulting builds. At higher temperatures (830 ºC) significant crack propagation was stimulated around porosities, when compared with samples that were stress-relieved at 600 ºC. In general, it was surmised that a high temperature oxidising environment can degrade fatigue performance, with severe oxidation occurring around areas of porosity, in the stress relieved DMD AISI 4340 steel, accompanied by reductions in ductility, and other measurable properties.

The processing effects of DMD on different Nickel alloys were also reviewed. In a study carried out by Cao et al. [46], Inconel 718 was deposited onto substrate materials from sheets of 1Cr18Ni9Ti steel and Inconel 718 respectively. The as-deposited microstructure was mainly comprised of finer columnar dendrites growing epitaxially from the substrate, in the vertical deposition direction. It was also reported that layer overlap rates

significantly influenced the size and distribution of the grains, resulting in a uniform microstructure upon recrystallization. In another study, the microstructures of DMD Inconel 625 were investigated by Dinda et al. [45], with Inconel 625 powder deposited onto a rolled Inconel 625 substrate plate. Longitudinal, transverse, and horizontal sections were extracted and inspected using optical microscopy and SEM techniques, but no defects, such as cracks, interfacial fusion errors, or pores were observed in the specimens. However, it was reported that the as-deposited microstructure, which primarily consisted of columnar dendrites, growing epitaxially from the substrate and incrementally, along the deposition direction, was significantly influenced by the laser scanning path, and was stable up to 1000 ºC, with fully recrystallized equiaxed microstructure visible at about 1200 ºC.

The effect of selected process parameters on single layers of laser-processed Inconel 718 powder, deposited onto a 1045 steel substrate, was studied by Wolff et al. [161]. Experiments were carried out with a DMG MORI LaserTec 65 3D hybrid additive and subtractive five-axis machine with varying parameters. Post-deposition analysis, including thermal imaging, material characterisation, and corresponding computational fluid dynamics (CFD) simulations, were performed. For DED of dissimilar materials, minimal dilution is preferred to stabilise gradients in composition, whilst achieving substantial interlayer bonding and fusion. Accordingly, the effects of energy density and powder mass flow rates on the dilution of deposited tracks were analysed. A depiction of the relationship between dilution and energy density is shown in Figure 2-13.

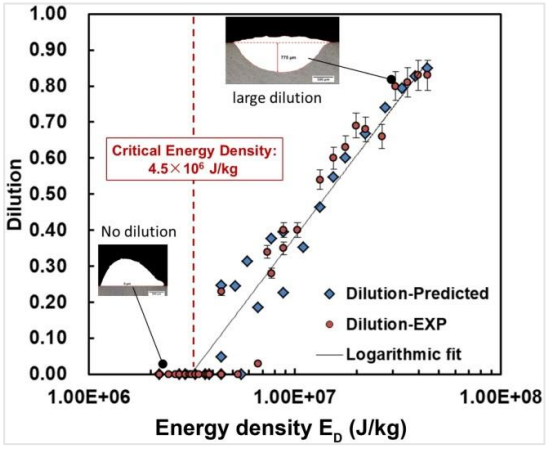

Figure 2-13. Comparison of empirical and predicted clad dilution values with energy density (Wolff et al. [161]).

Based on the combination of the equipment and material types investigated, and at a powder mass flow rate of 256 mg/s, and 1000 W laser power, a critical energy density of 4.5×10^6 J/kg for dilution was discovered. Energy density inputs lower than the established critical value were reported to have no observable effects on dilution, with logarithmic increases observed when energy density inputs were higher than the critical value. The effects of cooling rates on the melt pool geometry, and microstructure evolution in solidified deposits, were also evaluated. The localised primary and secondary dendrite spacing were determined and compared with cooling rates calculated from infrared (IR) thermography. An inverse power law relationship was observed between these variables, with lower dendrite spacing corresponding to higher energy density.

Parimi et al. [92] evaluated the characteristics of DLF Inconel 718 thin walls (20×0.7×10 mm), in order to simulate repair applications, and understand the influence of variations in the deposition path, and laser power on microstructure, grain structures, and intermetallic particle morphology development. Optical and scanning electron microscopy was used to investigate the porosity of the samples. Electron backscattered diffraction (EBSD) and x-ray spectroscopy techniques were also used for these investigations. Low porosity of about 0.2% was observed in the thin-walled samples, which increased to 0.8% as laser power increased. When low laser power was selected for deposition, the resultant microstructure consisted of fine and coarse grains with a weak texture. At higher power levels, which also resulted in the formation of Laves phase precipitates, carbides, and brittle delta (δ) phase, a strongly textured columnar structure was observed. In contrast, carbides and δ phase formation were not observed in low power samples, irrespective of the deposition path.

Bird and Hibberd [94] investigated the EBF^3 process for the fabrication of Inconel 718 components, for high temperature structural applications. The investigation was focused on determining the mechanical properties of EBF^3 deposits, and how to focus these properties to specific applications. The effect of post-EBF^3 heat treatment at different temperatures on the microstructure and mechanical properties were also investigated. For the as-deposited specimen, microstructural analysis, performed using optical microscopy techniques, revealed a fine dendritic structure, resulting from the rapidly solidified melt pool. At a high magnification, new dendrite colonies, formed at each boundary between adjacent deposition layers, were observed. Post-processing of the specimens, at lower heat treatment temperatures, did not appear to have a major effect on the microstructure. However, procedures completed at higher temperatures resulted in recrystallization and elimination of the original boundaries between deposited layers, which was attributed to the higher modulus reported for higher temperature heat treatment protocols.

Clark et al. [62] completed multi-pass linear depositions of Inconel alloy 718 using WAAM, and then fabricated a circumferential flange onto a ring rolled combustion casing, before performing microstructural analyses, using the Jeol 6100 and Phillips XL30CP SEM machines. The ultimate microstructural condition of the flange was determined to be highly dependent on deposition parameters and practice. It was reported that phases detrimental to mechanical properties, such as brittle laves and δ phases, which form through local chemical segregation, can be controlled via careful regulation of the cooling rate. In this case, fast freezing and minimal reheat was favoured throughout the process. At low magnification, extensive cracks, which transected multiple beads, were also reported within the flange, and it was inferred that crack orientations were initiated by a post deposition bi-axial stress field, imposed during cooling. At higher magnification, it was further noted that the local control of the crack path was clearly due to the deposited material microstructure, particularly at regions of dense laves precipitation, and shrinkage porosity, within overlap zones in the flange.

Taminger and Hafley [54] carried out a parametric study on the microstructural evolution of EBF^3 processed 2219 Al and Ti–6Al–4V walls. The build direction was optimised, with the wire always introduced into the leading edge of the molten pool. The translation speed, wire feed rate, and beam power were varied, to study

the effect of the processing energy density on the build quality and grain morphology. For the 2219 Al samples, the resultant microstructures varied from fine equiaxed grains to larger grain sizes and dendritic growth. When observed at a higher magnification, the samples also showed the formation of large columnar grains, growing epitaxially from the substrate, with evidence of α-β laths typical of the microstructures of α+β titanium alloys. In general, it was demonstrated that controlling the energy density, through careful selection of translation speed, wire feed rate, and beam power, can influence the resultant microstructure. Specifically, finer grained equiaxed microstructures can be obtained at lower energy densities, but this input condition corresponds to narrower bead widths and lower deposition rates. Conversely, a correlation was observed with higher energy density input and larger grains, including epitaxial growth from the baseplate in the Ti–6Al–4V samples, and pervasive dendritic microstructure in the 2219 Al grains and inter-pass regions. In addition, higher energy density input conditions resulted in higher deposition rates and wider bead widths.

Zhang et al. [162] performed deposition and rolling experiments using medium carbon 45 steel and Hybrid Deposition and Micro Rolling (HDMR) equipment on a Q235 steel plate with medium carbon 45 steel wire. The as-deposited and HDMR processed specimens were compared and the authors reported that:

- Coarse austenite grains with Widmanstatten structures were observed in the as-deposited specimens, but HDMR processed samples had refined and uniformly equiaxed grains, with the size down to ∅5.22 μm.
- Compared with as-deposition material, the HDMR process improved the hardness by 10.9%, tensile strength by 37.1%, and the elongation by 38.5%.
- Compared with investment casting, the HDMR process improved the tensile strength by 65.4%, and elongation by 107.7%.
- Compared with forging, the HDMR method improved the tensile strength by 12.9%, and total elongation by 5.9%.

Post-processing operations can also affect part and material microstructure as demonstrated in an investigation into the effects of different thermal and mechanical finishing operations on EBF3 processed 2219 Al pylons [93]. Following these operations, the resulting grain structure remained unaltered. However, a fine-grained equiaxed microstructure was observed, occurring at a constant depth of about 1 mm. Compared to the as-built material, the observed grains were much finer, and attributed to the post-processing electron beam glazing operation, which was implemented to improve surface quality.

2.4.4 Residual stress

Taminger et al. [131] investigated the surface residual stress in EBF^3 fabricated 2219 Al pylons. Illustrated in Figure 2-14, the measurements, which were obtained from the as-built sample via X-ray diffraction (XRD), showed moderate compressive residual stresses in the 0º direction, and low tensile residual stress in the 45º and 90º orientations. However, compressive stresses were induced in all directions by high-speed milling, wire EDM and glass bead blasting, which were used for post-processing the pylons. The electron beam glazing

process, also used for finishing parts, had no significant effect on the surface compressive residual stress in the 0º direction. Conversely, it induced high compressive stresses in the 45º direction and low tensile stress in the 90º direction, relative to the glazing direction, which was perpendicular to the build direction.

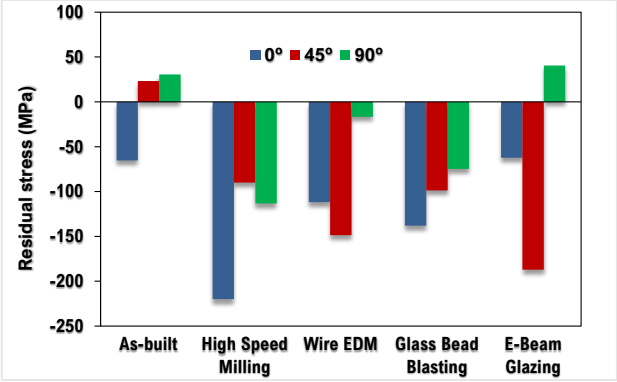

Figure 2-14. Surface residual stress measurements via XRD on EBF^3 fabricated pylons [93].

Cao et al. [46] used the Vickers micro indentation method for residual stress investigations in as-deposited samples of Inconel 718, fabricated with different overlap rates. Residual stresses between the overlap and inner-pass regions were compared. For these DED-LP samples, it was discovered that the residual stress in the overlap area was much higher, relative to the inner-pass area. Investigations, involving DMD AISI 4340 steel [43] showed that in all layers, the residual stress, which was measured using the XRD method, was lower in tempered specimens when compared to the as-deposited specimen. Also, the residual stress distribution, in the deposited layers and substrate, showed that the bending stress was compressive in the former, and tensile in the latter. In analytical and numerical studies on AISI 304 stainless steel, Aggarangsi and Beuth [163] reported that localised pre-heating strategies may be used to reduce residual stresses during the DED process. The numerical models accounted for temperature dependent material properties, including specific heat, thermal expansion coefficient, Young's modulus, yield stress, and latent heat of fusion, while excluding the effects of solid-state phase transformation. Two localised pre-heating approaches were modelled for the thin-walled AM features, involving the use of an additional heat flux, appropriately positioned ahead or behind the melt pool, and the application of a uniform pre-heating pass, to the deposition surface. The analytical and numerical models showed that the utilisation of a leading or trailing additional heat flux resulted in minimal changes in temperature distributions as the material cools behind the melt pool, with minor but noticeable reductions in maximum residual stress and temperature gradient. However, the application of uniform pre-heating, to the deposition surface, resulted in significant changes in temperature and residual stress distributions. A reduction of about 18% in maximum stress was predicted, where the top surface is heated to 400ºC (673K), prior to deposition.

Yan et al. [164] investigated the residual stress and warping of a stiffened Ti-6Al-4V panel produced by EBF^3. Two stiffeners of similar lengths (200×40×25 mm) were deposited on a single side of a flat plate, via longitudinal and transverse scanning patterns. Although the maximum deflection of the stiffeners, after

cooling, occurred at the corners, the deflection from the longitudinal track pattern was observed to be higher than that of the transverse track pattern. The deflection distribution correlated with predictions from an uncoupled thermo-mechanical finite element analysis (FEA) of the deposition, with a maximum deflection of 0.336 mm, located at the centre of the panel. Further FEA studies were carried out, to explore the deformation of a panel, following the deposition of stiffeners on both sides of the build plate. The analysis revealed that the maximum deflection was reduced by 63%, due to alternating depositions on opposite sides of the plate.

Thermally induced residual stresses and distortion are major concerns in MAM applications, particularly for large scale WAAM, because of the effects on resulting part tolerances and performance, notwithstanding the potential for causing premature failure. Different in- and post-process residual stress reduction strategies, such as the build pattern, deposition sequences, and pre-heating procedures were reported by Ding et al. [32]. However, the optimum strategy for reducing residual stresses during deposition still poses significant challenges. Colegrove et al. [165] investigated methods of reducing residual stress, distortion, and grain size in WAAM manufactured steel parts, by using a roller on each deposited layer. A purpose-built rolling rig was used to move a GMAW torch and a hydraulically loaded roller at a constant travel speed. Grade S355JR-AR steel parts were produced with profiled and slotted rollers, and later compared to the control "unrolled" samples. Elastic strains in the samples were measured using a neutron diffractometer. Detailed microstructure analysis was performed according to ASTM 112-96, and Vickers micro-hardness measurements were taken with a Zwick Roell Indentec hardness tester. The following observations were noted:

- Rolling can significantly reduce the peak residual stress in the longitudinal direction (from about 600 MPa to about 250 MPa) and the distortion in a straight AM wall.
- A slotted roller was found to limit the lateral deformation but provided more effective reduction in residual stress and distortion, with improved deposition efficiency, compared to rollers without lateral restraint.
- The microstructure of low carbon steel depositions consists of alternate layers of refined and non-refined ferrite, which are produced with each deposited layer, and this grain refinement is enhanced by rolling between subsequent layers.
- Comparisons of average hardness versus rolling load indicated that hardness is predominantly dependent on the rolling load, with increased hardness at higher rolling loads. However, this increase in hardness is attributed to work hardening, rather than the grain size.

Almeida [166] used neutron diffraction techniques to investigate the effect of repeated WAAM process thermo-mechanical cycles, on residual stress generation and distribution, in low carbon steel structures. Different multi-layer walls, comprised of 1, 2, 3, 4, 5 and 20 layers, were manufactured using a cold metal transfer (CMT™) welding torch on rectangular substrates (500×60×12 mm), with temperature measurements obtained via thermocouples, which were attached to the substrate. A unidirectional scanning pattern was employed during deposition. Subsequently, residual stress measurements were acquired using the spallation

source, ENGIN-X, located at the ISIS facility in Oxford, UK. Optical microscopy and Vickers hardness testing techniques were used for analytical purposes. The following observations were made:

- The residual stress in the initial layers were predominantly longitudinal in direction and significant in magnitude, owing to the clamping of the base plate and the non-uniform expansion and cooling in the material. The measured longitudinal residual stress ranged from 424 MPa near the base plate to 48 MPa at the fifth layer, for a wall with 5 layers.
- Repeated thermo-mechanical cycles from additional layers resulted in significant redistribution of the longitudinal stresses along the substrate and multi-bead, with residual stresses varying from tensile to compressive along the weld bead with additional layers.
- Upon the removal of the base plate, a near complete relaxation of elastic residual stress occurred along the multi-bead wall.
- Welding-induced distortion was observed in the plate with 20-deposited layers, attributed to the combination of mechanical constraint, non-uniform thermal loading, volumetric changes from solid-state phase transformation, and differential thermal expansion coefficients.
- Hardness indentation profiles were consistent with measured residual stress distribution along the substrate and as-deposited weld beads.

Other studies examining residual stress and distortion in WAAM Ti–6Al–4V structures [167,168] also confirmed that high tensile residual stress peaks (from ~450 to 500 MPa in this case) occur at the interface between the substrate and deposited material. As the build progresses, residual stress levels linearly decline, and gradually become compressive at the top of the build. For these linear WAAM deposits, the removal of the substrate was beneficial to the residual stress state of the build. Similarly, implementing varying levels of inter-pass rolling was also observed to have an overall reducing effect on residual stress and distortion, but contributed to significant increases in compressive residual stresses, occurring near the top of the wall. Honnige et. al. [169] introduced the concept of pinch-rolling to prevent lateral deformation in as-deposited walls, thus demonstrating how longitudinal residual stresses and distortion in linear WAAM builds may be eliminated.

2.4.5 Mechanical properties

Wolff et al. [161] investigated the micro-hardness of Inconel 718 powder deposited onto a 1045 steel substrate. Micro-hardness initially increased, with cooling rates normalised to specific energy density and at a maxima of 250 HV. Micro-hardness variations were also evaluated as a function of both the cooling rate and alloy composition, and it appeared that the latter had a more significant influence on micro-hardness than the former, with the cooling and dilution rates ranging from 1000 to 4000 K/s, and 0 to 0.9, respectively, thus indicating that minimal dilution is important for the conservation of high micro-hardness properties. In another study, Bi et al. [48] reported Vickers hardness values of between 610-690 MPa at the cross-section, and along the whole

height, of DMD deposited SS 316 walls. In comparison, an average hardness of 560 MPa was measured on an annealed 316L plate. Dinda et al. [45] also reported that relative to annealed samples, the high Vickers hardness measurements of as-deposited Inconel® 625 were high, with a narrow measurement range (254±6 HVN) attributed to variation in supersaturation of strengthening elements in the γ matrix. However, when investigating various annealing temperatures, it was reported that material hardness decreased with increasing annealing temperature. The average micro-hardness observed in as-deposited and heat treated DMD AISI 4340 steel from studies by Sun et al. [43] were 789.8 and 444.3 $HV_{0.5}$ respectively, indicating that heat treatment decreased the micro-hardness of the as-deposited part by about 43%. Indentation hardness (H_{IT}) and indentation elastic modulus (E_{IT}) values were also obtained via nano-indentation of the annealed and stress relieved DMD steels, with some variation observed in both H_{IT} and E_{IT} values, which are listed in Table 2-6.

Table 2-6: Comparison of nano-hardness (H_{IT}) and elastic modulus (E_{IT}) values in the as-deposited and stress-relieved DMD AISI 4340 steel, with annealed AISI 4340 steel plate at 23ºC [43].

Sample	Layer no.	Hardness (H_{IT}), GPa	Elastic modulus (E_{IT}), GPa
As-deposited DMD AISI 4340	1	6.845	218
	2	7.666	210
	3	8.247	284
Stress-relieved DMD AISI 4340	1	6.391	223
	2	6.929	206
	3	7.076	188
Annealed AISI 4340 alloy steel	-	2.236	200±10

The mechanical and fracture properties of DMD AISI 4340 steel were investigated by Sun et al. [43], with tensile test specimens used for evaluating mechanical properties, and lap shear and bend test specimens extracted for fracture property investigations. Tensile test specimens were prepared according to ASTM E8 [170], with lap shear and bend test specimens prepared according to ASTM D-3846 [171] and ASTM E290 [172], respectively. The average ultimate tensile strength (UTS) from seven stress relieved DMD AISI 4340 steel test samples was 1399 MPa, with an average failure strain of 1.665%. In comparison, the reported UTS and failure strain of annealed AISI 4340 steel were 745 MPa and 22% respectively. The fracture areas in the tensile specimens were devoid of necking, which confirmed the low engineering strain of the DMD deposited steel, with optical examination revealing a combination of ductile and brittle fracture surfaces.

Presented in Table 2-7, the average values of the shear strength and shear strain, for the stress relieved DMD AISI 4340 steel lap shear specimens, were reported as 512 MPa and 0.537% respectively, with the fracture surfaces also revealing a combination of ductile and brittle fracture. The average bending strength value, from four stress relieved DMD AISI 4340 steel bend specimens, was reported as 225 MPa, with observed interfacial fracture between layers alluding to the significance of fusion defects on bending performance.

Table 2-7: Ultimate strength and strain values of stress relieved DMD AISI 4340 steel.

Sample	Strength (MPa)	Strain (%)	Temperature (°C)
Tensile	1398	1.665	23
Lap shear	511	0.537	
Bend	225	-	

A comparison of DMD and wrought/cast material properties, from studies completed by Mazumder and Song [173] at the University of Michigan, is presented in Table 2-8.

Table 2-8: Comparison of material properties: DMD vs wrought/casting [173].

Material Condition	Temp (°C)	Tensile Strength (MPa)	Yield Strength (MPa)	Elongation (%)	Elastic Modulus (GPa)	Charpy Impact (J)	Hardness (HRC)
H13 (DMD)	23	1643	1407	8.4	197	12.9	54
H13 (Wrought)		1990	1650	9	207	13.6	53
316 SS (DMD)		678	515	43	177	178	23
316 SS (Wrought)		585	380	45	193	103	20

The mechanical properties of the EBF^3 processed Inconel 718 samples and the effect of post heat treatment on the mechanical properties were investigated by Bird and Hibberd [94]. Precision modulus tests were performed on specimens taken from as-deposited parts, in accordance to ASTM specification E111[174], and compared to reference properties for cast and rolled Inconel 718. Tensile tests were conducted for as-deposited and heat treated specimens, in accordance with ASTM E8 specifications [170]. The tensile properties of the samples fabricated at different deposition translation rates are shown in Table 2-9.

Table 2-9: Tensile properties of Inconel 718 EBF^3 deposited at 23 ºC [94].

Material	Modulus of elasticity, E (GPa)	Yield strength, YS (MPa)	Ultimate tensile strength, UTS (MPa)	Total strain (%)	Plastic strain (%)
EBF^3 Wall (127 cm/min)	160	580	910	23	22.4
EBF^3 Wall (190.5 cm/min)	157	583	917	23.3	22.7
EBF^3 Block (AD-T)	158.5.	612	985	31.3	30.8
EBF^3 Block (AD-B)	168	718	1055	20.8	20.1
EBF^3 Block (AD-T, HT-1)	164.8	945	1237	22.8	22.1
EBF^3 Block (AD-T, HT-2)	177.9	941	1132	21.8	21.2
EBF^3 Block (AD-B, HT-1)	167.5	948	1246	24.2	23.5
EBF^3 Block (AD-B, HT-2)	177.2	922	1123	22.6	21.9
Rolled	202	1206	1399	-	20.8
Cast	-	482	786	-	22.0

AD – as-deposited, AD-T – as-deposited-top, AD-B – as-deposited-bottom, HT – heat treatment.

The reported tensile properties of the wall samples fabricated at different deposition rates were similar, but the modulus (E) for EBF^3 was 20% less than that of rolled Inconel 718. The recorded YS and UTS of the EBF^3 processed alloy were ~35% and 50% less than rolled Inconel 718, but 20% higher than cast Inconel 718. In general, heat treatment resulted in more uniform properties in manufactured parts, with higher temperature heat treatments resulting in a higher modulus of elasticity, which was still low, relative to rolled Inconel 718.

Domack et al. [175] investigated the mechanical properties and resultant microstructure of EBF^3 processed 2219 aluminium alloy, based on different process variables. Tensile (YS and UTS) and elongation values were compared with typical handbook values for annealed (O temper) and naturally aged (T4 temper) sheet and plate, before and after heat treatment to T6 temper. The processing parameters are provided in Table 2-10.

Table 2-10. Process parameters for EBF^3 2219 Al depositions [175]

Parameter	Deposits		
	A1	A6	A6m
Unit deposition volume (cm^3/cm)	0.308	0.154	0.077
Energy per unit volume (kJ/cm^3)	254	532	532

The resulting mechanical properties are presented in Figure 2-15, which depicts the pre and post-heat treated EBF^3 processed samples in Figure 2-15(a) and Figure 2-15(b) respectively, with A1, A6 and A6m denoting the parameters described in Table 2-10. For pre and post–heat treated samples, the measurements in each orientation indicate that the material properties are isotropic, as shown in Figure 2-15(c).

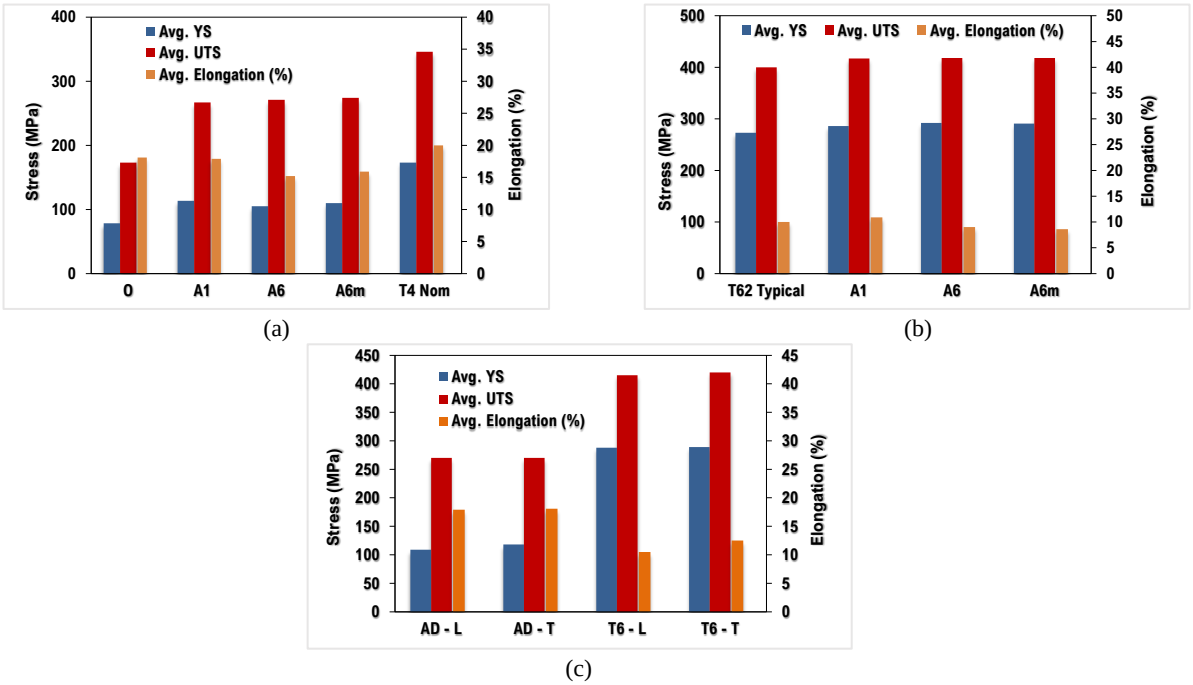

Figure 2-15. Comparison of tensile properties of EBF^3 deposited 2219 Al showing (a) as-deposited vs annealed (O) and naturally aged(T4), (b) heat treated deposits vs wrought T62 and (c) as-deposited vs heat treated in longitudinal (L) and transverse directions (T) [175].

The material properties of EBF^3 processed Ti-6Al-4V extra low interstitial (ELI), from parametric experimental studies by Taminger et al. [176] and Stecker et al. [177], are compared to the minimum specifications for AMS 4999 Ti-6Al-4V and AMS 4911 wrought Ti-6Al-4V, in Table 2-11.

Table 2-11. Comparison of mechanical properties of EBF^3 processed Ti-6Al-4V from experimental studies and the AMS 4999 Ti-6Al-4V minimum specification and wrought Ti-6Al-4V in AMS 4911.

Material	E (GPa)	YS (MPa)	UTS (MPa)	Elongation (%)	Reduction in area (%)
Ti-6Al-4V ELI (EBF^3) [176]	-	660	775	9.60	-
Ti-6Al-4V (EBF^3) [177]	116.52	848	923	13	35
Ti-6Al-4V (AMS 4999)	-	747	846	4.20	-
Ti-6Al-4V (Wrought) (AMS 4911)	113.8	880	950	14	-

Wanajara et al. [178] investigated the EBF^3 process for stainless steel, with 347 SS wire deposits on thin (1 mm) 321 SS substrates. As-built multi-layer deposits, measuring 100mm in length, were obtained and used

for material property characterisation. The shear punch test method was used to determine tensile properties, and micro-hardness was measured using a Vickers micro-hardness tester. The average hardness values, for measurements obtained from the deposits and substrate, are compared to published values for annealed materials in Table 2-12.

Table 2-12. Comparison of mechanical property for EBF[3] processed 321 SS and 347 SS

Material	YS (0.1%) (MPa)	UTS (MPa)	Elongation (%)	Reduction in area (%)	Hardness (HV)
321 SS (substrate)	242	591	-	68%	159.7±4.2
347 SS (deposit)	265	602	-	71%	166±3.7
321 SS (annealed)	240	585	55	65%	157
347 SS (annealed)	240	620	50	65%	167

Haden et al.[157] performed uniaxial tensile testing, micro-indentation hardness, and wear testing, on WAAM samples. The tensile properties, measured from samples taken at different locations within the deposited walls, are shown in Table 2-13.

Table 2-13: Tensile properties of WAAM processed 304 SS and ER70S mild steel at 23ºC [157].

Material	Yield strength (MPa)	UTS (MPa)
304 SS (TB1)	369	625
304 SS (TB2)	380	621
304 SS (TB3)	325	601
304 SS (TB4)	323	606
304 SS (TB5)	373	610
304 SS (TB6)	363	607
304 SS (TB7)	350	597
304 SS (TB8)	350	610
ER70S (V-TB 1-5)	265 ± 30	482 ± 4
ER70S (H-TB 1-5)	256 ± 37	475 ± 4
Wrought 304 SS	289	562 ± 58
Wrought ER70S	248	475.5 ± 75.5

TB - Tensile blanks, V – Vertical, H – Horizontal.

For the 304 SS specimens, the higher yield strength, observed along the weld deposition (i.e. x-orientation) and build height (i.e. z-orientation) directions, was attributed to the local thermal history and resultant mode of solidification [157]. Correspondingly, other researchers [179] observed a similar trend for the material hardness and wear rate, with specific values listed in Table 2-14.

Table 2-14. Vickers hardness and wear rate for WAAM processed 304 SS and ER70S mild steel at 23ºC [179].

Material	Vickers hardness (HV)	Wear rate (K), (mm^3/N·m)
304 SS (MB)	202.3	2.62
304 SS (MM)	209.2	1.21
304 SS (ME)	210.9	0.57
ER70S (MB)	142	-
Wrought 304 SS	200 ± 20	0.86
Wrought A36	146 ± 21	-

MB-Wall midline, beginning. MM-Wall midline, middle. ME-Wall midline, end.

Martina [180] reported a comprehensive set of material properties for various WAAM processed alloys, including orientation dependent mechanical properties, which were compared with wrought and cast material properties of the same alloys. The material properties for WAAM Ti–6Al–4V are shown in Table 2-15.

Table 2-15: Comparison of material properties: WAAM Ti–6Al–4V vs wrought/casting at 23ºC [180].

Material	Yield strength (MPa)	UTS (MPa)	Elongation (%)
Ti–6Al–4V (S-V)	810 ± 5	910 ± 5	23.0 ± 2.0
Ti–6Al–4V (S-H)	853 ± 10	946 ± 9	13.8 ± 1.2
Ti–6Al–4V (P-V)	871 ± 11	951 ± 6	15.0 ± 3.3
Ti–6Al–4V (P-H)	905 ± 12	982 ± 9	11.4 ± 1.4
Ti–6Al–4V (O-V)	802 ± 16	903 ± 16	14.8 ± 3.3
Ti–6Al–4V (O-H)	850 ± 9	948 ± 16	10.0 ± 1.5
Ti–6Al–4V (SUB)	950 ± 22.5	1033 ± 3	11.7 ± 0.65
Ti–6Al–4V (S-A)	883 ± 12	930 ± 10	17.8 ± 2.4
Ti–6Al–4V (P-A)	888 ± 12	968 ± 9	14.0 ± 2.1
Ti–6Al–4V (O-A)	827 ± 13	926 ± 10	12.3 ± 1.0
AMS 4999 (V, Additive)	758	855	6
AMS 4999 (H, Additive)	800	885	6
AMS 4928 (Wrought)	815	895	10
ASTM F1108 (Cast)	770	860	8

V - Vertical Orientation, H - Horizontal Orientation, S - Single Pass, P - Parallel Passes, O - Oscillating Passes, SUB – Substrate, A – Average Values.

The measured properties of WAAM processed Ti–6Al–4V were comparable to properties of wrought or cast Ti–6Al–4V, and fairly similar to measured properties of shaped metal deposition (SMD) Ti–6Al–4V materials reported by Baufeld et al. [181], with UTS values ranging from 925 to 1014 MPa, and strain at failure between 9 and 16%. Variations were typically attributed to differences in sample orientation and deposition patterns. The average measured properties of WAAM processed aluminium alloys, were reportedly comparable to wrought versions of the same alloys. The obtained measurements are provided in Table 2-16.

Table 2-16: Comparison of material properties: WAAM processed vs wrought Al at 23ºC [182].

Material	Yield Strength (MPa)	UTS (MPa)	Elongation (%)
2024 Al	185	287	12
2024-T6 Al	407	500	8.25
2024-T6 Al (wrought)	394	475	10
2319 Al	130	260	15.5
2319-T6 Al	309	455	13.6
2319-T6 Al (wrought)	295	415	10
4043 Al	68	178	19.2
5087 Al	134	280	21.2

The measured tensile material properties of WAAM processed mild steel, maraging steel and stainless steel are listed in Table 2-17. Significant improvement in the yield and ultimate tensile strengths were noted, after heat treatment of the maraging steel, with some decrease in elongation to failure. Some anisotropy is also evident in the reported properties of the stainless-steel samples (17-4 PH and 316L).

Table 2-17: Tensile material properties: WAAM processed steel at 23ºC [182].

Material	Yield strength (MPa)	UTS (MPa)	Elongation (%)
ER70S-6	435	530	30.6
ER80S-Ni1	430	525	30
ER90S-B3	580	900	16.9
ER120	730	925	23
Maraging Steel 250	810	1138	17
Maraging Steel 250 HT	1442	1520	9
Maraging Steel 350	1110	1485	14
Maraging Steel 350 HT	1770	1950	11
17-4 PH (V)	740	980	12.2
17-4 PH (H)	842	1010	11.5
316L SS (V)	300	582	43.6
316L SS (H)	298	512	40.5

V - Vertical Orientation, H - Horizontal Orientation, HT - Post Process Heat Treatment

The tensile properties of WAAM processed Inconel 718, enabled by CMT and PAW techniques, are provided in Table 2-18. For Inconel 718 samples obtained from both WAAM processes, these results indicate an orientation dependency, relative to the yield strength and UTS. Furthermore, post-process heat treatment significantly improved the strength, with loss of failure strain. However, the as-deposited values for yield and UTS are about 52% and 34% lower than AMS 5662 and AMS 5663 specifications for bars and forgings.

Table 2-18: Comparison of material properties: WAAM processed vs wrought Inconel 718 at 23ºC [182].

Material	Yield Strength (MPa)	Ultimate Tensile Strength (MPa)	Elongation (%)
IN718 (CMT, V-AD)	428 ± 11	803 ± 28	34.8 ± 3.9
IN718 (CMT, H-AD)	514 ± 17	824 ± 15	34
IN718 (CMT, V-HT)	889 ± 5	1233 ± 16	19.4 ± 2.8
IN718 (CMT, H-HT)	807 ± 1	1100	15.5 ± 0.3
IN718 (Plasma, V-AD)	506 ± 2	756 ± 7	28 ± 1.3
IN718 (Plasma, H-AD)	525 ± 7	817 ± 13	33.3 ± 2.5
IN718 (Plasma, V-HT)	791 ± 14	989 ± 6	12.6 ± 1.2
IN718 (Plasma, H-HT)	790 ± 9	1100 ± 78	14.7 ± 1.3
AMS 5662, AMS5663 Bars, Forgings.	1030	1275	12

AD – as-deposited; V - vertical orientation, H - horizontal orientation, HT - Post Process Heat Treatment, CMT – Cold Metal Transfer Process, Plasma – Plasma Arc Deposition.

In general, the strength development characteristics of MAM materials depend on several factors, as demonstrated by different researchers. While the alloy composition, type, and properties, in combination with the processing temperature, cooling rate, and conditions are key factors influencing MAM material characteristics, the deposition method and related strategies are also significant. For instance, Xu et. al., demonstrated the effectiveness of interpass rolling in enhancing the strength of Inconel 718 materials produced by WAAM [183]. In another study, Hönnige et. al. found correlations between the strength of 2319 aluminium walls, produced by WAAM, and the inter-pass rolling strategy utilised [169]. In essence, well implemented

thermomechanical strategies, especially during MAM operations, can enhance resultant strength characteristics of deposited materials and/or parts.

2.5 Factors influencing DED quality and performance

The underlying issues influencing the behaviour of DED components are evidently derived from the system, and its integral processing mechanisms, and other related process and operational variables. In consideration of these interrelated technical aspects on manufacturing quality and product performance, specific challenges and measures for improving process outputs were investigated. Focusing on DED processes, including DED-LP, EBF3 and WAAM processes, pertinent developmental factors are explored hereafter.

2.5.1 Processing mechanisms and effects

Presently, there are numerous diverse trade-offs that must be accommodated when considering the adoption of DED, including discrete sub-systems, energy sources, raw material options, and process parameters, notwithstanding the feedstock composition and characteristics. Furthermore, DED processed components are typically anisotropic, due to the layer-by-layer approach, which is characterised by heterogeneous nucleation, and rapid directional solidification, necessitating the development of strategies for managing evident issues.

Thompson et al. [52] developed a framework for assessing instantaneous energy and momentum transfer in DED-LP processes. Represented in Figure 2-16, the framework is predominantly focused on the thermal/fluidic phenomena, and accounts for the instantaneous occurrence of specified DED-LP events, while illustrating the possible paths for energy and/ or momentum transfer, as well as the effect of these physical events on the resulting microstructure and mechanical properties. The material properties, residual stress, porosity, surface roughness and geometric accuracy, and other quality and performance measures, are significantly influenced by complex and interdependent mechanisms, including the feedstock delivery and processing atmosphere, and the heating, melting, cooling, and solidification events. The inter-layer bonding and microstructure evolution are influenced by process variables, such as the layering parameters, including the layer thickness, deposition speed and duration. The advancements, challenges and physical attributes related to DED-LP processes were also considered, and the need for understanding the transport phenomena, inherent to these processes, and their influence on the resultant microstructure, was highlighted.

Other major challenges reported in the study include efficiency, process monitoring & control limitations, numerical modelling, determination of process parameters and physical properties of the material and heat source. The review concluded that a thorough understanding of the thermal/fluid aspects and associated thermal/mechanical properties, inherent to DED-LP processes, is necessary for their optimisation and ensuring consistent, high-quality outputs.

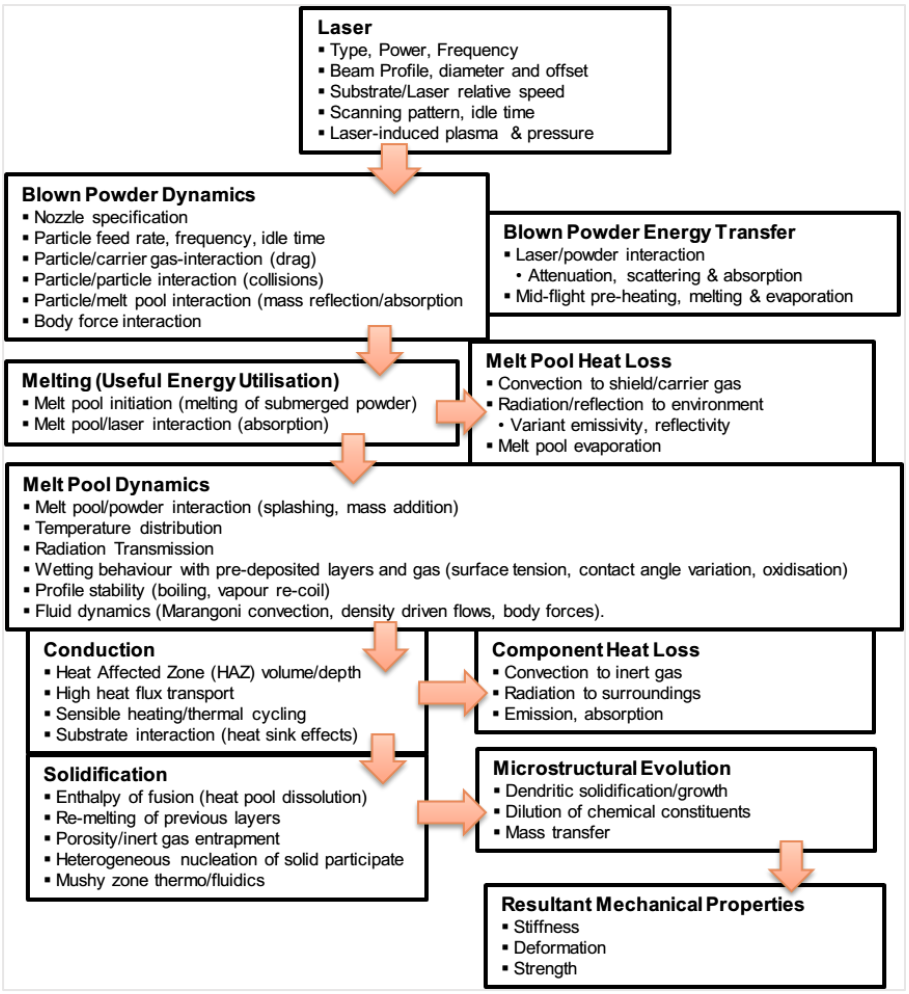

Figure 2-16. Framework for the assessment of energy/momentum transfer during LMD, showing instantaneous physical events [52].

Shamsaei et al. [184] examined the interrelationship between the mechanical characteristics and behaviour of parts fabricated via DED-LP. Focusing on process control and optimisation methods, the monitored part temperature and melt pool morphology were investigated. As a result, a framework showing the relationships between process parameters, thermal history, microstructure, and fatigue behaviour during DED-LP processes, was established. Presented in Figure 2-17, the framework depicts the heat and mass flow parameters distinctly from the machine translation parameters, to illustrate the direct effect of these inputs on the thermal history and solidification of DED-LP parts. In turn, these variables influence the resulting part microstructure, porosity, residual stress levels, and other directly dependent part properties that ultimately affect fatigue performance. Several areas were proposed for further holistic investigation, and to enhance understanding of the relationship between process parameters, thermal history, solidification microstructure, and mechanical properties of DED-LP fabrications. For specific applications, these investigations combine: comprehensive experimental data on cyclic strain and fatigue behaviour; effects of build orientation on tensile and fatigue behaviour; low cycle fatigue, variable amplitude fatigue, and multiaxial fatigue behaviour; and microstructural

sensitive fatigue models that consider the effect of surface condition, microstructure, porosity, and grain size and orientation on fatigue properties.

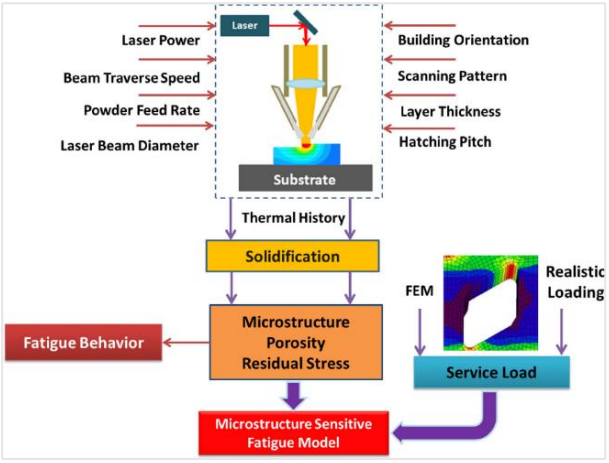

Figure 2-17. Framework for studying the interrelation of process parameters, thermal history, microstructure and fatigue behaviour of DED-LP (Shamsaei et al. [184])

While specific DED variables are crucial to understanding the relationship between process parameters and interrelated mechanisms, the DED-LP frameworks highlight critical commonalities, including the energy, feedstock, subsequent solidification phase, and resulting microstructure. Correspondingly, adequate real-time control of process parameters and associated variables is necessary, for obtaining the desired form and material properties, as well as a defect-free component.

2.5.2 Process monitoring and control

The undeniable effects of complex and interrelated processing mechanisms on quality and performance, observed in both commercial and non-commercial MAM capabilities, underscore the need for further improvements in process monitoring and control [63,85]. Mazumder et al. [44] developed a closed loop technique to control the bead height of DMD deposits. The closed-loop system was enabled by the visualisation and measurement of the surface deformation of the melt pool via the reflective topography technique, developed at the University of Illinois. A feedback loop was used to regulate the process parameters controlling the dimensions of deposited tracks. Three optical sensors, deployed at 120^{o} spacing from each other, were employed for closed loop feedback control of the build height, and to overcome any field-of-view related problems. The advantage of the height controller was demonstrated by depositing two overlapping cylinders, with and without the height control function. This procedure involved shutting off the laser while it traversed excessive build-up areas to control the height in overlapping regions, as illustrated in Figure 2-18.

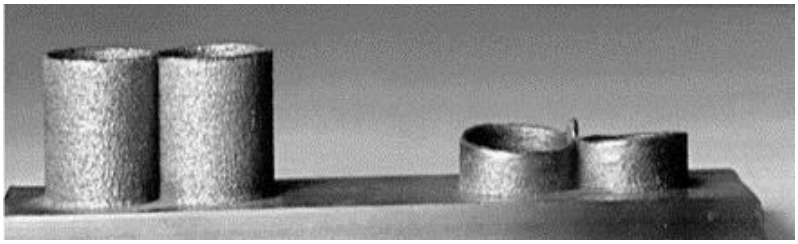

Figure 2-18. DMD fabrications with (left) and without (right) height controller by Mazumder et al. [44].

Closed- and open-loop control DMD deposition experiments, for 1100Al and H13 tool steel plates, were also carried out by the researchers, with the following observations:

- A consistent microstructure was observed throughout the fabricated sample, and a combination of decreasing specific energy, decreasing layer thickness, and increasing scanning speed, resulted in both finer grains and higher cooling rates, in the order of 10^5 K/s (ºC/s).
- Increasing the percentage overlap resulted in approximately 20% reduction in surface roughness, down from about 40 μm.
- Variation of the sensors in the feedback controller eliminated the directional dependence of the height controller during material deposition.
- The addition of two sensors had no significant effect on the material properties but reduced the surface roughness of the fabricated parts by 14 to 20%.

Wallace et al. [185] conducted a parametric study to evaluate the significance of input parameters on EBF^3 Ti–6Al–4V deposits. The parameters chosen were beam voltage, beam current, translation speed, wire feed rate, and beam focus. A design of experiments (DoE) approach was used to establish a set of 16 experimental combinations, for the evaluation of the relative performance of the selected parameters, on single and multi-bead EBF^3 deposits. The results of the analysis showed that translation speed is important to the resultant height and width, as variations in beam translation changes the specific volume of material deposited, and the amount of heat input during the process. Metallurgical analysis of samples with higher heat input showed a larger heat affected zone, which was attributed to simultaneous increase in bead width and reduction in bead height, measured in multi-bead stacks. The importance of the beam voltage and beam current, on the bead width and height, was identified as secondary to the translation speed. Increases in voltage or current resulted in increased energy input and associated enlargement of the molten pool surface area, thereby decreasing the height of the deposit. The wire feed rate (mass feed rate) was identified as strongly influential to the single and multi-bead heights, but less influential on bead widths. For this study, the beam focus was found to be the parameter of least importance, as variations in beam focus produced only small changes in the stack height, but no discernible change in stack width or the size of the heat affected zones.

Mazumder and Song [173] further enhanced the DMD closed-loop process control system to include temperature, composition, and microstructure control. The additional capabilities are summarised as follows:

- Temperature and cooling rate control: A dual colour pyrometer with operating wavelength, away from laser radiation wavelength, was deployed to monitor the melt pool temperature, with measurements fed back to a real-time controller, to track the melt pool temperature to a pre-set temperature profile. Monitoring the temperature, as a function of time, enabled cooling rate control, and implicit microstructure control. A closed-loop control system, incorporating geometry and temperature control, was implemented, and used for DMD processing of H13 tool steel. Other features included the ability to control heat input for complex geometries, to prevent under-fill or over-fill, and for improved geometric accuracy.
- Composition sensor: Real-time optical emission spectroscopy of the plasma plume, a by-product of laser induced plasma for DED-LP processes, enabled composition prediction. During DMD deposition of H13 tool steel, both chromium and iron atomic emission lines were observed, and comparisons with spectral lines of pure iron and chromium enabled the identification of the composition ratio of constituent elements.
- Microstructure sensor: A strong correlation was observed between the physical parameters of a plasma plume and the final microstructure. Further investigations showed that plasma characterisation just before solidification was a valid indicator for crystal structure. Based on this discovery, the development of a spectroscopic sensor, which monitors phase change during deposition, was proposed.

Smugeresky et al. [88] carried out a comprehensive evaluation of the effects of global closed-loop and open-loop variables, on the quality of functionally-graded depositions of several iron-based alloys, including iron, nickel, manganese, and austenitic steel, to demonstrate the capability of the LENS process. Initial depositions, carried out using gas atomised 316 SS as a baseline, confirmed that the LENS process is suitable for producing fully dense depositions using a standard alloy that had undergone extensive development for this process. The addition of sponge iron, which was introduced to form a graded composition, resulted in considerable porosity that could not be rectified by varying process parameters. However, open and closed-loop experiments with water atomised iron, and graded composition iron powders, produced better results. The effects of the alloying additions were measurable, but the microstructure was difficult to control. Challenges were attributed to the processing conditions required for closed-loop control system of the LENS hardware, which was based on a high-speed imaging technique that was specifically developed and calibrated for processing 316 SS. The additional alloying elements resulted in changes in emissivity, which saturated the sensor and, due to its effects on the laser power, caused deviations from the baseline. Expectedly, excessive porosity and associated variations in microstructure were observed in graded compositions of Iron-Manganese and Iron-Nickel alloys. This observation highlighted the difficulties in maintaining stable process compositions and porosity free deposits, even when in-process LENS parameters were varied. Nonetheless, open-loop experiments on Fe-Mn and Fe-Ni alloys demonstrated that in small samples, graded compositions can be achieved, with a 10% peak in the hardness of Fe-Ni alloys. In practise, the realisation of compositionally graded structures may be significantly hindered without a means of controlling complex phase transformations during deposition.

Taminger et al. [186] investigated the integration of real-time sensors in EBF^3, accounting for several interdependent factors affecting process outcomes. Seven major challenges hindering the acquisition of real-time sensor data for process monitoring and control purposes, were identified as follows:

- Deposition environment: requires miniaturised electronic sensors capable of operating in a vacuum environment and resistant to metal vapour deposition.
- Thermal transients: requires sensors capable of tracking and measuring thermal distributions in the molten pool.
- Dissimilar temperature and phase dependent physical properties of metal alloys (e.g. phase transition temperature, specific heat, density, thermal conductivity, viscosity, surface tension, vapour pressure and emissivity): require the deployment of wideband sensors to cater for a wide selection of metal alloys.
- Precise measurement of geometric variations in deposits, owing to imperfect combinations of heat and mass flow during typical deposition operations and/or events, including starts, stops and rapid directional changes. Adequate bead height sensor capability and location are also required to minimise accumulative errors from typical deposition operations.
- The effect of mass input (wire) orientation, elevation and relative machine translation on deposit geometry and subsequent part precision. Real time measurement of bead geometry is required to enable adjustment of processing parameters for precision enhancement.
- Sensors with wide fields of view and capability to track the hot/cold wire position are required, to minimise random process errors originating from wire feed inconsistencies, misalignment, rapid heating, and stiffness, due to fluctuations in the mass flow rate, and energy input, relative to the molten pool.
- Embedded real-time in-situ sensors may be required to detect, quantify, and repair defects that occur during deposition.

Five different hardware configurations (HC) were iteratively implemented over a decade, with varying degrees of success. The complementary metal-oxide semiconductor (CMOS), charge-coupled device (CCD), and short-wave IR (SWIR) detectors provided wider field of view and valuable thermal images for monitoring the challenges with the EBF^3 process. The sensor configuration HC2 had advantages in keeping the camera out of the chamber, although difficulties with heat damage to the fibre optic bundle led to the abandonment of this sensor configuration. The approach with sensor configuration HC3, which included a backscatter electron (BSE) detector, was also abandoned, owing to difficulties with the size and cost of the BSE detector and deficiencies in detecting thermal information. It was also learned from the first three sensors that the image sensor location was critical for adequate data acquisition for closed-loop process control. As such, methodologies that favoured the sensor configurations with internally mounted sensors (HC1, HC4 and HC5)

were adopted, owing to cost and miniaturisation. However, the more expensive SWIR sensor was the only sensor capable of measuring lower temperature for aluminium processing. Nevertheless, initial multi-layer deposition experiments with Ti-6Al-4V showed that the observable length of the molten pool doubled at a constant power and translation speed, illustrating the dependency between the process, geometry, and thermal history. The different sensor configurations investigated are detailed in Table 2-19.

Table 2-19. Sensor configurations and suitability for measuring EBF^3 process challenges [186].

Sensor Tech / **EBF^3 Process Challenge**	**Internally Mounted Near Infra-Red CMOS Camera (HC1)**	**Fibre Optic + Externally Mounted CCD Camera (HC2)**	**Internally Mounted BSE Detector (HC3)**	**Internally Mounted Near Infra-Red CCD Camera (HC4)**	**Internally Mounted Short-Wave IR (SWIR) Camera (HC5)**
Deposition Environment	Pinhole Optics with cold plate for cooling.	Pinhole with externally mounted fibre-optics	Full vacuum compatibility with vapour shield	Pinhole Optics + cold plate for camera cooling	Pinhole Optics + cold plate for camera cooling
Thermal Transients	Yes	Limited	No	Yes	Yes
Alloy Physical Properties/Melting range	NIR Signature	NIR Signature	N/A	NIR Signature	NIR Signature
Bead Height Measurement	Limited	Limited	Not demonstrated	Limited	Limited
Bead Width Measurement	Yes	Limited	Yes (Not demonstrated in real-time)	Yes	Limited
Wire / Molten Pool Tracking	Yes	Limited	Not demonstrated	Yes	Limited
Real-time Flaw Detection	Yes	Limited	Limited	Yes	Yes

Schematics of the instrument rings, designed around the electron gun for HC4 and HC5, are shown in Figure 2-19 (a) and Figure 2-19(b) respectively.

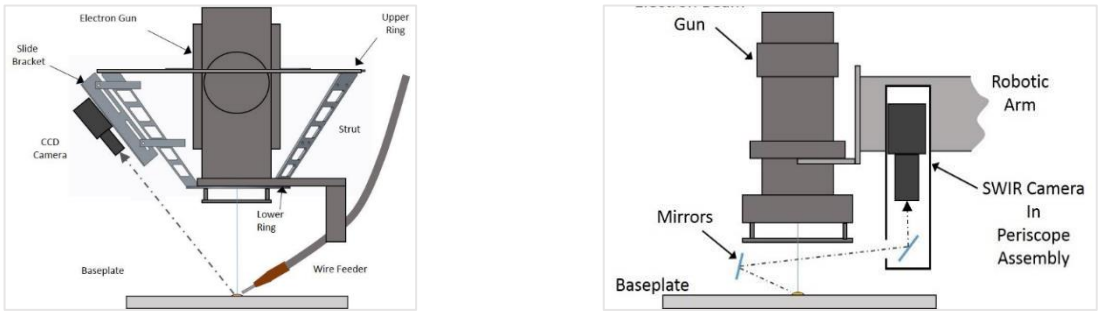

(a) (b)

Figure 2-19. Schematic diagrams of sensor configurations (a) HC4 and (b) HC5 used by Taminger et al. [186] for EBF^3 process monitoring.

Near-infrared (NIR) thermographs and line plots for higher melting temperature alloys 316 SS, Ti-6Al-4V and Inconel 625, obtained via HC4, are shown in Figure 2-20(a), with SWIR thermographs and line plot for lower melting temperature alloy 2219 Al, obtained via HC5, shown in Figure 2-20(b). Proposed areas for improvement include the development of algorithms to identify signatures linked to process challenges, and the establishment of closed-loop control system logic for real-time process refinement.

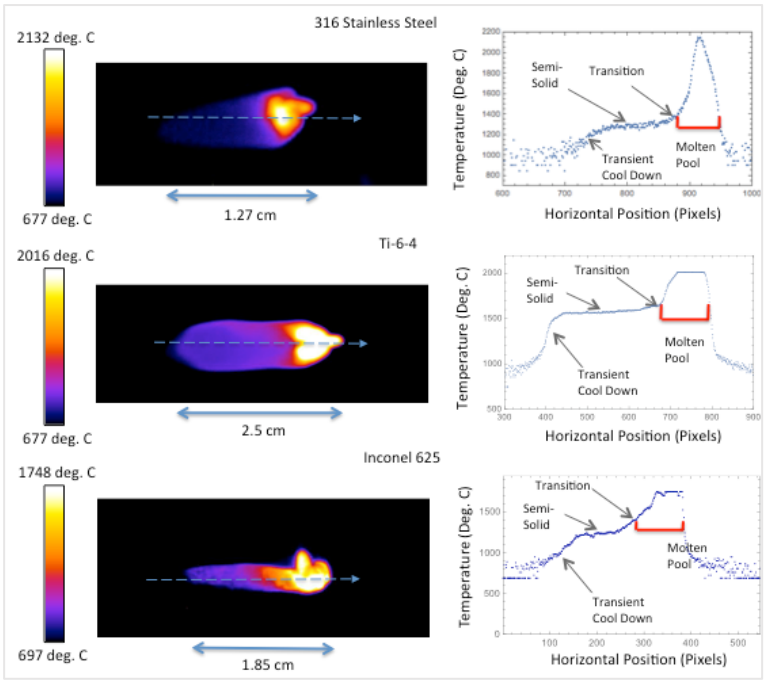

(a)

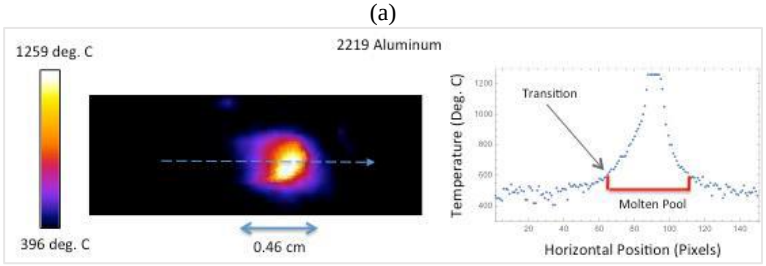

(b)

Figure 2-20. Thermal images and line plots showing deposition temperature variation during EBF[3] processing from (a) HC4 and (b) HC5 sensor configurations (Taminger et al. [186]).

Xu et al. [187] identified six major types of defects in WAAM produced components, namely, residual stress, structural distortion, cracking, lack of fusion, porosity and thermal dissipation, and based on these findings, proposed an in-situ multi-sensor model. A schematic of the proposed system is shown in Figure 2-21.

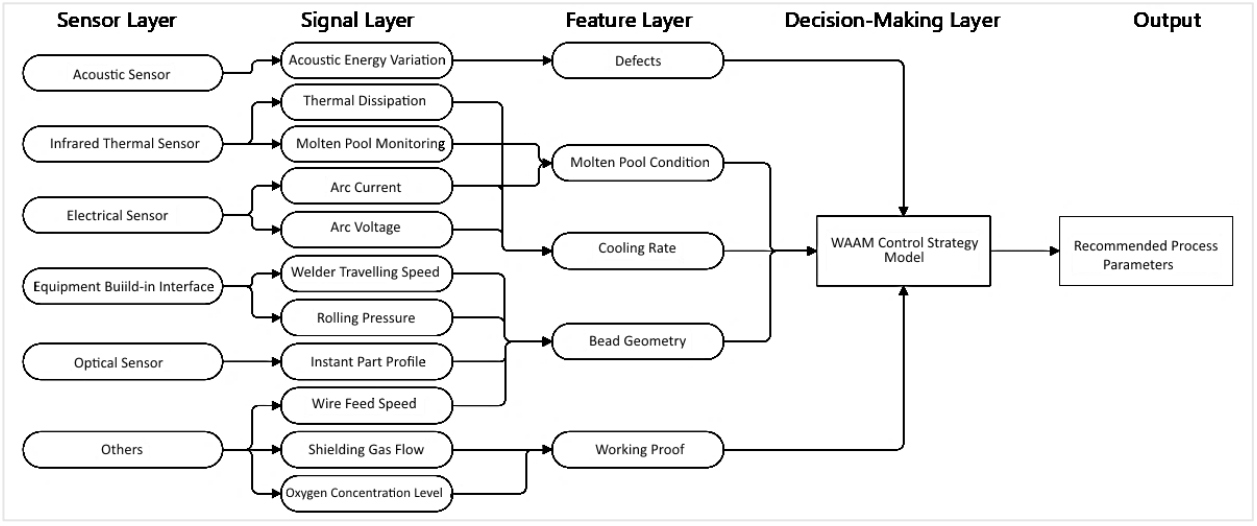

Figure 2-21.Schematic diagram of full state monitoring system for WAAM (Xu et al [187]).

The model (Figure 2-21) was developed with the aim of acquiring information from WAAM processes. Specifically, the different layers of the model were informed by the identified defect types, with residual stress, thermal dissipation and structural distortion attributed to the thermal history, while lack of fusion and porosity related issues were attributed to the process parameters. Cracks were also associated with residual stress.

An in-situ monitoring solution (iMUST), comprising a wire feed sensor, pyrometer, current sensor, oxygen sensor, shielding gas flow sensor, and two laser profilometers, was developed and incorporated into a high-value engineering (HiVE) WAAM machine. Experimental work was undertaken to examine the feasibility of the monitoring solution for WAAM. It was reported that complete point cloud information of a component, which may be used for the generation of a computer aided design (CAD) model for post processing, was successfully obtained. Voltage and current signal were recorded during the experiments. High frequency fluctuations and an increasing trend away from the nominal voltage was observed during monitoring. The high frequency fluctuation was attributed to circulated metal droplets melting and dripping, while the increasing trend was attributed to a slightly uneven bottom layer. It was postulated that the decreasing distance between the arc nozzle and the part was responsible for observed voltage increase. A Kalman filter was used to filter noise in the current signal and accurate current measurements were obtained, which is crucial for accurate energy input. The authors intend to use the voltage and current processing algorithm for the realisation of accurate voltage and current monitoring, in a closed-loop control system, which is being developed.

The different approaches investigated and proposed by researchers, indicate that the requirements for process monitoring and control remain unsatisfied, further underscoring present technological complexities, particularly when configuring necessary supplementary devices. The need for bespoke solutions also implies that there are persisting limitations in commercial capabilities, and that the performance of evaluated tools, where these exist, are below expectations, otherwise highlighting gaps for which there are no readily available solutions, to adequately support favoured MAM process monitoring and control strategies.

2.5.3 Substantiation and qualification of MAM outputs

Compared to contemporary approaches, the lack of suitably sized commercial MAM capabilities is an important contributing factor to the technology assimilation gap, as competitiveness can be restricted by capacity, which affects process, product, and production scaling [21,140,188–191]. Correspondingly, industrial similitude influences perceptions about the validity and, by extension, relevancy of manufacturing technologies. In practice, the utility of MAM research outputs, is influenced by the reliability of scale dependent parameters. While the scale may be volume and/ or weight dependent, pertinent parameters may be restricted either by the utilisation of ineffectually sized MAM capabilities or insufficient consideration of analogous scaling effects [192]. Therefore, appropriately acquiring scaling parameters in component design, manufacturing, performance, and safety studies, is a necessary initial step for demonstrating relevance and

validating the industrial applications to which these technologies aspire [22,191,193]. However, the precipitate deployment of DED capabilities, for different applications, can amplify existing inefficiencies, such that they become indistinguishable from persisting underlying issues. Similarly, when considering the capabilities to be deployed, the development process is highly challenging, because it involves managing distinct commercial, technological, technical, and human perspectives [194,195]. Furthermore, in an increasingly complex MAM landscape, the required system development expertise is often beyond the core capabilities of a single organisation or entity, which can affect visibility of important intersecting factors [196–198]. This complexity is exemplified in the DED capabilities used for larger builds [110], where bespoke configurations are the norm [199–202], and as demonstrated by the reported requirements and proposed solutions for process monitoring and control [44,186,187]. Nevertheless, highly integrated solutions, though complex, can offer significant benefits over utilising various separate technologies, particularly for distinct and unrelated SMRM tasks [203]. Accordingly, understanding the effects of scaling parameters and prior experiences shaping the developmental landscape, is important for realising comparable industrial MAM systems, processes, and products.

Presently, the usefulness of any MAM system extends beyond the product form and function, to the performance requirements, and related operational considerations. The qualification process, which is necessary for certifying that a component can be safely used and/or returned to service, is a critical requirement for MAM applications [204]. The substantiation process begins with the raw material input, which could be the powder or wire feedstock, depending on the DED process utilised, and encompasses the parameters and procedures used to create the resulting material or part. Correspondingly, the quality monitoring and control measures implemented during the manufacturing process, including the accumulation of related process data, are essential for traceability, verification of process outputs, and documentation purposes. However, when directly evaluating serviceable parts for verification purposes, destructive testing is not viable. Instead, and due to the high intrinsic value and criticality of parts, non-destructive evaluation (NDE) techniques are essential for the inspection and qualification process [205–207]. Part criticality is often defined in relation to the severity of failure condition or hazard, the designated function and operational state, and the subsequent effects on part integrity, performance and safety [208]. The combination of NDE technologies, tools, and techniques used for assessing failure conditions, and other safety related concerns, are generally classified based on the requirements, which could be related to either surface or subsurface issues [209].

Analysis of failure mechanisms revealed that common causes of manufacturing issues were attributable to either the material specification or the manufacturing process [210,211]. Reported manufacturing quality and material performance issues include poor dimensional accuracy and surface finish [48,93]; depletion of volatile alloying elements [94,156,157], chemical segregation and precipitation [43,62]; porosity, lack of fusion (LOF) defects and cracks [43,62,212]; deformation, distortion or warping, and residual stress [46,163]; and consequent variations in mechanical properties [94,157,180]. Based on these issues, both surface and subsurface NDE techniques are evidently required for validating DED outputs, but in-process monitoring and

control techniques can help to minimise or prevent such occurrences. In a further review of common failure mechanisms that initiate SMRM actions, fatigue was identified as the predominant cause [211]. In DED, the material or part susceptibility to fatigue is significantly influenced by the complex and interdependent processing mechanisms involved in the transformation of the feedstock. During the build process, both pre-existing and newly deposited layers typically undergo multiple non-uniform and very localised heating and cooling cycles. These rapid changes cause the material to expand and contract instantaneously, due to a volume difference between formed or solid and melted layers, the result being the build-up of residual stresses. Attributed to the material thermal history, other researchers have also identified residual stress and distortion as major causal factors in the susceptibility of DED materials and parts to fracture and fatigue [187,213,214]. Therefore, the analysis and explanation of distortion and residual stress, which is consistent with the utilisation of NDE methods for substantiation of manufacturing outputs, was identified as a key area for this study, particularly for planned SMRM actions. Correspondingly, it was necessary to review pertinent literature, to determine how predictive models could be implemented, to support verification proceedings.

Advanced digital technologies, including computer aided manufacturing (CAM) and other computer aided technologies (CAx), are undeniably beneficial, helping to increase productivity by enhancing understanding of quality and performance issues in traditional manufacturing, and MAM operations [215]. In general, AM modelling approaches are implemented in response to highlighted quality and performance related issues, observed in specific alloys and/or applications, with a predominant focus on the microstructure and mechanical properties of fabricated materials [33,161,216–223]. There is also significant interest in distortion and residual stress analysis, and the development of thermomechanical modelling approaches have significantly facilitated the investigation of the temperature history, and its effects in DED materials and parts [224,225]. Chen et al. [226] developed thermo-mechanical FEA models, incorporating the solid-solid phase change temperature of Ti-6Al-4V, in order to carry out parametric studies for controlling distortion during the EBF^3 deposition of a thin wall. The FE analysis showed the distributions of residual stress in the part and established a causal relationship between scanning patterns and distortion. Specifically, shrinkage distortion increased with scan current, while a dynamic current scheme decreased the maximum distortion along a specific build axis. Building on this explanation, the application of an elevated temperature boundary condition, below the solid-state phase transformation temperature, and at the bottom of the substrate, resulted in substantial reductions in the predicted distortion of the wall. This study demonstrates the potential value of such approaches for large-scale MAM, where significant distortions are similarly anticipated.

SMRM epitomises uncertainty, and under these conditions, the ability to enact different scenarios at an appropriate scale, select the optimal solution, and predict possible outcomes, to a reasonable degree of accuracy, is invaluable. Therefore, understanding the actual SMRM outputs that can be predicted, was necessary for devising a process verification strategy for this study. In this respect, NDE techniques allow for the substantiation of manufacturing outputs, using appropriate surface and subsurface methods, and increase

confidence in the empirical data used to explain and establish predictive models for improving SMRM solutions. However, it is challenging to establish, calibrate, and validate predictive models, due to the complexity of the processing mechanisms involved, computational resources required, and the lack of complete critical process data, which can ultimately lead to inaccurate results [224,227,228]. These shortcomings are typically investigated iteratively, by comparing experimental and NDE data with numerical model predictions, until the latter is in approximate agreement with the former, with relevancy underpinned by specific applications or actual situations. Nevertheless, the main purpose of adopting modelling techniques, for validating MAM system outputs, or closing the system-to-product loop, was to elucidate and refine insights about encompassing factors influencing the development of AM systems and procedures, primarily for large-scale MAM operations, and initially focusing on SMRM.

2.6 Managing supplementary manufacturing requirements

Supplementary manufacturing operations are necessary for creating and sustaining or extending the service life of valuable products. Although it is recognised that *value* is subjective, and associated definitions are influenced by mutual perspectives, for affected parties, the impacts are undeniable and measurable. Derived from issues encountered during the manufacturing process, when fulfilling designated functions, or between and within these situations, SMRM operations may involve the reworking, reprocessing, refurbishment, or upgrade of structures. However, underlying requirements are influenced by broader perspectives, which are explored in this section.

2.6.1 Factors influencing SMRM

There are varied causal factors influencing the management of supplementary requirements involving metallic structures. These factors, including raw material and manufacturing processes [229,230], and anomalous handling, loading and operating incidents [1–6], are compounded by other complex and interconnected issues. Although crosscutting issues typically affect different communal services infrastructures, the aerospace and energy industry sectors were specifically targeted due to the possibility to access relevant SMRM case studies more readily, and at the appropriate juncture of this study.

In energy, aerospace, and related services industries, with similar manufacturing requirements, the demand for large and ultra large components, via traditional manufacturing routes, such as forging and casting, is constrained by supply conditions. These components are typically imported, due to the lack of domestic capabilities to support local demands for various significant national and commercial ventures [210]. For applications in the energy sector, components are both heavy and large, with processing requirements that are often beyond the capacity of most suppliers [231,232]. The requirements for large but lighter aircraft components are customarily fulfilled by a small number of suppliers in the aerospace industry [233–235]. Hence, production schedules for available capabilities are often extended, due to technical and technological factors, including the complexity of the processes and procedures involved, resulting in long manufacturing

lead-times for these components [192,210,231,233]. The nature of international trade, which introduces other factors, including shipping modes, channels, ports, destinations, rates, applicable industry and trade regulations, also have a bearing on supply [236–240]. When combined with a strong industrial demand, these commercial challenges often translate to higher manufacturing and related costs [231,241]. Predictably, any reprocessing operation stemming from a supplementary requirement (SR) often exacerbates present commercial challenges, within existing supply chains.

In fulfilling industrial requirements, for higher performance materials, and improved safer designs, larger components are normally manufactured in multiple stages. The implication is that there are multiple points, both within and between different manufacturing operations and stages, in which SRs may occur. Within the process, problems may be inherent to the process itself, or attributable to input and control factors, as well as the process suitability for specific applications, a requirement subset with its own unique features and traits. Between manufacturing stages, selected processes will determine the type of problems encountered, which may be similarly classified based on process characteristics, inputs, control, and suitability, as well as initial state of the metallic structure or object before the next process is initiated [192,242]. Considering that distinct items, imported or produced by a restricted number of suppliers, will usually require additional operations upon arrival at specific destinations, the occasional risk of losing some or all of the accrued manufacturing value is inevitable [210]. For instances involving partial loss of value, irrespective of where losses are incurred, the supply conditions usually determine what happens next. Similarly, when the finished product is put into service, domestic supply conditions are critical for ensuring a rapid response to related demands.

The types of issues encountered at different manufacturing stages, which typically become evident in the realisation of product design requirements, are due to the interactions between the material and process, and the product form and its function [210,243,244]. Inadequate control of interactions between the material and the process increases susceptibility to various issues, including chemical segregation, microstructural inhomogeneity, and other material imperfections [210,242]. Between the product and its function, size and geometric limitations are some of the factors that influence intermediate product forms, which can affect subsequent processing steps. Production considerations include the susceptibility of intermediate parts to shape distortion, variability, accuracy, and other form related imperfections [242,245]. Product related issues are determined by interactions prior to, and when the product is in different use states and environments. In particular, performance is affected by inherent geometric characteristics, features, and latent design or manufacturing imperfections, which are revealed when a product is fulfilling its designated functions [243,244,246,247]. In other words, the probability and likelihood of encountering production or product related problems are dependent on these outlined factors, as well as other atypical causal factors. Thus, the ability to accurately detect and properly characterise imperfections is an important initial step in SMRM. When considering available recovery routes and supplier response rates, the types of requirements that can be

supported determines the management strategy that is subsequently selected for resolving detected or evident problems.

The ability to provide a quick and efficacious response to industry demands is impeded by several factors, including the determination of problems, during the part manufacturing and application stages [203,206,248]. Detectability requires complete and perpetual awareness of all aspects and conditions of the product within the manufacturing or use environment, such that necessary and appropriate mitigation measures may be applied in a timely manner. However, due to present technical and technological limitations, it is not practicable to have such broad and continuous cognizance. Instead, and at the determined manufacturing and service stages, preventative measures are applied, in conjunction with different inspection tools and techniques [248]. Although inspections are relevantly informed by design, functional and operational requirements, human and other factors do contribute to inspection related errors [7,248]. Even when inspections are judiciously completed, the detection sequence and timeframe are often retrospectively well-defined, because it is typically after an event has occurred that inspectors may have an enhanced understanding of causal factors [7,243]. Hence, timing, as well as the rapid detection and characterisation of manufacturing and service issues, are equally crucial for formulating a rapid response. Invariably, early awareness of typical issues will facilitate the determination of the types of requirements that can be supported within the accessible supply chain.

The feasibility of SMRM activities is judged on a case-by-case basis, and with integrity and safety being paramount, the decision to proceed is influenced by confidence in the suppliers ability to complete laborious operations, under possible deleterious working conditions [7,210,246]. Decision factors include unrestricted site access; the precision, control, portability, and versatility of capabilities; and personnel or human aspects, such as process know-how and competency [241,246–251]. However, relying on the supplier's judgement is a rather subjective exercise, as confidence will be based on supply conditions, which is determined not only in relation to current accreditations, but by the business circumstances at the point of demand. Between highlighted human, technical, and technological circumstances, is the prospect that numerous supplementary manufacturing requirements remain unfulfilled. Hence, there are potential benefits for suppliers capable of objectively meeting the need for operations that are insufficiently supported at the local or domestic level. From a commercial standpoint, some of these benefits are aligned with current engineering challenges, including how to establish circular economies, and efficiently manage pressing developmental and sustainability issues [8,9]. These perspectives are already shaping social movements, as well as national and international policies, which will likely influence how supplementary requirements for these designated long-lasting traditional infrastructures, as well as new AM developments, are managed in the future, alongside normal and unforeseen disruptive technological advancements.

2.6.2 SMRM tools and techniques

Due to the peculiarities and uncertainties surrounding SMRM, particularly for reworking operations, there are no set of tools and procedures presently applicable to all cases and scenarios [7]. Instead, end-to-end requirements are typically fulfilled using a suite of proven but distinct processes that are sufficiently adaptable to on-site and off-site requirements. For core requirements, complementary welding, forming, and hybrid or composite techniques, are primarily used in conjunction with supporting inspection, preparation, finishing and verification techniques [7,29,248–250,252]. For large metallic components, the appropriate solution may be permanent, as for cold or hot fusion processes, such as welding, or semi-permanent as applied when using patches, in consideration of pertinent design factors, material integrity, and safety requirements [7,249,251,253]. In-situ or on-site operations, implemented either during the manufacturing stage, or when the product is in service, are limited in scope, but can help to increase efficiency and minimise the impact of SMRM activities on otherwise streamlined operations and services [247]. Ex-situ or off-site operations are much broader in scope, particularly if a replacement is readily available, allowing sufficient time for suppliers to implement SMRM activities at an approved facility, where the mutability of the product, in this situation, is more critical than its location [7].

Establishing the need for direct intervention is an important early step in SMRM [248]. Primary investigative tools and techniques include both visual and other NDE methods, with the purpose of acquiring sufficient comprehensive data for analysing requirements and generating highly accurate and detailed specifications of the issue(s) to be resolved [7,206,254]. NDE data helps to determine subsequent SMRM steps, including the nature and feasibility of proposed interventions. Assuming there are no discrepancies that exclude the implementation of SMRM activities, then a restoration method, temporary or otherwise, is established [7,249,251,253].

The first procedure in the restoration process, is the cleaning operation. The area of interest is thoroughly cleaned and prepared, typically involving the removal of material and verification of this step, before proceeding with restoration. While actual intervention procedures may vary, depending on specific requirements, the sequencing and implementation of different operations are consistent with the purpose of making the component whole. Nonetheless, there is always a risk of further irremediable damage, due to the characteristically multifaceted operations and numerous interdependent variables to consider [7,210,248]. The type of structure, its purpose, characteristics of identified irregularities (i.e., type, location, point of origin, etc.) are typical interdependencies that influence estimation of the required SMRM effort, time, and costs. However, the human factor is a common denominator that significantly contributes to subjective SMRM experiences. Consequently, highly skilled operatives are needed for achieving consistent output quality. Individual ingenuity, though also subjective, may be necessary when there are no precedents, necessitating the design of multiple intervening steps that allow for the early implementation of mitigations [7,254]. Although

such interventions likely contribute to inefficiencies and prolonged lead-times in SMRM, they prevent the accumulation of issues that impede the successful implementation of requisite actions.

The final stages of SMRM involve the inspection and qualification of the product before it is returned to service. The substantiation process is encompassing, including all SMRM actions that have been performed, prior to certifying the part for use [7,248]. Different NDE tools and techniques are implemented at designated stages of the verification and validation process, with all materials, processes, procedures, and related activities properly documented, ensuring that traceability is maintained throughout, thus providing necessary evidence to support qualification and certification proceedings.

2.6.3 SMRM implications and AMT adoption opportunities

Irrespective of the causal factors, the top business implications of SMRM are cost and time. Compared to typical manufacturing, which commences under controlled initial conditions, involving relatively uniform pre-forms or components, and operations that are sequentially and optimally planned, SMRM starting conditions are highly variable. Consequently, the approach to SMRM is irregular, whereby expectations of typical manufacturing benefits and efficiencies are unrealistic. Notwithstanding the causal factors or starting conditions, replacing or scrapping products at this scale contributes to substantial material waste [253]. Already, the raw material for aircraft production and maintenance, repair, and overhaul (MRO) accounts for more than 0.5 million tonnes of metals [255,256], and about half of the global demand for titanium [257,258]. However, material yield remains relatively low, as only a fraction of the raw material is converted to finished products [255,256,259]. Low material conversion rates persist because of processing inefficiencies, which affects pre-forms or intermediate products, as well as secondary production operations and end-forms. Nevertheless, a significant proportion of the melt stock for new or replacement titanium products, and other non-ferrous raw materials, is now obtained from scrap metal [257,258]. There is also an increase in the utilisation of scrap steel, at ~0.5 billion tonnes, relative to crude steel production, which is up ~1.5 billion tonnes [260]. As the demand and value of all forms of raw material increases, and given that time is a factor in SMRM, the cost and affordability of new or replacement products will be affected by these trends.

Considering the daily operational costs and charges accrued, on top of the actual costs associated with SMRM, the financial implications can be quite significant, relative to the total business operating costs. The possibilities involve standardising the component and dealing with the resulting inefficiencies of a time-consuming material removal operation, or standardising supplementary task requirements, using appropriate inspection or reverse engineering techniques, before adapting subsequent operations [261–263]. Both options invariably add time and cost, but the former restricts activities to component-level requirements. Conversely, focusing on standardising tasks and optimising common operations, will encompass component-level requirements, while potentially expanding the scope for developing a combination of tools for rapid SMRM detection, characterisation, and resolution. In any case, when valuable and operationally critical products are

removed from service, pressure is exerted on the supply chain to complete necessary operations quickly, which can make it harder to track demand [264,265].

Though difficult to assess, the demand for SMRM is certain, and the market is undoubtedly significant, due to the natural life cycle or progression from CTG, for existing infrastructures, and particular circumstances confronting both developed and developing societies. Although the actual value is likely underestimated, available information on the average UK economic output suggests the domestic market is worth hundreds of millions of pounds [266]. In the transport industry, it is estimated that MRO activities generate about 40-50% of the aerospace industry revenue [259], with a forecast growth of approximately 3-5% or USD50-70 billion over the next decade [235]. Hence, reducing scrap rates, increasing productivity, and improving material yield, are important manufacturing priorities. In the energy sector, reductions in lead and maintenance times are key drivers, motivated by the need for a new generation of power plants, due to a significant number currently operating within their end-of-life window, with higher maintenance requirements [241,254,267]. Similarly, the requirement for longer operating aircrafts, and the re-use of serviceable materials, are especially aimed at reducing costs, tackling sustainability issues, and lessening the impact of manufacturing operations on the environment, particularly in relation to energy and resource intensity [268,269]. A further consideration, in securing approvals for component lifetime extensions, is the increased level or frequency of maintenance support required, what this entails, and the full implications for SMRM.

Challenges in SMRM stem from the interplay between highlighted commercial, technical, and technological factors, not least the applicable safety factors, costs, resources, and time involved. There are also variations in requirements and experiences, stemming from a combination of general and specific product, production, and service circumstances, including CTG factors. Thus, in both product manufacturing and use settings, specialist equipment or tools are sometimes required to complete specific operations [7]. These non-standard solutions can affect task complexity, resulting in more subjective domestic supply experiences, which can be financially burdensome, when considering the typical operational costs and efforts already dedicated to supporting current business demands more efficiently. However, the uptake of new approaches is typically done in a very conservative manner. As MAM technologies are increasingly deployed for applications where the product function and form are equally important, there is a need to ensure that selected processes are demonstrably suitable and effectual [28,76,109,268]. In general, the MAM deployment prospects, for SMRM purposes, are promising, due to the growing demand for new and improved infrastructures in both developing and developed nations [210,257,260]. Prime commercial targets include supplementary requirements currently deemed too complex or resource intensive, involving specialist tools and/or techniques, prolonged response times, obsolescence issues, or any combination of these scenarios. Therefore, the ongoing investigation of pertinent factors is necessary, to support the wider adoption of MAM technologies for different large-scale applications, particularly for SMRM.

2.7 Definition of requirements and priorities

Research priorities were defined in relation to the requirements for large-scale MAM technologies, which was meaningfully shaped by the initial focus on SMRM, while considering the broader scope and utility for such capabilities. The purpose of integrating a system was to facilitate MAM and SMRM investigations, and through this process, develop a framework to capture specific insights about the entire integration experience. As previously stated, such systems can offer significant benefits over utilising various separate technologies for SMRM, which typically involves several distinct and unrelated tasks that can increase the overall complexity, associated risks, and costs of required operations [203]. Thus, a single system that can be configured to purposefully link related aspects of work, such that the performance of combined solutions exceeds the sum of its constituent parts, is highly desirable. However, the systems integration process is highly challenging, as it typically involves combining different technologies from different suppliers, with the DED class of the additive manufacturing being a prime illustration [194,195,199]. WAAM techniques are ideally suited to a range of large-scale metallic applications but bespoke configurations are the norm [200–202]. In an evolving landscape, cooperation can enable the delivery of advantageous solutions that fully exploit the benefits of constituent tools and technologies, to maximise productivity [196–198]. Furthermore, the joint clarification of specific system, applications, and capability requirements, can enhance solutions, whilst reducing costs.

The alignment of different DED technologies with large-scale MAM operations was a key decision factor, in the selection of the WAAM process as the main technology underpinning system development activities and related investigations. Although different studies have demonstrated that WAAM output accuracy is low, when compared to DED-LP processes [48,153,154], other studies have shown that WAAM processes can be tailored, such that accuracy is prioritised over productivity [45,270,271]. At any rate, since different post-processing operations are often required for end-to-end SMRM, other factors, including process flexibility, were prioritised over post-processing requirements. Furthermore, when considering manufacturing quality and material performance challenges, the analysis of substantiation requirements revealed that irrespective of technology preferences, there were different cross-cutting surface and subsurface issues affecting all MAM processes [43,46,48,62,93,94,156,157,163,212].

Other considerations for an integrated MAM system, were evaluated in relation to present challenges and possible solutions described in Table 2-20. The outlined factors highlight broader aspects presently influencing the development of large-scale MAM systems and procedures. The initial focus on the application category, was symbolic of the hierarchical relationship between the technology and its utility, whereby relevancy is typically established via the utility of a particular technology, relative to its industrial application(s).

Table 2-20: Classification of general considerations influencing the development of the proposed large-scale MAM system.

System categories & factors		Development considerations
Application	Industrial AM capacity	Lack of suitably sized commercial AM systems and implications for processing capability and applications scope [38,272], including further industrialisation of AM, whereby industrial/ heavy engineering capacity can transform technical prospects and enhancing competitiveness [273,274].
	End-to-end process	CTG requirements, spanning 3D model to end-state component [38,195], and possibility to exploit AM, particularly DED, for increasing efficiency in industrial environments, including via integration of multi-stage operations involving single large-scale component or structure [273,275].
	Deployable productivity	Limitations of geographically constrained capability and potential for decentralised AM capability and capacity [276,277], including possibly deploying AM for task mechanisation, particularly in remote or harsh environments, as well as under challenging circumstances for task and personnel/ operatives [278].
Cost	Accessibility	Access (i.e. affordable and available industrial capacity) and other well-documented factors hindering wider AM adoption [272], and opportunities to develop more accessible AM capabilities, supported by increased understanding of technology and/or system gaps.
	Capital expenditure	Understanding budgeting constraints and impact on system acquisition plans, including incremental development needs driven by newer/ more advanced AM capabilities, and requirement to accelerate development of more robust approaches, and durable long-lasting systems [200,279].
	Operating expenditure	Understanding impact of tangible and intangible elements on operating expenses. Also, exploring standard solutions for reducing recurring expenses, and related business prospects for AM as a manufacturing service [275].
Features	Reconfigurability	Ability to modify equipment, including subsystems, and components to suit processing requirements for different applications, and alignment with broader considerations, prospects and emerging perspectives, including industry 4.0, circular economies, internet of things (IoT) devices, big data, etc. [280,281].
	Modularity	Understanding factors affecting independence of distinct subsystems/ modules within interdependent system boundaries, and how to support faster reconfiguration, upgrade, and maintenance, including the identification, diagnosis and rectification of system faults.
	Automation	Issues impeding realisation of fully automated/ operationally independent systems [282,283], and impact of underlying variability issues [280] on system dependability, as well as enablers for seamless integration of actual and digital/ virtual AM capabilities.
Complexity	Operability	Financial and technical implications of skills and training requirements for suitably qualified and fully competent AM personnel, including impact of complex solutions on safety, productivity, and efficiency, as well as related operational risks.
	Man-machine interface	Understanding of requirements to support transition to more advanced AM systems that are indistinguishable from their base technologies, with predominant focus on sustainable value creation and productivity via improved interfaces/ complex but easy to operate systems.
	Maintainability	Understanding of resources, expertise and technical support needed to maintain or restore manufacturing service continuity, with considerations for easily maintainable DED systems, to improve durability, overall efficiency and decrease downtime, thus negating the impetus for more costly replacements.

The cost category (Table 2-20) was the second most important consideration, because it determines affordability, particularly when seeking to acquire the desired features from which system functions are derived. Sequentially, the required system features can introduce further complexity, which can affect the procurement, integration, operation, and maintenance of the resulting amalgamated solution. Beyond the system, and relative to other DED processes reviewed, WAAM materials and parts were more susceptible to distortion and residual stress [168,284,285]. Hence, these topics were also prioritised, due to the potential implications on targeted MAM applications, and in consideration of planned substantiation activities. For large-scale MAM and SMRM operations, the identified processing issues emphasise the need for improved monitoring and timely control of underlying factors, and at critical stages, as well as the benefits of numerical modelling and simulation tools and techniques, for describing, explaining, exploring, and predicting interrelated causal factors.

The summary analysis (Table 2-20) demonstrates that the requirements and considerations for innovative metal fabrication systems are much broader than a single AM technology. However, it was necessary, and practical, to narrow the scope of investigations in alignment with the purpose of this study. Therefore, with MAM as the primary focus, and WAAM as an enabler, a top-level map of the main research requirements and priorities for this study was developed. This map is presented in Figure 2-22.

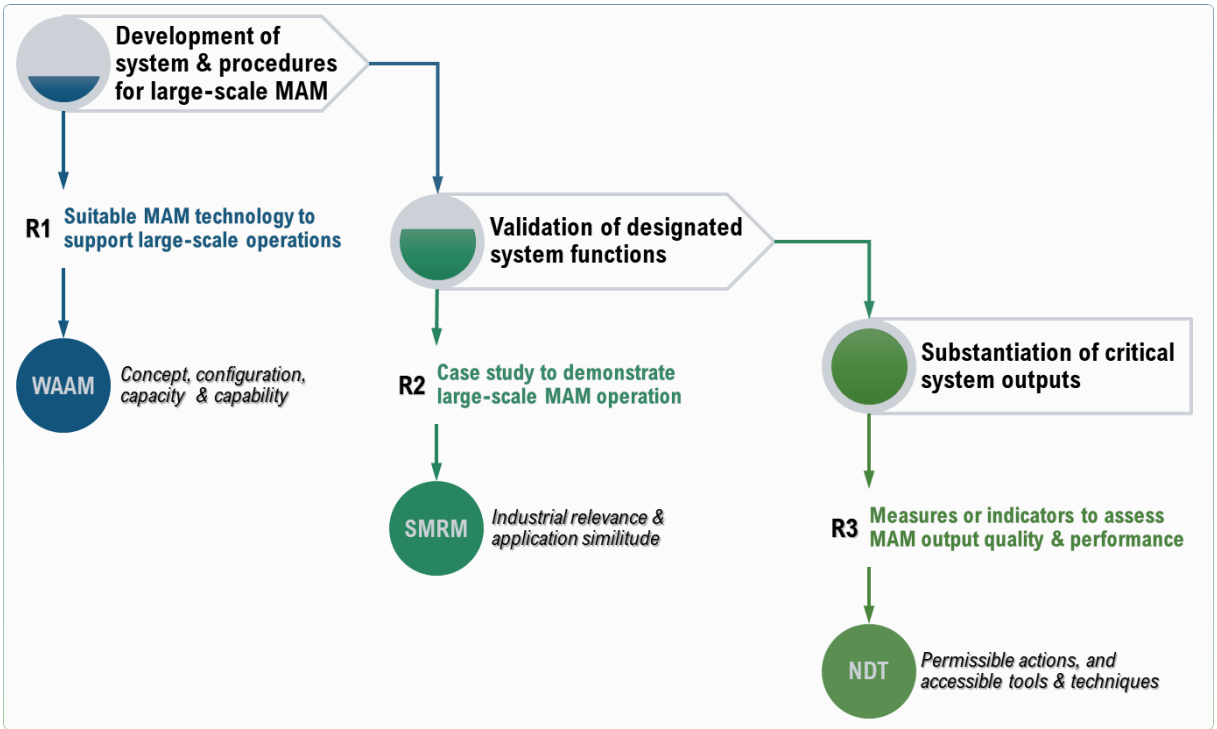

Figure 2-22. Mapping principal research requirements and priorities.

The map is used to emphasise the main research actions, which correspond to the GT framework data acquisition (DAQ) phase (Figure 1-1), as well as the specific requirements, *R1*, *R2*, and *R3*, and corresponding priorities supporting each action. The map also includes key considerations for defined priorities, due to the

influence of related factors on research implementation plans. System development requirements were underpinned by the WAAM process, which was selected for developing a large-scale MAM capability (*R1*). Correspondingly, an appropriately scaled, and industrially relevant case study was a crucial requirement (*R2*) when formulating the strategy for validating the system concept, configuration, and approach for large-scale MAM operations, underpinned by SMRM. The need for substantiable material and/ or part quality and performance (*R3*) influenced the prioritisation of non-destructive testing (NDT) methods, with distortion and residual stress identified as critical output measures. The main NDT/ NDE considerations were the allowable actions pertaining to the case study, and the accessible tools and techniques for implementing agreed development actions.

2.8 Theoretical basis

An investigation into the development of large-scale MAM system and procedures requires understanding of applicable design, systems, and related management theories. However, management aspects are influenced by a combination of industrial, organisational, situational, personnel, and other related factors, wherein a diverse and complex set of requirements must be accommodated within relevant multi-disciplinary domains. Hence, there are often gaps between stated requirements, technical specifications, and projected outcomes or deployed solutions. Due to the potential effects of these gaps on expected outcomes, the main challenge was to identify which developmental and procedural factors were most significant in the adoption and implementation of AM capabilities for various applications, including large-scale MAM and SMRM. Correspondingly, it was important to determine how to navigate anticipated complexities, organise highly unstructured qualitative, as well as quantitative data, and frame resulting information in a comprehensible manner, beginning with the definition of specific research requirements.

Specific needs can be challenging to articulate, due to differences between requisite attributes and multi-participant perspectives, notwithstanding that AM is a non-traditional approach, and SMRM strategies can be atypical. Hence, requirements management was a foundational theory applied throughout this study, to facilitate the translation of concepts into specifications, from which solutions were derived. Requirements management is principally concerned with the gathering, elicitation, expression, and formalisation of the statement of need, and is applicable across multiple domains, including system and product design and development activities [286–288].

Different complementary management approaches were equally important when implementing various research actions. Design principles were applicable to the management of system development activities and facilitated the translation of concepts into specifications, including the specification for a large-scale MAM system. Embedded in scientific methods, design is the cross-disciplinary process in which practitioners progress logically and sequentially, from specified need or problem statement to solution [289–292]. Thus, the purpose and primary objective of the design process is to derive a solution, which may take different

radical, evolutionary, analytical or synthetical forms. In other words, while that which is being created does not yet exist, following a methodical approach allows practitioners to create better solutions [289,291,293]. Compatibly, relevant manufacturing concepts were also adopted to support design activities. The principles of scientific management is an orthodox approach that emphasises efficiency through systematic management, and was especially developed to minimise waste, and overcome pervasive inefficiencies affecting both individual and corporate endeavours, in industrial and manufacturing establishments [294]. In this respect, inefficiency and waste are recurring themes linking both orthodox and contemporary manufacturing philosophies, which include various models for enhanced productivity, cost, quality, operations and supply chain management [295–299]. These issues affect both design and manufacturing endeavours and persist, due to different regional, organisational, cultural, behavioural, and implementation practices, as well as other internal and external drivers, including evolved organisational perspectives, informed by increased understanding of contributory factors, and technological advancements [294,299]. The main manufacturing concepts aligned with this study are lean manufacturing principles and its different mechanisms, which facilitate the practice of eliminating waste or non-value-added components, via a process of continuous improvement [300–304].

Causal modelling is one of the main statistical or numerical principles applied in different sections of this study. These mathematical models are used to represent causal relationships within individual systems [305,306]. In general systems theory, which also originates from the management discipline, the word "*system"* is an umbrella concept encountered in and simultaneously developed across multiple disciplines or scholarly domains [307–309]. The systems or holistic approach emerged as an alternative to reductionism, where inferences about the whole can be abstracted from isolated elementary parts, and instead focusses on the investigation of wholes, interdependence, and complexity, to account for systemic and emergent properties [307,308,310]. In systems dynamics, which is the concept most applicable to this study, the exploration of causality extends beyond systemic events and instead focuses on the attributable causal relationships between variables, in order to explain the behaviour of systems [311–314]. At any rate, the complexity of causal models is influenced by the thoroughness of the solution upon which inferences about causal relationships are founded, while actual causation is determined by the number of variables, and the measure of the degree of association between variables [311,315]. Hence, variables are referred to as the basic building blocks of causal models, while variability is defined as a measure of the degree to which values in a statistical data set, derived from individual systems, are distributed or dispersed [305,311,316]. In prevailing narratives, significant variability issues presently affecting MAM systems, processes, and outputs [52,56,85,94,157,175,317,318], remain insufficiently inclusive of the whole, whereby the empirical focus is mainly at the process-level [91,270,319–321]. However, this complex and multi-layer issue covers the configuration of the system; the procedures initiated in response to system configurations and associated constraints; the subsequent effects on system outputs; and the relationship between these elements. In this respect, causal descriptions, explanations, and predictions are concepts typically used when developing substantive theories. While causal models focus on

describing observable events, and explanatory models are used nearly exclusively for building and testing causal effects on interdependent variables, the goal of predictive modelling is to forecast the outputs for new observations from a given set of inputs [315,322]. Thus, causal and/ or numerical explanatory modelling approaches were most relevant for this study and applied in relation to planned substantiation activities. Correspondingly, mechanical engineering principles, particularly established concepts used to explain the response or mechanical behaviour of materials in metal forming operations, such as MAM, were adopted when developing specific numerical models. The implementation of modelling approaches has greatly benefitted from advanced computational software tools, which include pre-packaged computer codes. However, given the increasing reliance on these tools and techniques, understanding classical continuum mechanics theories is essential when formulating contemporary nonlinear continuum models [323]. Fundamental principles applicable to this study include the mechanics of materials, and the theory of plasticity.

After implementing various research actions, a mechanism was necessary for enhancing understanding of the functional relationships, interconnectedness, and intricacies of the overarching problems investigated. The objective was to ensure that insights about large-scale MAM systems and procedures, which were underpinned by SMRM, were properly extrapolated, well-construed, and concisely articulated. Hence, the framework research method allowed for the systematic acquisition, strategic analysis and mapping of data, and interpretation of resulting information, in accordance with key issues and themes identified throughout this study. The framework method is also derived from the mathematical field of statistics. The GT constant comparative method [324] was specifically selected because it allows for the verification of assumptions about technology adoption factors, whilst providing insights about major themes synthesised from amalgamated data. Thus, it was anticipated that by applying the GT framework method, the importance of evaluating developments in large-scale MAM, as outcomes that depend on the systems and processes adopted, as well as the procedures used to fulfil new or supplementary manufacturing requirements, will be elucidated.

The theoretical framework and respective domains supporting this study are presented in Figure 2-23. Beyond the explicit focus of this study, the theoretical framework highlights the connections between the GT approach and core principles shaping the main research ideas, related concepts, and investigations, and how these elements were incorporated. While the GT method encapsulated the overall research approach, applicable theories, tools, and techniques, including quality management principles and related process qualification considerations, were especially incorporated (Figure 2-23), to guide principal investigations, and obtain case data for identifying and organising the ideas and concepts emerging from this study.

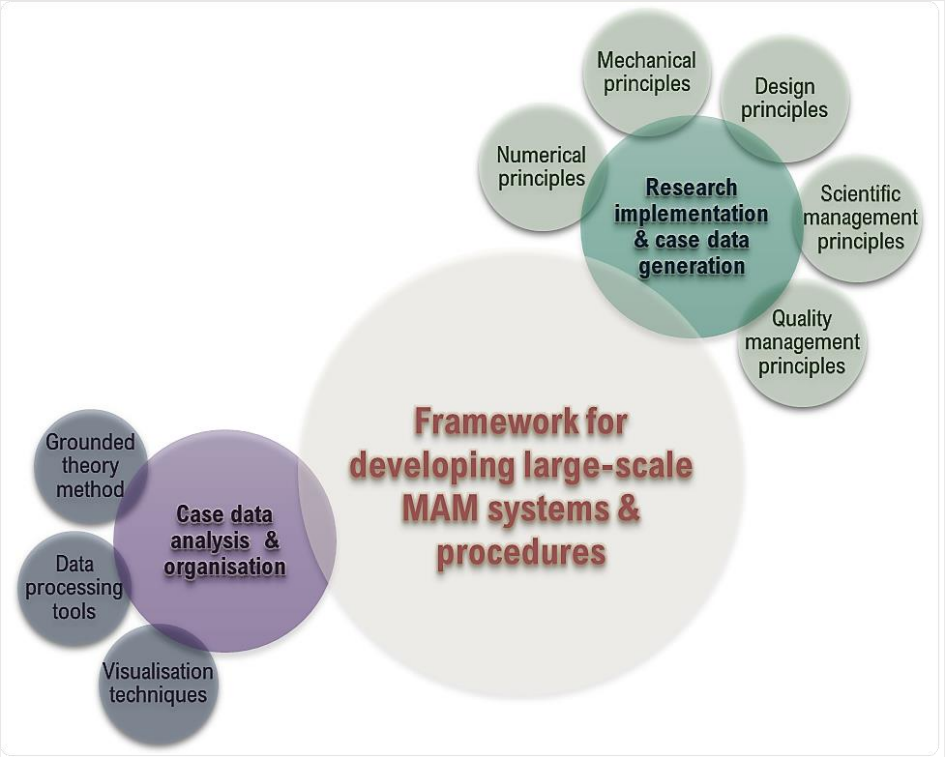

Figure 2-23. Principal theories and implementation.

2.9 Summary

In this chapter, the theoretical basis for this study and rational for adopting the GT framework method, to systematically investigate and organise emerging ideas about large-scale MAM systems and procedures, was established. Key organising principles and related concepts, encompassing design, mechanical engineering, statistical and management domains, were also explored, in consideration of system development, validation and substantiation plans.

Different AM technologies were originally investigated to identify capabilities that were aligned with the industrial focus on large metallic structures, before proceeding to characterise MAM technologies relative to the requirements for both original and supplementary manufacturing operations. Due to their strategic relevance, DED and PBF processes were selected from the MAM technology subclass and comparatively analysed based on current benefits, and limitations, before narrowing technology options for this study to the DED subclass. DED output quality and key performance indicators were further analysed, with WAAM subsequently selected as a significant enabler for large-scale MAM operations.

The topic of SMRM was introduced to underpin the overall development approach, whilst demonstrating the relevance of large-scale MAM capabilities. SMRM challenges and other interrelated business factors contributing to persisting industrial issues, including discrepancies between local supply conditions, global demand patterns and circumstances, and present technical and technological limitations were also explored.

Similarities between industry sectors were further evaluated, to clarify opportunities and prospects for MAM deployment, including for SMRM, where the combination of uncertainties surrounding specific requirements, non-standardised fixes, and other related constraints allow for the use of novel tools and techniques. Verification requirements were also reviewed alongside considerations for validating the system and procedures governing SMRM tasks, while highlighting typical issues affecting MAM materials and parts, comprising the different tools and techniques generally used for their characterisation. Different SMRM factors, including the primary objective of sustaining or restoring the inherent safety and reliability of existing metallic structures, necessitated the review of computational tools and techniques, to complement empirical activities and foreseen validation procedures. Numerical approaches were specifically considered to facilitate the description and explanation of WAAM output quality and performance related factors.

In the final section of this chapter, research requirements and priorities were outlined, to illustrate the relationship between the overall research strategy and planned investigations. In the next chapter, the overall approach for developing and validating a MAM system is presented, alongside initial investigations that were implemented to inform the overall development strategy.

CHAPTER 3

3 Method and Implementation

3.1 Introduction

The general research methodology presented in this chapter combines both qualitative and quantitative elements. Core research activities were designed to meet the central objectives of this study, and implemented in four distinct stages, including preliminary investigations, also documented in this chapter. Investigations were aligned with the overall research strategy, particularly the case data generation phase (Figure 1-1), with individual tasks and planned activities aimed at addressing the central objective of creating a GT framework. The main investigative stages and associated development tasks are outlined in Table 3-1.

Table 3-1: Core development tasks contributing to construction of concept GT framework

Task outline	Description	Implementation						
		AMRC	BAM	MIT	NAMRC	RR	SMD	PI*
Preliminary work	Study 1: Development and implementation of strategy for fabricating PoC part, including subsequent material					*CA*	*SPO*	*TDPI*
	Study 2: Development and implementation of DED strategy for depositing representative material samples,			*CA*			*SPO*	*TDPI*
	Study 3: Development and implementation of strategy for evaluating applications and procedures, including						*SPO*	*TDPI*
	Data collation and overarching analysis, including elucidation of related observations							
System development	Requirements analysis and concept development							*AD*
	BAM system implementation, including integration and commissioning		*SPO*		*SDA*			*TDPI*
	Post-implementation analysis, including related experiments.		*SDA*					*TDPI*
	Data collation and overarching analysis, including elucidation of correlations and observations							
System validation	Requirements analysis and SMRM strategy					*CA*		*TDPI*
	Reprocessing trials involving substrate, including machining and CT scanning	*SDA*	*SPO*		*SDA*			*TDPI*
	Reprocessing trials involving case study, including machining and inspection		*SPO*		*SDA*			
	Post-BAM analysis, including related material characterisation studies		*SDA*					*TDPI*
	Data collation and overarching analysis, including elucidation of related observations							
Verification of system outputs	Requirements analysis and modelling approach							
	Implementation of process models							
	Post-simulation analysis							
	Data collation and overarching analysis, including elucidation of correlations and related observations							

Key:
AMRC → Advanced Manufacturing Research Centre:- *Shane Smith, Steven Partoon, Graham Brook, Carl Wilson, & Chris Depledge*
BAM → BAM Team:- *Udisien Woy, Joe Cooper, Wei Guo, Samantha Biddleston, Jamie Todd & Alex Hanneman*
MIT → Massachusetts Institute of Technology:- *Tomasz Wierzbicki & Dirk Mohr*
NAMRC → Nuclear AMRC:- *Tom Parkin, Lewis Marsh, John Hilton, Robert Widdison, Jonathan Bramall, John Crossley, Andy Austin, Agostino Maurotto, Kevin Monaghan & Joe Hiley*
RR → Rolls-Royce plc:- *Daniel Clark, Steven Lawler , Richard Harlow*
SMD → SMD Team: - *Udisien Woy, Garry Hibbert, Joe Cooper & Vishal Patel.*
Principal Investigator (PI) → *Udisien Woy*
*Role/ task reponsibilities → AD - *Architect & developer* ; C- *Clarifications & approvals;* SDA - Specification, direction & assistance; SPO - *Set-up, programming & operation* ; TDPI - *Task development, planning & implementation*

For distinct tasks (Table 3-1), delegations were necessary to facilitate progress, whilst maintaining oversight of all implementation aspects, thus ensuring consistency with overall research objectives and strategy. Initial investigations provided first-hand experience of certain issues and specific insights, prior to the development and validation of a representative MAM system. Both preliminary and principal investigations, described in succeeding chapters, facilitated the generation of pertinent data to support the creation of a GT framework.

3.2 Preliminary studies

Different studies were completed to inform the main investigations underpinning the creation of the concept framework. These investigations were generally organised into formative and normative elements. Formative elements were focussed on directly verifying industrial drivers and challenges influencing the deployment of MAM technologies. These elements facilitated the refinement of requirements and priorities (section 2.6), which ultimately shaped the normative or prescriptive elements of this study, as outlined in the overall research strategy (Figure 1-1). The progression from preliminary to principal investigations is depicted in Figure 3-1.

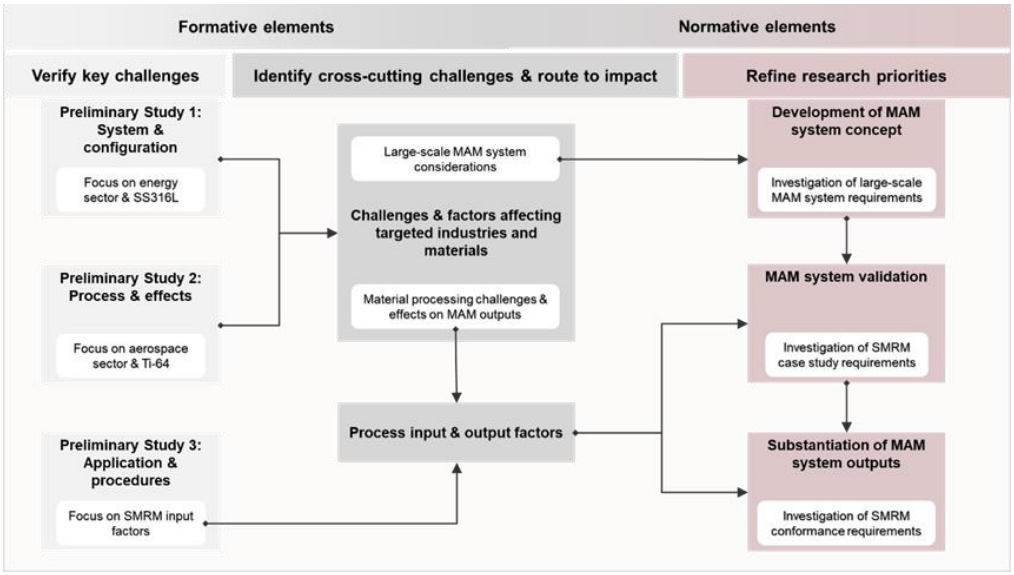

Figure 3-1: Formative and normative research elements and implementation strategy.

While formative investigations were instigated and collaboratively supported by industry and academic partners, normative studies were independently initiated and implemented in alignment with the distinctive research focus depicted in Figure 1-1. Formative aspects were opportunistically relevant and thus appropriately exploited for the benefit of normative research elements, by linking specific outputs and identifying commonalities between studies.

During the implementation of formative and normative investigations, two different DED capabilities were used; the proposed large-scale MAM capability, and the SMD capability, which were both configured for the WAAM process. However, all preliminary studies were completed using the SMD capability, with core investigations completed on the new system. This strategy allowed for the comparative analysis of developmental factors, at the relevant system, process, and application levels. As previously stated, the energy and aerospace industry sectors were targeted, due to the potential to access relevant SMRM case studies for validating the representative MAM system and related procedures. Correspondingly, two of the most significant engineering materials used in the targeted industry sectors, namely grade five titanium (Ti-6Al-4V or Ti-64) and low carbon stainless steel (316L) alloys, were strategically prioritised, for both preliminary and

principal investigations. This approach also facilitated the acceleration of core development phases and the framework construction process, due to the availability of baseline information for refining the system concept and validation procedures. Furthermore, the possibility to obtain relevant material property data, to support the development of numerical models, as part of SMRM verification procedures, was a potentially attractive prospect for this study, which was likely to involve one of the two alloys investigated.

3.2.1 Study 1: System and configuration factors

The limited capacity of MAM system is a well-known factor influencing wider industry adoption. Therefore, the purpose of this investigation was to validate the specific requirements for enhanced equipment capacity, with a predetermined focus on the energy industry sector and type 316L stainless steel (SS316L) alloy.

The feasibility study [63] was performed using an existing SMD capability, with the aim of producing a geometrically representative proof-of-concept (PoC) SS316L part. This industry-led collaboration was instigated with the goal of assessing the feasibility of utilising SMD to fabricate components used in the energy sector. From an industrial perspective, it was specified that novel manufacturing approaches were especially required to improve the manufacturability, processing times, material yield, and related costs associated with targeted components. It was also articulated that the main motivation was to support the development of AMTs, for the future fabrication of components used in this industry.

The primary experimental objective was to determine how to fabricate the required scaled-down industrial component, with a wall thickness of ~40mm, using DED technologies. Thus, when assessing the requirements for bulk or large-scale MAM capabilities, the part specifications and scaling considerations were crucial. The SMD capability used for the study is presented in Figure 3-2.

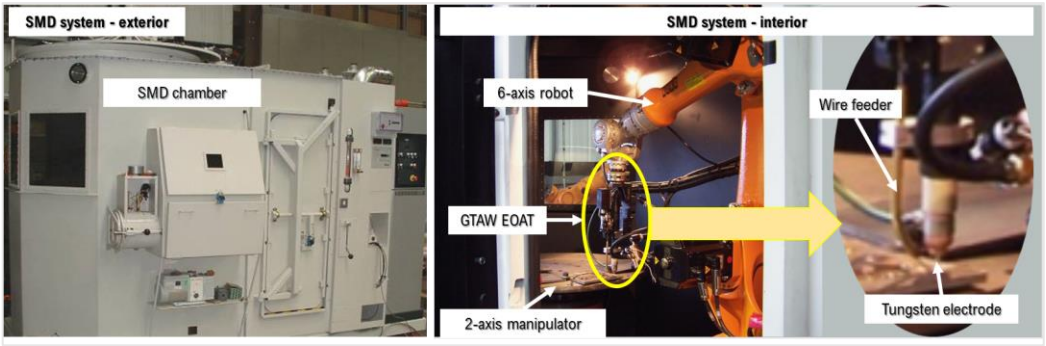

Figure 3-2: SMD capability for wire and arc deposition.

Configured with a GTAW end-of-arm-tooling (EOAT), the SMD manufacturing cell is comprised of a 6-axis robot and 2-axis manipulator, which can support a maximum component mass of 400 kg. When operating under an inert atmosphere, the fully sealed chamber ensures that argon purity is maintained at ~20 parts per million (ppm). The SMD kit also includes a camera, oxygen analysers, data logger, and other devices to facilitate process monitoring and data acquisition activities.

A DoE approach was applied when developing parameters for processing the PoC part. This method was enabled by MODDE, a statistical analysis software tool for planning and analysing empirical data, which was used in conjunction with Grasp10, an advanced process simulation tool developed by BYG Simulation, to enable the offline programming (OLP) of the SMD cell. The parameters for this study are summarised in Table 3-2.

Table 3-2: Experimental variables for PoC part.

Category	Type	Variable name	Values	Units
Input parameters	Quantitative	Current	160 - 320	Amps
		Voltage	12 - 14	Volts
		Arc gap	3 - 5	mm
		Travel speed	0.83 – 5.83	mm s^{-1}
		Wire feed	11.67 – 31.67	mm s^{-1}
	Constant	Wire diameter	1.2	mm
		Argon (torch)	15	l min^{-1}
		Oxygen levels	20	ppm
Layering parameters	Fixed	Step height	1	mm
		Overlap distance	2.5	mm
Outputs	Measured	Bead height	N/A	mm
		Bead width	N/A	mm

The itemised variables were used to generate experimental schedules, which were subsequently implemented. The main statistical outputs of this experimental design are depicted in Figure 3-3.

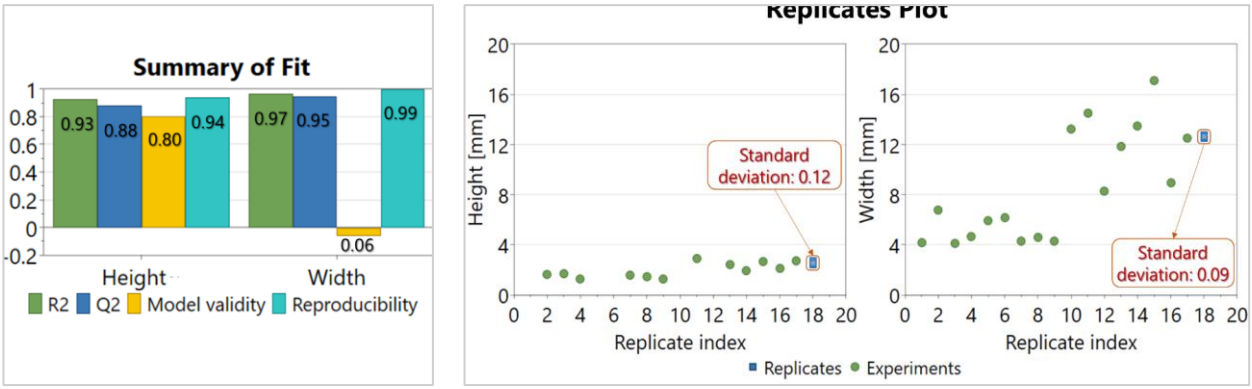

(a) (b)

Figure 3-3: Analysis of empirical (a) summary of fit and (b) replicates plots from SMD trials.

After quantifying empirical outputs, a summary fit plot was generated (Figure 3-3(a)), with distinct plot components i.e., the variance (R2), predictability (Q2), validity, and reproducibility, providing statistical insights about the resulting model. For each component, a value of 1.0 indicates a very good fit between the observed and predicted values. Correspondingly, the difference between R2 and Q2 should be <0.3 for very good models, and was well below this target, with specific values of 0.051 and 0.019 for the height and width respectively. Conversely, the model validity value was anomalously low (0.06) for one of the responses (Figure 3-3(a)), which typically occurs when replicate responses or outputs are almost identical, or if the model sensitivity is high. There were 3 replicate experiments in the schedule, and the plots revealed almost identical values, with nominal deviations between measurements (Figure 3-3(b)). Similarly, the model reproducibility values were very high for both the width (0.999) and height (0.938), implying that the model was dependable.

The aim of the next empirical phase was to validate process parameters and evaluate the build strategy for achieving the specified dimensions or wall thickness (40 mm) of the SS316L PoC part. Initially, predicted responses and related parameters from 2-dimensional (2D) contour and sweet spot plots were used to determine a suitable processing range as shown in Figure 3-4.

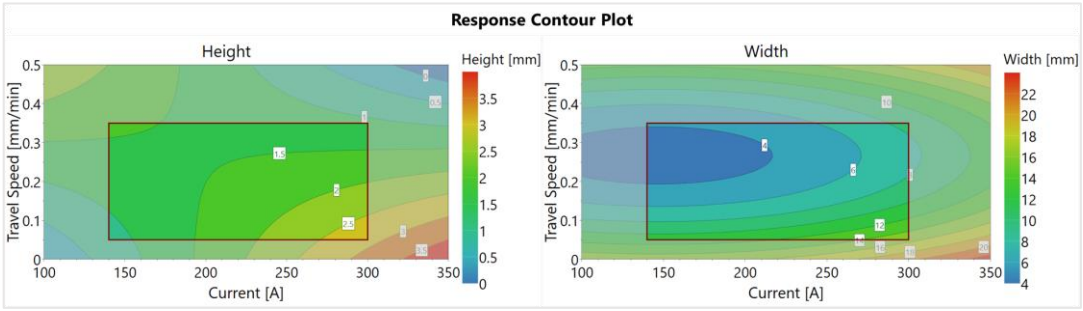

(a)

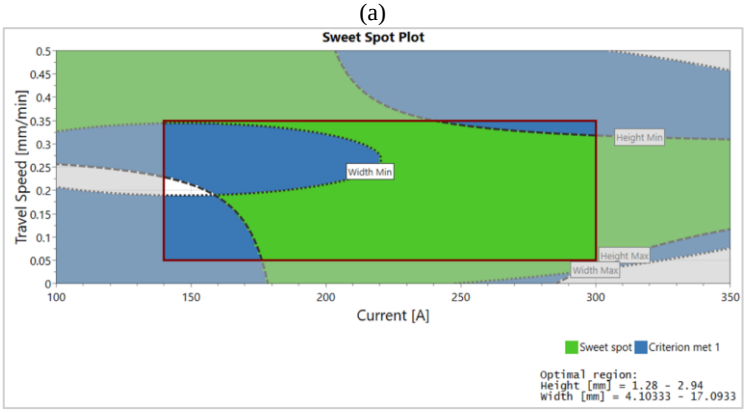

(b)

Figure 3-4: Analysis of (a) contour and (b) sweet spot plots from SMD trials.

For generated plots, the experimental limits, or quantified DED responses, are depicted in the regions bounded by red rectangles (Figure 3-4). The response plots (Figure 3-4(a)) show the relationship between the process parameters and empirical outputs, while the '*sweet spot*' or green areas (Figure 3-4(b)) indicate the optimal processing region. Conversely, blue regions indicate that a single criterion or response (i.e. height or width) has been met, with non-valid regions of the plot depicted in grey. Parameters were selected from the optimal region and iteratively assessed, based on the actual outputs from different trials, as shown in Figure 3-5.

Procedurally, ∅1.2 mm SS316L wire was typically used for depositions, in conjunction with 350 x 350 x 20 mm SS316L substrate plates. Although online programming techniques were efficacious when programming the equipment for initial trials (Figure 3-5(b)), the OLP environment (Figure 3-5(a)) is typically more efficient as build complexity increases. Single beads were deposited (Figure 3-5(b)) before evaluating multiple overlapping horizontal and vertical layer builds (Figure 3-5(c)). Due to observed LoF defects and excessive heat input (Figure 3-5(d)), different parameter combinations were evaluated to improve the build appearance. Correspondingly, statistical models (Figure 3-3) allowed for the extrapolation of pertinent information (Figure 3-4), including the sensitivity of derived empirical responses to process input variations, which resulted in significantly improved outputs (Figure 3-5(e)).

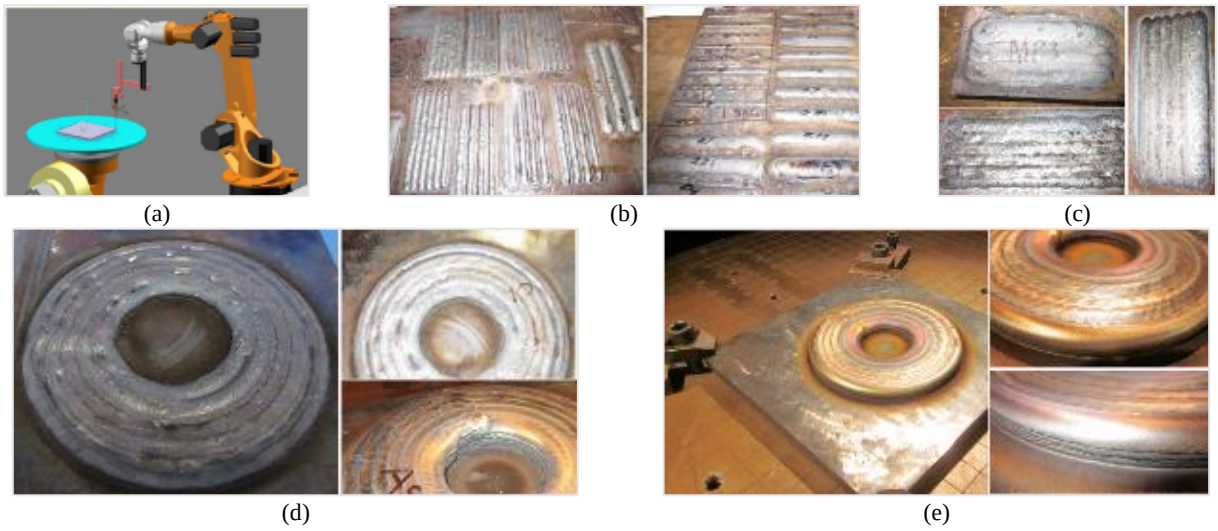

Figure 3-5: Progression from (a) typical set-up and OLP environment to (b) single bead (c) multi-pass/ multi-layer, (d) intermediate and (e) final trial builds, during PoC part development.

Following the successful completion of a representative build (Figure 3-5e)), and with dependable empirical data to support principal research requirements (Figure 2-22), evaluated parameters were selected for the PoC part, as summarised in Table 3-3.

Table 3-3. Parameters selected for producing PoC part using SMD capability.

Fixed parameters	**Values**
Welding current	190 A
Voltage	~13 V (at 4mm arc gap)
Travel speed	2.08 mm s^{-1}
Overlap distance	1.5 mm
Step height	1.25 mm

Similar procedures were implemented for the PoC part, including the use of OLP techniques, which facilitated the pre-build set-up and calibration, with each programme corresponding to the toolpaths for depositing the primary and secondary SMD structures of which the finished part was comprised. The primary structure was deposited vertically, onto a new substrate as represented in Figure 3-5(a), before rotating it horizontally, to facilitate the deposition of the secondary structure. The set-up, calibration and deposition procedures for the secondary structure were influenced by the accuracy of pre-existing SMD surfaces. Although the surface appearance was typical for this DED process, operational observations emphasised the need for more representative and accurate input data. In the development of multi-structure deposition strategies, with successive integral features involving unique structures or parts, the utilisation of representative inputs in OLP environments can significantly enhance efficiency, when resulting toolpaths are translated to actual scenarios. Furthermore, the relocation and clamping requirements when depositing individual structures, and between DED and machining operations, contributed to the total time required to complete this feasibility study. These multiple set-up procedures, both within and between processes, underscored the need for streamlining contiguous tasks and operations, to enhance overall efficiency.

In accordance with stated requirements, the final wall thickness (52mm) included machining allowances, with subsequent material inspection and characterisation requirements fulfilled by the industrial partner. The complete PoC part development summary is depicted in Figure 3-6.

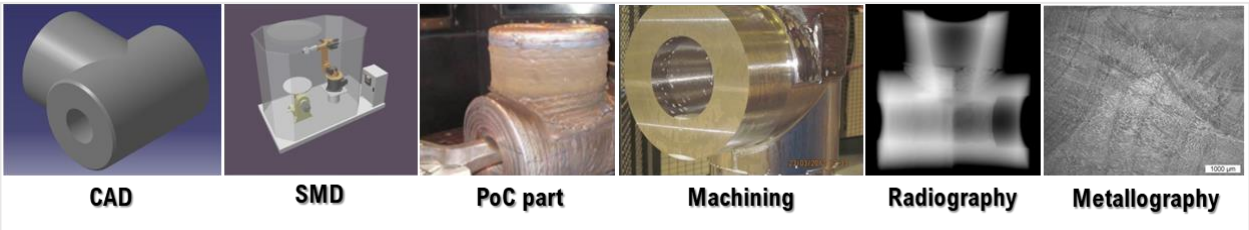

Figure 3-6: Summary of distinct stages in development of PoC part.

Weighing ~40kg, the PoC part deposition rate was 0.7kg/hr, requiring a total build time of about 60 hours, over multiple working shifts. Compared to previous SMD studies, the relatively low deposition rate was primarily influenced by the preferred continuous build strategy. Other factors, such as working patterns and related concerns, further accentuated the need for balancing operational and processing issues, alongside specific system requirements, including enhanced control of process variables, and fully automated/ unmanned capabilities to boost productivity. Correspondingly, discontinuities, defined here as any deliberate operational actions that manifestly interferes with the deposition process before the end goal is reached, are potential defect causal factors. The main sources of discontinuities for this build included the approach for achieving the desired part dimensions (i.e. multiple overlapping passes, both within and between overlapping layers), and the halting of operations to accommodate working patterns, necessitating the implementation of mitigation strategies. In general, observed issues were typically attributed to the process, deposition strategy, equipment, and related operating procedures. While different influencing factors were considered, necessary compromises, such as the scaling of the PoC part relative to the working envelop of the SMD capability, were permitted at the expense of industrial similitude for this application. Nevertheless, the objective of buttressing the informed need for relevantly scaled MAM systems, capable of performing meaningful and appropriately scaled studies, was achieved.

Procedurally, the outlined development steps, including the DoE phase, which was combined with a trial-and-error approach when validating selected parameters for the PoC part, underscored the need for advanced digital technologies to facilitate more efficient use of resources. Dependable process data is also required to support the implementation of these technologies, due to the insufficiency of available information, including historical SMD data initially harvested for this study. Other challenges, involving programming and deposition strategies, emphasised the need for more realistic digital representations and simulations capable of harnessing insights from DoE studies within OLP environments. Correspondingly, the need for greater processing flexibility was observed mainly in relation to restricted tooling, influenced by the build chamber size, and configuration of distinct system elements. Furthermore, set-up requirements for deposition and post-

processing phases emphasised the need for capabilities that support both core and related DED requirements more effectively.

Finally, the issue of control was a recurring theme throughout this study. Although there were subjective influencing factors, such as the preferred deposition and programming approaches, observed shortcomings validate the requirement for fully automated AM capabilities. Whether for typical MAM or SMRM operations, measures for adaptively controlling in-process variables are necessary for enhancing productivity and quality. Furthermore, a prescriptive approach, whereby performance is governed by the application and industry sector requirements, is not presently feasible, as demonstrated for this novel SMD application. In other words, due to uncertainties surrounding the properties and lack of long-term durability data for MAM materials, performance was determined based on the actual SMD outputs.

3.2.2 Study 2: Processing effects and implications

This work was completed as part of a joint material characterisation study, in collaboration with the Massachusetts Institute of Technology (MIT) Industrial Fracture Consortium (IFC). Compared to the previous study, the emphasis was on evaluating the performance of MAM materials to determine, independently of the application, the current safety envelop of these critical process outputs. The IFC's broader objective was to develop models to be implemented into finite element codes of commercial software releases. These interests were favourably aligned with the target industry sector (i.e. aerospace), and one of two potentially accessible alloys (i.e. Ti-6Al-4V) targeted for this study. While the alloy was predetermined by the partners, the proposed build specifications for representative material samples, which were recommended to suit the existing SMD capability, were approved, allowing for the implementation of planned investigations.

Preliminary trials were carried out using the SMD cell and equipment (Figure 3-2), with the objective of identifying parameters with which to produce sufficient material samples to aid performance evaluations. Considering existing capacity constraints, the geometric requirements for this study were less onerous, as the build specification was tailored to ensure sufficient SMD material samples were obtained for designated purposes. A MODDE enabled DoE approach was also implemented, and interactions between key process variables, including the material feed rate, and the current, voltage, and tool travel speed, were explored. The empirical factors and levels investigated are provided in Table 3-4.

Table 3-4: Experimental factors for preliminary Ti-6Al-4V SMD trials.

Factors	**Units**	**Levels**	
		Low	**High**
Current	Amps	109	115
Travel speed	m/s	0.005	0.025
Wire feed rate	m/s	11.67	31.67

Based on established SMD procedures and historical precedents for this alloy, other parameters, such as the Ti-6Al-4V wire diameter of ∅1.2, and arc gap of 4mm, were pre-set before trials. Compared to the previous

study, there was sufficient historical SMD data [181,325], which was appropriately exploited to enrich the data pool. The summary plots, generated from the amalgamated Ti-6Al-4V SMD data, is shown in Figure 3-7.

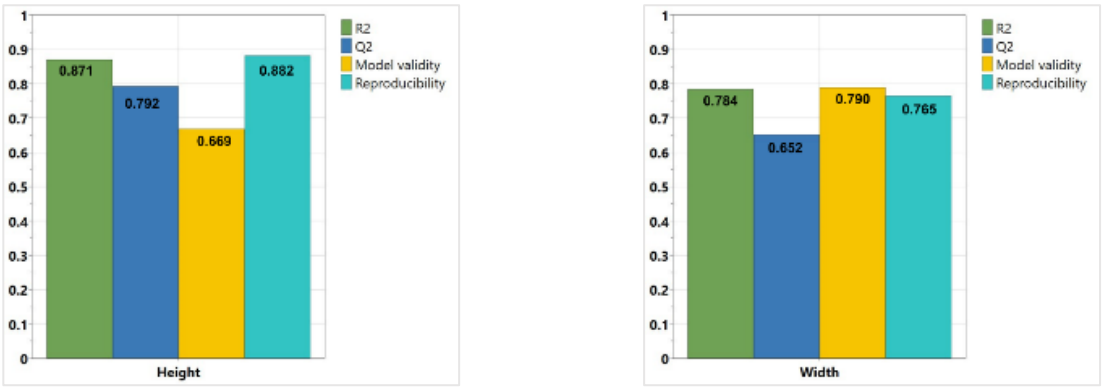

(a) (b)

Figure 3-7: Summary plots of measured (a) height and (b) width from SMD trials.

Analysis of the resulting summary plots revealed that the fit between observed and predicted values, for both height and width responses, were acceptable. Specific Q2 and R2 values indicated nominal variability, in relation to the build height and width, with an average difference of ~0.2 between these responses. Similarly, the difference between R2 and Q2 for this statistical model was well within the target range, and thus acceptable for subsequent trials. The contour and sweet spot plots, showing the relationship between experimental factors and the output responses from the amalgamated data set, are shown in Figure 3-8.

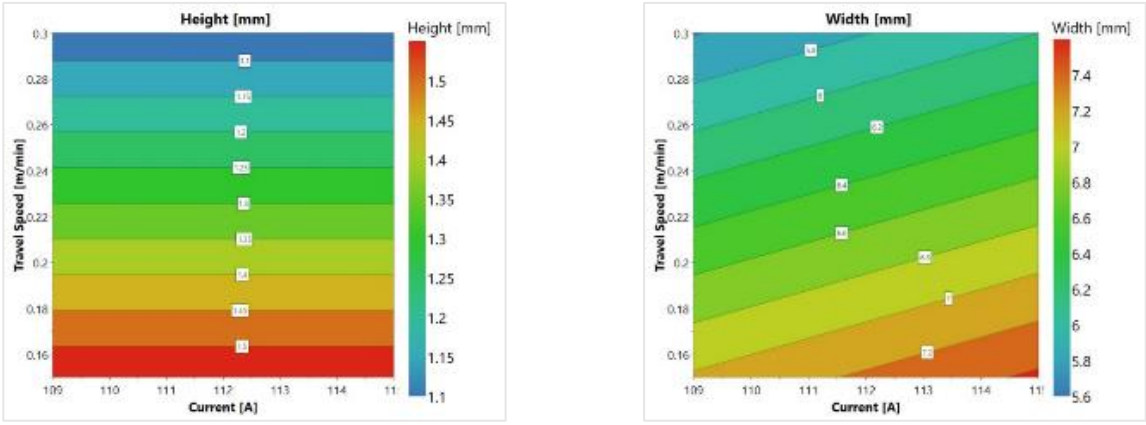

(a) (b)

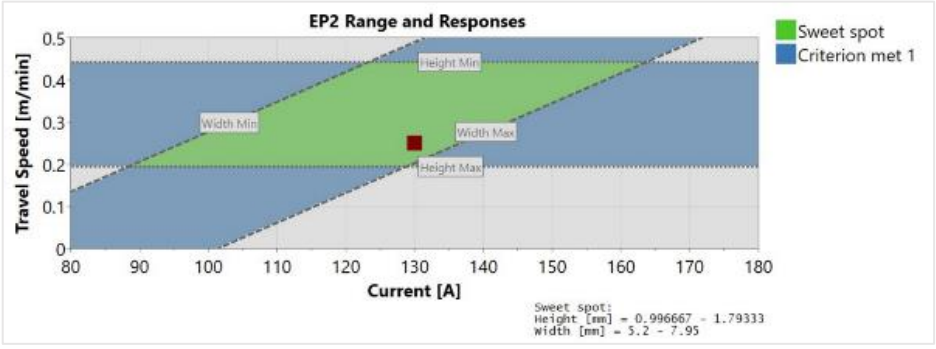

(c)

Figure 3-8: Contour plots of (a) height (b) width and (c) sweet spot for DED of Ti-6Al-4V.

The 2D contour plots display predicted values for the height (Figure 3-8 (a)) and width (Figure 3-8 (b)) based on a specific travel speed, current and wire feed rate. In general, there were noticeable differences in the plotted responses for Ti-6Al-4V, when compared to the previous SS316L study (Figure 3-4). For a given parameter set, the build height was more sensitive to changes in the travel speed, while the build width was more susceptible to the input current. These models were useful for predicting the ideal geometric characteristics of single beads and were used to identify suitable parameters for the final build. This build was based on the material sampling requirements, with a specified wall thickness of approximately 15mm. As with the previous preliminary study, it was determined that these trials could potentially accelerate the development of an accessible and relevant Ti-64 case study. The development progression for this study is depicted in Figure 3-9.

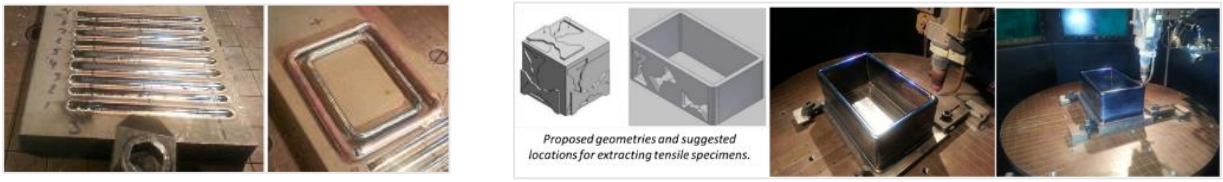

(a) (b)

Figure 3-9: (a) Evaluation of parameters for depositing (b) material samples for characterisation studies.

Various single beads were evaluated, followed by the test build of 2 distinct geometries (Figure 3-9(a)), which were deposited at a fixed wire-feed rate (18.33 mm/s), current (110 A), and travel speed (2.5 mm/s), before selecting parameters for the final build, measuring 296 mm × 182 mm × 120 mm, with an average wall thickness of 15 mm (Figure 3-9(b)). The structure, which was completed in ~15 hours, was achieved by depositing ∅1.2 mm grade 5 Ti-64 wire in 1 mm vertical increments, onto a 20 mm thick titanium substrate plate, at a fixed welding current of 170 A, travel speed of 5 mm/s, and average wire feed rate of 28.33 mm/s.

Compared to the trial phase, the final structures prepared for material performance evaluations were completed in an inert argon atmosphere, with O2 levels typically in the range of ~20 ppm or less. The plan for extracting individual specimens from the deposited structure (Figure 3-9(b)) was implemented as depicted in Figure 3-10.

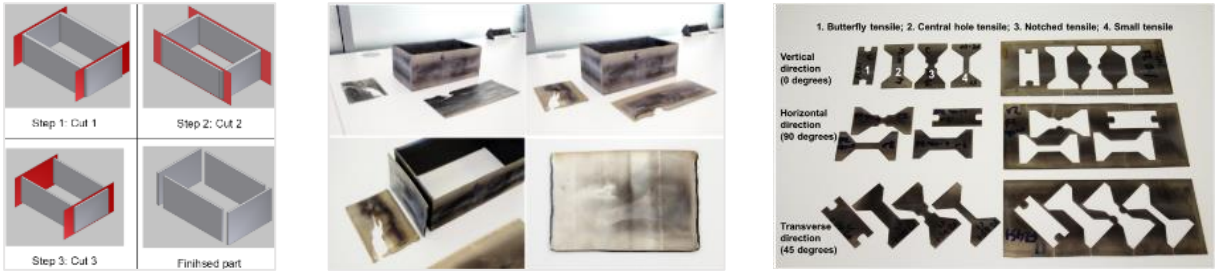

(a) (b) (c)

Figure 3-10: (a) Schematic for (b) material sampling and extraction of (c) tensile specimens.

Four different types of flat tensile specimens (Figure 3-10(c)) measuring 1.5 mm thick, were obtained from different locations (Figure 3-10(b)) of the build using wire EDM techniques. The material sampling protocol (Figure 3-10 (a)) was interpreted from stated requirements and facilitated the extraction of 72 different tensile

coupons for evaluating randomness in the fracture response of the SMD Ti-64 material. This external program involved material characterisation studies and was independently completed by academic partners.

In comparison to the previous SS316L study, the developmental speed was significantly facilitated by the availability of Ti-64 SMD data. However, when comparing the statistical models, there were noticeable differences in the plots generated due to more variability within responses evaluated for the Ti-64 builds, relative to the SS316L process data. In addition, the SS316L plots revealed a non-linear relationship between evaluated responses, when compared to Ti-64 plots, which predicted linear correlations between the inputs and outputs. Both models were contextually valid, but the data suggests that the reproducibility of the SS316L model was higher, thus predicted values were likely to be more accurate than the values obtained from the Ti-64 model. While the boundaries for processing investigated alloys were now defined, the safe limits for implementing these models were dependent on the specific requirements governing unique MAM applications, including the SMRM case study eventually selected for system validation purposes.

In terms of procedures, the relative simplicity of the Ti-64 geometry facilitated a more controlled implementation process, which was also enabled by previous SMD experience. However, the main observation was related to the material removal procedures, which provided further insights into post-processing considerations for DED materials, particularly in the as-deposited condition. Specifically, individual tensile specimens appeared flat (Figure 3-10(c)), but distortions were evident in the 1.5mm sheets (Figure 3-10(b)) from which material sections were extracted.

3.2.3 Study 3: System application and related procedures

MAM procedures are initiated in response to requirements and accomplished via configured inputs that control the functions or behaviours of the system, to produce the desired outputs. Hence, the purpose of this study was to understand the extent to which SMD procedures contributed to observations before, during, and after the process. Focusing on the material inputs, the feedstock for MAM processes were prioritised, and different types of available SS316L feedstock were evaluated.

A series of experiments were planned, to facilitate the characterisation of the different feedstock types, as enablers for large-scale MAM and SMRM operations. For this study, the parameters provided in Table 3-3 were re-used when evaluating input procedures involving SS316L feedstock materials. In opening experiments, the strip and wire input material forms were selected. Different sizes of these continuous feedstock types were securely fixed onto a substrate plate, as shown in Figure 3-11. For this phase, the trial set-up (Figure 3-11(a)) governed SMD procedures, which were analogous to PBF layering techniques, whereby the feedstock is positioned or spread across the build platform before applying heat, to melt and fuse distinct sections of each layer. The processing tool was utilised solely for melting the situated feedstock, resulting in the outputs presented in Figure 3-11(b), which also show the different material sections and conditions before and after melting. In the pre-tensioned state, material sections were manually straightened

and then tack welded onto the substrate, as specified, while the original/ preformed shapes were preserved when securing the remaining material sections.

(a) (b) (c)

Figure 3-11: Effects of feedstock (a) input variables and (b) deposition procedures on (c) process outputs.

Pre-tensioned wire sections snapped as soon as heat was applied, resulting in the displacements of wire segments. These effects were more pronounced for thinner wire sections, as evidenced by the misaligned section of un-melted wire identified in Figure 3-11(b). For the remaining wire sections, displaced segments remained in the vicinity of the pre-programmed toolpath and thus were subsumed within the build. Conversely, non-tensioned wire sections all melted without incident. Between wire sizes, differences were observed in relation to the droplet characteristics, depicted in build zones 1, 2, and 3 of Figure 3-11(c). As the wire diameter increased, so did the consistency of the droplets in the identified build zones. The breaking of pre-tensioned wire sections appeared to have the most significant influence on the formation of droplets (Figure 3-11(b)) as there were no discernible droplets observed in non-tensioned wire sections. Also, when comparing the outputs between continuous feedstock forms, there were no droplets observed in any of the outputs derived from strip material sections. Although both strip sections remained firmly secured to the substrate throughout, the edges of the pre-tensioned strip section, in the vicinity of the melt zone, was relatively smoother than the non-tensioned section, which was quite uneven. When comparing the resulting profiles, the pre-tensioned wire and strip sections were fairly straight and parallel along the edges of the build, while non-tensioned wire sections maintained a similar curved but precise profile, relative to the original outline of the preformed input.

Isolating the feeding mechanism demonstrated the significance of the feedstock inputs and related procedures on process stability, with droplets, which were indiscernible in strip sections, becoming more consistent with increasing wire diameter. The procedures also proved significant for analysing SMD process variations. Often measured in relation to the voltage outputs, the distance between the electrode and the workpiece or the arc gap, were typically attributed to changes across the surface of deposited layers. However, establishing similar input conditions, whereby a fixed arc gap was maintained relative to the secured feedstock sections enhanced understanding of causal factors. During the melting process, the snapping of pre-tensioned wire sections resulted in oscillations. Due to the proximity of the oscillating wire to the electrode, fluctuations were observed in the output voltage. Similarly, there were changes in the output voltage during the melting of the non-tensioned strip sections, which undulated throughout the process, resulting in rough edges. These observations

were pertinent when considering process control requirements, revealing that voltage sensitivity, as a measure of process stability, is influenced by the arc gap, evenness of deposition surface, relative rigidity of feedstock, and the electrode proximity to any tangible inputs during builds.

The next set of experiments involved using the SMD cell for comparative analysis of continuous and discontinuous feedstock forms. Originally configured for WAAM, wire was selected as the continuous feedstock, while powder was used as the discontinuous input form, to evaluate the effects of typical SMD procedures, due to these feedstock forms. The SMD capability was reconfigured for powder deposition by repurposing certain elements of the wire feeding mechanism, before establishing supplementary procedures. These procedures, mainly related to powder handling and operational safety, were maintained until comparative experiments were completed for both powder and wire feedstock. From a systems perspective, this exploratory approach allowed for enhanced understanding of factors influencing configuration decisions for different feedstock forms. At the application level, understanding the implications of such configuration decisions, was of significant interest. At any rate, utilising the SMD capability facilitated more direct comparisons between the two most common feedstock forms currently used in MAM. The differences between the original and reconfigured SMD capability are highlighted in Figure 3-12.

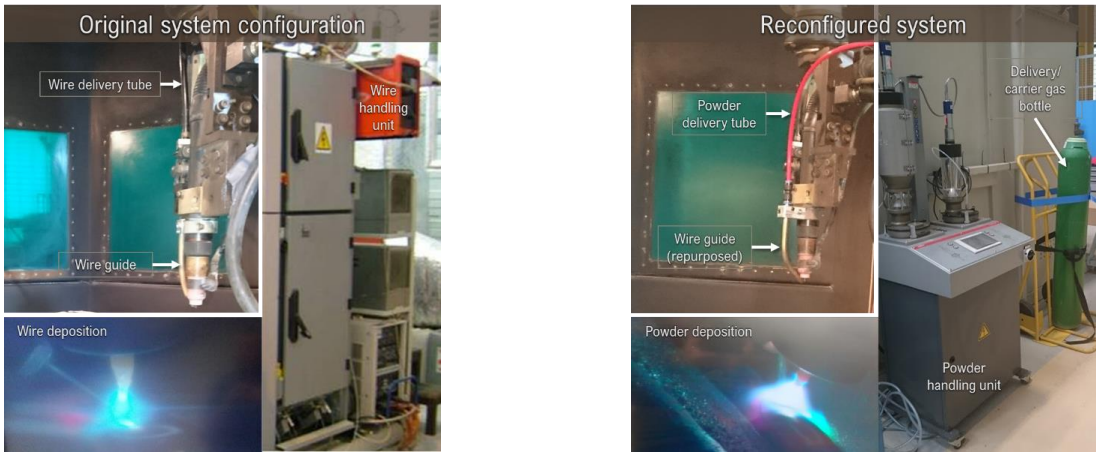

(a) (b)

Figure 3-12: SMD (a) configured for wire deposition and (b) reconfigured for powder deposition.

Minor modifications to the SMD capability were necessary, involving the integration of a portable Metco Twin 150 powder handling unit (Figure 3-12(b)). The powder delivery conduit was connected to this unit and fed through the wire guide via a pre-existing orifice in the SMD chamber. As trials involved SS316L alloy only, the same wire guide was repurposed for delivering powder feedstock to the fusion zone. After a quick functionality test, and with the delivery conduit in position, the orifice was properly sealed off to restore the chamber integrity, thus ensuring an inert atmosphere for depositions.

Statistical models (Figure 3-3) generated in the previous 316L study facilitated the evaluation of parameters for both powder and wire feedstock depositions. However, unlike the previous phase, which involved the

continuous solid 316L feedstock, and constrained to single layer deposits, multi-layer builds were envisioned for this phase. Correspondingly, parameters were evaluated for completing anticipated powder builds. Except for the specific variables governing distinct feedstock forms, all variables and procedures were established relative to the more demanding requirements for powder deposition, and subsequently maintained during the wire deposition process. The parameters used for this trial phase are presented in Table 3-5.

Table 3-5: Parameters for SMD SS316L powder and wire deposition trials.

Variables	**Powder**	**Wire**
Delivery mechanism	Blown (argon)	Mechanical feeding
Size	45-106 µm	Ø1.2 mm
Arc gap	3.5 mm	3.5 mm
Step height (Z+)	1.3	1.3
Material feed rate	190 g/hr	11.67 mm/s
Current	180 A	180 A
Travel speed	2.08 mm/s	2.08 mm/s

While the material feed rate and characteristics (i.e. continuous and discontinuous) were specific to the different types of feedstock, fixing related process and system variables, including the processing atmosphere within the SMD chamber, ensured that similar processing conditions were maintained. Although itemised variables for both feedstock types were identical, unique characteristics, such as the size, are reflected in the base units of measure.

Powder builds were completed as planned, before restoring the system to its original configuration and proceeding with wire depositions. The process involved depositing single, multi-pass and multi-layer material samples, as shown in Figure 3-13.

(a) (b)

Figure 3-13: SMD (a) powder and (b) wire builds in as-deposited condition.

Post-deposition, all builds were visually inspected, with wire deposits generally thinner and more precise, when compared to powder deposits. Furthermore, there were no perceptible surface imperfections in wire deposits, but dispersed particles were observed in the powder builds. Due to the manner of dispersion, combined with the lack of similar features in wire builds, the particles were attributed to powder granules

impinging affected surfaces. Cross-sections from each of the builds were macroscopically examined, with the resulting images from individual section shown in Figure 3-14.

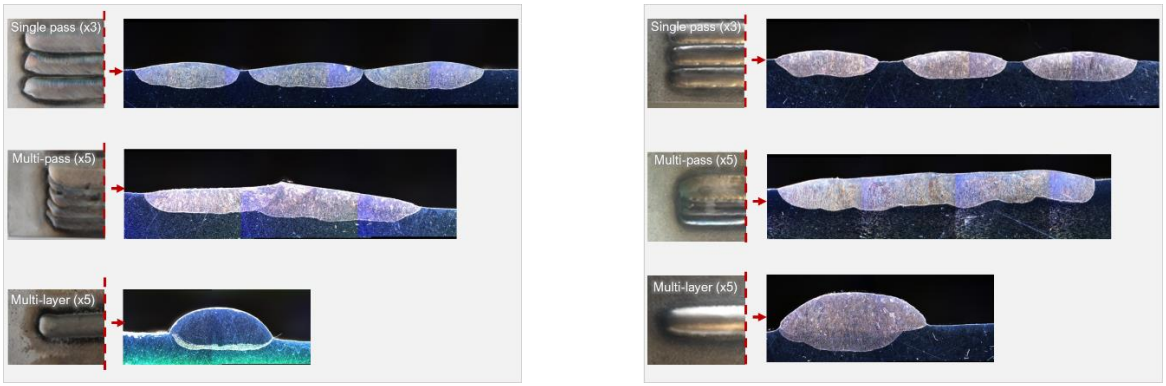

(a) (b)

Figure 3-14: Cross-sectioned (a) powder and (b) wire SMD materials.

Although builds were similarly spaced, when programming the toolpaths for deposition, powder builds (Figure 3-14(a)) were noticeably wider, particularly when compared to individual wire builds (Figure 3-14(b)). On the surface, the profiles of powder and wire deposits appeared similar, with satisfactory inter-pass and interlayer fusion observed in both samples. However, examination of the subsurface profiles showed that the powder deposits were more precise and relatively well-rounded, when compared to the wire builds. Other observable differences between the feedstock forms are highlighted in Figure 3-15.

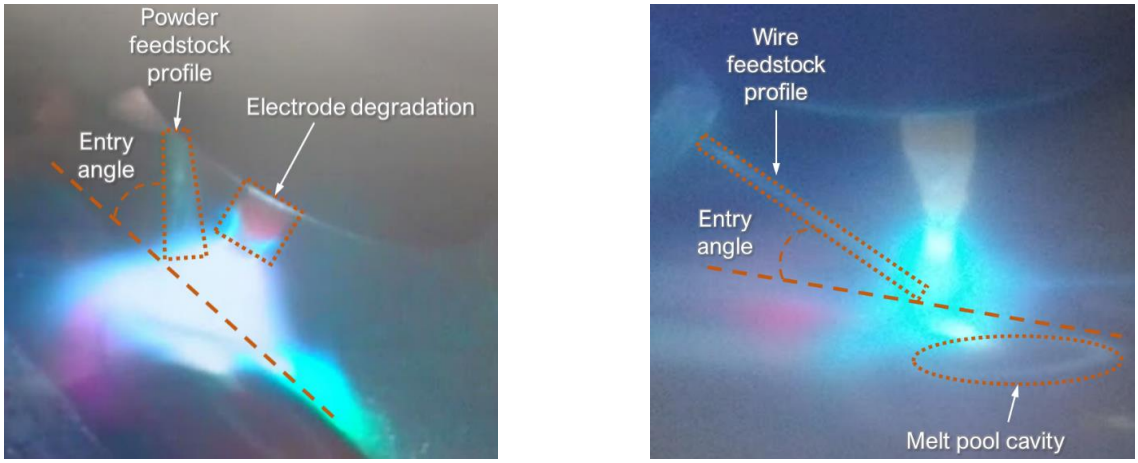

(a) (b)

Figure 3-15: Observable differences during the deposition of (a) powder and (b) wire feedstock.

When compared to the powder feedstock delivery angle (Figure 3-15(b)), the wire guide position was fixed, with the wire introduced at a shallower entry angle (Figure 3-15(b)), relative to the deposition surface, and melt pool, featuring a discernible cavity. This observation offers a likely explanation for the relatively rough subsurface profiles for the wire cross-sections (Figure 3-14(b)). Furthermore, the wire maintains a regular profile, which is consistent with the characteristics of this feedstock form, but the powder feedstock is dispersed as it exits the wire guide orifice. Noticeably, the dispersion of powder, observed on the surfaces of

the deposited material samples (Figure 3-14(a)), appeared to be the main causal factor in the contamination and degradation of the electrode. Powder dispersion also appears to have altered the arc characteristics, suggesting more tenuous links between the arc gap and voltage measurements. In contrast, the electrode for wire deposition showed only minor indications of degradation from the vapourised metal, hence the arc characteristics remained relatively unchanged. Distinctive blue and red colours were also observed in relation to both powder and wire depositions, which allows for the potential application of appropriate spectroscopic analysis techniques during the MAM process.

Compared to the previous phase, where the feeding mechanism was isolated, to determine the implication of this variable, reconfiguring the SMD cell to accommodate multiple feedstock forms emphasised the effects of related procedures on system behaviours and outputs. The SMD system was originally configured and optimised for wire deposition, and within the limited scope of this study, the focus was on evaluating the delivery of multiple feedstock forms, using the existing capability. The implemented procedures revealed that the feedstock form and entry angle influence the melt pool and resulting subsurface characteristics of deposits. For the powder feedstock, the dispersed material predominantly contributed to the rapid degradation of the electrode, thus amplifying the significance of feedstock proximity and input entry angle on process durability. For longer running operations, as anticipated for large-scale MAM applications, durability is an important variable, analogous to machining operations, whereby tool wear rates affect both cutting quality and efficiency, translating to higher manufacturing costs. As MAM technologies evolve, profitability will become increasingly important for competitiveness, thus necessitating further evaluation of cost factors, including deposition conditions and tool wear rates, as a measure of processing efficiency and material or part quality. Irrespective of the delivery mechanism, feedstock dispersal, which has other cost implications, proves the relative superiority of conversion rates presently achievable when using continuous input material forms.

This investigation demonstrated the possibility to utilise the arc, a heat source typically associated with the wire or other continuous feedstock forms, to deposit a discontinuous or granular material. However, considering the different types of continuous feedstock evaluated, it is worth stating that the decision to limit the exploratory scope was significantly influenced by the relative ease of incorporating the powder feeding unit into the existing SMD configuration. The powder feedstock was readily interchangeable and more easily accommodated within the original wire set-up. Correspondingly, switching from a discontinuous to a continuous feedstock form, or between continuous feedstock types, proved more challenging, due to the requirements for integrating the necessary hardware components to accommodate a different input form. Nevertheless, evaluating configuration requirements and perspectives elucidated how multiple feedstock forms may be incorporated within a single DED platform, to exploit distinct operational and processing advantages for different large-scale MAM and SMRM applications.

3.3 Main observations

Prior to implementing the main research activities, previously outlined requirements and priorities were re-evaluated, to accommodate insights from preliminary studies. Academic interests were influenced by current aerospace industry trends, particularly the performance of MAM materials, while the industrial focus was on forging a more rapid path for producing civil nuclear components, via the deployment of AMTs, such as AM. Notwithstanding the distinct processing requirements, and focus on different alloys, fracture toughness was identified as a common issue between studies. Specifically, measurements obtained from the PoC part revealed a large scatter in impact energies, which was a top priority for the industry partner [63], while the large spread of intra- and inter Ti-64 material properties shaped academic perspectives, when developing computational models to explain the fracture performance of MAM materials [64].

Fundamentally, fracture is the mechanical or forced separation of a solid, owing to the application of stress [326], while fracture toughness is a measure of resilience, which is determined in relation to the amount of energy a material can absorb before fracture occurs [326,327]. Compared to brittle materials, where the intrinsic energy, though nominal, is sufficient for fracture, considerably more energy is usually required when dealing with fracture occurring in structural alloys [326]. In other words, brittle fracture occurs without appreciable energy absorption or plastic deformation, whereas ductile fracture typically occurs after large plastic deformations in materials [328]. Ductility is desirable for durable performance, but can be affected by metal forming operations, due to residual or retained energy, which can compromise material toughness [329]. For the PoC part, which was characterised in the as-deposited condition, variations in measured impact energies were attributed to and underscore the significance of the material use-condition or state on mechanical behaviour, while reinforcing the benefits of post-MAM heat treatments [43,94,182]. Ultimately, strength and toughness are equally important when producing or maintaining structural alloys for use in the targeted industry sectors.

In mechanics of materials, mechanical behaviour is defined in terms of the different stress states which materials undergo and, as such, the general concept of stress must first be considered, when investigating mechanical properties, including fracture toughness [328,330]. Conversely, strain is defined as the deformation of a material due to the application of stress, thus large plastic deformations result in irreversible plastic strain or permanent distortion [328,330]. Whether evident, as observed in the Ti-6Al-4V SMD specimens (Figure 3-10) or otherwise, evaluating the relationship between the material stress state and the resulting strain was an important objective, due to the potential implications for the resilience and durability of MAM materials. This focus is consistent with previously defined priorities (Figure 2-22), particularly for large-scale MAM operations, where longer build durations are anticipated, or in SMRM, where localised operations can affect the integrity of the entire part.

Although specific processing requirements were influenced by the alloys under investigation, where feasible, similar empirical approaches were maintained, except during powder deposition trials, which necessitated the modification of the SMD system and related procedures. When compared to the PoC part, which proved challenging due to previously highlighted factors, including geometric complexity and sizing requirements, the implementation process was relatively easier for the Ti-6Al-4V builds. These challenges underscored the need for more flexible and suitably sized MAM capabilities, to ensure similitude at both system and application levels. Preliminary studies, in conjunction with literature surveys, proved particularly useful for clarifying system configuration and related implementation factors, including the strategy for substantiating system outputs. Accordingly, principal research requirements and priorities were implemented in three parts, encompassing system development activities, outlined in *Chapter 4*, system validation approaches, presented in *Chapter 5*, and *Chapter 6*, which covers the strategy for verifying the system outputs.

3.4 Summary

The purpose of this chapter was to describe preliminary studies that were implemented to elucidate cross-cutting issues in MAM operations, whilst exploring a route to impact, neither specific to a particular industry sector nor alloy, but instead focused on commonalities within the purview of a robust manufacturing system. Initial outputs were invaluable for broadly articulating specific shortcomings at the system-level, identifying critical performance related issues at the process-level, and increasing understanding of important technical and procedural factors at the application-level. These insights were also useful for directly verifying the requirements on which the specifications for a representative MAM system were based.

In the following chapter, activities undertaken during the development of a large-scale OA MAM system are described.

CHAPTER 4

4 Development of an OA MAM System

4.1 Introduction

This chapter introduces one of three foundational parts of this study and focuses on the development of an OA system for MAM. The primary aims were achieved using different approaches, which were initiated as part of the development process, involving the definition of requirements, concept development, evaluation of enabling technologies, and commissioning of the embodied solution. Potential system applications are also explored in this chapter, alongside considerations for maintenance, inspection, verification testing, and continuous improvement (MITC) aspects, which are integral to this development.

4.2 Requirements analysis

Different perspectives were explored when determining the requirements for the MAM system. The business, technology, and procurement perspectives were encapsulated within the statement of need, which was necessary for initiating procurement activities. While business and technology requirements were primarily shaped by the operation context and potential utility of the system, procurement requirements were influenced by previously highlighted supply chain factors. On the other hand, the material to be investigated (Ti-6Al-4V) was determined by the industrial case study, which was especially selected to demonstrate how scalable systems can potentially expand the scope of possible MAM applications. The requirements also allowed for the exploration of the research hypothesis that *the lack of suitably sized MAM capabilities is a crucial factor limiting the adoption and competitiveness of MAM technologies for critical high-value industrial application.*

4.2.1 Business perspective

The business perspective was evaluated in relation to the core function of the organisation within which this study was completed. The core business function is advanced manufacturing research (AMR), and the goal was to assess verified industry needs and insights from preliminary studies, relative to the AMR context underpinning the MAM system deployment. Furthermore, having prioritised the need for increased capacity, exploiting technological areas of consensus was desirable, for enhancing the utility and commercial prospects of the deployed system. Therefore, common elements that facilitate MAM operations were initially used, to establish and organise basic system requirements supporting current and evolving AMR needs.

Basic system components, which were identified from literature surveys, include the material feedstock, energy source, and mechanical systems which control deposition feeds and speeds, as well as the manipulation of the deposition tool and/or part. These three common MAM system components determined the general

technological requirements, while the selected process (i.e. WAAM) determines the specific processing requirements and operational procedures. Other development decisions and considerations, including the cost, configuration options, safety, and maintenance requirements, are also derived from basic and related MAM system components, and the selected WAAM process.

Irrespective of the specific AMR technologies or capabilities offered, all businesses operate within a supply chain whose outputs can be tailored in response to demand. However, supply conditions and related industrial activities are typically well regulated, such that businesses must consider other factors, beyond specific technological requirements or demand patterns. Hence, requirements were analysed in relation to key factors influencing technology adoption strategies, particularly in AMR settings, as depicted in Figure 4-1.

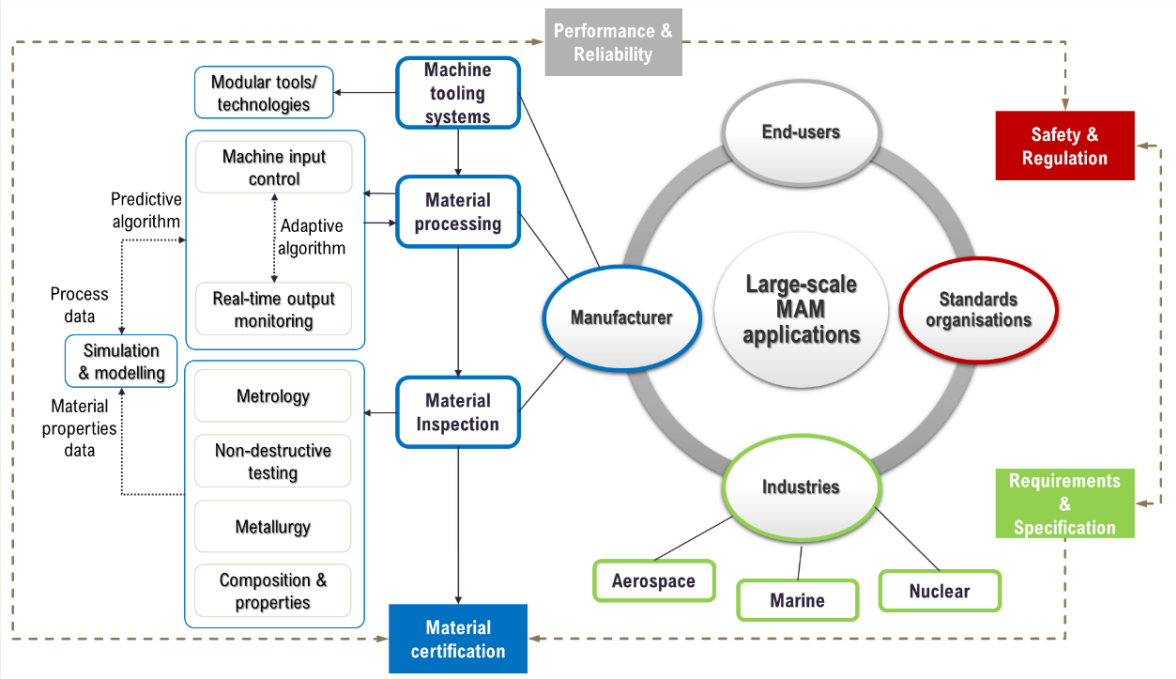

Figure 4-1: Business requirements and considerations.

Basic system requirements were influenced by business factors, embodied by the *Manufacturer*, while the *Industry* and *End-user* or *Customer* functions determine the performance and certification requirements that must be considered for MAM products. Mapping these relationships emphasises the need for adherence to required industry standards and protocols, which regulate the use of MAM facilities, processes, and products. Presently, product applications, manufacturing specifications and related regulatory activities are constrained by limited understanding of material or part quality and performance. Although technological limitations of selected MAM processes contribute to documented issues, the *Manufacturer* is still responsible for demonstrating facility, process, and product adequacy. Adequacy is typically achieved by controlling interrelated manufacturing and process factors, which are ultimately influenced by the basic system components, as well as the highlighted tooling, processing, and inspection requirements that enable MAM operations.

4.2.2 Technology perspective

Considering the significance of the *Manufacturer's* responsibility, the focus of this section was on determining how to manage the business requirements, when preparing the system specification, and initiating procurement activities. The three common MAM elements, otherwise known as the basic system components, allowed for the evaluation and categorisation of different technologies or high-priced artefacts (HPA). In this context, HPA are defined as items deemed to be of significant economic value. For this study, the threshold for each HPA was fixed at £50k. Derived from available MAM hardware acquisition data (Figure 2-7), the amount is equivalent to about 10% of the lower average cost, ranging from ~£0.5 to ~£1M, for this dataset.

The business perspective (Figure 4-1), including end-to-end processing requirements for MAM operations, were also considered, and other technologies for enhancing the system utility and prospects were evaluated. For common and specific system components, it was rationalised that different HPAs will be distinctly incorporated, with each HPA representing a single system unit or module. Thus, these units or modular HPAs were separately investigated, to assess the specific features required to achieve the basic MAM functionality. Information was obtained from typical industry sources, including OEM publications and other relevant documentation, as well as extensive interactions with suppliers. The resulting information, which was used to support development decisions, includes the main system features and functions derived from required technologies or HPAs, which were subsequently organised into distinct categories, as presented in Table 4-1.

In general, requirements were evaluated in relation to identified features, available options, and specific considerations, which were broadly organised into the S*ystem and automation*, *EOAT* and *Related* categories. Automation is a primary enabler for the build or layering process in MAM operations, hence robotic, gantry, and part manipulation requirements were prioritised, before assessing EOAT requirements and options. For metal deposition, and the preferred WAAM process, typical arc technologies for processing the wire feedstock were evaluated, before considering other EOAT for augmenting MAM operations, including 3D inspection capabilities. Technology availability, maturity, limitations, and affordability were also considered, alongside business and industry factors. While the decision to proceed with WAAM helped to focus the process on commercial off the shelf (COTS) solutions or arc technologies capable of being integrated as EOAT, the core business function influenced the evaluation of technologies capable of supporting end-to-end MAM operations.

The plans for this capability, including other EOAT extend beyond the common MAM and WAAM elements outlined in Table 4-1. However, within the available budget and development scope of this study, the required HPA that were procured include hardware components, comprising the articulated and gantry robots, a positioner or part manipulator, the GTAW or metal deposition EOAT, and a 3D scanner. Other requisite features, including essential software components, were also procured to secure basic system functions.

Table 4-1: A non-exhaustive list of MAM system requirements and considerations [331–351].

Requirements	**Features, options, and considerations**		
System & Automation	**Programming and control**	**Decision factors**	
	Numerical	G-Codes can be generated from CAM software but limited solutions for AM applications.	
	Robot	Various programming languages (C++, Pascal, etc.) and can be customised via application programming interfaces (API).	
	Robots (including gantry)		
	Types of industrial robots	**Articulated variants**	**Features and capabilities**
	Articulated (1 twisting & 2 or more rotary joints)	Shelf	Suitable for foundry applications
	Cartesian (3 prismatic joints/ axes)	Pedestal	Payload
	Cylindrical (1 or more rotary & prismatic joints)	Inverted or ceiling	Flexibility/ reach
	Polar (1 twisting & combination of 1 or more rotary and linear joints)		Accuracy
	Selective Compliance Articulated Robot Arm (SCARA) (2 parallel joints)		Cooperating robot or cobot applications (i.e. Cartesian + articulated)
	Delta (Jointed parallelograms connected to base)		Mounting options
	Part manipulation		
	Positioners/ configurations	**Multi-axis variants**	**Features and capabilities**
	Turning rolls	Rotary turntable	Suitable for robot and arc applications
	Bench/ floor	Skyhook	Load capacity
	Multi-axes		Accuracy
	Head/tailstock		Tilt
			Continuous rotation
End of arm tooling (EOAT)/ end-effectors	**Metal deposition EOAT**		
	Arc technologies	**GTAW variants**	**Features and capabilities**
	Plasma	Standard GTAW	Suitable for automation/ mechanised applications
	Metal Inert Gas (MIG)	K-TIG®	Deposition rate
	Metal Active Gas (MAG)	TOPTIG®	Precision/ accuracy
	Gas Tungsten Arc Welding (GTAW)		Stability
			Flexibility
			Compactness
			Hot/ cold wire
			Feature resolution (i.e. bead characteristics)
	Geometric inspection EOAT		
	Imaging technologies	**3D scanning variants**	**Features and capabilities**
	Photogrammetry	Structured light	Suitable for robot applications
	3D scanning	Laser	Large volume calibration, inspection and validation
			On-machine geometric inspection
			Digitised point cloud (reverse engineering)
			Resolution
			Accuracy
			Stability
			Non-contact
Related/ Other	**Technology specialisations**	**Expertise**	**Association**
	OEM	Systems integrator	Pre-existing organisational relationship
	Service / technology provider	Developer	

4.2.3 Procurement perspective

Organisational procurement functions were developed for generic use and were primarily focussed on interpreting the typical needs of the customer. However, due to a combination of factors, including the peculiarities of OA systems, anticipated acquisition challenges, and other complexities associated with capital

undertakings, it was necessary to supplement existing protocols. Procurement requirements were analysed to ensure that the organisational and strategic functions underpinning this study were streamlined.

Factors influencing the different stages of the procurement process were derived from observations and insights acquired from interaction with different suppliers and OEMs. The resulting procurement perspectives and functions are depicted in Figure 4-2.

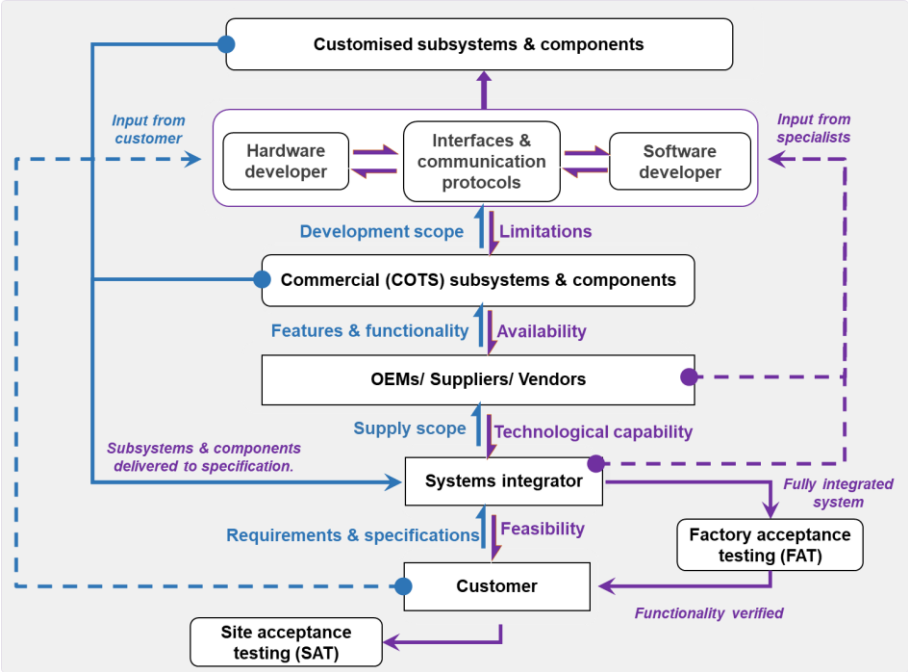

Figure 4-2: Procurement requirements and functions.

Organisational functions were embodied by the *Customer*, while strategic procurement functions, which also overlaps with the *Customer* role, include the *Systems integrator* and *Suppliers* of both COTS and customised technologies. A customer-driven approach was adopted to facilitate the tendering process, which ensured that requirements for defined procurement functions were properly interpreted within the relevant business or strategic context. This decision was influenced by the preferred OA configuration, which was considered appropriate for this development, particularly in relation to the AMR business context. Conversely, relying on specialist input helped to manage organisational expectation, when considering the feasibility of integrating specific solutions, based on the current availability, benefits and limitations of required technologies. For COTS solutions, this involved verifying that within the supply scope, the required features and functions were readily available. Otherwise, feasibility was determined in relation to the system development scope, which was tailored according to the requirements for this OA MAM platform, and for AMR purposes. The highlighted types and flow of information between each of the required functions was also critical to the development process. For key functions (Figure 4-2), the emphasis was on clarifying and pushing the system concept and requirements, and directly dealing with specialists, to draw on their experience and expertise, particularly when assessing customised HPAs, and prior to initiating procurement actions.

Factory acceptance tests (FAT) were completed according to external protocols, and at specific product integration levels, while site acceptance test (SAT) protocols were developed based on integrated capabilities. the FAT scope was limited to witnessing basic equipment functions, and identifying issues to be rectified, prior to the onsite installation and commissioning phase. While specific activities are reported in subsequent sections, the distinct product specifications used to develop SAT procedures, facilitated the analysis of related factors, and supported the construction of the GT framework. Interrelated aspects of the procurement process were also considered when defining developmental roles and responsibilities, which were based on defined procurement functions and requirements management strategy. Mainly, this activity involved demonstrating how specific interactions between key functions facilitated the actualisation of the envisioned large-scale OA MAM platform. The defined roles and responsibilities, supporting development tasks (Table 3-1), are presented in Figure 4-3.

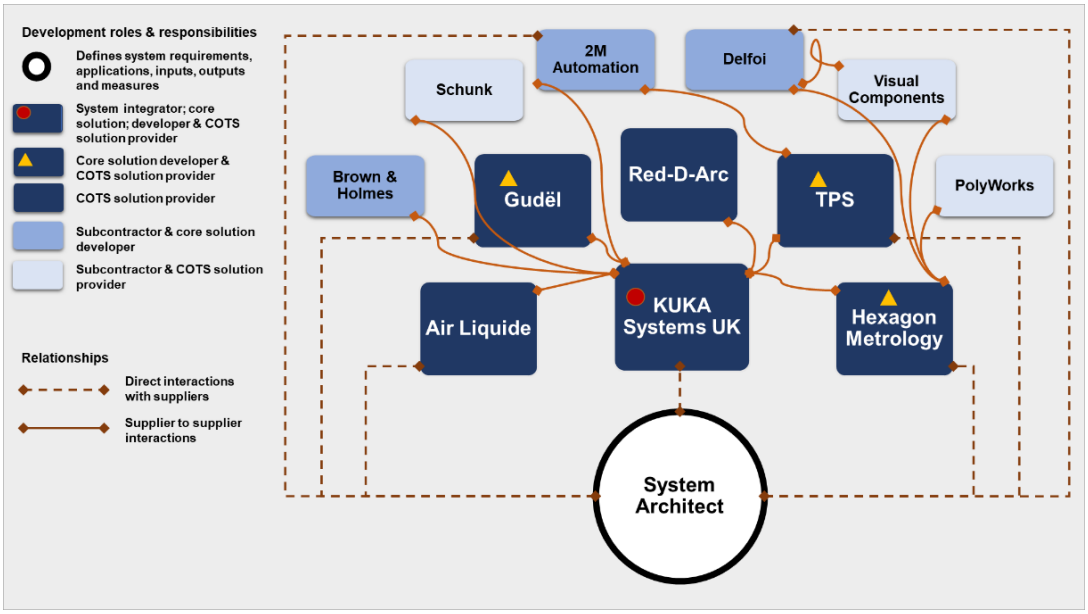

Figure 4-3: Definition of development roles and responsibilities.

The process of identifying potential development partners was facilitated by factors outlined in Table 4-1. A customer driven approach was maintained, with the voice of the customer represented by the system architect or planner. As the system architect for this development, responsibilities included developing the concept, prior to coordinating and directing implementation activities towards the realisation of the envisioned solution, which facilitated the clarification of interactions observed between development partners. For instance, it was evident, from the number of specialists directly and indirectly involved in development activities, that the requirements for the system were beyond the expertise of a sole supplier. Furthermore, only the top-level functions of each partner were typically captured in submitted bids, with gaps in critical elements supporting core or top-level functions underscoring the complexity of the MAM supply chain. In practise, it was typical for the primary supplier of full turnkey solutions to subcontract certain specialisations to other parties, while focusing on their primary areas of expertise. Between contracting parties, secondary suppliers were identified,

but the relationship, scope of involvement, and technical contributions to planned developments, were not often elaborated. Nevertheless, the need for direct communication with developers involved in this undertaking was foreseen. Irrespective of designated roles, maintaining direct links at key procurement phases was useful for clarifying technical requirements and acknowledging specific contributions, thus eliminating superfluous interpretative layers between the architect, developer, and/or supplier functions.

4.3 Concept development

When applying design principles to defined problems, the solution development process or steps are typically outlined, but precise implementation details are not often provided because each problem is different, necessitating a tailored approach. This consideration was most important when implementing the concept development phase, which is the mechanism that allowed for the encapsulation of meaning, via the organisation of the general characteristics associated with the actual problem or circumstances. In this case, the specific circumstance under investigation is the concept of an OA MAM system. Five general attributes were used to capture the basic idea or concept, beginning with the term used to refer to the system; its objective or purpose; the types of activities planned; how planned activities will be performed; and the anticipated system benefits. Broadly based on the analysed requirements, and specific considerations presented in Table 4-1, these attributes, including the overarching OA MAM system concept, are separately explored in the succeeding sections.

4.3.1 Bulk additive manufacturing (BAM)

The initial development goal was to derive a simple and evocative term that encapsulated the designated system function. Hence, the term *bulk additive manufacturing*, also known by the acronym *BAM*, was deemed sufficiently evocative about the prospective system functions, and used to convey meaning to the concept of a large-scale MAM system. While the word *bulk* denotes the anticipated size or scale of the manufacturing operation, *additive*, in this context, is presently synonymous with, and has specific connotations when describing the manufacturing method utilised. For the GT framework, the gaol was to determine how the BAM concept, and factors influencing system development, design, and integration approaches, could facilitate the identification of unifying themes that captured the essence of OA MAM systems.

The overarching BAM concept essentially symbolises an OA system capable of supporting large-scale MAM, and other related value-adding operations, via interchangeable EOAT. Correspondingly, the concept of modularity was used to convey meaning to the requirement for interchangeability, which was applicable to the EOAT approach, as well as other modular elements of the system that could be reconfigured to enhance productivity. The feasibility of the concept of reconfigurability was demonstrated via the integration of a portable powder feeding unit with the SMD system (Figure 3-12), which facilitated the interchangeable deposition of wire and powder feedstock. The main advantages of a reconfigurable OA system, particularly within an AMR setting, include flexibility, which is highly desirable, due to the previously outlined challenges

associated with the production of large structures. Specifically, discrepancies between local supply conditions, global demand patterns, and uncertainties in an evolving landscape, require greater responsiveness at multiple levels, including the system, which is what is being referred to, when discussing flexibility. Thus, modularity, reconfigurability, and flexibility are characteristics of the overarching BAM concept, aimed at facilitating more rapid responses to changing requirements, involving low-volume high-value products, within AMR facilities.

A COTS approach was used to encapsulate the system integration concept, whereby COTS solutions were preferred for the integration of higher-level modular solutions, as opposed to a lower-level strategy, where more fragmented solutions are the norm. However, the acquisition of modular COTS solutions, and other distinct elements of this multi-technology capability, does not solve the problem of how to integrate and configure these components into a fully functional system. Similarly, ownership of such a system does not address the issue of how to deploy it for intended industrial applications. Hence, it was necessary to establish the desired characteristics and other interrelated concepts that were required to achieve the central functions and primary purpose for which the BAM system was created.

4.3.2 Purpose and applications

The system applications or similitude concept was explored by linking the requirements for large-scale MAM capabilities to the potential for its utilisation. Here, it is assumed that MAM applications are undeniably broad, but industrially similar. Thus, the requirement for increased capacity and scalability extends beyond typical use-case scenarios. In developing this approach, it was evident that focusing on specific applications or industry sectors was likely to limit the utility of the system. Therefore, the goal was to conceive a solution that would satisfy requirements for a system whose specific applications were yet to be defined. Correspondingly, the concept for possible BAM applications was broadly informed by the AMR context, and fundamental requirements for improving the manufacturability and maintenance of large components typically fabricated from distinct preforms. These preforms are traditionally associated with casting and forging techniques, which can produce near-net shape (NNS) structures, thus influencing the exploration of commonalities between these processing technologies and their typical applications.

In developing the BAM concept, foundry business activities and applications were investigated to identify concrete commonalities between distinct techniques and typical applications. However, due to fundamental differences in processing mechanisms and operations, the focus was on identifying similarities between the bulk and/or large structures produced by selected foundry businesses [188,189,191,352]. Compatibly, the concept of similitude was developed in relation to representative equivalents, including the tangible and non-tangible characteristics derived from foundry capabilities, as well as the dynamic similarities upon which specific applications depend. In particular, the geometric or physical characteristics of these applications were determined by foundry capabilities, which facilitate the realisation of the dimensional context of products and

their applications. It was rationalised that evident commonalities were appropriate when describing general characteristics attributable to potential BAM applications.

Publicly available information about manufacturing businesses specialising in forging and casting processes were analysed to identify pertinent industrial baseline characteristics. This evaluation, involving different foundry businesses linked to various industries, including the target sectors (Figure 4-1), yielded unstructured multidimensional data, which included pertinent industrial capabilities. Data was collated from over 250 randomly selected foundry businesses, which enabled the identification of 18 discrete variables attributable to foundry products, including preforms, intermediate shapes and finished components. The specific values declared for each variable were aggregated and subsequently organised as presented in Table 4-2.

Table 4-2: Preliminary assessment of common variables associated foundry operations [353–383].

Item	Variable	Forging (open-die)	Forging (closed-die)	Casting	Average (range)	Unit of measure
1	Size control accuracy	3.5	1	-	2.25	millimetres
2	Gas Furnace Volume	-	-	5.265	5.265	Cubic metres
3	Quench Volume	367.5	-	10.315	188.9075	Cubic metres
4	Build height	7.4875	-	4.2	5.84375	meters
5	Width	2.84	2.5	6.5	3.9466667	meters
6	Build Length	11.3875	5	11.5	9.2958333	metres
7	Gas Furnace Diameter	10	-	-	10	metres
8	Gas Furnace Depth	16.9	21	-	18.95	metres
9	Electric Furnace Diameter	2.5	1.6	3.7	2.6	metres
10	Electric Furnace Depth	17.875	13	21.5	17.458333	metres
11	Quench Depth	15.12	-	10.75	12.935	metres
12	Build Mass	94.4	3.00625	92	63.135417	metric tonnes
13	Lifting/ service crane (Load Limit)	79.333333	8.25	70.4	52.661111	metric tonnes
14	Manipulator	122.33333	32	-	77.166667	metric tonnes
15	Press capacity	6946.1538	18593.634	-	12769.894	metric tonnes
16	Gas Furnace Capacity	96	60	78.25	78.083333	metric tonnes
17	Electric Furnace Capacity	20	20	90	43.333333	metric tonnes
18	Heat Treatment Temperature	1050	1000	1300	1116.6667	ºC

The aggregated data was further organised, in relation to both qualitative and quantitative characteristics of unique variables, such as the diameter, before synthesizing information about common application attributes relevant to MAM systems. Specifically, common qualitative elements were combined and then grouped according to base units of measure (Table 4-2), resulting in six different and representative categories. Finally, quantitative aspects were incorporated by averaging discrete publicised value for each category. Thus, the physical characteristics and related attributes for industrially equivalent MAM system applications were defined.

The synthesised attributes and categories are listed in Table 4-3, with supplementary information, used to elucidate the concept of similitude, graphically represented in Figure 4-4.

Table 4-3: Definition of common attributes associated with foundry applications.

Attributes	Description
Accuracy (millimetres)	Typical size control or form accuracy of fabricated components.
Dimensions (millimetres or meters)	Basic geometric data, including linear and size.
Mass (metric tonnes)	Mass of typical components fabricated.
Temperature (degree Celsius)	Includes aggregated data on forging, casting and heat treatment temperatures.
Volume (cubic meters)	Data about volumetric capacity, including furnaces.
Working load (metric tonnes)	Includes aggregated data on component manipulation and lifting capacity.

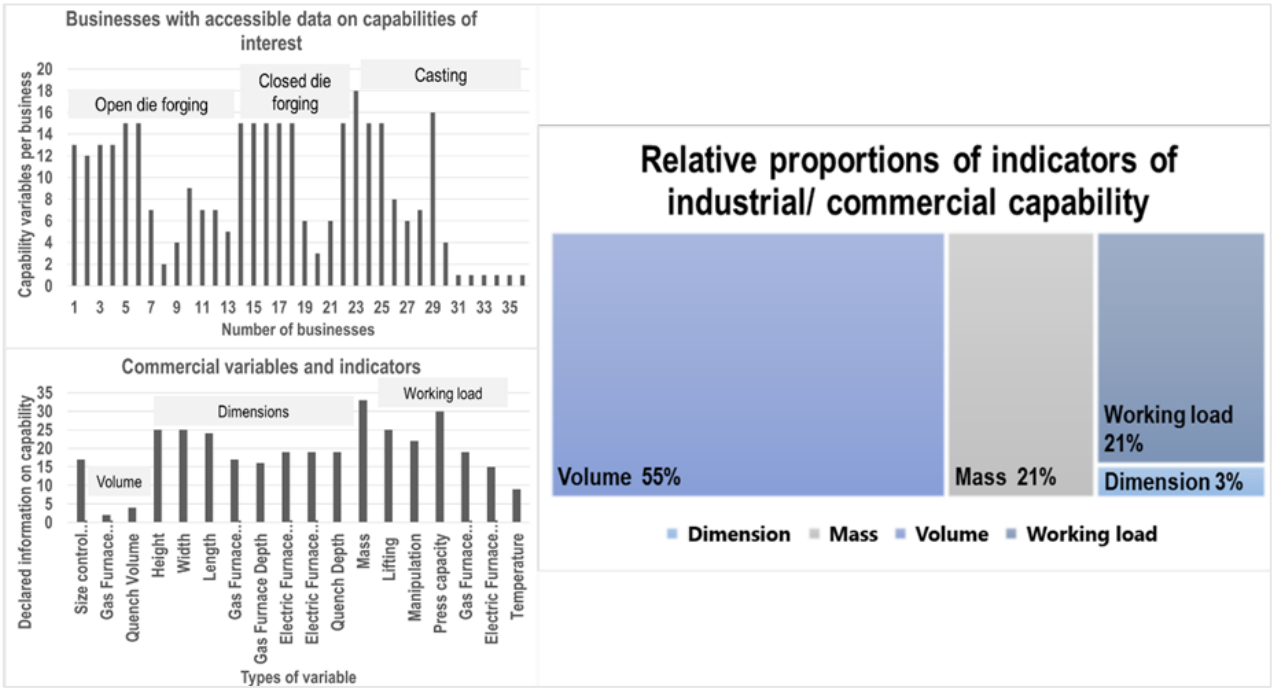

Figure 4-4: Representative characteristics underpinning industrial foundry applications.

While collated data provided a means for quantifying some of the required characteristics for industrial MAM systems (Table 4-3), the resulting chart (Figure 4-4) illustrates the relationship between industrial forging and casting capabilities and characteristics. It revealed the hierarchical prominence of the volumetric capacity or product scale, which buttresses its significance as a key commercial and technical enabler for industrial applications. The relative positioning of other geometric characteristics, typically determined by specific application and design requirements, also underscored the commercial significance of these variables for foundry businesses. It was rationalised that advertising practices, particularly decisions about the types of information businesses publicised, likely influenced profitability, due to the potential to invite enquiries and attract potential customers. The product mass, for instance, was the second most significant piece of easily accessible information, particularly for forging operations, and was typically publicised alongside the available press capacity. The working load was also identified as a key commercial attribute in casting and forging applications, closely linked to the component mass and similarly valued, relative to the publicised

commercial hierarchy and application significance. Another important variable, aggregated within the averaged value of the working load (Figure 4-4), was the lifting capacity. In practise, industrial requirements may exceed this capacity, due to limited infrastructure for lifting/ handling, and is regulated accordingly. Likewise, large-scale MAM operations will be restricted by available infrastructure for lifting and handling. In conjunction with observations from preliminary studies, these considerations influenced the EOAT concept. Further to managing in-process handling and manipulation requirements, relative to a stationary build platform or product, different tools may be integrated as necessary, for completing contiguous pre- and post-processing tasks and operations within the BAM cell.

Due to variations in advertising practices and related consistency issues, it was challenging to obtain complete foundry product data. Hence, accessible information was screened to enhance the homogeneity, comprehensiveness, and overall quality of retained data. Following this approach, only a few businesses surveyed (~13%) publicised sufficient information to meet the inclusion criteria. Specifically, the bar chart, displayed in the top left corner of Figure 4-4, shows the number of businesses and unique capability variables evaluated, while distinct characteristics, shown in the bottom left corner, are organised according to the categories presented in Table 4-3. Between manufacturing techniques, it was observed that most businesses publicised information concerning the mass, dimensions and working load. In contrast, it was more challenging to obtain volumetric data, without directly engaging businesses, which was beyond the study scope. Nevertheless, the impact of direct engagement on reporting habits were also considered, alongside the possibility to improve specific data. Ultimately, documenting actual observations yielded useful insights about current advertising practices, as well as preliminary data for establishing a realistic baseline for BAM applications. Overall, more comprehensive capacity data was obtained from forging businesses, in comparison to manufacturers of castings, with the latter attributed to the need for specific design input from customers.

When analysing common manufacturing characteristics (Table 4-3), the *size control accuracy* (i.e. ± 2 mm), *temperature* (i.e.1117 ºC) and *press capacity* (at 11023 mt) were excluded, due to significant asymmetry in the stated values and/ or base units of measure, relative to other class variables. Distinctive attributes, such as the *press capacity* for forging, were not directly relevant to the BAM applications concept, while *temperature*, though essential, is dependent on the processing requirements for specific alloys. Thus, such attributes were not scrutinised. However, *size control accuracy* is both desirable and pertinent to MAM product quality and remains a crucial advantage in the selection of foundry techniques for producing large structures. Consequently, the NNS concept was explored as an important feature of MAM applications, and typical foundry products were sampled, to establish the possible scope for related BAM applications. Product characteristics that influenced the envisioned applications concept, relative to the requirements for MAM, were drawn from different sources, including the product examples shown in Figure 4-5.

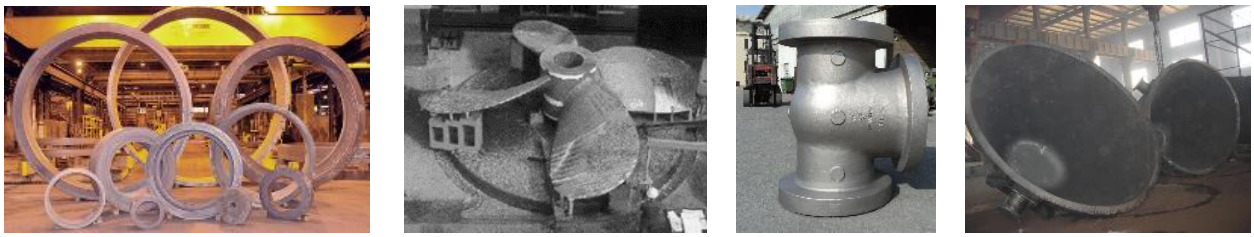

(a) (b) (c) (d)

Figure 4-5: Different (a) forged rings [384] and cast (b) marine propeller [385] (c) valve component [386] and (d) melting steel slag pots for steel plants [387].

The depicted foundry applications are prime examples for large-scale MAM, which may potentially include tooling for forging and casting operations, and SMRM operations within foundry facilities. Further to extending the service life of products derived from these processes, SMRM may enable the remanufacturing and recovery or repurposing of castings and forgings that may otherwise be scrapped, as well as for extending the service life of products derived from these processes. Focusing on the typical dimensional accuracy currently achievable (Table 4-2), relative to the size of typified foundry products (Figure 4-5), NNS characteristics were evaluated as shown in Figure 4-6.

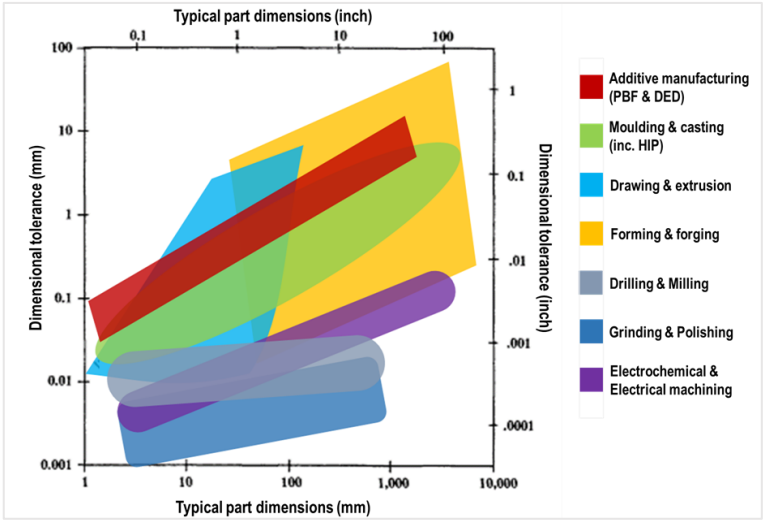

Figure 4-6: Typical manufacturing tolerances adapted from [388].

The dimensional tolerance chart was adapted by incorporating information about PBF and DED technologies, which were derived from literature surveys (Table 2-1). Subsequently, representative regions were colour coded to emphasise overlapping similarities and obvious distinctions between conventional and MAM techniques. In general, manufacturing tolerances are influenced by typical part dimensions, with similarities observed between regions representing MAM and casting techniques. Overall, the achievable tolerances for castings were much tighter but quite varied, relative to the capability of the selected process, such as precision cast products, where the dimensional or form accuracy is relatively superior to other casting techniques. As part dimensions increased, so did the overlapping similarities between forging, MAM, and casting techniques,

but there were much larger variations in achievable forging tolerances. These variations were attributed to a combination of factors, including the selected process (e.g. closed versus open die forging). For MAM, achievable tolerances were similarly influenced by the selected process, which is supported by literature findings, as summarised in Table 2-1, and typified by the artefacts shown in Figure 4-7.

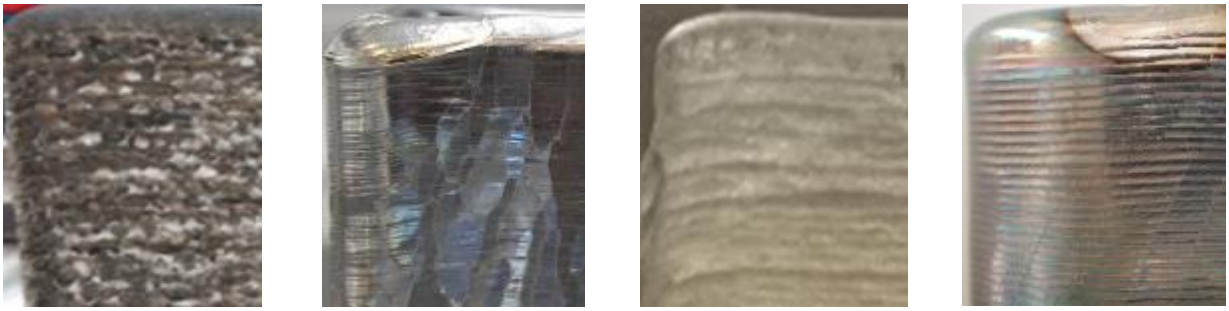

(a) (b) (c) (d)

Figure 4-7: Typical resolution for DED outputs derived from (a) IN718-powder (b) Ti-64 wire (c) IN718-wire and (d) Ti-64 wire feedstock materials.

The artefacts (Figure 4-7) were retrospectively selected from relevant organisational examples to underscore the effects of the processing mechanisms on output form accuracy. Derived from different DED capabilities, feedstock types and alloys, the resulting surfaces are characteristic of the layering approach, exhibiting varying degrees of unevenness, with lower build resolutions, typically in the range of ~1mm, and consistent with literature findings (Table 2-1). Nevertheless, size control accuracy is important and was used to define aspirational characteristics (Table 4-3) and boundaries for MAM outputs. Correspondingly, the ideal commercial characteristics for envisioned applications and, by extension, the specific attributes for industrial AMR applications, were extrapolated. Desirable attributes were organised into four categories, namely the product, geometry, mass, and thermal characteristics. Specific values were derived from aggregated commercial data (Figure 4-4), which was enriched with input from literature surveys (Table 2-1). The desirable attributes and equivalent ranges for large-scale MAM systems and applications are presented in Table 4-4.

Table 4-4: Definition of desirable MAM system attributes for industrial applications.

		Target values			Unit of measure
Attributes	**Description**	**Minimum**	**Average**	**Maximum**	
Product	Height/ depth	1	14	21.5	m
	Width/ diameter	1.5	7	23	m
	Volume	2.25	97	650	m^3
Mass	Component	0.10	70	400	mt
	Manipulation	0.25	77	400	mt
Geometric	Dimensional tolerance (NNS)	10	5	1	mm
	Size control accuracy	10	2	1	mm
Thermal	Processing temperature	1600[1]			^oC
	Latent heat of fusion[2]	500			kJ/ kg

Notes:
[1]It is possible to use additive manufacturing for transition and other metal (e.g. Tungsten and Tantalum).
[2]The temperature required to heat a specific quantity of a substance, at constant pressure, to induce a state change (i.e. from solid to liquid).

Irrespective of the services offered, averaged values for defined attributes were typically within range of declared foundry capacities (Table 4-2). However, and relative to publicised data, the averaged component mass value (Table 4-4) was disproportionately high, with asymmetry issues, between distinct values, further compounded by low data availability. While the average and maximum attribute values for this data set were often beyond the capacity of most suppliers, target minimum values (Table 4-4) were typical for sampled businesses. Correspondingly, deploying industrially equivalent capabilities in an AMR setting is advantageous for enhancing understanding of scaling parameters and related effects in large-scale MAM applications. Therefore, when pondering appropriate capacities for industrially competitive MAM capabilities, defined attributes and typical minimum target values were used to establish threshold limits for the BAM system.

4.3.3 Functions and attributes

In line with system requirements and considerations (Table 4-1), automation aspects of this development were conceived before other requirements. During preliminary studies, it was observed that accessibility issues were exacerbated by the positioning of the robot and by extension, the EOAT, relative to the deposition platform. The challenge with this established configuration concept was the potential to limit the deposition strategy or options, as observed during the development of the PoC part. Hence, it was desirable to minimise or eliminate this issue. The BAM configuration concept was based on siting the robot in a manner that enabled the EOAT to have full and complete access to the build platform and/or component, thus enhancing the possibility and prospects for both locational and situational deployment of MAM capabilities. While modularity, reconfigurability, and flexibility were introduced in relation to the overarching OA MAM system concept, the intermediate focus was on describing the configuration concept and specific attributes enabling BAM system functions.

Although flexibility is intrinsic to the kinematic (i.e. gantry and robot) modules or components, the goal was to maximise the EOAT flexibility and range, within the operational boundaries of the system. In this context, the SMD system was constrained and thus inefficient, due to relying on attaching extension brackets or other similar fixtures to achieve the desired EOAT range, which was determined on a case-by-case basis. For the BAM system, flexibility was achieved by combining and synchronising the movements of the gantry and articulated robots. This configuration concept enabled macro-movements during the global positioning of the EOAT via the gantry, with the articulated arm providing more precise or micro-movements during the deposition process. Depending on the application, these functions could be interchanged or combined as required, to fulfil specific BAM functions. Furthermore, the idea of tethering the robot to the gantry was aimed at achieving additional range and manoeuvrability, ensuring that the working perimeter or build envelop was entirely accessible. An illustration of the configuration concept, for maximising the BAM system flexibility, is shown in Figure 4-8.

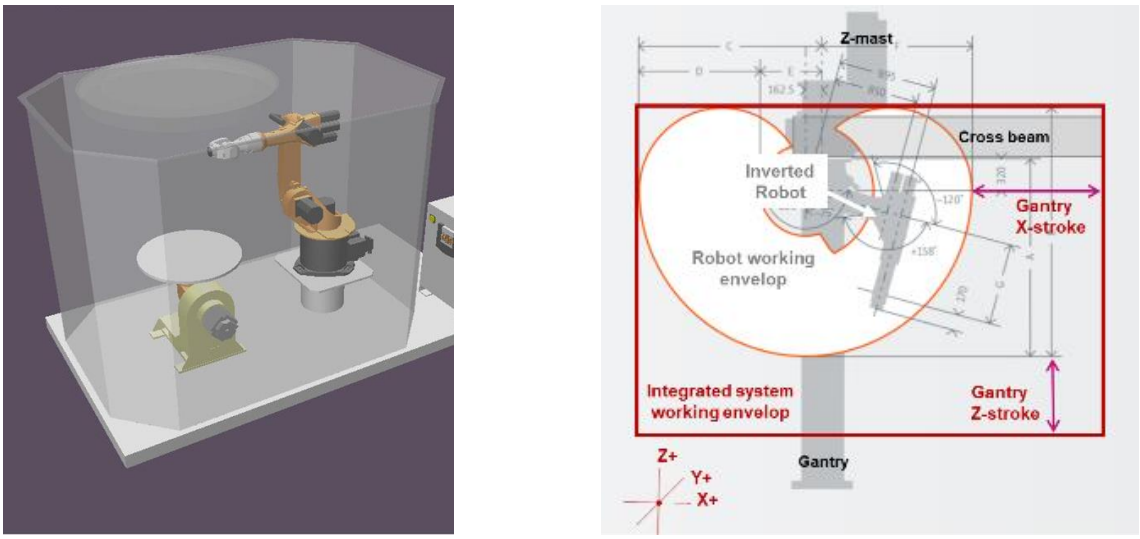

(a) (b)

Figure 4-8: (a) SMD configuration and (b) BAM concept - adapted from OEM publication [389]

The SMD configuration concept for the WAAM process comprised a pedestal robot and positioner, which were both tethered as illustrated in Figure 4-8(a). In comparison, the BAM concept (Figure 4-8(b)), which also includes a tethered positioner, introduces a gantry system, in conjunction with an articulated robot, to enhance access and manoeuvrability. In this configuration, the flexibility and range of the inverted robot is maximised, via the additional movements afforded by the gantry, in the X, Y and Z directions. Further to eliminating the need for operationally inefficient applications-based modifications to the EOAT, as observed for the PoC part, the designated working envelop was entirely accessible, thus enabling the envisioned 360º coverage of components to be processed within the operational boundaries/ working envelop of the integrated system.

The concept of modularity was motivated by insights gleaned when investigating capability and procurement needs and enabled by a COTS based approach. From a design perspective, modularity was realised as a function of the distinct COTS modules or solutions, which facilitated the organisation of different features and functions required to support end-to-end MAM operations, including performance evaluations, and system management and maintenance strategies. Actual BAM functions were primarily derived from the GTAW unit, robot arm, gantry system, component manipulator, and possible EOAT options, including the 3D scanner, with an automatic tool changer enabling interchangeability (Table 4-1). As a primary system function and enabler for MAM, automation was similarly conceived as a feature of the seamless interactivity between digital and physical environments. However, due to the potential impact of digital inputs on system performance and process outputs, as observed during preliminary studies, this function is under development. Nevertheless, the basic concept for a fully automated solution that readily links virtual and real environments, while algorithmically and adaptively controlling system inputs, in response to feedback from real-time process monitoring devices (Figure 4-1), was explored in an ensuing section.

When exploring designated system functions, the GTAW unit, comprising the feedstock material feeding and heating elements, and robots, including the articulated and gantry units, were classed as primary system modules, because they directly enable the WAAM process. While the manipulator or build platform is essential for AMR applications, it was viewed as an optional primary module, due to the possibility to deploy such capabilities for SMRM, and other in-situ applications. Conversely, the automatic tool changer, comprising the EOAT attachments and docking station, did not meet the HPA criteria, but enabled the concept of interchangeable EOAT, involving both primary and secondary system modules, such as the 3D scanner, which was integrated to support MAM operations. Correspondingly, the concept of interchangeability was applicable to the WAAM process, where different arc energy sources or feedstock forms may be used, as well as the distinct operations envisioned for the BAM cell. Secondary modules were especially introduced to enhance BAM efficiency by exploiting enabling technologies capable of supporting contiguous operations involving a single component or part. The implementation of the 3D scanner was especially motivated by challenges encountered when developing the PoC part, as well as broader MAM and SMRM considerations, including the anticipated benefit of initiating the WAAM process based on accurate digital representations. This idea involved creating scans from actual objects within the BAM environment, transferring the resulting data to the OLP environment for toolpath planning and simulation, generating the corresponding program for automated builds, and subsequently creating scans to facilitate the verification of BAM outputs.

4.3.4 Mechanisms and complexity

Beyond specific requirements for the proposed system, it was desirable to understand the intrinsic complexity of MAM capabilities, which influence *how* MAM activities are performed. Therefore, the objective of this investigation was to explore deterministic factors that influence OA system complexity. Having surveyed literature to assess the relative effects of different processing mechanism on MAM outputs (section 2.3), the focus was on exploring these mechanisms and related concerns. Thus, different technological options, founded on basic or common elements that enable MAM processes were evaluated, before organising the resulting information relative to the energy source or heat input, the feedstock types, and mechanisation components typically associated with MAM capabilities. Focusing on processes within the DED technology subclass (Figure 2-1), a non-exhaustive list of the distinctive elements or subcomponents associated with these three components, or core elements, were itemised.

For illustrative purposes, only 7 options and 23 related items or subcomponents typically associated with MAM capabilities were considered, with individual options categorised in relation to core components (i.e. energy, feedstock, and mechanisation) currently associated with selected technologies. For instance, when configuring a DED system that relies on a power beam, this energy source determines the functional requirements for configuring an electron beam gun or laser head (Figure 2-3.). Thus, the discrete elements supporting this option include the subcomponents for generating, shaping, guiding, and focusing the beam to provide the required power density for the DED process. Conversely, for a GTAW-based DED system, the high frequency mode initiates and maintains the arc, while the electrode guides, shapes, and focuses the arc

energy. The energy source also dictates the prerequisites for its safe and efficacious operation, including the processing atmosphere or conditions. Next, material shielding requirements are also influenced by the latter, while the selected feedstock option determines whether mechanical or fluidic subcomponents are required for transporting the raw material input to the deposition site. Finally, the mechanisation option determines how the process is controlled, typically via CNC or robotic controllers, with essential subcomponents selected to support either option. As other system components or options, and the number of related subcomponents accumulate, and the bill of materials (BOM) is expanded, the resulting structure becomes increasingly complex, thus influencing configuration decisions. The illustrative selections are presented in Table 4-5.

Table 4-5: Example of core components and distinct elements used for configuring DED systems.

		Primary Components						
		Energy source options			**Feedstock options**		**Mechanisation options**	
Subcomponent		**Arc**	**Laser**	**E-beam**	**Powder**	**Wire**	**Robot**	**CNC**
Thermal input	Generator	✓	✓	✓				
	Anode			✓				
	Beam protection		✓	✓				
	Cathode	✓		✓				
	Collimating lens		✓					
	Deflector coil			✓				
	Electrode	✓		✓				
	Focusing coil			✓				
	Focusing lens		✓					
	Optical fibre		✓					
	Power source	✓	✓	✓				
	Plasma/ shielding gas	✓						
Condition	Vacuum chamber			✓				
	Vacuum generator			✓				
	Work chamber	✓	✓	✓				
Consumable input	Carrier gas				✓			
	Delivery system				✓			
	Drive system/ motor					✓		
	Hopper				✓			
	Nozzle				✓	✓		
	Plasma/ shielding gas	✓			✓			
	Spool					✓		
Control	Articulated/ kinematic system						✓	
	Cartesian coordinate system						✓	✓
Total	**23**							

The magnitude and complexity of configuration issues were demonstrated by hypothetically determining the number of unique DED systems that could be configured from a limited number of inputs, represented by the itemised core components (Table 4-5). Assuming ‘n’ is the total number of objects required for configuring a unique DED system, and ‘r’ represents the possible options or items per object, of which only 7 were enumerated in Table 4-5, then the basic system requirements may be represented as shown in Table 4-6.

Table 4-6: Possible system configurations for basic system options.

Required components (r)	**Thermal input (T)**			**Feedstock (F)**		**Automation (A)**	
Objects or options	Electric arc	Laser beam	Electron beam	Powder	Wire	Robot	CNC
Object no. (n)	1	2	3	1	2	1	2

For any system, the number of core components, 'r' will be less than 'n', which implies that for a given number of components ('r'), there are different ways to combine ('C') or configure a unique DED capability. Thus, the combinations 'C', or number of ways in which each option or object 'n', may be chosen from the list of required items 'r', to create a unique DED capability, can be expressed as a binomial coefficient:

$$\binom{n}{r} = C(n,r) = \frac{n!}{(n-r)!\,r!}, (r < n) \tag{4-1}$$

The required thermal input (T), with three objects, was expressed as $C(n_T, r_T)$; the required feedstock input (F), with two objects, was expressed as $C(n_F, r_F)$; and the automation input (A), also with two objects, was expressed as $C(n_A, r_A)$. Therefore, based on the component requirements and options given in Table 4-5, the possible configuration options for a DED system were calculated as follows:

$$\begin{aligned} C(n_T, r_T) \times C(n_F, r_F) \times C(n_A, r_A) &= \frac{3!}{(3-1)!\,1!} \times \frac{2!}{(2-1)!\,1!} \times \frac{2!}{(2-1)!\,1!}, \\ &= 3 \times 2 \times 2 = 12. \end{aligned} \tag{4-2}$$

Hypothetically, there are 12 unique ways to configure the DED system, based on a relatively crude BOM, derived from narrow selection of core components. From a design perspective, the primary purpose of the initial concept development phase is to generate different concepts that embody the specified solution, having clarified the requirements, and before proceeding with a particular concept on which the final solution is based. This characteristically creative process is non-prescriptive, hence there are no requirements or stipulations governing the number of concepts that can be generated to arrive at a *good* solution. This exercise demonstrates how the concept generation phase may be creatively as well as systematically approached. Beyond the generation of a range of possible ideas or unique configuration, it also underscores the correlations between the BOM structure, and the intrinsic complexity of the resulting system.

Decisions made during the concept development phase can significantly affect the cost and other aspects of the final solution, and potentially constrain future developments and/or modifications involving established solutions. Thus, from a technological perspective, and when considering the concept of reconfigurability, there are potential benefits to exploring unique configuration possibilities derived from a more comprehensive and fully representative list of MAM options. The generation of additional concepts, from which a well-considered solution may be developed, can help to improve design outcomes. However, not all solutions are likely to be viable, and presently, it is not evident how the 12 unique configuration concepts can be generated efficiently, to ensure that conceptualisation activities result in desired developmental outcomes. Nevertheless, the optimal

configuration for long-lasting and adaptable systems was a key consideration, and the focus was on developing an optimisation strategy to facilitate the evaluation of currently available MAM options for deriving a unique system concept. While the evaluation of specific business, technology, and procurement requirements, allowed for the simplification of the development process, and refinement of the configuration concept, there were other decision factors underpinning the selection of derivatives, including system utilisation prospects.

4.3.5 Utility and value

The utility and value of the BAM system were of utmost importance due to the financial implications of this undertaking. As such, it was desirable to explore key ideas influencing the initial capital expenses (capex) and subsequent operating expenses (opex) for MAM system. In developing this idea, the main considerations were the impact of design decisions on costs and vice-versa, and in relation to system configuration options (Table 4-5) and implications for potential applications (Figure 4-7).

The decision to utilise COTS solutions was advantageous for estimating capex, because cost elements, facilitated by investigations into HPAs and related technologies (Table 4-1), were more easily quantified. Furthermore, for customised COTS and similar solutions with relatively opaque cost elements, technological precedents offered a basis for capex estimations. Hence, there were no obvious conceptual advantages to exploring this theme any further. Conversely, aggregated costs that directly influence opex, as well as profitability, which is linked to the utility and value of the system, are typically more challenging to estimate. Primarily, the appropriate context, such as the envisioned AMR requirements for actual applications, is essential for estimations, due to variations between specific instances or use cases and product features, as well as anticipated manufacturing volumes.

In manufacturing, the direct material, labour, and equipment are well recognised as the main cost drivers in industrial operations. From a product perspective, the opex is linked to the business rates, and production costs per unit, and influenced by the labour and equipment used to complete manufacturing operations. Furthermore, the requirements for developing and validating approaches for large-scale MAM applications, as exemplified by the feasibility study involving the PoC part, are related cost elements that affect opex. However, considering the dependencies between the product context and production requirements, and the broader focus on the GT framework, it was neither practical nor beneficial to investigate these subjective cost elements. On the other hand, the direct material is a major product input and manufacturing cost driver, while the ability to maximise material utilisation is a perceived commercial advantage of MAM techniques. Therefore, the direct material was used as a basis for exploring how the feedstock choice and utilisation influence DED costs and vice versa.

There are correlations between the relative cost of the system, its related temporary (e.g. feedstock) and linked (e.g. consumables) components, and the proportions in which these elements are incorporated. The consumables are relatively cheaper and replaced more often than other subcomponents of the system, whereas the feedstock, such as the wire used for the WAAM process, is typically more expensive than the consumables,

but accrues value as it passes through the system. While the preference for WAAM predetermined the choice of feedstock, this decision was influenced by cost, as well as other literature survey insights, such as the associations between wire and large-scale DED applications. Nevertheless, the motivation for the framework was much broader than a single feedstock variant. Consistent with preliminary studies, the direct materials currently used for MAM were organised into solid and granular variants. These classifications facilitated comparative analysis of relative costs, involving relevant data obtained from previous organisational studies.

Initially, differences between the amounts of raw material processed and the actual amounts subsumed within the finished product were evaluated. Known as the material yield or BTF ratio, in the aerospace industry sector, this important business metric is widely accepted for evaluating direct material utilisation. For the wire feedstock, data on direct material utilisation was lacking because this variable is not typically or widely monitored at present, as the yield is perceived to be negligible, a view supported by *Preliminary Study 3*, where both feedstock types were compared (Figure 3-15). Conversely, the powder feedstock utilisation is monitored as part of standard organisational practices, as a significant amount of un-melted/ un-fused powder typically remains in the build vicinity after deposition. Classed as *used* material, its utility is determined by its condition, and whether it can be directly reused. At any rate, the combination of data availability, and utilisation insights, influenced the initial investigative focus on the powder yield.

The yield variance (σ) of the powder feedstock was determined by calculating the sum of the squared difference between the feedstock data (x_i) set, and the data set average ($\bar{x}$), divided by the number (n) of data points, or the sample size, minus one. The variance is expressed as follows:

$$\sigma^2 = \frac{\sum(x_i - \bar{x})^2}{n-1} \tag{4-3}$$

Material utilisation data was obtained from previous development studies completed at the Nuclear AMRC, to demonstrate the potential implications of the raw material choice in a real business setting. Historical information was screened, to identify random samples of high-quality data, which is presented in Table 4-7.

Table 4-7: Actual data set used for calculating the yield variance of powder feedstock.

Set1	**Deposited mass (g)**	**Actual part mass (g)**	$\boldsymbol{x}$	$\boldsymbol{\bar{x}}$	$\boldsymbol{x_i - \bar{x}}$	$\boldsymbol{(x_i - \bar{x})^2}$
$\boldsymbol{x_1}$	319.3	301	18.3		-4	18
$\boldsymbol{x_2}$	320	300	20		-3	6
$\boldsymbol{x_3}$	322.7	299	23.7		1	1
$\boldsymbol{x_4}$	322.7	298	24.7		2	5
$\boldsymbol{x_5}$	322	296	26		3	12
$\sum$	-	-	112.7	22.54	-	42

For this preliminary assessment, the sample size (n) of the identified data set or *Set1*, (Table 4-7) comprised five data points. The values in column x represent the difference between the deposited and actual mass of the powder feedstock utilised. The actual powder variance (σ_p^2) was calculated as follows:

$$\sigma_p^2 = \frac{42}{5-1} = 10.6 \tag{4-4}$$

The targeted mass of the actual sample was ~299±2 g. However, due to observed inefficiencies or waste, during the powder deposition process, the yield variance across this data set was 10.6.

The standard deviation or square root of the variance, which is expressed in the same units as the base data, was also calculated. For the actual powder feedstock utilised, the standard deviation (σ_p) was derived as follows:

$$\sigma_p = \sqrt{\frac{\sum(x_i - \bar{x})^2}{n-1}} = 3.3\ g \tag{4-5}$$

Set1 data was acquired during the development of parameters for completing the referenced study. However, these short runs were not representative of the typical powder utilisation during the subsequent DED operation for actual builds. Hence, a representative data set for a typical part build was also sampled for comparative purposes. Similarly, historical data from previous organisational studies were screened, before identifying the data set, *Set2*, shown in Table 4-8.

Table 4-8: Standard deviation for powder feedstock based on representative part build.

Data sets	**Starting/deposited feedstock mass (kg)**	**Actual utilisation/ part mass (kg)**	x	$\bar{x}$	σ^2	σ
Set1 (average values)	0.30	0.30	0.02	0.3	10.60	3.30
Set2	50.00	19.80	30.20	y	z	$\sqrt{z}$

The referenced part was typical for studies completed within the organisation, and consistent with the envisioned requirements for AMR applications. The data was acquired as part of typical operating procedures, which facilitated the observation of factors likely to influence the yield variance at the targeted industrial scale, where similar production volumes are anticipated, and actual data sets are likely to be equally unique. Analogous to the procedures for generating *Set1* data, it was assumed that typical optimisation studies were performed prior to the actual build.

In order to determine the variance, it was necessary to establish a relationship between datasets *Set1* and *Set2*. Then, the mean value (y), variance (z), and the standard deviation ($\sqrt{z}$) for *Set2* were extrapolated as follows:

$$\frac{1.49}{19.80} = \frac{0.3}{y}$$

$$\therefore y = \frac{19.80 \times 0.3}{1.49} = 16 \quad (4\text{-}6)$$

For *Set2*, the variance and standard deviation values obtained were 250 and 2 respectively. Between data sets, the values were relatively lower for *Set2*, than for *Set1*, which implied that during the continuous deposition operation for the referenced build, material utilisation significantly improved.

A lower yield variance is desirable because of its implications on direct material requirements and costs for the process development and production phases, as well as for specific product volumes. Furthermore, irrespective of the material type (i.e. granular or solid), the outlined development phases (i.e. parameter development and part build) were typical, which implied that for low-volume large-scale operations, the overall costs will be determined by all developmental phases. Thus, the wire remained the preferred direct material option for BAM. Nevertheless, and further to the qualitative insights from preliminary studies (Figure 3-15), the powder utilisation data provided a quantitative basis for assessing the granular feedstock yield relative to the direct material inputs.

Due to lack of data concerning the wire, comparisons between solid and granular material types, remained at the qualitative level, and were supported by insights from literature surveys. Other relevant organisational information was especially incorporated, not to inform the development of the concept, but with the specific purpose of generating pertinent data to create a GT framework, in accordance with the ultimate objective of this study. When considering the desirable attributes for large-scale MAM applications (Table 4-4), the typical part resolution was identified as an important quality measure, due to the implications of part finishing requirements. Correspondingly, the focus of this task was on the ability to create relatively NNS parts, which is a distinct processing advantage. Assessing part resolutions allowed for the comparative analysis of pertinent factors affecting the perceived utility and value of MAM applications, due to the material or feedstock option.

The relative implications of the manufacturing output quality were evident, when examining representative DED part resolutions, as depicted in Figure 4-7. These images were obtained from relevant studies, which were completed using different DED capabilities at the Nuclear AMRC. The sample depicted in Figure 4-7(a) was deposited from IN718 powder feedstock, which was processed in enclosed chamber, via robotic-laser DED, but utilising local shielding only, while Figure 4-7(c) shows an IN718-wire sample similarly processed, under local shielding conditions, via robotic-arc DED. Figure 4-7(b) depicts a titanium alloy Ti-64 wire sample processed in a vacuum via CNC electron-beam DED, while Figure 4-7(d), also fabricated from Ti-64 wire, was processed in the SMD chamber under both a localised and globally controlled inert argon atmosphere.

When comparing the representative samples, and from observations during preliminary studies, it was evident that the material transmission mechanisms significantly affected the product yield (Figure 3-12). Due to the

granular characteristics of the powder feedstock, pressurised inert gas is required for controlling the precise transmission and dispersal of fine powder particles to the melt region, which is also locally shielded with an inert gas. Conversely, a mechanical delivery system is required to transmit the continuous solid wire feedstock to the melt region, which is similarly shielded. However, the effects of the material transmission mechanism on the resulting part resolution were negligible, relative to the processing environment. In particular, the different wire samples (Figure 4-7(b) and Figure 4-7(d)), processed under vacuum and inert conditions, appeared shiny and more precise than the wire (Figure 4-7(c)) and powder (Figure 4-7(a)) samples that were processed using only local shielding techniques. Between the different feedstock types, both involving the same type of alloy (i.e. IN718) and similarly produced using argon as a local shield, the appearance of the wire sample (Figure 4-7(c)) was more visually appealing than the powder sample (Figure 4-7(a)). There were also similarities between the outputs, mainly in relation to the characteristic layers visible in each sample, with distinct layers more noticeable in samples processed within a globally controlled environment, thus establishing possible correlations between the processing (vacuum and inert) environment and the preciseness of outputs. These observations are consistent with findings from *Preliminary Study 3*, which resulted in builds that were similarly precise along the edges, as depicted in Figure 3-13. Although, when comparing the material input forms, similar inert conditions resulted in a glossier appearance for wire builds, relative to the outputs from the powder feedstock. The build resolution also has broader implications on fatigue properties, due to established correlations between the application criticality, surface condition, and the potentially detrimental effects on the durable performance of end-use parts.

From an operational standpoint, these insights were useful for qualifying the relative economic value of the direct material input and output quality. The main observations include differences in the feedstock delivery mechanisms, and common requirements for creating, monitoring, and sustaining the processing environment, for both solid and granular materials. The effects of distinct variables were particularly evident when comparing the different capabilities utilised for processing these alloys, particularly between outputs involving similar alloys (i.e. Ti-6-Al-4V) and feedstock (i.e. wire). Incorporating independently generated, yet verifiable organisational data, ensured that consequent inferences were realistic and representative of MAM approaches. Practically, it enabled the qualification of the relationship between the choice of feedstock, processing efficiency, product quality, cost, and related system considerations. There appeared to be stronger cost correlations between the processing conditions afforded by the different MAM capabilities and the resulting visual quality of builds, which was consistent with literature findings. In essence, globally controlled inert or vacuum environments resulted in relatively superior outputs, when compared to builds completed under localised shielding circumstances only. The outputs of different feedstock types of a particular alloy, processed under similar DED conditions, were also evaluated. From this perspective, the relative cost of distinct builds were perceived to be disproportionate, when considering the configuration options (Table 4-5) and typical part resolutions (Figure 4-7), because power beam (i.e. electron and laser) systems are significantly more expensive than arc-based solutions. On the other hand, the dull appearance of the as-deposited powder samples, relative

to the wire builds, allude to the possible effects of powder dispersal on solidified areas of the build, notwithstanding the potential effects of spatter, affecting both wire and powder depositions (Figure 3-15). However, the need for a post-processing operation was established relative to the requirements and priorities for this study.

In terms of the framework, exploring cost factors provided a more holistic understanding of this element, relative to the broader utility and value of MAM systems. Correspondingly, if the DED build quality remains the same, then equivalent operating expenses would be incurred for similar products, irrespective of the choice of feedstock. There were obvious correlations between the delivery mechanisms, and the material form and yield, which generally improved when optimised for a specific application. For large-scale MAM applications, the granular feedstock material yield is important due to the potential and relatively disproportionate cost implications. Hence, impressions of utility and value were explored, as part of the solution optimisation strategy, and relative to the overall BAM concept, and prioritised WAAM technique.

4.3.6 Optimisation strategy

The purpose of this phase was to adequately screen concepts and define the criteria to support development decisions, based on the different factors influencing the final BAM solution. The evaluation criteria were defined relative to important developmental factors, namely the (1) potential system utility; (2) technological complexity; (3) cost of distinct technologies; and (4) time required for this development. Due to funding constraint and related development considerations, including a very rigid procurement-to-delivery schedule, the organisational cost and time were classed as critical decision factors. These constraints influenced decisions about the specific configuration options, particularly when considering the lead time and specific costs of distinct solutions, including COTS items. In other words, the preferred approach (i.e. WAAM) was established, but specific solutions were constrained by the available budget. Correspondingly, system complexity was determined by the preferred configuration options, but utility derives from its purpose, and the potential applications it enabled. Thus, relying on the alternatives presented in Table 4-5, and the four itemised factors, the overall aim was to achieve the best development outcomes for the BAM system.

From an organisational perspective, the objective was to maximise system utility, whilst minimising development time and cost, thus improving the overall value of this undertaking. The design/ development focus was on minimising complexity, through a higher level of modularity, to maximise integration efficiency. However, maximising utility, via the EOAT and reconfigurability concepts, was incompatible with the objective of minimising system complexity. Similarly, minimising cost would impact both utility and complexity, with strong correlations between the latter and integration efficiency. Due to the combination of the development context and particular circumstances, a multi-objective optimisation approach was adopted, requiring an appropriate optimisation tool whose outcomes adequately supported budget justifications and procurement decisions.

The Lean Manufacturing Six Sigma prioritisation matrix was adopted for this optimisation exercise and implemented as illustrated in Figure 4-9. The prioritisation matrix is a management tool typically used to support decision-making. It was specifically adopted for evaluating the four defined optimisation factors or decision criteria, and subsequently balancing optimisation outcomes against the development budget and procurement justifications. The full analytical criteria method, which is appropriate when relatively few criteria and options are involved, was selected for this optimisation exercise, and implemented based on defined optimisation criteria, core technology configuration options (Table 4-5), and was further informed by literature and supplier surveys.

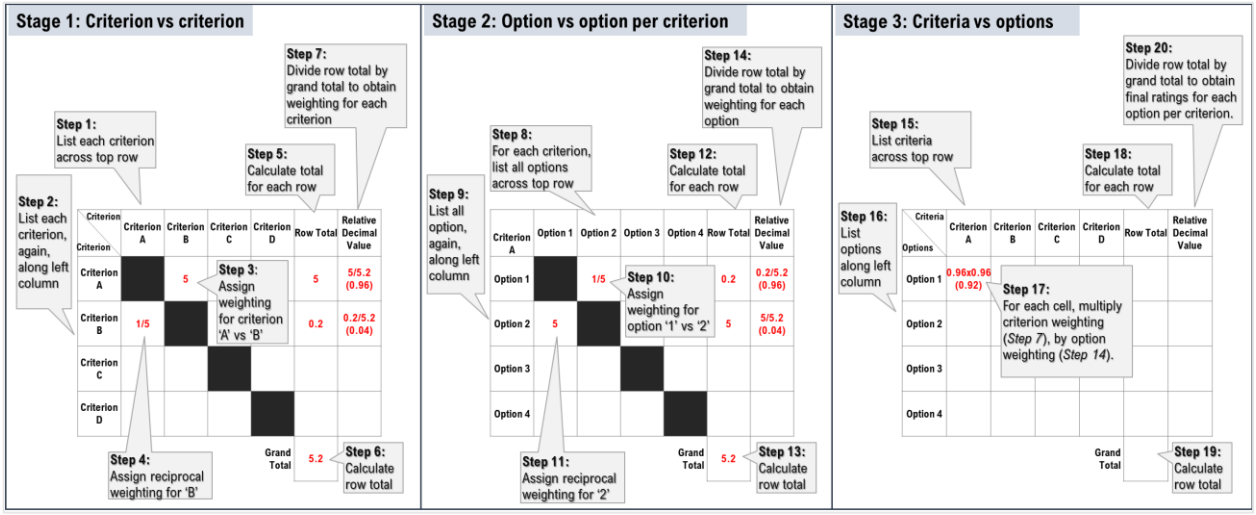

(a)

Optimisation Criteria

Criterion	Cost	Time	Value	Complexity	Row Total	Relative Value
Cost		1	1/10	1/10	1.2	0.03
Time	1		1/5	1/10	1.3	0.03
Value	10	5		5	20	0.47
Complexity	10	10	1/5		20.2	0.47
Grand Total					42.7	

Criterion weighting
1 = Equally important
5 = More important
10 = Much more important
1/5 = Less important
1/10 = Much less important

(b)

Energy options

	Cost	Arc	Laser	E-Beam	Row Total	Relative Value
Cost		1/5	1/10	1/10	0.4	0.03
Arc	5		5	10	20	0.73
Laser	10	1/5		5	5.2	0. 25
E-beam	10	1/10	1/5		0.3	0. 01
Grand Total					20.5	

Option weighting for cost criterion
1 = Equally important
5 = More important
10 = Much more important
1/5 = Less important
1/10 = Much less important

(c)

Summary matrix

	Options	Cost	Time	Value	Complexity	Row Total	Relative Value (Ranking)
Energy	Arc	0.02	0.02	0.34	0.35	0.73	0.25 (1)
	Laser	0.01	0.01	0.12	0.12	0.25	0.09 (2)
	E-beam	0.00	0.00	0.01	0.01	0.01	0.00 (3)
Feedstock	Powder	0.00	0.01	0.02	0.45	0.48	0.16 (2)
	Wire	0.03	0.01	0.45	0.02	0.50	0.17 (1)
Control	CNC	0.00	0.01	0.45	0.02	0.48	0.16 (2)
	Robot	0.03	0.01	0.02	0.45	0.51	0.17 (1)
	Grand Total					2.96	

Ranked development options summary	
Energy	Arc
Feedstock	Wire
Control	Robot

(d)

Figure 4-9: (a) Main steps in the implementation of the Six Sigma prioritisation matrix for evaluating development (b) criterion versus criterion and (c) option versus option, enabling the creation of a (d) decision summary matrix for the BAM system.

The illustrated approach (Figure 4-9(a)) was initiated by listing the optimisation criteria, and weighting each criterion relative to another (Figure 4-9(b)), before similarly comparing each option per criterion (Figure 4-9(c)). When evaluating options for a specific criterion, a similar rating scale was typically applied, as depicted in Figure 4-9(c) for the energy options and cost criterion. For assigned weightings, higher values

signify the relative importance of the criterion or option under consideration, with reciprocal values assigned to denote a lower priority. All feedstock and motion control options were similarly assessed for each criterion (i.e. Time, Value and Complexity), as shown in *Stage 2* (Figure 4-9(a)), before generating the summary matrix (Figure 4-9(d)), to decide which options to pursue. For the energy option, the *arc energy source* was highly ranked, relative to the defined criteria. However, based on similar considerations, the final ratings were much closer for the feedstock and control options, with the *wire feedstock form* and *articulated robot* ultimately selected, thus formalising the core options for the BAM system.

The optimisation matrix was mainly implemented to enhance confidence that selections were well informed. It facilitated a more considered review of the defined development objectives and pertinent factors. Correspondingly, important constraints, i.e. cost and time, were appropriately evaluated within this context, whilst ensuring that the objectives of maximising utility, as a mechanism for deriving value, and minimising integration complexity, were satisfied.

4.4 Implementation of BAM concept

This section covers the interpretation of the BAM concept, which allowed for the specification of the different system components that were subsequently integrated. The basis for procurement decisions and other considerations that influenced the final solution, which embodied the BAM concept, is also explained. In general, the funding and scheduling requirements influenced the implementation process, while the integration strategy was developed based on crucial factors, including the availability of funds and the envisioned integration end state for the final solution. The details of the implementation strategy are provided in the following sections.

4.4.1 Specification of solutions

The design and development objectives were to derive a solution for large-scale MAM operations, and the resulting BAM system can be described as a product or solution that is both evolutionary and analytical. Analytical forms were embodied by the COTS solutions specified, while evolutionary product forms were derived in response to customisation requirements. In general, the development specifications, which embodied the different concepts described in previous sections, were used to establish how to implement the design concept, while the implementation itself was based on the functional design specification (FDS). Derived from the design specification or concept requirements, the purpose of the FDS was to specify the features, functions and procedures underpinning the system performance, and was provided by the supplier or developer of individual and/ or modular solutions. The concept requirements, which included both analytical and evolutionary solutions that were procured from the different suppliers (Figure 4-3), also provided an initial basis for evaluating and approving technical decisions arising from the interpretation and implementation of the FDS phase. The design specification for the BAM system is outlined in Table 4-9.

Table 4-9: Hardware requirements.

Requirements	Description/ functions
GTAW equipment.	GTAW-based DED solution for deposition of wire feedstock.
Integrated manipulation and processing capability	Reconfigurable robotic cell with multi-sided access capable of accommodating multiple end-effectors for DED of large metal structures.
Supplies	Power supply to electrical devices
	Compressed air to supply pneumatic systems
	Inert gas to shield material (local and trailing)
Process monitoring	Vision system to monitor melt pool and arc gap
	Oxygen sensor to monitor gas purity in vicinity of melt pool.
	Mechanism for recording input parameters including current, voltage and wire-speed
	Infrared sensors to monitor (inter-pass) temperature
	Thermal camera displays real time video images of arc, melt pool or puddle, and base metal

The procurement and approval processes were normally based on outlined requirements (Table 4-9), particularly for customised COTS and bespoke solutions, but OEM specifications were typically accepted for approved COTS solutions. The specifications compilation process for items, including HPAs, was relatively orthodox, compared to the approach for bespoke solutions, which included software requirements. The latter were typically coupled with required hardware solutions in a manner that did not often satisfy specifications for the BAM system. Furthermore, it was recognised that the progression from a fully integrated, to a fully automated system, was significantly beyond the mere amalgamation of different system components. Instead, both integration and automation states were strongly influenced by the solution, a representation of the developers' perspective, which may be focussed and comprehensive, yet limited, in view of stated requirements and specifications. Conversely, the need for higher quality MAM outputs was informed by issues identified from literature surveys and preliminary studies and motivated the envisioned concept for an integrated digital platform (Figure 4-1).

The requirements for an adaptable standalone solution, capable of virtually linking BAM system components and auxiliary devices, irrespective of the model or brand, were analysed. The specification for the digital solution, which mirrored the OA configuration of the real BAM platform, was subsequently developed to accommodate multiple solutions (S) or EOAT. As with the real system, the focus was on the end-to-end process, based on a platform that allowed for the monitoring, measurement, and automatic control of processes associated with each solution. The concept for real-time monitoring and control of the BAM process, is depicted in Figure 4-10.

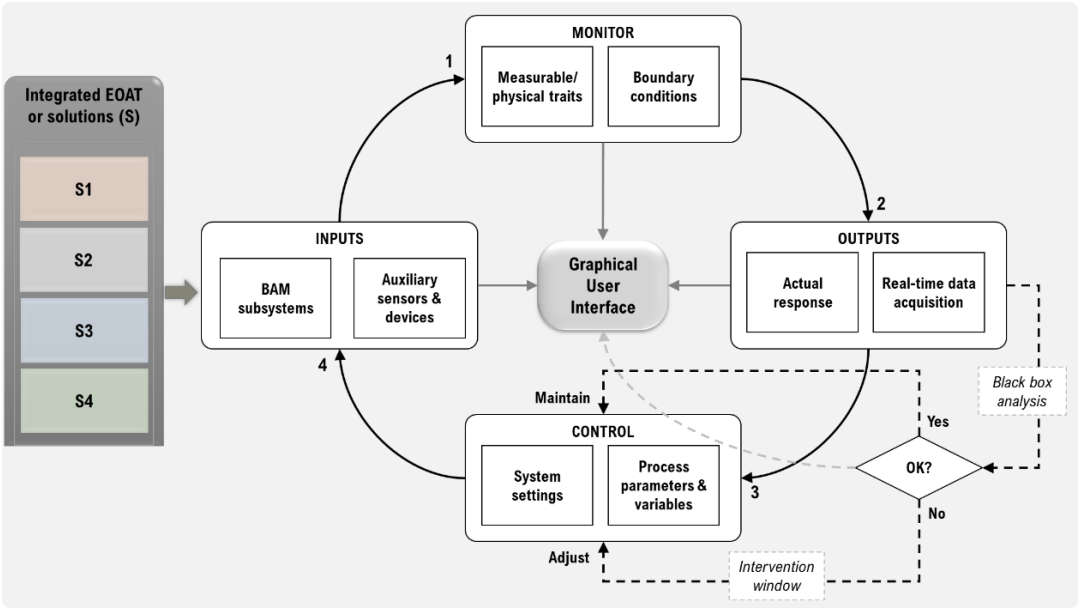

Figure 4-10: Concept for monitoring and control of the BAM system.

The idealised concept requirements are outlined below.

- Step '1': monitoring devices are utilised to detect BAM system inputs.
- Step '2': the status, conditions and resulting characteristics are measured and recorded.
- Step '3': actual outputs are automatically analysed against measures and indicators.
- Step '4': inputs are algorithmically controlled to improve reliability and quality.

The purpose of the graphical user interface (GUI), and underlying infrastructure, is to enable system-process-operator interactions via the monitoring of inputs and responses; acquisition and logging of pertinent process data for permanent records; and capturing activity logs to enable the (re)programming, troubleshooting and interrogation of the distinct solutions and associated subcomponents of the BAM system. Compared to the in-situ monitoring solution (iMUST) proposed by Xu et al [187], the idealised concept also allows for system-process interactions, whereby process outputs or data logs are utilised to support instantaneous analytics and timely feedback for controlling system inputs, independently of the operator.

The depicted black-box approach (Figure 4-10) was preferred for combined response monitoring and performance diagnostics. It was created to ensure that the need for manual operator interventions during the process was eliminated. Otherwise, system-process interactions were likely to enhance the precision and timing of responses, both within and between integrated solutions, thus reducing the need for human intervention. Essentially, if interventions were necessary, as defined by established manufacturing quality criteria, then the responsiveness of the system was more likely to result in actions that were more precisely and readily implemented, relative to direct operator actions. At the very least, this approach would enhance operator efficiency as necessary. The design/ development requirements, for realising the BAM software concept, are summarised in Table 4-10.

Table 4-10: BAM software requirements.

Requirement	Description
Standalone process management system	Solution that interfaces with distinct subsystems and instrumentation for overall system monitoring and control.
Integrated user interface	To display monitored system and process variables and parameters in real-time.
Active system monitoring	To track system and process variables in real-time.
Unique database	For acquiring multi-usable data at variable sampling rates for permanent records.
Customisable software	For reprogramming and calibration of specific input and/or output fields critical to control of monitored variables.
Data analytics	For analysing equipment and instrumentation data to identify specific issues affecting efficiency, quality, and productivity.

The preferred customised solution was prioritised over the existing capabilities of separate subsystems, from which, it was envisioned, that necessary inputs would be obtained. Furthermore, concept requirements were subject to similar considerations previously outlined in relation to the *optimisation strategy*. However, the selection process was relatively easier, with the overriding concern being the compatibility of solutions, and the overall system functionality, within the allocated budget, time limit, and related development constraints.

4.4.2 Technical feasibility

When evaluating concept requirements, the technical feasibility assessment process was especially developed in response to observations and insights acquired from interactions with suppliers, and supported procurement and implementation activities, whilst taking into consideration, the broader GT framework requirements. The feasibility assessment was supported by a decision matrix, and the process involved analysing the proposed BAM concept requirements and justifications. It was particularly useful for clarifying and/or approving pertinent aspects of the FDS issued by development partners. The matrix is presented in Figure 3 26.

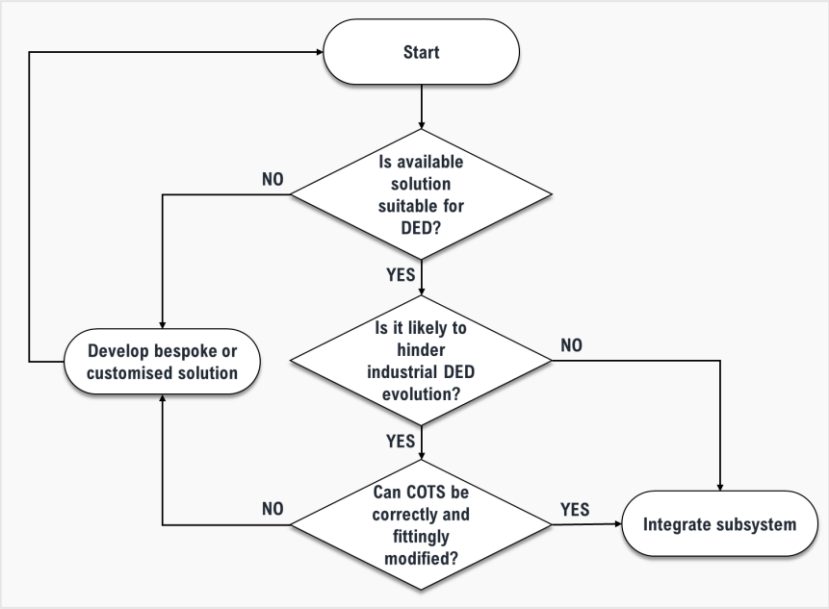

Figure 4-11: Decision tree to support implementation of BAM system concept.

The decision matrix initially allowed for the identification and analysis of COTS solutions. In essence, if specified features (i.e. real and virtual) were available, compatible, and enabled current and potential prospects for the BAM capability, then the decision was to proceed with integration. Otherwise, the concept requirements, such as the one developed for the software solution (Figure 4-10), were developed. Following the feasibility assessment of the technology integration state and readiness level, and if it was not possible to modify available COTS solutions, then a customised approach was necessarily adopted.

It was rationalised that the preferred approach of integrating COTS solutions was likely to have a relatively lower integration risk profile than that of customised solutions. Consequently, the possibility of completing the planned undertaking, within a relatively shorter timeframe, was expected to improve, due to the utilisation of proven and available technologies, supported by publicly available information, outlining the value, benefits, and limitations of established solutions. For instance, the customised solution for component manipulation was especially developed due to the COTS solution not meeting the concept requirements. Specifically, compatibility issues were identified, necessitating significant and expensive upgrades, to meet concept requirements. Furthermore, it was determined that even with significant modifications, future modifications would be necessary to meet evolving MAM requirements, due to limitations imposed by the original design. Consequently, the concept and specification for a ready-to-integrate solution was developed, resulting in a fully integrated 11-axis BAM system. The customised solution is depicted in Figure 4-12.

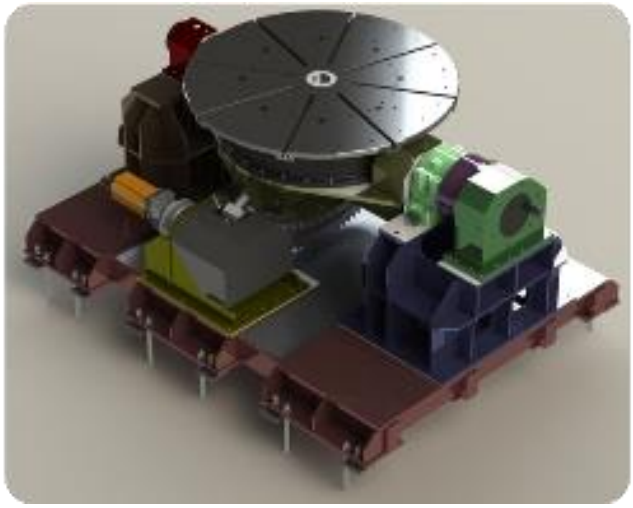

Figure 4-12: 3D model of bespoke 2-axis manipulator for the BAM system.

When developing concept requirements, it was evident that not all desirable MAM system attributes were attainable. Further to the integration state of the manipulator, the size, and manipulation capacity, including the load limit and related performance indicators, were important design requirements. The main consideration was the specified system boundaries, which was constrained by the available or allocated factory space for siting the BAM capability. Consequently, the specified solution (Figure 4-12) exceeded the minimum class value, but fell short of the average values defined for the component mass attribute (Table 4-4).

In general, the mass of distinct components and/or load capacity were important when evaluating the technical feasibility of distinct elements of the BAM system, particularly for EOAT. This consideration influenced how different concepts and requirements were implemented when configuring the system, ensuring that it was functional, yet safe to operate. Nevertheless, the specified load limit for the manipulator was adequate, relative to pre-existing organisational capabilities, and for conducting appropriately scaled investigations within the defined AMR context.

The preferred GTAW solution (Table 4-1) was also adapted, because it was not possible to modify or control process parameters without using the OEM interface. However, unlike the manipulator, it was determined that this solution could be successfully adapted. Hence, design requirements were derived from the concept illustrated in Figure 4-10. The upgraded solution, which maintained the OEM front-end/ operator interface, was coupled with an initial back-end solution that facilitated the connection of related hardware and software components, thus fulfilling the basic requirements for *Step* 1 (Figure 4-10). Accordingly, the procurement strategy for both ready-to-integrate and/or customised COTS solutions (Figure 4-2) were implemented, with due consideration given to the final integration state of the different solutions subsequently integrated.

A basic analysis of the current integration status revealed that approximately 35% of the modular solutions or HPA integrated within the BAM system were customised. The analytical data for this study included COTS solutions that did not possess the requisite features, mainly due to the specific concept requirements. This study also underscored the complexity of the MAM supply chain, as exemplified by the number of partners (Figure 4-3) involved in the development of individual BAM solutions. While customisations were necessary to achieve concept requirements, which were aligned with defined research challenges, the supply conditions, including interrelationships observed between contracting parties, had a significant bearing on the modularity or wholeness of top-level solutions that were integrated. Specifically, when customising solutions, both primary and affiliated contractors often participated in developmental proceedings, even when the required expertise was evidently beyond the scope of involvement. Observationally, and considering that bids were submitted in response to the concept requirement for modular or complete solutions, it appeared that the parties involved did not perceive solutions as elements of a whole, but as standalone components cooperating with other components as part of the top-level solution. Consequently, further complexities were introduced, affecting solution development and implementation phases, as well as related management processes, particularly when operating and maintaining the BAM system. Nevertheless, this analysis demonstrates that developing an OA MAM system based entirely on the integration of COTS solutions is not feasible at present.

The data supporting the analysis of the current BAM system integration status is summarised in Table 4-11, alongside important decision factors and considerations.

Table 4-11: Scope of supply and current integration state of DED capability.

	Item	Supplier	Integration state		Purpose and related procurement decision factors
			COTS	Customised	
1	Gantry robot	Güdel	✓		Standard gantry frame and components (includes standard KUKA components to facilitate integration).
2	Articulated Robot	KUKA Systems UK	✓		Standard foundry robot equipment and components.
3	Manipulator	Red D Arc	✓		Standard positioner to establish basic capability for semi-automated part manipulation.
		Brown & Holmes		✓	Customised unit assembled using combination of customised and standard components (includes standard KUKA components) for compatible and fully integrated 11-axis system directly controlled via robot interface.
4	GTAW equipment	Air Liquide	✓		Standard TOPTIG equipment/ end-effector modified with standard JACKLE WIG 500i direct current (DC) power source and customised weld controller compatible with robot controller.
		TPS		✓	
5	3D geometric scanner	Hexagon Metrology	✓		Standard portable profile scanner/ end-effector to generate input DED data for volumes up to 60m (Ø) in a single set-up.
6	Multi-tool docking station	KUKA Systems UK		✓	Customised solution to facilitate end-to-end processing by supporting multiple end-effector tooling for related processing requirements.
7	Automatic tool changer	Schunk	✓		Standard solution with compatible interfaces linked directly via the robot control system for automating tool change, enhancing operator safety and increasing efficiency between tasks.
8	Virtual platform	2M Automation		✓	Customised tool for capturing and connecting contextual information across all integrated equipment and processes to support strategic decisions to enhance industrial DED applications
9	WorkVisual software	KUKA Systems UK	✓		Standard interface and programming tool for offline development, online diagnosis and maintenance.
10	Polyworks	Polyworks	✓		Standard solution for acquiring point cloud data from 3D scanner to control part dimensions, diagnose and prevent manufacturing issues.
11	CAD/CAM functions	Visual Components	✓		Standard Visual Components for workspace and component modelling and simulation with customised tool for DED process planning and simulation.
		Delfoi-Oy		✓	

4.4.3 Integration strategy

The BAM system integration process, which included previously mentioned FAT and SAT phases, was significantly enabled by decisions made during the definition of concept and functional design requirements. The actual process was completed in two distinct stages over a two-year period, with the main output being the fully integrated 11-axis BAM system. In the initial phase, the focus was on establishing the foundations or basic building blocks for BAM operations, while the subsequent phase was focused on attaining the desired level of integrated functionality. The development timeline and activities are depicted in Figure 4-13.

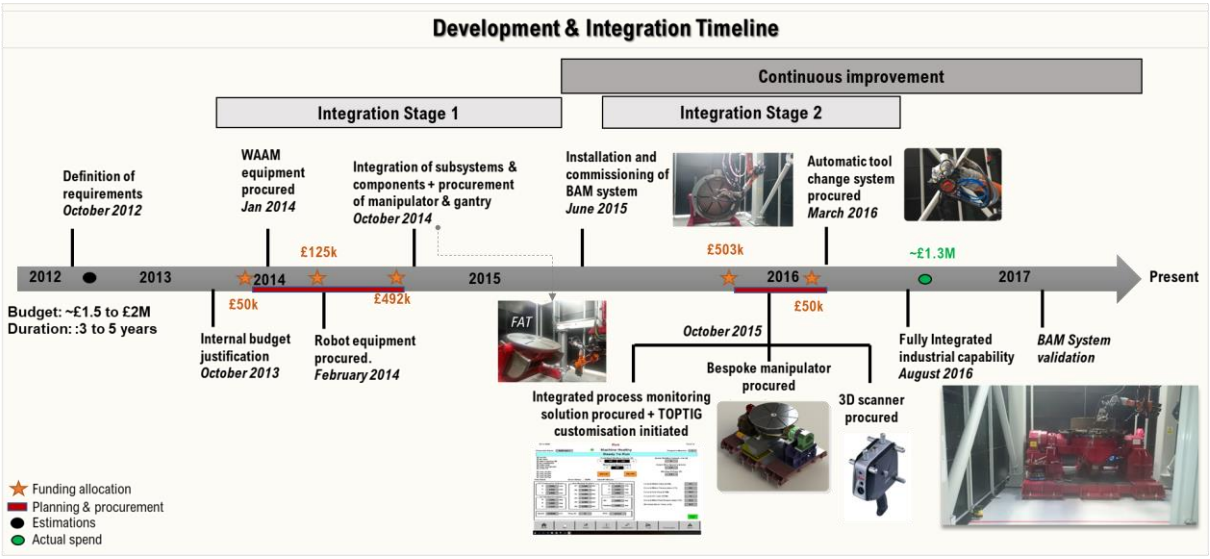

Figure 4-13: BAM system development timeline and milestones.

The estimated cost and duration for this multi-staged process was based on insights from literature surveys, and independent investigations completed as part of preliminary studies, and were used when preparing justifications to support internal funding decisions [390]. Excluding preparatory work, the actual duration was about 2.5 years, and the sum of ~£1.3M was required to complete the distinct stages depicted in the timeline (Figure 4-13). While the actual development costs are representative for this type of OA-DED system, the timeline was dependent on specific internal and development circumstances. The main internal factor was funding allocation and defrayment conditions applicable to this development, while external considerations include the lead-time, particularly for customised solutions. Nevertheless, and after completing development stages '1' and '2', the desired level of integrated functionality was achieved, whereby the movements of all subsystems were synchronised, thus enabling typical operations, including the implementation of BAM system validation actions.

Maintaining oversight of internal and external factors affecting the systems integration process was essential to the success of this development. For instance, within the scope of supply, the subsystems, or modules, integrated at distinct stages, were prioritised in a manner that ensured that basic system functionality was

maintained, which facilitated limited system trials, pending the integration of other solutions. This building blocks approach was sufficiently flexible, and allowed for the accommodation of supplementary requirements, to attain and/or enhance basic functionality, with due consideration for the immediate system requirements, its overall utility, and previously outlined developmental factors. A prime example is the introduction of a manipulator in *stage 1*, which enabled BAM operations to proceed, albeit independently of other modules, but was later substituted in *stage 2* for a customised solution (Figure 4-13), which enhanced the operability of the system. Similarly, the 3D scanner was introduced to enhance BAM operations by enabling the inspection of components, both before and after the deposition process.

Post-implementation, the focus was on increasing understanding of specific system attributes and causal relationships. These relationships, arising from the integration approach, unique configuration concept, as well as the distinct technologies and customised solutions currently integrated, provided valuable insights, which will support the transition from a fully integrated state to a fully automated system. Thus far, the BAM platform has been utilised to complete different organisational projects, including the system validation studies reported in the following chapter. In the intermediate sections of this chapter, specific implementation activities and related observations are described in relation to the main system components, including the robots, EOAT, manipulator, and digital platform presently utilised for BAM operations.

4.4.4 Robotic subsystems

The integration sequence was influenced by earlier decisions and considerations that helped to minimise the potential for human interpretation errors, and similar assembly-related issues. This focus was influenced by the Poke Yoke technique, a Six Sigma tool from the Lean manufacturing discipline that focusses on efficiency via error-proofing. For instance, the specifications for the inverted and gantry robots logically determined the integration sequence for this subassembly, while the concept of modularity enabled efficiency by keeping the component count low for each solution. The subassembly integration sequence is shown in Figure 4-14.

(a) (b)

Figure 4-14: BAM system configuration concept developed as (a) 3D model prior to (b) implementation.

During the installation process, the gantry robot was assembled, based on the concept design (Figure 4-14(a)), before the articulated robot was mounted onto the base of the gantry (Figure 4-14(b)). Next, the WAAM EOAT was attached to the base of the articulated robot, after which related peripherals were installed.

Management considerations were generally motivated by the need to minimise complexity, mainly by streamlining operations between integration phases, integrated modules, and suppliers, and was facilitated by investigations completed during the concept development stage. For instance, establishing automation as the primary enabler and basis for MAM operations (Table 4-1), predetermined the basic integration protocols during this phase, as well as the types of interactions that subsequently occurred between and within the different elements of the system. Accordingly, the articulated robot was integrated as the primary automation or controlling system, with the gantry robot incorporated as a secondary external unit, whereby each axis of the gantry was assigned a unique external or 'E' identifier, within the primary system controller.

4.4.5 End-of-arm tooling (EOAT)

The tool-docking module is a unique system feature that embodies the concept for end-to-end MAM operations. Essentially, multiple end-effectors can be introduced within the BAM platform, which, in addition to enabling the end-to-end processing of metallic structures, can be designated as a testbed for evaluating new EOAT for MAM. The functionality of new EOAT may be assessed in relation to the overall contributions to the value of MAM products, or for assessing integration states of base technologies being considered for other integration projects. Currently integrated EOAT are shown alongside the tool docking station in Figure 4-15.

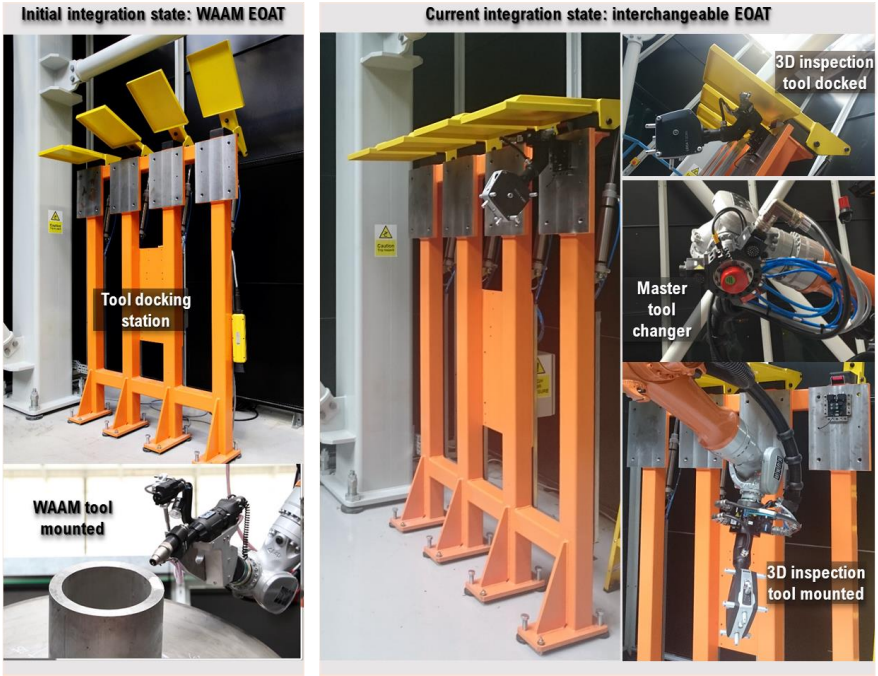

Figure 4-15: Implementation of tool docking station to support multi-EOAT concept for BAM applications.

The docking system was especially introduced as an automation enabler, facilitating efficiency via automatic tool interchanges between contiguous BAM operations involving large components. Furthermore, controlling human-machine interactions in this manner can improve operational safety. This system includes the master tool changer, which is attached directly to the robot, as shown in Figure 4-15, and can accommodate any new EOAT introduced to the BAM system, by interfacing with secondary units attached to different tools. However, only two end-effectors are presently integrated; a TOPTIG™ EOAT, which enables the MAM process, and a 3D scanner, for geometric and/or surface inspections.

Based on the multi-tool concept for end-to-end BAM operations, which was consistent with specifications for a digital platform (Figure 4-10), the plan was to have the MAM EOAT docked alongside other tools supporting non-MAM operational requirements. However, due to developmental considerations, mainly the cost and time implications when developing the solution for connecting and disconnecting supplies (i.e. power, air, etc.), to switch between EOAT, a compromise was necessary. Effectively, the MAM tool was docked at the base of the robotic subassembly, which negated the imminent need to resolve connection and supply issues. In contrast, the modularity of the 3D inspection EOAT was ideally suited to the multi-tool concept, as it was designed to be utilised as a handheld or mounted solution, making it relatively easy to integrate this item. Presently, and in addition to existing tools, the docking station can accommodate three additional end-effectors or EAOT, to support BAM operations.

4.4.6 Component manipulation

The specification for the bespoke manipulator was comparable to the semi-automated COTS solution, previously implemented in stage one (Figure 4-13). However, while the earlier focus was on establishing basic BAM system capabilities, stage two was mainly concerned with ensuring the full integration and co-operation of relevant modules or subassemblies. Thus, practicality was a key consideration when developing the functional design specification for the customised manipulator. The implementation approach was relatively straightforward and involved siting the COTS manipulator in its designated position, which was maintained when swapping this component for the customised solution, as shown in Figure 4-16.

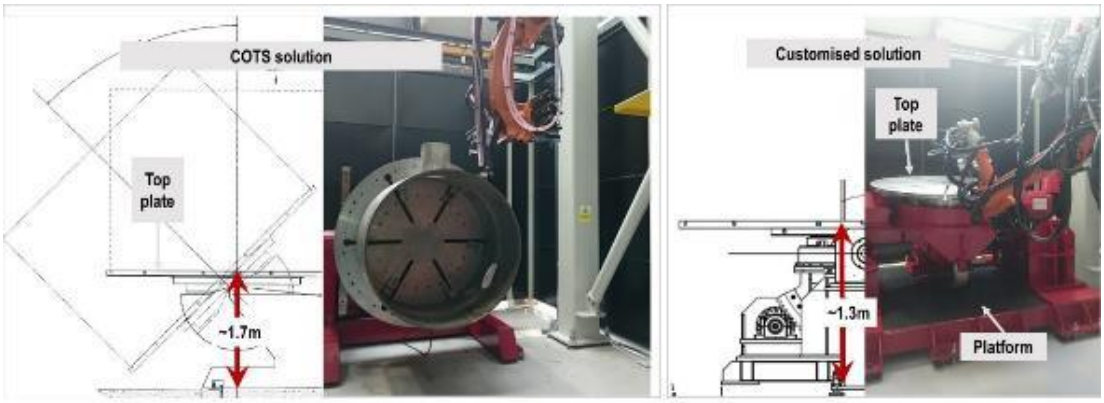

Figure 4-16: Transition from COTS to customised solution for fully integrated BAM system.

Relative to the COTS solution, the customised manipulator, which was reduced in height, and more closely aligned with the concept requirements. This reduced height requirement was influenced by considerations for access to the build platform during BAM, and improved specific operations, including equipment set-up procedures. The main differences between the COTS and customised solutions include the dimensions, as the width of the customised solution was lengthened to accommodate the reduced height requirement, and the operational aspects. This 2-axis item was also integrated as an external secondary unit of the 6-axis articulated robot. Following the integration of the 3-axis gantry robot, available unique 'E' identifiers were similarly assigned to each axis of the manipulator, resulting in the fully integrated 11-axis BAM platform.

4.4.7 Virtual platform

The objective of this stage was to implement a digital solution that accurately detected and monitored key variables, which was a crucial step toward achieving the envisioned concept for controlling the BAM process (Figure 4-10). The underlying logic was that the ability to detect, monitor and acquire process data, would establish a basis for the proposed control strategy, thus facilitating the forecasting of process performance and associated issues. The current solution is presented in Figure 4-17.

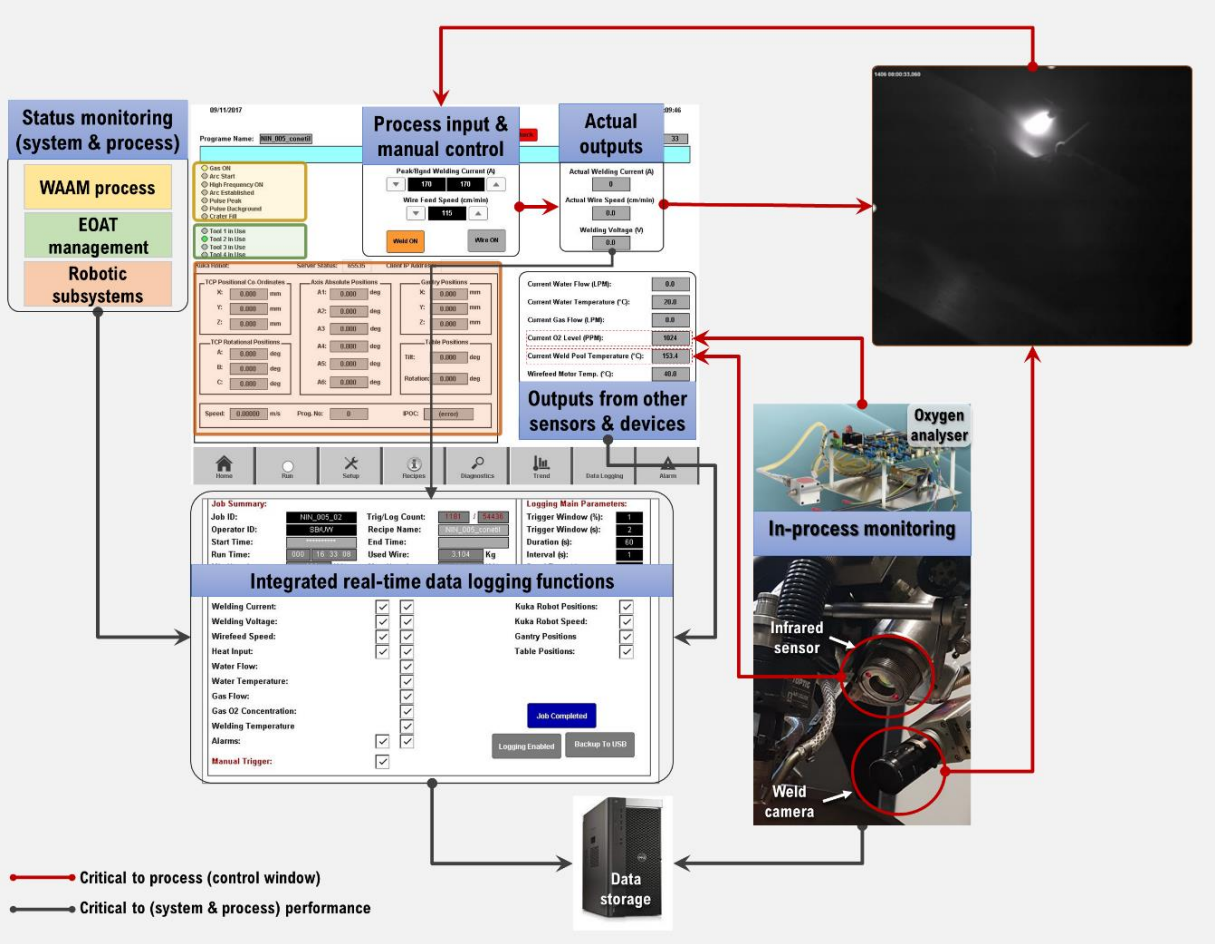

Figure 4-17: Implementation of BAM virtual platform concept.

The basic solution was developed in relation to specific BAM requirements, and in consideration of broader issues affecting MAM process control strategies. However, previously highlighted internal and external constraints influenced the management approach for this phase. Essentially, the concept requirement was based on an adaptable solution, comprising the basic elements for establishing the foundations on which future requirements could be developed. The platform also allows for the monitoring of BAM operations and the system status. During the WAAM process, the functions of the GTAW equipment, including the arc properties, are closely monitored. The digital platform also indicates which tool is currently selected via the EOAT management functions, using designations that correspond to the current capacity of the tool docking station (Figure 4-15), and tracks the current position of the EOAT, relative to the workpiece, and via the movements of the gantry, robot, and manipulator. Presently, the outputs from detection capabilities, including infrared sensors and other devices, are manually tracked, to determine when interventions may be necessary, to improve process and output quality. Although detection and monitoring capabilities are basic, they enable the operator to exercise a degree of control over the process. Furthermore, this digital solution has facilitated the integration of the requisite system and process perspectives, allowing for the acquisition of real-time process data, to facilitate historical analysis and predictive studies, notwithstanding the potential to support future development plans for large-scale MAM.

4.5 Post-implementation analysis

The main purpose of this section is to provide details about post-implementation activities that were undertaken prior to the validation of the BAM system. The main objective was to establish that the functional requirements for the BAM system had been met, while exploring other relevant considerations influencing the development of MAM systems and procedures. Hence, a systems approach was adopted for this phase.

In systems engineering, black boxes are simplistic models used to describe complex systems at high levels of abstraction, and may be implemented, with or without complete knowledge of all system mechanisms. The black box approach was adopted during the evaluation of BAM system functions. Subsequently, other related systems approaches were used to analyse interdependencies between system variables, systemic events, emergent traits, and causal factors. The primary aim was to enhance understanding of how BAM system inputs, and functions, were transformed into desired outputs.

4.5.1 System dynamics

The system dynamics approach was used to explore dependencies between distinct BAM system variables. As with previous systemic investigations, and consistent with the overall research strategy for developing the GT framework, the system, component or application, and process perspectives, were separately explored. These distinct perspectives were represented at three levels, namely the global, intermediate, and local levels, which were used to organise associated variables, when mapping system boundaries. As part of this process, dynamic models were constructed to clarify interrelationships and interdependencies between system

variables, which was useful for understanding how systemic events and traits are derived. Furthermore, and considering the potential for information asymmetry concerning MAM systems, these models also facilitated the comparative evaluation of core BAM operations, ensuring that attributable causal relationships in MAM systems were correctly characterised.

4.5.1.1 Functional testing

The black box approach allowed for the clarification of BAM system functions and was specifically explored via acceptance test (i.e. FAT and SAT) protocols, which were implemented during the outlined development and integration phases (Figure 4-13). In order to establish the functional state of the integrated system, pertinent documentation, including BAM concept requirements and specifications (Table 4-9 and Table 4-10), OEM product specifications for COTS solutions, and the FDS used for customised solutions, were reviewed. Afterwards, internal documents were specifically created to support the evaluation process [391–393]. The black box implementation strategy for the BAM system is depicted in Figure 4-18.

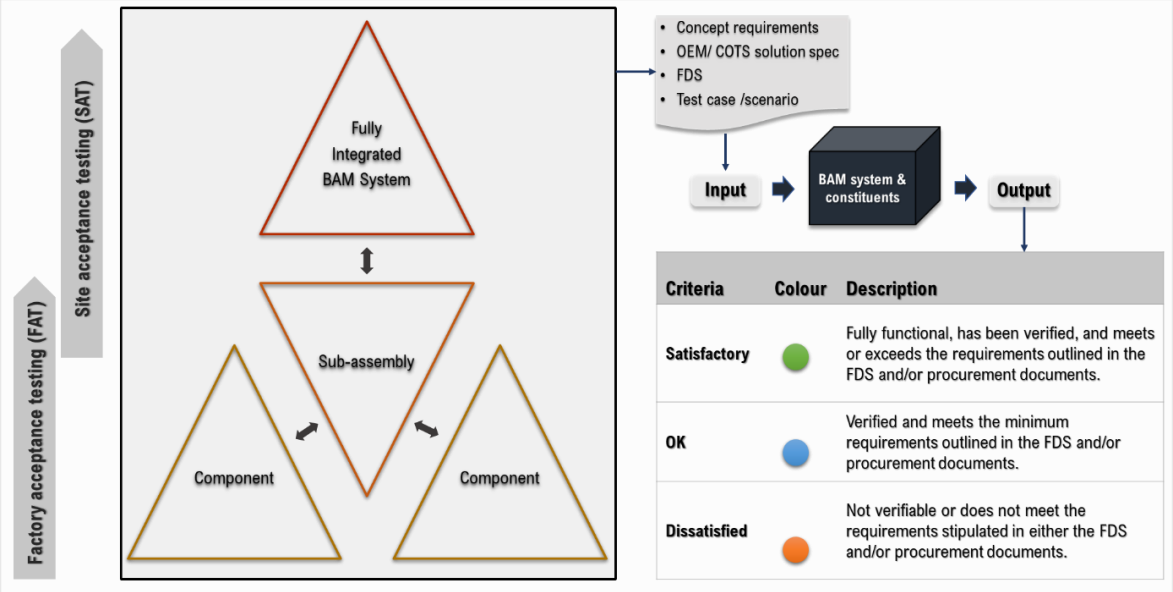

Figure 4-18: BAM functional testing strategy and related system acceptance criteria.

Actual acceptance testing procedures involved specifying the functions to be observed, which were the designated inputs for the black box, observing these functions during SAT and FAT activities, and interpreting test results or black box outputs. For customised solutions (Figure 4-13), it was also necessary to evaluate certain constituent elements upon which the fully integrated system functionalities were predicated. Thus, specific black box tests were implemented as building blocks, whereby individual system components or modules were situated at the base, subassemblies at the intermediate level, and the fully integrated BAM system at the highest level of the pyramid (Figure 4-18).

The FAT phase was limited to witnessing basic system functions, due to the availability of different components, including subassemblies or modular solutions from different suppliers. For FATs, the emphasis was on customised HPAs, while SAT procedures involved designing test cases or scenarios as needed, to assess separate or integrated system functions. In all instances, the focus was on establishing a simple and clear basis for justifying the developmental progression from procurement to fully functional system. Correspondingly, acceptance criteria were defined prior to the implementation of functional tests. The criteria were rudimentary, but adequate, when considering the level of abstraction, and the relatively limited scope typically associated with functional tests. The specific functional tests that were completed for this development, corresponding to previously outlined building blocks or pyramid levels, are depicted in Figure 4-19.

Figure 4-19: Black box implementation status following FAT and SAT protocols.

FATs may be performed on fully integrated equipment, but due to the nature of open architecture developments, it was not possible to do so for the BAM system, with FAT activities remaining at the base (i.e. component) and intermediate (i.e. subassembly) levels. SAT activities were typically implemented at the intermediate and highest (i.e. BAM system) levels of the pyramid. For development instances where there were no corresponding FAT activities, the outlined testing strategy (Figure 4-18) was still maintained, such that associated subsystems or components were properly isolated, for separate on-site verification testing. Subsequently, these isolated elements were (re)integrated before evaluating overall system functionality. Occasionally, certain system functions, such as those associated with the virtual platform, could only be evaluated on-site, after all other system inputs had been fully integrated. Under these circumstances, extended

test protocols were initiated, typically in response to issues that were observed to impede system functions [392]. In general, the goal was to ensure that the requirements for the desired functionality had been met, and that the test outcome was either ‘OK’ (i.e. blue) or ‘satisfactory’ (i.e. green), as outlined in the acceptance criteria (Figure 4-18).

The decision to proceed with FATs was mainly influenced by the maturity of the solution and related costs. Essentially, if a non-COTS solution and HPA was being developed, then FAT was completed, otherwise, on-site testing was acceptable. On this basis, the customised positioner (Figure 4-16) was the only component-level solution that was evaluated in a factory setting. However, the actual FAT was limited in scope because integrated system functions could only be evaluated on-site, after installing the positioner. Consequently, an orange status was initially awarded after FAT proceedings, and eventually upgraded to green, after completing functional tests on the fully integrated system.

At the intermediate level, basic factory tests were completed for the robotic and GTAW subassemblies or modular solutions. A blue status was awarded, after robotic subassembly tests, indicating minimum requirements had been met, while the GTAW module and COTS positioner remained orange, because it was necessary to upgrade both items to meet concept requirements, as outlined in the system development and integration timeline (Figure 4-13). Furthermore, it was not possible to safely verify GTAW functions due to factory limitations. Hence, related components were isolated during the SAT, to allow for the evaluation of specific functions, before re-introducing these components, and verifying integrated functions. This progressive approach was adopted for assessing both WAAM and 3D inspection functions, and further substantiated lower-level tests, allowing for the upgrade of overall system status from ‘OK’ to ‘satisfactory’.

The virtual platform is conceptually equivalent to the fully integrated BAM system, hence positioning it at the highest-level. As previously stated, it was not possible to assess virtual platform functions until all associated components or inputs, which includes the outputs from all relevant solutions supporting the core processes presently integrated, were accessible. Thus, SAT protocols were implemented after actual supporting functions were verified. The initial focus was on the WAAM process because the virtual solution was primarily developed to support GTAW operations, and was upgraded by the developer, to accommodate the EOAT concept, and related management functions derived from robotic subsystems and monitoring features. However, only minimum concept requirements were fulfilled, with the overall test status of ‘OK’.

During the implementation of the functional test strategy, different factors were observed to have varying degrees of influence on acceptance test proceedings. For instance, capacity was a recurring issue, observed at distinct facilities in which the FAT procedures were completed. The overall height of the BAM system (Figure 4-14) could not be accommodated, due to the restricted building capacity or headroom at the test site. Similar restrictions necessitated supplementary arrangements on the part of another supplier, due to the overall mass of the customised positioner (Figure 4-16) exceeding the site lifting capacity, thus underscoring the

significance and implications of capacity issues on large-scale operations. The interrelationships between suppliers also had a significant bearing on the integration states of solutions, which ultimately influenced the outcomes of functional tests. In general, similar technologies from different suppliers were relatively easier to integrate, and test, when predefined roles and responsibilities were agreed by all parties. Conversely, insufficiently clarified expectations, such as the need for appropriate access to interrelated system elements by all developers, provided greater scope for competition, which impeded efficacy and impacted progress. These issues emphasise the need for a higher degree of standardisation, whereby technology integration experiences are less subjective, to the interrelations and perspectives of development partners, but remain focused on the interfaces and cooperation between the technologies that are supplied. Understandably, there are various commercial, legal, and other related factors influencing these observations, including the competitiveness of individual organisations in the supply chain. Invariably, and as observed during the development of the BAM system, these factors can impede the pace of development for both OA and commercial MAM technologies, potentially narrowing the integration focus, even when distinct technologies may have exceeded requirements.

4.5.1.2 System boundaries

In system dynamics, the identification of key variables is a crucial initial step when exploring the boundaries of a system, and was facilitated by combined insights from literature surveys, preliminary studies, and FAT activities. Determining how WAAM inputs effected changes, in response to interactions between variables, at different levels of the system, was especially important due to its hierarchical position in this development. Hence, the main emphasis was on WAAM, with 3D inspection operations providing a comparative basis for understanding systemic issues at the global, intermediate, and local perspectives.

The global perspective and related boundaries encompass the variables and interrelationships that are typically observed at the integrated system level. Evident variables and interdependencies include the supporting infrastructure, raw materials, supplies, processing requirements and individuals that provide the necessary global inputs. At this level, some interactions, such as the component and accompanying data, are transitory, because they typically interact with the system for a specific purpose, and are subsequently removed, or permanently excluded from the system boundaries afterwards. Whereas other inputs, such as the manipulator, are classed as permanent fixtures within the system, these inputs are also subject to transitory changes. For instance, when contemplating changes within system boundaries at this level, the manipulator state is altered when a component or substrate is introduced, prior to the initiation of core WAAM or 3D inspection operations, thus affecting its load bearing capacity. Similarly, the supplies (i.e. power and compressed air) required to effect changes to the manipulator state, and also for WAAM and 3D processes, are transitory. These inputs are initiated in response to processing or component requirements, and affect interactions observed beyond this perspective. The integrated BAM system perspective is depicted in Figure 4-20.

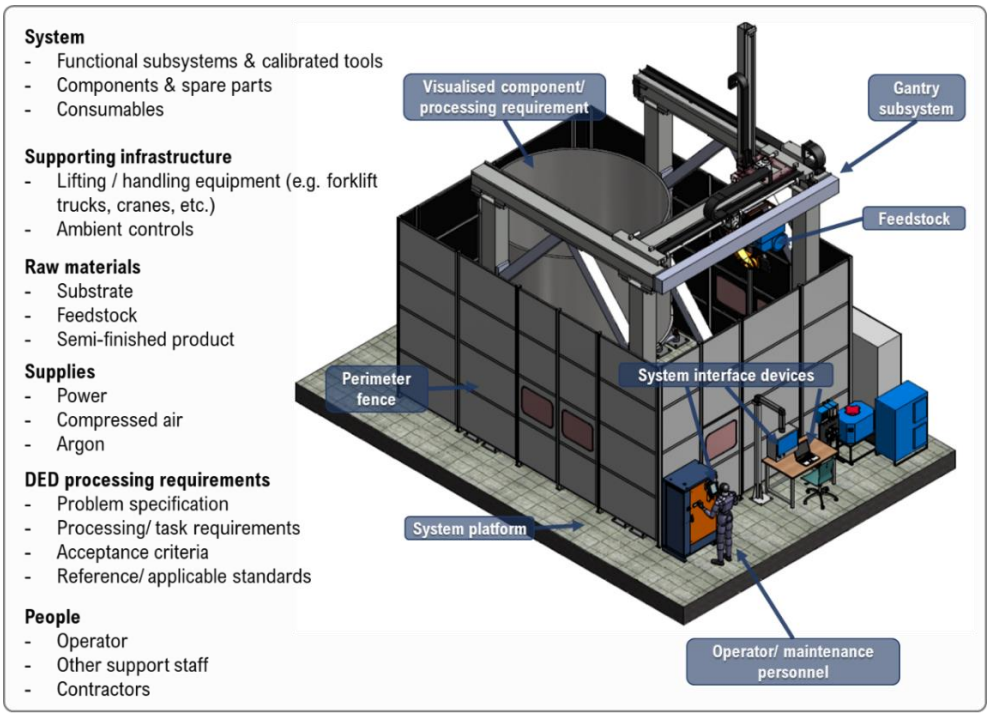

Figure 4-20: Typical interactions observed within global system boundaries.

The intermediate perspective was focused on interactions at the component level, as shown in Figure 4-21. The processing requirements and specifications (Figure 4-20) drive changes at this level. In response to task requirements, the component is prepared accordingly by introducing new elements to the system, such as the dial test indicator (DTI) and clamps, necessary for aligning the component and securing it to the manipulator. However, these intermediate elements are also transitory, and typically excluded at the appropriate juncture.

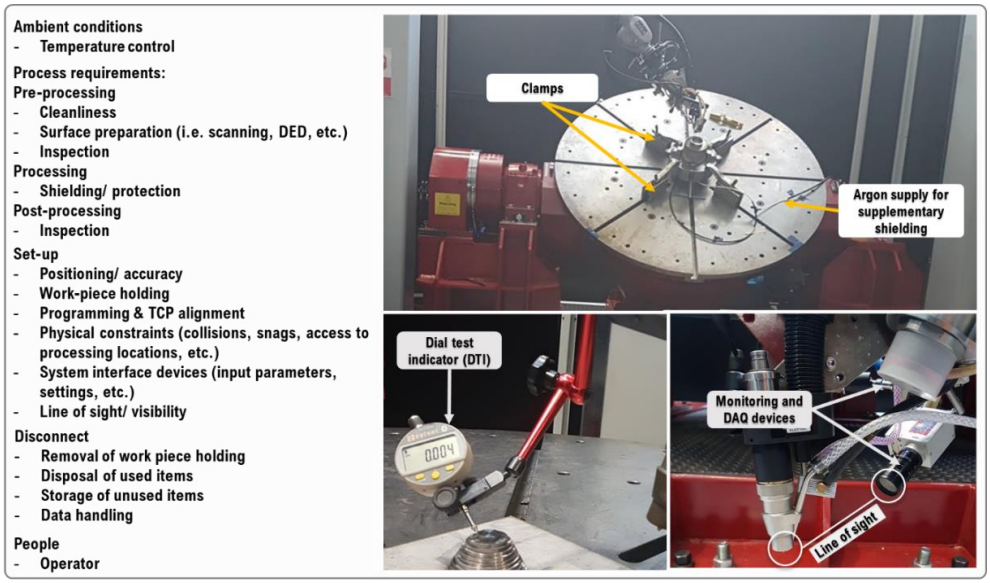

Figure 4-21: Intermediate perspective on typical interactions at the component levels.

While the DTI is removed as soon as the component is properly aligned and securely clamped onto the manipulator, the clamps remain in position, fulfilling an important purpose within the intermediate

perspective. Similarly, the manipulator, which is now positioned at an appropriate angle to facilitate access, has attained a new operational state, further changing the characteristics of this subsystem. Specifically, and relative to the previous state, the load bearing capacity of the manipulator is influenced by its current state and will be similarly affected by any further changes to its intermediate orientation and/or movements. Relative to the 3D inspection process, which is mainly about obtaining information, the WAAM process adds material to existing structures, or the build platform. At the targeted operating scale for the BAM system, such additions represent significant intermediate level changes. Likewise, the requirements for supplies, such as argon and power (Figure 4-20), as well as the intensiveness of the operation, will result in further systemic changes. Compared to the 3D inspection process, these requirements will be more substantive for WAAM, with longer processing durations reflected, for instance, in both higher energy requirements and power consumption patterns, notwithstanding the raw material inputs required for the deposition process.

Exploring the interdependencies between subsystems and modules at this level also highlighted the cascading effects of global events, such as the introduction of a component, on intermediate system functions. In this instance, the manipulator facilitates the positioning and alignment of the component, thus enhancing accessibility during core operations. However, these actions equally and directly affect the manipulator capacity. Thus, the potential impact of such intermediate state changes, particularly in relation to process reliability and other measurable in-situ and ex-situ manifestations of manufacturing quality, necessitate due consideration, particularly for larger components and associated protocols.

Activities at the global and intermediate levels, are usually completed while the system is in a limited operational state. Conversely, interrelated local processing phenomenon and conditions are specific to integrated processes and associated EOAT requirements. These elements represent the most critical level of the system, due to the proximal and direct influence on process outcomes. For WAAM and 3D inspection operations, proximity was defined relative to the melt pool vicinity, and scanning regions respectively, where the cumulative effects of global and intermediate events are most evident.

At the local level, system input parameters are typically determined by 3D inspection or WAAM processing requirements, with monitoring devices facilitating both in- and ex-situ observations. Specifically, sensory devices receive real time inputs based on local state changes, such as an increase in component temperature, with feedback from these devices initiating further actions, by the system and/or the operator functions. These actions, which allow for changes to input parameters, are aimed at improving system performance and/or process consistency. When acquiring monitoring data or measurements from permanent devices, which include all sensors associated with the WAAM process, as well as during 3D inspections, when this process is enabled, actual objects are requisite change agents. In other words, there must be an object undergoing changes at this level. Hence, measurements are classed as transitory system elements because they are dependent on changes to the state or condition of objects within local system boundaries. However, the measurements obtained from these events result in the creation and accumulation of both usable and unusable data, which

initiates further actions at intermediate and global levels. These actions necessitate additional resources for handling, processing, and storing pertinent system, process, and component data, which has broader implications for MAM activities that are likely to be more pronounced at scale, notwithstanding contributions that are directly attributable to manufacturing endeavours. While the latter was beyond the scope of this study, each level of the system was further explored based on the dependencies between identified variables. The local perspectives for the WAAM and 3D inspection operations are depicted in Figure 4-22.

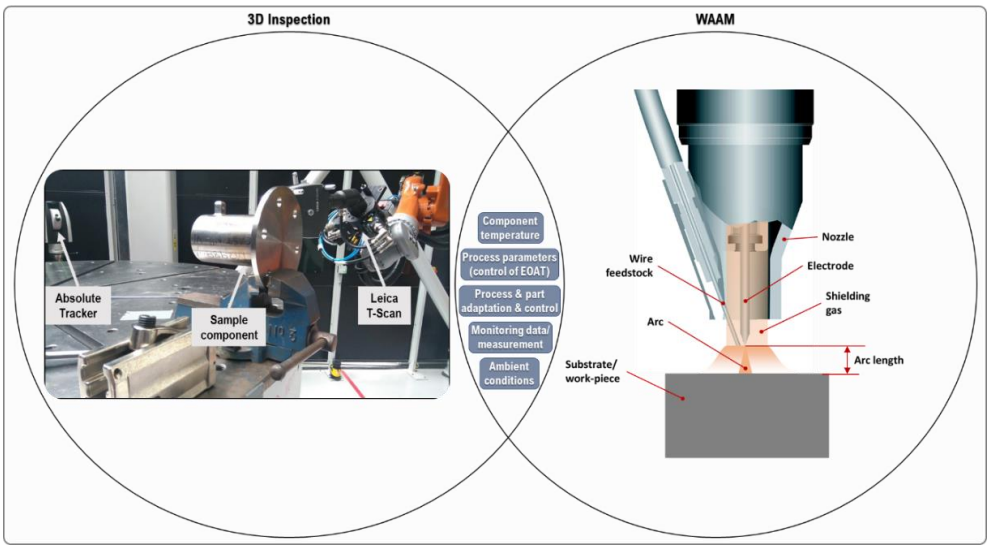

Figure 4-22: Local perspective on typical interactions observed at the process level.

4.5.1.3 Process interdependencies

In system dynamics, the premise on which attributable causal relationships are established, between time dependent variables, is important for demonstrating that correlations and dependencies do exist. Hence, the interactions within defined system boundaries were explored, relative to the global (Figure 4-20), intermediate (Figure 4-21), and local (Figure 4-22) perspectives, to clarify dependencies between selected variables. Focusing on events likely to influence systemic behaviours, the relative effects of specific actions were explored via core BAM operations, and distinct system variables associated with the WAAM and 3D inspection processes. The methodology involved mapping how the system handled specific inputs, such as the feedstock for WAAM operation, to produce the desired output, before establishing dependencies between the distinct system elements involved in this chain of events.

Logic tools are typically used to model discrete events, and process dependencies, and were adopted for creating the stock and flow diagrams, which depict the primary feedback loops in the BAM system. *Stocks* or *accumulators* are defined as the elements of a system that can be accumulated or depleted, while *flows* are transitional elements whose discrete and time-bound actions induce measurable changes (i.e. increase or decrease) to *stocks*. In other words, *flow* behaviours are attributable to *stock* events. In this study, *stocks* represent the BAM subsystems or modules that change states during the operation of the system, while *flows*

are the elements, which may be tangible or intangible, that induce change. The stock and flow diagram for the WAAM process is presented in Figure 4-23.

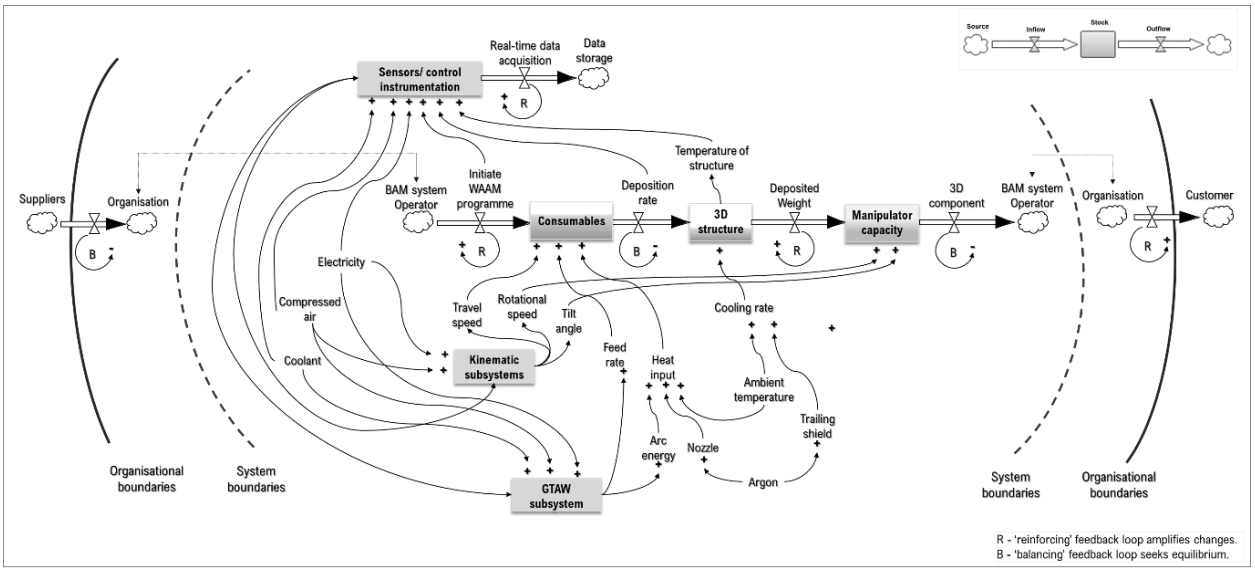

Figure 4-23: Basic representation of systemic events during WAAM operations.

Using the global, intermediate, and local perspectives as inputs, variables were organised according to the type of element (i.e. stock or flow) being considered, before connecting relevant feedback loops. Connections were used to establish associations between specific variables and events, to facilitate the identification of systemic patterns of behaviour. The different types of elements and interactions are presented relative to their direct influence on the WAAM process. The diagram illustrates the chain of events that are set in motion when the system is utilised for deposition or build operations, how these events are connected, and the consequent effects. Accordingly, the focus was on the aspects of the system directly observed during the WAAM process, as well as the broader links and supporting infrastructures enabling specific events. For instance, the manipulator load capacity is not presently monitored, but at the targeted scale, the load distribution will become increasingly important, as the build characteristics (i.e. mobility, size, and mass) of the deposited part change, thus affecting the behaviour of this system variable. Furthermore, changes in the part manipulation strategy, during deposition, are likely to affect the melt pool behaviour or flow characteristics of the molten material. When planning the build strategy, and based on these examples, such insights may be incorporated to ensure that the specified load limits are not exceeded, at the global level. At the local level, the strategy may also be adapted to ensure that material flow characteristics, due to any positional changes required at different locations of the build, are fully accounted for, at the intermediate or part level. Another example is the global and local temperature of the part or structure, which changes over time, in response to the sustained or reinforced application of heat during the WAAM process. Tracking this event can support the development of a control strategy that properly anticipates the causal effects of this event within the system boundaries.

The stock and flow diagram for the 3D inspection process is presented in Figure 4-24.

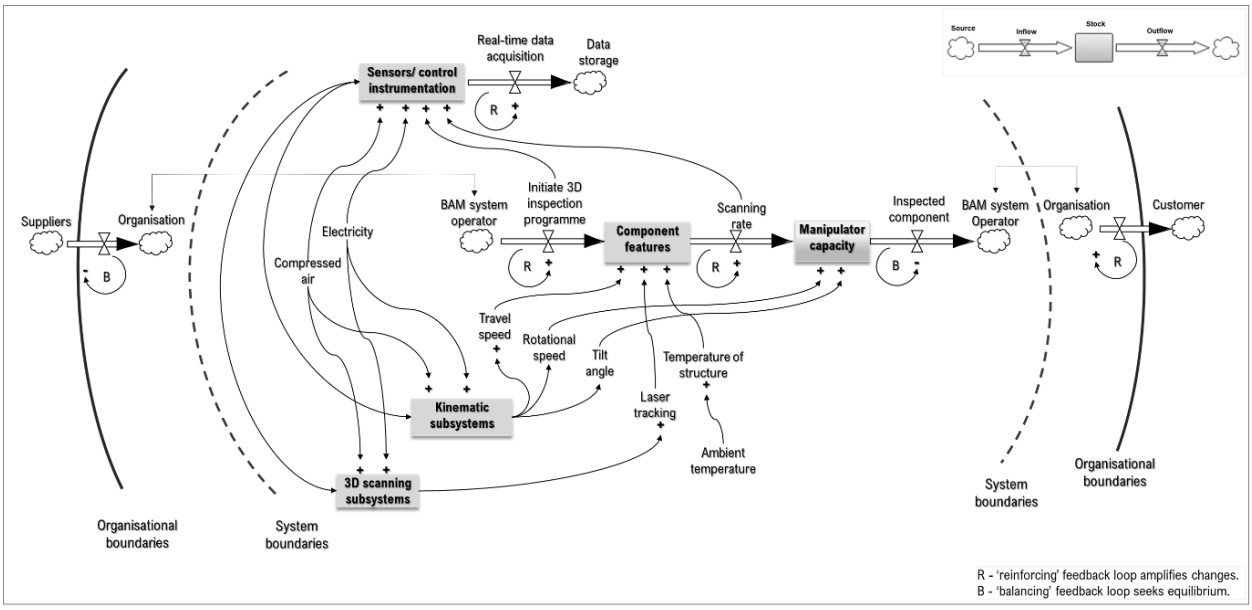

Figure 4-24: Basic representation of systemic events during 3D inspection operations.

For automated inspection operations, where both field of view and line of sight remain critical for vision systems, the focus was on events encapsulated within the local perspective. Although there were relatively fewer variables to consider when mapping inspection operations, systemic interactions for both inspection and WAAM operations were comparable, because the BAM system is fully integrated. For operations involving a specific component, the systemic requirements for WAAM, including the combined energy and resources utilised during the process, and any resulting data and by-products generated, are likely to be more intensive when compared to the inspection process. On the other hand, the scanning approach can result in the accumulation of substantive amounts of data, requiring necessary computational resources, to support both integral and related inspection activities, including data management strategies, more efficiently.

The basic stock and flow diagrams, introduced for the WAAM and 3D inspection processes, may be converted into simulation models, to assess different application scenarios, and further enhance understanding of the potential effects of systemic changes. The simulation models can support the analysis of connecting system events, and potentially enhance understanding of changes that may occur, due to the requirements for pre- and post-processing operations on WAAM components and end-use parts. Within defined system boundaries and envisioned applications, such models can also facilitate the evaluation of interactions involving typical system elements, as well as possible reconfiguration events. For the GT framework, the focus was on clarifying the relative differences between core BAM operations, to support inferences about the variables, events, and behaviours attributable to the MAM process.

4.5.2 Performance analysis

Requirements for manufacturing systems, such as the BAM platform, and the initiation of subsequent actions and operations in response to these requirements, usually precede systemic events and mapped behaviours.

Hence, the initial focus was on describing the current actions and operations that can be initiated within established system boundaries, and to enhance understanding of the system behaviour, relative to anticipated activities. A manufacturing capability map was used to depict the ideal workflow and strategy for MAM structures, involving both pre- and post-processing considerations. Supported by core development objectives, the purpose was to streamline contiguous tasks and resources (Figure 4-1) around typical manufacturing requirements. The BAM system capability map is depicted in Figure 4-25.

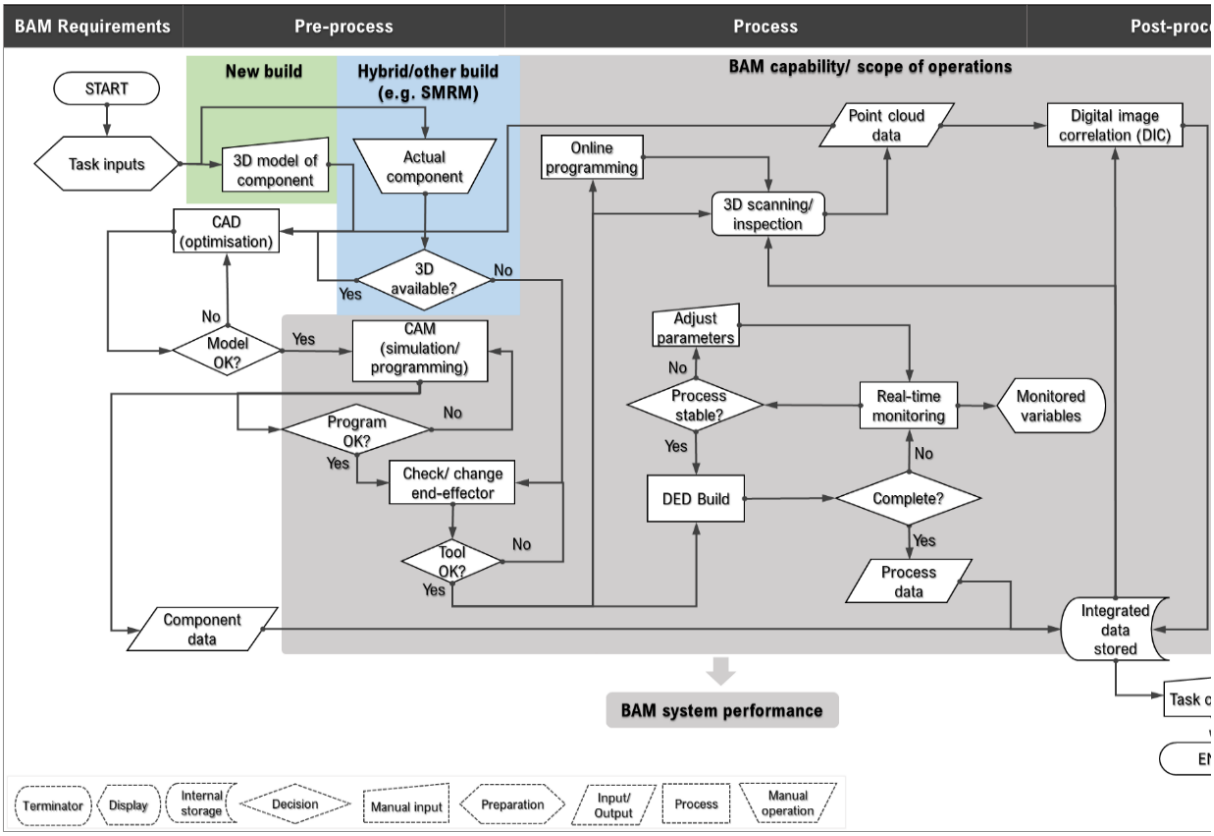

Figure 4-25: Mapping the BAM system capability and process workflow.

The map elucidates how BAM system capabilities were strategically organised, relative to the requirements for industrial MAM components, and corresponding tasks and operations that can be completed. Presently, the system can receive digital inputs in the form of CAD models or tangible objects, such as substrates, or components for hybrid or SMRM operations. The CAD inputs can be processed, utilising accessible digital capabilities (Table 4-10). The digital outputs derived from this phase enable the generation of requisite inputs, such as the toolpaths used for the deposition or inspection of 3D objects. Correspondingly, the 3D inspection EOAT can directly generate inputs (i.e. point cloud data or scans) from actual components, which may be utilised to initiate the BAM process. In the absence of suitable CAD data, which is typical of some envisioned application scenarios, particularly for SMRM, the direct data generation approach is advantageous. For hybrid builds or reprocessing applications, including SMRM, the inspection EOAT can also be utilised to verify actual component dimensions and tolerances before the WAAM process. Post-deposition, this capability can

facilitate the comparative assessments of geometric quality and/ or dimensional accuracy, based on pre-existing component information, such as scans, or, if available, CAD models. The current scope of operations is also depicted in Figure 4-25, to highlight some of the factors influencing the BAM system performance.

Having mapped the overall system capabilities, based on WAAM and 3D inspection operations, other Six Sigma tools were adopted for subsequent analyses. Specifically, the stability and capability of these BAM processes were investigated, to enhance understanding of correlations between the product output quality and important process characteristics, derived from the system and its established functions. Stability is a measure of process consistency, while capability is used to assess variations in a process, relative to its specifications. Stability and capability assessments were also useful for establishing the product or output specification limits and obtaining insights about systemic traits. Technically, system variables influence process consistency, which affects Six Sigma product quality. In practice, the product specification limits are dictated by the customer, with important characteristics governed by actual applications and stipulated requirements, such as agreed tolerances. However, process control remains within the manufacturer's purview, hence the goal was to assess stability and capability, including systemic aspects, before proceeding with validation activities.

4.5.2.1 WAAM process

Since there are other factors influencing the WAAM process, particularly within an AMR context, the objective was to assess process consistency in relation to important systemic functions. Configuration elements (Table 4-5), including the energy source, automation, and feedstock, were considered for capability and stability assessments, because essential WAAM functions, namely the arc energy, EOAT travel speed, and wire feed rate inputs, are derived from these components. The heat input for the WAAM process is derived from an electrical arc energy, which is a function of the travel speed, current, and electrical potential difference, or arc voltage. From a systemic standpoint, arc stability is influenced by the consistency of the input current and voltage, as well as other interrelated system and process parameters that ultimately influence output quality. In essence, the arc energy is an important variable whose characteristics facilitate the uniform transfer of the wire feedstock during WAAM operations. Thus, the wire feed and arc energy were selected for evaluating the stability of the process, which normally precedes process capability assessments.

The process consistency was assessed by quantifying variations between discrete measurements of actual (output) and set (input) values used for the WAAM process. Using a ∅3.2 mm electrode, at a fixed arc length of 3mm, corresponding to a voltage input value of 13V, discrete measurements obtained during the deposition of 250mm single beads were analysed. While the wire feed, current and travel speed input values are typically set independently, and prior to deposition, the voltage is associated with the arc length or distance between the tungsten electrode and the work piece (Figure 4-22), as well as other interrelated variables such as the inert gas chemistry, and is set using a fixed gauge. The summary data for the process is presented in Table 4-12.

Table 4-12: Sample data for evaluating WAAM process characteristics.

Wire feed rate (mm/min)		Current (Amps)		Voltage (V)	Travel speed (mm/min)
Set	Actual	Set	Actual	Set	Set
1000	998	160	163	13	960
900	899	200	200	13	1200
800	800	180	182	13	1200
800	802	180	181	13	840
750	752	150	150	13	840
1000	1002	155	153	13	840
1000	1001	200	199	13	960
800	800	200	198	13	960
700	703	160	162	13	1200

The voltage (V), current (I), and travel speed (v) are components of the arc energy. Hence, systemic variance was analysed in relation to the arc energy and the wire feed rate. The arc energy (AE) was derived according to the equation in ASME Section IX and AWS D1.1 2020, which is expressed as follows:

$$AE = \frac{60VI}{1000v} \left(\frac{kJ}{mm}\right) \tag{4-7}$$

After determining the AE, the variance between the set and actual values, for both the wire feed rate and AE, were calculated. While set and actual values were utilised when evaluating the wire feed rate (WFR), the voltage and travel speed were fixed (Table 4-12), thus derived AE values were based on the difference between the set and actual current for this phase. The WAAM variance charts are presented in Figure 4-26.

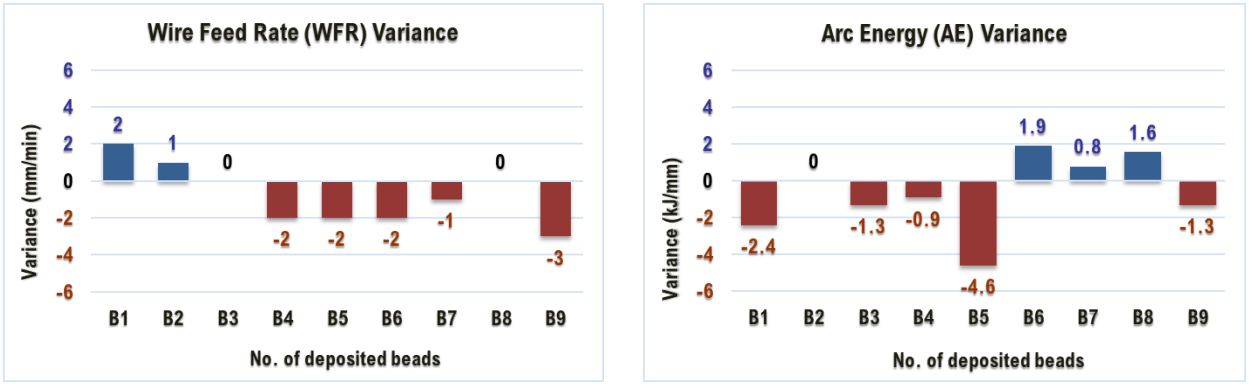

(a) (b)

Figure 4-26: Analysis of WAAM (a) wire feed (b) arc energy variance.

The charts revealed that for both the wire feed rate and AE variables, actual values were generally higher than the requested or set values. For the WFR, the maximum and minimum variance of 2mm/min and 3mm/min appears to be negligible for the range of values investigated (Table 4-12), but the cumulative effects may prove significant, depending on the specific applications, and as more layers are deposited over time. Similarly, the significance of the maximum (0.002 kJ/mm) and minimum (-0.005 kJ/mm) AE variances, depends on the application, but were deemed insignificant in this case, due to the very low values recorded. However, the heat

input is usually tailored to the requirements of the material being processed, such that if the AE variance is within the recommended range for a specific alloy, then the likely effects on the outputs will be negligible. Nevertheless, it was evident that for these important variables, system outputs or actual values tended to be higher than the requested or set values. Hence, control measures are necessary, particularly for the heat input. Although the AE is the main variable driving heat input fluctuations, efficiency is determined by how much of the supplied AE is converted during the WAAM process. Thus, key influencing factors, include the component design, the base technology (i.e. GTAW) enabling WAAM, and processing environment. Ultimately, it is the dependencies between these system, process, and application variables, that govern WAAM operations and outputs.

The stability of the process was also evaluated in relation to the WFR and AE variables. In Six Sigma, stability is inferred from statistical process control (SPC) charts, after determining the mean (μ), upper control limit (UCL), and lower control limit (LCL) values for the process. Also known as Six Sigma lines, the UCL and LCL represent the statistical process or tolerance limits, which should be plus or minus 3 Sigma (±3σ) for a well-controlled process. The tolerance limits were calculated as follows:

$$UCL = \mu + 3\sigma$$
$$LCL = \mu - 3\sigma \quad (4\text{-}8)$$

SPC charts were plotted for the WFR and AE variables using the discrete WAAM data set presented in Table 4-12. The resulting charts are presented in Figure 4-27.

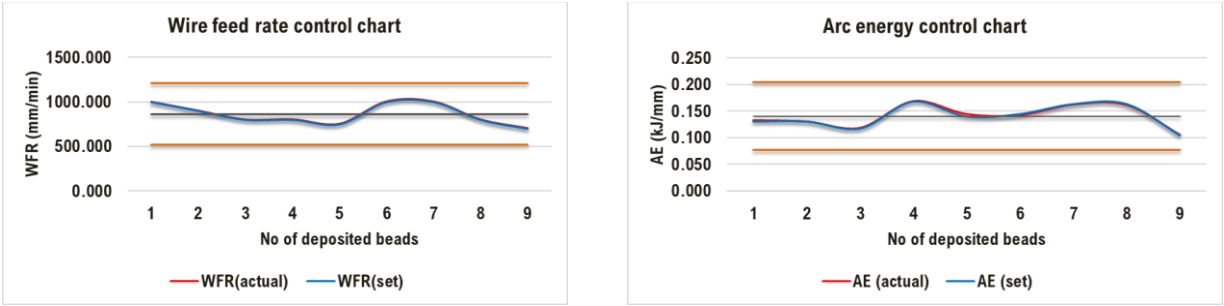

(a) (b)

Figure 4-27: Process control chart for (a) WFR and (b) AE variables used for single layer deposits.

For both charts (Figure 4-27), variations were observed around the centre line (μ), but for distinct variables, maximum and minimum values were within the desired control limits, with UCL and LCL values of ~73J/mm and ~253 J/mm for the AE, and ~1203mm/min and 514mm/min for the WFR. While common cause variations are typical, and thus expected in statistically controlled processes, other variations, including unpredictable or inconsistent responses that exceed control limits, may be indicative of abnormalities. These non-common or special cause variations typically warrant further investigation, to identify underlying causes. Nevertheless,

the control charts, derived from this discrete WAAM data set, revealed that important characteristics were within specific control limits, thus demonstrating the stability of the process, while establishing a basis for tracking and continuous improvement of BAM operations.

4.5.2.2 3D inspection process

Relative to the SMD system, with preliminary studies providing insights into WAAM operations and important process variables, the lack of contextually relevant data was a key consideration when evaluating the 3D inspection process. Introduced to support WAAM operations, the developmental objective was to define important inspection characteristics, derived from inspection requirements, covering pre- and post-processing tasks, as depicted in the BAM capability map (Figure 4-25). The empirical aim was to generate preliminary inspection data for comparative analysis, whilst exploring systemic factors influencing inspection procedures. Correspondingly, it was important to enhance understanding of factors in the implementation of the concept and approach for utilising interchangeable EOAT to support contiguous MAM operations.

A pre-existing hybrid-SMD component, created by depositing a flange and boss onto a solid round bar [63], was selected because it included a variety of protruding and recessed features, as well as relevant surfaces that were suitable for both new and hybrid WAAM builds. The combination of surfaces and features typified possible inspection scenarios envisioned for the BAM system and was broadly representative of inspection challenges likely to be encountered. The hybrid SMD component is shown in Figure 4-28.

(a) (b) (c)

Figure 4-28: (a) CAD model for fabricating (b) hybrid-SMD component to support (c) 3D inspection analysis.

It was assumed that the selected SMD component (Figure 4-28(b)) was representative and accurate, relative to the original CAD model (Figure 4-28(a)), and the inspection outputs generated from the component. Inspection data (Figure 4-28(c)) was obtained according to specifications, using both the BAM system, and a coordinate measuring machine (CMM), which provided a basis for comparison. Although access to the CAD model ensured that accuracy was independently verifiable, it was recognised that in some instances, such as for SMRM actions involving obsolescence issues, reverse engineering may be the only viable option. For

scanning operations, complete component data was required to facilitate analysis of the areas of interest. This requirement dictated the implementation of distinct scanning operations and tasks, such as the part orientation and EOAT configuration, mainly to ensure that line of sight was maintained, when acquiring data from the mounted component (Figure 4-22). Multiple 3D scans were obtained by manually rotating the component between scans, before capturing data from targeted surfaces and features as necessary. Subsequently, the different scans were merged, to create a single 3D object, as shown in Figure 4-28(c).

For the CMM process, a ball stylus was used to obtain specified measurements. The procedure involved selecting the inspection property, such as the diameter of the cylinder, before probing designated inspection areas. Each feature was probed multiple times to acquire sufficient data for subsequent analysis. Inspection variables were used for comparing CMM and 3D scan data, with CAD measurements establishing the specified or set values for each variable. The component variables and measurements are provided in Table 4-13.

Table 4-13: Actual and set values of hybrid component used for evaluating inspection process variables.

Features	**Variables**	**Datum**	**Measurements (mm)**			
			CAD	**CMM**	**3D standard scan (3DSS)**	**3D extra fine scan (3DXFS)**
Cylinder 1	Diameter	-	100.00	102.62	102.64	102.66
	Cyclindricity	-	0.00	0.11	0.43	0.56
Cylinder 2	Diameter	-	15.00	8.13	7.84	7.86
	Cyclindricity	-	0.00	0.22	0.27	0.37
Plane 1	Flatness	-	0.00	0.02	0.18	0.21
	Perpendicularity	Cylinder 1	0.00	0.29	0.28	0.45
Plane 2	Flatness	-	0.00	0.04	0.11	0.18
	Parallelism	Plane 3	0.00	0.11	0.14	0.36
	Perpendicularity	Plane 5	0.00	0.06	0.11	0.23
Plane 3	Flatness	-	0.00	0.08	0.12	0.20
Plane 5	Flatness	-	0.00	0.02	0.20	0.25
	Perpendicularity	Plane 3	0.00	0.05	0.20	0.32
Radius 1	Radius	-	15.00	9.41	9.66	9.22
	Radius	-	15.00	9.27	9.27	9.37

The BAM system offers different scan settings (i.e., 3DSS and 3DXFS), which were both used to obtain the values shown in Table 4-13. While this output allowed for the analysis of the component form and accuracy, relative to the capability of both measurement systems, the focus was on enhancing understanding of the pre- and post-build requirements for WAAM operations, based on the consistency of intermediate process inputs. The variance between CAD and actual values was calculated, before identifying important inspection characteristics and geometric features (Table 4-13). The resulting variance charts are presented in Figure 4-29.

There were noticeable differences between CAD and actual measurements (Figure 4-29(a)), particularly in relation to the size of distinct geometric features whose measurements significantly exceeded the target CAD values. For these features, mainly the pre-formed round bar, as well as the as-deposited and subsequently machined features of the hybrid part (Figure 4-28(b)), differences were attributed to the manufacturing allowances typically associated with fabrication processes, including forming, MAM, and machining

operations. The manufacturing allowances are typically dependent on and established relative to the process capability, as previously discussed in relation to the NNS concept (Figure 4-6).

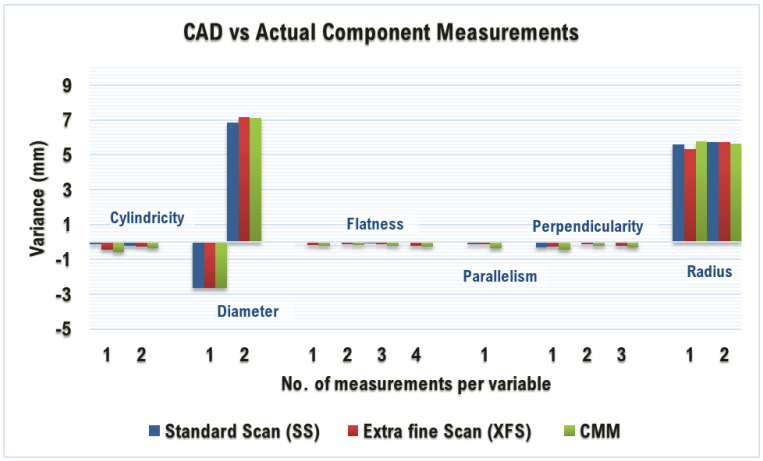

(a)

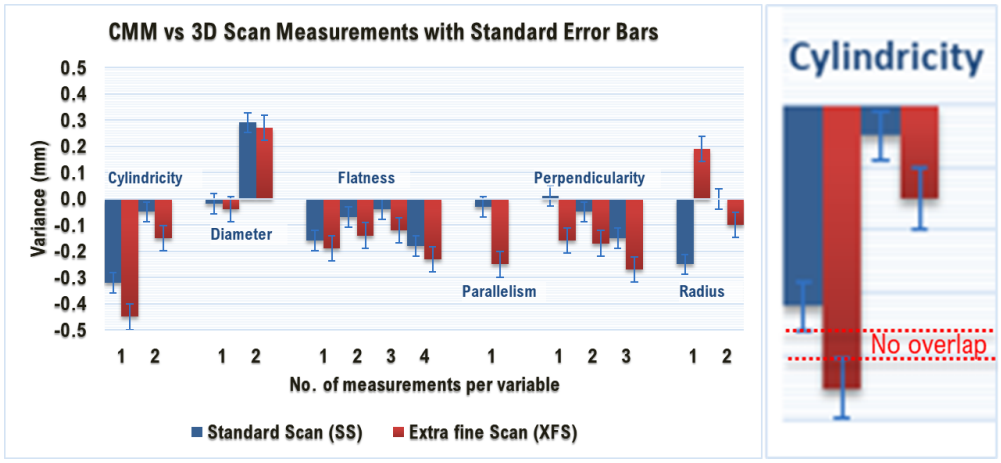

(b)

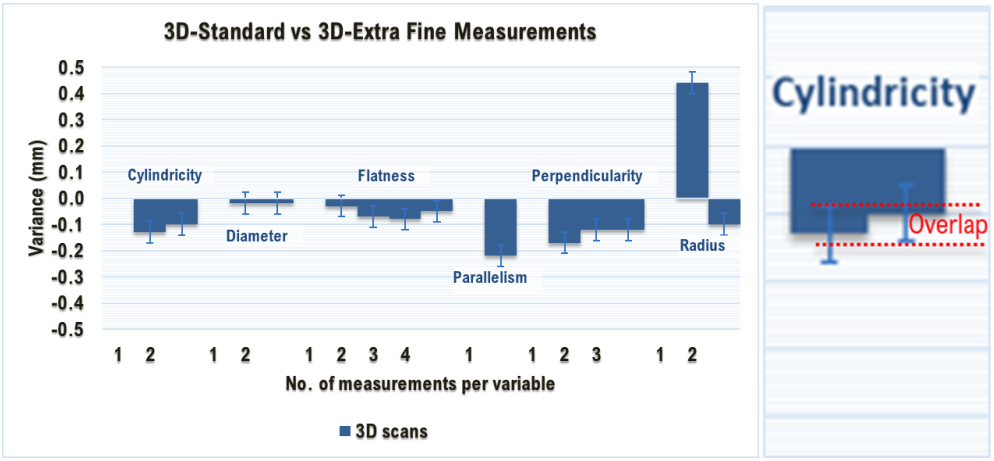

(c)

Figure 4-29: Variance charts comparing (a) CAD data and actual measurements (b) CMM and 3D scan measurements and (c) 3D scan measurements at different scanning resolutions.

When considering form-related measurements, which were obtained from the surfaces associated with fabricated features, the differences between actual and CAD measurements were nominal. Mainly, the need

for accurate input data was evident, particularly in relation to hybrid builds and SMRM operations, where varying starting conditions can have a significant and cumulative impact on manufacturing output quality. Similarly, when comparing actual measurements (Figure 4-29(b) and (Figure 4-29(c)), the incorporation of standard error bars, which measures the standard error for all values in a given dataset, was useful for describing the precision of the inspection techniques utilised. Due to the relative spread and variability of sampled data, the variance chart comparing CAD and actual measurements (Figure 4-29(a)) was excluded. For actual outputs, the overlap between error bars representing distinct measurements or values can provide indications about the relative precision of the different inspection techniques. In this case, there were more overlapping error bars observed between the 3DSS and 3DXFS (Figure 4-29(c)), when compared to the number of non-overlapping bars between CMM and 3D scans (Figure 4-29(b)), highlighting correlations between the inspection capability, and measurement sensitivity. There were also correlations between the number of points that were sampled during 3D scans and the resulting measurement accuracy, which was most evident when comparing 3DSS and 3DXFS scans (Figure 4-29(c)). The inspection procedures were similar for both scans, but more data points were sampled using the 3DXFS setting (~40ppmm^2 or 36,417,155 million points), compared to the 3DSS setting (~16ppmm^2 or 1,471,232 million points), which were significantly higher than average values for similar CMM operations (~280).

Compared to the 3D scanning procedure, the probing process was significantly facilitated by the prior definition of the inspection property variable, in conjunction with requiring a minimum number of points, to construct inspected objects. Based on the complexity of features, the required number of points typically ranged from 1 to 6, with the latter being applicable to most 3D objects. Though marginal, the effects of rounding or approximation errors were also evident when comparing the discrepancy between CMM and 3D scan data (Figure 4-29(b)). Nevertheless, it was obvious that the measurement accuracy or precision improved when sufficient data was sampled during the inspection process, with 3D scans undoubtedly representing the actual profile of the hybrid component much more realistically, than the CMM process, where fewer points were used to algorithmically generate pre-designated features. These insights offer a possible explanation for the non-overlapping error bars observed between 3D and CMM measurements, with differences mainly attributed to inspection techniques, and procedures. In the end, the size, form, and related geometric characteristics remain important (Figure 4-29(a)), when considering inspection requirements for WAAM.

In exploring the identified geometric characteristics, the radius and diameter were classed as size-related features, while associated variables (i.e. cylindricity, flatness, parallelism and perpendicularity) were included in the form-related category. CAD values were excluded from the latter because the variance was valueless or zero. In other words, these outputs did not reflect the true or actual measurements of the hybrid component. Thus, only actual measurements (Table 4-13) were utilised when determining the control limits for the inspection process. Correspondingly, the 3DXFS outputs were relatively more precise, due to the higher

sampling rate and more detailed information acquired over similar inspection areas, and were used to derive baseline values (i.e. μ, UCL, and LCL). The resulting process control charts are presented in Figure 4-30.

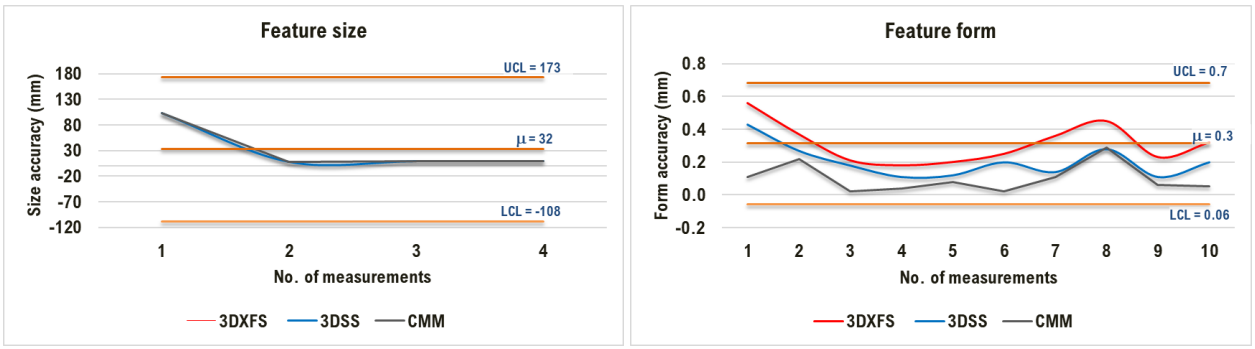

(a) (b)

Figure 4-30: 3D inspection process control chart for feature (a) size and (b) form related variables.

Based on the 3DXFS measurements for this data set, the charts indicate that all values were within the established control limits for the 3D inspection process. The range of values recorded in the feature size category (Figure 4-30(a)) are representative of typical engineering structures, where vast differences often exist between the minimum and maximum dimensions in a single component. However, distinct size measurements were comparable and consistent for similar features, irrespective of the inspection capability, settings, or procedures, particularly for 3D scans. Conversely, there were more obvious differences between form-related values obtained for similar features (Figure 4-30(b)), which supports previous observations about the precision of the different inspection techniques (Figure 4-29). Relative to the size category, the variances between the form class values were significantly smaller, with greater deviations observed in relation to the 3DXFS data set (0.015mm), compared to 3DSS (0.010mm), and CMM (0.008mm) measurements.

While scanning precision is affected by the stability of the system, and the speed at which the EOAT travels, during the acquisition of scan data, the accuracy of the 3D inspection process, which was the driver for this study, is affected by the surface condition of the inspected object, as well as full and clear access to all inspection areas. For this investigation, the robot was programmed to travel at a speed of 0.2 ms^{-1}, to allow sufficient time to acquire data from designated areas of the hybrid SMD part. In terms of productivity, the total number of points captured during the 3DXFS inspections significantly increased the post-processing time, while only marginally enhancing the overall measurement accuracy. This observation is perhaps most evident for the feature size category, where both CMM and 3D scan measurements were similar (Figure 4-30(a)). Conversely, while form related measurements were not so critical for this study, the potential effects of form variabilities warrant further investigation, when deploying this approach for critical applications. Ultimately, both size and form-related factors are potentially significant for all WAAM operations. Size-related factors include oversized or undersized products, with previously discussed considerations, such as manufacturing allowances, affecting intermediate products forms used as inputs to the process. However, the effects of feature

form variations are typically more localised, as observed in relation to the 3D scans, where capturing more data points over a small accessible area, generally yields significantly more accurate information.

Presently, the effects of WAAM process variations can be detected ex-situ via NDE techniques, or by in-situ monitoring of changes in system outputs, such as voltage fluctuations, while noting that interrelated mechanisms can contribute to unexpected changes in monitored outputs. Similarly, it may be assumed that the intermediate products used for new, or hybrid builds, including SMRM applications, are within tolerance, and that set-up procedures can help to minimise variability, but this exercise demonstrates the significance of form input characteristics in MAM operations. For SMRM applications, differences between the initial condition of the intermediate product or preform, relative to the original specifications are to be expected. However, variabilities stemming from any combination of the arc characteristics, input material or feedstock, feeding mechanism, and profile of target objects, will undoubtedly have a cumulative impact on process control strategies, and ultimately, the resulting product or part quality. Therefore, inspection data can be utilised to minimise variability, or facilitate the identification of important variables to be controlled, during large-scale MAM operations, and at both ends of the process.

In the present BAM configuration, the 3D scanner effectively captured relatively accurate data about the hybrid SMD component, and the implementation of different inspection techniques facilitated direct comparisons of the actual data. This approach facilitated the verification of the specified ranges for the BAM EOAT, which is nominally accurate to ±60 µm, and at distances over 8.5m. When considering the minimum criteria for the feature size accuracy involving large components (Table 4-4), and the NNS concept, the inspection tool satisfies the requirements for targeted applications, including SMRM. Irrespective of how the BAM inspection data is deployed, either as a DED process enabler, or for broader verification purposes, this study also demonstrates the value of the 3D inspection concept, for end-to-end MAM applications.

4.5.2.3 Systemic performance

The auditing of system logs is one of the most prevalent methods for assessing system performance and was adopted for this exercise, with the aim of gathering further insights about systemic behaviours, relative to designated system functions (Figure 4-19). Consistent with this focus, the overall performance of the BAM system was prioritised over specific tasks, processing requirements, or applications, involving either 3D inspection or WAAM operations. Systemic data was obtained from integral capabilities, as well as core BAM operations, and associated procedures and operator actions, to enhance understanding of the context underpinning correlations between procedures, operator actions, systemic events, and related performance. The aggregated data included records obtained during core operations and activities that automatically triggered logging functions. Within this scope, different organisational projects, which were initiated as part of the ongoing development of this OA MAM platform, provided pertinent inputs, observations, and insights for this exercise. Correspondingly, architype scenarios and applications for BAM are depicted in Figure 4-31.

Figure 4-31: Exploring BAM capabilities and applications.

Focusing on the targeted application scale, the exemplars in Figure 4-31 were initiated to enhance understanding of the capability and limitations of the BAM platform. The possibilities for different application scenarios were explored, including feature additions, analogous to the hybrid SMD part (Figure 4-28), and for the fabrication of entirely new structures.

Due to the co-dependencies between the kinematic subsystems enabling both WAAM and 3D inspection operations (Figure 4-23 and Figure 4-24), associated event data were directly acquired from the KUKA system logs. Designated the primary logbook (PLB), available data were downloaded as text (.txt) files, which contained different entries that were organised according to predefined event types and classes. The sampled PLB data is summarised in Table 4-14, and further analysed as depicted in Figure 4-32.

Table 4-14: Overall summary data from primary system logbook (PLB).

Event Type	**Description**	**Total events**	**Event Class**		
			Information	**Warning**	**Error**
Boot	Attributed to during boot procedures and depicted as black arrow icon	2062	86.66%	0.00%	13.34%
User action	Occurs during user operation and depicted as hand icon	1891	94.50%	5.34%	0.16%
Process	Generated by programs and depicted as hammer icon	1724	100.00%	0.00%	0.00%
System	Attributed to the robot kernel and depicted as robot icon	1831	99.84%	0.16%	0.00%
Start-up	Attributed to installation events and depicted as wrench icon	562	6.58%	93.42%	0.00%
Operation	Occurs during system operation and depicted as looped circular arrow icon	1672	100.00%	0.00%	0.00%
	Total events entries logged	**9742**	8835	629	278
	Event class distribution (%)		90.69	6.46	2.85

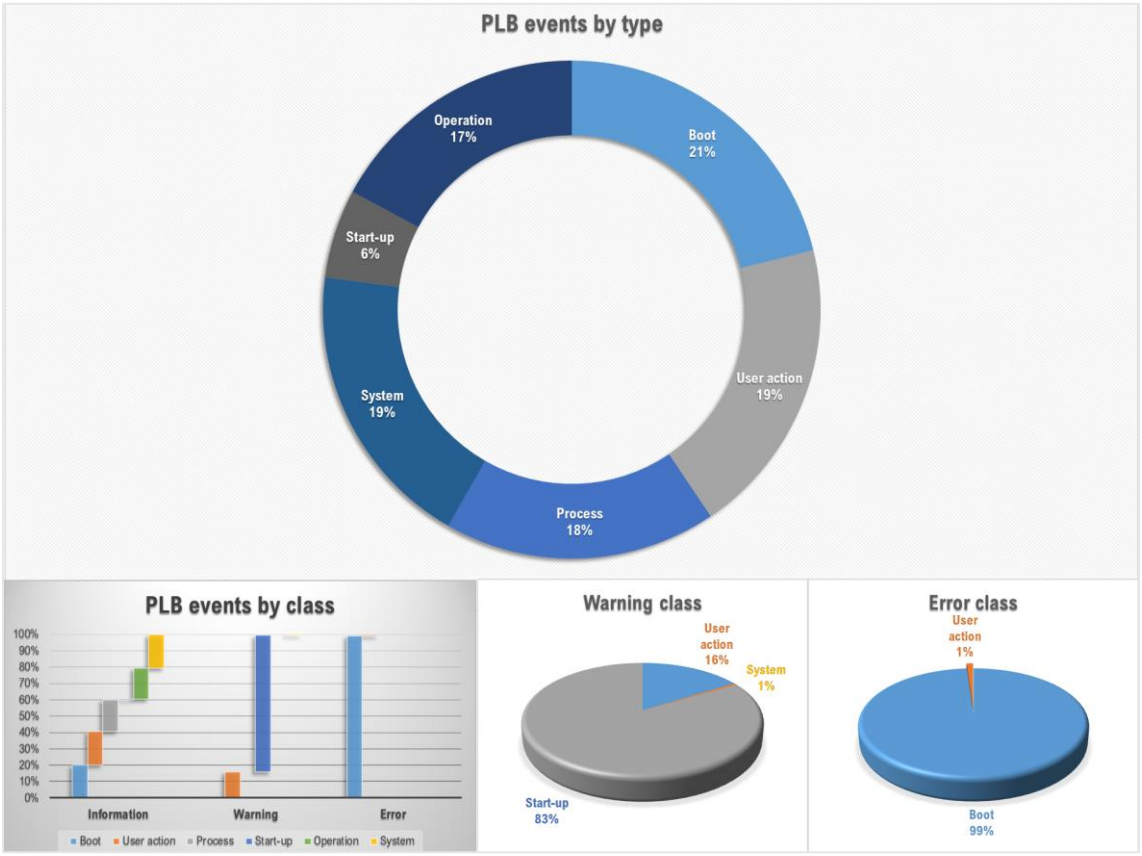

Figure 4-32: Analysis of PLB data by event types and classes.

For KUKA system elements, event classes are also predesignated, with associated data logged accordingly. The downloaded PLB included nearly 10,000 unique entries, filtered by type, and further organised according to designated event classes, namely *Information, Warning* and *Error*. *Information* class events are identified by a blue square, within which the event icon is bounded, with a yellow circle representing *Warning* class events, while a red octagonal depicts events logged under the *Error* class. Evaluating the data distribution in the event class revealed that over 90% of automatically logged entries were *Information* related, while the *Warning* and *Error* classes respectively accounted for approximately 7% and 3% of the total number of events recorded.

Analysing the PLB entries by event types revealed that *Boot* related events were dominant in this category, while *Start-up* events accounted for a small fraction (~6%) of the total events logged, with other entries distributed relatively evenly across the remaining categories. Analysing data entries by class, revealed that there were no *Warning* or *Error* related events automatically logged for *Operation* and *Process* event types. However, *User action* events featured in both *Warning* and *Error* classes, while *User action* and *Boot* event types were entirely responsible for all events recorded under the *Error* class, which is potentially significant from an operational standpoint. While *User action* events can be directly traced to specific operator actions, most events filed under the *Error* class were *Boot* type events, which typically occur without warning, causing a system shutdown. Whereas the former may be addressed via relevant procedures, which may involve further

enhancement of operator skills, system shutdowns can impede the identification and troubleshooting of underlying issues, particularly if pertinent information is irretrievably lost, and often with limited recourse.

The PLB was screened to identify relevant entries for exploring the context and performance implications of selected events. Representative entries from the different event classes were randomly selected, based on the completeness of available PLB records. The sampled events are presented in Table 4-15.

Table 4-15: Sample PLB data for different event classes.

Log entry number (Event type, Event class)	**Date and time**	**Event description**	**Affected module & message number**
Entry 2774 (User input, Information)	2017-09-12 09:27:18'844	File RobotData.xml copied from RDC to hard drive	Module: RDC Message number: 81
Entry 1685 (System, Warning)	2019-03-05 14:32:17'701	Axis E1 acceleration not programmed	Module: System Message number: 1412
Entry 2108 (System, Error)	2017-10-05 10:15:10'598	Drives off, intermediate circuit voltage still charged	Module: System Message number: 220

During BAM operations, the user must take immediate action to resolve events recorded under the *Information* and *Warning* classes, thus it was rationalised that events recorded under these classes were less likely to impact system performance. For instance, *Information* class events, such as *Entry 2274* (Table 4-15), are typically resolved by acknowledging the displayed information. In this case, it is indicated that a specific file, 'RobotData.xml' was copied from one location to another. Conversely, understanding events in the *Error* class is a priority, due to the potential operational and related systemic implications. The *Warning* provided in *Entry 1685*, indicates that a programming issue was prohibiting all active commands, and was resolved by inputting the acceleration for the external gantry axis, 'Axis E1'. Some events can be traced to specific subsystems, such as the *Resolver Digital Converter* (RDC). Mentioned in *Entry 2774* (Table 4-15), it was determined that the RDC is an internal storage location. The assigned message number can also facilitate the investigation of such events. For event *Entry 2108*, the error message number (i.e., 220) was referenced when investigating the issue, and revealed that an error that prohibited the operation of the system had occurred. A typical excerpt from the KUKA system manual is provided in Figure 4-33.

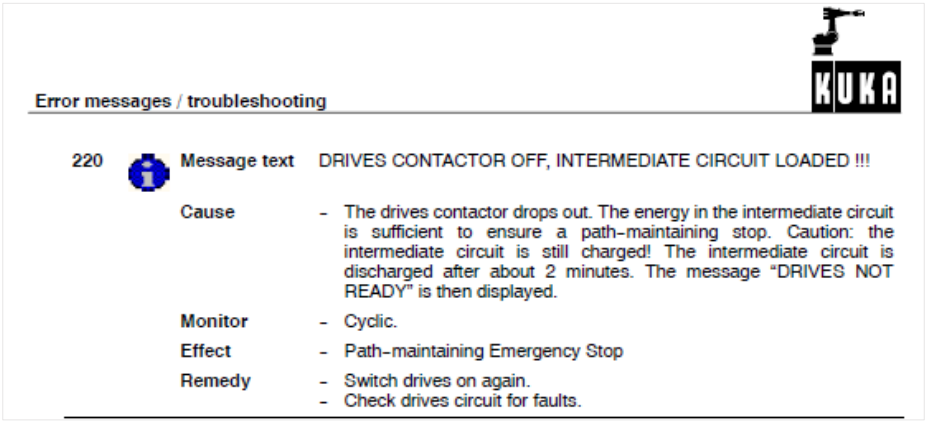

Figure 4-33: Typical entry in OEM manual to support troubleshooting of system errors [394].

Current OEM manuals, if available and/or accessible, typically include details about previously documented issues, which would otherwise necessitate further independent investigation, to find an effective resolution. For enumerated events, the manual typically includes a brief description of the cause, effects, and possible remedies.

When reviewing the manual for *Error* 220, from event *Entry 2108* (Table 4-15), it was noted that the motor contactor drives were off, due to a residual charge in the intermediate circuit. This issue was resolved by waiting for a few minutes, as recommended in the message text, before resuming BAM operations. Although the message text states that the fault lies with the *Drives Contactor* (Figure 4-33), there is no further information about why this event has occurred. Due to such information gaps, the PLB was augmented with supplementary data, mainly obtained from the GTAW unit, and associated entries, contained in a designated secondary logbook (SLB), and further supported by entries captured in the operators logbook (OLB).

The SLB data was derived from the virtual platform (Figure 4-17), and includes common event entries, such as the date, time, and description of affected subsystems. However, unlike the PLB, there were no predefined event types or classes associated with automatically logged SLB entries, or dedicated manuals to support troubleshooting endeavours. For associated SLB subsystems, detected issues were typically resolved by acknowledging displayed message, resetting alarms, performing specific actions, and/ or rebooting the affected module. Typical outputs from the SLB and OLB are provided in Figure 4-34.

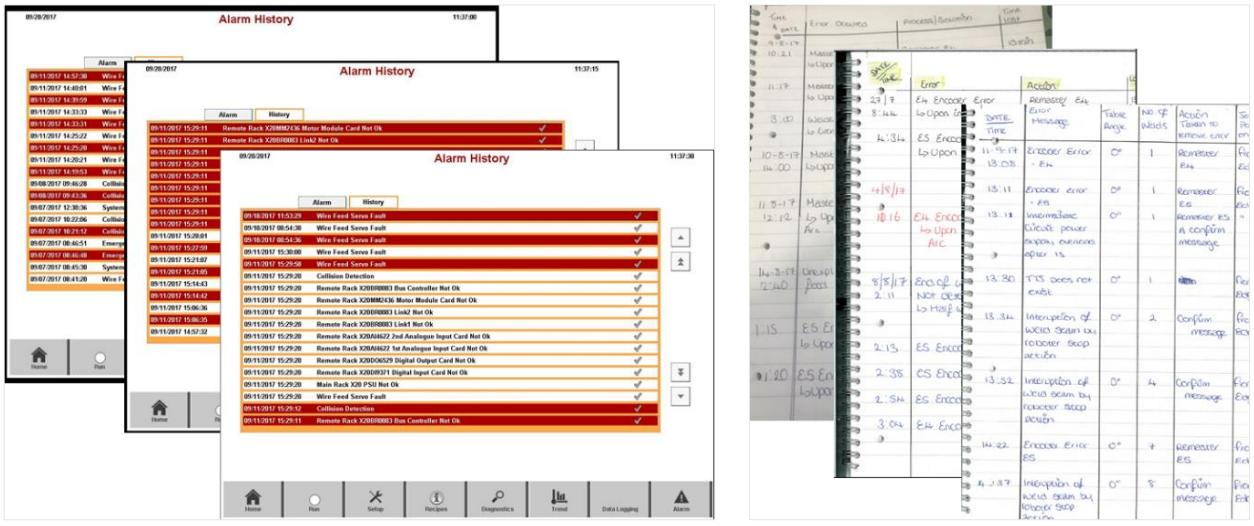

(a) (b)

Figure 4-34: Actual outputs from the (a) SLB and (b) OLB.

SLB event details and logging parameters were fixed (Figure 4-34(a)), but OLB requirements evolved over time, to include system downtime and related observations (Figure 4-34(b)). In general, OLB records of pertinent observations affecting operations included common details, such as the event time, description, and effects, as well as the subsequent operator responses, or actions required to restore normal system functions. Although the underlying causes of SLB events were not often evident, or sufficiently explained (Figure 4-33), documenting specific actions in the OLB, allowed operators to quickly resolve previously encountered issues. Invariably, and without the benefit of OLB entries, more time was required to resolve problems.

When reviewing the PLB and SLB, the lack of contextual clarity about automatically logged events directly influenced manual data logging procedures, which were initiated and maintained, via the OLB, with the sole purpose of documenting pertinent information about system events from the operator's perspective. Following a disruptive event, and consistent with the BAM monitoring and control requirements (Figure 4-10), relevant information was recorded in the OLB, thus supporting the continued development of the basic solution (Figure 4-17) already implemented. Correspondingly, the benefits of a more consolidated events monitoring approach were further explored, to enhance understanding of BAM limitations and identify developmental requirements.

A review timeframe was established, based on the integrity and completeness of available system records. Initially, related event data from the OLB and SLB (Figure 4-34) were converted into the desired format, before manually aggregating pertinent entries, from all three sources, into a single spreadsheet. The combined PLB, SLB and OLB entries were then organised, before analysing the outputs, as depicted in Figure 4-35.

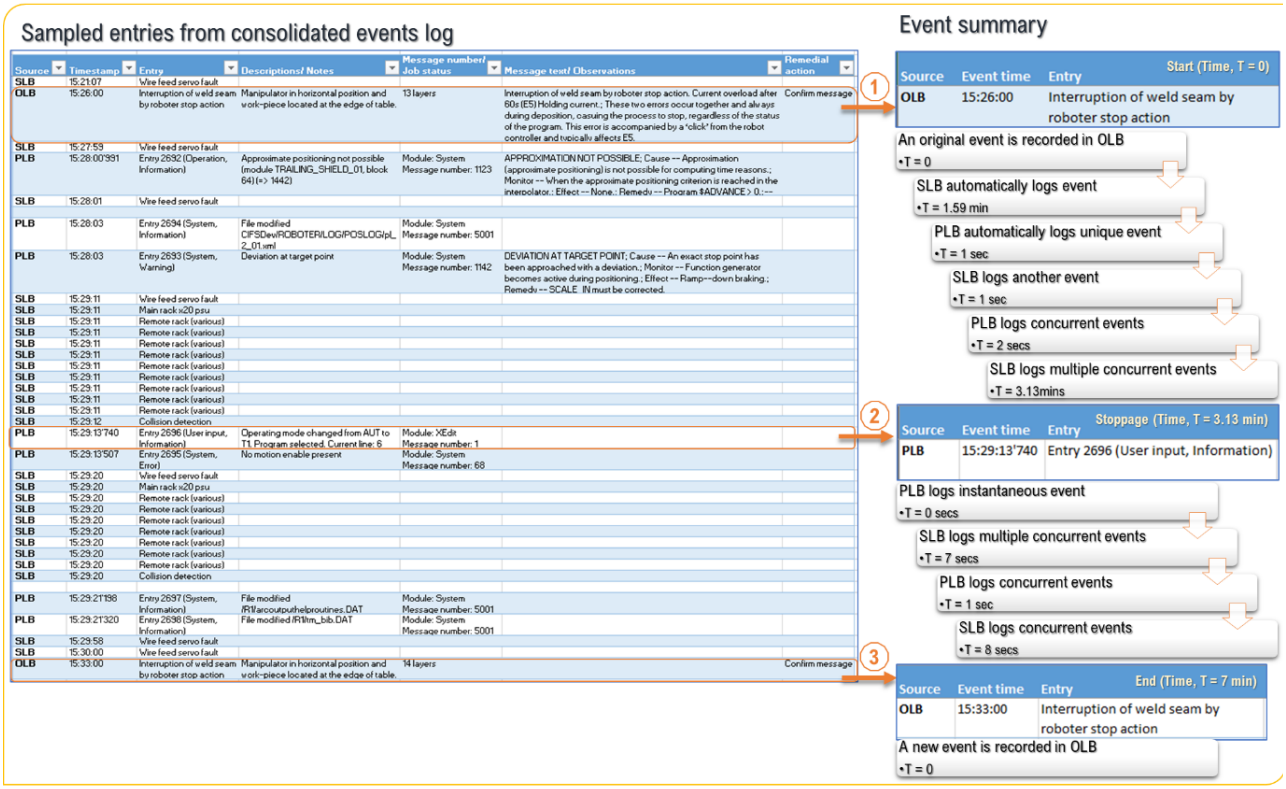

Figure 4-35: Manual consolidation and analysis of BAM systemic events.

Chronologically, the timeline suggests that moments after the operator logged an original event in the OLB, as identified in '1', multiple events were subsequently logged in the SLB and PLB, culminating in a system error ~3 minutes later (Figure 4-35). However, operator events are typically logged in response to observations or specific issues that halt operations, while automatic logging functions are triggered by systemic events and logged instantaneously. Hence, the issue identified in '1' had occurred prior to the operator's actions, which were automatically logged in the PLB as depicted in '2'. In the interlude between '1' and '2', further events were automatically logged in both the PLB and SLB, but more recurring issues were captured in the SLB.

Furthermore, it was observed that prior to the original OLB entry in '1', an event had also been automatically logged in the SLB, and at point '3', the new event recorded in the OLB is preceded by another SLB event. This pattern indicates a probable correlation between the systemic issue being investigated, and the subsystems associated with SLB, which subsequently triggered automatic logging functions in both the SLB and PLB, but corroborating studies were beyond the scope of planned investigations. Nevertheless, the OLB indicates that both issues in '1' and '3' were resolved by confirming the displayed message.

In the analysis of system events, temporal factors can affect perceptions about the relevance of harmonised data, relative to the overall performance and dominant traits, as observed in the BAM environment. Perceptions are due to the aggregation of different perspectives, derived from both manual and automatically logged entries. For instance, when considering the main event classes identified in the PLB (Table 4-15), it was noted, in the OLB, that user input events were typically resolved in less than 60 seconds. System events were usually resolved in about 5 minutes, while system errors, particularly when they caused system shutdowns, required ~15 to 30 minutes. It was also observed that the operator's skill had the most significant impact on resolution actions, with highly skilled operators requiring less time, on average. In all instances, productivity was often impacted by lack of awareness about underlying causes, or insufficient information, to support the appropriate instantaneous response. While the effects of certain events and related traits are unavoidable at this level of integration, the consequences can be managed via proper documentation of systemic data, standardisation of logged event entries, and improvements in the automatic recognition of trends and patterns.

From a developmental standpoint, the inclusion of observational data from the operator, and the manual aggregation of inputs from heterogenous data sources, are important considerations. The event reporting sequence and context are equally important, as these factors can impede the analysis of trends, patterns, and related systemic issues. Correspondingly, improved data management strategies, including data retention practices, and specific policies governing such decisions, are associated concerns. Mainly, it was observed that exponential data growth, enabled by ubiquitous data gathering capabilities, is not presently matched by an equivalent approach for automatically and perceptively processing valuable manufacturing data, which like any resource, has much broader implications beyond the BAM system and organisational boundaries. For the BAM system, ensuring that the data landscape is relevantly streamlined and enriched, particularly through discerned understanding of specific gaps, is important. For instance, due to the relationship between definite variables and naming conventions used for individual subsystems or modules, some data discontinuities, gaps, and overlaps, were identified when comparing outputs from different sources (Figure 4-35). Thus, the goal of automatically identifying, organising, analysing, and correlating information to facilitate the management of systemic issues, and support the comprehension of causal factors via the SLB, is only partially fulfilled.

The SLB presently embodies the basic functions of the virtual platform (Figure 4-17), which supports the algorithmic approach for process monitoring and control (Figure 4-10). It also provides a real-time convening

function, helping to ensure that systemic events are properly and accurately logged, which is useful for promptly elaborating and relevantly exploiting heterogenous system data. Although the platform is still under development, this evaluation demonstrates the benefits of a consolidated approach (Figure 4-35) for interpreting systemic performance, particularly during normal and abnormal circumstances. Correspondingly, pre-emptive strategies can be developed, whereby established causal relationships facilitate the analysis of performance issues, based on actual or hypothetical/ what-if scenarios. Primarily, complementary information, such as knowledge of specific tasks and distinguishing attributes, as well as the inputs from the OLB and OEM manuals, significantly enhanced the interpretation of resulting data. Specifically, the platform was developed to facilitate the continuous homogenisation of information, provide meaningful insight into patterns and issues, and enable the identification of opportunities to improve systemic performance and operational efficiency.

4.5.3 Emergent characteristics

In systems thinking, emergent properties are necessary adaptations that typically enhance the durability of a system in the environment within which it operates. However, due to unpredictable behaviours, such adaptations may be detrimental to the durable performance and maintainability of complex engineering systems. Therefore, the emerging traits, as well as other behaviours resulting from the integration of the distinct configuration options or BAM system modules, were investigated. Motivated by the observed effects of the interactions between system components, where events logged in response to triggers resulted in unpredictable responses, with unintended consequences on performance and productivity (Figure 4-35), the goal was to enhance understanding of observed BAM system behaviours and their underlying traits.

Building on designated system functions, the true characteristics of the BAM system were evaluated in relation to the main features and general requirements associated with both WAAM and 3D inspection operations. Insights were drawn from the black box testing approach, which elucidated system functions (Figure 4-18); the stock and flow diagrams used to map system interactions (e.g. Figure 4-24); and subsequent performance evaluations, which enhanced awareness of process conformance and related systemic issues (Figure 4-27 and Figure 4-35). These activities were especially useful for highlighting associations between distinct BAM system features, designated functions, and specific behaviours typically observed during the implementation of tasks. Depicted in the capability/ process map (Figure 4-25), different tasks were separately implemented to obtain desired system outputs, mainly the 3D objects and inspection data, thus enabling the documentation and evaluation of observable behaviours and resulting performance. Subsequently, distinguishing system features and associated functions were organised into different overarching categories or traits, related to observed behaviours. The resulting categories of features and related functions are presented in Table 4-16.

The BAM system is comprised of basic supporting *structures* that enhance the mobility and reconfigurability of interconnected modules, such as the gantry and articulated robot. In conjunction with these structures, *conversion systems*, provide the requisite WAAM and 3D process characteristics, which ensure that principal

BAM functions are fulfilled. Accordingly, *transmission mechanisms* rely on interdependencies between the different *structures*, such as the individual subsystems, auxiliary devices, and so on. However, in addition to transmitting desired functions (e.g. supplying electrical energy to the electrode), undesirable traits (e.g. electromagnetic interference) were observed, indicating that certain subsystems were transmitting outside the prescribed transmission paths or channels. In this case, strong correlations were observed between the malfunctions of certain system modules, and the initiation of the arc (Figure 4-35). Such issues underscore the importance of *transmission* mechanisms and their influence on the *control* of traits affecting system performance, particularly when measures, implemented to *regulate* and/or minimise their impact on interconnected elements, prove ineffectual. For this analysis, a distinction is made between *control*, the response of the system to inputs and outputs, and *regulation*, the means, mechanisms, or devices through which control is achieved.

Table 4-16: Preliminary list of technical characteristics and functions of the BAM system.

Technical traits	Functions
Structures	For protection, support, and mobility of tool and/or component during 3D or DED processes, as well as the system itself.
Transmission (e.g. wire, feedstock, signals, etc.) system	Creates paths between elements to facilitate the circulation of services/ inputs (e.g. argon, energy, data, etc.), including waste extraction/ removal of by-products.
Conversion/ transformation systems	Agents that enable change of substances from original to new state/form (e.g. feedstock to 3D component; actual to digitised/ virtual part; arc energy to heat; etc).
Sensors/ receptors	For sensing, acquisition and measuring of stimuli mainly in responses to changes within structures, conversion, and transmission mechanisms.
Control systems or controllers	Effects changes in response to inputs and outputs, to stabilise linked structures, transmission, and conversion mechanisms.
Regulators	Provides feedback to controllers, for monitoring and calibration of other traits, including quality critical conversion elements (i.e. repeatability and accuracy).
Intuitive/ intelligent systems	The main driving/ dominant features that automatically process information from interconnected systems to maintain normal functions.

Intuitive elements, including event triggering and DAQ functions, can influence perceptions about observed system behaviours and attributable causes. Presently, the lack of a fully automated feedback system is a hindrance to certain BAM functions, such as the wire feed rate during the WAAM process, which relies on manual interventions for necessary in-process adaptations. Consequently, the *regulator* reaction time is subjective because it relies on the operator's skill, which can result in a higher degree of variability in *controlling* observed behaviours or traits that are often evident in the subsequent output quality. However, within the allocations for this undertaking, incorporated system interfaces and existing operational protocols were crucial for minimising the effects of observed issues. Therefore, integrated system *receptors* (Figure 4-17), which facilitate manual interventions, will be retained, until such a time as the full virtual platform concept, including specific requirements and approaches for automation and regulating entities, can be implemented.

When describing known causal relationships, assumptions about inherent system variables and traits can generally influence perceptions about systemic behaviours. However, certain interactions are unknowable, due

to hidden or overlooked variables, which makes it challenging to establish correlations between emergent traits, systemic events, and system variables, including changes to the values associated with these variables. Instead, it is usually when integrated elements of the system interact, to fulfil designated functions, that observed traits can be evaluated. In this instance, the *transmission* of electro-magnetic waves from the high frequency generator to other subsystems, was the most predominant trait identified within the complex BAM environment, due to the amplification of specific behaviours that were observed when initiating the arc. Between interconnected system elements, operator actions, and systemic issues, *intuitive* mechanisms are key automation priorities, in conjunction with *control* and *regulating* entities, due to their influence on system traits and observable behaviours, and ultimate impact on performance, productivity, and system output quality.

4.6 Main observations

The development of a concept for a reconfigurable OA MAM system was facilitated by established engineering rules, and complementary management and statistical principles. The approach involved specifying the requirements from relevant perspectives, which emphasised the need for a perspectives management strategy to support all development phases. Managing different perspectives underpinning system requirements is consistent with the focus on high-level solutions that enhance development outcomes. The main considerations, including the characterisation of requirements and representative functions, were motivated by the different organisational procedures, and diverse internal and external factors encountered, when analysing system development requirements.

The development of specific concepts was primarily underpinned by technology, application, function, and related considerations, which highlighted necessary trade-offs and compromises. The industrial requirement for suitably sized MAM capabilities is established but ill-defined, due to a lack of pre-determined specificity on sizing requirements. Thus, the technology selection criteria and definition of desirable system attributes were equally crucial for clarifying the basis on which development requirements were progressed and subsequently measured. The need for managing complexity was also highlighted, relative to the fragmented integration landscape, stemming from the requirement for multiple non-standard and/or proprietary solutions, as well as the necessary intra- and inter-process protocols enabling interactivity between distinct hardware and software components. Ultimately, transforming a concept into an actual specification for an OA MAM system necessitated the balancing of multiple competing objectives, to achieve the optimal outcome for this development.

The implementation of the BAM concept, and current integration state of the resulting system, was determined by the scope of supply, which was supported by the specifications derived for both COTS and customised solutions. However, there were several constraints influencing the development of the system, which necessitated compromises, to achieve a satisfactory overall outcome. Technologically, it was often necessary to balance the limitations of current solutions, and expected and potential integration challenges, with the

transitionary and envisioned final integration state for the BAM system. Organisational considerations included the cost and internal capacity, relative to the allocated budget, time limit, and available footprint for the BAM system. Hence, a decision tree was developed and implemented, in conjunction with other pertinent information, to justify development preferences. Other identified implementation factors, and developmental considerations for industrial MAM capabilities, include the need for reconfigurable solutions, relative to the deployment of disruptive evolving technologies within persistently unpredictable supply chains. Importantly, a transition management strategy can help to navigate disruptions, as well as related evolving and unpredictable circumstances, alongside other barriers that hinder technology adoption.

The commissioning of the BAM system was an important developmental milestone, which was underpinned by the functional testing strategy and acceptance criteria, defined in relation to the desired integration state. The FAT and SAT phases further accentuated the significance of integration factors, including the interconnections between technologies and interrelationships between suppliers, while alluding to various commercial, legal, and related supply chain considerations influencing individual business competitiveness. Key development considerations include the need for a higher degree of standardisation between modular cooperating technologies. Further to supporting the development of high-level solutions, including the provision of toolboxes and similar interfacing technologies, these developments should efficiently and expeditiously facilitate necessary interconnectivity in integrated settings.

The full integration of the BAM system allowed for the clarification of system boundaries and process interdependencies, and enhanced understanding of the system dynamics, which was evaluated to underpin performance analysis, undertaken at the process and systemic levels. Based on the current BAM capability map, the consistency of the WAAM and 3D inspection processes were demonstrated, using sampled process data from pertinent investigations. These investigations were completed as part of ongoing development proceedings, and facilitated the generation of related system data, to support systemic evaluations. Together, these studies demonstrated the significance of both technology and human factors in BAM operations, while supporting the strategic need for managing heterogenous data sources and corresponding requirements, to improve systemic performance and operational efficiency. Furthermore, considerations for emerging characteristics also highlighted the need for more intelligent, adaptable, and enduring industrial MAM systems, which is important, particularly in an evolving technology landscape.

4.7 Summary

The BAM system development and implementation strategy was described in this chapter, which is one the main elements underpinning the GT framework construction. Investigations were structured around the requirements, related concepts, and specifications for the system, including the analysis of developmental outcomes. In *Chapter 5*, an industrial SMRM case study is introduced. This case study is integral to the BAM system validation approach, and is described hereafter.

CHAPTER 5

5 BAM System Validation

5.1 Introduction

This chapter covers the methodology for validating the BAM system. The objective was to demonstrate that this representative system could fulfil designated tasks and requirements for industrially relevant MAM applications, including SMRM operations. The adopted case study approach was based on a titanium alloy aerospace component, selected to underpin validation studies. The details of specific activities, involving the development of SMRM tasks, related reprocessing trials, and subsequent analysis of the BAM system outputs, are described in the following sections.

5.2 Requirement analysis

Describing the specific SMRM activities to be implemented was important, when assessing how to validate the BAM system, and deploy DED for relatively complex reprocessing operations on metallic structures. Reprocessing is defined here as any deliberate operation or action that discernibly alters the physical and related characteristics of a structure. It may include the addition of features, and alteration or repurposing of a pre-existing component, in a manner that preserves and/or enhances its intrinsic value. Correspondingly, complexity is defined as the combination of associated factors and variables influencing specific operations, including the type, location, and proximity of integral features, relative to the location and characteristics of the regions or surfaces of the structure to be reprocessed.

Due to their industrial significance in various high-value manufacturing applications, and consequent maintenance requirements, alloys 316L SS and Ti-6Al-4V were initially considered for system validation studies. These alloys, which have been the focus of various MAM investigations, were also used for preliminary studies. Ultimately, the selection of alloy Ti-64 was influenced by the availability of a suitable artefact, which satisfied the technical criteria for this study, both in terms of the component size (i.e. large) and application or task specification (i.e. SMRM). Fundamentally, the artefact provided the relevant industrial context for validating the BAM system and the different concepts which it embodies, whilst testing the research supposition that *MAM technologies can adequately support relatively complex SMRM operations*.

5.2.1 Component and task specification

When supplying the artefact, the specific technical information provided by the industrial partner was restricted to its geometric parameters, with other pertinent details withheld for commercial reasons. Within the agreed SMRM scope, activities necessary for preparing the component and completing specified reprocessing

operations via DED were permitted. However, post-DED activities were restricted to NDE/ NDT techniques. Hence, supplementary validation activities were necessary, and planned accordingly, to further corroborate BAM system outputs.

Different considerations influenced the selection of the case study, including the alloy, geometric specifications, and availability, which was most important. Comprised of different investment cast and joined parts, and over 3000 precise features produced to aerospace tolerances, the component mass, diameter, and height, were approximately 200 kg, ∅1200mm and 900m, respectively, with a wall thickness of ~8mm in the regions of interest. Owing to the combination of its size, distinct fabrication techniques, different geometric shapes, and numerous features, this single valuable entity fit the definition of a component that was both large and complex, thus conforming to the set criteria for validation studies.

The task specification was informed by earlier investigations, which revealed that fatigue and cracks were common factors influencing reprocessing requirements in serviceable metallic structures, and major contributors to SMRM costs. However, it was necessary to establish the actual basis for SMRM, relative to factors that were directly applicable to the selected case study. Consequently, representative features, in the form of voids or cavities, were introduced to the surfaces of interest, via appropriate material removal techniques, to satisfy task input requirements, and establish the basis for impending reprocessing operations.

5.2.2 Processing considerations

It is generally accepted that titanium alloy Ti-6-Al-4V, from which the selected aerospace component was fabricated, has excellent forming and welding characteristics. However, Ti-6-Al-4V is highly reactive at elevated temperatures, making it susceptible to contaminants in the environment, which can cause, for example, embrittlement or loss of ductility. Consequently, an environment that is clean, tightly controlled, and affords adequate shielding, is essential when working with this alloy, particularly during reprocessing operations. From a structural standpoint, elevated processing temperatures also increase the risk of distortion and residual stresses, which can compromise the quality and integrity of the workpiece. Hence, adequate control of related factors was an important consideration when developing the SMRM approach. However, as the BAM processing environment is presently underdeveloped, and whilst specific solutions are being evaluated for the next development phase of this platform, an intermediate solution was required for shielding the component.

In general, the scope of SMRM activities is relatively narrow, even though the value of target components is usually high, and manufacturing lead-times for new products are typically long. Therefore, when deploying the BAM system for reprocessing tasks, the intention was to deliberately introduce specified features in relatively difficult to access regions of the component. The aim was to mimic industrially representative conditions, whereby non-optimal scenarios increase the level of task complexity, whilst providing ample opportunity to observe consequent AMT requirements. This strategy also allowed for the evaluation of related

technical, technological, and economic factors that were likely to limit the potential scope and applicability of the BAM system, for SMRM. The main considerations guiding validation activities, included how to: access the regions of interest during reprocessing operations; minimise the risk of damage or significant distortion, to the underlying structure; adequately control the conditions likely to affect the material composition and properties; achieve consistent outputs for similar reprocessing tasks; and increase efficiency when implementing SMRM strategies, whilst minimising associated costs.

5.3 Development of SMRM approach

Preliminary trials were completed on substrates, to inform the reprocessing strategy involving the titanium Ti-6Al-4V alloy case study. The objective was to proceed with BAM validation tasks, informed by data that could be easily obtained and objectively assessed, to facilitate comparisons within and between trial phases. The selection of substrates with similar wall thicknesses, relative to targeted reprocessing sites involving the case study, was an important early decision that bridged preliminary investigations and reprocessing trials. Principally, baseline parameters and related insights from the SMD trials were used to establish the initial BAM approach, with further trials initiated as necessary, to support specific task requirements.

5.3.1 Measurement and data acquisition plan

Actual measurements were required to support the development of the proposed SMRM strategy, and initial BAM trials allowed for the acquisition of pertinent process data. The decisive focus on real-time temperature and strain data was motivated by planned supplementary validation activities involving the artefact, which were necessary and in line with the agreed supply conditions. The DAQ approach, including the general set-up and monitoring devices utilised, is illustrated in Figure 5-1.

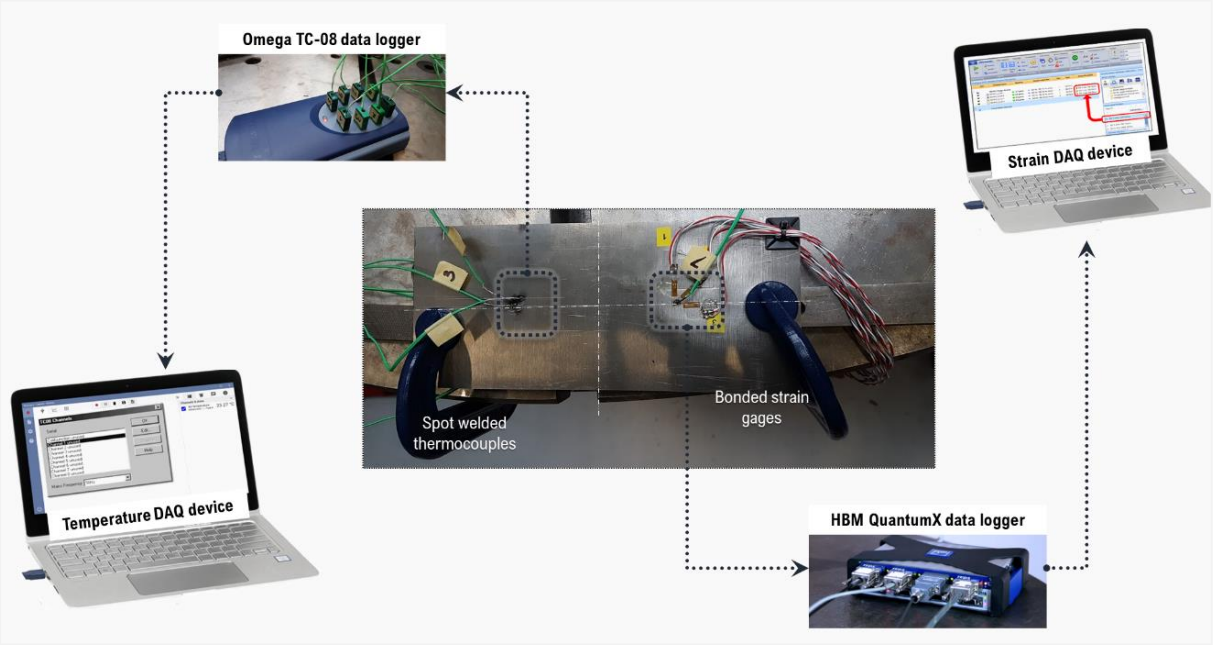

Figure 5-1: Set-up for real-time monitoring and data acquisition.

Two separate computers were used when setting-up DAQ devices for real-time process monitoring. Temperature measurements were acquired by means of an Omega TC-08 data logger. This device has eight input channels, measures temperatures within the range of –270 to +1820 °C, and samples data at a rate of up to ten measurements per second. Before acquiring data, K-type thermocouples (1 mm in diameter) were spot welded onto the surfaces of interest, and subsequently connected to the input channels of the data logging device. PicoLog 5 data logging software was used to set up DAQ parameters, and for recording measurements.

Direct strain measurements were acquired using HBM Catman DAQ software. In total, 13 strain gauges with 120 Ω resistors were used to obtain actual measurements from both the substrate, and the artefact. In line with specifications, the gauges were bonded onto substrate surfaces, which were specially prepared to improve adhesion, before directly connecting each one to a QuantumX data logger. This eight-channel device was set-up to acquire measurements at the recommended sampling frequency of 5 Hz.

Process monitoring procedures were implemented in separate stages. Initially, temperature measurements were acquired and analysed, to support the approach for concurrently acquiring temperature and strain data. Subsequently, both strain gauges and thermocouples were attached to designated surfaces (Figure 5-1), to enable the simultaneous monitoring and acquisition of corresponding measurements. The main experiments, and specific measurement procedures, are outlined in the following sections.

5.3.2 Design of experiments (DoE)

Process parameters from preliminary studies were initially verified, due to the differences between the SMD and BAM capabilities, and experiments involving titanium alloy. While SMD trials were performed in an enclosed space and fully sealed chamber, the present BAM environment is much more expansive, including only a perimeter fence. There were other differences, such as the substrate specifications, and designated SMD operations, relative to the focus of validation studies involving the BAM system. Conversely, DED trials involving both SMD and BAM capabilities were completed on geometrically similar substrates, with the SMD process parameters used to initiate BAM trials. The SMD study also yielded pertinent data for augmenting the BAM process, which was verified based on the geometric characteristics of the outputs from both systems.

Dedicated investigations were also necessary to support SMRM operations. Due to the anticipated localised effects of the heat input during reprocessing operations, the characteristics of the stationary arc were evaluated to develop a strategy to govern the start and end of reprocessing operations. The experimental procedure involved using a 10.5 mm thick titanium substrate to assess how much material was displaced by a stationary arc, over the specified duration. The experimental design factors for this study are summarised in Table 5-1.

Table 5-1: Summary of factors and corresponding levels tested in Phase I BAM trials.

Factors		**Levels**	
Type	**Variable**	**Low**	**High**
Quantitative	Current [A]	100	130
	Arc Length [mm]	2.5	3.5
Constant	Voltage [V]		~13
	Dwell time (s)		10
	Argon [l/min]		13

The ∅3.2 mm by 150 mm long, 2% thoriated tungsten electrode used for depositions, was sharpened to the OEM recommended vertex angle of 40°. This variable was maintained at a fixed value, while the arc length was varied to determine its effects on the substrate. The trial procedure involved initiating and maintaining a stable arc for the specified duration and repeating this process at varying arc lengths and currents, until all experimental runs were completed. The trial outputs are presented in Figure 5-2.

(a) (b)

Figure 5-2: Arc outputs on (a) substrate material and subsequent (b) optical scans.

Due to human error when inputting the required parameters, experiments 1, 2, and 3 were repeated, with an asterisk (*) used to denote repeat experiments, as shown in Figure 5-2(a). Optical 3D measuring techniques were used to acquire scans of the resulting arc profiles (Figure 5-2(b)), which were subsequently quantified by measuring the diameter and height of the displaced material, relative to the plane/ surface of the substrate.

The summary plot for this experimental design indicated that there was a good fit between the predicted and measured values of the resulting model. The summary plot values are presented in Table 5-2, with the corresponding contour and sweet spot plots provided in Figure 5-3.

Table 5-2: Values of predicted versus observed responses for evaluating effects of arc on substrate.

Responses	**Variance (R2)**	**Predictability (Q2)**	**Model validity**	**Reproducibility**
Height	0.901	0.852	0.959	0.861
Diameter	0.781	0.698	0.947	0.698

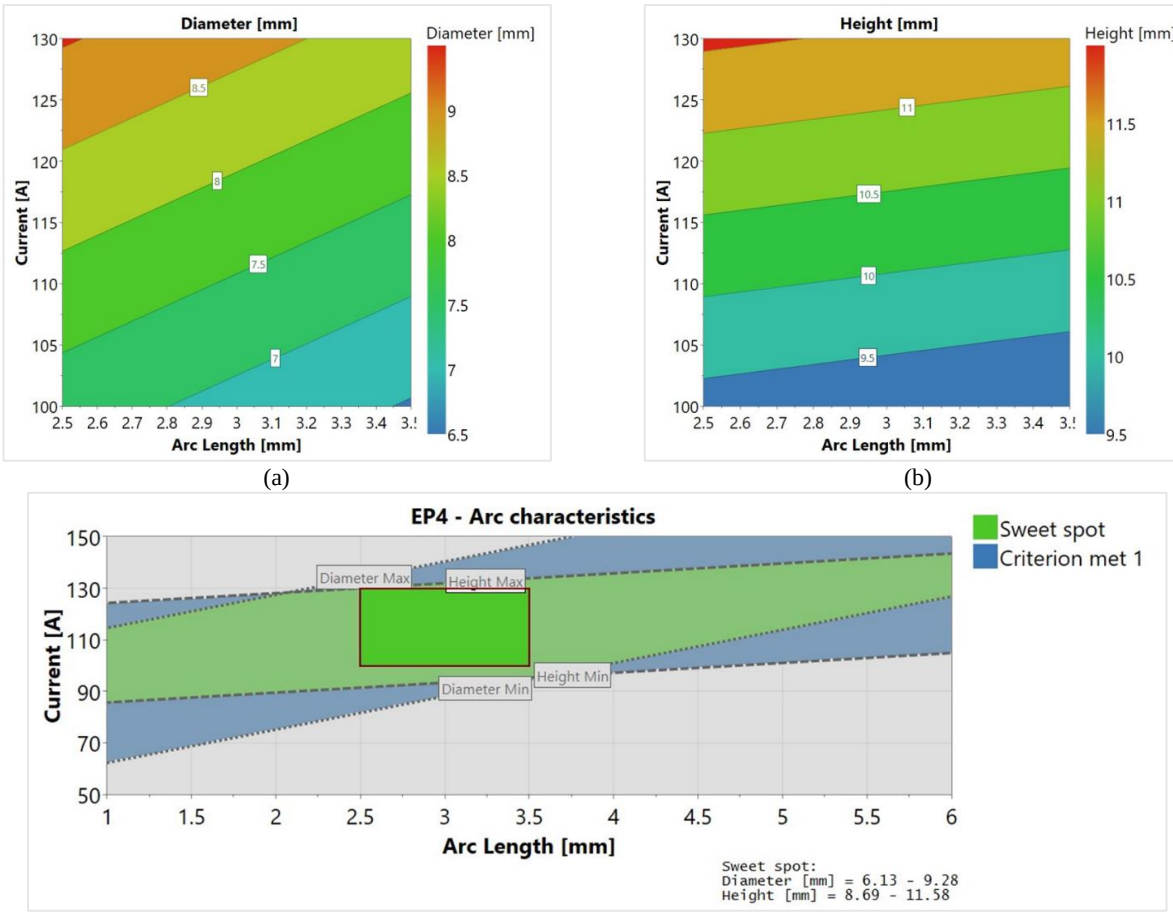

Figure 5-3: Contour plots arc output (a) diameter and (b) height and associated (c) sweet spot plot.

The contour plots illuminate the relationship between the arc input parameters and resulting characteristics, indicating that both the arc diameter (Figure 5-3(a)) and height (Figure 5-3(b)) increase, with increasing currents and arc lengths. However, when extrapolating this information (Figure 5-3(c)), the diameter, which is represented by dotted lines, appeared to be more sensitive to changes in the arc length. The dotted lines slope upwards, and at a much steeper angle, relative to the parallel lines representing the height, whose limits are represented by dashed lines. The plots indicate the stable arc regions, and for SMRM operations, the goal was to reduce the amount of displaced material, such that its effects were negligible, particularly at arc termination sites. For the BAM system, other considerations included the stability of the process as the arc length increased, as well as the lag between the ignition and stabilisation of the arc. However, this important sequence, which is controlled by the minimum possible duration required between interacting subsystems, was observed to have the most significant impact on the outputs. For specific SMRM tasks, the priority was to maintain a fixed arc length of ~3.5 mm or less, for the shortest possible duration and lowest permissible amperage, at the start and end of the process.

Focusing on the defined SMRM task requirements and specifications, different experiments were performed to screen and verify parameters for depositing single beads onto a flat substrate, before assessing other technical factors likely to influence SMRM procedures. The reprocessing strategy is depicted in Figure 5-4.

(a) (b) (c) (d)

Figure 5-4: Reprocessing strategy involving (a) characterisation of single beads (b) evaluation of different types of features (c) specification of SMRM task inputs and (d) development of in-process monitoring technique.

Initially, trials performed using SMD data were repeated to verify single bead characteristics (Figure 5-4(a)). Related trials were also completed to evaluate different types of representative features (Figure 5-4(b)), before specifying the dimensions of features (Figure 5-4(c)) eventually transferred to the case study, with DAQ plans initiated (Figure 5-4(d)), to facilitate verification procedures. The details of each trial are provided hereafter.

5.3.3 Temperature mapping

The purpose of temperature mapping trials was to quantify the workpiece temperature, relative to the heat input parameters, and evaluate temperature gradients in the vicinity of the melt pool, including its effects on the workpiece. Correspondingly, the variables incorporated within this experimental phase were expanded from previous titanium alloy trials, to facilitate the evaluation of interrelated factors. For reprocessing and related trials involving flat substrates, process input variables are summarised in Table 5-3.

Table 5-3: Summary of parameters and corresponding levels tested.

Factors		**Levels**	
Type	**Variable name**	**Low**	**High**
Quantitative	Current - peak [A]	100	130
	Current - background [A]	-	78
	Wire feed rate (mm/s)	9.17	28.33
	Travel speed (mm/s)	0.005	0.015
	Mechanical weaving-displacement (mm)	1	4
	Mechanical weaving-amplitude (mm)	2	3
Constant	Voltage [V]	~11	
	Arc Length [mm]	3	
	Dwell time (s)	10	
	Argon [l/min]	~14	
	Argon pre-flow (s)	2	
	Argon pre-flow (s)	2	

The interactions between the variables (Table 5-3) were evaluated using different substrates. Adopting a grid pattern, thermocouples were attached to ~10 mm thick substrates. Beforehand, each substrate was machined, to improve the flatness of parallel surfaces, before proceeding to drill the required holes. The specifications used for preparing the initial set of planar substrates (PS) are depicted in Figure 5-5.

The schematic depicted in Figure 5-5(a) was provided for the preparation of substrates, which were supplied as shown in Figure 5-5(b). The hole depths were designed to facilitate the acquisition of temperature data relative to the material thickness. Due to human error, it was necessary to redrill the holes in PS01-2, which resulted in slight deviations from the original schematic. However, such recurrences, whether attributable to

the system or operator, demonstrate how issues develop relative to distinct value adding operations along the SMRM chain, as well as the overall and specific consequences. In this case, the deposition toolpaths were easily adapted to accommodate offsets, thus enabling the substrate to be utilised for designated purposes.

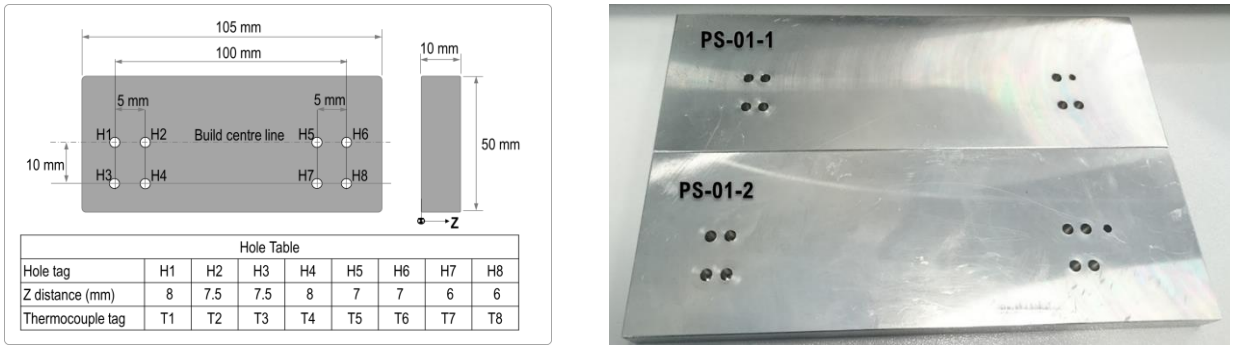

Hole Table								
Hole tag	H1	H2	H3	H4	H5	H6	H7	H8
Z distance (mm)	8	7.5	7.5	8	7	7	6	6
Thermocouple tag	T1	T2	T3	T4	T5	T6	T7	T8

(a) (b)

Figure 5-5: (a) Schematic for preparing (b) substrates for temperature mapping trials.

Thermocouples were subsequently attached to drilled holes, to map the subsurface temperature at the different depths identified in Figure 5-5(a), before securing the substrate to the BAM positioner. The set-up for temperature mapping trials is presented alongside the outputs in Figure 5-6.

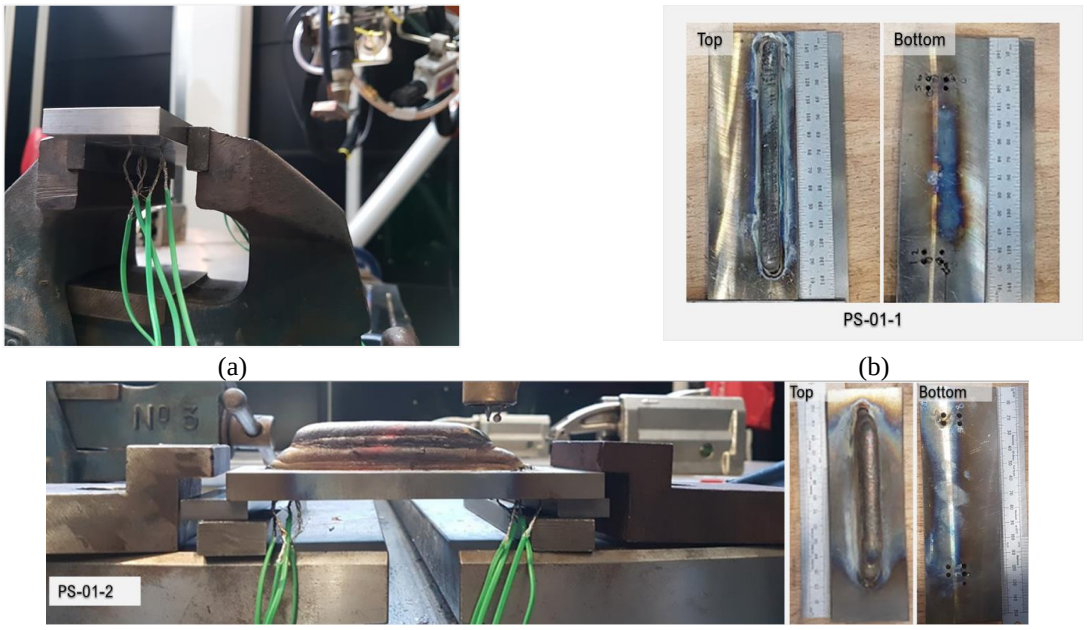

(a) (b)

(c)

Figure 5-6: BAM (a) set-up for temperature mapping trials and outputs (b) PS01-1 and (c) PS01-2.

Substrates PS01-1 and PS01-2 were respectively set-up, as shown in Figure 5-6(a) and Figure 5-6 (c), to ensure that thermocouple functions were relatively unimpeded. Material was subsequently deposited, as shown in Figure 5-6 (b) and Figure 5-6 (c), to facilitate the acquisition of pertinent temperature data. Due to the lack of dedicated BAM shielding solutions, all experiments were performed under localised argon circumstances, which is known to have a noticeable effect on the appearance of deposited layers (Figure 4-7), as observed in

relation to trial outputs, particularly for PS01-2. Nevertheless, the objective of mapping the evolving substrate temperature, in response to the process input parameters, was achieved. For all experiments (Figure 5-6), the tool was perpendicularly aligned to the substrate, with a 45-degree rotation applied to facilitate continuous deposition of multiple layers, with the wire leading or trailing the arc as it traversed the plane of the substrate. The emphasis was on acquiring data during single and multi-layer depositions, and to establish the build temperature steady state, thus determining the functional limits or sensing boundaries of this DAQ approach. However, due to performance issues, some of which were explored as part of systemic evaluations (Figure 4-35), the build was terminated prematurely. Other experiments were eventually performed to map the temperature distribution at varying distances from a fixed toolpath on substrate PS-02. The aim was to establish the temperature measurement boundaries, relative to the locations of different sensors, whilst exploring the potential effects of the arc energy on the substrate during depositions. The trial set-up is shown in Figure 5-7.

Thermocouple (T) locations on PS-03

Set S1	Distance from CL- Set T1 (mm)	Set S2	Distance from S2* (mm)	Set S3	Distance from S3 (mm)
TC-01	25	TC-01	-5	TC-01	-5
TC-02	50	TC-02	25	TC-02	25
TC-03	75	TC-03	50	TC-03	50
TC-04	100	TC-04	75	TC-04	75
TC-05	10	TC-05	105	TC-05	105
TC-06	20	TC-06	0	TC-06	0
TC-07	30	TC-07	50	TC-07	50
TC-08	40	TC-08	100	TC-08	100

- *S1*/S2*/S3* : Start/ arc-on position for Set S1, Set S2, and Set S3;*
- *CL : Centre line.*

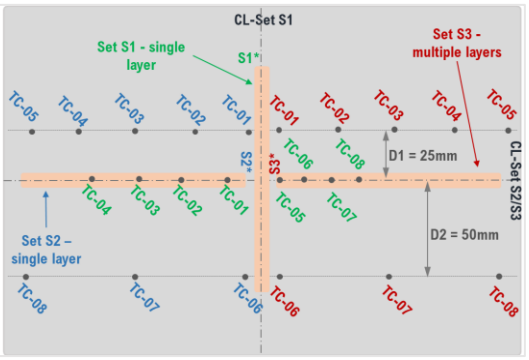

(a)

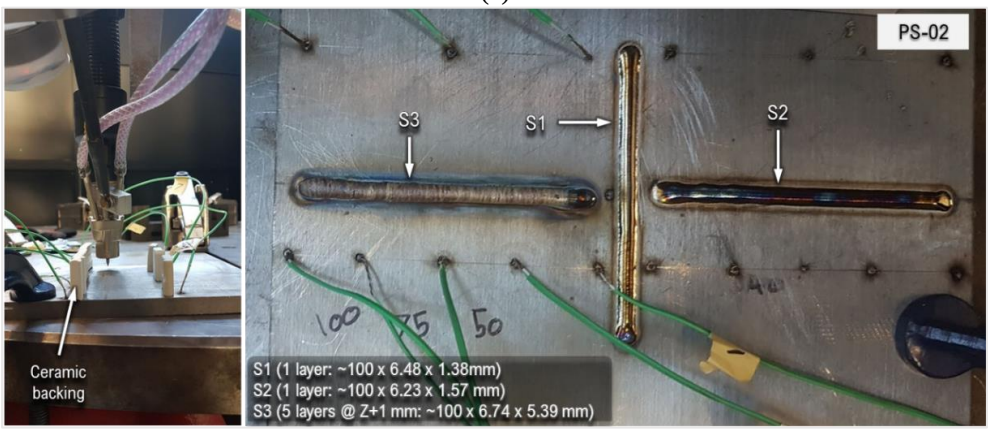

(b)

Figure 5-7: (a) Schematic for preparation of substrate and (b) setup for temperature mapping trials on PS-02.

Thermal data was obtained during autogenous passes, and for single and multi-layer builds, according to sets S1, S2 and S3 (Figure 5-7(a)). The goal was to mimic likely reprocessing scenarios, whereby a pre-heating pass may precede the deposition process. Thus, data was captured for autogenous passes, before repurposing the substrate and repositioning thermocouples to acquire data for single layer sets S1 and S2 respectively. This procedure was repeated for the final set, S3, which involved the continuous deposition of multiple layers. Before each trial, ceramic backing was strategically positioned to shield thermocouples from the direct effects of the arc, as depicted in Figure 5-7(b). Compared to PS01-2 (Figure 5-6), which was completed with similar

build parameters, the visual appearance of build PS02-S3 was significantly improved, as previously identified performance issues had been resolved. The temperature mapping trial outputs are depicted in Figure 5-8.

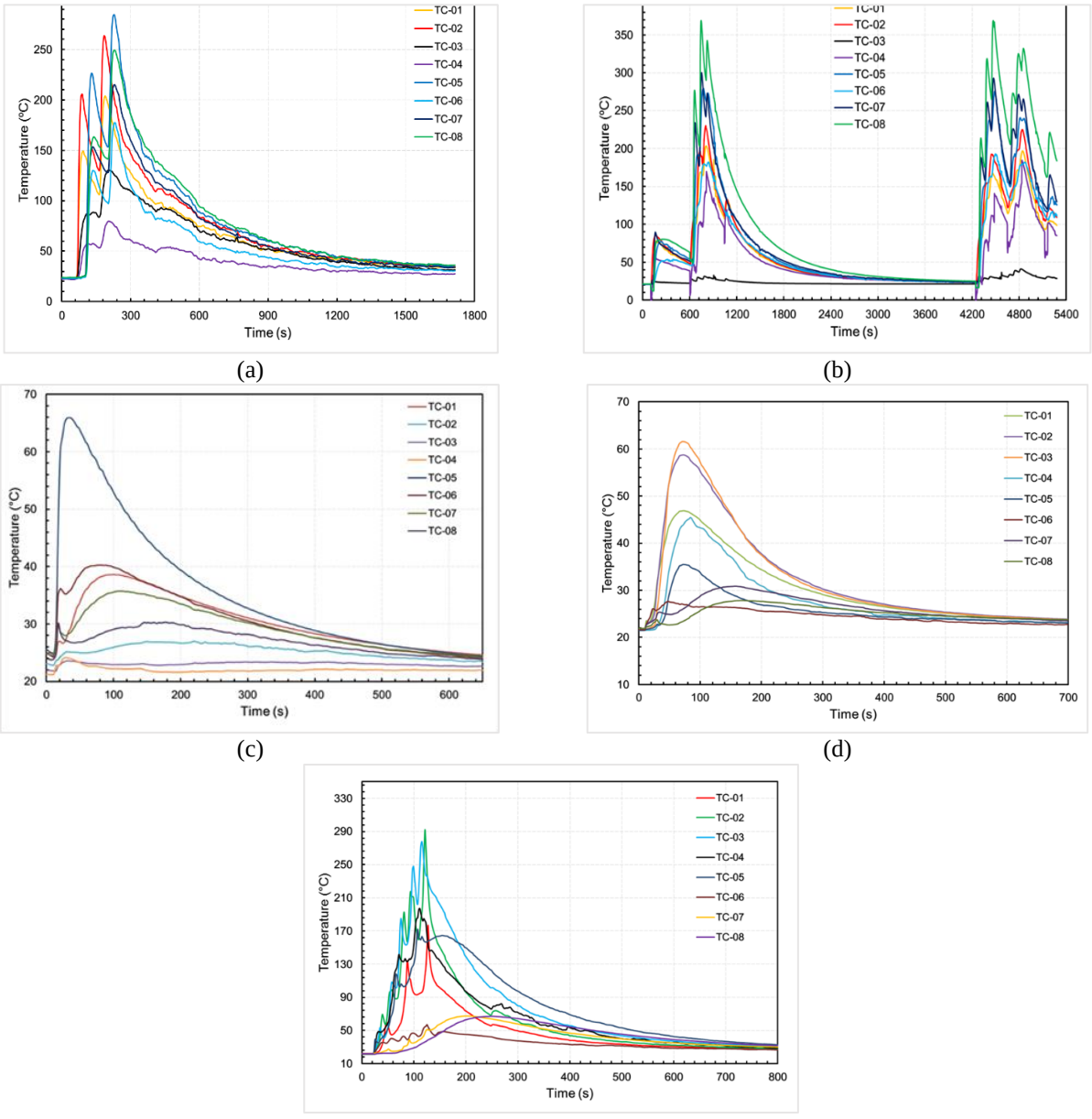

Figure 5-8: Representative temperature plots for substrates (a) PS01-1 (b) PS01-2 (c) PS02-S1 (d) PS02-S2 and (e) PS02-S3.

For similar builds, the resulting temperature profiles were comparable, with the maximum temperatures typically rising to ~290 °C for a single layer (Figure 5-8(a) and Figure 5-8(e)), and >350 °C for multi-layer builds (Figure 5-8(b)). Measurements obtained from multi-layer builds that included a pre-heating or autogenous pass, implemented prior to the deposition of initial layers, were comparable to the outputs derived from substrates to which similar procedures were applied, with maximum temperatures typically under 70 °C (Figure 5-8(c) and Figure 5-8(d)). In general, outputs were characterised by rapid heating and cooling cycles, which were more pronounced for multi-layer builds. Correspondingly, evident correlations between the

number of deposited layers, the part or substrate design parameters, and the cooling rate, were corroborated by the duration between the maximum and minimum values recorded. Furthermore, the EOAT orientation appears to have contributed to observed unevenness in resulting temperature profiles. Specifically, the data acquired with the wire leading the arc, resulted in temperatures rising and falling more evenly (Figure 5-8(a)) than plots derived from data acquired with a 45-degree tool orientation (Figure 5-8(b)), which was preferred for continuous deposition. It was also observed that substrates clamped directly onto the BAM manipulator (Figure 5-7(a)), cooled faster than substrates that were elevated during depositions.

5.3.4 Concurrent temperature and strain mapping

Due to the dependencies between the system input parameters, the output temperature and resulting strain responses, trials involving the latter were reserved until this stage. The aim was to establish and quantify correlations between the actual temperature of the workpiece, derived from process input parameters, and the consequent strain response. Six strain gauges (SG) were bonded onto substrate surfaces, using an adhesive compound, before spot welding thermocouples (TC) in different locations, for real-time monitoring of related variables. The experimental set-up for PS03 is shown in Figure 5-9.

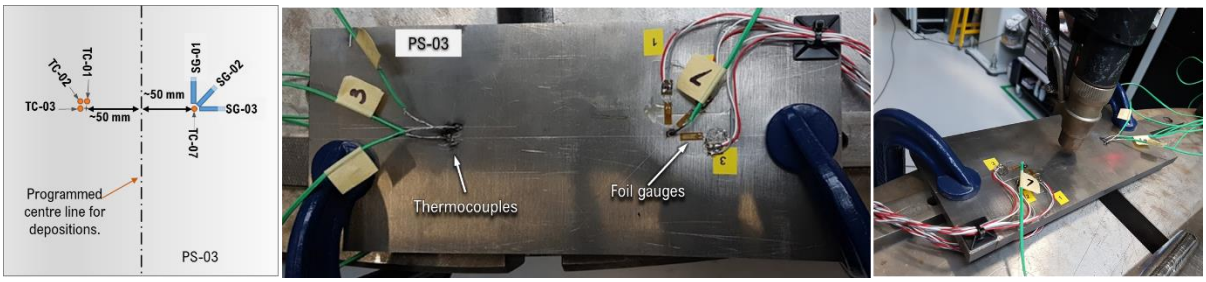

Figure 5-9: Schematic and set-up for simultaneous monitoring of temperature and strain on PS-03.

All sensors were tagged and connected to DAQ devices, as illustrated in Figure 5-1. Strain gauges SG-01, SG-02 and SG-03, were attached at 0, 45, and 90 degrees around a central point, which was located approximately 50 mm from the designated centre line of the workpiece (Figure 5-9), to enable the possible isolation of strain components in the stated directions. Thermocouples TC-01, TC-02, and TC-03, were similarly configured about the centre line and aligned to mirror strain gauge positions. An additional sensor, TC-07, was positioned at the centre of the strain gauges, to monitor temperatures in this vicinity. The remaining 3 gauges (i.e. SG-04, SG-05 and SG-06) and 4 thermocouples (i.e. TC-04, TC-05, TC-06, and TC-08), were attached in a parallel configuration, to the bottom surface of the substrate, for capturing opposing responses. The substrate was then clamped onto the BAM positioner (Figure 5-9), before proceeding with real-time measurements.

An initial layer was deposited, before allowing a cooling period of ~45minutes, the duration required to return the substrate to ambient temperature. For the final deposition, comprising 2 additional layers, a continuous deposition strategy was adopted, hence the procedures and tool configuration used for PS03(S3) was maintained. The outputs, corresponding to the distinct stages of this trial, are illustrated in Figure 5-10.

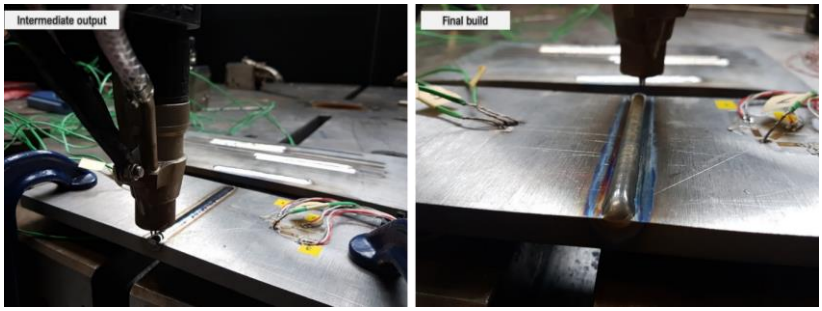

Figure 5-10: Outputs from trials on PS03.

The intermediate and final builds were both completed under localised argon circumstances, and the strain gauges appeared unaffected by the procedure. The resulting builds were relatively consistent between the two stages, with precisely formed outputs that were visually comparable to the builds shown in PS02. The concurrent measurements obtained from trials involving substrate PS03, are plotted in Figure 5-11.

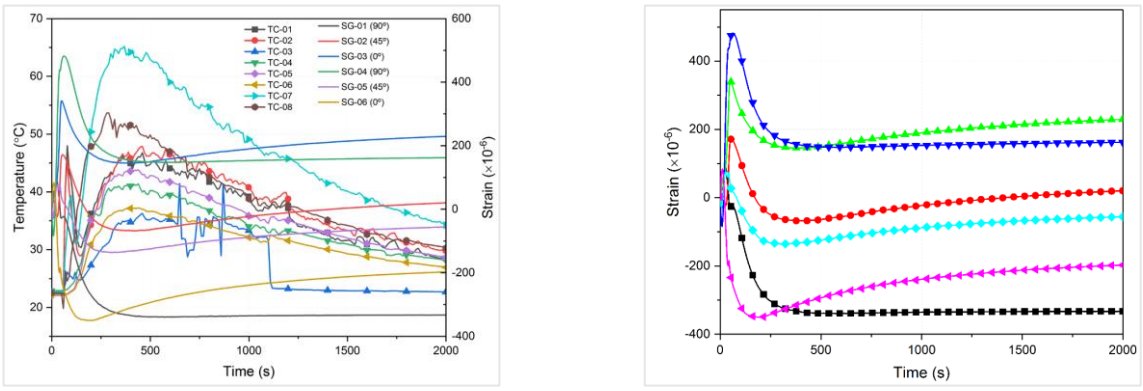

(a) (b)

Figure 5-11: Representative plots of (a) temperature and (b) strain measurements obtained from the substrate.

The acquired data establishes how the underlying structure responded to thermal inputs. The magnitude of each response was of significant interest, due to the potential effects on the structure during reprocessing operations. Autogenous passes, which correlated to the initial responses acquired, were specifically implemented to test the functionality of the sensors attached to the substrate (Figure 5-11). However, representative plots reveal detectable changes in the substrate, with the maximum strain (>400 με) corresponding to the maximum substrate temperature event (<70 °C).

5.3.5 Reprocessing trials on Ti-6Al-4V substrates

The final set of experiments were initiated to inform the specification of features, which were eventually introduced to the titanium alloy structure. Considering the direct SMRM requirements, these features, typically prepared using machining or other appropriate material removal techniques, established the starting conditions and inputs for actual reprocessing tasks. From an operational standpoint, and before finalising the requirements specification, it was desirable to have some variation between distinct restoration tasks, to enhance understanding of practical issues, including the input parameters, output quality, and reproducibility, when

reprocessing similar features. For expediency, design variables were limited to the width, depth, length, and radiuses of distinct features. The design inputs for preliminary reprocessing trials, performed on set PS04, are presented in Figure 5-12.

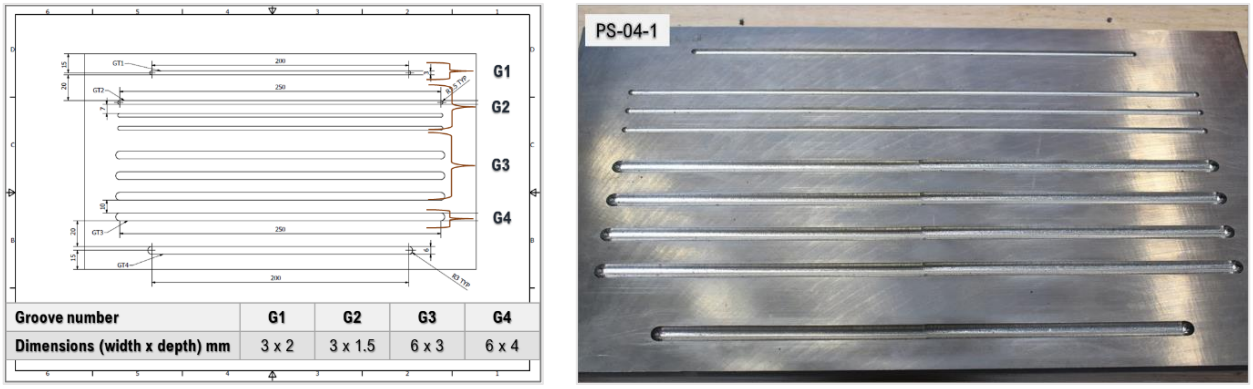

Groove number	G1	G2	G3	G4
Dimensions (width x depth) mm	3 x 2	3 x 1.5	6 x 3	6 x 4

(a) (b)

Figure 5-12: Specification of (a) preliminary inputs for reprocessing trials and (b) machined substrate PS04.

The different feature types and replicates were to be machined according to the specifications provided in Figure 5-12(a), but due to an omission during the preparation of substrates, some machined features, in PS04-01, were misaligned (Figure 5-12(b)). The impact of this error was judged to be low, relative to the purpose and criticality of planned trials. Hence, the substrates were used to evaluate reprocessing factors, including the programming approach and overall deposition strategy. The outputs for PS04 are depicted in Figure 5-13, with the experimental summary data provided in Table 5-4.

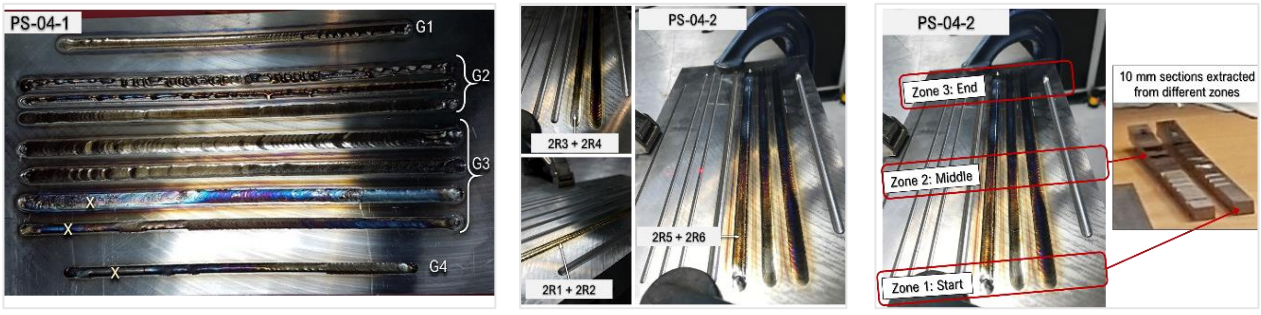

(a) (b) (c)

Figure 5-13: Reprocessing trial on (a) PS04-01 and (b) PS04-02 and subsequent (c) extraction of cross-sections.

An ‘x’ was used to denote experiments that were excluded, due to incorrect input parameters being applied (Figure 5-13(a)). The remaining PS04-01 trials were valid, and related outputs provided sufficient insights to proceed with PS04-02. When preparing flat substrates for reprocessing experiments, the preferred approach of consecutive machining of specified features, maximised the available trial surfaces, and enhanced efficiency, due to reduced set-up and processing times. However, the proximity of machined features impeded the planned acquisition of supplementary data via thermocouples, as shown in the original measurement set-up (Figure 5-1). Instead, a handheld IR thermometer facilitated instantaneous DAQ during reprocessing trials.

Table 5-4: Summary of variables evaluated during reprocessing trials on substrate set PS04.

Fixed variables	Travel speed: 0.15 mm/min Arc gap: 3 mm (Voltage ~12-14 V*) Argon pre-flow & post-flow duration: 2 secs Argon (torch): 17 l/min (O2 level ~3 ppm*)									
Independent Variables	***PS04-01 (305mm x 165mm x 10mm)***				***PS04-02 (305mm x 165mm x 10mm)***					
	Run 1 (1R1)	**Run 2 (1R2)**	**Run 3 (1R3)**	**Run 4 (1R4)**	**Run 1 (2R1)**	**Run 2 (2R2)**	**Run 3 (2R3)**	**Run 4 (2R4)**	**Run 5 (2R5)**	**Run 6 (2R6)**
Deposition pattern	MWT	MWT	MWT	MWT T	MWT T-RP	MWT T-CP	RP	CP	T45-CD	T45-CD
Weave length	5	4	-	3	3	3	-	-	-	-
Amplitude/ deflection (mm)	1.5	1.25	-	1	1	1	-	-	-	-
Weave angle (º)	90	90	-	90	90	90	-	-	-	-
Pulse (s)	0.4 on/ 0.4 off	-	-	-	-	-	-	-	-	-
Wire feed rate (mm/s)	9.17	9.17	9.17	9.17	12.5	12.5	12.5	12.5	12.5	12.5
Peak Current (A)	130	115	130	130	130	130	130	130	130	130
Base Current (A)	78	115	130	130	130	130	130	130	130	130
Dependent variables										
Visual inspection	OK	OK	OK	OK	Acceptable	Acceptable	Acceptable	Acceptable	Acceptable	Acceptable
Start temperature (ºC)	23-25	23-25	23-25	23-25	23-25	153	192	153	23	35
Max temp (ºC)	-	-	-	-	153	210	153	215	40	240
Number of layers	1	1	1	1	1	1	1	1	1	1
Notes					Temperature recorded <1-minute post-deposition.	Temperature recorded <1-minute post-deposition.	Temperature recorded ~ 5 minutes post-deposition	Temperature recorded <1-minute post-deposition.	Temperature recorded ~ 15 minutes post-deposition.	Max temperature recorded ~10 minutes post-deposition and 50mm from centreline. Temperature ~55 ºC at ~15 minutes post deposition.

Key: MWT (Mechanical weaving - Trapezoid); RP (root pass); CP (cap/ finishing pass); T45-CD (Torch/ EOAT positioned at 45º - Continuous deposition).
(*) Derived variables

Manual procedures were maintained throughout this phase, to facilitate monitoring of the substrate condition before and after each trial, whilst augmenting specific knowledge of related operational factors. Each feature was restored and visually inspected, before proceeding with the next feature, until all PS04-01 trials were completed. The outputs from G3 or groove type 3 (Figure 5-13(a)), corresponding to 1R3 (Table 5-4), were visually acceptable. 1R3 was also deposited without weaving the EOAT, resulting in a much flatter profile, when compared to feature 1R4, which was of equal dimension. Thus, focusing on type G3 features only, the parameters used for 1R3 were selected for subsequent reprocessing trials on PS04-02 (Figure 5-13(b)). For these trials, the wire feed rate was increased to ensure that sufficient material was deposited to completely fill the void. Different deposition patterns were also utilised, with weaving passes resulting in much wider deposits, in 2R1 and 2R2, when compared to the other passes. Similarly, continuously depositing the initial and finishing layers in 2R5 and 2R6, increased the width of deposits, relative to the slightly narrower outputs derived from consecutively depositing 2R3 and 2R4. The outputs (Figure 5-13(b)), resulting from different deposition patterns, were generally acceptable, as reprocessed features were visually similar, with relatively even build profiles and groove edges. However, due to slight indentations or end imperfections, noted in relation to 2R5 and 2R6, concerns about weaving the EOAT in restricted spaces, and the resulting oversized features, relative to the specifications of G3, a serial layering approach was preferred.

Material cross-sections were extracted from the mid- and end zones of PS04-02 (Figure 5-13(c)), via laser cutting techniques. The extracted sections were inspected using x-ray computed tomography (CT) scanning techniques, to assess the subsurface condition of restored features, particularly at the interfacial regions and/ or fusion lines, between the deposited and base materials. The resulting CT scans are presented in Figure 5-14.

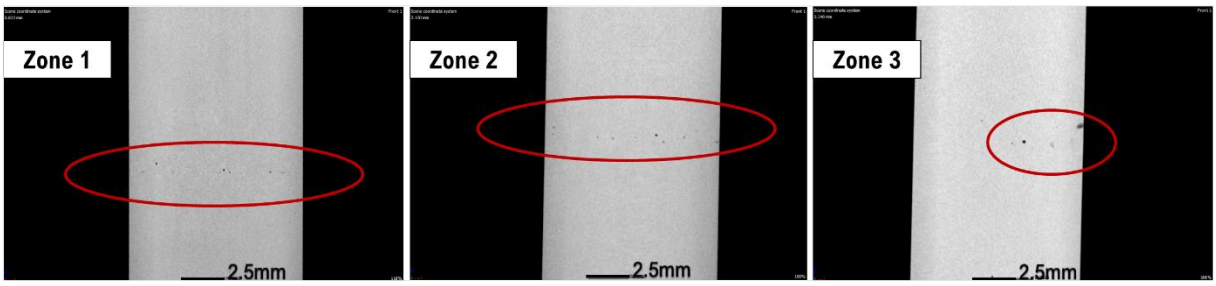

Figure 5-14: Typical subsurface imperfections in reprocessed material specimens.

From visual inspections, it appeared that reprocessed features were properly fused, but indications were observed in the different inspection zones (Figure 5-14). Normally, acceptance criteria are defined by industry and may vary, depending on the industry, application, and specific in-house standards. Typically, certain material flaws, including linear, lack of fusion, and through wall indications, are not permitted, but rounded or spherical material indications, such as chain porosity, may be accepted. Acceptability is usually determined relative to the maximum size, quantity, and minimum spacing between adjacent indications. In this instance, the scans revealed a few evenly distributed and regular shaped indications that were typically ≤50 microns, which is relatively small, when considering the specified dimensions of distinct features (Figure 5-12). From

a quality perspective, these indications were well within the limits specified in ISO 5817:2014, which addresses welding quality levels of imperfections for different alloys, including titanium.

While CT scans were particularly useful for corroborating the reprocessing strategy on which subsequent trials were based, the size of the aerospace component exceeded the capacity of the equipment, precluding it from further substantiation activities. Recurring capacity issues, also observed during FAT/SAT stages, further underscored the significance and potential implications of such limitations, on SMRM operations. Undeniably, this important inspection technique was invaluable for qualifying trial outputs and underpinned the decision to modify the specification of features to be reprocessed. For the final geometry, design modifications mainly involved increasing the feature depth to width ratio, from 1:2 to 1:5, as depicted in Figure 5-15.

(a) (b) (c) (d)

Figure 5-15: Standardisation of (a) SMRM requirements and (b) specification for machining of features before proceeding with reprocessing operations on (c) PS05-01 and (d) PS05-02.

The representative features were machined to specification (Figure 5-15(a)), using additional substrate set PS05, shown in Figure 5-15(b). The corresponding trial outputs revealed visible edge imperfections for outputs PS05-01 (Figure 5-15(c)), which were unacceptable. Flaws were attributed to the distinctions between substrate sets PS04 and PS05, with wall thicknesses of approximately 8mm and 10mm, respectively. Consequently, the experimental design was further augmented by combining process data from preliminary *Study 2* (section 3.2.2), with screened titanium alloy DED data from previous organisational studies. Focusing on reprocessing task requirements and the specified groove dimensions of ~10mm (Figure 5-15(a)), the enriched data set was used to create a new contour plot, to identify a different set of parameters, based on the model predicted responses, presented in Figure 5-16.

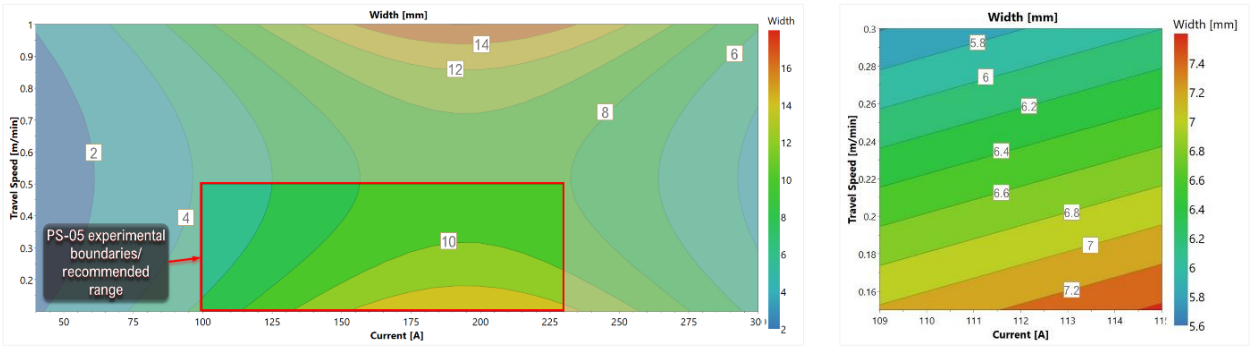

(a) (b)

Figure 5-16: Comparison of contour plots derived for (a) PS-05 and (b) preliminary SMD trials.

The original SMD contour plot (Figure 5-16(b)) showed that at a fixed travel speed, the width of depositions generally increased in response to an increasing current and vice versa. However, enriching the data pool for PS05 resulted in a contour plot (Figure 5-16(a)) that bore striking similarities to the responses observed in preliminary investigations (Figure 3-3), in which a stable region was identified, allowing for the selection of parameters for processing the SS316L PoC part. For PS05, the contour plot was similarly extended, beyond the verified experimental boundaries or range, to elucidate the relationship between screened parameters and responses. A new parameter set was selected, to match the desired width of the standardised features, before proceeding with PS05-02. The current and wire feed rate were increased from 130 to 150 A, and 12.5 to 20 mm/s, respectively, while the travel speed was ultimately reduced to 0.13 mm/min, to maintain a similar deposition height/ profile. Although there were indentations at the end of the run, attributed to a combination of the substrate and groove dimensions, relative to the programmed toolpath for the build, the modified parameters evidently and satisfactorily improved the visual appearance of the reprocessed substrate, PS05-02 (Figure 5-15(d)), which was the main objective of this trial. The outputs were also consistent with predicted responses for selected parameters (Figure 5-16(a)). However, the benefits of further reprocessing trials were relatively limited, due to evident correlations between the substrate dimensions, specific inputs, and qualified outputs. Accordingly, the new dimensions for standardised features, in conjunction with other process parameters associated with PS05-02, were maintained for the case study. As with previous reprocessing trials, the outputs from set PS05 were also retained to support further investigations.

5.3.6 Inspection and analysis

Inspection procedures were implemented to validate trial outputs, and further rationalise observations pertinent to the GT framework. Correspondingly, outputs from reprocessing trials were repurposed to obtain material samples in the as-deposited, restored, and as-supplied substrate conditions. The secondary objective was to characterise the resulting material properties, due to the highlighted development state of the BAM capability, and the potential implications for the case study, including the task requirements, and processing consideration. Specifically, the stipulated conditions of supply further narrowed the analytical scope of planned investigations, and as such, it was necessary to establish other means of corroborating system outputs, within the defined empirical scope and stated boundaries.

Further to increasing confidence in underpinning decisions, evaluating the fittingness of the overall SMRM strategy for reprocessing tasks was necessary, before proceeding with the case study. In conjunction with visual inspections, completed at relevant trial stages, the main verification tools, and techniques, implemented for related activities, including material characterisation studies, are discussed hereafter.

5.3.6.1 Bulk material characterisation

A Zeiss Axiocam digital camera was used to inspect specimens obtained from reprocessed BAM samples (Figure 5-15). The extracted specimens were prepared using a Struers AbraPol-20 automatic grinding and

polishing machine. Samples were initially ground flat, using a 120-grit silicone paper. This procedure was repeated for a further 5-minutes, using a 250-grit silicone paper, with a grinding force of ~100 N, and rotating holder and disc speeds of 50rpm and 300 rpm respectively. A rotating holder and disc speed of 50rpm, and a force of 80 N were applied to samples, which were polished for ~5 minutes, using a 9 μm diamond suspension, followed by a final ~7 minutes oxide polish, with a 2 μm fumed silica suspension. Microscopic images were obtained to assess the as-supplied (AS-C), and as-deposited (AD-C) material conditions, as well as the heat affected zones (HAZ) of the reprocessed substrate. The acquired optical images are shown in Figure 5-17.

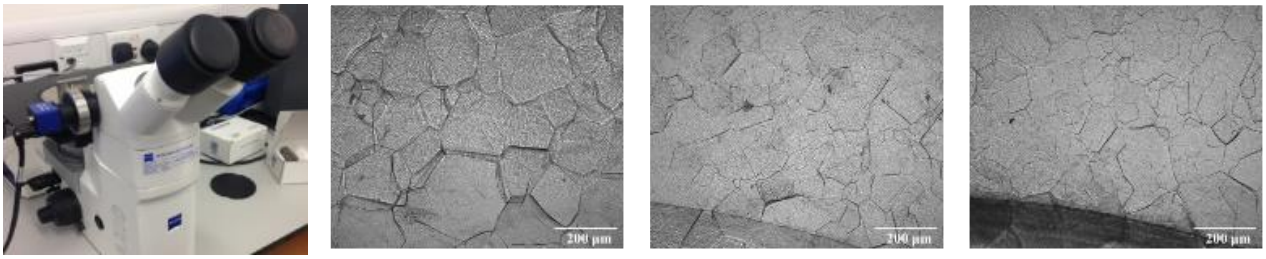

Figure 5-17: (a) High-resolution digital camera for analysis of typical microstructures in the (a) AD-C (b) HAZ and (c) AS-C materials.

The grain structure of both deposited and substrate materials were clearly visible in polished samples obtained from substrate PS-05. Material imperfections were also evident, indicating the inherent nature of material processing issues. When evaluating the grain sizes, larger structures were observed in AD-C materials, when compared to the finer microstructures of the AS-C and HAZ specimens. A higher number of grain boundaries are desirable due to measurable correlations to the material strength. However, strength, stiffness, and ductility are equally significant, due to the implications of these characteristics on durable performance. Therefore, the mechanical properties of materials obtained from BAM trials were also evaluated.

5.3.6.2 Microhardness mapping

The microhardness mapping was completed on substrate PS05 (Figure 5-15), using a Tukon 2500 microhardness tester. Measurements were obtained using a test load of 0.5 kg, which was applied for a duration of 15 seconds, and at 0.2 mm intervals. Micro-hardness tests were completed on sample set PS05, before and after the restoration process (Figure 5-15), to determine variations is these derived system outputs. Pre-deposition, measurements were obtained from locations near the centre and at the edge of the groove (GE) and from the corner of the sample (SC). Post-deposition, these approximate locations, designated reprocessed GE or RGE, and reprocessed SC (RSC), were maintained to quantify the effects of reprocessing operations on the samples PS05-01 and PS05-02.

The experimental set-up and outputs are shown in Figure 5-18, alongside designated locations from which measurements were obtained. The pattern for mapping designated zones (Figure 5-18(c)), mirrored the configurations used when attaching strain gauges to substrates (Figure 5-9). This arrangement provided a basis

for evaluating the sufficiency of such approaches for basic material characterisation, with measurements facilitating comparative analysis of representative variations in restored samples.

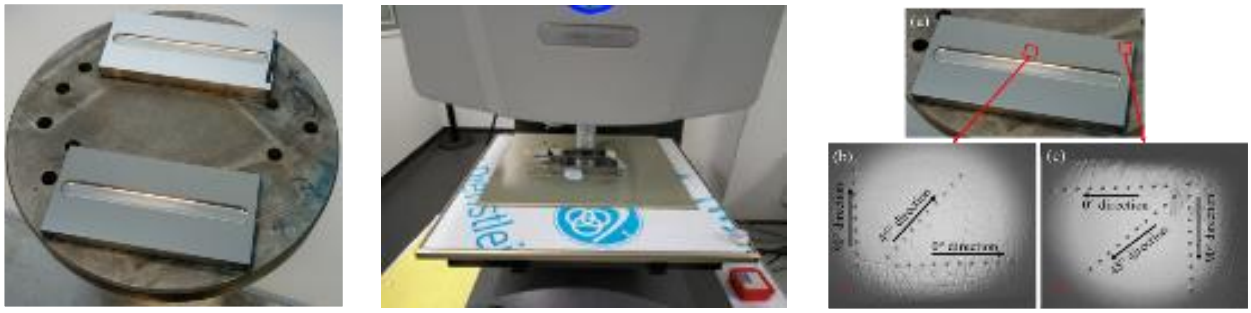

(a) (b) (c)

Figure 5-18: (a) Set-up for polishing and (b) micro-hardness testing at (c) specified locations on PS-05.

The approach also anticipates the use of portable hardness testing devises, which may be integrated with the BAM platform, to obtain measurements, albeit with relatively lower sampling rates, to support the envisioned concept for end-to-end SMRM operations. The resulting measurements are plotted in Figure 5-19.

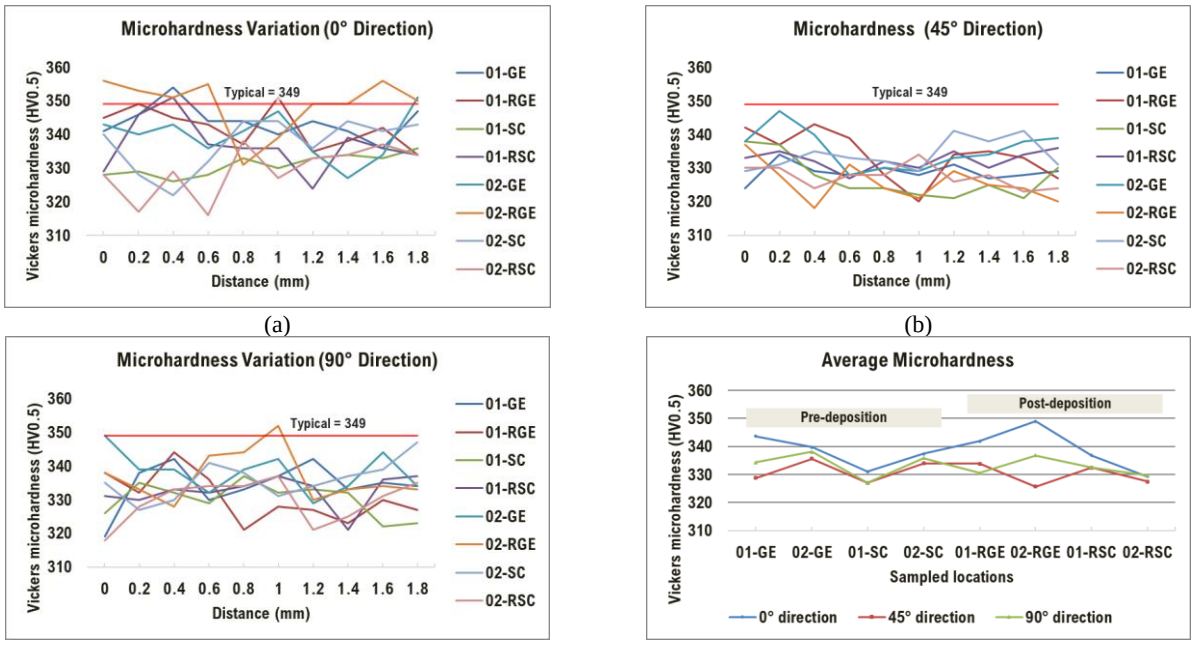

(a) (b) (c) (d)

Figure 5-19: Analysis of micro-hardness variation in (a) 0° (b) 45° and (c) 90° directions, for samples PS05-01 and PS05-02, including (d) summary plot of microhardness variation in each direction.

Typical handbook values (i.e., 349 HVN) for Grade 5 titanium were used for comparative purposes. Pre-deposition, the averaged micro-hardness of substrates PS05-01 and PS05-02 varied between ~330 to ~345 $HV_{0.5}$, irrespective of the direction or location, with trends indicating less resistance to localised deformations, particularly in the 45° direction (Figure 5-19(d)). Material resistance typically increased after reprocessing operations, particularly in the 0° direction, where the maximum average value (~349 $HV_{0.5}$) was recorded at location 02-RGE for PS-05-2, compared to corresponding measurements acquired along the 45° (~326 $HV_{0.5}$)

and 90° (~337 $HV_{0.5}$) directions. However, the variance was greater between distinct measurements obtained after reprocessing operations, ranging from approximately 326 to 349 $HV_{0.5}$ (Figure 5-19(d)).

Measurements related to distinct directions were consistent with overall trends, with the maximum value (~356 $HV_{0.5}$) recorded in the 0° direction, followed by the 90° and 45° directions, where maximum values obtained were ~352 $HV_{0.5}$ and 347 $HV_{0.5}$ respectively. Considering all substrates were similarly prepared, variations at different locations were attributed to related procedures, with both machining and reprocessing operations likely contributing to higher resistance levels, typically occurring at GE locations (Figure 5-19(d)).

5.3.6.3 Tensile testing

Small sized uniaxial tensile specimens (ASTM-E8/E8M Specimen 3) were extracted from both as-deposited and reprocessed materials, corresponding to trial phases PS01 (Figure 5-6) and PS05 (Figure 5-15). For reference purposes, further specimens were also extracted from the substrate material, before proceeding with tests on the resulting specimens as depicted in Figure 5-20.

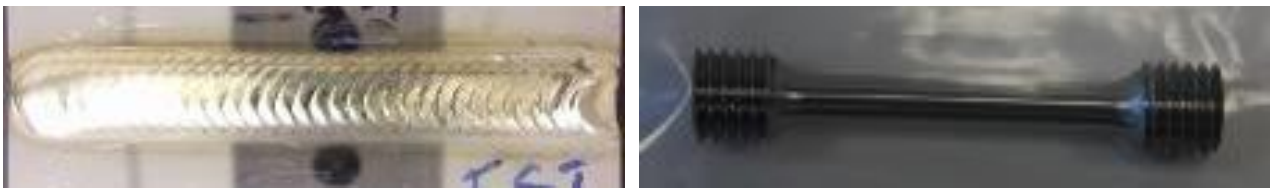

(a) (b)

Figure 5-20: (a) Material extracted from restored BAM sample for (b) uniaxial tensile specimen

The test samples (Figure 5-20(b)), of 30mm gauge length and 6mm diameter, were extracted in the transverse direction from deposited, reprocessed and substrate materials. Tensile tests were performed at room temperature, using a hydraulically operated 50 kN Instron universal testing machine, pulling at a rate of 4 mm/min. uring the tensile test, elongation was recorded using an extensometer, with stress-strain diagrams for each sample obtained from the inbuilt monitoring and data gathering facilities.

Consistent with the GT approach, test results were further analysed to establish the relative properties of representative SMD materials obtained from preliminary studies (section 3.2.2), and from extracted BAM materials derived from trials involving PS01 and PS05. The results are presented in Figure 5-21.

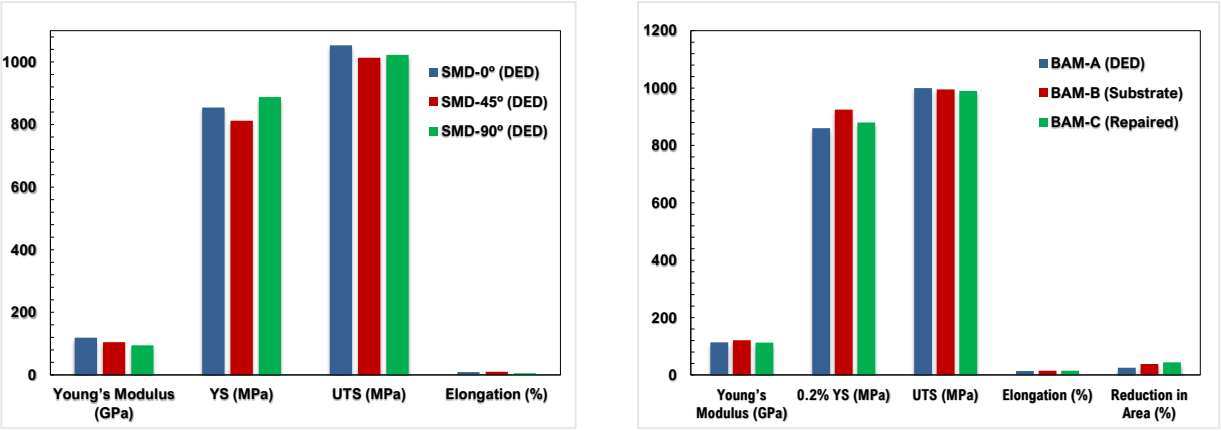

(a) (b)

Figure 5-21: Comparison of tensile properties of (a) SMD and (b) BAM specimens.

For SMD experiments and flat tensile specimens, the averaged UTS value was higher for samples extracted in the deposition or SMD-0° direction (~1053 MPa), than for samples extracted in the SMD-45° (~1014 MPa) and SMD-90° (~1022 MPa) orientations. The yield strength was typically higher in the transverse or SMD-90° orientation, with a maximum value of 941 MPa, compared to 836 MPa and 891 MPa for SMD-45° and SMD-0° directions respectively. These results correspond with averaged elongation values, measured at ~5%, 9% and 10% for SMD-90°, SMD-45° and SMD-0° accordingly. Young's modulus values were also consistent with higher material stiffness in the build direction (119 GPa), with lower values obtained from the SMD-45° (105 GPa) and SMD-90° (94 GPa) directions respectively. For cylindrical BAM specimens, the UTS value slightly higher in the as-deposited condition, BAM-A (~1000 MPa), relative to the substrate, BAM-B (~995 MPa) and restored material, BAM-C (~990 MPa). Similarly, there were very small differences between the Young's modulus and elongation values, and only slight differences in the measured reduction in the cross-sectional areas of fractured specimens. In contrast, the measurements revealed more obvious variations in the yield strength for specimens obtained from the BAM-A (~860 MPa), BAM-B (~925 MPa), and BAM-C (~880 MPa) materials. When comparing SMD and BAM materials, the UTS values were typically higher in SMD materials, but similar yield strengths were obtained for the BAM-A and SMD-0° specimens, and for BAM-C (repaired) and SMD-90° specimens, with the maximum values obtained from the substrate (BAM-B).

5.4 SMRM case study

The actual validation of the BAM system for large-scale applications was underpinned by SMRM operations involving a Grade 5 titanium aerospace component, with preliminary and reprocessing trials informing the overall strategy. Related factors, including the siting of features, and the method of extraction from designated reprocessing regions, were also explored. Identified regions were defined in relation to the primary structure and integral features of the component, including the distinct edges associated with these features, and the intersections between separate features and the primary structure. The primary focus was on clarifying system

validation requirements, and preparing the artefact for related SMRM operations, which involved specifying representative features and developing the reprocessing strategy for BAM tasks, as depicted in Figure 5-22.

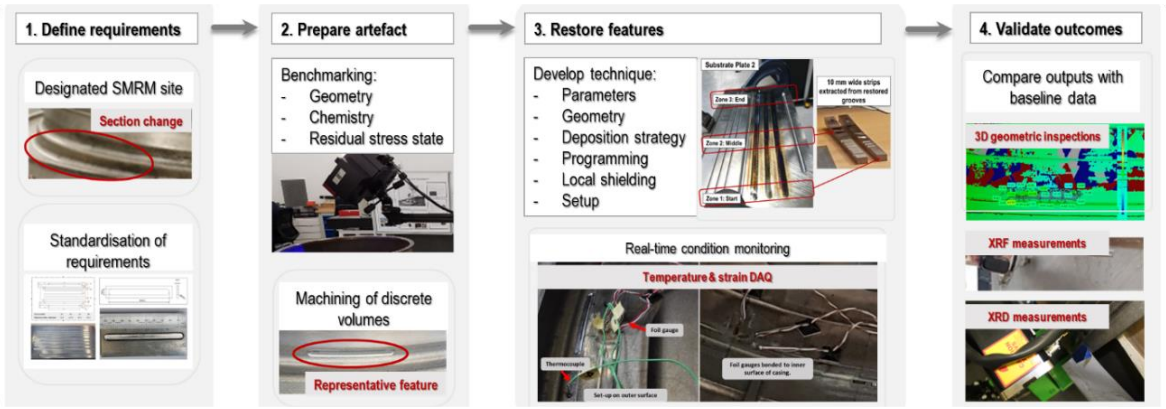

Figure 5-22: Overview of SMRM scope and implementation strategy.

The strategy for this case study, which is further elaborated in subsequent sections, provides and outline of the main SMRM operations and implementation stages. Developed in consideration of the supply scope, the component was first inspected, to quantify the as-received condition, before defining exact SMRM requirements underpinning investigations. Then, a series of representative and standardised features were machined into designated areas around the circumference of the component, thus establishing the basis for subsequent reprocessing operations. Finally, different NDT methods were adopted, to acquire corresponding data for comparative assessments.

5.4.1 Preparation of component

The as-received component was visually inspected before proceeding with other benchmarking activities. The actual inspection methods, which are detailed in the relevant sections, established the original state of the component. The specified features were to be extracted from locations with adjacent features, and/or sited between distinct component sections. However, tooling-related restrictions, necessitated modifications to this approach. Features were sited in more accessible locations and sufficiently distanced from impeding edges and/or other features, before proceeding with machining operations, which were to be completed in accordance with specifications (Figure 5-15). The plan was to evenly space features around the circumference of the component, but due to similar tooling considerations, a further compromise was necessary. These concessions also highlighted the effects of accessibility issues, stemming from the technological or capacity limitations during the implementation of SMRM operations. Ultimately, the revised machining specifications predetermined the starting conditions and input parameters for BAM system validation activities.

In total, 6 features were specified for machining operations, with due consideration given to the proximity of distinct features and spacing requirements for accommodating real-time monitoring appurtenances during reprocessing operations. The preparatory steps for adjoining operations are shown in Figure 5-23.

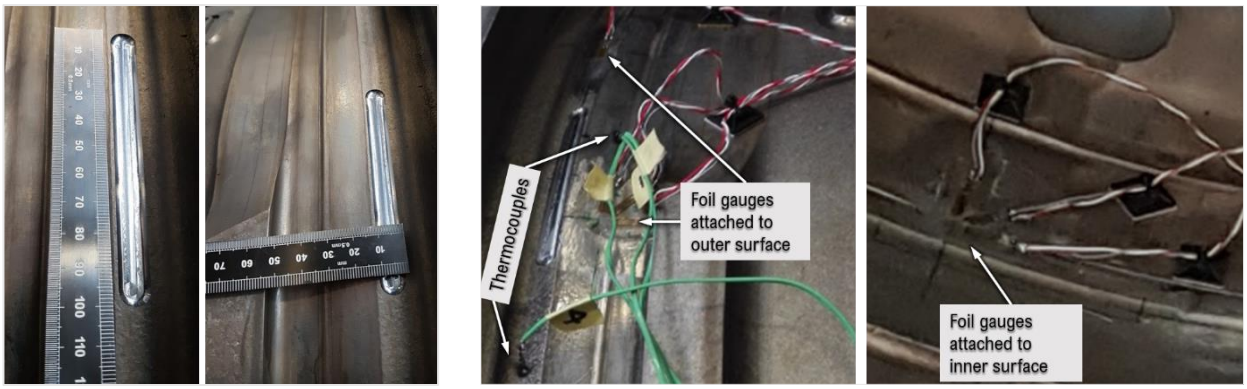

(a) (b)

Figure 5-23: Preparation for reprocessing of (a) standardised feature(s) and (b) in-process monitoring setup.

The machined volume, shown in Figure 5-23(a), is typical of the inputs used for validating the BAM system. After machining, each feature was visually inspected to verify compliance with specifications, before transferring the component to the BAM system. Next, target surfaces were cleaned and degreased, to facilitate the attachment of different sensors required for in-process monitoring of predetermined variables. Thermocouples were used to sample data from two different features, while strain gauges were attached to only one of the features (Figure 5-23(b)) for concurrent monitoring and DAQ. However, due to the specifications governing the siting of machined volumes, it was not possible to attach sensors in the specified locations linked to the feature being monitored. This consideration, and related concerns, highlight the need for advanced non-contact tools to instigate more robust condition monitoring strategies. Furthermore, the generation of high integrity data from such strategies are potentially advantageous to the development of simulation models for MAM, particularly for relevantly scaled research and properly validated outputs. In this instance, offset distances on measurement surfaces were restricted to locations that afforded sufficient allowances for the proper attachment of sensors, particularly for foil gauges (Figure 5-23(b)). The different sensors were attached to the component, according to revised specifications for the preferred measurement locations, after which it was transferred to the BAM platform, to commence reprocessing operations.

5.4.2 BAM set-up and programming

The component was lifted onto the 2-axis BAM manipulator and secured in position, using universal clamps, before tilting the manipulator into a horizontal position. Then, the robot was positioned directly above the component, ensuring that the EOAT was perpendicularly orientated, to facilitate deposition in the wire leading configuration. Between distinct reprocessing tasks, the manipulator was rotated to facilitate consecutive access to each of the machined volumes or features (Figure 5-23(a)). Compared to the SMD capability, which dictated the dimensions of PoC part, the 200 kg component, and associated dimensions (∅1200 x 900 mm), were well within the specified load and dimensional capacity of the BAM platform, and thus easily accommodated. Conversely, OLP capabilities are being developed for the BAM system, while the bespoke SMD solution was fully functional. Accordingly, related BAM programming task were performed online, when generating deposition toolpaths for experiments. However, set-up procedures were relatively easier, as the double access

doors in the perimeter fence allowed unrestricted access to the BAM positioner, whose movements, in conjunction with the gantry, significantly facilitated the macro-positioning of the robot. Subsequently, the articulated robot similarly enabled the more efficient micro-positioning of the EOAT, relative to the component. The extended reach afforded by the gantry ensured that designated component areas were easily accessed during programming, and for subsequent reprocessing tasks.

While the SMD capability offered an inert atmosphere, it was necessary to evaluate localised shielding options for the BAM system. The SMD kit included temporary shielding solutions, but these items were purposefully designed, and thus not suitable to be repurposed. Instead, a dedicated BAM solution was specially devised to ensure adequate shielding conditions were maintained during reprocessing operations. The equipment set-up, including the case study and provisional shielding solution used for trials, is shown in Figure 5-24.

(a) (b) (c)

Figure 5-24: (a) Component set-up relative to (b) EOAT with trailing shield, and (c) clamping solution.

For both SMD and BAM capabilities, the requirement for temporary shielding solutions, emphasised the compounding implications of non-standard EOAT designs, and requirements governing the particulars of an application (Figure 5-24(b)), on set-up times and costs. Other factors, such as the clamping or work holding requirements (Figure 5-24(c)) also have technical and financial implications. Invariably, specialised solutions will be required for scenarios where there are no discernible locating points or appropriate work holding solutions to meet exact requirements. In this instance, there were suitable locating points on the BAM positioner, for accommodating a range of work holding solutions via different holes and slots, together with pre-existing component features, which helped to ensure that the workpiece was properly secured. Thus, the BAM system requirements for work holding and part manipulation, to facilitate the automation of consecutive operations on the different features of a single component, were satisfied.

5.4.3 Reprocessing trials on titanium artefact

Before each operation, features (Figure 5-23(a)) were cleaned using lint free cloths, acetone, and isopropanol, to remove all traces of grease and other surface contaminants. Due to the restrictions on post-DED operations, in-process monitoring measures were crucial when implementing restoration tasks. Equally, the strategy for real-time monitoring and DAQ was especially devised to support process validation, and it was necessary to verify that the devices attached to the component (Figure 5-23(b)) functioned as intended. The verification procedures involved implementing an autogenous pass using the lowest permissible input current of 40 A, while other parameters were maintained as defined for PS-05-2. Test runs were typically completed, before

depositing material into the designated feature. Visual inspections were completed between autogenous passes and initial layers, before proceeding to deposit a subsequent final layer, as necessary.

During reprocessing operations, the BAM EOAT was normally programmed to traverse the designated segment of the component, with the wire leading the arc, while the component remained stationary. However, it was desirable to evaluate the systemic effects of rotating the part relative to a stationary EOAT. Accordingly, a programme was specifically created and used in conjunction with equivalent input parameters for this trial, with the wire stationed behind the arc, but feeding in this same direction as the component, which was rotated in an anti-clockwise manner. This procedure resulted in excessive material build-up at the end of the feature, due to the molten metal flowing in the direction in which the component was rotated, and pooling at the end of the feature, where depositions were terminated. While changes to the flow characteristics of molten material were anticipated, owing to the exploration of systemic events via stock and flow diagrams (Figure 4-23), the specific effects of such changes remained indeterminate until afterwards. The detectability of this event was influenced by the limited field of view afforded by monitoring devices, thus underscoring the benefits of discrete event modelling for MAM applications. Nevertheless, it was demonstrated that, with proper procedures in place, the BAM system can handle operations involving both stationary and/ or rotating components. The operator's perspective, including related task and procedures, is presented in Figure 5-25.

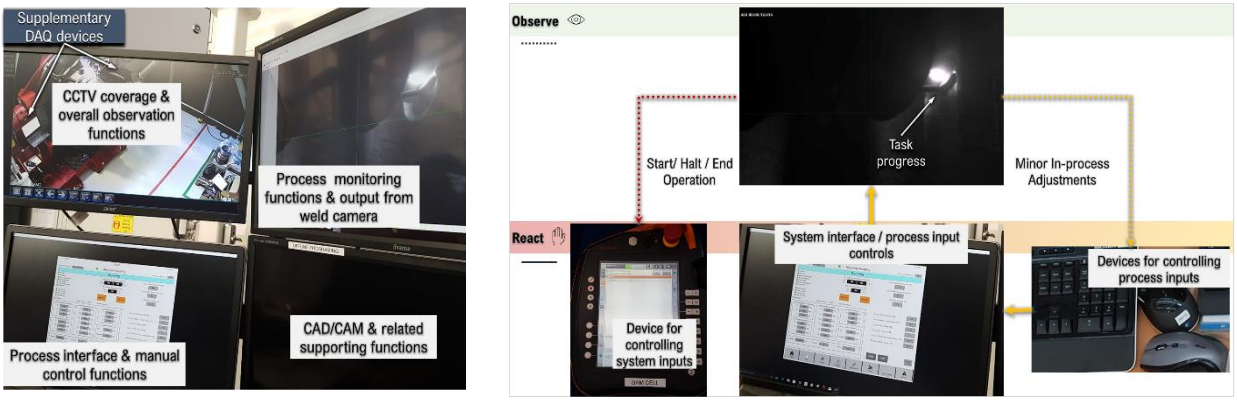

(a) (b)

Figure 5-25: BAM (a) operator perspective and corresponding (b) procedures during reprocessing operations.

In the current developmental state, the BAM virtual platform concept (Figure 4-17), in conjunction with the dedicated kit depicted in Figure 5-25, support important operator functions. Correspondingly, considerations for adaptive process control algorithms, as outlined in relation to the business perspective (Figure 4-1), are brought into focus, as the operator's perspective is limited to observable events. The operator must be aware of all critical functions that influence imminent decisions, as well as the response rate to manifest issues. Presently, closed circuit and weld cameras (Figure 5-25(a)) respectively provide the intermediate (Figure 4-21) and local (Figure 4-22) perspectives of elements within the system boundaries. The operator remains alert while observing these inputs, prepared to take rapid action as necessary, whilst continuously assessing the build as it progresses (Figure 5-25(b)). These onerous expectations may be sustained over long durations, as

was necessary during the *PoC* part build, and further accentuates the need for more intuitive MAM systems, to support decision making, and related operator and systemic functions.

While operating the BAM system, maintaining set parameters and procedures is desirable for achieving the best outcomes, but not often practicable, particularly in AMR settings, due to more variable circumstances when compared to traditional production settings. For the case study, similarities between reprocessing tasks offered an ideal basis for proceeding with established parameters and procedures, but important decisions were informed by actual outputs, due to critical geometric differences between the planar and cylindrical surfaces. The parameters for trials involving PS05-2 (Figure 3 63) were selected, with visual inspections completed immediately after depositions. The objective was to verify that the edges of reprocessed features were no longer visible, indicating that the deposited and base materials were appropriately blended. Subsequently, the component was rotated, with online programming techniques used to modify the toolpath as necessary, including the start and end positions for each feature. This process was repeated, until all tasks were completed.

Post-DED, restored features were individually inspected following similar procedures as outlined for benchmarking operations. Afterwards, the component was despatched in the as-deposited state, to the industrial partner, thus concluding planned SMRM actions directly involving this artefact. The details of inspection and analytical procedures are provided in the following sections.

5.4.4 Inspection and analysis

Adhering to the conditions of supply, relevant pre- and post-DED data were obtained via different NDT methods. The purpose of benchmarking the component was to provide baseline data for evaluating the relative effects of completed SMRM operations, while elucidating related factors applicable to the framework. System outputs derived from non-invasive analysis, including geometric, and compositional data, were evaluated, together with data obtained from in-process monitoring of the component during reprocessing operations.

5.4.4.1 In-process data

The measurements obtained from the thermocouples and strain gauges, attached to the titanium component during reprocessing operations, are presented in Figure 5-26. The resulting temperature plot (Figure 5-26(a)) includes a momentary dip in temperatures, which rapidly falls and rises again within seconds, in a window that coincides with the cessation of argon from both sources. As previously stated, an initial autogenous phase was implemented to test the functionality of the sensors attached to both artefact and substrate surfaces. However, input parameters for reprocessing operations were significantly more demanding. Furthermore, considering the proximity of the gauges, relative to the toolpath and areas under observation, and the condition of the devices after deposition, the reliability of the acquired data was in doubt. Nevertheless, the peak strain value (~400 με) coincided with the window within which the maximum temperature of ~110 °C was measured.

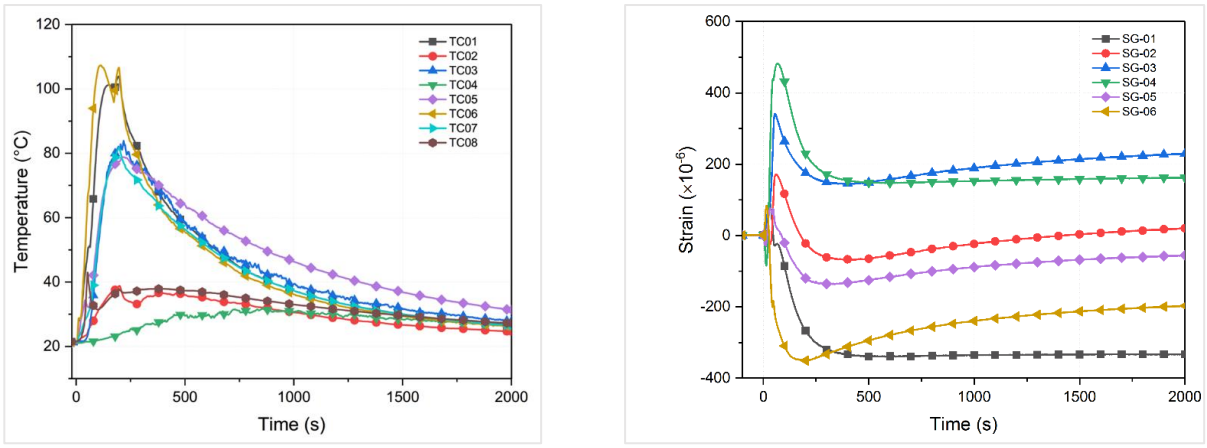

(a) (b)

Figure 5-26: Representative plots of (a) temperature and (b) strain measurements obtained from the artefact

When considering the proximity of the probes to reprocessed areas, and measurements obtained from trials involving substrate PS03 (Figure 5-9), the maximum temperature appeared relatively low (< 110 °C). The larger component surface area, and utilisation of a trailing shield, were assumed to be likely contributing factors. This observation is perhaps most evident, when considering the argon post-flow procedures. For previous builds, maintaining the argon flow for 2 seconds, prior to and immediately after depositions, appeared to have nominal effects on cooling (Figure 5-11), when compared to the component, which was simultaneously cooled for extended periods, with argon flowing from both the supplementary trailing shield and the EOAT.

5.4.4.2 Visual inspection

Visual inspections were completed at different stages of the SMRM process, including directly before and after reprocessing operations. The typical SMRM input and output circumstances are depicted in Figure 5-27.

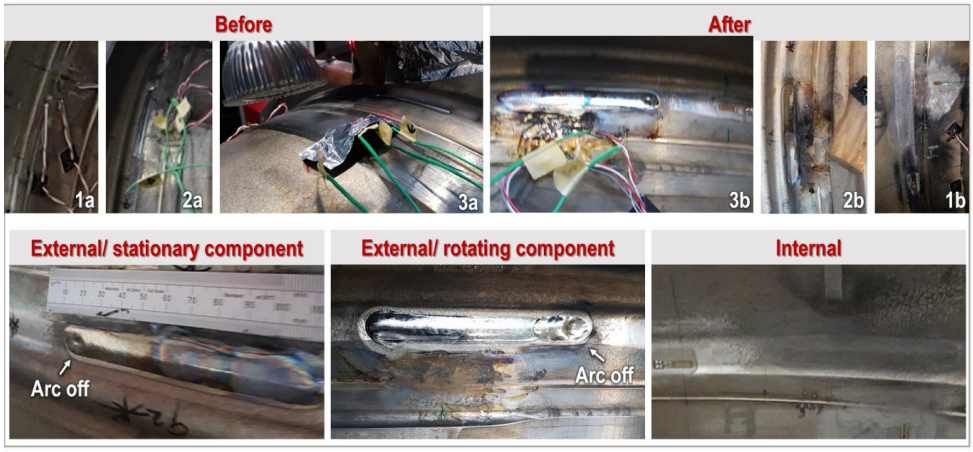

Figure 5-27: Typical appearance of restored features on artefact.

Based on the visual quality of the deposited material and surrounding areas, as seen in relation to the *internal* and *external* images (Figure 5-27), it appeared that the local shielding solution was only partially effective. Presently, the WAAM EOAT is configured with different supplementary kit, including the visible lightbulb shown in image *3a* (Figure 5-24(b)). Further to illuminating the areas under observation, it enhances the

outputs from the weld camera (Figure 5-25(a)) and thus, the operator's viewpoint. Hence, shielding solutions were more narrowly focused and developed in consideration of vital operator functions derived from the kit. When evaluating the dynamics of the system, similar concerns were also identified at the local perspective, for the 3D inspection EOAT (Figure 4-22), which relies on the scanning field of view, and a clear line of sight between the tracker and scanner, during inspections. These limitations can affect normal operator and/ or system functions and warrant further investigation, due to the evident need to balance competing objectives. Specifically, it was apparent that a more encompassing solution, for the WAAM EOAT and requisite kit, was necessary, to ensure that stated objectives for this application were achieved. However, within the scope and resources for this study, the operator functions were prioritised. Incidentally, the trial completed whilst rotating the component did not compromise operator functions, but significantly improved shielding outcomes (Figure 5-27), which was attributed to sufficient coverage of reprocessed areas at crucial thermal phases. The alternate procedure also indicates how the present BAM configuration may support specific objectives, while a more robust shielding solution is developed, with due consideration given to thermal and related factors.

The resulting *external* build (Figure 5-27) was representative of the condition of reprocessed features, and filled the groove entirely, extending beyond the edges of the volume in all directions. Material allowances, or overbuilds, were tolerated in anticipation of subsequent machining operations, which were beyond the scope of this study. Furthermore, depositions were terminated just beyond the edge of each feature, but there were obvious indentations at some locations, that coincided with where the arc was extinguished. Similarly, these effects were exaggerated for alternate trials, as seen in *External/ rotating component* image (Figure 5-27), which also shows the material build-up at the opposite end of the feature. This feature was reprocessed, after a dressing operation with portable tools, and in accordance with original procedures for other features. However, it highlighted the limitation and challenges associated with the scope of reprocessing trials, whilst demonstrating the significance of scalability for industrial applications. In particular, the combination of geometric differences between the substrates and case study, implementation of manual programming approaches, and specific strategies investigated, including the arc characteristics, are likely contributory factors. The previously highlighted effects of the material feeding mechanism on detectable voltage changes (section 3.2.3), as well as the impact of form accuracy on variability issues (section 4.5.2.2), also bring into focus the significance of the programming procedures, particularly when establishing the arc gap. The effects are manifest in the ensuing arc indentations, with a likely cascading effect on subsequent interactions between system and process variable, and potential implications for WAAM quality and costs.

Another obvious difference between the pre- and post-WAAM conditions was the appearance of the component, as observed in *2b* and *3b* (Figure 5-27). The associated images depict the measures taken to protect foil gauges, which involved the application of a heat resistant foil tape, prior to deposition. After the tape was removed, discolorations were observed in the areas where the adhesive compound had been applied, to secure the gauges onto the component, indicating that these devices were likely compromised. However, all the

gauges secured to internal surfaces and one of the sensors on the external surface, located ~50mm away from the reprocessed feature (Figure 5-27), remained intact. Considering the evident consequences of these supplementary devices, and necessary actions to remove all traces, as well as the potential implications for component durability, they appear to be of limited utility. Conversely, when focusing on the objective and purpose of this input for supplementary validation activities, such data is invaluable in AMR/ R&D settings.

5.4.4.3 Geometric inspection

Geometrical optical measuring (GOM) techniques were used to acquire geometric data from the component, to facilitate nominal actual comparisons. The geometric inspection approach was similar for benchmarking and post-WAAM operations. However, due to the developmental state of the BAM system upon receipt of the component, coupled with uncertainties surrounding specific progression plans for multiple EOAT, initial scans of the component were obtained using the ATOS III system. The BAM inspection solution, comprising a Hexagon Leica T-Scan 5/ Absolute Tracker AT-960 combo, and the GOM ATOS III system, are both classed as industrial non-contact 3D scanning technologies, capable of obtaining detailed, precise, and repeatable geometric resolutions at high speed. Nevertheless, the decision to proceed with the ATOS system ensured that planned end-to-end SMRM operations (Figure 5-22) were completed within the supply timeframe. Specifically, other scheduled non-BAM operations, including the machining of features, were progressed accordingly and importantly, similar pre- and post-DED inspection procedures were maintained. Consistently, the same tool and techniques were also utilised for evaluating the arc characteristics (section 5.3.2), prior to reprocessing trials involving flat substrates. The set-up for 3D geometric DAQ is presented in Figure 5-28.

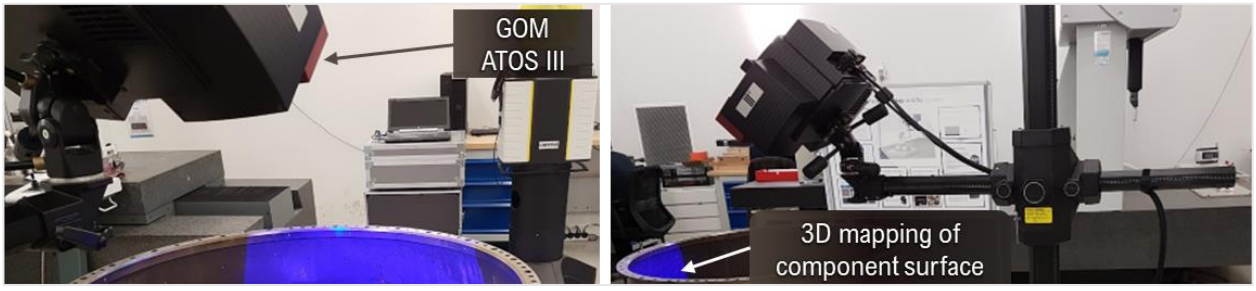

Figure 5-28: 3D geometric inspection and DAQ procedures.

Although it was prudent to proceed with geometric inspections via other means, it was important that a comparable optical 3D measuring technique was utilised. The 3D mapping and post-processing approaches for the selected GOM ATOS III system and BAM 3D EOAT, a T/Scan and an Absolute Tracker AT-960 combo, were similar, as were the core objectives, which was to quantify the effects of reprocessing operations. Relative to the CMM used for earlier comparative studies, which required various attachments to complete the specified range of operations, the GOM system was quite adequate for this validation task. Accordingly, the entire component was scanned, in the original condition, and after reprocessing operations, to obtain the specified 3D geometries. The typical outputs of this process are depicted in Figure 5-29.

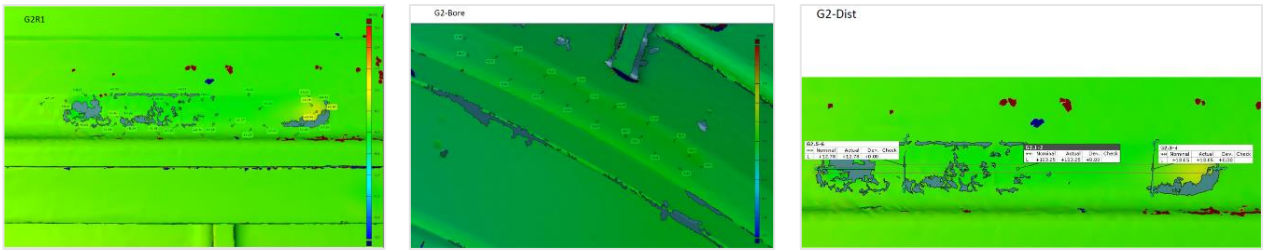

(a) (b) (c)

Figure 5-29: Measurement of (a) external and (b) internal deviations and (c) overall feature dimensions.

After acquiring the scans, original and post-DED output files were merged to facilitate the acquisition of deviation and overall measurements, using the GOM Inspect software. Deviation measurements were obtained by randomly sampling multiple points across the external (Figure 5-29(a)) and corresponding internal (Figure 5-29(b)) surfaces, before quantifying overall dimensions (Figure 5-29(c)). The latter was based on the farthest observable build outlines or edges, with inspection outputs subsequently used for geometric analysis. Focusing on each reprocessed feature, the geometric inspection outputs are presented in Figure 5-30.

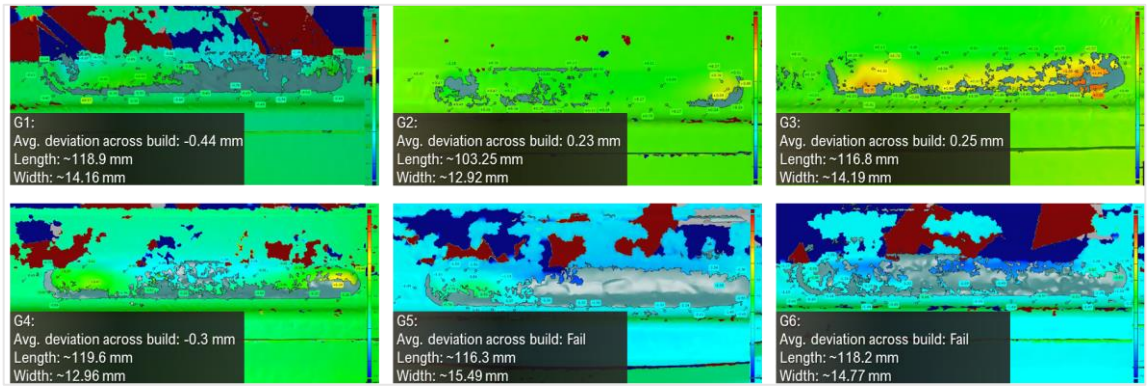

Figure 5-30: Characterisation of geometric outputs from 3D inspection data

Measurements were typically obtained from green or valid inspection areas, while avoiding red, blue, and other sections that revealed the underlying component, due to incomplete on missing information, which was only evident after merging initial and subsequent scans. In general, overall measurements corroborated visual observations, with deviations between baseline and reprocessed geometries typically less than 0.5 mm across the build. The overall dimensions of reprocessed features also exceeded original specifications (Figure 5-15), ranging from ~103 mm to ~120mm along the build, and from ~13 mm to 15 mm across. The deviation between original and reprocessed features was more challenging to ascertain, particularly for G5 and G6, due to incomplete scan data. Nevertheless, quantified surface variations and disparities were already evident from visual inspections, and attributed to the task inputs and parameters, including related inspection procedures. Specifically, the manual programming, and set-up of individual reprocessing tasks, likely contributed to measurement variations in outputs derived from the integrated BAM scanner and standalone GOM system, highlighting common procedural attributes between the different systems utilised, separately from WAAM or 3D inspection operations. The inspection operations relied on the independent acquisition of scan data, with

post-processing steps, including the merging and subsequent alignments of distinct scans performed afterwards, which further emphasised existing dependencies between the output quality and input scan data, as well as procedures completed before and after inspection operations.

5.4.4.4 Compositional analysis

The x-ray fluorescence spectrometry (XRF) elemental analysis technique was used to assess the relative effects of the reprocessing operation on the component. A 20 kV X-MET8000 series was used to obtain measurements from different locations of the artefact. Spectrum data was acquired by aiming the handheld device at designated surfaces for the requisite 10-15 seconds, with output data transferred to a PC for analysis. The specified sampling locations for measurements are shown in Figure 5-31.

(a) (b) (c)

Figure 5-31: XRF characterisation of (a) as-supplied (b) restored and (c) HAZ material sections of artefact.

Preliminary measurements were randomly sampled (Figure 5-31(a)), while post-DED inspection data was obtained from the reprocessed and surrounding regions (Figure 5-31(b)) of the component. Acquired compositional data were evaluated based on automatically detected elements, and different regions containing representative compositions of the artefact were analysed, relative to the respective conditions of outer surfaces (Figure 5-32). Due to the focus on the effects of the reprocessing operation, measurements were directly sampled from the as-supplied component (C), as well as from the restored/ reprocessed (R) regions, and the HAZ (H) as depicted in Figure 5-31. The analytical outputs are presented in Figure 5-32.

The specification for ASTM Grade 5 titanium was used for comparative purposes, and the actual V content (Figure 5-32(b)) was within the expected range. The remaining total composition (Figure 5-32(d)) was also below the maximum specification for each measurement instance, with distinct Al measurements (Figure 5-32(a)) typically within the expected range. Fe levels occasionally exceeded the maximum specifications, with higher values typically observed in measurements obtained from the as-supplied component (C2, C3, C4 and C5), and the HAZ (H2 and H4). In comparison, all measurements obtained from reprocessed regions were within specified tolerances, as depicted in Figure 5-32(c). According to the specification, the Ti content is usually determined by difference, hence measurements were compared with derived values. While three coincident measurements were observed (at locations H, C2 and R4) actual measurements were typically higher than derived outputs, even when accounting for XRF detection errors, typically in the range of ±0.25 Wt.%.

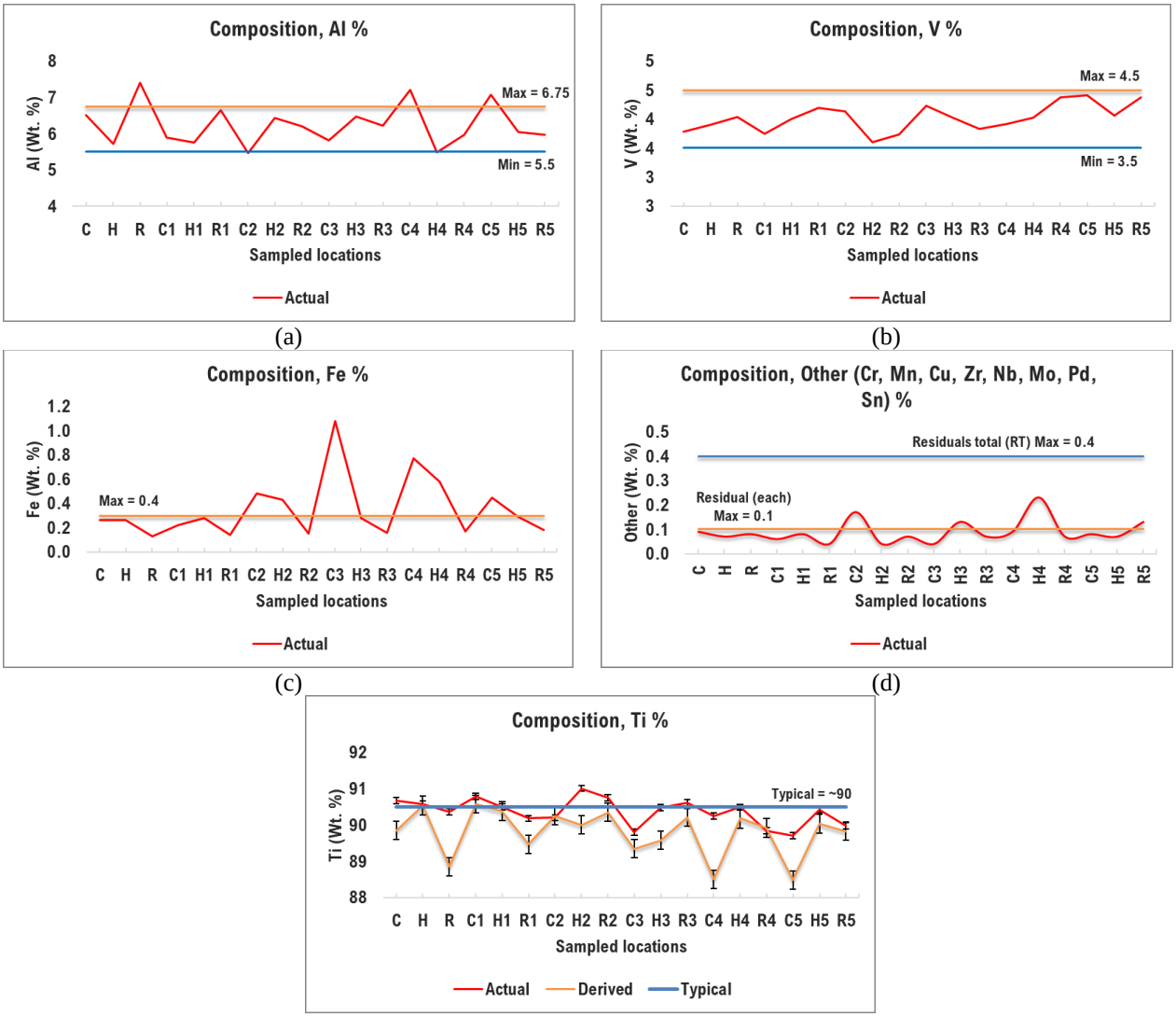

Figure 5-32: Analysis of artefact based on (a) Ti (b) Al (c) V (d) Fe and (e) other elements detected by XRF.

5.4.4.5 Residual stress mapping

A residual stress x-ray diffraction (XRD) analyser, the Proto LXRD® system, was used to assess the residual stress state of the component. The measurement set-up and sampled locations are shown in Figure 5-33.

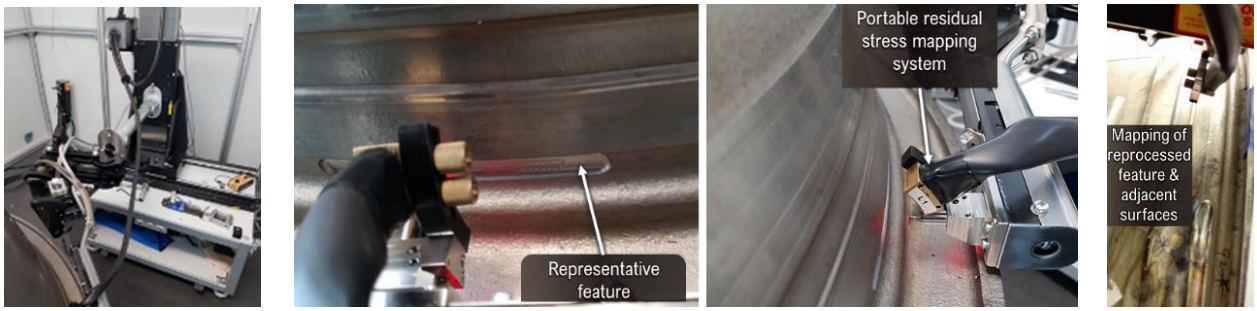

Figure 5-33: Measurement (a) set-up for assessing (b) machined and (c) reprocessed component conditions.

This modular XRD system offers significant flexibility, which facilitates residual stress mapping and complex measurements involving large components. Measurements were obtained before and after WAAM operations, to quantify the relative effects of the process on the component. Due to the specified material removal technique, it was desirable to quantify the effects of machining operations on the component stress state, hence measurements were obtained from both machined (Figure 5-33(b)), and reprocessed features (Figure 5-33(c)). For comparative purposes, measurements were also sampled from other areas of the component, to quantify the as-supplied condition.

The measurement schematic and analytical results are presented in Figure 5-34, which clarifies the approach for quantifying circumferential residual stresses in the artefact, along paths C and E, with the effects of different procedures qualified relative to the geometric input for reprocessing operations (Figure 5-34(a)). Focusing on the reprocessed groove, measurement directly obtained from machined features (Figure 5-33(b)) are depicted alongside measurements obtained from the reprocessed regions and beyond (Figure 5-34(b)). Consistent with literature findings, compressive stresses were recorded for all machined features or grooves (i.e. G1, G2, G3 and G4), typically in the region of ~560 to 660 MPa.

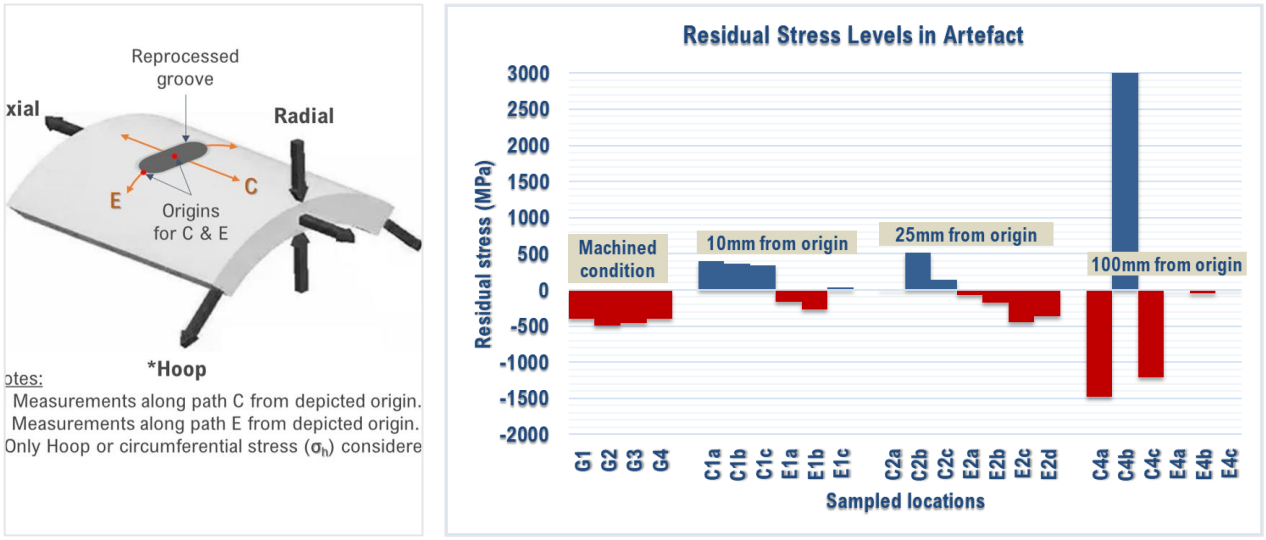

(a) (b)

Figure 5-34: XRD of artefact based on (a) measurement schematic and (b) resulting residual stress levels.

Measurements sampled from locations approximately 100mm from origins C and E (Figure 5-34(a)), were representative of the as-supplied condition, and belonged to the distinct structures of which the component was comprised, as documented in section 5.2.1. Although there were discrepancies between measurements along path E, greater variations were observed between the maximum (3117 MPa) and minimum (-1473 MPa) values, along path C. Conversely, measurements obtained nearer the reprocessed regions typically alternated between compressive and tensile residual stresses, with relatively lower values recorded closer to the reprocessed groove. In these regions, the maximum compressive stress (-450 MPa) occurred ~25 mm from origin C, with tensile stress levels in a similar location increasing to about 520 MPa. Furthermore, measurements along E were almost entirely compressive, with measurements at E4 ranging from -12 to -42

MPa. Compressive stresses were typically constrained to location C4, which belonged to an adjoining structure of the artefact, and included measurements acquired ~100 mm from origin C.

5.4.4.6 Dye penetrant inspection

All reprocessed features were inspected using the specified dye penetrant inspection (DPI) technique, to detect surface breaking flaws. The procedure involved cleaning the inspection area with acetone and a solvent-based remover, before applying a penetrant over the test area. After allowing the requisite contact time of ~15 minutes, a developer was applied to provide good colour contrast, relative to detected indications on test surfaces. Inspections were completed within the allowed 30-minute window, and at ~5 minutes viewing intervals. Post inspection, the component was wiped down, using a solvent-based remover, to eliminate all traces of penetrant and developer from inspection areas. The inspection records are depicted in Figure 5-35.

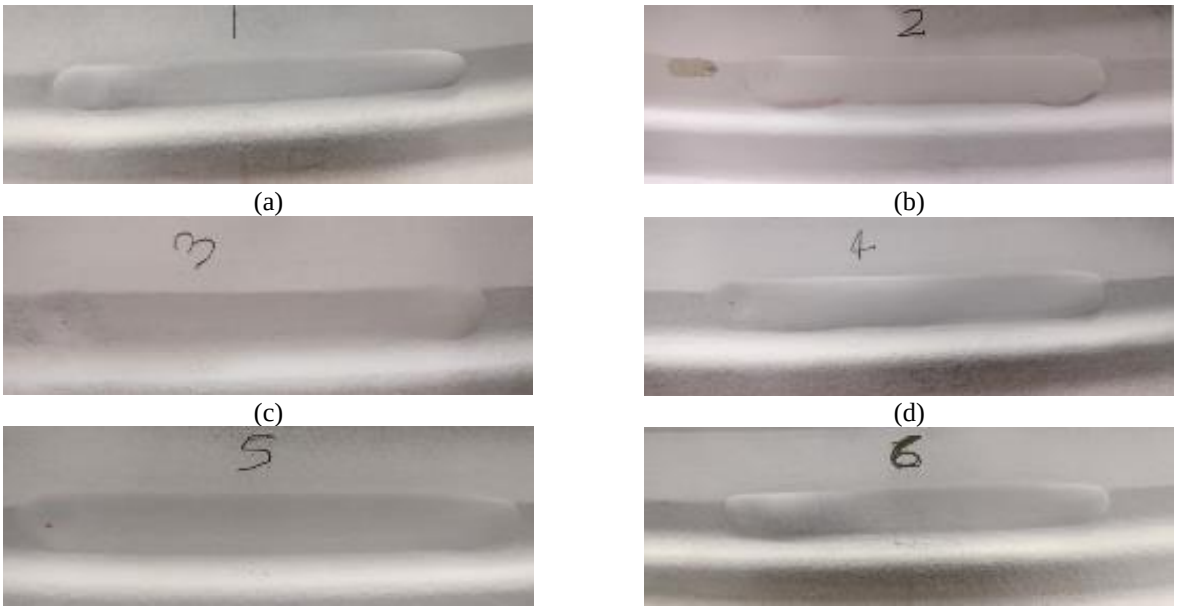

(a) (b) (c) (d) (e) (f)

Figure 5-35: NDT of reprocessed features namely grooves (a) G1 (b) G2 (c) G3 (d) G4 (e) G5 and (f) G6.

There were obvious similarities between the outputs, particularly in relation to the profiles, which appeared relatively flat in the middle with distinctly bulging ends. Correspondingly, the arc termination spots were also evident and relatively more pronounced in some features, as shown in Figure 5-35 (c), Figure 5-35(d), and Figure 5-35(e). Procedures implemented during the set-up and deposition of initial and subsequent layers, including online programming of toolpaths for reprocessing features, and the manual modification of start and end positions for each feature, between reprocessing tasks, likely contributed to observed imperfections. Correspondingly, necessary manual interventions were implemented at the BAM operator's discretion, in response to specific observations, which were also informed by visual inspections completed at each stage.

The DPI outputs underscore the benefits of OLP, in conjunction with the 3D EOAT concept and approach involving specific CAD inputs, particularly for BAM enabled SMRM operations. Nevertheless, case study

outputs were relatively consistent, and generally in line with the requirements and considerations for this study, particularly for the underlying structure, as corroborated by the different inspection techniques and outputs.

5.5 Post-validation analysis

While post-implementation activities (section 4.5) were focused on verifying and objectively validating system functions, in an operational setting, and for intended purposes, the objective of this phase was to establish that the BAM system effectively fulfilled the requirements for which it was developed. In this case, the verification of the BAM system for large-scale MAM, including SMRM operations, in an AMR setting.

The outputs from BAM trials, involving the substrates and the SMRM case study, were assessed, relative to the intended purpose and desirable attributes of the system (section 4.3.2), as well as the actual SMRM requirements. The main task considerations (section 5.2), including how to access specific locations, minimise risk to the underlying structure, and control processing conditions to achieve consistent results, also provided a qualitative basis for validating system outputs, which are explored in the following sections.

5.5.1 Overall capability

The defined attributes for industrial MAM capabilities (Table 4-4), which were derived from foundry business data, were used to establish the relative positioning of the BAM system. Focusing on DED technologies promoted for MAM and SMRM, available system data from literature was evaluated alongside the actual DED systems used for this study. The working load and volume capacity were prioritised, from commercially significant attributes of foundry capabilities (Figure 4-4), while mass and dimensional attributes were excluded as these variables are application dependent. The target minimum values defined for these attributes were used to determine the deviation from this baseline. Beforehand, pertinent DED system data obtained from literature (Table 2-1) were aggregated based on the heat source. The resulting classes, including BAM, SMD, and other DED technologies, namely DED-EB, DED-WA, and DED-LP/LW, corresponding to the electron beam (EB), wire arc (WA), laser powder (LP) and laser wire (LW) variants, were analysed as shown in Figure 5-36.

When comparing aggregated and derived outputs, it was observed that DED capabilities tended to emphasise the build volume, as evidenced by the null values recorded against the working load attribute, which was often underreported or lacking in extant literature. This oversight represents a potential gap in the marketing of DED capabilities, and perhaps alludes to the perceived maturity of such systems, relative to their current adoption for industrial applications. Based on the variance chart, the BAM system compared favourably against other DED capabilities, and the commercial foundry inputs, from which baseline values were derived. It exceeded minimum target values in the categories evaluated, and easily accommodated the case study. The DED-EB class exceeded the minimum target volume, while the SMD capability satisfied the working load capacity requirements for the case study. Although, other DED variants did not meet the minimum targets for evaluated

attributes, the WAAM of an excavator arm (Figure 2-6) demonstrated that for OA configurations in particular, it was possible to develop solutions that were industrially competitive, for technologies within this DED class.

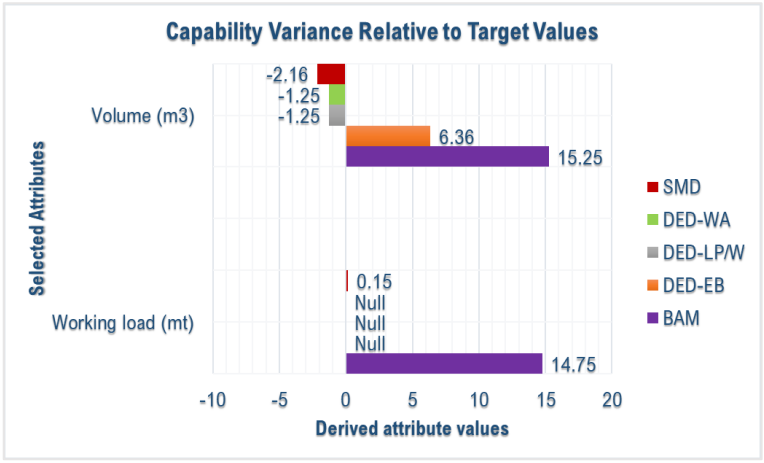

Figure 5-36: Relative industrial positioning of BAM, SMD and other DED capabilities.

Preliminary capability data was based on pertinent commercial considerations, which enumerated the requirement for large-scale MAM systems. Correspondingly, the OA BAM platform satisfied the minimum targets for established commercial attributes, was of an appropriate scale, and can support industrially relevant MAM activities within an AMR context, as demonstrated via the SMRM case study.

5.5.2 Challenges and limitations

There were evident shortcomings and related challenges when validating the system for SMRM. For instance, the need for an appropriate processing environment was already established, but owing to the current BAM development state, a temporary solution was implemented to meet basic shielding requirements. The task requirements and criticality also necessitated the configuration of supplementary devices to support the validation of system outputs. Facilitated by different trials, the efficacy of certain approaches underpinning the reprocessing strategy, though limited due to geometric disparities and related concerns, were necessary, as replicating actual SMRM circumstances is not often feasible when developing solutions.

Evidently, the BAM platform can meet basic functional requirements for SMRM (Figure 5-37(b)), and new large-scale builds (Figure 4-31), but specific examples were selected to underscore the observable effects of present limitation. Presented in Figure 5-37, the examples include the effects and efficacy of shielding solutions. When evaluating different outputs, the benefits of adequately controlled processing environments were reinforced, as outputs obtained from reprocessing operations completed under adequate shielding conditions, were generally glossier in appearance, relative to materials obtained from trials, where only local and/ or inadequate shielding strategies were utilised, resulting in comparatively dull outputs. Conversely, the more complex surfaces of the component dictated the set-up procedures for supplementary devices, contributing to the resulting appearance of the component, as well as the likely degradation of device functions.

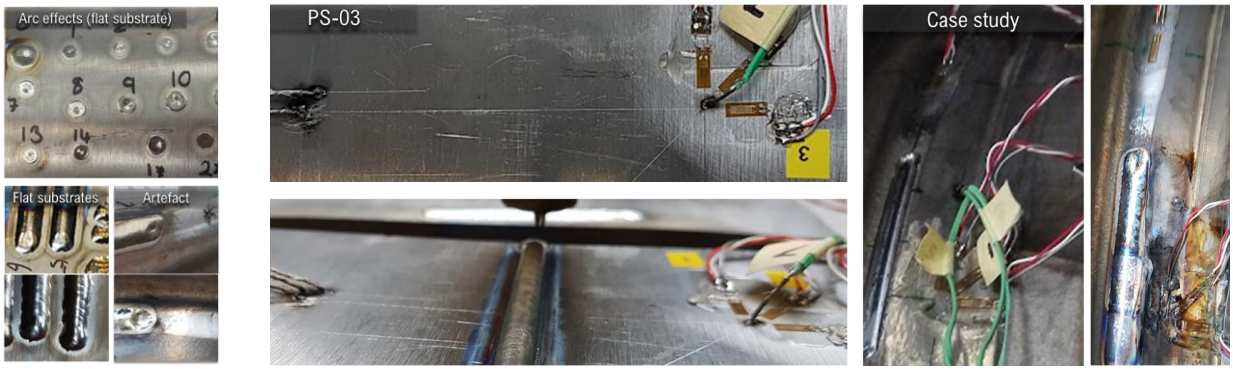

(a) (b)

Figure 5-37: System (a) dependent and (b) derived outputs

Configuration issues stemmed from the need for more robust in-process control strategies, for generating requisite data to support the development of predictive process models, and similar digital approaches, to enhance MAM prospects. It is worth noting that configuration was a cross-cutting theme, affecting access to, and subsequent monitoring and control of interrelated variable for different operations, including adequate field of view and unimpeded line of sight for GOM and BAM 3D inspections, the cameras, and other devices configured for condition monitoring purposes during DED. The concept of configuration was initially explored in relation to the different mechanisms and interrelated complexities, arising from core technology options, i.e., energy, mechanisation, and the feedstock material. Thus, expanding the system configuration scope, to support the exploration of possible input combinations, including fixed and transitory devices, without unduly compromising access to the component or impeding necessary tasks, should improve functionality, and enhance overall system utility.

As previously discussed, the arc (Figure 5-37(a)) is a critical process variable, due to the interdependencies between associated parameters or system inputs. Investigating the arc characteristics, elucidated its compounding effects on experimental variables and related procedures, including the transferability of approaches. There were significant improvements between arc trials, and subsequent experiments for evaluating selected parameters, which were all implemented on flat substrates. However, these improvements were not replicated on the artefact, mainly due to geometric differences, programming techniques, and related procedures. These observations further validate the need for the proposed BAM inspection approach, whereby actual scan or point cloud data is used to facilitate end-to-end SMRM, as well as other contiguous MAM operations. Other factors, such as the relative proximity of the arc to supplementary devices, as observed in relation to the component (Figure 5-37(b)), can also have adverse effects, including, in this case, potentially unreliable/ unusable output data, due to the condition of the sensors, after reprocessing operations. Consequently, process interdependencies were further explored via subsequent trials which were designed to quantify the system outputs, temperature, and strain, which were dependent and/or derived from its inputs.

Correlations were observed between the deposition strategy and the stability of process outputs, whereby changes in the tool orientation and wire entry angle, relative to the substrate, and associated procedures, such

as the work holding or clamping arrangement, were detectable in resulting temperature profiles. Considering the boundaries of the sensing or DAQ approach, and relative to dependent system outputs, such as the build temperature and number of deposited layers, acquired measurements were generally consistent, with similar maximum temperatures recorded for autogenous passes (<70 °C), single layers (~290 °C) and multiple layer builds (350 °C) on different substrates. Conversely, other empirical factors, including the design parameters, shielding approach, sensor configuration and specific procedures, were identified as key sources of variation that likely contributed to relatively lower component temperatures of ~110 °C for single layer builds. While there are advantages to monitoring variables and related characteristics, to fully comprehend the effects on materials and parts, particularly for reprocessed structures, the benefits of the strategy implemented in this study remain uncertain, relative to the practicalities and resources required for such an undertaking.

5.5.3 Outputs and implications

The capabilities of manufactured products are derived from the properties of the materials and alloys of which they are comprised. Thus, the tensile properties of BAM materials were investigated, to provide early indications about the relative characteristics of representative outputs. The specification for Grade 5 titanium, was used to support this analysis, with relevant data obtained from various sources, as presented in Table 5-5.

Table 5-5: Comparison of Ti-6Al-4V tensile properties.

Material	YS (MPa)	UTS (MPa)	Elongation (%)
SMD-0º (DED)	854	1053	9.08
SMD-45º (DED)	812	1013	10.075
SMD-90º (DED)	887	1022	5.25
BAM-A (DED)	860	1000	13.59
BAM-B (Substrate)	925	995	14.76
BAM-C (SMRM)	880	990	14.91
EBF3 (ELI) [258] [259]	660	775	9.6
EBF3 [259]	848	923	13
AMS 4999	747	846	4.2
AMS 4911	880	950	14
ASM (Cast) [389]	896	1000	8
ASM (Cast + HIP) [389]	869	958	10
ASM (Wrought) [389]	880	950	9
WAAM (SUB) [40]	950	1033	11.7
WAAM (S-A) [40]	883	930	17.8
WAAM (P-A) [40]	888	968	14
WAAM (O-A) [40]	827	926	12.3
AMS 4999 (Vertical, Additive) [40]	758	855	6
AMS 4999 (Horizontal, Additive) [40]	800	885	6
AMS 4928 (Wrought) [40]	815	895	10
ASTM F1108 (Cast) [40]	770	860	8

S - Single Pass, P - Parallel Passes, O - Oscillating Passes, SUB – Substrate, A – Average Values.

In general, the averaged values obtained from BAM materials were within range of the specifications for this alloy, and comparable to other sampled tensile property data. The main outliers include the EBF^3 (ELI) material, due to the lower yield (660 MPa) and UTS (775 MPa) values, when compared to maximum YS value

(950 MPa) and UTS value (1053 MPa), obtained from the WAAM (SUB) and SMD-0º (DED) materials respectively. Similarly, the AMS 4999 material appears to be quite brittle, owing to the relatively low elongation value (4.2 %), when compared to the significantly higher value of the WAAM (S-A) material (17.8%). These variations were attributed to the specimen types, sampling direction, and other manufacturing process variables associated with the different techniques used for fabricating the referenced materials. Nevertheless, product functionality, and durability in service, are influenced by broader considerations, some of which were already explored in previous chapters, including effects of the relative spread of measurements, obtained from a single build, on fracture performance. Thus, the investigation of both specific (i.e., to a material or product) and general (i.e., across all materials and products) variances, can enhance understanding of the behaviours and tendencies of distinct technologies, and unique material processing factors, whilst providing further insights into how the predictability of MAM outputs may be improved.

5.6 Main observations

The foremost restriction on pre-and post- BAM operations was the portability of accessible tools, which necessitated the relocation of components to and from the BAM cell, to facilitate planned tasks. Within system boundaries, accessibility was also a key consideration for the main and supplementary devices configured for SMRM. Material variabilities, which were quantified geometrically, elementally, microstructurally, and mechanically, for different alloys and DED capabilities, were intrinsically linked to interdependent system and process variables and derived outputs. In some cases, variations were incorporated as an essential part of the process, such as the DoE involving multiple variables, and investigating the potential of different feedstock for reprocessing operations. In other instances, variations across data sets were derived from the system and related process interdependencies. Hence, the emphasis on absolute variations in DED appears to be at the expense of tolerable variations, which can be acceptable, if within the agreed and relevant specifications.

The specimens extracted from different DED materials were tested and analysed according to specific standards, some of which involved different geographically distributed capabilities. Although some of the distinct values, involving similar alloys, significantly exceeded and/or did not meet requirements, the averaged values for the bulk materials revealed good overall agreement between experimental programmes. In some cases, bulk material properties from SMD and BAM specimens, were generally within, or near the expected range of values, provided in the referenced standards. In addressing significant variations, establishing DoE objectives that reduce deviations between the maxima and minima of a data set is desirable. While geometric responses, such as the bead characteristics, may be readily evaluated using metrology and other laboratory tools, quantifying microscopic responses, in real-time or otherwise, is more demanding. Hence, more expensive tooling and/ or the integration of other supplementary technologies is required, for more timely tracking of responses.

Other notable outcomes include the effects of operational procedures and process inputs on output quality. The use of non-destructive testing techniques significantly enabled the early identification of geometric flaws, particularly at the interfaces between deposited and existing structures. However, it was observed that technological limitations could influence the efficacy of such techniques. For specimens used to assess reprocessing methods, it was necessary to cut-up samples before NDT. This operation appeared counterintuitive, but was necessary to suit the inspection requirements, based on the available equipment. While it is certain that some operational issues may be overcome, by modifying certain aspects of the SMRM strategy, these concessions become even more critical when technological limitations prevail. For example, although the toolpath programming technique may be modified to eliminate LOF defects, if OLP features are not suitable, particularly for complex scenarios, then further R&D may be necessary. This additional effort ensures that available tools and particular features can be satisfactorily adapted, to address specific issues.

5.7 Summary

In this chapter, the reprocessing strategy, and empirical procedures, implemented when validating the BAM system, are described. Anticipated and emerging issues were also explored, to elucidate some of the limitations and benefits of the proposed approach for large-scale MAM and SMRM applications. In *Chapter 6*, the computational models developed as part of the overall SMRM strategy are described. This third phase, is integral to principal system development and validation investigations, and aimed at further substantiating empirical observations, particularly in relation to the case study.

CHAPTER 6

6 Substantiation of BAM Outputs

6.1 Introduction

This chapter focuses on the verification of selected Ti-6Al-4V outputs, which were derived from BAM system validation activities. Process modelling and simulation techniques were adopted to facilitate numerical analysis of actual reprocessing trials. The investigative aim was to establish numerical models for predicting the effects of DED reprocessing operations on metallic structures. The finite element modelling (FEM) method was specifically selected to facilitate the prediction of temperature and strain responses observed during BAM trials. The primary objective was to demonstrate the compliance of numerical models with selected trials involving the titanium aerospace case study described in *Chapter 5*, while exploring the broader utility of the FEM approach for supporting SMRM operations. The FEM approach, including the codes, features, element formulations, assumptions, and related considerations, are discussed in the relevant sections of this chapter.

6.2 Requirements analysis

In order to assure that the intrinsic value of serviceable metallic infrastructures is preserved, outcomes of SMRM operations need to be substantiated. However, the requirements for these critical and typically low volume high-value applications are such that a trial-and-error approach may be the only viable route to achieving the desired outcomes, which is a relatively high-risk strategy, and subject to the supply conditions, including the personnel involved. Therefore, the objective of this supplementary activity was to validate certain aspects of the SMRM approach, by corroborating empirical outputs with numerical predictions, and exploring related risk factors, due to the strategy implemented during reprocessing trials. While NDT techniques provided a practicable means of assessing the artefact, other accessible inspection capabilities, such as the CT scanner, which proved very useful for inspecting restored substrates (Figure 5-14), were limited to items ~50 kg by ∅500 mm. Consequently, numerical simulations were ideal for dealing with the more complex problem of understanding, and thus inferring pertinent details from predictions about the effects of operations involving the artefact. The FEM method was also crucial for devising a generic SMRM approach.

Due to the differences between the artefact and substrate geometries, the focus was on sequentially developing predictive models, that were aligned with specific areas of interest. Further to augmenting data acquired from post-DED inspection operations, the latter also influenced the adoption of a concurrent validation strategy for the artefact. Specifically, empirical, analytical, and numerical approaches were implemented independently of each other. Accordingly, empirical trials were completed, and outputs were analysed for different substrates and the artefact, before proceeding with numerical studies.

As the acceptability of numerical studies depends on the validity of predictive models, actual data acquired from empirical studies, involving both the substrate and artefact, were used to demonstrate the conformance, accuracy, and reliability of the analysis.

It was desirable to have good correlation between experimental data from BAM trials, and predictions from numerical models, which were developed using realistic input parameters obtained from the former. However, due to the necessarily iterative development approach, the BAM OA platform lacked certain functions for capturing comprehensive process data. The goal was to achieve an acceptable outcome, while testing the research hypothesis, that *process simulation and modelling techniques can significantly improve SMRM outcomes*. For this study, model predictions that were within a reasonable range of actual measurements, were deemed acceptable.

6.3 Modelling approach

The general modelling procedures, for describing and subsequently predicting the effects of reprocessing trials, involving both the substrate and artefact, were iterative, due to underlying assumptions about precise inputs and variables that were inherent to the problem under investigation. The specific model formulations and development details are provided hereafter.

6.3.1 Physical models

The physical models used for investigations were derived from experiments described in the previous chapter. Specifically, experiments involving temperature and strain measurements, derived from substrates PS02 and PS03, were selected for the development and validation of numerical models. The model configuration for PS02, and the actual substrate used for temperature mapping trials, are shown in Figure 6-1.

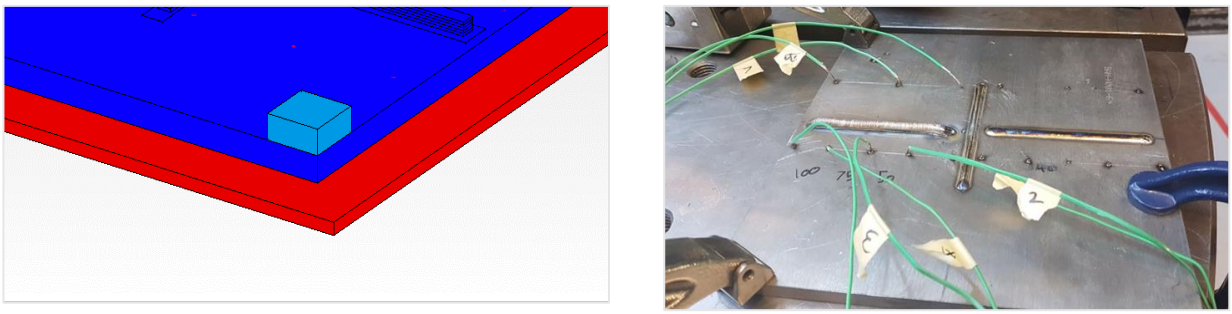

(a) (b)

Figure 6-1. (a) Model configuration and (b) actual substrate set-up for PS02.

For PS03, where surface strain in the substrate was monitored, the asymmetric clamping arrangement obliged the use of a full model, in lieu of half symmetry. Accordingly, the virtual and actual arrangements used for concurrent temperature and strain measurements on substrate PS03, are depicted in Figure 6-2.

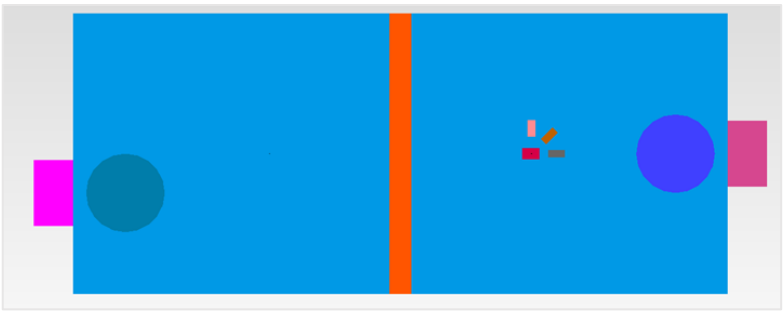

(a)

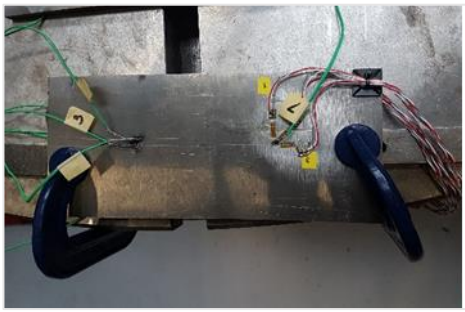

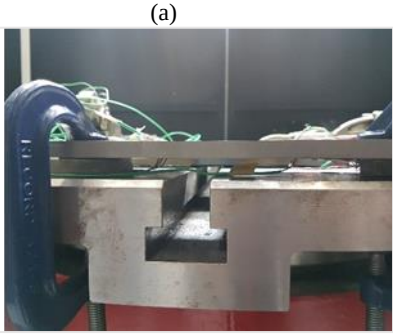

(b) (c)

Figure 6-2. (a) Full geometry FEA set-up for modelling PS-03 and (a) images of actual substrate plate showing asymmetric clamping arrangement and (c) first layer/ initial build.

6.3.2 Finite element method (FEM)

A commercial non-linear finite element software suite, MSC.Marc [395], was used for the implementation of all numerical modelling in this study. MSC.Marc includes a series of tightly incorporated programs that are suited to the analysis of non-linear engineering problems. A schematic of the components of the software suite and inter-related routines is shown in Figure 6-3.

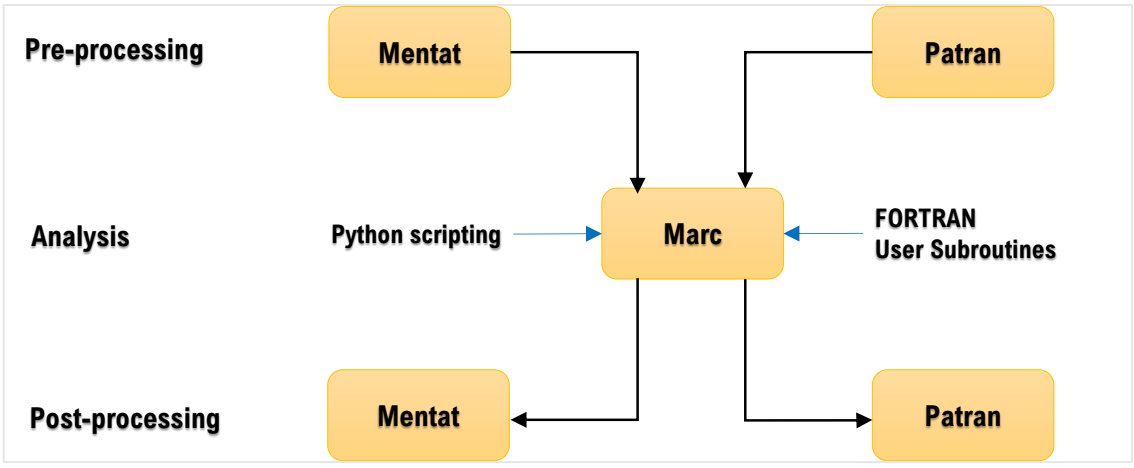

Figure 6-3. The Marc system [395].

The main components of the suite include MSC.Patran or MSC.Marc Mentat, for pre and post processing through a graphical user interface (GUI); MSC.Marc for analysis, extensible via special routines and FORTRAN based user subroutines; and Python, which is used as a scripting language.

6.3.3 Heat source specification

The addition of thermal energy in a weld or metal deposition analysis is specified through specialised boundary conditions and may be specified via two different techniques:

- Modelling the heat input as a multi-dimensional varying volumetric flux that is applied to the substrate and filler elements.
- Modelling the heat input as a multi-dimensional varying temperature boundary condition, applied to the nodes of the filler elements.

In this study, the multi-dimensional varying volumetric heat flux option was selected. The most common model is the double ellipsoid heat source model, proposed by Goldak et. al [396,397]. This model has been successfully used in several studies [398–402], to model the heat input from an arc-based heat source. The Goldak double ellipsoid heat source model prescribes a Gaussian distributed volumetric heat flux, defined in both 2D and 3D moving frames of reference, as [403]:

$$q_f(x,y,z) = \frac{6\sqrt{3}f_f Q}{abc_f\pi\sqrt{\pi}} \exp\left(\frac{-3\mathrm{x}^2}{\mathrm{a}^2}\right) \exp\left(\frac{-3\mathrm{y}^2}{\mathrm{b}^2}\right) \exp\left(\frac{-3\mathrm{z}^2}{\mathrm{c}^2}\right)$$
$$q_r(x,y,z) = \frac{6\sqrt{3}f_r Q}{abc_r\pi\sqrt{\pi}} exp\left(\frac{-3x^2}{a^2}\right) exp\left(\frac{-3y^2}{b^2}\right) exp\left(\frac{-3z^2}{c^2}\right) \quad (6\text{-}1)$$

Where q_f and q_r are the heat flux rates per unit volume in the front and rear molten pools respectively;
$Q = \eta VI$ is the applied power;
a is the molten pool width along the tangent direction x;
b is the molten pool penetration depth along the arc direction y;
c_f and c_r are the forward and rear molten pool lengths in the weld path direction z;
f_f and f_r are dimensionless factors which denote the forward and rear heat input fractions, given by:

$$f_f = \frac{2}{\left(1 + \frac{c_r}{c_f}\right)}$$
$$f_r = \frac{2}{\left(1 + \frac{c_f}{c_r}\right)} \quad (6\text{-}2)$$

A graphical depiction of Goldak's double ellipsoid heat source configuration, and the power distribution function along the local x-axis, is shown in Figure 6-4. The heat source dimensions can be varied as functions of time or distance. The model was further extended for metal deposition modelling [404] through techniques, such as the addition of other heat source models, for more thorough heating of the filler material. Consequently, the combined heat source efficiency is divided between the double ellipsoidal heat source, and the heat source for heating the filler material only. Previous studies [405,406] indicate that the arc efficiency

(η) for GTAW is between 50% and 82%, with molten filler metal droplets contributing about 38-42% of the power supplied to the work piece.

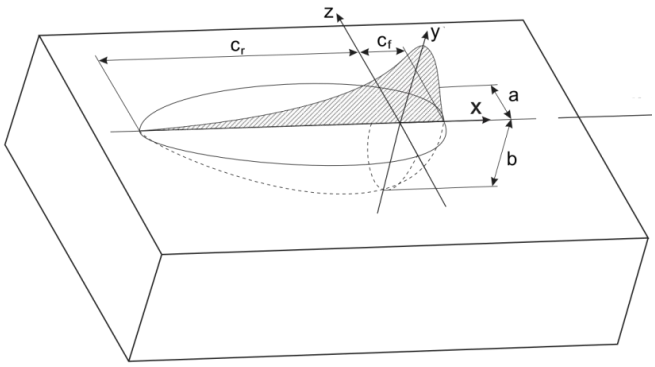

Figure 6-4. Goldak's double ellipsoidal heat source model and power distribution function in a local coordinate system [395,396,407].

In these studies, a combined heat source model was applied, comprising the Goldak double ellipsoidal heat source, with a Gaussian distribution, and the cylindrical shaped constant volume heat source, implemented in MSC.Marc. The latter is exclusively used to heat filler elements, with the possibility to incorporate the wire in either a trailing or leading translation mode.

Theoretically, the total heat input applied through the heat flux is equal to the power, Q. However, due to numerical integration errors, over the element integration points, and errors from integration over a finite domain, the magnitude of the applied volumetric flux is typically 0.85 to 0.9 of Q, even with a very fine mesh. However, the volumetric heat flux may be altered, to account for integration errors and obtain an equivalent value for Q, for the total heat input in the finite element domain through the auto scaling option in MSC.Marc,

6.3.4 Toolpath definition

Three possibilities exist for the definition of the path and orientation of the moving heat source in MSC.Marc; through text input, direct input or via user subroutines. This is used to determine a local coordinate system for the moving volumetric heat flux. In this study, the traversal path and orientation of the deposition head were modelled by the definition of a toolpath reference curve, which consists of n discrete points, equally positioned along the toolpath, as shown in Figure 6-5.

(a) (b)

Figure 6-5. (a) Global coordinate system and (b) local coordinate system for the moving heat source by transformation of the global coordinate system [403].

6.3.5 Material deposition

There are two methods supported in MSC.Marc [395], which may be utilised for the dynamic addition of filler elements and associated boundary conditions, namely:

- The **quiet element method**, where the filler elements with scaled down material properties are all included at the beginning of the analysis. The coefficient of thermal expansion is set to zero, and all other material properties, except for the yield stress, specific heat capacity and thermal density, are scaled down by a default scale factor of 10^{-5}, or through a user defined scale factor. Volumetric heat fluxes, and other distributed or point thermal loads on the quiet elements, are ignored, until awakened by a moving heat source. When triggered by the heat source motions, the thermal properties are fully restored over the specified thermal activation time, while the filler elements remain mechanically quiet, until the next step or increment in the analysis. However, the quiet element method is numerically sensitive, and prone to ill-conditioning, thus it is not recommended for large amounts of added material [220].

- The **deactivated element method**, where the filler elements are completely deactivated and are not displayed in the post file at the beginning of the analysis. It is only after creation, by a moving heat source, that filler elements are thermally activated and displayed in the post file. At the next increment, or after the user specified thermal activation time has expired, elements are activated mechanically. The delay between the thermal and mechanical activation prevents excessive generation of mechanical stresses and strains during the temperature ramp-up period. While the deactivated method is less numerically sensitive, and does not result in ill-conditioning problems, the interior nodes of deactivated elements do not move with the rest of the model, which can lead to distorted filler elements.

It is worth noting that some authors [396,397,408] have recommended the incorporation of at least 5 elements, spread across the radius of the fusion zone, for more accurate predictions of thermal gradients in both the fusion and heat affected zones. Hence, the inbuilt MSC.Marc adaptive meshing function was used to refine the molten pool mesh automatically, via the automated node in box criterion. This feature uses the current location of the moving heat source and molten pool dimensions to adaptively re-mesh the nodes and associated elements in the HAZ. Alternatively, a user defined node in box criterion or a temperature gradient-based criterion may be used. The automated option was selected for this study.

The simulation of metal deposition onto substrates was accomplished by using the robust contact algorithm in MSC.Marc, which allows contact bodies to be easily modelled, without the use of special contact or gap elements. A glued ‘bonded’ contact constraint condition was used to attach the deposited layers onto substrates, and subsequent deposits to pre-existing layers, which enabled the bonding of contact bodies with dissimilar meshes in a computationally efficient manner. In a coupled thermo-mechanical analysis, the glued ‘bonded’ contact condition ties all displacement, and temperature degrees of freedom of a node of the added layer, onto a segment of the substrate in the contact patch. Thus, a continuous displacement and temperature

field is maintained through the contact interface, for 2 or more contact bodies [395,409]. The temperature constraint between two glued 'bonded' contact bodies of dissimilar meshes, is illustrated in Figure 6-6.

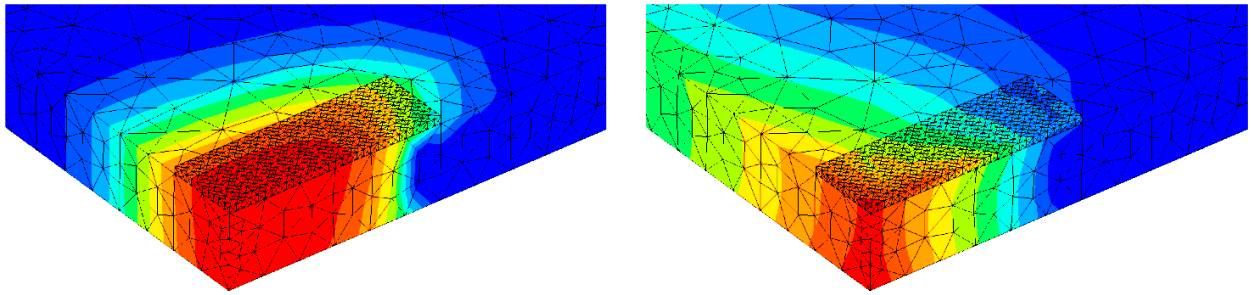

(a) (b)

Figure 6-6. Illustration of (a) temperature fields and (b) displacement fields between two glued 'bonded' contact bodies of dissimilar meshes and non-coincidental nodes.

6.3.6 Non-linearity

Welding and metal deposition operations are non-linear physical processes thus, sources of non-linearity were considered in the model development. The main sources considered in this study include the material, geometric, contact, and non-linear boundary conditions, which are further discussed in the following sections.

Non-linear material considerations include temperature, solid-liquid phase, solid–solid phase, and time dependence of the thermal and mechanical properties of the alloy(s) investigated. The MSC.Marc multi-physics input procedure, in which physical material properties can be linked to a table or function, was utilised. A subset of material data, used as a function of temperature in a heat transfer analysis, is shown in Table 6-1.

Table 6-1. Temperature dependent material properties for heat transfer analysis.

Analysis type	**Material property**	**Function**
Heat transfer	Density	$\rho(T)$
	Conductivity	$K(T)$
	Specific heat capacity	$c_p(T)$
	Latent heat	$Q(T)$

Analogous to welding techniques, WAAM is typically associated with high levels of transient thermal processing, and engineering alloys typically exhibit changes in mechanical and thermal properties, which are dependent on the rate of cooling from high temperatures. These properties are dependent on the instantaneous temperature, preceding thermal history, and the internal microstructure of the material. The microstructural evolution is also dependent on the rate of change of temperature. Furthermore, changes in the microstructure (e.g., grain growth) precipitates/solutes, recrystallisation, and phase structure, are accompanied by volume changes. Consequently, adequate modelling of the microstructure evolution is important for the determination of distortion and durability, and to inform requirements for the heat treatment of components manufactured or reprocessed using DED techniques. Although the significant material property characterisation studies and literature surveys, necessary for generating and/ or obtaining requisite data for each alloy under consideration,

were beyond the scope of this study, the requirements for a robust thermo-mechanical-metallurgical (TMM) analysis were explored, as schematically represented in Figure 6-7.

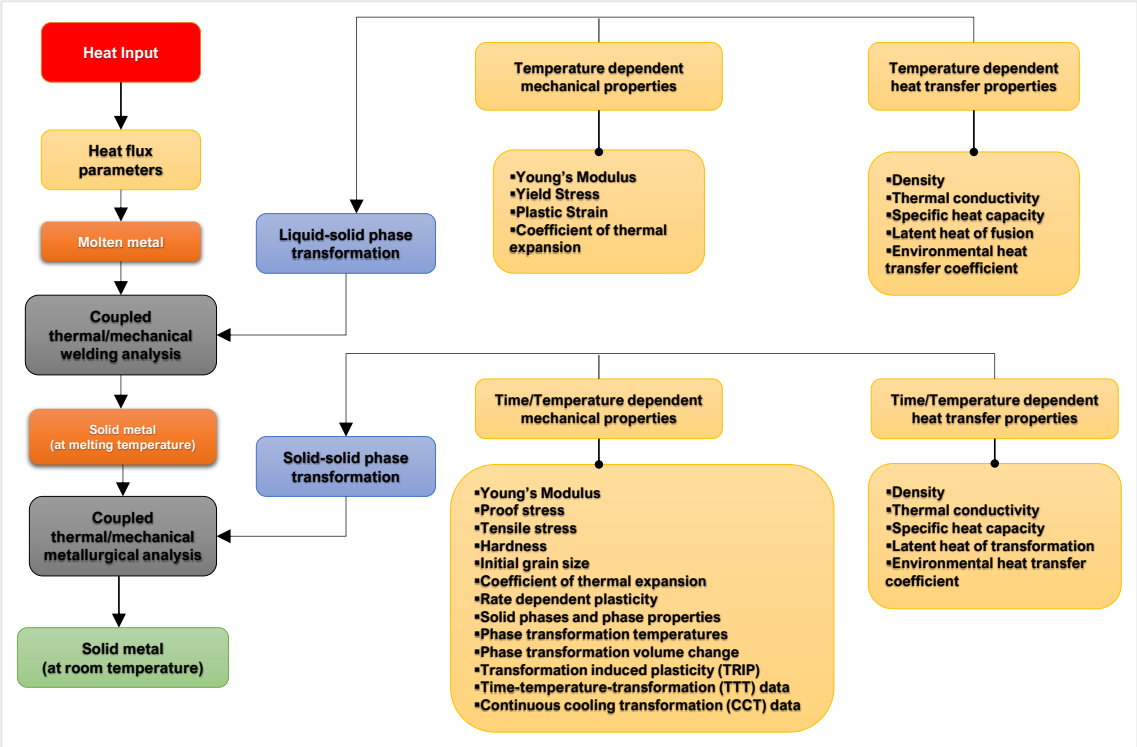

Figure 6-7. Schematic of time and temperature dependent material properties considered for TM and TMM analyses.

Geometric non-linearity is widely recognised as a contributor to changes in structural behaviour and loss of structural stability, and was considered in this study, due to the fluctuating thermal environment, and its effect on the material, and deposition of layers. The updated Lagrangian approach was specified for all the analyses carried out. This updated version, calculates initial stress and geometric stiffness matrices, based on the current element deformed shape at each increment, as opposed to the total Lagrangian approach, which is based on the original element geometry [395].

Fundamentally, loaded surfaces or structures will deform and change in response to any applied load. For the metal deposition process, which involves fluctuating distributed loads and fluctuating load bearing surfaces occurring at each increment of the analysis, variations in the load bearing surface area, or orientation, will result in changes in either the load applied, or the loading conditions at each increment. This effect was accounted for by activating the follower force parameter in MSC.Marc [395], which forms both the pressure stiffness and pressure terms, based on the current deformed configuration at any time during the analysis.

6.3.7 Element choice and meshing strategy

The choice and number of elements, and associated node locations directly influence the accuracy of finite element results, including temperature, stress, strain, and deformed shapes. Thus, factors such as element type, mesh density, contact conditions, heat source, deposition path, geometric and material non-linearity were

iteratively considered in the meshing strategy employed. MSC.Marc has an extensive library of regular and special elements. The regular element library includes 2D solid, 3D solid, plate, beam, and shell elements. The special element library also includes composite continuum, gap, friction, interface, and multi-physics elements [410].

For the TM models implemented in this study, Marc *element type 7*, with assumed strain formulation, (i.e., 8 node hexagonal 3D solid continuum elements) and *type 134 tetrahedral elements*, were used for the added material and substrate. The elements with assumed strain formulation were especially chosen for their enhanced ability to capture bending, relative to conventional elements [395,411].

A local adaptive mesh refinement procedure was used to generate a finer mesh in the molten pool and HAZ, to improve the accuracy of responses resulting from high thermal gradients, at reduced computational costs. This local adaptive meshing strategy was applied to every element with at least one node within the region defined by the moving volumetric flux.

6.3.8 Symmetry

For some of the FEA models, existing geometric and loading symmetry was exploited for computational efficiency. Symmetry can only be considered if the original and deformed shapes are symmetrical. Thus, given the idealised nature of models employed to mimic experimental samples, half symmetry was utilised for some models where the loading was also symmetrical about the longitudinal axis, as illustrated in Figure 6-8.

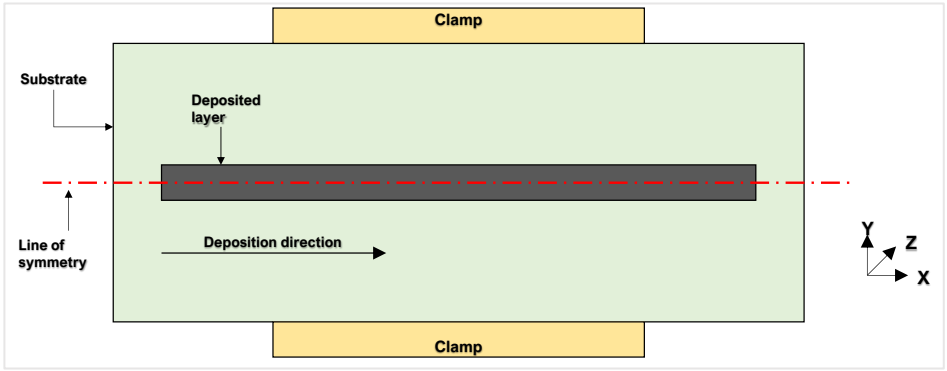

(a)

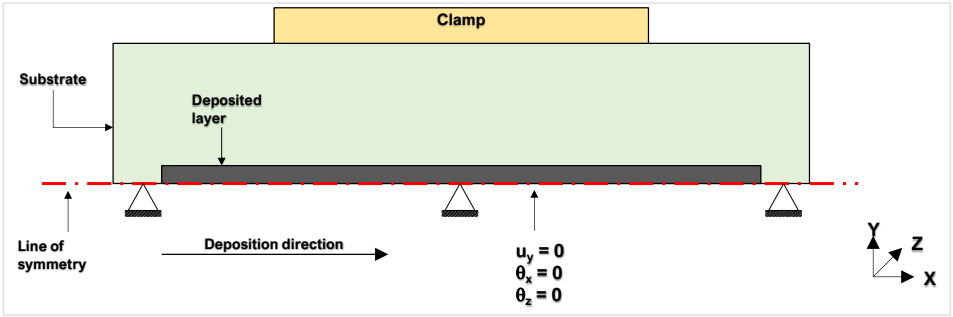

(b)

Figure 6-8. Longitudinal symmetry used for geometry simplification showing (a) full geometry and loading direction and (b) half symmetry geometry and loading direction.

6.3.9 Modelling techniques and assumptions

The geometry of some MAM components is difficult to mesh, in the as-deposited state, given the variations in the width and thickness of deposited layers, and the effects of thermal reprocessing on the resultant component. In practice, it is common to simplify the model geometry, to reduce mesh complexity, and utilise computational resources more efficiently. Therefore, idealised geometrical configurations were used to represent the deposited materials. Some of the simplifications and modelling assumptions are listed below.

- The deposited layers were assumed to be perfect throughout the length and width of the depositions. Similarly, subsequent layers were assumed to be of equivalent dimensions as previous layers.
- Excess material, deposited at the beginning and end of the toolpath traversal, were assumed to be the same size and shape.
- Depositions were assumed to be perfect cuboids, and the corresponding rate of material deposition was assumed to be constant.
- The speed of the deposition head was assumed to be perfect during deposition, although it is well known that there is acceleration and deceleration in the traversal of robot-actuated EOAT [100].
- Metal vaporisation was assumed to be negligible.
- The convection flow of the liquid in the molten pool was partially accounted for by artificially increasing the conductivity about the liquidus temperature of the alloy [220,412,413].
- Dynamic adaptive mesh refinement was used in the region of the molten pool for each model, for increased resolution of the high thermal gradients, in comparison to a static mesh scheme.
- The effect of localised forced convection, due to the shielding gas, was incorporated in the model by applying the forced convection parameters away from the molten pool and HAZ, to prevent spurious temperature resolutions within these elements.
- A scheme to track the evolution of temperature dependent material and mechanical properties was applied per loadcase timestep, such that the maximum change allowed, per increment in nodal temperature, did not exceed the change in temperature dependence of the material property, as shown in Table 6-2.

Table 6-2. Temperature increment allowed in each loadcase timestep for Ti-6Al-4V.

Temperature range (°C)		**Permissible temperature increment per loadcase timestep (°C)**
Lower bound	Upper bound	
0	950	100
950	1670	50
1670	2500	200

- All residual stresses within the physical substrates and artefact were ignored in the models, as it is not currently possible to accurately measure and map the residual stress field with adequate resolution, for incorporation into FEA models.

6.4 Implementation of process models

The implementation of different models was facilitated by data from pertinent sources, including empirical studies and literature surveys. Results from trials were screened as necessary, to obtain sufficient and complete data, while relying on previous studies to augment model input parameters and improve predictive accuracy.

6.4.1 Model calibration

The heat input model parameters were estimated and calibrated through the use of thermographs of the molten pool [414], measurements of the substrate temperature at specific points using thermocouples [408] during deposition, and the measurement of the resultant bead width from each experiment. These measurements were used to adjust the heat input model parameters in an iterative manner. The previously reported temperature measurements are compared with the FEA predictions in this section.

A video annotation and motion measurement tool, Kinovea [415], was used for video and thermograph analysis, with acquired images, depicting how heat input parameters were estimated, shown in Figure 6-9.

(a) (b)

Figure 6-9. Time coded images used for the estimation of molten pool dimensions: (a) arc extinguishing point and (b) estimated molten pool dimensions as the arc is extinguished. Arc properties 130A, 13V, 3 mm arc gap

The calibrated heat source parameters used for some of the simulations in this study, are listed in Table 6-3, which includes details of the only parameters, a, b and c, that were calibrated with respect to the estimated molten pool dimensions.

Table 6-3. Values of heat source parameters

	Heat source parameters							
Experiment	a **[mm]**	b **[mm]**	c_f **[mm]**	c_r **[mm]**	**Voltage [V]**	**Current (A)**	**Efficiency,** η	**Deposition speed [mm/s]**
PS02	5.37	10	3.6	5.2	13.4	130	0.75	5
PS03 (L1)	4.25	8	4.5	10	12	130	0.75	2.5
PS03 (L2 & L3)	4.25	8	4.5	10	16.7	130	0.75	2.5
Substrate	-	-	-	-	12.4	130	0.75	2.5
Artefact	5.5	4	4.25	15	11.9	148	0.75	1.61

6.4.2 Material properties

The mechanical and thermal properties of Ti-6Al- 4V, which were used for this study, are shown in Figure 6-10. The thermal conductivity of 7 $W{\cdot}m^{-1}{\cdot}°C^{-1}$ at 25°C was varied with temperature, and increased to a value above the liquidus temperature (1660°C) to account for convective stirring in the molten pool [396,397,413]. The specific heat capacity was also varied with temperature, with solid-liquid phase transformation accounted for via a latent heat of fusion of 365 kJ/kg, with solidus and liquidus temperatures of 1604°C and 1660°C respectively.

Heat loss occurs on all free surfaces of the model via convection and radiation. The material properties for natural and forced convection were adapted from the work of Heigel et al [416,417], with 10 $W{\cdot}m^{-2}{\cdot}°C^{-1}$ used for free convection, and 65 $W{\cdot}m^{-2}{\cdot}°C^{-1}$ used in areas of localised forced convection, simulating heat losses from the shielding gas. Heat transfer to the environment, via radiation, was adapted from Boivineau et al [418], and is temperature dependent, as shown in Figure 6-10(b).

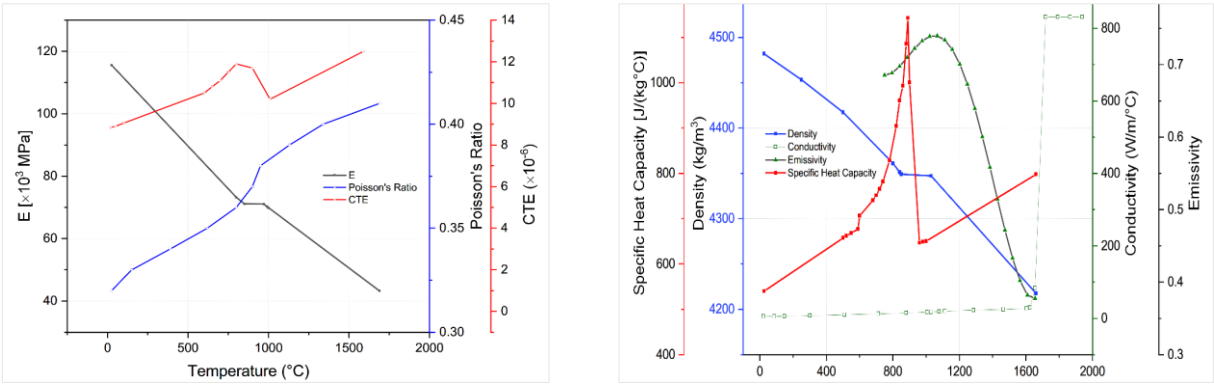

(a) (b)

Figure 6-10. Temperature dependent (a) mechanical and (b) thermal properties of Ti-6Al-4V

The flow stress curves used in the TM models, were adapted from several sources[408,419–421], including calculations using JMAT Pro by Sente Software [422], and are shown in Figure 6-11.

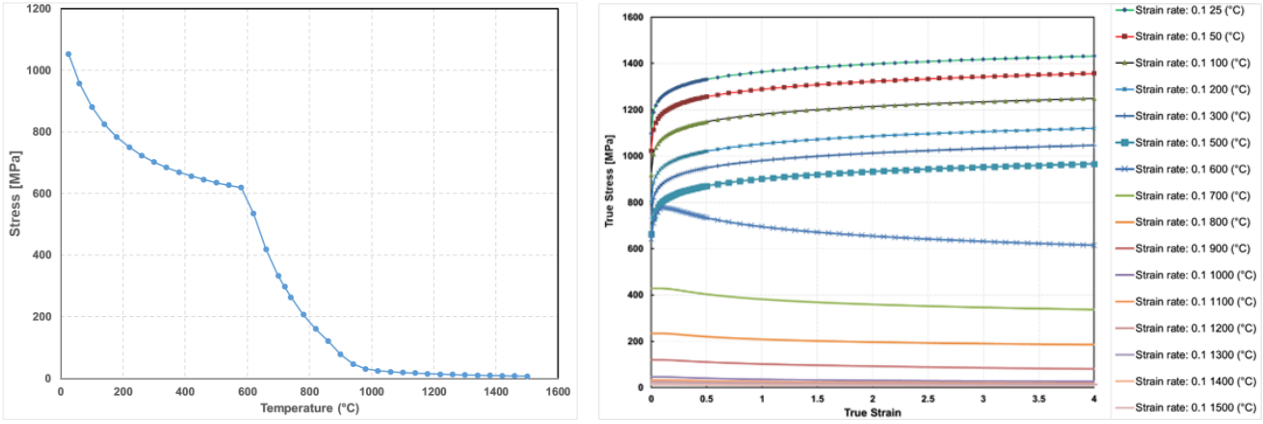

(a) (b)

Figure 6-11. Temperature dependent Yield Stress and flow stress curves for Ti-6Al-4V.

The solid-solid phase transformation (microstructure evolution) was not considered in this study, due to restrictions on post-reprocessing operations involving the artefact. Consequently, only thermal and TM analyses were performed, to support inferences about the possible effects of the WAAM process on the Ti-6Al-4V substrates and artefact.

6.4.3 Thermal model verification for substrate PS02

A thermal finite element model was used to model heat transfer for comparison with the temperature mapping data acquired during experiments. The model consisted of 22,220 hexagonal heat transfer elements (element type 43), used for the substrate PS02, and deposition sets S1, S2 and S3 (Figure 5-7) i.e. PS02:S3. For computational efficiency, and to ensure adequate heat transfer via conduction, the positioner was modelled as a flat plate of dimensions 300×300×5 mm, with 2938 tetrahedral elements (element type 136). The bottom of the plate was fixed at 22°C, the assumed ambient temperature for this model. The substrate was glued to the build plate via a mesh independent tie, or glue contact condition, and a temperature constraint was applied between the substrate and the plate. The clamps were modelled as rigid contact bodies, which were glued to the substrate.

The deactivated elements scheme for filler elements was used for this model. The load case history for PS02 is listed in Table 6-4, while the mesh configuration is shown in Figure 6-12.

Table 6-4. Deposition sequence for PS-02.

Loadcase (LC)	Arc stabilisation time (s)	Deposition time (s)	Tool path direction	Delay time (s)	Description
LC01	1.5	20	+Z	0	Autogenous run
LC02	0	0	-	1800	Cool down to below 30°C
LC03	1.5	20	+Z		Deposition of layer S1
LC04	0	0	-	1800	Cool down to below 30°C
LC05	1.5	20	+Z		Deposition of layer S2
LC06	0	0	-	1800	Cool down to below 30°C
LC07	1.5	100	+Z		Deposition of layers S3(1-5)
LC08	0	0	-	1800	Cool down to below 30°C

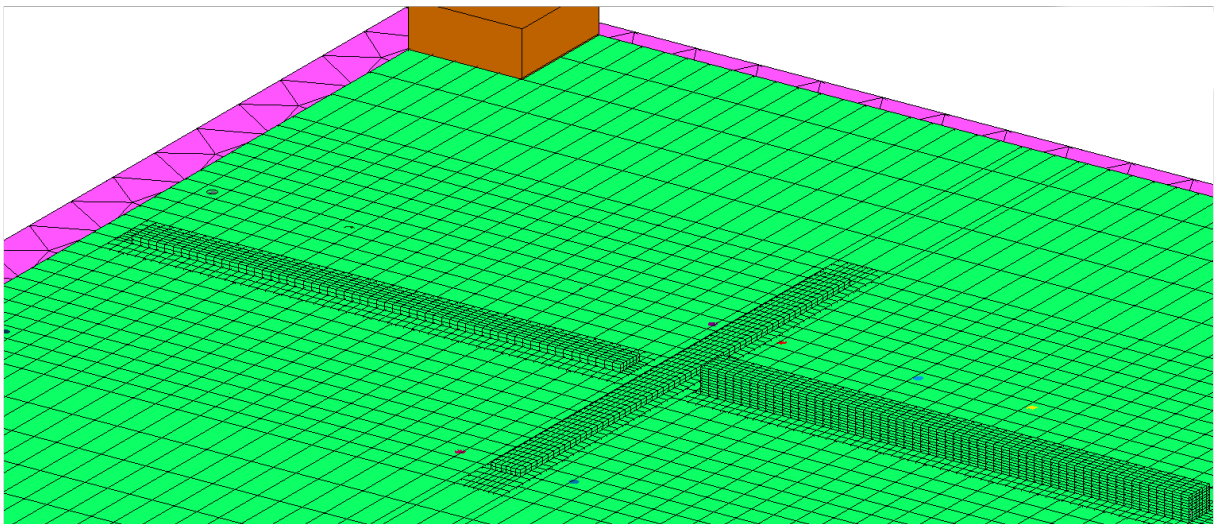

Figure 6-12. Mesh configuration PS02

The depicted mesh configuration (Figure 6-12) was used for predicting the temperature field for substrate PS02, deposited layer S3, and loadcase LC03, or PS02_S3LC03. The temperature distribution shows the molten pool for pre-deposited layers S3L01and S3SL02, with elements above 1655°C. The locations of the thermocouple TC05 for each S3 deposition sequence, is marked by a red dot, as shown in Figure 6-13.

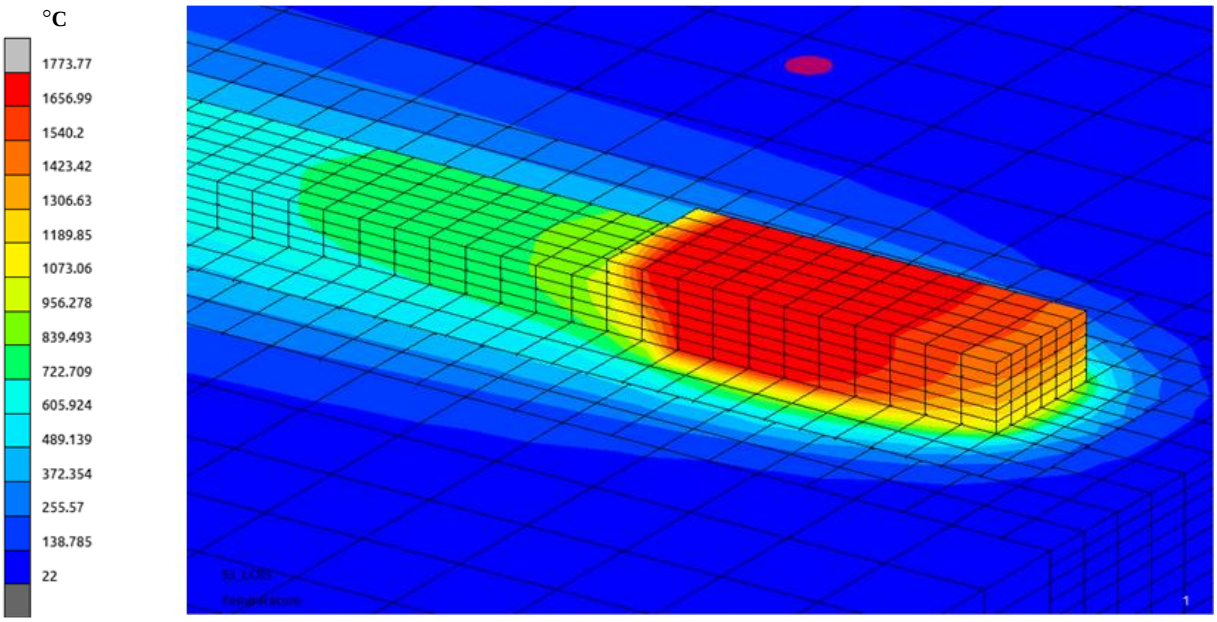

Figure 6-13. Temperature field during deposition of PS02:S3LC03

The predicted temperatures from the thermal model and experimental readings obtained from thermocouples TC01-TC08, and for deposition sequences, PS02-S1, PS02-S2 and PS02-S3, are compared in Figure 6-14. Overall, there were good correlations between peak measurements and predictions, except for thermocouple TC-05, relating to experiments PS02:S2 (Figure 6-14 (d)), and PS02:S3 (Figure 6-14 (f)). Discrepancies were mainly attributed to modelling assumptions, including the method of applying localised forced convection parameters away from the molten pool, and the proximity and location of devices during trials (Figure 5-7).

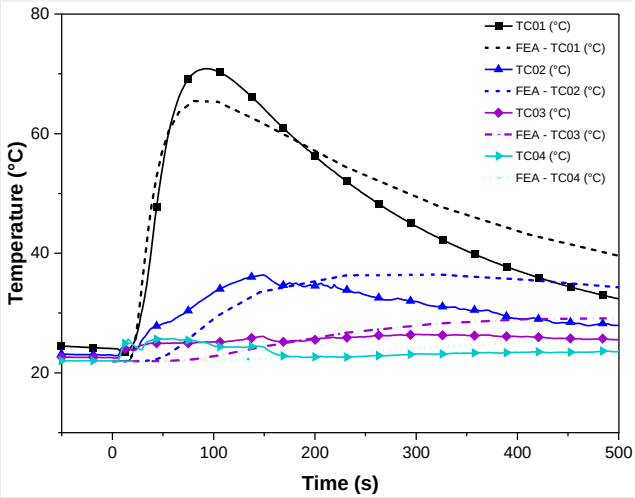

(a)

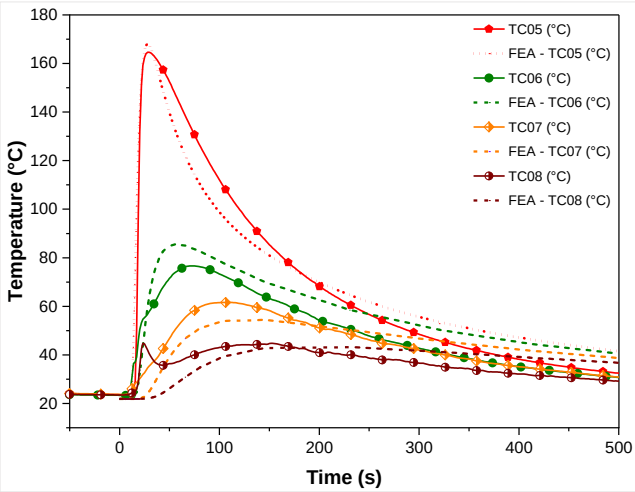

(b)

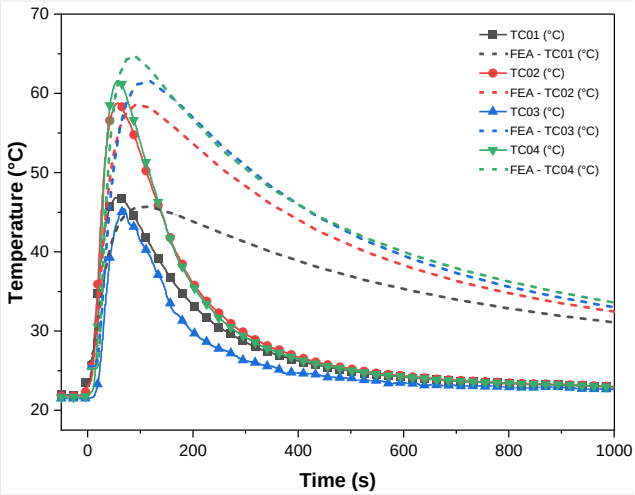

(c)

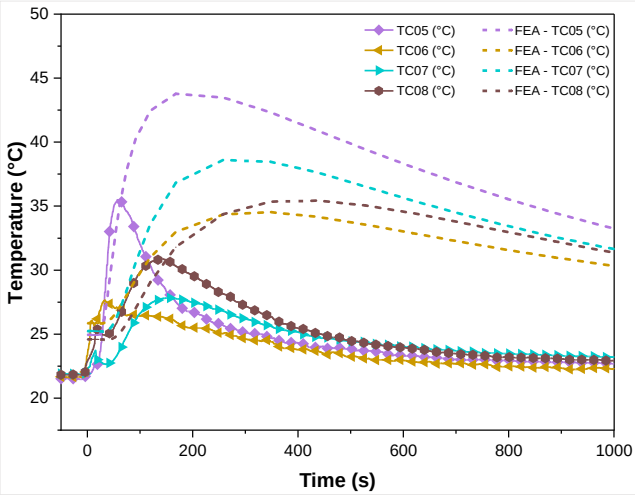

(d)

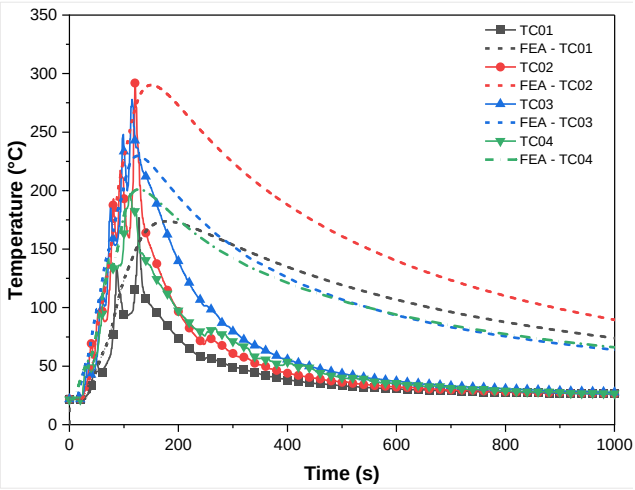

(e)

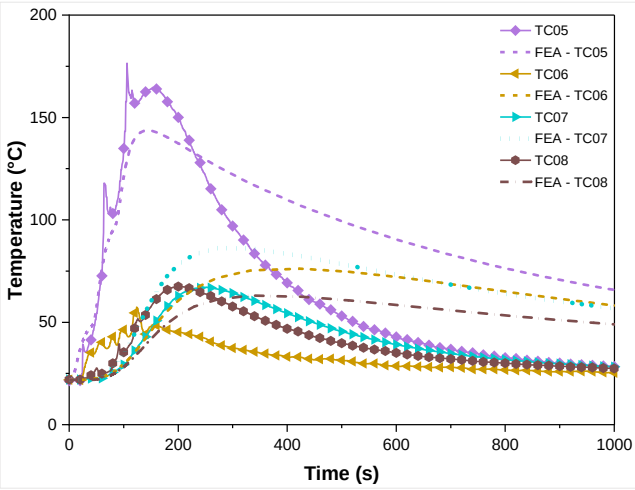

(f)

Figure 6-14. Comparison of measured and predicted temperatures for PS02:S1 (a) & (b), PS02:S2 (c) & (d), and PS02:S3 (e) & (f).

6.4.4 Thermo-mechanical model verification for substrate PS03

Coupled thermo-mechanical finite element analyses were used to simulate DED experiments, based on the outputs depicted in Figure 6-2. The representative FE model for PS-03 simulations consisted of an element size of 0.5 mm in the deposition areas. Adaptive mesh refinement was used to further improve the mesh density, in the area bounded by the volumetric heat source, by a factor of 4, and improve the prediction of the temperature distribution within the molten pool. The substrate dimensions, thermocouple and strain gauge locations, and the clamping configuration for the idealised FEA geometry, are shown in Figure 6-15.

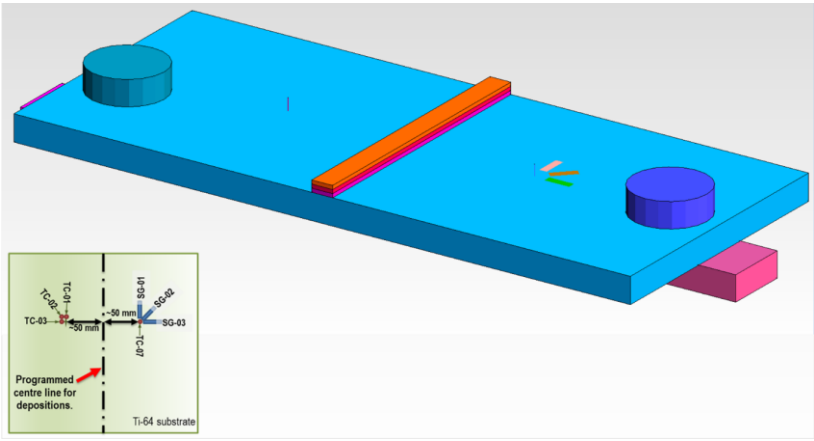

Figure 6-15. FE model for PS-03 with representative contact bodies and schematic for locating strain gauges and thermocouples

The depositions were performed in three sequences, with the timing for each sequence, which is reflected in the FE model. The details of each deposited layer, or subsequent delay phase, which is represented as a loadcase in the model, is provided Table 6-5.

Table 6-5. Deposition sequence for PS-03.

Load case (LC)	Arc stabilisation time (s)	Deposition time (s)	Tool path direction	Delay time (s)	Description
LC01	2	40	+Z	0	Deposition of Layer 1
LC02	0	0	-	3840	Cool down to below 30°C
LC03	2	40	+Z		Deposition of Layer 2
LC04	0	40	-Z	-	Deposition of Layer 3
LC05	0	0	-	3840	Cool down to below 30°C

The measured and predicted temperature distributions, during LC01 and LC02, corresponding to the top and bottom of the substrates at the previously described locations, are shown in Figure 6-16(a) and (b). Although computed values are higher for both cases, with a difference of about 9°C at TC-07, and about 16°C at TC-07, there is good overall agreement in the shape of the temperature distribution curves between the computed and measured values. Furthermore, the gradients for predicted and acquired measurements, for loadcase LC01, occurring over the initial 42 seconds (Figure 6-16), are comparable.

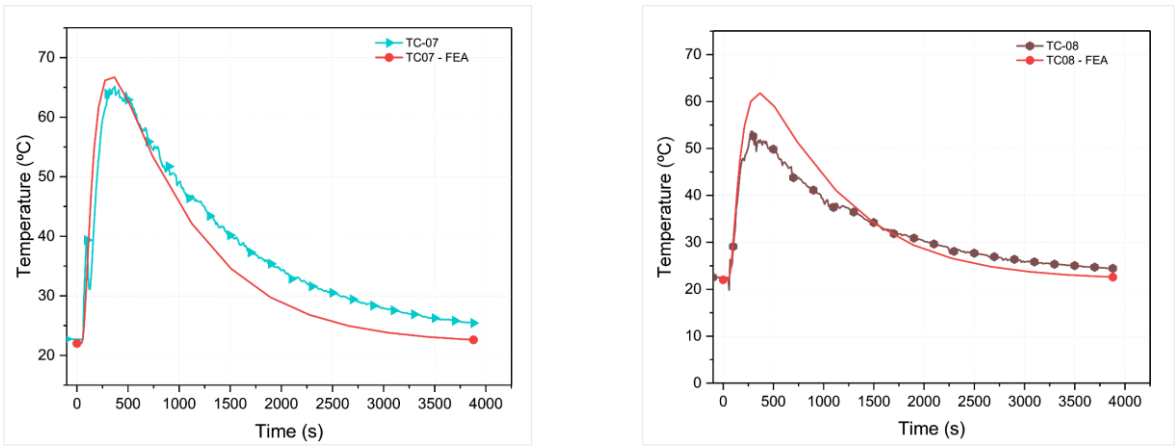

(a) (b)

Figure 6-16. Comparisons of measured and predicted temperature history at location of thermocouples at the top (TC-07) and bottom (TC-08) of the substrate during LC01 and LC02.

The comparisons of predicted and experimentally measured transverse strain (ε_{zz}), at the locations SG01 and SG04, are shown in Figure 6-17.

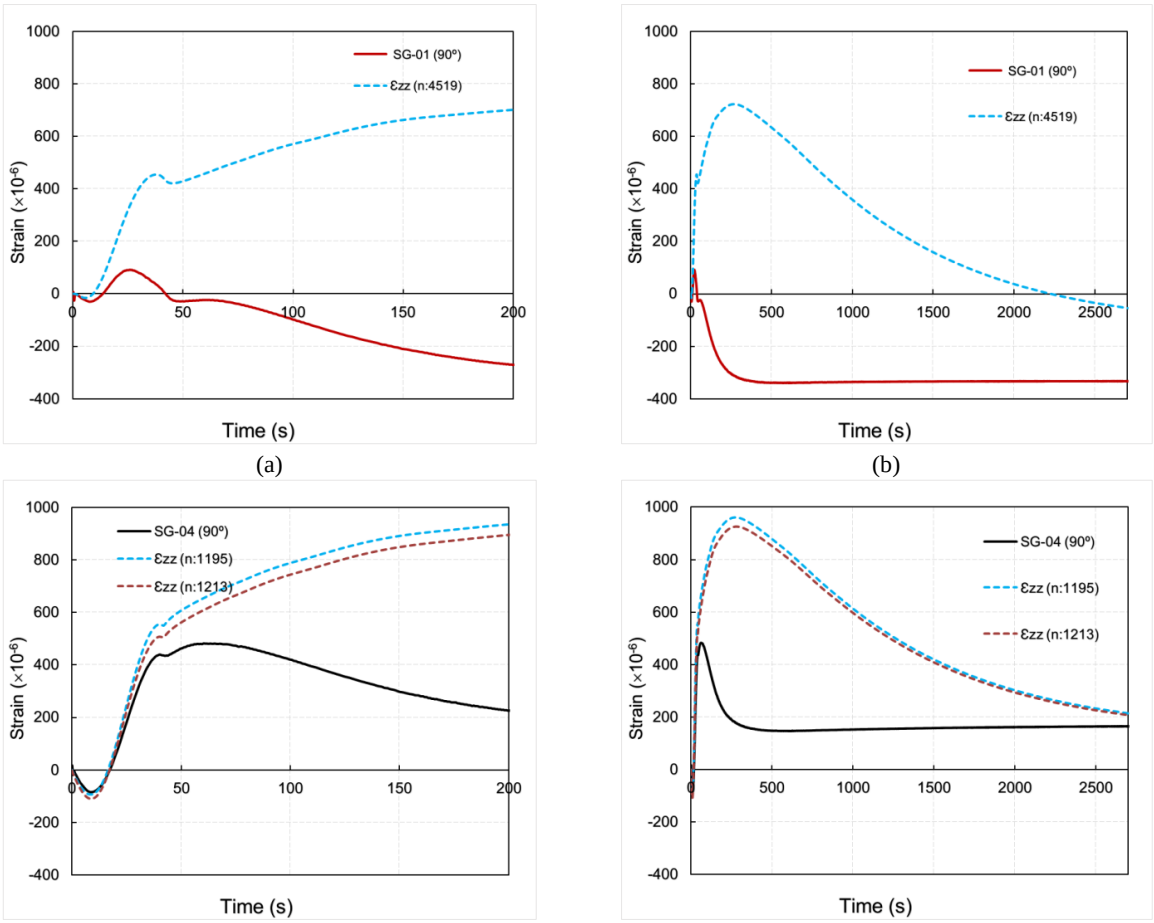

(a) (b)

(c) (d)

Figure 6-17. Measured vs. predicted transverse strain distribution (εzz) at experimental locations showing the (a) short and (b) long timescales for SG01 respectively, and the (c) short and (d) long timescales for SG04.

In Figure 6-17(a), the strain distribution during the initial 200 seconds for combined load cases LC01 and LC02 is shown for SG01, with the entire duration shown in Figure 6-17(b). This duration was selected because of the relatively short timescale (~42 seconds) when energy is introduced to the system. The predicted strains are much higher than the recorded strains during the initial phase, and for the entire timescale considered. However, changes in the distribution were coincidental for both curves.

The comparisons of measured and predicted transverse strains at SG04 are shown in Figure 6-17(c) and (d), using the same timescales previously described. Additional strain distributions from nearby nodes were added, given the relative area of strain gauges compared to extrapolations from nodal points. For SG04, the predicted strains compare favourably with the measured strains for the duration representing the deposition loadcase LC01. Although the inflexion points along both curves are coincidental, the predicted strain magnitude was much higher over the remaining timescale, when compared with actual measurements.

The comparisons of transverse shear strain (ε_{zx}) measurements and predictions, at SG02 and SG05, are shown in Figure 6-18.

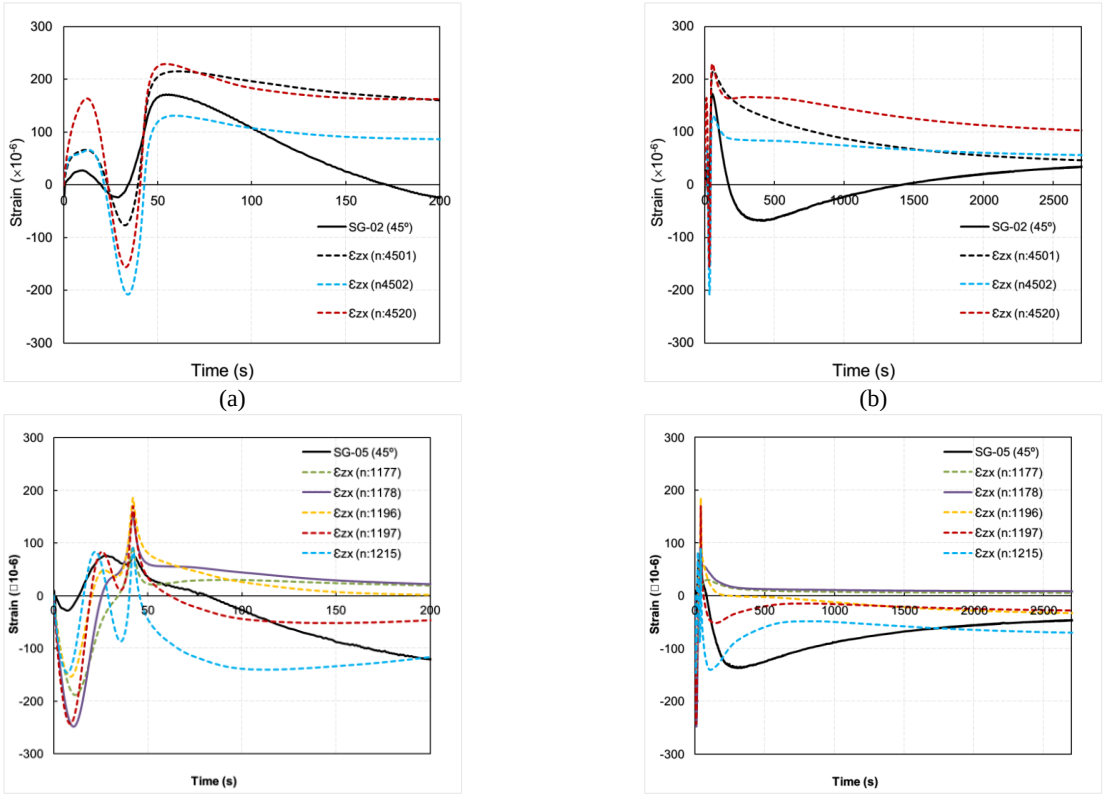

Figure 6-18. Measured vs. predicted transverse shear strain distribution ((ε_{zx}) at experimental locations showing (a) short and (b) long timescales for SG02 respectively, and (c) short and (d) long timescales for SG05.

The predictions compare favourably with the measured strains for both timescales considered. Given the approximate nature of the model, and the modelling assumptions, strain predictions from adjacent nodes within an area equal to that of the experimental rosette arrangement were included. The strain history profiles show

alternating positive (tensile) and negative (compressive) strains during LC01, which correspond to the energy input phase of the timescale under consideration. The direction of the strain profiles from SG02 (Figure 6-18(a) and (b)) and SG05 (Figure 6-18(c) and (d)) also mirror each other in the initial phase, and are similar for LC02.

The comparisons for measured and predicted longitudinal strains, at SG03 and SG06 are shown in Figure 6-19.

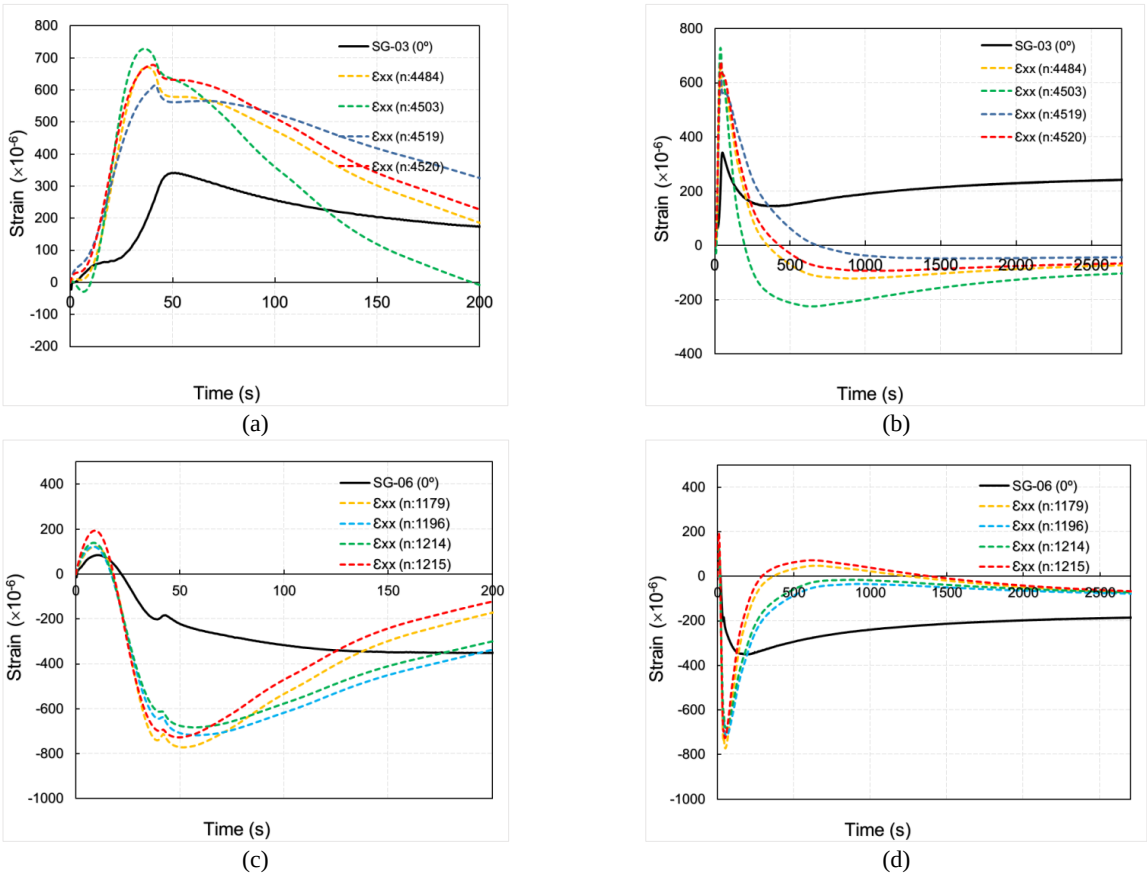

Figure 6-19. Measured vs. predicted longitudinal strain distribution ((εxx) at experimental locations showing (a) short and (b) long timescales for SG03 respectively, and (c) short and (d) long timescales for SG06.

The overall shape of the predicted evolution of longitudinal strains at SG03 (Figure 6-19(a) and (b)) compares well with the measured strains over both timescales considered. However, predicted values are about 2 times higher than the measured peaks along the timescale. A similar trend is observed in Figure 6-19(c) and (d) for strain comparisons at SG06, with measured peaks along the history curve much lower than the maximum predicted strains during the period of energy input into the system. While the distributions were different, predicted strain magnitudes over the remaining timescale were lower, relative to the measured strains, which may suggest similarities in the total strain energy at the end of the timescale.

The predicted and measured temperatures for LC03 and LC04 are shown in Figure 6-20(a) and (b), for TC-07 and TC08 respectively.

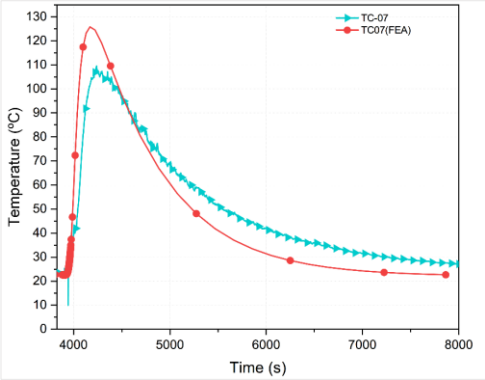

(a)

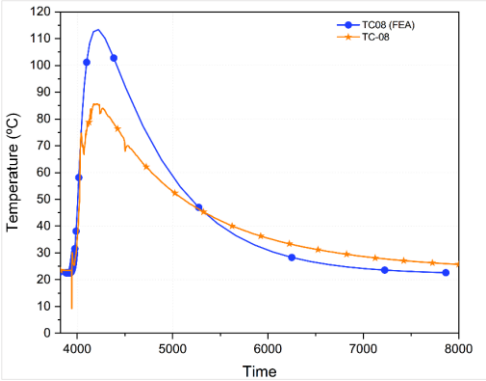

(b)

Figure 6-20. Comparisons of measured and predicted temperature history at location of thermocouples glued to the top (TC-07) and bottom (TC-08) of the substrate during LC03-LC05.

The peaks of measured and predicted temperatures during the deposition phase are comparatively higher than the values obtained in the previous deposition phase. This phase, which lasts for ~84 seconds for LC03 and LC04, corresponds to the increased energy input relative to LC01. Although the gradients were similar during the energy input phase, the maximum temperatures recorded at TC-07 and TC-08 were lower than the predicted values by about 15°C and 25°C respectively. This variation was attributed to errors in the estimation of convection coefficients for the model, compared to realistic effects of cooling from the shielding gas in experimental conditions, as well as experimental measurement errors, and necessitates further investigation.

The predicted and measured temperatures for SG01 and SG04, and LC03-LC05, are shown in Figure 6-21.

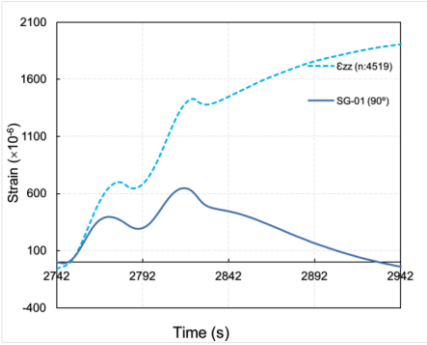

(a)

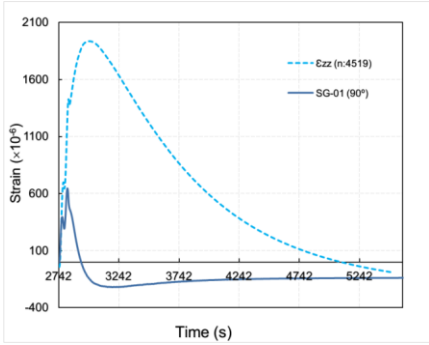

(b)

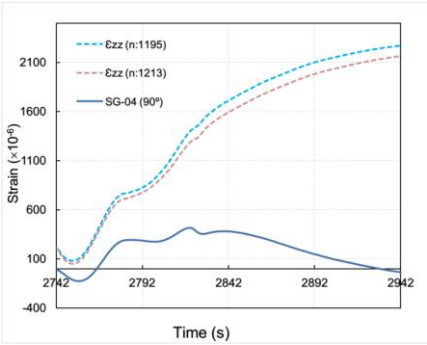

(c)

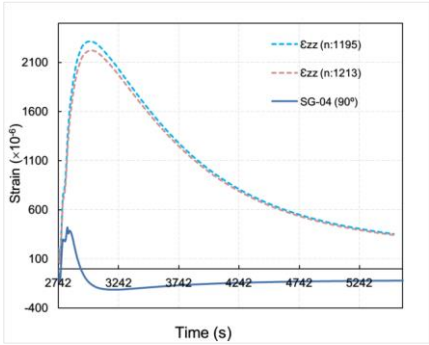

(d)

Figure 6-21. Measured vs. predicted transverse strain distribution (ε_{zz}) at experimental locations during LC03-LC05 showing (a) short and (b) long timescales for SG01 respectively, and (c) short and (d) long timescales for SG04.

The differences in measured and predicted transverse strains for the duration of LC03-LC05 for SG01(Figure 6-21(a) and (b)), and SG04 (Figure 6-21(c) and (d)), follow the same trend observed in Figure 6-16, but with higher maximum predicted values, attributable to the increased energy input during this period.

The predicted and measured transverse shear strain (ε_{zx}) distributions, for the duration of LC03-LC05, are shown in Figure 6-22.

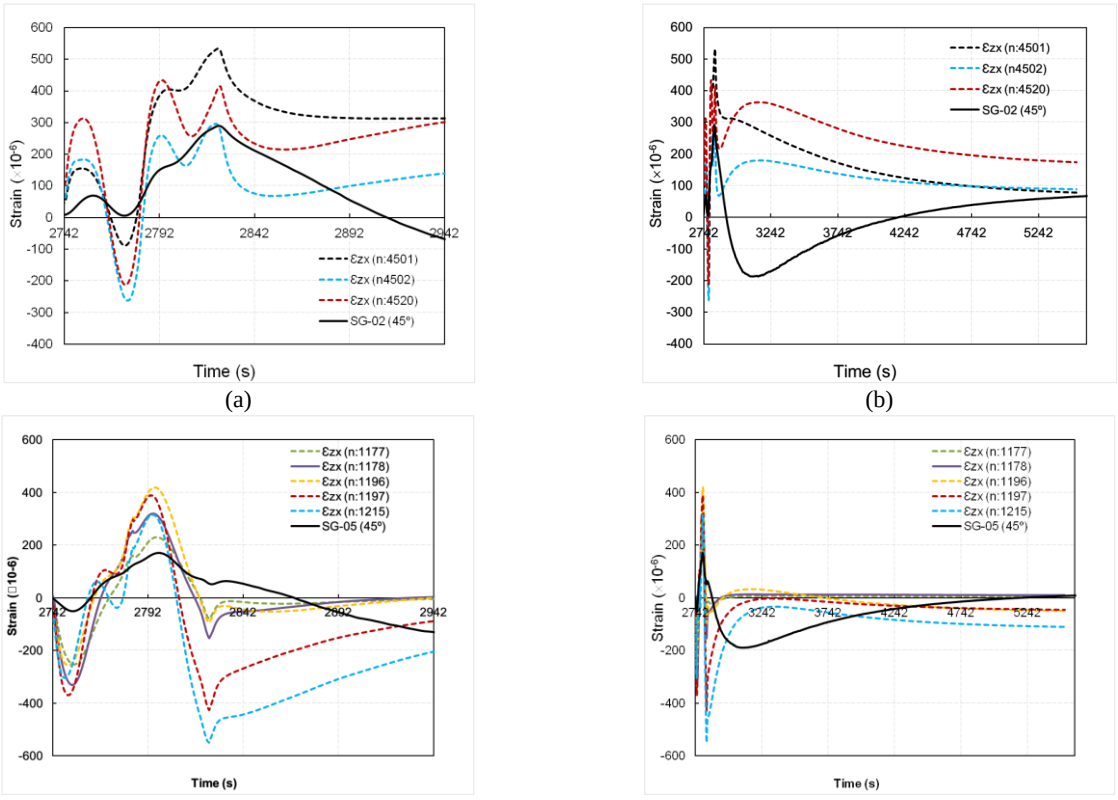

Figure 6-22. Measured vs. predicted transverse shear strain distribution (ε_{zx}) at experimental locations during LC03-LC05 showing (a) short and (b) long timescales for SG02, and (c) short and (d) long timescales for SG05.

The strain distributions are comparable, in terms of magnitude and shape for SG02 (Figure 6-22(a) and (b)), and SG05 (Figure 6-22(c) and (d)) respectively. The distributions from adjacent nodes in the equivalent area of the model, representing the surface area covered by the strain gauge, indicates minor variability in the strain distribution in the selected areas. The measured and predicted strain evolution also mirrors the evolution for LC01 and LC02, with distinctly higher values corresponding to the increase in energy density.

The trend for the transverse strains, shown in Figure 6-23, is repeated in the comparison of measured and predicted longitudinal strains (ε_{xx}) for the duration of the load cases LC03-LC05, as shown in Figure 6-19. Although the shapes of the history plots are similar, and peaks corresponding to multiple depositions are clearly visible, the models for SG03 (Figure 6-23(a) and (b)) and SG06 (Figure 6-23(c) and (d)) overestimate the measured peak values by a factor of 5.

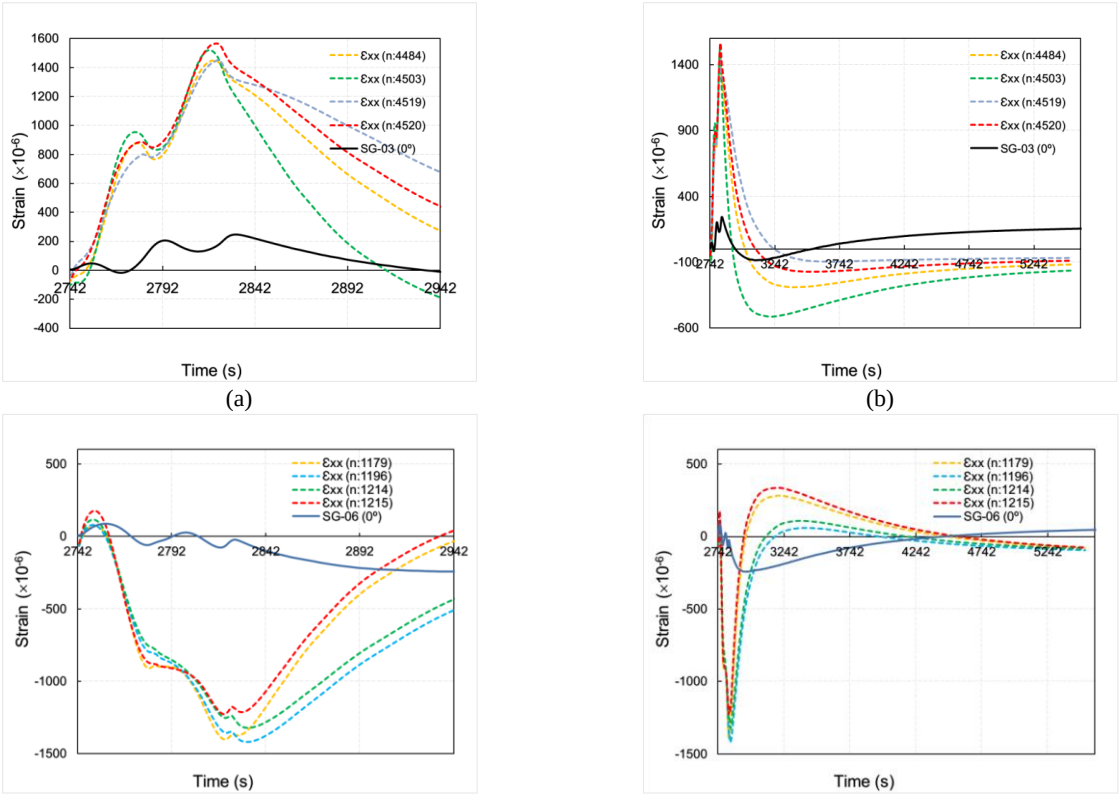

Figure 6-23. Measured vs. predicted longitudinal strain distribution (ε_{xx}) at the experimental locations during LC03-LC05 showing (a) short and (b) long timescales for SG03 respectively, and (c) short and (d) long timescales for SG06.

6.4.5 Modelling DED reprocessing operation on Ti-6Al-4V artefact

The DED operation on the Ti-6-Al-4V artefact was investigated, using coupled thermo-mechanical models and similar techniques to those used in the analysis of PS-02 and PS-03. Due to commercial sensitivities, only a section of the artefact was considered for this part of the study. The selected section is shown in Figure 6-24.

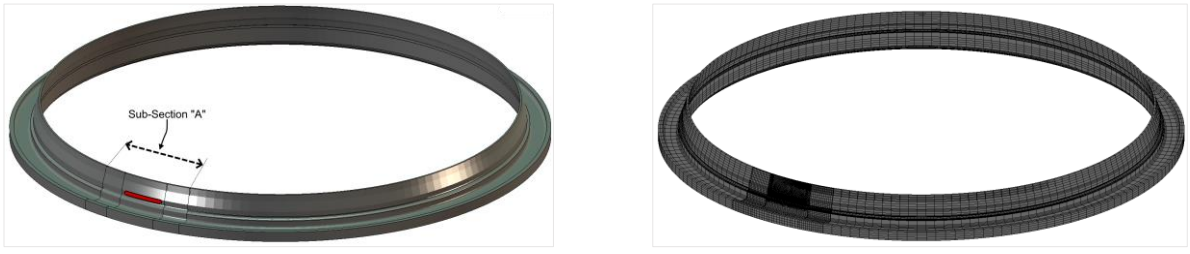

Figure 6-24. (a) Defeatured artefact model section with representative groove, showing sub-section “A”, and (b) artefact model section mesh.

The designated section was defeatured via the removal of stiffeners, ports, and other special or identifying features, whilst retaining critical dimensions and important geometric characteristics, including machined grooves, as inputs for the model. The resulting structure was analysed as shown in Figure 6-24(a), with the meshing strategy implemented for computational efficiency, as shown in Figure 6-24(b). Specifically, the

focus was on modelling the reprocessed region of the artefact to which sensors were applied, with a more refined mesh used in *Sub-Section "A"* (Figure 6-24(a)), to enhance the accuracy of model predictions. The geometric characteristics of the groove were also modified, with defeatured fillet areas introduced at the base and each end of the groove, before applying a mesh to the area, as illustrated in Figure 6-25.

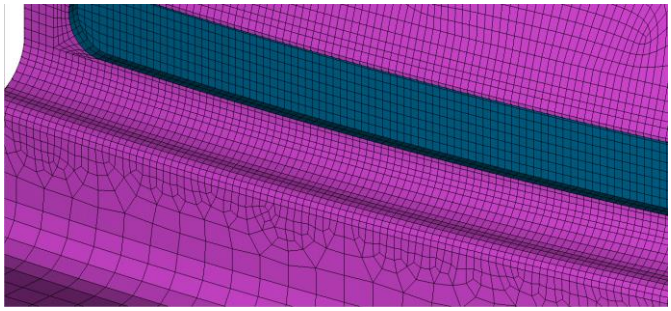

Figure 6-25. Close-up of *Sub-Section "A"* with representative mesh.

Key parts of the simplified model, comprising the filler elements representing the deposited material volume, the mesh section, and combined elements and mesh in the area under consideration, are depicted Figure 6-26.

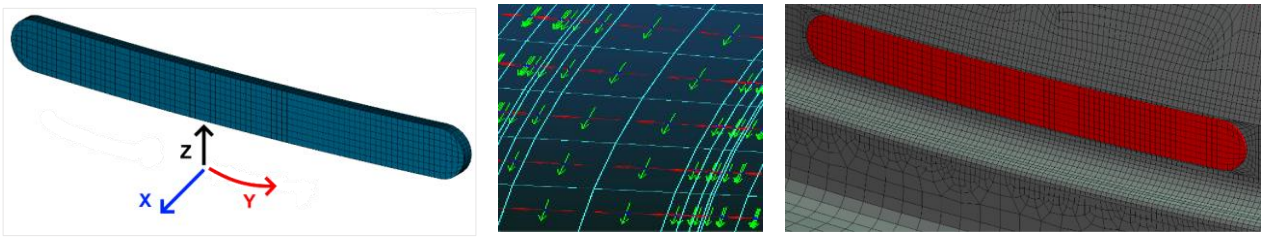

(a) (b) (c)

Figure 6-26. Close-up of (a) groove filler elements and local coordinates, (b) mesh section with element orientations, and (c) elements and mesh in combined filler and groove area.

Due to the large surface area to volume ratio of the entire section selected for modelling, the mesh was progressively dense in areas of interest (Figure 6-26(c)). The entire volume of the filler elements for the groove and the combined groove and filler element mesh are displayed in Figure 6-26(a) and (b) respectively. Mesh independent ties or glued contact was used to join the mesh of the entire section as a congruent body for finite element analysis. The entire mesh consisted of 65682 nodes and 45,349 hexagonal, type 7, 8 node brick elements, with assumed strain formulation. The orientations of all elements were realigned from the global *XYZ* direction to local coordinates (Figure 6-26(a)), such that the element *XYZ* outputs were in the radial, circumferential and axial (cylinder length) directions. The quiet element filler addition method was used in this case, to avoid excessive mesh distortion and solution convergence difficulties arising from the two heating and cooling passes that were applied during the reprocessing operation.

In order to prevent rigid body motion during the simulation, the nodes around the base of the artefact model section were secured using RBE2, a multipoint constraint element which was linked to a node at the circumferential centre of the modelled section, thus mimicking the supporting blocks and clamps used to

secure the artefact to the positioner (Figure 5-24 (c)). Conversely, the nodes around the top circumference of the section were held with RBE3 links, to a node at the circumferential centre, such that the model section was not over constrained. Unlike RBE2, a kinematic rigid coupling that adds stiffness to a model, the distributed RBE3 coupling allows independent movement based on the respective local stiffness, which is a more realistic representation of the problem being simulated.

The video of the entire BAM operation was analysed using Kinovea, which enabled the precise reproduction of the actual sequence of distinct reprocessing events. The resulting data, which corresponds to the different loadcases that were considered when modelling the events, was important for enhancing the accuracy of predictions, and understanding the effects of DED process on restored features (Figure 5-27). The load cases derived from the Kinovea analysis are listed in Table 6-6.

Table 6-6. Deposition sequence of events during the artefact DED reprocessing operation

Load case (LC)	Event	Next event	Duration (s)	Description
LC01	Arc ignition	Arc stable	1.5	Arc stabilisation time
LC02	Arc stable	Tool translation	0.7	Translation delay
LC03	Tool translation start	Tool translation stop	59	Autogenous pass at 0.476kW power
LC04	Tool translation stop	Arc off	1.9	Arc off delay after tool translation.
LC05	Cooling	Arc ignition	1800	Cool down to below 30°C
LC06	Arc ignition	Arc stable	1	Arc stabilisation time
LC07	Arc stable	Filler addition	1	Filler addition delay
LC08	Filler addition	Tool Translation	0.8	Tool translation delay
LC09	Tool translation start	Tool translation stop	58	Deposition pass at 1.716kW power.
LC10	Tool translation stop	Filler stop	0.9	Filler end delay
LC11	Filler stop	Arc off	0.15	Arc dwell delay
LC12	Arc off	Cool to 25°C	2700	Cool down to below 30°C

Coupled thermo-mechanical FE analyses were employed to simulate the DED reprocessing of the artefact. A staggered solution procedure, including previously described modelling considerations, was implemented before comparing actual measurements with predicted results, as presented in Figure 6-27.

The measured and computed temperature history at the thermocouple locations shown in Figure 6-27 (a) for load cases LC01-LC04, during the reprocessing operation, are displayed in Figure 6-27 (b), (c) and (d). While the computed temperature history compared favourably with the experimental values close to the tool path trajectory (TC01), the magnitude of the temperature history curve at point TC04, at ~50mm away from the edge of the reprocessed section, was underestimated. This discrepancy was attributed to differences in the thermal mass of the artefact, relative to the simplified/ defeatured model section.

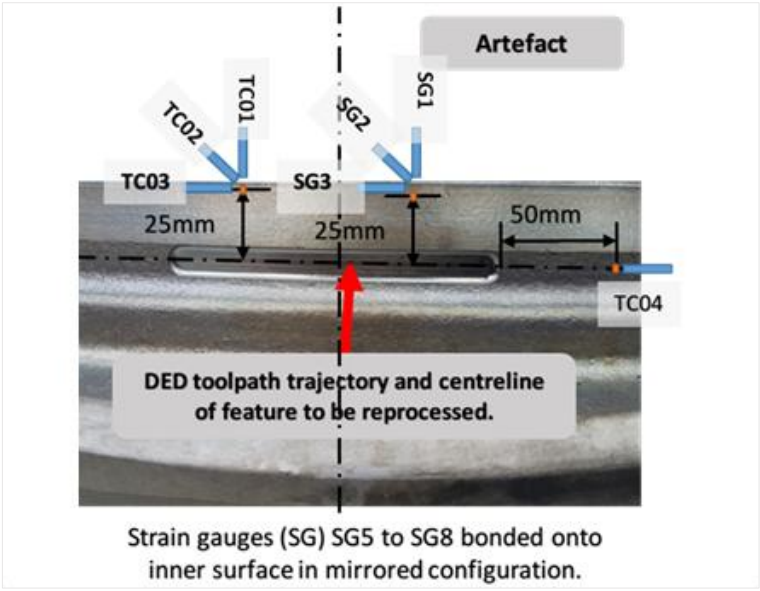

(a)

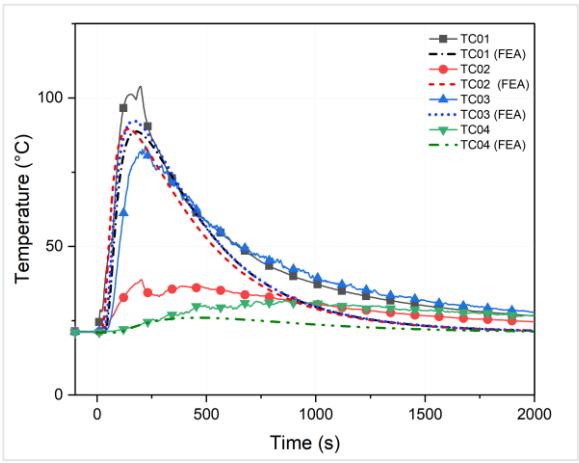

(b)

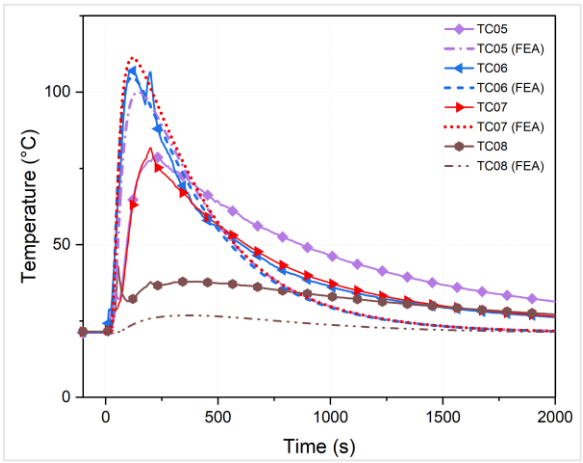

(c)

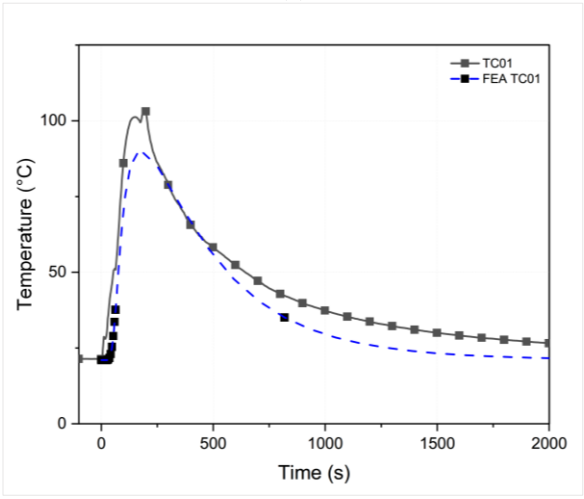

(d)

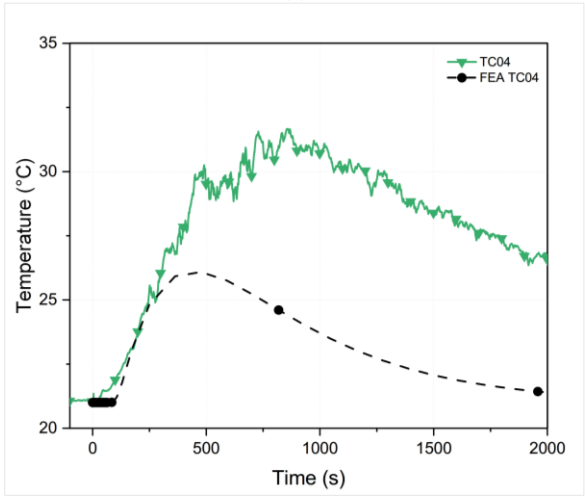

(e)

Figure 6-27. Measured vs. predicted temperature evolution during loadcase LC03 (autogenous pass) in the reprocessing procedure: (a) thermocouple locations on the artefact, (b) temperature history at thermocouples TC01 – TC04, (c) temperature history at thermocouples TC05 –TC08, (d) TC01 only and (e) TC04 only.

The predicted temperature evolution, for different loadcases or reprocessing events, are shown in Figure 6-28.

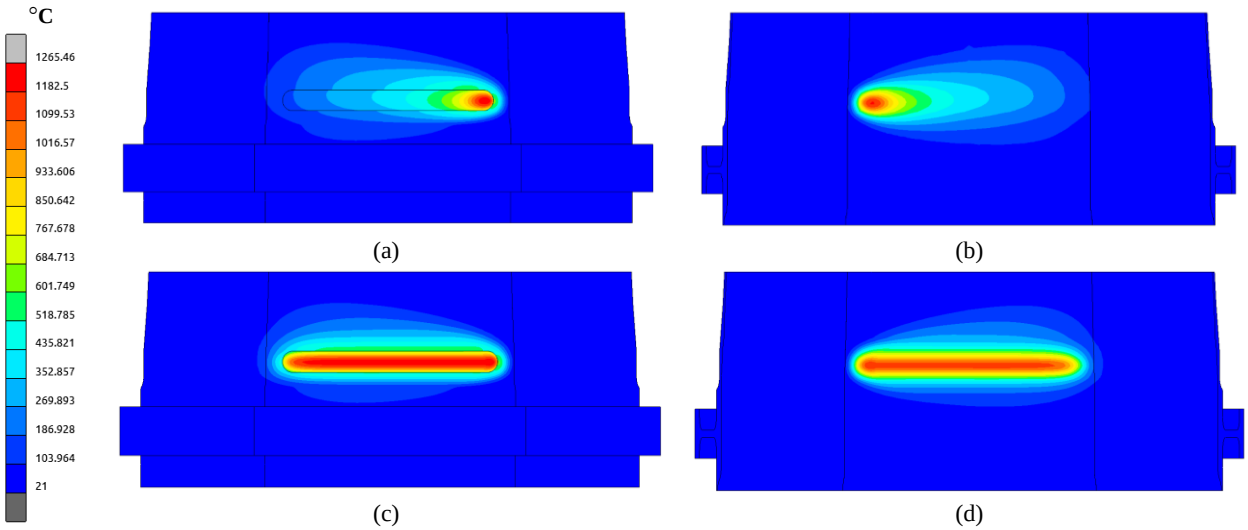

Figure 6-28. Computed temperature map of (a) the front and (b) rear of the reprocessed zone during LC04, near the end of the autogenous pass and the computed peak temperature of the (c) front and (d) rear of the reprocessed zone.

Contour plots of the predicted temperature evolution during and at the end of the autogenous pass (LC04) for sub-section "A", of the modelled artefact section, are shown in Figure 6-28(a) and (b), for the front and rear of the reprocessed zone. The numerical analysis predicts temperatures higher (above 1200 °C) than the β-transus temperature of Ti-6Al-4V (980°C-1000°C) [64,423], at the given power and translation speed.

The predicted peak temperature for the same area and load cases (LC03-LC04) is shown in Figure 6-28(c). and (d) for the front and rear of the reprocessed zone, and indicates that the entire length of the groove, and through the thickness of the component at that area, exceeds the β-transus temperature of the material.

The strain measurements from the autogenous pass (LC01-LC04) of the reprocessing procedure are compared with the computed strain predictions, from the same region (indicated in Figure 6-27(a)) on the artefact section in Figure 6-29. Multiple line plots of computed strain are presented, to match the cross-sectional area of the physical strain gauges. Overall, and except for the strain histories at SG01 and SG05, the magnitude of the strains recorded during the heating pass (the initial 63 seconds on each line plot), tends to be lower than the predicted strains at each strain gauge location, followed by a convergence during the cooling period.

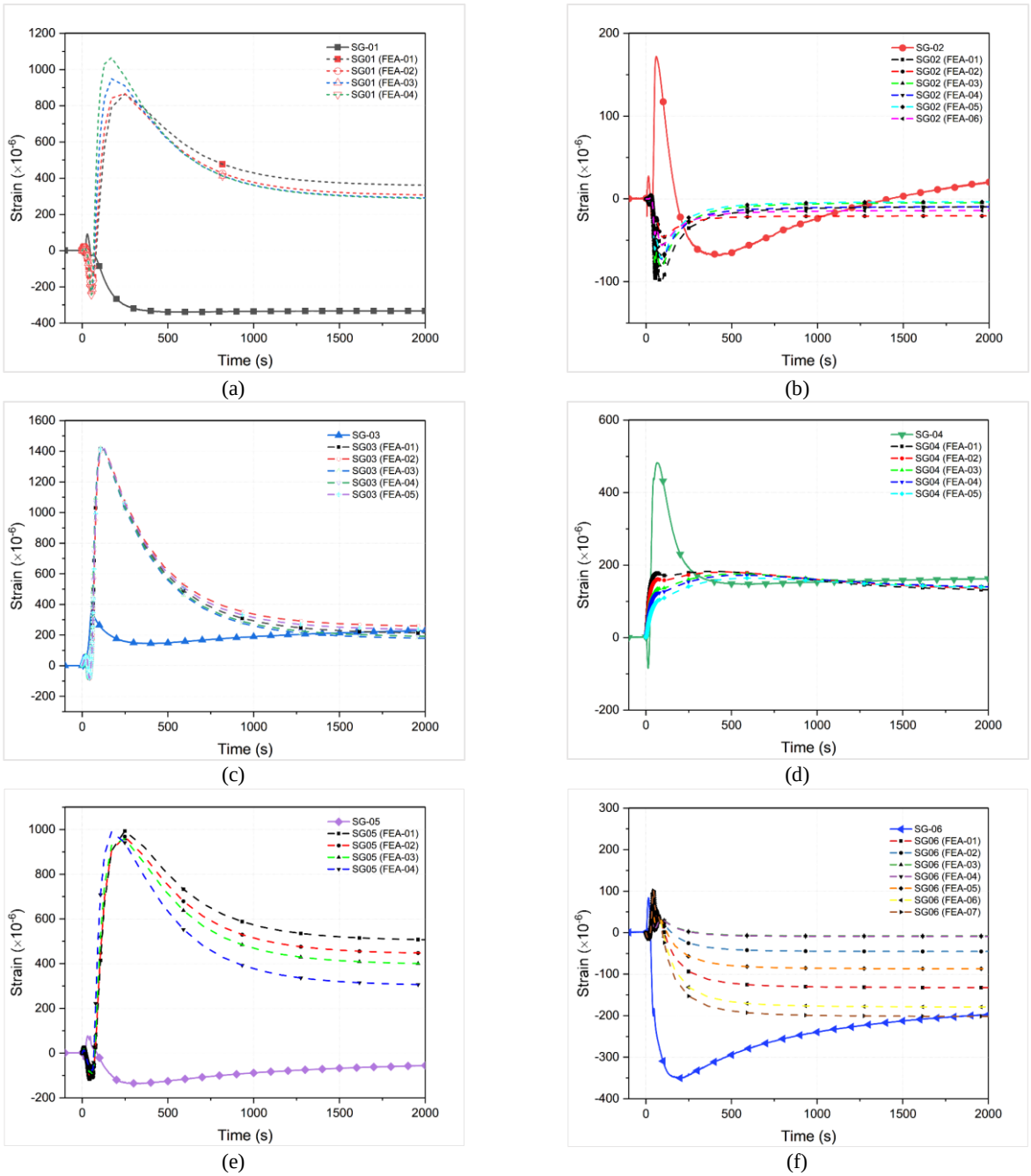

Figure 6-29. Measured vs. predicted strain evolution during load cases LC01-LC04 (autogenous pass) in the reprocessing procedure: (a) SG01(ε_{33}), (b) SG02 (ε_{23}), (c) SG03(ε_{22}), (d) SG04(ε_{22}), (e) SG05 (ε_{33}) and (f) SG06(ε_{23}).

As reported in chapter 5, the suspected failure of the adhesive bonding the strain gauge sensors to the artefact, despite attempts at heat shielding, likely caused the loss of sensor functions, for the deposition pass (LC06-LC11). However, XRD techniques were also used to quantify the residual stress in reprocessed areas. The measurement locations are indicated in Figure 6-30(a), with the results presented in Figure 6-30(b) and (c). The numerically predicted residual hoop stress (σ_{22}) results compare favourably with the XRD measurements, given the resolution of the technique, coupled with the differences between the artefact, and the heavily defeatured model section. The results indicate high levels of tensile and compressive stress (>400 MPa) above the reprocessed area. A similar trend is observed in the horizontal direction, away from the reprocessed area.

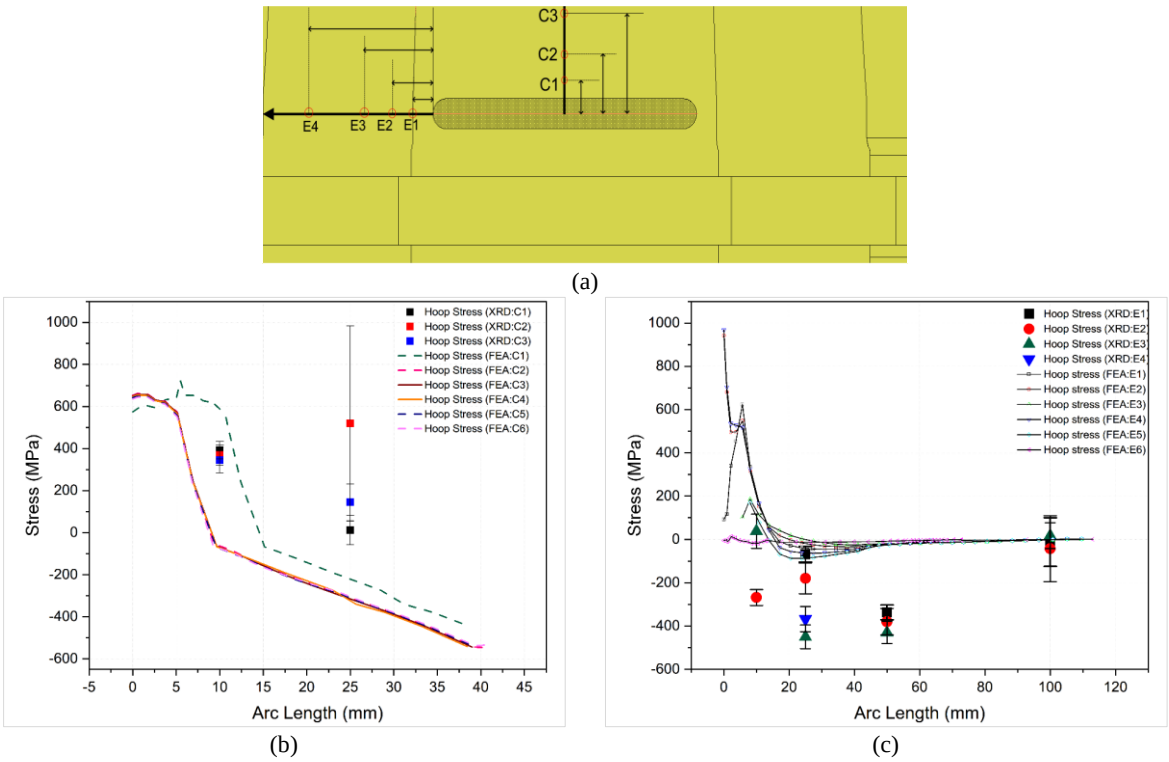

Figure 6-30. (a) Locations of post deposition residual stress measurements in the artefact, (b) comparison of measured and computed residual stress in the circumferential or hoop direction (σ_{22}) along paths C and (c) E.

Other reprocessing procedures were analysed using the FE model, to assess the predictive capability of the model in the optimisation of future reprocessing scenarios. Contour maps of the peak temperature predictions of the front and rear sections of the groove area during the metal deposition phase of the reprocessing procedure (LC08: t = 31s) are shown in Figure 6-31 (a) and (b).

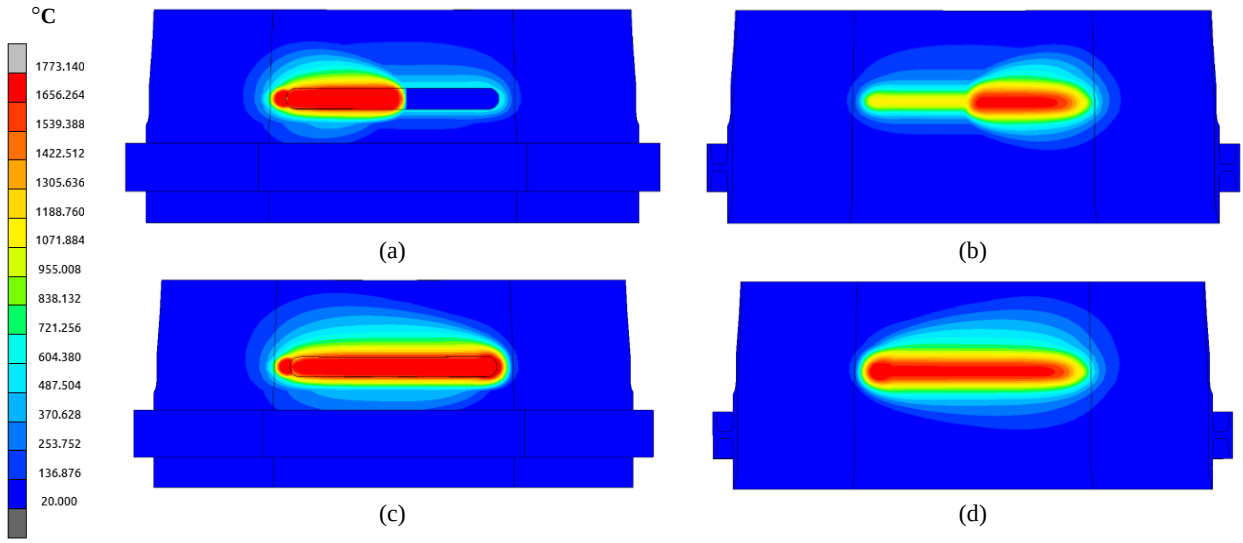

Figure 6-31. Predictions of peak temperature during the reprocessing operation at LC08:t=31s, (a) at the front profile of sub-section "A", (b) rear profile of sub-section "A", (c) front profile after LC11, (d) rear profile after LC11.

The inactive quiet elements, yet to be activated at that time, can be seen in Figure 6-31 (a), with peak temperatures of 1773°C, indicating areas where full melting occurred during the procedure. Of concern is the

area at the beginning of the toolpath, on the left-hand side, where full melting of the artefact is predicted (LC06-LC07), owing to the stationary nature of the EOAT for 2 seconds, to allow for arc stabilisation and wire feed initiation. The model also predicts peak temperatures close to melting, at the rear side of the artefact, ranging from 1422-1539°C, far exceeding the predicted peak temperature of about 1200°C, during the autogenous pass, and approaching the melting temperature of the material, as shown in Figure 6-31 (b). In Figure 6-31 (c) and (d), the peak temperatures predicted for the entire deposition phase of the reprocessing procedure are shown (end of LC11).

The images in Figure 6-32(a) and (b), show the HAZ in the rear of the process zone for grooves G5 and G2 of the artefact, respectively, after reprocessing, indicating possible oxidation and evaporation of alloying metals, previously investigated by several authors [424–427]. During this reprocessing operation, there were no supplementary provisions for shielding the entire artefact in an inert atmosphere or other protective measures, due to insufficient evidence, from previous experiments (PS01-PS03). The HAZ at the rear of the groove G2, after a cleaning procedure, is shown in Figure 6-32 (c).

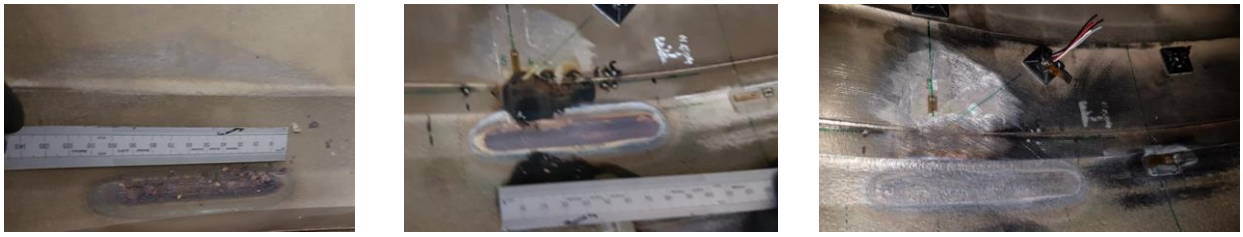

(a) (b) (c)

Figure 6-32. Reprocessed regions of artefact, including (a) HAZ at grooves G5 and appearance of G2, in (b) original and (c) intermediate conditions, prior to inspection.

The predicted hoop stress (σ_{yy}) and von Mises (σ_{Mises}) stress contours for the model sub-section "A", at the end of the reprocessing procedure (end of LC12), are shown in Figure 6-33.

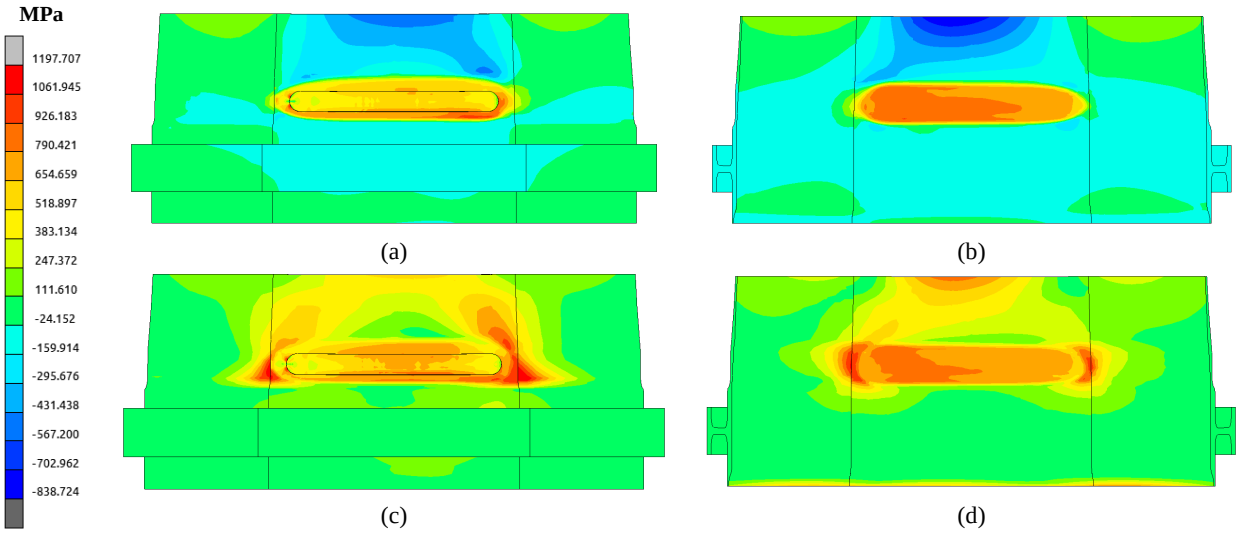

Figure 6-33. Predicted residual stress distribution in sub-section "A" after LC12; hoop stress (σ_{yy}) at (a) front profile, (b) rear profile, von Mises stress (σ_{Mises}) at (c)front profile and (d) rear profile.

The predicted hoop stress levels exceed 500 MPa at the edges of the groove, with a compressive stress state above the grove area, also exceeding 500 MPa, as shown in Figure 6-33(a) and (b). Similar stress levels were measured via XRD, as shown in Figure 6-30. The equivalent von Mises stress contours (Figure 6-33(a) and (b)) indicate stresses approaching or exceeding the elastic limit of the material at 25°C, for the front and rear profiles of the modelled sub-section.

Line plots of the von Mises stress state predicted in the model sub-section, at the commencement and cessation of cooling (entire duration of LC12) at the location "X-X*" on the front profile, and "Y-Y*" at the rear profile (indicated in Figure 6-34(a) and (b)), are shown in Figure 6-34 (c) and (d). In general, the model predicts that cooling after the reprocessing procedure induces high levels of stress in the component, across the groove length, and throughout the thickness/ walls of the component (in excess of 400 MPa).

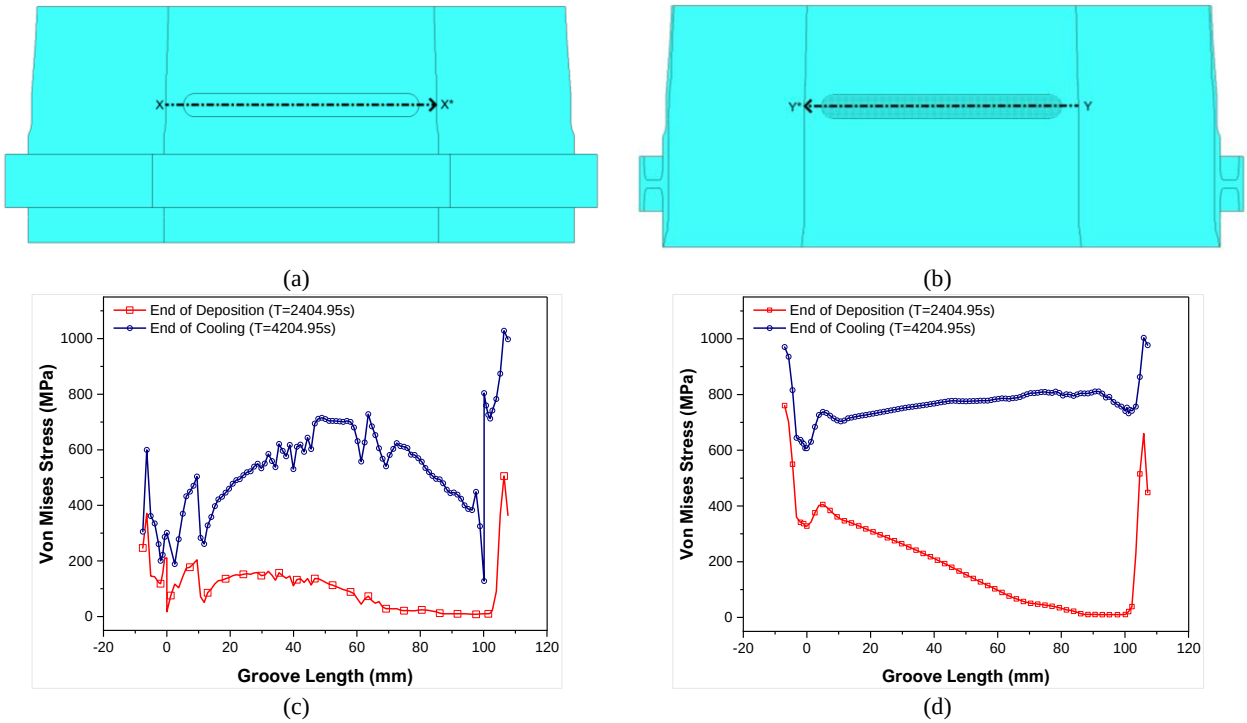

Figure 6-34. Predicted von Mises stress distribution in sub-section "A" during LC12 at the (a) front profile and (b) rear profile. The location of the line plots are (a) profile "XX*" and (b) profile "Y-Y*", respectively.

In Figure 6-35, the predicted equivalent plastic strains after LC12, and at the front (Figure 6-35(a)) and rear profile, (Figure 6-35(b)) of the sub-section, are shown, with corresponding line plots at the chosen profiles showing the effects of cooling on plastic strain. The line plots across profiles "X-X*" and "Y-Y*" indicate little change in plastic strain across the length of the groove, except at the left edge of the groove where a significant increase is predicted (up to 20% strain).

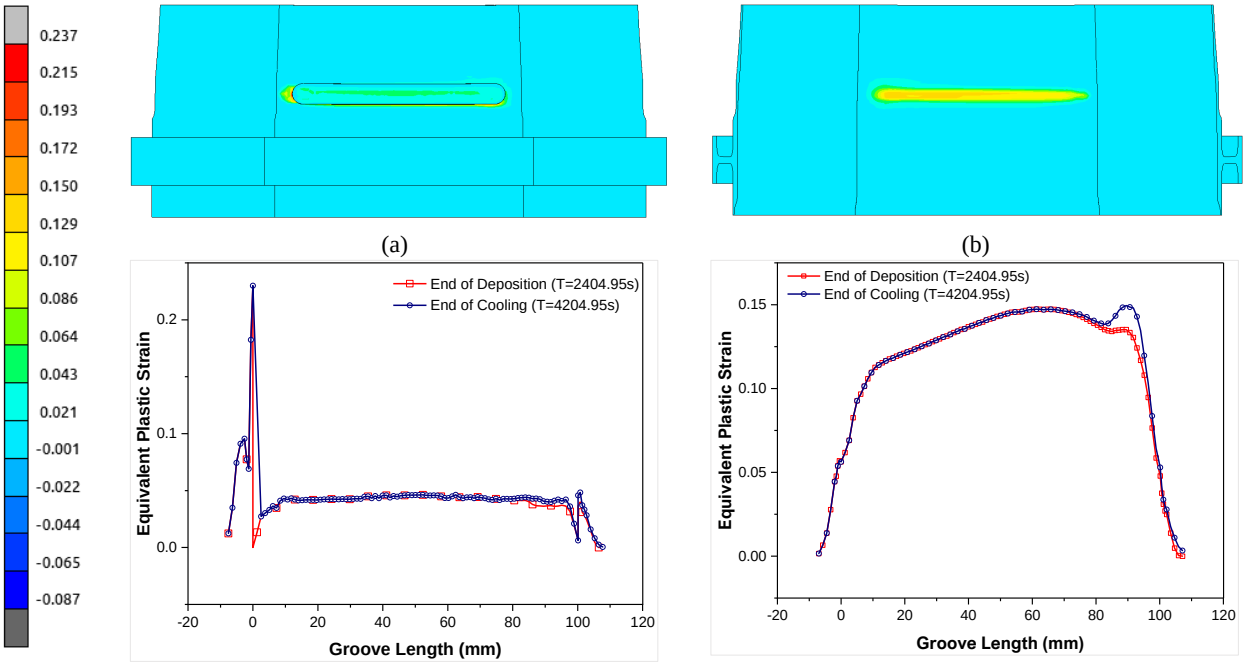

Figure 6-35. Predicted equivalent plastic strain distribution in sub-section "A" during LC12 at the (a) front profile, (b) rear profile , line plots along (a) profile "XX*" and (b) profile "Y-Y*", respectively.

The predictions of the resultant displaced shape after reprocessing on the model section, and after cooling (end of LC12), are shown in Figure 6-35.

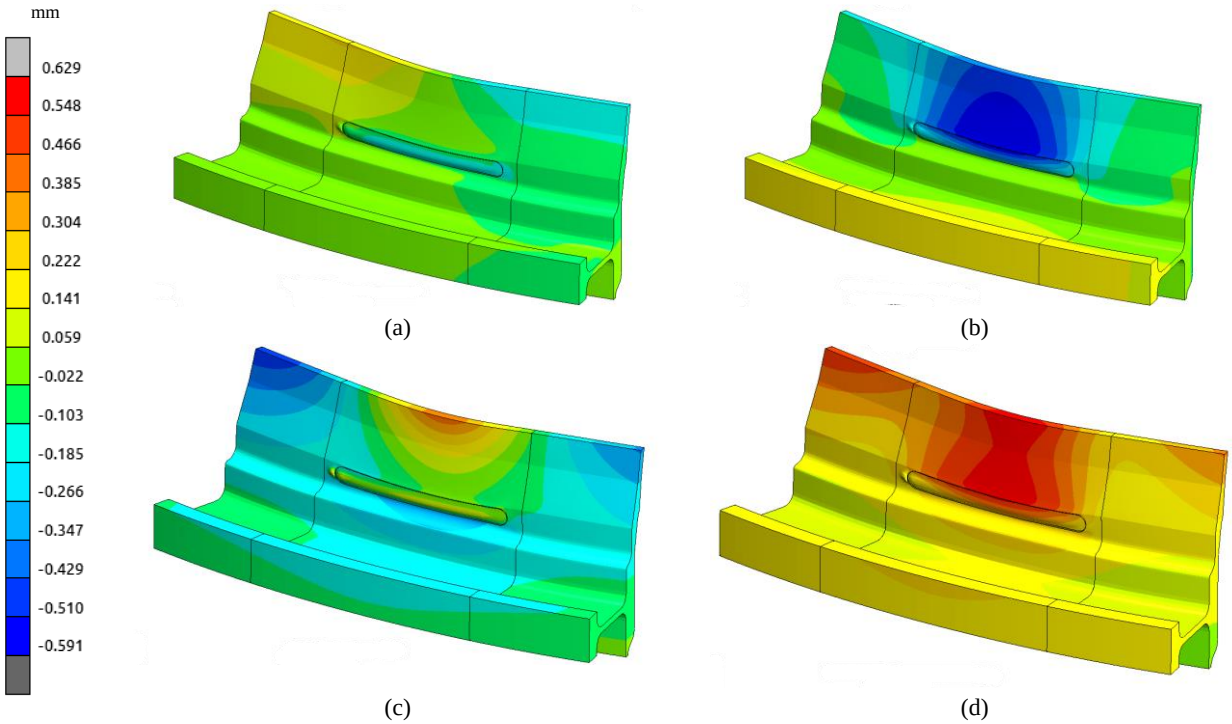

Figure 6-36. Predicted displacement in sub-section "A" after reprocessing; (a) radial displacement (d_{xx}), (b) circumferential or hoop displacement(d_{yy}), (c) axial displacement (d_{zz}) and (d) combined displacement.

The displaced shape was artificially magnified by a factor of 5, for better visualisation. The model sub-section was displaced in the radial direction (d_{xx}) by a magnitude of -0.185 mm to 0.141mm, with low radial

displacement in the groove vicinity as shown in Figure 6-35(a). The prediction of circumferential displacement (d_{yy}) ranges from -0.591 mm above the groove, to 0.22 mm in the circumferential ridge. The widest variation is predicted in the axial direction (d_{zz}), from between -0.591mm at the top left edge of sub-section "A", to about 0.5 mm at the top middle edge, above the groove HAZ area. The contour plot of resultant displacement shows a complex variation of distortion, especially directly above the reprocessed area. There is also relative distortion, seen at the left edge of the groove, and coinciding with the beginning of the toolpath translation.

6.5 Main observations

Three different models were developed, one thermal and two coupled thermo-mechanical models, to simulate the DED process effects on substrates PS-02 and PS-03, as well as the artefact. The primary objective was to supplement validation activities by exploring the dependencies between the process input parameters and related effects. The heat input is a critical variable due to its dominant effects on derived responses. Hence, the goal was to assess the effects of this significant variable on the surrounding areas of the material that was subjected to DED operations.

Consistent with the reprocessing approach, models were initially developed using outputs derived from substrate materials before proceeding with the artefact. The results from these models were comparable to the experimental results derived from the actual substrates (i.e. PS-02 and PS-03), which facilitated the development of the models for predicting responses in the artefact. Although the model representation of the artefact was de-featured and heavily modified, for previously stated reasons, and based on the modelling assumptions, the actual and predicted strain, stress, and temperature compared favourably. The observations, particularly in the HAZ, revealed the potential for oxidation in the inner surfaces of the component, which underpins the need for a more fitting environment, or at the very least, a localised shielding strategy for all areas likely to be affected by reprocessing operations. Furthermore, the model predictions revealed the effects of the autogenous pass on the artefact, which was implemented to assess the device functionality. However, this input is potentially detrimental to SMRM proceedings, due to the need for further post-processing or heat treatment of the artefact to mitigate the effect of the additionally induced thermal-residual stresses.

Notwithstanding the model assumptions and simplifications, it was evident that the FEA model was useful for predicting the effects of the experimental variables investigated. Furthermore, these models can support the overall SMRM strategy, by facilitating the implementation of more representative (geometric and process) input parameters, while enhancing understanding of systemic correlations between interacting variables, beyond experimental boundaries.

6.6 Summary

Coupled thermo-mechanical FEA models were used to assess the temperature, stress, strain, and distortion associated with reprocessing operations via DED. The techniques, considerations and methodology used for this modelling study were described, with the assumptions, simplifications, and factors necessary for adequate modelling of metal DED processes. In this study, only coupled thermo-mechanical effects were considered, while the effects of metallurgy, microstructure and solid-state phase transformation were neglected, due to difficulties in obtaining material properties necessary for adequate modelling of the metallurgical phenomena.

Temperature and strain data obtained experimentally was compared to modelling predictions of temperature and strain, with mixed results. This is attributed to the modelling simplifications and inability to adequately depict experimental conditions such as forced convection near the molten pool. The resulting models were moderately accurate in predicting the timeline or historical trends in the experimental data. Modest agreement was also found between the magnitudes of measured temperature and strain and the model predictions.

In the next chapter, the proposed GT framework for OA MA systems and procedures is presented. The synthesising of framework categories, with system concepts, development and validation activities, and other investigations completed in previous chapters, providing necessary structure and context for the framework.

CHAPTER 7

7 Framework Construction

7.1 Introduction

The purpose of the framework is to establish the development priorities for large-scale MAM systems and outline related procedures for enhancing efficiency and productivity. Ultimately, the goal of all manufacturing endeavours, whether in an AMR setting or otherwise, is to create value, which is fundamentally expressed via the product or application to which manufacturing technologies and services are partially or wholly applied. Correspondingly, this framework was constructed to underpin development decisions that prioritise higher technical functions and innovations that can truly transform large-scale MAM systems and operations. Here, the overall hypothesis is that *the GT method is appropriate for constructing a development framework*.

7.2 Transformation of case data

The goal was to further refine framework inputs based on the specific topics targeted in this study. Focusing on value creation as a key driver for this development template, a logic model was created to describe overarching business or commercial factors that were considered. This model is presented in Figure 7-1.

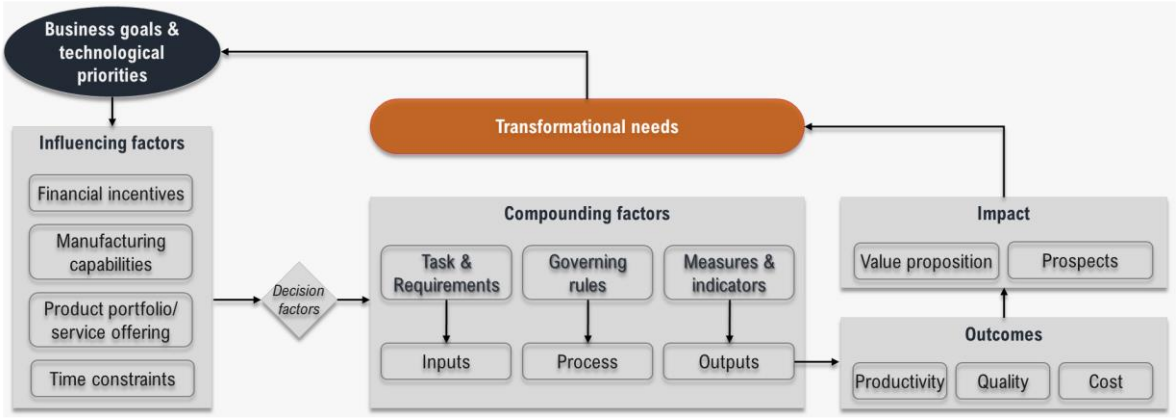

Figure 7-1: Business logic model for adoption of industrial MAM systems.

The model highlights broader perspectives influencing requirements for OA MAM systems. Primarily, manufacturing goals and priorities are key business considerations in the adoption of AM and investment in new systems. The direct impact of new technologies on business competitiveness, is influenced by the manufacturing outcomes, while the value proposition is informed by measurable outputs, relative to the performance and limitations of manufacturing capabilities. For instance, an incremental approach may be desired, but will lengthen the development timeline, and may increase overall costs. Conversely, a radical

approach that successfully converts manufacturing inputs to high quality outputs, may be riskier, but can shorten the integration timeline, even as underpinning needs or requirements are transformed and dictate current priorities. Both approaches are valid, but decisions influencing the inputs configured in the final solution, will affect the level of innovation and manufacturing outcomes, as well as the impact on the business. Therefore, supporting important development decisions, whilst saving valuable time and minimising associated costs, are primary aims for the proposed framework. Equally, while important or high-level development functions are influenced by system constituents and integration factors, inefficiencies occur when the resulting capability interacts with designated applications and governing procedures. Thus, clarity of purpose was prioritised, when determining how to organise framework categories.

7.2.1 Purpose

When clarifying the framework purpose, insights were drawn from subtractive manufacturing technologies, particularly machining. The singular focus on efficient and precise material removal is retrospectively illuminating, and it was evident that similar clarifications are needed for additive manufacturing technologies. *Precision* casting is another example of how clarifications have sufficiently distinguished manufacturing technologies, relative to their purpose. To emulate the machining example, if the goal were merely to create 3D structures efficiently and precisely, via the layer-by-layer addition of material, then the value creation criteria, which is judged relative to the manufacturing outputs, would have been satisfied, as it is for machining. However, the value of MAM products currently extends beyond their precise and efficiently created forms, which establishes the need for expounding the singular and evolved technological focus. The maxim, *clarity is borne of purpose*, is apt, in the sense that if the purpose is to deploy MAM products for critical applications, then the technology focus must be clearly grounded, and singularly focused on this purpose.

Necessarily, MAM should be efficient, and precise, but its outputs should also reflect the equivalent need for form, function, and durable performance, relative to its operational or service parameters. In the opening sections of *Chapter 2*, the need for 3D printers, which enabled greater design freedoms, was introduced, as a key milestone marking the transition from *form*, as evidenced by the earliest examples of WAAM being used for crafting, to *function*, where AM prototypes were primarily used to support design functions. Here, a distinction is made between the ability to efficiently and repeatably sustain predetermined manufacturing conditions for specified products, and at the desired production volumes, versus the more artistic expressions derived from the earliest MAM examples. Presently, the transition from *function* to *durable performance*, whereby vested parties are increasingly concerned with demonstrating the suitability of MAM for critical applications, is in progress, and it is intended that the proposed framework can support this transition. Thus, identified system integration factors, and related procedures governing implementation activities, were explored, to bring into focus, the relevance and alignment of this study, with the overall framework.

7.2.2 System development and integration factors

The definition of size, relative to the volumetric and mass attributes, was important when determining how to specify the dimensions for the BAM system. The subsequent implementation approach, based on COTS solutions, was preferred for standardising, and accelerating the development and efficient integration of enabling technologies and tools. While the resulting BAM system fulfilled its designated purpose, broader considerations include cross-functional requirements for OA MAM systems, which may be utilised for SMRM operations. Pertinent development factors explored in this study were organised as depicted in Figure 7-2.

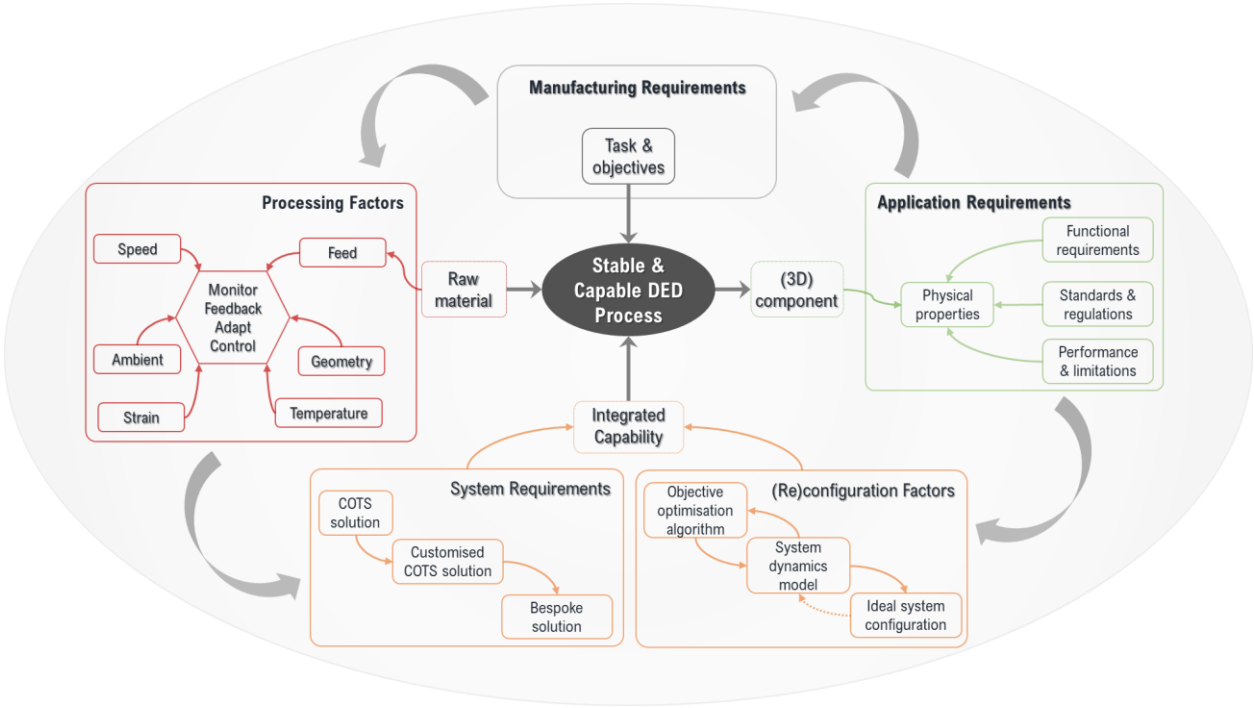

Figure 7-2: Mapping development considerations for OA MAM systems integration.

Development factors were informed by the gaps identified between the requirements for the BAM capability, and the outcomes realised via system integration and validation activities. The map combines the intrinsic (i.e., developed for a specific platform) and acquired (i.e., generalised for multiple platforms) characteristics. These elements were captured to emphasise the technological requirements for manufacturing large metal structures via MAM, which are further elaborated below.

- Structural / application requirements: to help define and understand the problem and constraints.
- Manufacturing requirements: to help define, analyse, and prioritise technological solutions.
- Processing factors: to focus design and development efforts on the specific details of the solution that is needed to adequately fulfil manufacturing requirements.
- System requirements and (re)configuration factors: to aid the construction, integration, and implementation of a sustainable technological solution for DED.

The primary system input is the feedstock material, which is processed to create the 3D structure from customer specifications, taking into consideration the functional and operational requirements for the end-products. The manufacturing requirements determine the factors to be controlled during the process, but technological limitations may restrict monitoring activities, as was observed when implementing reprocessing tasks. The gaps between the observable, and controllable processing factors, was affected by the lack of suitable real-time in-process monitoring devices.

The map (Figure 7-2) also incorporates the business (i.e. optimisation algorithm) and system priorities (i.e. dynamics model), to generate an ideal system design, including considerations for durable performance, application requirements, task specifications, applicable criteria, and enabling system features and functions. Due to the interrelations between the system, process and component or application, the overall system configuration, including strategies for control, monitoring, and in-situ DAQ, are also important, as are related operation and maintenance considerations. For SMRM, related considerations were further explored as depicted in Figure 7-3.

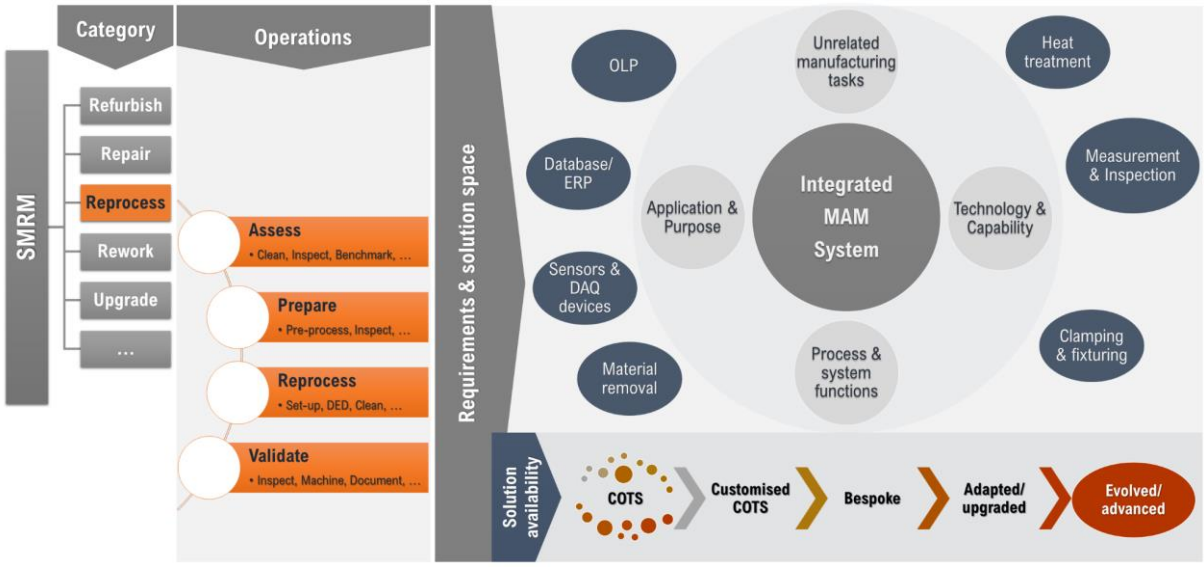

Figure 7-3: MAM system application and SMRM task considerations.

The different tasks and specific operations that may be considered, when integrating systems, especially for SMRM purposes, are outlined. Informed by observations from this study, highlighted solutions are logically organised, based on the possibility of integrating COTs solutions for enhancing efficiency, versus the time domain, which realistically considers the availability and readiness of solutions to be integrated.

7.2.3 System application and governing procedures

The SMRM strategy, which was enabled by the BAM system, evolved from experimental and numerical investigations, involving the industrial case study. The key insights from this work are summarised below.

- Due to the underdeveloped capability for in-situ monitoring, it was difficult to track instantaneous changes across the entire artefact, during the DED operation. However, measurements obtained from strategically located sensors, subsequently enabled the development of models for predicting temperature and strain. These models were useful for observing designated areas, but also revealed much broader effects. For example, the effects of the forward fraction of the heat source, at the ends of a segment or discontinuous layer, were more carefully observed than was possible via the weld camera. The specific limitations of this device, which is attached to the robotic arm, were previously explored. Nevertheless, they facilitated localised events monitoring, from which selected responses concerning reprocessing trials were inferred.

- For computational models, developing dedicated strategies for capturing certain operational issues, such as the effects of objects within proximity of the electrode, which were only evident when reviewing acquired recordings after DED operations, may be impractical, resource intensive, or insufficiently informed, relative to the perceived benefits. When considering that the goal is to obtain an approximate solution to underlying problems, other empirical principles, such as Pareto rules, can strategically support efforts to maximise the impact of available resources.

- The main limitation in the development of process models, that may be adopted for DED applications, was the resources required to generate requisite data. However, reliance on publicised information, not specifically generated and/ or properly vetted for the factors under investigation, such as the temperature and time-dependent material properties required for this study, may similarly affect modelling outcomes. Related considerations, including how much real time information can be acquired and processed by the operator, further underscore the utility of tracking critical parameters, such as the current, travel speed, and wire feed rate. When appropriately applied, monitoring tools and techniques can support the implementation of process models, by facilitating the optimisation of deposition strategies and related control measures, to enhance productivity, whilst helping to assure the quality of resulting DED products.

- In the design of experiments, particularly for SMRM applications, which pose unique challenges when compared to new builds, factors, such as the geometry, defect characteristics, and location, as well as the initial condition of the part or structure before restoration, may be screened to account for both modelling and experimental variables and responses. Practical considerations and issues may be informed by experiments, with FE models used to support more in-depth parametric and optimisation studies, before conducting more focused and representative experiments. to validate model predictions.

Based on the outlined observations and identified issues, it is evident that standalone experiments or process models, are insufficient when investigating SMRM challenges, particularly when considering the main findings from completed reprocessing operations involving the artefact. Accordingly, combining experience, experimentation, and modelling, allowed for more comprehensive understanding of task requirements, whilst highlighting potential risk factors. Thus, the proposed approach for SMRM is illustrated in Figure 7-4.

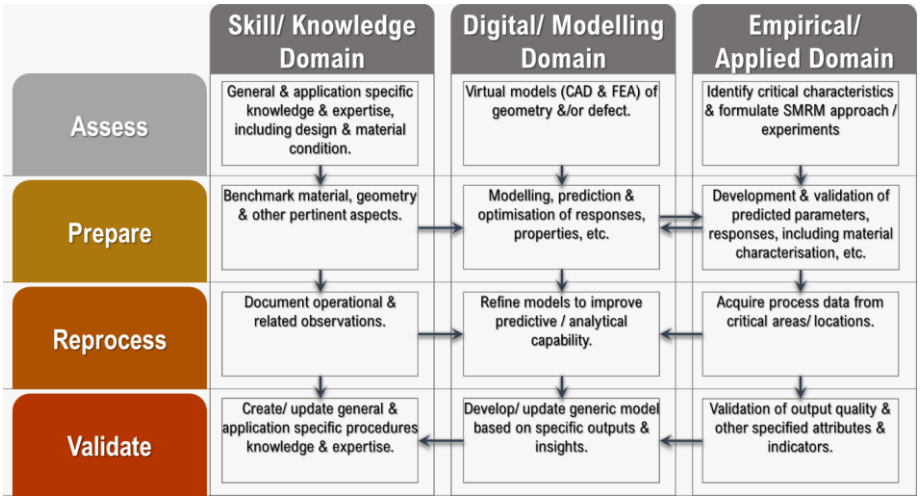

Figure 7-4. Consolidated strategy for DED-enabled SMRM operations.

Key considerations were organised around distinct operations, along the knowledge, digital, and applied domains (Figure 7-4). In the development of SMRM strategies for specific applications, critical areas may be identified along the operation sequence, and prioritised across each of the distinct domains. For the BAM system, the virtual platform concept aspires to an approach that appropriately integrates both numerical and empirical domains, with relevant expertise, to derive more optimal outcomes. Correspondingly, enabling digital and manufacturing tools, and technologies, may be adopted for future iterations of the BAM platform.

7.3 Codification strategy

The coding approach was informed by enhanced understanding of specific issues, and emphasises the functions of the framework, as a *development tool*, or *enabler*, for the creation of large-scale MAM systems and procedures. However, the ability of the system to create value, which remains central to development activities, supersedes the creation of the system itself. Similarly, the singular purpose of the system, relative to its application, supersedes the designated MAM technology on which it is based, and so on, and so forth. The main categories supporting the framework are explored in Figure 7-5.

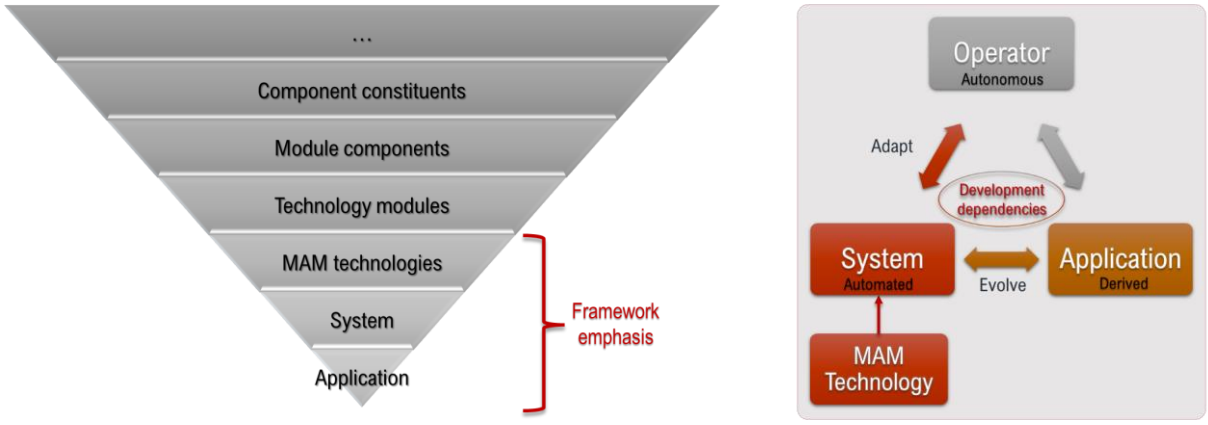

(a) (b)

Figure 7-5. Framework (a) code drivers and (a) dependencies.

The defined areas of focus were the system, technology, and application, which are highlighted in Figure 7-5(a). However, the application, and resulting characteristics, performance, and behaviours, are derived from the system, which receives, interprets, and translates user inputs. In this respect, the system is a dependent but automated entity, in so far as it responds to commands initiated by the operator, who in this chain, remains independent of both system and application. However, the operator's autonomy is constrained by the governing (system and application related) procedures that must be followed to create value, thus establishing the cycle of dependency, as depicted in Figure 7-5(b). This distinction was necessary, when emphasising developmental priorities, to intuitively support autonomous (operator) functions, which often adapt to evolving system/ application circumstances. Furthermore, the system is dependent on and thus constrained by the architect and/or developers' vision, as well as the different technologies and/or modules of which it is comprised. Similarly, its functions are constrained by previously explored factors, including scalability and capacity. These insights offered a lens through which research data was initially viewed, and helped to clarify specific interests, whilst supporting the deductive coding phase, based on a predefined set of themes.

7.4 Thematic analysis

The main recurring themes, spanning all research activities described in previous chapters, are *requirements and specifications.* While it is recognised that there are different perspectives influencing these requirements, and ultimately, system development outcomes, it is not often clear what they are, or how they are managed. Due to the implications of ill-defined or insufficiently clarified perspectives on development outcomes, the concept of *technical perspectives management* is proposed. Primarily driven by insights and observations from the implementation of core development tasks and related investigations, this theory can complement requirements management, by clarifying development roles and functions, relative to organisational and task objectives, as well as projected outcomes. The goal is to ensure that the outcomes reflect the optimal solution for creating value. The premise is that if system development outcomes are predetermined, it follows that the main and central functions of the system should be prioritised, over distinct subsystems, and defined development roles, responsibilities, or certain perspectives.

The basic tenets of the proposed *technical perspectives management theory* are described as follows:

- Every stakeholder or participant has a different perspective, but not all are unique and/or valid.
- Validity is relative to the universal objectives and alignment of unique and common perspectives, dominant or otherwise, to specific requirements.
- Requirements is both an overall and layered concern, and must be managed thus, alongside the applicable perspectives that influence and underpin the resulting specifications.

In other words, different perspectives are unified via a shared vision, but the outcomes may not reflect essential functions due to the dominant perspectives driving the development of solutions. These different perspectives are baked into every layer, and thus often inseparable from the specifications underpinning the shared vision.

In this case, experience of the SMD/ WAAM process influenced the development of the OA BAM system, but adopting a systemic view, enabled by the GT framework approach, facilitated the exploration of broader issues, which enhanced understanding of the significance of different perspectives, in the realisation of stated requirements. The system development experience also provided new insights into the realities surrounding development ambitions, including elucidating specific limitations, relative to the selected MAM technology, and its application for SMRM. At the process level, validating the system enhanced understanding of perspectives influencing demand and supply factors, including the need for harmonising common views, whilst evaluating unique considerations on technological and/ or technical merits, in line with the purpose of value creation. At the product level, the verification approach allowed for greater conceptual clarity, particularly in relation to in- and ex-situ qualification requirements. Beyond these experiences, the goal is to acknowledge and subsequently manage considered perspectives more efficaciously, alongside well-defined requirements, and in response to properly and concisely expounded problems. A preliminary outline of the proposed *technical perspectives management concept* is illustrated in Figure 7-6.

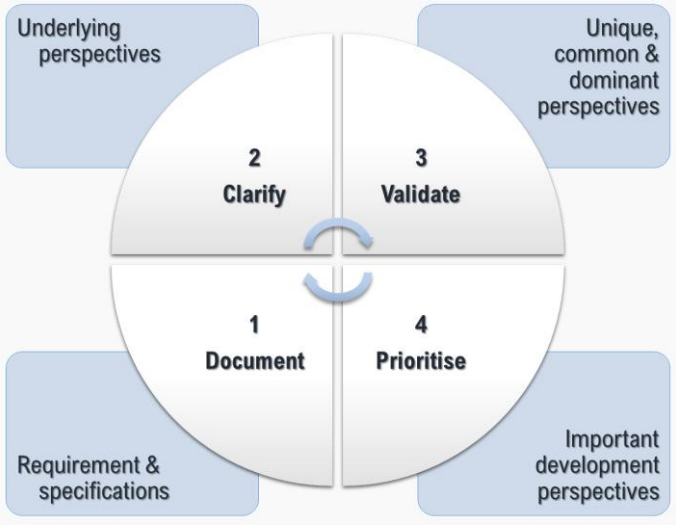

Figure 7-6. Principles of the technical perspectives management concept.

The proposed approach complements established *requirements* and *change* management philosophies, by further clarifying the four main steps for navigating the development of complex systems in an evolving landscape. In other words, the need to *document, clarify, validate,* and *prioritise* discernments underpinning requirements and specifications. It is also intended that this approach will support the implementation of the resulting framework, via enhanced understanding of the impact of each requirement, on the overall solution.

When reviewing the outputs of this study, a manual deductive thematic analysis technique was implemented, due to awareness of the general themes or codes that were of interest. Consistent with the GT codification process, and with preceding chapters as the primary source of case data for this activity, selected codes were initially identified through keyword searches, and gradually expanded to include other pertinent codes, which were eventually organised into categories. A visual representation tool, WordItOut [428], was used for initial

data transformations, which involved generating a word cloud from elected keywords associated with the focus and purpose of the framework, before proceeding with further thematic evaluations, as depicted in Figure 7-7.

Figure 7-7. Exploring emerging themes and ideas using a word cloud and keyword tags.

The coding contexts were further analysed to enhance specific insights, with keyword tags emphasising the dominant terms used in preceding chapters (Figure 7-7). For brevity, related keywords were aggregated, before highlighting some of the terms associated with different tags. There were also cross-cutting themes identified, including cost and time, with associations between keyword tags, related terms, and specific contexts, further demonstrating the validity of important development themes and ideas. Related topics were converged around the compromises and interventions that were necessary, due to encountered limitations and challenges, different influencing factors, and resulting impacts, as well as the direct and projected implications explored. Based on preliminary research outputs, the emerging themes and refined categories are presented in Table 7-1.

Table 7-1: Organisation of emerging framework themes and categories

Common themes	Consolidated themes	MAM Categories		
		Application	*System*	*Technology*
Commercial & business	Adoption considerations			
Supply chain & geographical				
Definitions, requirements, perspectives specifications, standards & criteria	Compliance factors			
Organisational & management				
Technology & technical	Evolutionary factors/ adaptation functions			
Autonomy, automation & control	Features and functions			
Characteristics & performance				
Procedures & protocols	Operational factors			
Productivity, efficiency, cost, & sustainability				
Socio-economic				
Data management & documentation	Systemic factors			
Performance & events				
Stability & reliability				

While the primary objective was to develop the framework for MAM *systems* and *procedures*, the main categories (Table 7-1) were especially focused on the applications, systems, and specific technologies that

enable different MAM tasks and operations. When implementing the SMRM case study, the application largely influenced the procedures that were adopted. Similarly, procedures were developed after the BAM system was established, and in consideration of the preferred technology, specific reprocessing tasks, and application requirements, which determined how the system was deployed, as well as the processing considerations that were investigated. These investigations informed necessary task modifications and provided further insights into related system and processing requirements for the preferred MAM technology, while demonstrating how procedures are cross-cutting, intricately linked to system applications, and consistent with the purpose of value creation, the main reason new systems and technologies are typically developed.

7.5 Theoretical framework

The framework contents were derived from the main categories and identified themes, itemised in Table 7-1. These essential inputs were consolidated and organised to establish development priorities. The foundational framework, proposed to support the development of MAM systems and procedures, is presented in Figure 7-8.

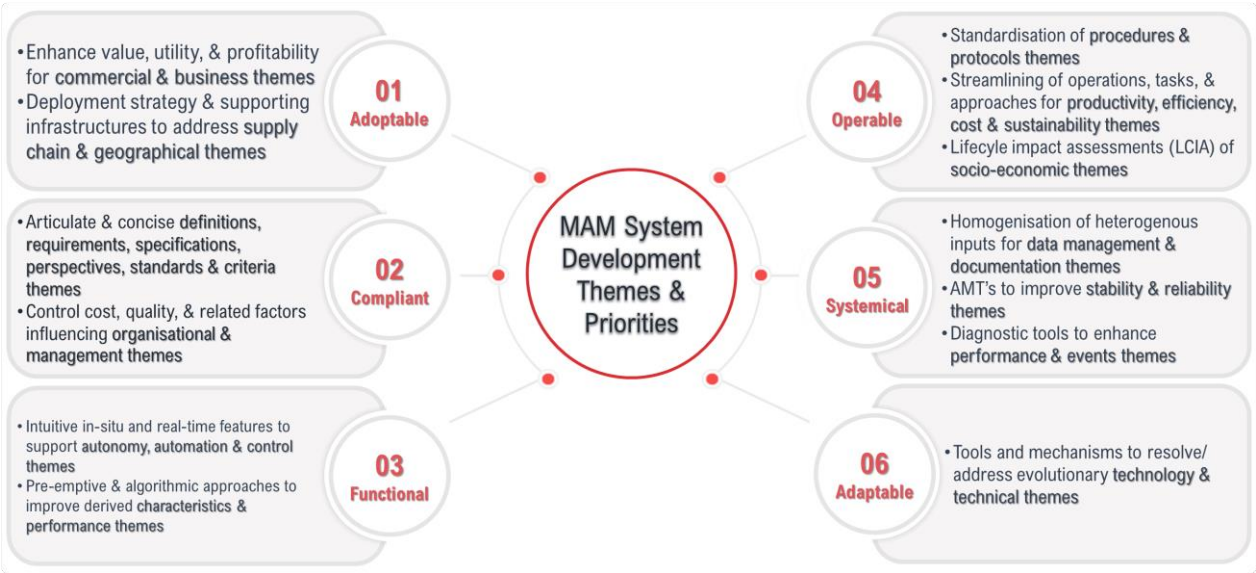

Figure 7-8. Framework for developing MAM systems and procedures.

1) **Adoption** was prioritised due to the potential for MAM technologies to address a range of manufacturing challenges, including broadening the scope of SMRM, and bridging the disparities between global demand patterns and local supply conditions, to reduce cost and lead times.

2) **Compliance** is equally important for ensuring that MAM capabilities adhere to and complement existing manufacturing and business infrastructures. Thus, ambiguities must be resolved when distinguishing MAM from traditional and similar approaches, to ensure that specific latencies are properly explicated.

3) Different features and **functions** are required to support and enhance current MAM operations. However, due to the impact on quality, autonomous functions must be adequately supported, alongside automation and control features, and associated factors.
4) **Operating** procedures and protocols are locally developed but have broader implications for the sustainability of (additive) manufacturing endeavours. Moreso, these factors affect cost, productivity, and efficiency, which further impacts other prioritised themes, alluding to a need for more central governance.

5) **Systemic** issues are prevalent and often underreported. The lack of pertinent data and underutilisation of available or publicised information, which is often topically focused, and thus lacking full context of interrelated aspects within system boundaries, makes it more challenging, yet increasingly important, to ensure that MAM capabilities, processes, and applications, are holistically and measurably improved.

6) The *additive* approach is an established manufacturing method. Therefore, in conjunction with other priorities outlined above, (reconfigurable) MAM systems that evolve and **adapt** in response to technological and technical factors, will help to ensure that future systems are long-lasting, and support the clear and distinguishing purpose, for which these capabilities are developed.

7.6 Summary

The concept framework for developing large-scale MAM systems and procedures was presented in this chapter. Aimed at supporting important development decisions, saving valuable time, and minimising associated costs, the GT framework identifies the introductory development themes and priorities emerging from this study. Case data obtained from investigations described in preceding chapters were manually consolidated, and codified, before thematically analysing the resulting information. Within this scope, exploring development, integration, and validation activities, helped to establish determinants and verify initial deductions about MAM systems and procedures, thus allowing for the definition of distinct framework elements.

The framework identifies development priorities, associated themes, and related considerations, including the need for *adoptable* MAM technologies to further enhance utility and broader prospects, whilst assuring *compliance* at relevant business and industry levels, and ensuring that requisite features and *functions* measurably enhance *operability*. Correspondingly, enhanced understanding of *systemical* factors will facilitate the development of more relevant and targeted procedures, for more *adaptable* future systems. Furthermore, a four-step technical perspectives management approach, for *documenting*, *clarifying*, *validating*, and *prioritising* underpinning system requirements and specifications, was introduced, to complement development activities, and support the implementation of the proposed framework.

In the next chapter, the overall research strategy and outcomes are discussed, relative to the distinct investigations and outputs upon which the resulting framework was founded.

CHAPTER 8

8 Discussion

8.1 Introduction

General impressions of the overall research strategy, core investigations, and resulting GT framework, are described in this chapter. Structured around core development stages and tasks, discussions are particularly focused on notable findings and corresponding interpretations of the main approaches and research outputs. The aim was to explain how planned investigations facilitated the realisation of defined objectives, by providing further insights into the main ideas, assumptions, limitations, and implications of this study.

8.2 GT research strategy

The overall aim was to construct a GT framework, to support the development of large-scale MAM systems and procedures. The GT approach has been predominantly applied to sociology-based qualitative research, but was especially selected due to its flexibility, which allowed for the incorporation of relevant qualitative and quantitative principles, and the different contexts, explored within this study. However, lack of familiarity about the subject matter and the need for a great deal of unstructured and diverse data, which requires a significant amount of time and resources to collate, are notable issues that can affect GT research outcomes. While considerable time and resources were still required to gather data for the framework, there have been significant advancements in data analytics since the GT method was introduced. Other factors that may unduly influence data collation, analysis, and interpretation, which are intricately connected to the framework, include the researcher's objectivity and significant personal agency. Therefore, skilful management of the entire process is essential, and systematic data gathering tools and techniques were typically prioritised, alongside careful handling and interpretation of findings, to obtain deeper and less subjective insights. Furthermore, deductions were informed by familiarity with explored topics, as well as direct experience of specific issues, demonstrated via relevantly incorporated studies.

When implementing the GT approach, directly deriving insights from investigations can be advantageous, over approaches or ideas that are further removed from the data or specific principles to be verified or refuted. However, the method of progressively combining and comparatively assessing information was beneficial, ensuring that evaluations and connected extrapolations, were informed by established principles and ideas that remained connected, via the systematic analyses of heterogenous case data. Ultimately, the framework incorporates perceptions from literature surveys, experiences from system development and validation studies, as well as other pertinent and direct interactions and observations, which shaped the overall analysis and interpretation of the main research outputs.

8.2.1 System development

The principles governing system design and development activities are well established and were corroborated when developing the BAM system. The system integration concept was based on a COTS approach, which was preferred for maintaining a high-level of modularity and standardisation within subsystems, whilst lowering the integration risk-profile, via the implementation of proven solutions. However, it was observed that procured COTS solutions were generally adequate, but not always wholly suited to more specialised requirements, with necessary modifications applied as needed to achieve a fully functional and integrated solution. While the overall system configuration was influenced by typical MAM applications, the focus was on implementing features that enhanced synergy, and improved the workflow between contiguous operations. The deployment of such capabilities, for wide ranging manufacturing tasks enabled by the MAM process, was also considered, due to interconnected application requirements and issues, including the movement of artefacts between different requisite operations, and planning of necessary resources. Therefore, the BAM architecture was developed with the distinguishing aim of utilising integrated functionalities to minimise artefact movements, by completing necessary operations within a single geographically situated or deployable platform. Compatibly, a flexible and modular configuration concept was developed, to enhance the synergy between tasks, by providing multi-sided access to artefacts, in conjunction with the integration of different EOAT for completing related tasks, thus reducing disruptive changeovers between operations.

In general, system requirements were organised relative to targeted applications, then desired functionalities, before exploring the consequent complexity and cost implications of preferred solutions. The evaluation of typical structures manufactured via forging and casting techniques facilitated the identification of geometric similitudes, which provided a much needed and quantifiable basis for classifying MAM systems. Variables associated with foundry operations were also referenced, when defining industrially relevant criteria for large-scale MAM operations, and specifying requirements, desired features, and different options underpinning system integration objectives. It was demonstrated that system configuration concepts can be effective capability differentiators but contribute to further complexity, as evidenced by the number of possible permutations derived from a relatively small number of options, which were also assessed, in consideration of the financial incentives and other pertinent factors influencing this development. An optimisation matrix tool allowed for more objective evaluation of decision factors, including the utility, integration complexity, configuration options, cost of distinct technologies, and time for configuring the overall solution. For basic MAM system elements, namely the energy, feedstock and control options, the optimisation objectives of maximising utility and value at cost, while minimising configuration complexity and time, were achieved.

Compared to other unique requirements, the procurement specifications for COTS technologies were relatively easy to describe. A technical feasibility assessment instrument, which was developed to distinguish customisation needs, based on defined concepts or existing solutions, was crucial for supporting the procurement strategy, with a dedicated decision tree further augmenting clarifications about the scope of

supply and related development activities. In general, adopting established management, logic, and quality tools, were particularly useful when implementing the BAM system concept. Focusing on HPA, modular capabilities were integrated in two distinct phases, primarily dictated by allocated funds, internal procurement procedures, and external factors, including the availability of solutions. Presently, the fully integrated 11-axis system is equipped with different EOAT, for WAAM and 3D inspection operations, but solutions for monitoring and control are somewhat limited, due to a combination of unique development requirements and underdeveloped capabilities. It was also recognised that supplementary requirements might be at cross-purposes with established functionalities. For example, while existing features create operational synergy between inspection and deposition capabilities, the integrated gantry and articulated robots are unsuited to contact operations (i.e., machining). Therefore, additional EOAT requirements necessitate further investigation to determine how additional tools may be introduced, without compromising the established integration state or system functions.

Scientific and other management principles were also adopted for objectively and effectively demonstrating that the BAM system conformed to its specifications, thus paving the way for other planned investigations, including the validation of the BAM system for large-scale operations. A range of development projects were completed as part of broader validation activities and facilitated the collation of generic data for assessing system and process performance. Although the sample size for these studies was relatively small, the data was representative of the issues under consideration. WAAM process control charts revealed common cause variations, which are typical. From the data set, 97% of the obtained process values occurred within established upper and lower bounds, as defined by Six Sigma quality, thus demonstrating that BAM system outputs can be predicted reliably. Inspection capabilities were similarly evaluated, to demonstrate process reliability, with representative surfaces and geometries measured and verified against established criteria for large-scale MAM operations. Culminating performance evaluations involved reviewing system event logs, which were supplemented with manually logged information, to identify systemic factors influencing productivity and processing efficiency. Based on the interactions between modules, it was evident that certain system characteristics dominated observed performance and related issues at different levels. Globally, the availability of infrastructures (e.g. lifting crane) and resources (e.g. consumables), to support planned operations, were some of the issues influencing the scheduling of activities, while localised factors, including the deposition strategy, parameters, and conditions, contributed to overall productivity. Between and within these perspectives, intermediate (e.g. set-up) and sub-local (e.g. arc control) factors affected productivity and output quality, notwithstanding certain dominant system traits influencing documented events, with varying implications. While system notifications were usually acknowledged in less than a minute, system warnings and errors typically required ~10 to 45 minutes to resolve. In general, productivity was severely affected by machine downtime, particularly if multiple system errors occurred. The resolution of issues typically depended on the operator's skill, with effectiveness enhanced by the initiated practice of documenting previous encounters and experiences in the OLB or supplementary logbook.

Overarching considerations include the need for substantial resources, which lengthened the development time, but underscored the benefits of the different management approaches that were adopted or especially developed for this study. For instance, implementing the technical feasibility assessment tool and decision tree, alongside the optimisation matrix tool, was necessary to support the overall development objectives, whilst maintaining focus on the integration strategy and functionality of the system, irrespective of resource constraints or development duration. The adoption of design principles also ensured adherence to best practice, but in the field of AM, where a range of commercial solutions are readily accessible, carefully curating important distinguishing features, beyond the basic configuration and core elements for MAM systems, can be advantageous. For the BAM system, and other OA MAM solutions, these considerations highlight opportunities for creating original templates that can be replicated and further enhanced. This perspective was explored when developing the BAM system concept, particularly in relation to the specific features, configurations, and approaches that can enable adjoining large-scale MAM operations. While OA MAM solutions require enhancements, much like the upgrades applied to commercial solutions, the flexibility of the latter, and the emphasis on a reconfigurable setup, implies that improvements can be more readily implemented. In practise, there were technological and commercial barriers, and specific supplier circumstances influencing the process. For commercial solutions, documented factors include the adverse consequences of end-users not adhering to OEM specifications for feedstock materials or independently modifying the system. Similarly, when implementing the BAM system concept, it was observed that the required expertise remained beyond the capability of most suppliers, highlighting the importance of the supply chain. This observation is buttressed by current developments, whereby business mergers and acquisitions are enabling OEMs to provide more vertically integrated MAM solutions. For OA platforms in particular, these issues further underscore the need for standardisation, which will improve technological prospects, whilst enhancing cooperation between development partners; a necessary step towards ensuring that the templates for new MAM systems are more focused on open challenges.

8.2.2 System validation procedures

Different experimental programmes were initially completed to verify processing challenges and investigate identified performance issues. For these investigations, statistical models were developed to predict process parameters for achieving desired outputs, based on a given set of empirical variables and responses. One of three initial studies, which involved the characterisation of a stainless-steel component, fabricated using a pre-existing MAM system, revealed large variations in impact energy within this single product. A second study, involving the fabrication of titanium alloy using the same MAM system, also revealed deviations in the fracture performance of resulting materials, underscoring the need for both mitigation and verification strategies to manage MAM related issues, which can indiscriminately affect product performance, irrespective of the deposited material or alloy. The final study, also involving stainless steel, was mainly organised around the practical aspects of reprocessing operations, including the possibility to incorporate different feedstock

forms, for new MAM products, as well as for SMRM purposes. Powder, wire, and strip metal input forms were selected and especially investigated to inform the development of a generic SMRM strategy. Experiments involving these different feedstock forms highlighted the significance of the application sequence for related material and heat inputs, on dependent variables such as the visual appearance of resulting builds. While process stability may be assessed relative to detected changes in the output voltage, the reliability of this approach is dependent on other factors, including the feedstock characteristics. It was observed that the lack of stiffness and/or the mechanical feeding mechanism, which was evident when comparing the different feedstock input conditions and resulting outputs, are key contributory factors. These investigations were all completed using the pre-existing and established SMD capability and process, thus providing a comparative basis for objectively verifying BAM outputs.

Verification studies were mainly based on an industrial aerospace case study, and an iterative approach was adopted to facilitate the development of an effective SMRM strategy. Informed by earlier investigations, planned titanium Ti-6Al-4V alloy trials were initially focused on how to mitigate the potential effect of designated reprocessing operations on the selected aerospace case study. For instance, arc responses were evaluated to minimise the localised effects of this dependent variable, while other trials were aimed at managing the effects of distinct operations on the reprocessed structure. Trials were completed to map the temperature at different locations on flat substrates, and enhanced understanding of heating trends and decay patterns during the DED process. The recorded peak temperatures matched the detection of heat in the substrate, typically occurring ~2 s after igniting the arc, with other correlations observed in relation to the build duration, consisting of the deposition and dwell times, per and between layers. While the need for managing rapid temperature changes was evident, other considerations, such as the geometric characteristics and relative rate of cooling, as well as the number of deposited layers and processing environment or conditions, affected the overall strategy for specific SMRM tasks and operations. Primarily, the relationship between temperature and strain was quantified by capturing real-time data from thermocouples and strain gauges. This approach was beneficial for verification purposes, with good correlations between the observed trends for the thermal (i.e. heating and cooling) and strain (i.e. expansion and contraction) cycles, but validated the need for non-contact monitoring devices, due to the potential implication of direct sensing on the integrity of monitored structures. Certain factors, such as the introduction of a temporary trailing shield, and the application of different clamping configurations, appeared to have a degree of influence on substrate cooling rates, and on the efficacy of shielding solutions, which was essential for the investigated alloy. Cooling times were typically longer for operations involving samples that were suspended in air, than for samples that were clamped directly onto the BAM positioner and exposed to bigger surface areas, highlighting the significance of the primary cooling method (i.e. via conduction, (forced) convection, or radiation), during SMRM operations. Other trials revealed the extent to which the overall strategy, accounting for the investigated geometry and deposition patterns, such as mechanical weaving, affects output quality.

For empirical studies, output verification procedures involved both destructive and non-destructive methods. All samples were visually inspected, and for selected trials, visually acceptable outputs were progressed for further evaluations. CT scans revealed imperfections occurring in restored geometries, while demonstrating the influence of design related factors on output quality. The latter is consistent with convention for reprocessing tasks, where the depth to width ratio of the input geometry, is an important design consideration, and should be defined, relative to the selected reprocessing technology, and for specific applications. Mechanically, Vickers hardness tests revealed directional variations in reprocessed samples, with nominal changes in the measurements obtained before and after DED operations. The UTS values obtained from different builds were typically higher in BAM samples, when compared to material specimens evaluated in both the restored and as-supplied conditions. These results were compatible with micro-hardness characterisations, as similar changes were observed in measurements derived from post-restoration material samples. The elongation values for restored and substrate materials were similar, but the yield was ~5% lower for the restored sample, with values typically within range of the specification for Grade 5 titanium (Ti-6Al-4V), thus demonstrating the capability of the BAM system for fulfilling the requirements for MAM operations.

8.2.3 Process verification procedures

Supplementary procedures were implemented, due to restrictions on the aerospace case study, and the need to verify that other important processing factors influencing the outputs were accounted for. Accordingly, coupled thermo-mechanical FEA models were developed using MSC.Marc. The goal was to assess the effects of the process on the aerospace components, mainly focusing on temperature, stress, strain, and distortion, whilst enhancing understanding of broader factors affecting restoration applications. For preliminary models, representative scenarios were evaluated based on temperature measurements obtained from sample set PS01, and simultaneously acquired temperature and strain data, obtained from PS03. Certain modelling assumptions and simplifications were necessary when implementing the different aspects of the model, including the geometry, material, loading conditions. The focus was on establishing the thermo-mechanical effects of reprocessing operations, but the metallurgical phenomena and related aspects were excluded from these initial models, due to difficulties in obtaining the requisite material properties, with well documented issues, including resource and technical requirements, contributing to present challenges in this field. Nevertheless, comparisons of the predicted and measured temperature and strain data revealed mixed results, which were mainly attributed to earlier simplifications and necessary assumptions about the process, such as the deduced effects of forced convection near the melt pool, relative to actual experimental conditions. In general, there were correlations between experimental and predicted historical trends, but differences were also observed in relation to the magnitudes of actual and computed peak temperature and strain values.

The incremental development of the overall SMRM strategy, which was facilitated by both empirical and numerical studies involving the Ti-6Al-4V samples and aerospace component, allowed for the exploration of broader considerations. The experimental programmes, and preliminary numerical models, facilitated the

formulation of the strategy for combining experience with digital manufacturing capabilities, to minimise the risks associated with reprocessing operations. For instance, the prioritisation of high-risk activities, identified from analytical insights and observations during empirical studies, was numerically corroborated. It was observed that ~2 seconds after arc ignition, the anticipated spike in localised temperatures, which were more pronounced at the end of a segment or build, was corroborated by process models, verifying the need for adequate management of the arc initiation and termination strategies, when depositing discrete layers, as well as for continuous builds. The temperature profile in the middle segment was expectedly different, but generally consistent with the conduction of heat from the build vicinity and surrounding areas, as observed during experiments, and verified by process models. For smaller segments and reduced builds, the shortened processing duration restricts the time available for in-process modifications, and likely contributes to higher defect occurrences, further accentuating the need to enhance autonomous functions. Related factors, such as the length of build segments, were equally important considerations contributing to quality issues. Other observations include the overall effect of temperature on the magnitude and direction of strain, and resulting residual stresses, as well as typical operational considerations for cleaning, handling, and inspections.

For verification studies, the principal focus was on qualifying generic factors and representative scenarios, to reduce the time for assessing and implementing an SMRM solution most suited to a specific requirement. In the current manufacturing landscape, computer aided engineering (CAE) tools offer manufacturers a means of minimising risks and increasing efficiency, which is consistent with the overall SMRM strategy. The goal was to determine when and how digital manufacturing capabilities may be combined with empirical approaches, to manage the risks associated with critical SMRM tasks and operations. Focusing on factors that significantly affect output quality, the preliminary models were primarily used to demonstrate how DED procedures, involving the aerospace case study, were further verified. Generally, it is intended that specific strategies will be tailored in accordance with the requirements dictated by actual SMRM scenarios.

8.3 Concept framework

The outputs from outlined system development and validation activities, were especially important when establishing the framework, which was focused on the main topics investigated, namely *MAM*, *systems*, and *procedures*. The GT research principles were applied throughout the study, but the latterly focus was on establishing the framework structure and content, relative to its purpose for supporting value creation, which was predominantly explored via the implementation of the BAM system and industrial case study. During the data gathering phase, the documentation of observations and experiences, alongside qualitative and qualitative case data, was prioritised, to facilitate open coding of the resulting information. A further analysis was similarly completed after concluding development and validation studies, to obtain a more holistic perspective than was possible when implementing separate research activities. The objective was two-fold; to enrich the case data through the consolidation and analysis of specific insights, and to further refine ideas about the main framework topics.

Different requirements were analysed to harmonise business, system, and application insights, and a logic model was used to explore the business perspective, which was expanded to account for other important factors, such as the impact of MAM technologies on transformational needs. System integration insights were also assessed, which allowed for the identification of cross-functional requirements that remained broadly consistent with overall development plans. Specific SMRM tasks highlighted factors influencing integration prospects, with limitations mainly stemming from the availability, suitability, and readiness of required solutions. Analysis of actual procedures, facilitated the clarification of crucial gaps, affecting the implementation of development and validation activities, and culminating in the proposed strategy for DED-enabled SMRM operations. These activities preceded the main coding phase, also known as selective or axial coding, which involved manually consolidating the research data, to deductively derive the main themes emerging from this study. Correspondingly, maintaining analytical consistency can be challenging when implementing the GT approach. Mainly, the iterative and constant comparative method, in conjunction with other strategic considerations outlined in previous sections, including familiarity with the topics under investigation, were crucial for achieving theoretical data saturation. Such implementation risks, including the possibility of insufficient data for reaching theoretical saturation, or informing deductions about investigated topics, were also important, and influenced the comprehensiveness of the study, which provided new insights and ideas. While a deductive approach was preferred, due to familiarity with the topics, which was enhanced by direct experiences and observations, it imposed a relatively narrower focus. Thus, a more generic review of the case data, and other pertinent studies, may allow for further refinement of the framework.

When creating the framework content, manual searches for specific keywords facilitated the data compilation process, but the consolidated information was iteratively analysed using a combination of data processing tools, resulting in different topically focused categories, from which the main framework ideas emerged. One of the main philosophies emerging from this study was derived from greater conceptual clarity about design and development requirements. In particular, the need for updating, upgrading, or customising manufacturing systems is typically informed by different technical perspectives that are not always appropriately documented or captured, which can limit understanding of non-evident but critical insights supporting requirements and specifications. Similarly, modified procedures usually evolve from specific needs that are not often captured, particularly when adapted on the fly, or in relation to certain circumstances. Hence, the technical perspectives management concept focuses on *documenting*, *clarifying*, *validating*, and *prioritising* developmentally important requirements affecting both systems and procedures, and was proposed to complement established theories adopted for this study, and support the implementation of the framework. Correspondingly, the defined framework themes reflect the early ideas evolving from this study, including the need for *adoptable*, *compliant*, *functional*, *operable*, *systemical*, and *adaptable* solutions. In conjunction with other well-documented factors, related considerations can support the development of MAM solutions, for critical high-value metallic applications. For preliminary framework themes and priorities, immediate considerations

include the clarification of requisite inputs, for implementing the framework, and the development of specific action plans, to support its validation.

8.4 Summary

In this chapter, the main investigations and resulting contributions, including specific approaches, and associated theoretical and methodological considerations applicable to this study, were critically appraised. In particular, the benefits and limitation of the GT research method were explored, to demonstrate how the principal objective of constructing a framework, to support the development of large-scale MAM systems and procedures, was achieved. The significance of planned system development and validation activities, including empirical and numerical investigations involving an aerospace SMRM case study, which allowed for the corroboration of other established philosophies and principles adopted, was also discussed. Specifically, the need for systematically and analytically managing the research was emphasised to demonstrate how the subjectiveness of the GT approach was countered, when drawing inferences from this study. The principal research outputs, including the GT framework and technical perspectives management concepts, were also described. These preliminary outputs reflect the main ideas emerging from this study and offer a basic template for future MAM systems.

In the next and concluding chapter, the main findings of this work are summarised. Recommendations and plans for future work are also outlined.

CHAPTER 9

9 Concluding Summary

9.1 Principal outcomes

The primary objective of creating a GT framework to support the development of MAM systems and procedures was achieved via various activities, including the implementation of the BAM system concept. The embodied concept, and other significant research milestones, enhanced understanding of important development priorities. The GT approach, together with adopted principles, philosophies, and strategies, also facilitated the systematic evaluation of case data, which enabled the identification of emerging development themes. The transformation of the BAM system, into a utility for high integrity applications, including SMRM, culminated in a defining framework and other key findings, which are summarised in the following sections.

Concept framework: From a developmental perspective, implementing this study within an AMR environment undeniably influenced how different investigations were conducted. However, key system and process development and validation phases, including distinct SMRM actions, were crucial for ensuring that framework themes and priorities were properly informed, and realistically reflect where resources may be expended to maximise the value and impact of MAM solutions. Critically, the present approach to fragmented but connected MAM issues, which are often, and perhaps necessarily explored in isolation or separately, is inefficient. Thus, the main contribution of this work is the identification and effective organisation of important concerns, presently affecting both commercial and bespoke systems, under the umbrella of a concept framework for developing large-scale MAM systems and procedures. The technical perspectives management concept is another important output from this study, and complements proposed development priorities, including the need for specific and measurable objectives when adopting the framework. In developing requirements and specifications for future MAM solutions, more carefully considered inputs can illuminate general and unique focus areas, while shaping decisive actions in line with defined themes and priorities.

Systems integration and COTS solutions: While solution availability and maturity were equally important procurement decision factors, it was verified that COTS solutions are not always wholly suited to a range of requirements for new MAM systems. For the BAM system, modularity was prioritised, but engendered a segregated asset management strategy, which had significant implications for the operation and maintenance of the single entity representing the embodied solution. Although vertical integration and standardisation approaches are typical reactive modes when presented with incompatibility and related issues, it is recognised that an evolutionary approach is necessary in the development OA MAM systems, and horizontal integration can be an important accelerator for technological advancement in this field. When utilising this approach,

standard peripheral devices, or plug and play interfaces, may be developed alongside other identified priorities that enable highly specialised and more efficient functions. Nonetheless, the BAM concept validated the benefits of a COTS-enabled integration approach, facilitated by readily available and modular solutions. Compared to similar activities involving customised solutions, COTS technologies typically posed fewer risks, thus minimising associated integration complexities, whilst accelerating the development pace. Accordingly, it was demonstrated that highly customised MAM systems can be configured via optimised architectures that combine end-user requirements, technology options, and features tailored for specific (SMRM) applications, while exploiting the potential benefits of different (re)configuration concepts.

Management of systemic factors: Modularity is an enabler for more reconfigurable architectures, but the potential benefits of this concept and approach can be limited by the interactivity between the operator and the system, as well as the interactions between system modules. Typically, issues stemming from non-compliance events are investigated through a process of elimination, which often involves isolating affected modules from the integrated whole. Thus, latent flaws that manifest due to operational interdependencies may be underestimated, overlooked, or remain undetected. When dealing with these non-compliance scenarios, dominant operational characteristics may also have a disproportionate and system-wide effect on rule-based responses, with implications for separate modules and overall system functions. For observed systemic issues, even when pertaining to COTS solutions only, the mechanisms supporting root-cause analysis were either lacking or underdeveloped, thus validating the need for more resilient solutions, equipped with universal rules that govern the dynamic responses of integrated systems. Specifically, consolidated capabilities that include features for operational status monitoring, automatic event logging, and troubleshooting facilities, with heterogenous data handling capabilities, can facilitate more effectual management of interdependent issues.

Derived system features and characteristics: The conceivable applications for DED capabilities, such as the BAM platform, are wide-ranging. However, verified cross-cutting challenges, including the fracture performance of the materials and components derived from initial studies, remain priorities, as there are opportunities for extending the durability of serviceable infrastructures via the development of more flexible MAM strategies. Predominantly informed by arc-based DED processes, preliminary investigations were focused on certain practicalities, including the possibility of interchangeably utilising different metal feedstock forms to suit specific application requirements and supply circumstances. These early trials accentuated the effects of the material application technique and modified melting sequences on the geometric accuracy and surface quality of resulting 316L builds. It was also demonstrated how interchangeable feedstock inputs, in conjunction with deposition parameters and strategies, can enhance broader technology prospects, particularly for SMRM operations. Experiments involving continuous and granular feedstock forms also revealed further insights about specific form factors and associated characteristics, including the relative rigidity of continuous feedstock, which can increase susceptibility to positional-related processing concerns, such as the wire feedstock stiffness, input position, or entry angle.

Compared to the powder feedstock, intrinsic wire characteristics can be further compounded by the feeding mechanisms, which dictate the input orientation and related parameters, with cumulative and often evident variations in the outputs, thus validating the requirement for coaxial solutions that effectively mitigate such issues. The effects of the build duration, on the wear rate or degradation of mechanical components directly involved in the material delivery sequence for both continuous and granular forms, were also observed, alongside related process monitoring considerations for arc-based technologies, including the practice of utilising arc voltage control (AVC) solutions. Specifically, objects in proximity of the electrode, expected or otherwise, can effect detectable changes in voltage outputs, which raises reliability concerns. For systems configured with AVC solutions, or other advanced monitoring capabilities, the detection of and response to relative changes should account for both expected and unique sources of discrepancies, particularly over longer processing durations, where variances may exceed the specified control limits for a stable MAM process. Furthermore, as MAM systems become increasingly sophisticated and more widely accepted, addressing exacerbating and underlying productivity, quality, and performance related variability issues, can give businesses a competitive edge.

Verification and validation requirements: Preliminary investigations were focused on the verification of pertinent challenges, while core development strategies were aimed at demonstrating desired system functions at a generic level, and establishing the suitability of the BAM platform, for designated large-scale MAM applications. Systemic investigations involved the generation, collation, organisation, and analysis of pertinent system data, derived from WAAM and 3D inspection operations, and confirmed the conformance of these processes to BAM specifications. Interconnected observations, including the need for consolidated approaches, to support analysis and control of both tangible and intangible sources of inconsistency, also revealed how operations were more broadly impacted by activities within and beyond system boundaries. Having demonstrated that the system could fulfil basic MAM functions, the focus was on validating the platform for large scale MAM operations. The targeted SMRM applications was based on an industrial case study for which a titanium alloy aerospace component was designated, and the empirical objective was to devise a suitable restoration strategy, beginning with the verification of discrete factors affecting measurable DED outputs. Temperature and strain responses were specifically targeted, and the former was evaluated without (autogenous) and with feedstock input. Compared to autogenous passes, the introduction of the feedstock significantly increased the duration and magnitude of the overall substrate temperature, which was anticipated. However, the orientation of the EOAT during deposition also had a measurable impact on the substrate temperature, further emphasising the need for solutions that effectively limit or eliminate positional and/or orientational issues. Mapping the magnitude, duration, and relative changes in directional strain components also corroborated previous studies, with peak temperatures characteristically coinciding with peak strain values in designated substrates.

SMRM case study: In general, DED parameters were developed in consideration of the alloys investigated, and then optimised for specific trials or to suit the application circumstances. Incorporating available process data improved experimental design outcomes while saving time, due to increased confidence in the reliability of selected process parameters and the consistency of resulting builds. Post-DED, CT scans of visually acceptable builds, derived from restoration trials, revealed a small number of subsurface indications, mainly attributed to the geometric parameters, thus demonstrating the implications of effective product design inputs and related parameters, on SMRM tasks. The BAM platform proved capable of satisfactorily restoring voids on Ti-6Al-4V substrates, but dependencies between actual application and system variables, and experimental outputs further validated the need for acceptance criteria to govern dedicated reprocessing tasks and related strategies. Equally, these insights facilitated the development of the SMRM strategy for operations directly performed on the Ti-64 aerospace component, and corroborated previous studies by revealing when, where, why, and how certain tasks affect SMRM outcomes. For instance, persisting accessibility issues necessitated compromises when completing machining operations on the component, thus underscoring the need for more flexible solutions, such as the BAM platform. Conversely, combining essential ancillary monitoring and shielding solutions with the BAM EOAT, emphasised the need for more compact and/or less intrusive solutions to address accessibility and related line-of-sight issues hindering the effective deployment of advanced tools.

Reprocessing procedures: The goal of the SMRM case study was to ensure adequate access to the component, basic control of reprocessing conditions, and mitigate risks to the underlying structure, whilst achieving consistent outputs for similar tasks. The main verification procedures involved both destructive and non-destructive testing techniques, but due to the conditions of supply, only NDT procedures were permitted for the aerospace component. NDT verification procedures, including visual, GOM, XRF, L-XRD and DPI techniques provided both qualitative and quantitative information, confirming that for this large-scale MAM application, the BAM platform had met the general requirements and specifications for designated SMRM tasks. While evident imperfections were corroborated by GOM inspection and DPI data, which highlighted geometric inaccuracies and distinct features, such as arc indentations, there were no significant quality issues observed. For XRF and L-XRD operations, measurements were evaluated in relation to baseline values obtained from the as-received component and/or prior to the implementation of reprocessing operations. There were nominal discrepancies between baseline and post-DED values of primary alloy constituents Ti, Al and V, and trace amounts of other elements found in all inspected regions were each < 0.3 Wt. %. Across different inspection zones, the Fe content typically exceeded the maximum specification (~0.3 Wt. %) for Grade 5 titanium, with the highest (1.08 Wt. %) and lowest (0.13 Wt. %) measurements obtained from the as-supplied and reprocessed areas respectively. Geometrically, no significant distortions were observed after reprocessing operations, but XRD measurements revealed higher residual stress levels in different regions of the component, from about -12 to -382 MPa, relative to baseline measurements, which ranged from approximately -560 to -735 MPa. Destructive examinations were also completed on representative BAM materials and

Vickers hardness measurements revealed nominal variations across the sampled regions, with hardness typically increasing by about 10-20 $HV_{0.5}$ post-DED, compared to values obtained from the HAZ (~349 $HV_{0.5}$) and as supplied (330-340 $HV_{0.5}$) substrate conditions. The tensile properties of uniaxial specimens obtained from representative Ti-64 samples, were also examined, and the YS was typically higher in substrate materials (>900 MPa). Conversely, the as-deposited (860 MPa) and reprocessed (880 MPa) BAM materials were in good agreement with standard wrought, cast, and AM materials, with values ranging from 815 MPa to 880 MPa, 770 MPa to ~900 MPa, and ~750 to 800MPa respectively. Thus, the actual manufacturing procedures and condition of the test material remain important determinants in the prediction of material behaviour.

Process verification: Due to commercial restrictions on post-DED tests on the aerospace component, supplementary verification procedures were necessary and further enhanced understanding of the effects of reprocessing operations. Specifically, thermo-mechanical models were developed to predict temperature, strain, and distortion responses in the reprocessed Ti-6Al-4V materials and components. Although the magnitude was overestimated, predictions showed good correlations concerning the effects of sequential addition of mass and energy into the system. Discrepancies were attributed to necessary simplifications and assumptions applied during the development of the models. In lieu of other quantifiable indicators, which is typical for serviceable parts and critical structures, model predictions provided useful insights about the overall SMRM strategy. In this instance, commercial restrictions were further compounded by technology availability and technical limitations. Hence, the localised and broader effects of DED operations, including the heat input and its potential effects within and beyond HAZs, may be parametrically investigated to obtain valuable insights that supplement other measurements obtained from empirical studies. The utilisation of process models is also important for evaluating deposition strategies, and discovering more effectual ways of controlling processing effects, by exploring the impact of adopted procedures, which can help to anticipate potential problems and mitigate risks during reprocessing operations. Ultimately, combining experience, experimental and modelling approaches proved most effective, by allowing for the consolidation of more in-depth information used to identify critical factors and variables, which is an important foundational step when developing solutions to SMRM problems.

9.2 Future work

The BAM system is a development platform and as such, it may be used for typical MAM applications or as a testbed, to support the development of enabling COTS technologies and other emerging solutions. Accordingly, an iterative approach will be maintained to facilitate gradual, sustainable, and enduring improvements, whilst prioritising functional and operational requirements for completing basic MAM tasks, even as new features are implemented, and different applications explored. This strategy is desirable for ensuring that enhancements are properly investigated, and augment accrued benefits, in terms of the overall architecture and utility of integrated capabilities. Key areas for future development are summarised below.

Concept framework: The proposed framework includes specific themes and related development priorities that extend beyond the basic requirements for the BAM system. Thus, when articulating actual requirements and specifications, further elaboration of definitive problems, and clarification of specific actions and related strategies, are necessary and will be explored, to maximise the utility of the framework, particularly for OA MAM platforms.

Data analytics: In the development of more robust MAM systems, data analytics is important, but appropriate control mechanisms for DED operations depend on the ability to monitor and interpret key performance indicators from measurements taken at different stages of the process, and from the system. Furthermore, real-time process data can provide meaningful insights about important indicators, but such activities generate big data sets. Thus, dedicated analytic tools for proactively and instantaneously deciphering continuous streams of heterogenous data will be evaluated, to improve the quality of algorithmically driven system inputs and interrelated process responses. From a systems perspective, investigation of consolidated events monitoring approaches should facilitate the management of derived functions, while supporting troubleshooting and maintenance activities. Beyond this study, strategies are also required for managing available MAM data, due to the utility of such inputs, particularly for activities within AMR settings.

Process monitoring and control: Intuitive process monitoring tools and adaptive control techniques are essential for planned system enhancements, and a strategy for combining process monitoring and data analytics with insights about the features and traits of the BAM capability, is being investigated. This work, which involves detecting, accurately measuring, and algorithmically interpreting data to support adaptive control of system inputs, as well as autonomous functions that are entirely fulfilled by the operator at present, should facilitate more timely and accurate control of process inputs.

Modelling and simulation: Complementary modelling and simulation activities will be initiated, to augment adaptive control strategies, with thermo-mechanical-metallurgical (TMM) models developed to facilitate more accurate prediction of realistic parameters and processing conditions that fulfil MAM requirements. Specifically, the preliminary models presented in this study will be further developed, necessitating extensive literature reviews to support parametric material characterisation studies, and enhance understanding of different processing conditions, task scenarios and related effects. For specific applications, shorter development times, fewer processing errors, and more effective MAM strategies are anticipated benefits.

System (re)configuration: The need for access during SMRM operations and related configuration concerns are equally important from an operational standpoint. Accessibility issues and related observations highlight the need for expanding the configuration concept, which will enhance condition monitoring strategies that inform adaptive control measures. Specifically, it was determined that it was possible to derive multiple unique configurations from a limited set of core inputs. However, the application was prioritised, and the BAM cell accordingly optimised, with the main emphasis placed on the EOAT itself, and the effective deployment of

the WAAM process. Thus, expanding the configuration concept to accommodate modular solutions, including supplementary devices to support monitoring activities, is more consistent with the systems approach and requirements for access during envisioned MAM operations.

BAM development priorities: Other development priorities include the investigation of algorithmic approaches to support machine learning, which will be progressed alongside enhancements for EOAT interfaces and interconnectivity, and specific improvements to the DED tool and processing environment that are imminently crucial. These enhancements, including the integration of supporting technologies and related investigations, should measurably improve the BAM platform, translating to better outcomes and overall utilisation prospects.

9.3 Closing remarks

In a fragmented and rapidly evolving technology landscape, where different interest groups are influenced by often competing commercial and/ or technical priorities, emerging issues and similarly disruptive advances can threaten the maturation and resilience of future MAM solutions. The diverse perspectives from which defined priorities are considered, can also influence how interconnected challenges and opportunities are managed. Therefore, adopting consolidated approaches, such as the GT framework resulting from this study, can enhance understanding of mutual perceptions bolstering the state of the art, whilst directly and deliberately fostering more reasoned actions, during the development of MAM systems and associated procedures.

References

[1] Adamczuk RR, Seume JR. Early Assessment of Defects and Damage in Jet Engines. Procedia CIRP 2013;11:328–33. https://doi.org/10.1016/j.procir.2013.07.022.

[2] Paul Seidenman, David Spanovich. How Bird Strikes Impact Engines. Inside MRO 2016. http://www.mro-network.com/maintenance-repair-overhaul/how-bird-strikes-impact-engines (accessed February 18, 2018).

[3] Maleque MA, Salit MS. Mechanical Failure of Materials. Materials Selection and Design, Springer, Singapore; 2013, p. 17–38. https://doi.org/10.1007/978-981-4560-38-2_2.

[4] Bhaumik SK, Rangaraju R, Venkataswamy MA, Bhaskaran TA, Parameswara MA. Fatigue fracture of crankshaft of an aircraft engine. Engineering Failure Analysis 2002;9:255–63. https://doi.org/10.1016/S1350-6307(01)00022-X.

[5] Krstic B, Rasuo B, Trifkovic D, Radisavljevic I, Rajic Z, Dinulovic M. An investigation of the repetitive failure in an aircraft engine cylinder head. Engineering Failure Analysis 2013;34:335–49. https://doi.org/10.1016/j.engfailanal.2013.08.013.

[6] Makhlouf ASH, Aliofkhazraei M. Handbook of Materials Failure Analysis with Case Studies from the Aerospace and Automotive Industries. Butterworth-Heinemann; 2015.

[7] Moedano J. A STUDY ON THE PRACTICAL APPLICATION OF REPAIR DEVELOPMENT METHODS FOR AEROSPACE COMPONENTS n.d.:83.

[8] Nations U. Global Issues. United Nations n.d. https://www.un.org/en/global-issues (accessed July 29, 2021).

[9] 15 Global Challenges – The Millennium Project n.d. http://www.millennium-project.org/15-global-challenges/ (accessed July 29, 2021).

[10] Ford S. The Emergence of Additive Manufacturing Introduction to the Special Issue of Technological Forecasting and Social Change n.d.:7.

[11] Wohlers T, Gornet T. History of additive manufacturing 2014:34.

[12] Goehrke S. Why Are Investors Pouring Millions Into 3-D Printing? Forbes 1970. https://www.forbes.com/sites/sarahgoehrke/2019/01/25/why-are-investors-pouring-millions-into-3-d-printing/ (accessed November 30, 2021).

[13] 3D Printing Industry Awards 2019 Materials Company of the Year Update. 3D Printing Industry 2019. https://3dprintingindustry.com/news/3d-printing-industry-awards-2019-materials-company-of-the-year-update-148031/ (accessed November 30, 2021).

[14] Hype Cycle for 3D Printing, 2017. Gartner n.d. https://www.gartner.com/en/documents/3759564/hype-cycle-for-3d-printing-2017 (accessed August 13, 2021).

[15] Glaser BG, Strauss AL. The Discovery of Grounded Theory: Strategies for Qualitative Research. Transaction Publishers; 2009.

[16] Timonen V, Foley G, Conlon C. Challenges When Using Grounded Theory: A Pragmatic Introduction to Doing GT Research. International Journal of Qualitative Methods 2018;17:1609406918758086. https://doi.org/10/gd32dp.

[17] ISO/ASTM 52900:2015(en), Additive manufacturing — General principles — Terminology n.d. https://www.iso.org/obp/ui/#iso:std:iso-astm:52900:ed-1:v1:en (accessed May 30, 2019).

[18] ASTM F2792-12a Standard Terminology for Additive Manufacturing Technologies. ASTM International, West Conshohocken, PA.; n.d. https://doi.org/10.1520/F2792-12A.

[19] International Organization for Standardization. ISO/TC 261 - Additive manufacturing n.d. https://www.iso.org/committee/629086.html (accessed July 3, 2017).

[20] ASTM International. Committee F42 on Additive Manufacturing Technologies n.d. https://www.astm.org/COMMITTEE/F42.htm (accessed July 3, 2017).

[21] Residual Stress Characterization and Control in the Additive Manufacture of Large Scale Metal Structures, 2017, p. 455–60. https://doi.org/10/gcsgww.

[22] Hu X, Nycz A, Lee Y, Shassere B, Simunovic S, Noakes M, et al. Towards an integrated experimental and computational framework for large-scale metal additive manufacturing. Materials Science and Engineering: A 2019;761:138057. https://doi.org/10/gmtphj.

[23] Taminger KM, Domack CS. Challenges in Metal Additive Manufacturing for Large-Scale Aerospace Applications. In: Kinsella ME, editor. Women in Aerospace Materials: Advancements and Perspectives of Emerging Technologies, Cham: Springer International Publishing; 2020, p. 105–24. https://doi.org/10.1007/978-3-030-40779-7_8.

[24] A Comprehensive List of all the Metal 3D Printer Manufacturers. 3Dnatives 2021. https://www.3dnatives.com/en/metal-3d-printer-manufacturers/ (accessed August 2, 2021).

[25] Best metal 3D printers in 2021: comprehensive overview. Aniwaa n.d. https://www.aniwaa.com/buyers-guide/3d-printers/best-metal-3d-printer/ (accessed August 2, 2021).

[26] Duda T, Raghavan LV. 3D Metal Printing Technology. IFAC-PapersOnLine 2016;49:103–10. https://doi.org/10.1016/j.ifacol.2016.11.111.
[27] Billberg A, Blom R, Holke O. Research and development of additive manufactured bladed disks 2017.
[28] Witzel J, Schrage J, Gasser A, Kelbassa I. Additive manufacturing of a blade-integrated disk by laser metal deposition. ICALEO 2011;2011:250–6. https://doi.org/10/gmtphh.
[29] Liu R. Repair of metallic components using hybrid manufacturing n.d.:128.
[30] Frazier WE. Metal additive manufacturing: a review. Journal of Materials Engineering and Performance 2014;23:1917–28.
[31] Uriondo A, Esperon-Miguez M, Perinpanayagam S. The present and future of additive manufacturing in the aerospace sector: A review of important aspects. Proceedings of the Institution of Mechanical Engineers, Part G: Journal of Aerospace Engineering 2015;229:2132–47. https://doi.org/10/ggcqv5.
[32] Ding D, Pan Z, Cuiuri D, Li H. Wire-feed additive manufacturing of metal components: technologies, developments and future interests. The International Journal of Advanced Manufacturing Technology 2015;81:465–81. https://doi.org/10/f7r78h.
[33] Stavropoulos P, Foteinopoulos P. Modelling of additive manufacturing processes: a review and classification. Manufacturing Rev 2018;5:2. https://doi.org/10/ggcqvq.
[34] Shah K, Haq I ul, Khan A, Shah SA, Khan M, Pinkerton AJ. Parametric study of development of Inconel-steel functionally graded materials by laser direct metal deposition. Materials & Design (1980-2015) 2014;54:531–8. https://doi.org/10/f5kxqv.
[35] Wang H, Jiang W, Valant M, Kovacevic R. Solid Freeform Fabrication Based on Micro-Plasma Powder Deposition n.d.:12.
[36] Liu R, Wang Z, Sparks T, Liou F, Newkirk J. Aerospace applications of laser additive manufacturing. In: Brandt M, editor. Laser Additive Manufacturing, Woodhead Publishing; 2017, p. 351–71. https://doi.org/10.1016/B978-0-08-100433-3.00013-0.
[37] Gibson I, Rosen DW, Stucker B, others. Powder Bed Fusion Processes. Additive manufacturing technologies, vol. 238, Springer; 2010.
[38] Gao W, Zhang Y, Ramanujan D, Ramani K, Chen Y, Williams CB, et al. The status, challenges, and future of additive manufacturing in engineering. Computer-Aided Design 2015;69:65–89. https://doi.org/10/gctpcv.
[39] Riza SH, Masood SH, Wen C. 10.11 - Laser-Assisted Additive Manufacturing for Metallic Biomedical Scaffolds. In: Hashmi S, Batalha GF, Van Tyne CJ, Yilbas B, editors. Comprehensive Materials Processing, Oxford: Elsevier; 2014, p. 285–301. https://doi.org/10.1016/B978-0-08-096532-1.01017-7.
[40] Gu DD, Meiners W, Wissenbach K, Poprawe R. Laser additive manufacturing of metallic components: materials, processes and mechanisms. International Materials Reviews 2012;57:133–64.
[41] Ruan J, Sparks TE, Fan Z, Stroble JK, Panackal A, Liou F. A review of layer based manufacturing processes for metals. Proceedings of the Solid Freeform Fabrication Symposium, 2006, p. 233–45.
[42] Karunakaran KP, Suryakumar S, Chandrasekhar U, Bernard A. Hybrid rapid manufacturing of metallic objects. International Journal of Rapid Manufacturing 2010;1:433–55.
[43] Sun G, Zhou R, Lu J, Mazumder J. Evaluation of defect density, microstructure, residual stress, elastic modulus, hardness and strength of laser-deposited AISI 4340 steel. Acta Materialia 2015;84:172–89. https://doi.org/10/f6zfm3.
[44] Mazumder J, Dutta D, Kikuchi N, Ghosh A. Closed loop direct metal deposition: art to part. Optics and Lasers in Engineering 2000;34:397–414. https://doi.org/10.1016/S0143-8166(00)00072-5.
[45] Dinda GP, Dasgupta AK, Mazumder J. Laser aided direct metal deposition of Inconel 625 superalloy: Microstructural evolution and thermal stability. Materials Science and Engineering: A 2009;509:98–104. https://doi.org/10/dnd4cn.
[46] Cao J, Liu F, Lin X, Huang C, Chen J, Huang W. Effect of overlap rate on recrystallization behaviors of Laser Solid Formed Inconel 718 superalloy. Optics & Laser Technology 2013;45:228–35. https://doi.org/10/ggcqvz.
[47] Bhattacharya S, Dinda GP, Dasgupta AK, Natu H, Dutta B, Mazumder J. Microstructural evolution and mechanical, and corrosion property evaluation of Cu–30Ni alloy formed by Direct Metal Deposition process. Journal of Alloys and Compounds 2011;509:6364–73. https://doi.org/10.1016/j.jallcom.2011.03.091.
[48] Bi G, Gasser A, Wissenbach K, Drenker A, Poprawe R. Characterization of the process control for the direct laser metallic powder deposition. Surface and Coatings Technology 2006;201:2676–83. https://doi.org/10/bzx8df.
[49] Hong C, Gu D, Dai D, Gasser A, Weisheit A, Kelbassa I, et al. Laser metal deposition of TiC/Inconel 718 composites with tailored interfacial microstructures. Optics & Laser Technology 2013;54:98–109. https://doi.org/10/ggcqvv.
[50] Lewis GK. Directed Light Fabrication--A Laser Metal Deposition Process for Fabrication of Near-Net Shape Components. Los Alamos National Laboratory; 1997.
[51] Milewski JO, Lewis GK, Thoma DJ, Keel GI, Nemec RB, Reinert RA. Directed light fabrication of a solid metal hemisphere using 5-axis powder deposition. Journal of Materials Processing Technology 1998;75:165–72. https://doi.org/10.1016/S0924-0136(97)00321-X.

[52] Thompson SM, Bian L, Shamsaei N, Yadollahi A. An overview of Direct Laser Deposition for additive manufacturing; Part I: Transport phenomena, modeling and diagnostics. Additive Manufacturing 2015;8:36–62. https://doi.org/10/gd7gqw.
[53] Taminger K, Hafley RA. Electron beam freeform fabrication: a rapid metal deposition process. 2003.
[54] Taminger KM, Hafley MRA. Electron Beam Freeform Fabrication for Cost Effective Near-Net Shape Manufacturing. NASA Langley Research Center, Hampton, Virginia; n.d.
[55] Hafley RA, Taminger KM, Bird RK. Electron Beam Freeform Fabrication in the Space Environment. 45th AIAA Aerospace Sciences Meeting and Exhibit, 2007, p. 8–11.
[56] Bandari YK, Lee Y, Nandwana P, Richardson BS, Adediran AI, Love LJ, et al. Effect of Inter-layer Cooling Time on Distortion and Mechanical Properties in Metal Additive Manufacturing (AM). Oak Ridge National Lab.(ORNL), Oak Ridge, TN (United States); 2018.
[57] Heralić A, Christiansson A-K, Lennartson B. Height control of laser metal-wire deposition based on iterative learning control and 3D scanning. Optics and Lasers in Engineering 2012;50:1230–41. https://doi.org/10.1016/j.optlaseng.2012.03.016.
[58] Zhang YN, Cao X, Wanjara P, Medraj M. Oxide films in laser additive manufactured Inconel 718. Acta Materialia 2013;61:6562–76. https://doi.org/10/f4993g.
[59] Govekar E, Jeromen A, Kuznetsov A, Kotar M, Kondo M. Annular laser beam based direct metal deposition. Procedia CIRP 2018;74:222–7. https://doi.org/10.1016/j.procir.2018.08.099.
[60] Kotar M, Fujishima M, Levy G, Govekar E. Initial transient phase and stability of annular laser beam direct wire deposition. CIRP Annals 2019. https://doi.org/10.1016/j.cirp.2019.04.118.
[61] DebRoy T, Wei HL, Zuback JS, Mukherjee T, Elmer JW, Milewski JO, et al. Additive manufacturing of metallic components – Process, structure and properties. Progress in Materials Science 2018;92:112–224. https://doi.org/10.1016/j.pmatsci.2017.10.001.
[62] Clark D, Bache MR, Whittaker MT. Shaped metal deposition of a nickel alloy for aero engine applications. Journal of Materials Processing Technology 2008;203:439–48. https://doi.org/10/bvrcs4.
[63] Woy U, Jones S, Gault R, Ridgway K, McCluskey R. Evaluation of Shaped Metal Deposition (SMD) for applications in the energy industry. High Value Manufacturing: Advanced Research in Virtual and Rapid Prototyping, CRC Press; 2013, p. 619–22. https://doi.org/10.1201/b15961-113.
[64] Tancogne-Dejean T, Roth CC, Woy U, Mohr D. Probabilistic fracture of Ti–6Al–4V made through additive layer manufacturing. International Journal of Plasticity 2016;78:145–72. https://doi.org/10/f8bhcw.
[65] Martina F. Additive manufacturing: current status and future developments 2013.
[66] Xiong J, Lei Y, Chen H, Zhang G. Fabrication of inclined thin-walled parts in multi-layer single-pass GMAW-based additive manufacturing with flat position deposition. Journal of Materials Processing Technology 2017;240:397–403. https://doi.org/10/ggcqv2.
[67] Ding D, Pan Z, Cuiuri D, Li H. A multi-bead overlapping model for robotic wire and arc additive manufacturing (WAAM). Robotics and Computer-Integrated Manufacturing 2015;31:101–10. https://doi.org/10.1016/j.rcim.2014.08.008.
[68] Yang D, He C, Zhang G. Forming characteristics of thin-wall steel parts by double electrode GMAW based additive manufacturing. Journal of Materials Processing Technology 2016;227:153–60. https://doi.org/10/ggcqv3.
[69] Wu B, Pan Z, Ding D, Cuiuri D, Li H, Xu J, et al. A review of the wire arc additive manufacturing of metals: properties, defects and quality improvement. Journal of Manufacturing Processes 2018;35:127–39. https://doi.org/10/gfmm3h.
[70] Williams SW, Martina F, Addison AC, Ding J, Pardal G, Colegrove P. Wire + Arc Additive Manufacturing. Materials Science and Technology 2016;32:641–7. https://doi.org/10/gfz2hd.
[71] Arcam EBM. EBM Hardware. Arcam AB n.d. http://www.arcam.com/technology/electron-beam-melting/hardware/ (accessed May 30, 2019).
[72] DMLS Technology for Metal 3D Printer n.d. https://www.eos.info/en/industrial-3d-printing/additive-manufacturing-how-it-works/dmls-metal-3d-printing (accessed August 12, 2021).
[73] Keshavarzkermani A, Sadowski M, Ladani L. Direct metal laser melting of Inconel 718: Process impact on grain formation and orientation. Journal of Alloys and Compounds 2018;736:297–305. https://doi.org/10/gfj4qv.
[74] Bhavar V, Kattire P, Patil V, Khot S, Gujar K, Singh R. A review on powder bed fusion technology of metal additive manufacturing. In: Badiru AB, Valencia VV, Liu D, editors. Additive Manufacturing Handbook. 1st ed., CRC Press; 2017, p. 251–3. https://doi.org/10.1201/9781315119106-15.
[75] Niu HJ, Chang ITH. Selective laser sintering of gas atomized M2 high speed steel powder. Journal of Materials Science 2000;35:31–8.
[76] Niklas Wahlström, Oscar Gabrielsson. Additive Manufacturing Applications for Wind Turbines. Master of Science. Royal Institute of Technology (KTH), 2017.
[77] plc R. Renishaw: Additive Manufacturing Solutions Centres. Renishaw n.d. http://www.renishaw.com/en/additive-manufacturing-solutions-centres--37039 (accessed August 12, 2021).

[78] Concept Laser | GE Additive n.d. https://www.ge.com/additive/who-we-are/concept-laser (accessed August 12, 2021).
[79] Arcam EBM. Electron Beam Melting - EBM Process, Additive Manufacturing. Arcam AB n.d. http://www.arcam.com/technology/electron-beam-melting/ (accessed May 30, 2019).
[80] Arcam EBM. EBM Hardware. Arcam AB n.d. http://www.arcam.com/technology/electron-beam-melting/hardware/ (accessed May 30, 2019).
[81] Pfeiffer Vacuum. 3D Printing 2020. https://www.pfeiffer-vacuum.com/filepool/file/application-reports/brochure_3d-printing_en.pdf;jsessionid=4BAC8BE62D2827633CA3494499BCFF1D-n1?referer=2613&request_locale=en_US (accessed November 25, 2021).
[82] Niklas Wahlström, Oscar Gabrielsson. Additive Manufacturing Applications for Wind Turbines. Master of Science. Royal Institute of Technology (KTH), 2017.
[83] About Arcam | GE Additive n.d. https://www.ge.com/additive/who-we-are/about-arcam (accessed August 12, 2021).
[84] Letenneur M, Kreitcberg A, Brailovski V. Optimization of Laser Powder Bed Fusion Processing Using a Combination of Melt Pool Modeling and Design of Experiment Approaches: Density Control. JMMP 2019;3:21. https://doi.org/10.3390/jmmp3010021.
[85] Krishnan M, Atzeni E, Canali R, Manfredi D, Calignano F, Ambrosio E, et al. Influence of post-processing operations on mechanical properties of AlSi10Mg parts by DMLS. High Value Manufacturing: Advanced Research in Virtual and Rapid Prototyping: Proceedings of the 6th International Conference on Advanced Research in Virtual and Rapid Prototyping, Leiria, Portugal, 1-5 October, 2013, CRC Press; 2013, p. 243.
[86] Kok Y, Tor SB, Loh NH. Comparison of two metallic additive manufacturing technologies: selective laser melting and electron beam melting 2014.
[87] Todorov E, Spencer R, Gleeson S, Jamshidinia M, Kelly SM. America Makes: National Additive Manufacturing Innovation Institute (NAMII) Project 1: Nondestructive Evaluation (NDE) of Complex Metallic Additive Manufactured (AM) Structures: Fort Belvoir, VA: Defense Technical Information Center; 2014. https://doi.org/10.21236/ADA612775.
[88] Smugeresky JE, Atwood CJ, Gill DD. New low cost material development technique for advancing rapid prototyping manufacturing technology. 2007. https://doi.org/10.2172/926378.
[89] de Lima MSF, Sankaré S. Microstructure and mechanical behavior of laser additive manufactured AISI 316 stainless steel stringers. Materials & Design 2014;55:526–32. https://doi.org/10.1016/j.matdes.2013.10.016.
[90] Knapp CM, Lienert TJ, Chen C, Kovar D. Additive Manufacturing of 1018 Steel: Process Observations and Calculations n.d.:11.
[91] Ma M, Wang Z, Wang D, Zeng X. Control of shape and performance for direct laser fabrication of precision large-scale metal parts with 316L Stainless Steel. Optics & Laser Technology 2013;45:209–16. https://doi.org/10.1016/j.optlastec.2012.07.002.
[92] Parimi LL, A. RG, Clark D, Attallah MM. Microstructural and texture development in direct laser fabricated IN718. Materials Characterization 2014;89:102–11. https://doi.org/10/ggcqwk.
[93] Taminger K, Hafley RA, Fahringer DT, Martin RE. Effect of Surface Treatments on Electron Beam Freeform Fabricated Aluminum Structures 2004.
[94] Bird RK, Hibberd J. Tensile Properties and Microstructure of Inconel 718 Fabricated with Electron Beam Freeform Fabrication (EBF (sup 3)) 2009.
[95] Wanjara P, Brochu M, Jahazi M. Electron beam freeforming of stainless steel using solid wire feed. Materials & Design 2007;28:2278–86. https://doi.org/10/b3v5cj.
[96] Demir AG. Micro laser metal wire deposition for additive manufacturing of thin-walled structures. Optics and Lasers in Engineering 2018;100:9–17. https://doi.org/10/ggcqvx.
[97] Froend M, Riekehr S, Kashaev N, Klusemann B, Enz J. Process development for wire-based laser metal deposition of 5087 aluminium alloy by using fibre laser. Journal of Manufacturing Processes 2018;34:721–32. https://doi.org/10/gd67fc.
[98] Xu X, Mi G, Luo Y, Jiang P, Shao X, Wang C. Morphologies, microstructures, and mechanical properties of samples produced using laser metal deposition with 316L stainless steel wire. Optics and Lasers in Engineering 2017;94:1–11. https://doi.org/10/ggcqv4.
[99] Motta M, Demir AG, Previtali B. High-speed imaging and process characterization of coaxial laser metal wire deposition. Additive Manufacturing 2018;22:497–507. https://doi.org/10/ggcqvr.
[100] Yashwanth Bandari, Stewart W Williams, Jialuo Ding, Filomeno Martina. Additive manufacture of large structures: robotic or CNC systems? 26th International Solid Freeform Fabrication Symposium, Austin, Texas: n.d.
[101] Williams SW, Martina F, Addison AC, Ding J, Pardal G, Colegrove P. Wire + Arc Additive Manufacturing. Materials Science and Technology 2016;32:641–7. https://doi.org/10.1179/1743284715Y.0000000073.
[102] Dutta B, Froes FS. The additive manufacturing (AM) of titanium alloys. Metal Powder Report 2017.

[103] Herzog D, Seyda V, Wycisk E, Emmelmann C. Additive manufacturing of metals. Acta Materialia 2016;117:371–92. https://doi.org/10/f8384s.
[104] New manufacturing milestone: 30,000 additive fuel nozzles | GE Additive 2022. https://www.ge.com/additive/stories/new-manufacturing-milestone-30000-additive-fuel-nozzles (accessed November 26, 2021).
[105] Hauser C. Case Study: Laser Powder Metal Deposition Manufacturing of Complex Real Parts 2014.
[106] Qiu C, Ravi GA, Dance C, Ranson A, Dilworth S, Attallah MM. Fabrication of large Ti–6Al–4V structures by direct laser deposition. Journal of Alloys and Compounds 2015;629:351–61. https://doi.org/10.1016/j.jallcom.2014.12.234.
[107] Santangelo M, Silwal B, Purdy A. vibration assisted robotic hot-wire gas tungsten arc welding (GTAW) for additive manufacturing of large metallic parts. Solid FreeForm Symposium, Austin, 2016.
[108] Zhao H, Zhang G, Yin Z, Wu L. A 3D dynamic analysis of thermal behavior during single-pass multi-layer weld-based rapid prototyping. Journal of Materials Processing Technology 2011;211:488–95. https://doi.org/10.1016/j.jmatprotec.2010.11.002.
[109] Dey NK. Additive manufacturing laser deposition of Ti-6Al-4V for aerospace repair application. Missouri University of Science and Technology; 2014.
[110] Greer C, Nycz A, Noakes M, Richardson B, Post B, Kurfess T, et al. Introduction to the design rules for Metal Big Area Additive Manufacturing. Additive Manufacturing 2019;27:159–66. https://doi.org/10.1016/j.addma.2019.02.016.
[111] Tofail SAM, Koumoulos EP, Bandyopadhyay A, Bose S, O'Donoghue L, Charitidis C. Additive manufacturing: scientific and technological challenges, market uptake and opportunities. Materials Today 2018;21:22–37. https://doi.org/10/gc6dhj.
[112] Khajavi SH, Partanen J, Holmström J. Additive manufacturing in the spare parts supply chain. Computers in Industry 2014;65:50–63. https://doi.org/10.1016/j.compind.2013.07.008.
[113] Frazier WE. Metal additive manufacturing: a review. Journal of Materials Engineering and Performance 2014;23:1917–28.
[114] Duda T, Raghavan LV. 3D Metal Printing Technology. IFAC-PapersOnLine 2016;49:103–10. https://doi.org/10.1016/j.ifacol.2016.11.111.
[115] Baumers M, Dickens P, Tuck C, Hague R. The cost of additive manufacturing: machine productivity, economies of scale and technology-push. Technological Forecasting and Social Change 2016;102:193–201.
[116] Thomas DS, Gilbert SW. Costs and Cost Effectiveness of Additive Manufacturing. National Institute of Standards and Technology; 2014. https://doi.org/10.6028/NIST.SP.1176.
[117] Aliakbari M. Additive manufacturing: State-of-the-art, capabilities, and sample applications with cost analysis. 2012.
[118] Martinaa F. Additive manufacturing: current status and future developments 2015.
[119] Wohlers TT. Wohlers Report...: 3D Printing and Additive Manufacturing, State of the Industry, Annual Worldwide Progress Report. Wohlers Associates Incorporated; 2014.
[120] Knapp CM. Los Alamos National Laboratory's Approach to Metal Additive Manufacturing. Los Alamos National Lab. (LANL), Los Alamos, NM (United States); 2016. https://doi.org/10.2172/1242923.
[121] Ruan J, Sparks TE, Fan Z, Stroble JK, Panackal A, Liou F. A review of layer based manufacturing processes for metals. Proceedings of the Solid Freeform Fabrication Symposium, 2006, p. 233–45.
[122] Legzdina D, Adams R, Godfrey D. Additive Manufacturing of Titanium Alloys at Honeywell Aerospace n.d.
[123] Norsk Titanium | Technology n.d. https://www.norsktitanium.com/technology (accessed July 4, 2019).
[124] Cunningham CR, Flynn JM, Shokrani A, Dhokia V, Newman ST. Invited review article: Strategies and processes for high quality wire arc additive manufacturing. Additive Manufacturing 2018;22:672–86. https://doi.org/10.1016/j.addma.2018.06.020.
[125] Yashwanth Bandari, Stewart W Williams, Jialuo Ding, Filomeno Martina. Additive manufacture of large structures: robotic or CNC systems? 26th International Solid Freeform Fabrication Symposium, Austin, Texas: n.d.
[126] Cunningham CR, Wikshåland S, Xu F, Kemakolam N, Shokrani A, Dhokia V, et al. Cost Modelling and Sensitivity Analysis of Wire and Arc Additive Manufacturing. Procedia Manufacturing 2017;11:650–7. https://doi.org/10.1016/j.promfg.2017.07.163.
[127] Norsk Titanium | Technology n.d. https://www.norsktitanium.com/technology (accessed July 4, 2019).
[128] Legzdina D, Adams R, Godfrey D. Additive Manufacturing of Titanium Alloys at Honeywell Aerospace n.d.
[129] Dawes J, Bowerman R, Trepleton R. Introduction to the Additive Manufacturing Powder Metallurgy Supply Chain. Johnson Matthey Technol Rev 2015;59:243–56. https://doi.org/10.1595/205651315X688686.
[130] Cunningham CR, Flynn JM, Shokrani A, Dhokia V, Newman ST. Invited review article: Strategies and processes for high quality wire arc additive manufacturing. Additive Manufacturing 2018;22:672–86. https://doi.org/10.1016/j.addma.2018.06.020.

[131] Baumers M, Dickens P, Tuck C, Hague R. The cost of additive manufacturing: machine productivity, economies of scale and technology-push. Technological Forecasting and Social Change 2016;102:193–201.
[132] Baumers M, Tuck C, Wildman R, Ashcroft I, Rosamond E, Hague R. Combined build-time, energy consumption and cost estimation for direct metal laser sintering. The Twenty-Third Annual International Solid Freeform Fabrication (SFF) Symposium – An Additive Manufacturing Conference, Austin, Texas: 2012, p. 932.
[133] Baumers M. Raw material pricing and Additive Manufacturing 2014.
[134] Manogharan G, Wysk RA, Harrysson OLA. Additive manufacturing–integrated hybrid manufacturing and subtractive processes: economic model and analysis. International Journal of Computer Integrated Manufacturing 2016;29:473–88. https://doi.org/10/ggcqvs.
[135] Thompson MK, Moroni G, Vaneker T, Fadel G, Campbell RI, Gibson I, et al. Design for Additive Manufacturing: Trends, opportunities, considerations, and constraints. CIRP Annals 2016;65:737–60. https://doi.org/10/f85q6d.
[136] Aliakbari M. Additive manufacturing: State-of-the-art, capabilities, and sample applications with cost analysis. 2012.
[137] Strauß H. AM Envelope / The potential of Additive Manufacturing for façade construction n.d.:278.
[138] Baumers M, Tuck C, Wildman R, Ashcroft I, Hague R. Shape Complexity and Process Energy Consumption in Electron Beam Melting: A Case of Something for Nothing in Additive Manufacturing?: Shape Complexity and Energy Usage in 3D Printing. Journal of Industrial Ecology 2017;21:S157–67. https://doi.org/10.1111/jiec.12397.
[139] Jackson MA, Van Asten A, Morrow JD, Min S, Pfefferkorn FE. A Comparison of Energy Consumption in Wire-based and Powder-based Additive-subtractive Manufacturing. Procedia Manufacturing 2016;5:989–1005. https://doi.org/10/ggcqvw.
[140] Bekker ACM, Verlinden JC, Galimberti G. Challenges in Assessing the Sustainability of Wire + Arc Additive Manufacturing for Large Structures n.d.:11.
[141] Lawrence A, Thollander P, Andrei M, Karlsson M. Specific Energy Consumption/Use (SEC) in Energy Management for Improving Energy Efficiency in Industry: Meaning, Usage and Differences. Energies 2019;12:247. https://doi.org/10.3390/en12020247.
[142] Baumers M, Tuck C, Wildman R, Ashcroft I, Hague R. Energy inputs to additive manufacturing: does capacity utilization matter? EOS 2011;1000:30–40.
[143] Kellens K, Yasa E, Dewulf W, Duflou J. Environmental assessment of selective laser melting and selective laser sintering. Going Green-Care Innovation: From Legal Compliance to Energy-Efficient Products and Services, Paper 2010:5.
[144] Faludi J, Baumers M, Maskery I, Hague R. Environmental impacts of selective laser melting: do printer, powder, or power dominate? Journal of Industrial Ecology 2017;21:S144–56. https://doi.org/10/gcmxcb.
[145] Wilson JM, Piya C, Shin YC, Zhao F, Ramani K. Remanufacturing of turbine blades by laser direct deposition with its energy and environmental impact analysis. Journal of Cleaner Production 2014;80:170–8. https://doi.org/10/f6fvdt.
[146] Huang R, Riddle M, Graziano D, Warren J, Das S, Nimbalkar S, et al. Energy and emissions saving potential of additive manufacturing: the case of lightweight aircraft components. Journal of Cleaner Production 2016;135:1559–70.
[147] Morrow WR, Qi H, Kim I, Mazumder J, Skerlos SJ. Environmental aspects of laser-based and conventional tool and die manufacturing. Journal of Cleaner Production 2007;15:932–43.
[148] Vayre B, Vignat F, Villeneuve F. Metallic additive manufacturing: state-of-the-art review and prospects. Mechanics & Industry 2012;13:89–96. https://doi.org/10/ggcqwb.
[149] Atzeni E, Iuliano L, Marchiandi G, Minetola P, Salmi A, Bassoli E, et al. Additive manufacturing as a cost-effective way to produce metal parts. In: da Silva Bártolo P, de Lemos A, Pereira A, Mateus A, Ramos C, Santos C, et al., editors. High Value Manufacturing: Advanced Research in Virtual and Rapid Prototyping, CRC Press; 2013, p. 3–8. https://doi.org/10.1201/b15961-3.
[150] Piili H, Happonen A, Väistö T, Venkataramanan V, Partanen J, Salminen A. Cost Estimation of Laser Additive Manufacturing of Stainless Steel. Physics Procedia 2015;78:388–96. https://doi.org/10.1016/j.phpro.2015.11.053.
[151] Cunningham CR, Wikshåland S, Xu F, Kemakolam N, Shokrani A, Dhokia V, et al. Cost Modelling and Sensitivity Analysis of Wire and Arc Additive Manufacturing. Procedia Manufacturing 2017;11:650–7. https://doi.org/10/gdz4fd.
[152] Stecker S, Lachenberg KW, Wang H, Salo RC. Advanced electron beam free form fabrication methods & technology. American Welding Society Conference, Missoula, MT, Nov, vol. 17, 2006, p. 35–46.
[153] Li Y, Huang X, Horváth I, Zhang G. GMAW-based additive manufacturing of inclined multi-layer multi-bead parts with flat-position deposition. Journal of Materials Processing Technology 2018;262:359–71. https://doi.org/10.1016/j.jmatprotec.2018.07.010.

[154] Li Y, Sun Y, Han Q, Zhang G, Horváth I. Enhanced beads overlapping model for wire and arc additive manufacturing of multi-layer multi-bead metallic parts. Journal of Materials Processing Technology 2018;252:838–48. https://doi.org/10/gcp8r7.
[155] Ehigiator O. Investigation of wire and arc additive manufacturing methods for high integrity, high productivity fabrication of large steel structures. Thesis. 2021.
[156] Wang Z, Denlinger E, Michaleris P, Stoica AD, Ma D, Beese AM. Residual stress mapping in Inconel 625 fabricated through additive manufacturing: Method for neutron diffraction measurements to validate thermomechanical model predictions. Materials & Design 2017;113:169–77. https://doi.org/10/ggcqv7.
[157] Haden CV, Zeng G, Carter FM, Ruhl C, Krick BA, Harlow DG. Wire and arc additive manufactured steel: Tensile and wear properties. Additive Manufacturing 2017;16:115–23. https://doi.org/10.1016/j.addma.2017.05.010.
[158] ASM Handbook, Volume 1: Properties and Selection: Irons, Steels, and High-Performance Alloys - ASM International n.d. https://www.asminternational.org/home/-/journal_content/56/10192/06181G/PUBLICATION (accessed November 12, 2019).
[159] Bönisch M. Structural properties, deformation behavior and thermal stability of martensitic Ti-Nb alloys. 2016.
[160] Maresca F, Curtin WA. The austenite/lath martensite interface in steels: Structure, athermal motion, and in-situ transformation strain revealed by simulation and theory. Acta Materialia 2017;134:302–23. https://doi.org/10.1016/j.actamat.2017.05.044.
[161] Wolff SJ, Gan Z, Lin S, Bennett JL, Yan W, Hyatt G, et al. Experimentally validated predictions of thermal history and microhardness in laser-deposited Inconel 718 on carbon steel. Additive Manufacturing 2019;27:540–51. https://doi.org/10/ggcqv6.
[162] Zhang H, Jian H, Wang G, Qi H, Xie Y. Research on Microstructure and Properties of Medium Carbon Steel Parts Manufactured by HDMR Technology 2015.
[163] Aggarangsi P, Beuth JL. Localized preheating approaches for reducing residual stress in additive manufacturing. Proc. SFF Symp., Austin, 2006, p. 709–20.
[164] Yan W, Yue Z, Zhang J. Study on the residual stress and warping of stiffened panel produced by electron beam freeform fabrication. Materials & Design 2016;89:1205–12. https://doi.org/10/f73wbd.
[165] Colegrove PA, Coules HE, Fairman J, Martina F, Kashoob T, Mamash H, et al. Microstructure and residual stress improvement in wire and arc additively manufactured parts through high-pressure rolling. Journal of Materials Processing Technology 2013;213:1782–91. https://doi.org/10/gfsb84.
[166] Almeida DF, Martins RF, Cardoso JB. Numerical simulation of residual stresses induced by TIG butt-welding of thin plates made of AISI 316L stainless steel. Procedia Structural Integrity 2017;5:633–9. https://doi.org/10/ggcqwh.
[167] Martina F, Roy MJ, Szost BA, Terzi S, Colegrove PA, Williams SW, et al. Residual stress of as-deposited and rolled wire+arc additive manufacturing Ti–6Al–4V components. Materials Science and Technology 2016;32:1439–48. https://doi.org/10.1080/02670836.2016.1142704.
[168] Szost BA, Terzi S, Martina F, Boisselier D, Prytuliak A, Pirling T, et al. A comparative study of additive manufacturing techniques: Residual stress and microstructural analysis of CLAD and WAAM printed Ti–6Al–4V components. Materials & Design 2016;89:559–67. https://doi.org/10/f73gxq.
[169] Hönnige JR, Colegrove PA, Ganguly S, Eimer E, Kabra S, Williams S. Control of residual stress and distortion in aluminium wire + arc additive manufacture with rolling. Additive Manufacturing 2018;22:775–83. https://doi.org/10.1016/j.addma.2018.06.015.
[170] ASTM E8 / E8M-16a Standard Test Methods for Tension Testing of Metallic Materials. ASTM International, West Conshohocken, PA.; n.d. https://doi.org/10.1520/E0008_E0008M-16A.
[171] ASTM D3846-08(2015) Standard Test Method for In-Plane Shear Strength of Reinforced Plastics. ASTM International, West Conshohocken, PA.; n.d. https://doi.org/10.1520/D3846-08R15.
[172] ASTM E290-14 Standard Test Methods for Bend Testing of Material for Ductility. ASTM International, West Conshohocken, PA.; n.d. https://doi.org/10.1520/E0290-14.
[173] Mazumder J, Song L. Advances in Direct Metal Deposition 2013:6. https://doi.org/10/ggcqvt.
[174] ASTM E111-98 Standard Test Method for Young's Modulus, Tangent Modulus, And Chord Modulus. ASTM International, West Conshohocken, PA.; 1998.
[175] Domack MS, Taminger KM, Begley M. Metallurgical Mechanisms Controlling Mechanical Properties of Aluminium Alloy 2219 Produced by Electron Beam Freeform Fabrication. Materials science forum, vol. 519, Trans Tech Publ; 2006, p. 1291–6.
[176] Taminger KM, Hafley RA. Electron beam freeform fabrication (EBF3) for cost effective near-net shape manufacturing 2006.
[177] Stecker S, Lachenberg KW, Wang H, Salo RC. Advanced electron beam free form fabrication methods & technology. American Welding Society Conference, Missoula, MT, Nov, vol. 17, 2006, p. 35–46.
[178] Wanjara P, Brochu M, Jahazi M. Electron beam freeforming of stainless steel using solid wire feed. Materials & Design 2007;28:2278–86. https://doi.org/10.1016/j.matdes.2006.08.008.

[179] Haden CV, Zeng G, Carter FM, Ruhl C, Krick BA, Harlow DG. Wire and arc additive manufactured steel: Tensile and wear properties. Additive Manufacturing 2017;16:115–23. https://doi.org/10.1016/j.addma.2017.05.010.
[180] Filomeno Martina. Recap of WAAM Mechanical Properties 2019.
[181] Baufeld B, Van der Biest O, Gault R. Additive manufacturing of Ti–6Al–4V components by shaped metal deposition: microstructure and mechanical properties. Materials & Design 2010;31:S106–11. https://doi.org/10/dwmrxw.
[182] Filomeno Martina. Recap of WAAM Mechanical Properties 2019.
[183] Enhancing mechanical properties of wire + arc additively manufactured INCONEL 718 superalloy through in-process thermomechanical processing. Materials & Design 2018;160:1042–51. https://doi.org/10.1016/j.matdes.2018.10.038.
[184] Shamsaei N, Yadollahi A, Bian L, Thompson SM. An overview of Direct Laser Deposition for additive manufacturing; Part II: Mechanical behavior, process parameter optimization and control. Additive Manufacturing 2015;8:12–35. https://doi.org/10/gddmz9.
[185] Wallace TA, Bey KS, Taminger KM, Hafley RA. A design of experiments approach defining the relationships between processing and microstructure for Ti-6Al-4V. DTIC Document; 2004.
[186] Taminger KM, Domack CS, Zalameda JN, Taminger BL, Hafley RA, Burke ER. In-process thermal imaging of the electron beam freeform fabrication process. In: Zalameda JN, Bison P, editors., Baltimore, Maryland, United States: 2016, p. 986102. https://doi.org/10/ggcqwm.
[187] Xu F, Dhokia V, Colegrove P, McAndrew A, Williams S, Henstridge A, et al. Realisation of a multi-sensor framework for process monitoring of the wire arc additive manufacturing in producing Ti-6Al-4V parts. International Journal of Computer Integrated Manufacturing 2018;31:785–98. https://doi.org/10/ggcqv8.
[188] Thomas E. Blejwas. Trends in Large-scale Testing of Reactor Structures. Transactions of the 17th International Conference on Structural Mechanics in Reactor Technology (SMiRT 17), Prague, Czech Republic: IASMiRT; 2003.
[189] Jha A, Sedaghati R, Bhat R. Dynamic Testing of Structures Using Scale Models. 46th AIAA/ASME/ASCE/AHS/ASC Structures, Structural Dynamics and Materials Conference, American Institute of Aeronautics and Astronautics; 2005. https://doi.org/10.2514/6.2005-2259.
[190] Kenton W. Cottage Industry is manufacturing on a small scale. Investopedia n.d. https://www.investopedia.com/terms/c/cottage-industry.asp (accessed August 13, 2021).
[191] Ramu M, Prabhu Raja V, Thyla PR. Establishment of structural similitude for elastic models and validation of scaling laws. KSCE J Civ Eng 2013;17:139–44. https://doi.org/10/gfx6tp.
[192] Hanus R. HEAVY STEEL CASTING COMPONENTS FOR POWER PLANTS "MEGA-COMPONENTS" MADE OF HIGH CR-STEELS. Materials for Advanced Power Engineering 2010:10.
[193] Rubenchik AM, King WE, Wu SS. Scaling laws for the additive manufacturing. Journal of Materials Processing Technology 2018;257:234–43. https://doi.org/10/gnnt2x.
[194] Molina A, Rodriguez CA, Ahuett H, Cortés JA, Ramírez M, Jiménez G, et al. Next-generation manufacturing systems: key research issues in developing and integrating reconfigurable and intelligent machines. International Journal of Computer Integrated Manufacturing 2005;18:525–36. https://doi.org/10/bhqt68.
[195] Huang Y, Leu MC, Mazumder J, Donmez A. Additive Manufacturing: Current State, Future Potential, Gaps and Needs, and Recommendations. Journal of Manufacturing Science and Engineering 2015;137:014001. https://doi.org/10/gctr4b.
[196] Mahmood K, Karaulova T, Otto T, Shevtshenko E. Performance Analysis of a Flexible Manufacturing System (FMS). Procedia CIRP 2017;63:424–9. https://doi.org/10/gfx776.
[197] O'Grady PJ, Menon U. A concise review of flexible manufacturing systems and FMS literature. Computers in Industry 1986;7:155–67. https://doi.org/10/c9v8q9.
[198] Lee WB, Cheung CF, Li JG. Applications of virtual manufacturing in materials processing. Journal of Materials Processing Technology 2001;113:416–23. https://doi.org/10/dg3vw4.
[199] Monzón MD, Ortega Z, Martínez A, Ortega F. Standardization in additive manufacturing: activities carried out by international organizations and projects. Int J Adv Manuf Technol 2015;76:1111–21. https://doi.org/10/gfx782.
[200] Beaman JJ, Atwood C, Bergman TL, Bourell D, Hollister S, Rosen D. Additive/Subtractive Manufacturing Research and Development in Europe: Fort Belvoir, VA: Defense Technical Information Center; 2004. https://doi.org/10.21236/ADA466756.
[201] Adebayo A. CHARACTERISATION OF INTEGRATED WAAM AND MACHINING PROCESSES n.d.:262.
[202] Wang Z, Palmer TA, Beese AM. Effect of processing parameters on microstructure and tensile properties of austenitic stainless steel 304L made by directed energy deposition additive manufacturing. Acta Materialia 2016;110:226–35. https://doi.org/10/f8kmk6.
[203] Bremer C. Automated Repair and Overhaul of Aero-Engine and Industrial Gas Turbine Components 2005:841–6. https://doi.org/10/b7vcqz.

[204] Rodrigues TA, Duarte V, Miranda RM, Santos TG, Oliveira JP. Current Status and Perspectives on Wire and Arc Additive Manufacturing (WAAM). Materials 2019;12:1121. https://doi.org/10/gkp5vp.
[205] Davis JR, editor. Metals Handbook Desk Edition. ASM International; 1998. https://doi.org/10.31399/asm.hb.mhde2.9781627081993.
[206] Bartha B. Nondestructive Evaluation Applications for Failure Analysis. In: Miller BA, Shipley RJ, Parrington RJ, Dennies DP, editors. Failure Analysis and Prevention, vol. 11, ASM International; 2021, p. 0. https://doi.org/10.31399/asm.hb.v11.a0006758.
[207] Hauk V. Structural and Residual Stress Analysis by Nondestructive Methods: Evaluation - Application - Assessment. Elsevier; 1997.
[208] Mauri G. INTEGRATING SAFETY ANALYSIS TECHNIQUES, SUPPORTING IDENTIFICATION OF COMMON CAUSE FAILURES n.d.:193.
[209] Albishi A, Ramahi OM. Detection of Surface and Subsurface Cracks in Metallic and Non-Metallic Materials Using a Complementary Split-Ring Resonator. Sensors (Basel) 2014;14:19354–70. https://doi.org/10/gcfrxr.
[210] Jinwu K, Tianyou H, Baicheng L. Review of production status of heavy steel castings and key technologies for their manufacture in China. CHINA FOUNDRY 2008:6.
[211] Findlay SJ, Harrison ND. Why aircraft fail. Materials Today 2002;5:18–25. https://doi.org/10/bkjrwt.
[212] Ahlfors M. Hot Isostatic Pressing for Metal Additive Manufacturing 2020. https://doi.org/10/gnnt24.
[213] Lu X, Lin X, Chiumenti M, Cervera M, Hu Y, Ji X, et al. Residual stress and distortion of rectangular and S-shaped Ti-6Al-4V parts by Directed Energy Deposition: Modelling and experimental calibration. Additive Manufacturing 2019;26:166–79. https://doi.org/10/ggcqwf.
[214] Kandil FA, Lord JD, Fry AT, Grant PV. A Review of Residual Stress Measurement Methods - A Guide to Technique Selection. n.d.:45.
[215] Rosen DW. Computer-Aided Design for Additive Manufacturing of Cellular Structures. Computer-Aided Design and Applications 2007;4:585–94. https://doi.org/10/gj5rrb.
[216] Duranton P, Devaux J, Robin V, Gilles P, Bergheau JM. 3D modelling of multipass welding of a 316L stainless steel pipe. Journal of Materials Processing Technology 2004:7. https://doi.org/10/bb2t7w.
[217] Traidia A, Roger F, Guyot E, Schroeder J, Lubineau G. Hybrid 2D–3D modelling of GTA welding with filler wire addition. International Journal of Heat and Mass Transfer 2012;55:3946–63. https://doi.org/10/gk87ks.
[218] Graf M, Hälsig A, Höfer K, Awiszus B, Mayr P. Thermo-Mechanical Modelling of Wire-Arc Additive Manufacturing (WAAM) of Semi-Finished Products. Metals 2018;8:1009. https://doi.org/10/gjw38x.
[219] Ding J, Colegrove P, Mehnen J, Ganguly S, Sequeira Almeida PM, Wang F, et al. Thermo-mechanical analysis of Wire and Arc Additive Layer Manufacturing process on large multi-layer parts. Computational Materials Science 2011;50:3315–22. https://doi.org/10/bskv78.
[220] Lindgren L-E, Hedblom E. Modelling of addition of filler material in large deformation analysis of multipass welding. Commun Numer Meth Engng 2001;17:647–57. https://doi.org/10/bkfgm5.
[221] Galan-Lopez J, Naghdy S, Verleysen P, Kestens LAI, Coghe F, Rabet L, et al. Mechanical behavior and texture prediction of Ti-6Al-4V based on elastic viscoplastic self-consistent modelling. IOP Conf Ser: Mater Sci Eng 2015;82:012027. https://doi.org/10/gjw39n.
[222] Tan P, Shen F, Li B, Zhou K. A thermo-metallurgical-mechanical model for selective laser melting of Ti6Al4V. Materials & Design 2019;168:107642. https://doi.org/10/gjw387.
[223] Lu X, Lin X, Chiumenti M, Cervera M, Li J, Ma L, et al. Finite element analysis and experimental validation of the thermomechanical behavior in laser solid forming of Ti-6Al-4V. Additive Manufacturing 2018;21:30–40. https://doi.org/10/ggcqwd.
[224] Hajializadeh F, Ince A. Short review on modeling approaches for metal additive manufacturing process. Material Design & Processing Communications 2020;2:e56. https://doi.org/10/gnnt23.
[225] Heigel JC, Michaleris P, Reutzel EW. Thermo-mechanical model development and validation of directed energy deposition additive manufacturing of Ti–6Al–4V. Additive Manufacturing 2015;5:9–19. https://doi.org/10/ggcqv9.
[226] Chen Z, Ye H, Xu H. Distortion control in a wire-fed electron-beam thin-walled Ti-6Al-4V freeform. Journal of Materials Processing Technology 2018;258:286–95. https://doi.org/10.1016/j.jmatprotec.2018.04.008.
[227] Heigel JC. Thermo-Mechanical Model Development and Experimental Validation for Directed Energy Deposition Additive Manufacturing Processes n.d. https://etda.libraries.psu.edu/files/final_submissions/10633 (accessed November 10, 2021).
[228] Biegler M, Marko A, Graf B, Rethmeier M. Finite element analysis of in-situ distortion and bulging for an arbitrarily curved additive manufacturing directed energy deposition geometry. Additive Manufacturing 2018;24:264–72. https://doi.org/10/gnnt22.
[229] Wilby AJ, Neale DP. Defects introduced into Metals during Fabrication and Service. MATERIALS SCIENCE AND ENGINEERING-Volume III 2009;5:48.
[230] Ortiz AF, Rodríguez SA, Coronado JJ. Failure analysis of the engine cylinder of a training aircraft. Engineering Failure Analysis 2013;35:686–91. https://doi.org/10.1016/j.engfailanal.2013.06.010.

[231] David Sandusky, David Gandy. Welding and Fabrication Innovations Mitigate Reactor Pressure Vessel Embrittlement in Nuclear Plant Construction. POWER Magazine 2014. https://www.powermag.com/welding-and-fabrication-innovations-mitigate-reactor-pressure-vessel-embrittlement-in-nuclear-plant-construction/ (accessed November 12, 2019).
[232] Voronenko BI. Hydrogen and flakes in steel. Met Sci Heat Treat 1997;39:462–70. https://doi.org/10/d7x2nx.
[233] Wyman O. MRO Survey 2017: When Growth Outpaces Capacity n.d. https://www.oliverwyman.com/our-expertise/insights/2017/apr/mro-survey-2017.html (accessed November 12, 2019).
[234] Deppe G, Koch R. Supporting the Decision Process for Applying Additive Manufacturing in the MRO Aerospace Business by MADM n.d.:12.
[235] Wyman O. 2017 – 2027 Fleet & MRO Forecast n.d. http://www.oliverwyman.com/our-expertise/insights/2017/feb/2017-2027-fleet-mro-forecast.html (accessed February 18, 2018).
[236] Surugiu M-R, Surugiu C. International Trade, Globalization and Economic Interdependence between European Countries: Implications for Businesses and Marketing Framework. Procedia Economics and Finance 2015;32:131–8. https://doi.org/10/ghc33n.
[237] Corbett JJ, Winebrake J. The Impacts of Globalisation on International Maritime Transport Activity n.d.:31.
[238] Tongzon J. The Challenge of Globalization for the Logistics Industry: Evidence from Indonesia. Transportation Journal 2012;51:5–32. https://doi.org/10/gmtphn.
[239] International Maritime Shipping: The Impact of Globalisation on Activity Levels. ResearchGate n.d. https://doi.org/10.1787/9789264072916-5-en.
[240] Kherbash O, Mocan ML. A Review of Logistics and Transport Sector as a Factor of Globalization. Procedia Economics and Finance 2015;27:42–7. https://doi.org/10/d6cv.
[241] Heavy Manufacturing of Power Plants - World Nuclear Association n.d. https://www.world-nuclear.org/information-library/nuclear-fuel-cycle/nuclear-power-reactors/heavy-manufacturing-of-power-plants.aspx (accessed November 12, 2019).
[242] Failures Related to Metalworking 2002. https://doi.org/10/gmtphq.
[243] Esaklul KA. Handbook of Case Histories in Failure Analysis, Volume 1. ASM International; 1992.
[244] Failure Analysis and Prevention 2002. https://doi.org/10/gmtphp.
[245] Zheng K, Politis DJ, Wang L, Lin J. A review on forming techniques for manufacturing lightweight complex—shaped aluminium panel components. International Journal of Lightweight Materials and Manufacture 2018;1:55–80. https://doi.org/10/gfj4qj.
[246] Thompson BD, Badgley RH, Hartranft JJ. Experience From Expansion of On-Board Maintenance for Marine Gas Turbines. Volume 2: Aircraft Engine; Marine; Microturbines and Small Turbomachinery, Toronto, Ontario, Canada: American Society of Mechanical Engineers; 1989, p. V002T03A008. https://doi.org/10/gmtphm.
[247] Outland T, Rogers D, Awiszus G. SPLIT CASING DESIGN FACILITATING IN-SITU REPAIR AND MAINTENANCE n.d.:3.
[248] Gramopadhye AK, Drury CG. Human factors in aviation maintenance: how we got to where we are. International Journal of Industrial Ergonomics 2000;26:125–31. https://doi.org/10.1016/S0169-8141(99)00062-1.
[249] Counselman R. Repair Welding of Castings 2008. https://doi.org/10/gmtphf.
[250] Nichol CI, Pace DP, Larsen ED, McJunkin TR, Clark DE, Clark ML, et al. Yucca Mountain Waste Package Closure System Robotic Welding and Inspection System. Nuclear Technology 2011;176:138–46. https://doi.org/10/gmtphk.
[251] Rodrigues D, Lavorato P. Maintenance, Repair and Overhaul (MRO) Fundamentals and Strategies: An Aeronautical Industry Overview. IJCA 2016;135:21–9. https://doi.org/10/d4mb.
[252] Popoola LT, Grema AS, Latinwo GK, Gutti B, Balogun AS. Corrosion problems during oil and gas production and its mitigation. Int J Ind Chem 2013;4:35. https://doi.org/10/gj267q.
[253] Nov 30, Seidenman 2015 Paul, MRO DJS| I. Next-Gen Jets Driving New Repair Technology Trends n.d. http://aviationweek.com/advanced-machines-aerospace-manufacturing/next-gen-jets-driving-new-repair-technology-trends (accessed February 26, 2018).
[254] Internationale Atomenergie-Organisation, editor. Heavy component replacement in nuclear power plants: experience and guidelines. Vienna: IAEA; 2008.
[255] Cox M, Bihlman B. Aeromaterials: Past, Present and Future. MMTA 2015.
[256] October 13, 2015, Bill Bihlman. Aerospace materials and design. Aerospace Manufacturing and Design 2015. http://www.aerospacemanufacturinganddesign.com/article/amd1015-aerospace-materials-design-outlook/ (accessed February 26, 2018).
[257] Michael C. Gabriele. World Titanium Industry Supply & Demand Overview - International Titanium Association n.d. http://www.titanium.org/news/314739/World-Titanium-Industry-Supply--Demand-Overview.htm (accessed February 18, 2018).
[258] An outlook for titanium metal. Thomas Hohne-Sparborth October PDF Free Download n.d. https://docplayer.net/150944301-An-outlook-for-titanium-metal-thomas-hohne-sparborth-october-2017.html (accessed November 20, 2021).

[259] Additive Manufacturing for the Aircraft Industry: A Review n.d. https://www.longdom.org/open-access/additive-manufacturing-for-the-aircraft-industry-a-review-18967.html (accessed August 19, 2021).
[260] WORLD STEEL RECYCLING IN FIGURES 2015 – 2019 Steel Scrap – a Raw Material for Steelmaking n.d. https://www.bir.org/publications/facts-figures/download/643/175/36?method=view (accessed September 13, 2021).
[261] Kumar A, Jain PK, Pathak PM. Reverse Engineering in Product Manufacturing: An Overview. In: Katalinic B, Tekic Z, editors. DAAAM International Scientific Book, vol. 12. 1st ed., DAAAM International Vienna; 2013, p. 665–78. https://doi.org/10.2507/daaam.scibook.2013.39.
[262] Verim Ö, Yumurtaci M. Application of reverse engineering approach on a damaged mechanical part, 2020. https://doi.org/10/gmtphd.
[263] Tut V, Tulcan A, Cosma C, Serban I. Application of CAD / CAM / FEA , reverse engineering and rapid prototyping in manufacturing industry 2010. https://www.semanticscholar.org/paper/Application-of-CAD-%2F-CAM-%2F-FEA-%2C-reverse-and-rapid-Tut-Tulcan/ee0b94f98a2a4621811cf017c52babb5802abd59 (accessed August 19, 2021).
[264] Wells C. The Forging of Compressor and Turbine Blades. The Development of Gas Turbine Materials, Springer, Dordrecht; 1981, p. 207–28. https://doi.org/10.1007/978-94-009-8111-9_8.
[265] Lee HJ, Strahan N, Boyd E. Turbocharger Jet Engine Build and Engineering Analysis 2016.
[266] Turnover in UK production and Great Britain services industries: monthly production and services turnover - Office for National Statistics n.d. https://www.ons.gov.uk/businessindustryandtrade/manufacturingandproductionindustry/datasets/topsiproductionandservicesturnover (accessed August 19, 2021).
[267] Plans for New Nuclear Reactors Worldwide - World Nuclear Association n.d. https://world-nuclear.org/information-library/current-and-future-generation/plans-for-new-reactors-worldwide.aspx (accessed August 19, 2021).
[268] Saboori A, Aversa A, Marchese G, Biamino S, Lombardi M, Fino P. Application of Directed Energy Deposition-Based Additive Manufacturing in Repair. Applied Sciences 2019;9:3316. https://doi.org/10/gg7r35.
[269] Wyman O. 2017 – 2027 Fleet & MRO Forecast n.d. http://www.oliverwyman.com/our-expertise/insights/2017/feb/2017-2027-fleet-mro-forecast.html (accessed February 18, 2018).
[270] Liberini M, Astarita A, Campatelli G, Scippa A, Montevecchi F, Venturini G, et al. Selection of Optimal Process Parameters for Wire Arc Additive Manufacturing. Procedia CIRP 2017;62:470–4. https://doi.org/10.1016/j.procir.2016.06.124.
[271] Dinda GP, Dasgupta AK, Mazumder J. Texture control during laser deposition of nickel-based superalloy. Scripta Materialia 2012;67:503–6. https://doi.org/10.1016/j.scriptamat.2012.06.014.
[272] Bhattacharjya J, Tripathi S, Taylor A, Taylor M, Walters D. Additive Manufacturing: Current Status and Future Prospects. In: Bayro-Corrochano E, Hancock E, editors. Progress in Pattern Recognition, Image Analysis, Computer Vision, and Applications, vol. 8827, Cham: Springer International Publishing; 2014, p. 365–72. https://doi.org/10.1007/978-3-662-44745-1_36.
[273] Frank LK. The Significance of Industrial Integration. Journal of Political Economy 1925;33:179–95. https://doi.org/10/bzfst2.
[274] The American Society of Mechanical Engineers. 71-ALCOA-50000-ton-Hydraulic-Forging-Press.pdf 1981.
[275] Beiderbeck D, Deradjat D, Minshall T. The Impact of Additive Manufacturing Technologies on Industrial Spare Parts Strategies 2018. https://doi.org/10/gfx8c5.
[276] Beiderbeck D, Deradjat D, Minshall T. The Impact of Additive Manufacturing Technologies on Industrial Spare Parts Strategies 2018. https://doi.org/10/gfx8c5.
[277] McNulty CM, Arnas N, Campbell TA. Toward the Printed World: Additive Manufacturing and Implications for National Security n.d.:16.
[278] McNulty CM, Arnas N, Campbell TA. Toward the Printed World: Additive Manufacturing and Implications for National Security n.d.:16.
[279] David Santos González, Almudena González Álvarez (Fundación Prodintec). ADDITIVE MANUFACTURING FEASIBILITY STUDY & TECHNOLOGY DEMONSTRATION. European Defence Agency; 2018.
[280] Brettel M, Friederichsen N, Keller M, Rosenberg M. How Virtualization, Decentralization and Network Building Change the Manufacturing Landscape: An Industry 4.0 Perspective 2014;8:8.
[281] Lasi H, Fettke P, Kemper H-G, Feld T, Hoffmann M. Industry 4.0. Bus Inf Syst Eng 2014;6:239–42. https://doi.org/10/gfx8dd.
[282] Mourtzis D, Doukas M. Design and Planning of Manufacturing Networks for Mass Customisation and Personalisation: Challenges and Outlook. Procedia CIRP 2014;19:1–13. https://doi.org/10/gfx8d9.
[283] Vogel-Heuser B, Fay A, Schaefer I, Tichy M. Evolution of software in automated production systems: Challenges and research directions. Journal of Systems and Software 2015;110:54–84. https://doi.org/10/gfx8df.

[284] Ahmad SN, Manurung YH, Mat MF, Minggu Z, Jaffar A, Pruller S, et al. FEM Simulation Procedure for Distortion and Residual Stress Analysis of Wire Arc Additive Manufacturing. IOP Conf Ser: Mater Sci Eng 2020;834:012083. https://doi.org/10/gjw38w.
[285] Dong P, Hong JK, Bouchard PJ. Analysis of residual stresses at weld repairs. International Journal of Pressure Vessels and Piping 2005;82:258–69. https://doi.org/10.1016/j.ijpvp.2004.08.004.
[286] Lindgaard G, Dillon R, Trbovich P, White R, Fernandes G, Lundahl S, et al. User Needs Analysis and requirements engineering: Theory and practice. Interacting with Computers 2006;18:47–70. https://doi.org/10/dsk8c3.
[287] Requirements Engineering: A Good Practice Guide | Wiley. WileyCom 2022. https://www.wiley.com/ (accessed November 3, 2021).
[288] Nuseibeh B, Easterbrook S. Requirements engineering: a roadmap. Proceedings of the conference on The future of Software engineering - ICSE '00, Limerick, Ireland: ACM Press; 2000, p. 35–46. https://doi.org/10/b5hfzg.
[289] Cross N. A History of Design Methodology. In: Vries MJ, Cross N, Grant DP, editors. Design Methodology and Relationships with Science, Dordrecht: Springer Netherlands; 1993, p. 15–27. https://doi.org/10.1007/978-94-015-8220-9_2.
[290] Penny RK. Principles of engineering design. Postgraduate Medical Journal 1970;46:344–9. https://doi.org/10.1136/pgmj.46.536.344.
[291] Hurst K. Engineering Design Principles. Butterworth-Heinemann; 1999.
[292] Linda A. Universal Principles Of Design 1970.
[293] FUNdaMENTALS of Design 2014. http://pergatory.mit.edu/resources/fundamentals.html (accessed December 31, 2021).
[294] Taylor FW. The Principles of Scientific Management. 1st World Publishing; 2005.
[295] Jacobs FR, Chase RB. Operations and supply chain management. Fourteenth edition. New York: McGraw-Hill/Irwin; 2014.
[296] Groover's Principles of Modern Manufacturing: Materials, Processes, and Systems, SI Version, 6th Edition, Global Edition | Wiley. WileyCom n.d. https://www.wiley.com/en-ie/Groover%27s+Principles+of+Modern+Manufacturing%3A+Materials%2C+Processes%2C+and+Systems%2C+SI+Version%2C+6th+Edition%2C+Global+Edition-p-9781119249122 (accessed December 31, 2021).
[297] Drucker PF. The Emerging Theory of Manufacturing. Harvard Business Review 1990.
[298] Crandall RE, Crandall W. How Management Programs Can Improve Organization Performance: Selecting and Implementing the Best Program for Your Organization. IAP; 2015.
[299] Pindur W, Rogers SE, Suk Kim P. The history of management: a global perspective. Journal of Management History 1995;1:59–77. https://doi.org/10.1108/13552529510082831.
[300] Hines P, Holweg M, Rich N. Learning to evolve: A review of contemporary lean thinking. International Journal of Operations & Production Management 2004;24:994–1011. https://doi.org/10.1108/01443570410558049.
[301] Lean Thinking: Banish Waste and Create Wealth in Your Corporation by James P. Womack 1970. https://www.goodreads.com/book/show/289467.Lean_Thinking (accessed December 31, 2021).
[302] A Brief History of Lean. Lean Enterprise Institute 1970. https://www.lean.org/explore-lean/a-brief-history-of-lean/ (accessed December 31, 2021).
[303] Jones D, Roos D, Womack J. The Machine That Changed the World. Lean Enterprise Institute 1970. https://www.lean.org/store/book/the-machine-that-changed-the-world/ (accessed December 31, 2021).
[304] Bicheno J, Holweg M. The Lean Toolbox, 5th edition. A handbook for lean transformation. 2016.
[305] Hitchcock C. Causal Models. In: Zalta EN, editor. The Stanford Encyclopedia of Philosophy. Summer 2020, Metaphysics Research Lab, Stanford University; 2020.
[306] Greenland S. The Logic and Philosophy of Causal Inference: A Statistical Perspective. In: Bandyopadhyay PS, Forster MR, editors. Philosophy of Statistics, vol. 7, Amsterdam: North-Holland; 2011, p. 813–30. https://doi.org/10.1016/B978-0-444-51862-0.50026-5.
[307] Mele C, Pels J, Polese F. A Brief Review of Systems Theories and Their Managerial Applications. Service Science 2010;2:126–35. https://doi.org/10.1287/serv.2.1_2.126.
[308] Montuori A. Systems Approach. In: Runco MA, Pritzker SR, editors. Encyclopedia of Creativity (Second Edition), San Diego: Academic Press; 2011, p. 414–21. https://doi.org/10.1016/B978-0-12-375038-9.00212-0.
[309] Marchal JH. On the Concept of a System. Philosophy of Science 1975;42:448–68. https://doi.org/10.1086/288663.
[310] Green J. The Application of Black Box Theory to System Development n.d.:18.
[311] Schaffernicht M, Empresariales FDC. 1 Causality and diagrams for system dynamics n.d.
[312] Weiner B. Heider, Fritz (1896–1988). In: Smelser NJ, Baltes PB, editors. International Encyclopedia of the Social & Behavioral Sciences, Oxford: Pergamon; 2001, p. 6650–4. https://doi.org/10.1016/B0-08-043076-7/00257-6.
[313] Schaffernicht M. Causal loop diagrams between structure and behaviour: A critical analysis of the relationship between polarity, behaviour and events. Systems Research and Behavioral Science 2010;27:653–66. https://doi.org/10.1002/sres.1018.

[314] System Dynamics Methods: A Quick Introduction 1970. https://www.public.asu.edu/~kirkwood/sysdyn/SDIntro/SDIntroduction.htm (accessed January 25, 2022).
[315] Boyle RP. Causal Theory and Statistical Measures of Effect: A Convergence. American Sociological Review 1966;31:843–51. https://doi.org/10.2307/2091663.
[316] Measures of Variability. The SAGE Encyclopedia of Communication Research Methods, 2455 Teller Road, Thousand Oaks California 91320: SAGE Publications, Inc; 2017. https://doi.org/10.4135/9781483381411.n333.
[317] Qiu C, Adkins NJE, Attallah MM. Microstructure and tensile properties of selectively laser-melted and of HIPed laser-melted Ti–6Al–4V. Materials Science and Engineering: A 2013;578:230–9. https://doi.org/10/f4577z.
[318] Åkerfeldt P, Pederson R, Antti M-L. Microstructure and mechanical properties of laser metal deposited Ti-6Al-4V. vol. 3, Social Sciences Academic Press (China); 2012, p. 1730–4.
[319] Shipley H, McDonnell D, Culleton M, Coull R, Lupoi R, O'Donnell G, et al. Optimisation of process parameters to address fundamental challenges during selective laser melting of Ti-6Al-4V: A review. International Journal of Machine Tools and Manufacture 2018;128:1–20. https://doi.org/10/gc8mkg.
[320] Lockett H, Ding J, Williams S, Martina F. Design for Wire + Arc Additive Manufacture: design rules and build orientation selection. Journal of Engineering Design 2017;28:568–98. https://doi.org/10/gfx8dm.
[321] Kozamernik N, Bračun D, Klobčar D. WAAM system with interpass temperature control and forced cooling for near-net-shape printing of small metal components. Int J Adv Manuf Technol 2020;110:1955–68. https://doi.org/10/gjw38v.
[322] Shmueli G. To Explain or to Predict? Statist Sci 2010;25. https://doi.org/10.1214/10-STS330.
[323] Bowen RM. Introduction to continuum mechanics for engineers. New York: Plenum Press; 1989.
[324] Chun Tie Y, Birks M, Francis K. Grounded theory research: A design framework for novice researchers. SAGE Open Med 2019;7:2050312118822927. https://doi.org/10/gf4wkn.
[325] Brandl E, Michailov V, Viehweger B, Leyens C. Deposition of Ti–6Al–4V using laser and wire, part I: Microstructural properties of single beads. Surface and Coatings Technology 2011;206:1120–9. https://doi.org/10/d4z4pn.
[326] Fracture Toughness and Fracture Mechanics 2000. https://doi.org/10.31399/asm.hb.v08.a0003305.
[327] Kenny P, Campbell JD. Fracture toughness an examination of the concept in predicting the failure of materials. Progress in Materials Science 1968;13:135–81. https://doi.org/10.1016/0079-6425(68)90020-0.
[328] EN380: Naval Material Science and Engineering 1970. https://www.usna.edu/NAOE/academics/en380.php (accessed January 6, 2022).
[329] Bieber C, Bjelkengren C, Ryu J, Varga A. PLASTIC DEFORMATION IN MATERIALS PROCESSING n.d.:7.
[330] Jenkins C, Khanna S. Mechanics of Materials: A Modern Integration of Mechanics and Materials in Structural Design. Elsevier; 2005.
[331] COMAU. COMAU Robotics. n.d.
[332] Butcher, B.D.R. Robots vs. CNC Machine Tools: The Software Edge 2006.
[333] Wang, L., Y. Tian, and T. Sawaragi. Case-based automatic programming in robotic assembly production. Industrial Robot: An International Journal 2011;38:86–96. https://doi.org/10.1108/01439911111097887.
[334] Robotmaster. Programming CNC machines versus robots n.d.
[335] Bruno Siciliano, O.K. Springer Handbook of Robotics. Springer; n.d.
[336] Joni, A. EMC - The Enhanced Machine Controller Project 2006. http://linuxcnc.org/docs/html/index.html. (accessed August 19, 2022).
[337] Frederick M. Proctor, John Michaloski. Enhanced Machine Controller Architecture Overview 1993.
[338] Robotworx. Robotics and Automation 1970. http://www.robots.com/.
[339] Paul G. Ranky. Collaborative, synchronous robots serving machines and cells. Industrial Robot: An International Journal 2006;30:213–7. https://doi.org/10.1108/01439910310473915.
[340] Bennett Brumson. What's New with Robots in Electronics and Semiconductors? Robotic Industries Association 2010.
[341] Bogue R. Robots in the nuclear industry: a review of technologies and applications. Industrial Robot: An International Journal 2011;38:113–8. https://doi.org/10.1108/01439911111106327.
[342] Developing rugged robots for the nuclear industry. New Electronics 1970. https://www.newelectronics.co.uk/content/features/developing-rugged-robots-for-the-nuclear-industry/ (accessed August 19, 2022).
[343] Sands D. Cost effective robotics in the nuclear industry. Industrial Robot: An International Journal 2006;33:170–3. https://doi.org/10.1108/01439910610659079.
[344] KUKA. KUKA Automation - Robotics 2011. http://www.KUKA-robotics.com/united_kingdom/en.
[345] 11: The KUKA Robot Programming Language. Dr Stienecker's Site 2010. https://drstienecker.com/tech-332/11-the-kuka-robot-programming-language/ (accessed August 19, 2022).
[346] ABB. ABB Robotics 2011. http://www.abb.co.uk/product/us/9AAC910011.aspx?country=GB.

[347] Diarmuid Pigott. HOPL : an interactive roster of programming languages. Murdoch, Western Australia : Murdoch University, School of Information Technology 1995. https://www.worldcat.org/title/hopl-an-interactive-roster-of-programming-languages/oclc/262298622 (accessed August 19, 2022).
[348] KAWASAKI. Kawasaki Robotics 2010. http://www.kawasakirobotics.com/.
[349] Mitsubishi. MELFA Robots 2010. http://www.mitsubishi-automation.com/.
[350] OTC. OTC Daihen 2011. http://www.daihen-usa.com/.
[351] NACHI. Nachi Robotic Systems 2011. http://www.daihen-usa.com/.
[352] None N. Review Of Piping And Pressure Vessel Code Design Criteria. Technical Report 217. C. F. Braun and Co., Alhambra, CA (United States); 1969. https://doi.org/10.2172/4031361.
[353] Sheffield Forgemasters - Technical Capabilities.pdf 2020.
[354] Lebronze alloys. Lebronze Alloys 1970. https://www.lebronze-alloys.com (accessed August 19, 2022).
[355] Inc CF. Forging Capabilities - Canada Forgings Inc. - Open and Closed Die Forging in North America. Https://WwwCanforgeCom 1970. https://www.canforge.com/capabilities/ (accessed August 19, 2022).
[356] Lampson J. Open Die Press Forging. Independent Forgings and Alloys 1970. https://independentforgings.com/capabilities/open-die-forging/press-forging/ (accessed August 19, 2022).
[357] Closed die forging parts from high performance metals | Aubert & Duval. Aubert&Duval Site 1970. https://www.aubertduval.com/products/forgings-aerospace-titanium-steel-aluminum-superalloy-closed-die-hammer-drop-forge/ (accessed August 19, 2022).
[358] Forging | 1 kg - 80 Tonnes | Somers Forge 1970. https://www.somersforge.com/capabilities/forging/ (accessed August 19, 2022).
[359] Pilsen Steel n.d. http://www.pilsensteel.cz/en/forge_shop/ (accessed August 19, 2022).
[360] Mineral Processing Equipment | Manufacturing Capability | CITIC HIC 2022. https://citicheavyindustries.com/capabilities.html (accessed August 19, 2022).
[361] Products and Services 1970. http://www.uniones.com/forged-engineered-products/servicesoffers/ (accessed August 19, 2022).
[362] The best production equipment for rolled rings - euskalforging n.d. https://euskalforging.com/en/process-production-equipment/production-equipment (accessed August 19, 2022).
[363] special_steel_production.pdf 2014. http://dnepropress.net/files/pdf/special_steel_production.pdf (accessed August 19, 2022).
[364] admin. Forging. Forja Rotec Srl 1970. https://www.forjarotec.ro/services/forging/ (accessed August 19, 2022).
[365] Bay-Forge - FOMAS Group 1970. https://www.fomasgroup.com/production-network/bayforge (accessed August 19, 2022).
[366] Wyman Gordon - Home 1970. https://www.wyman.com/ (accessed August 19, 2022).
[367] Forging. Mettis Group | Innovative Forging Solutions 2016. https://www.mettisgroup.com/integrated-solutions/forging/ (accessed August 19, 2022).
[368] Drop-forging (aluminum, steel, stainless steel) | Richter Formteile. Richter 1970. https://www.richterformteile.com/en/products-and-procedures/drop-forging/ (accessed August 19, 2022).
[369] Bifrangi UK Process Capabilities 2020. http://www.bifrangi.co.uk/process-capabilities.html (accessed August 19, 2022).
[370] Casting Capacity. Norton Cast Products 2022. https://www.nortoncast.com/production-capacity/ (accessed August 19, 2022).
[371] Fabricated Castings - Goodwin Steel Castings 1970. https://www.goodwinsteelcastings.com/goodwin/scope/fabricated-casting (accessed August 19, 2022).
[372] Laister D. Bonds Heavy Casting. Business Live 2020. https://www.business-live.co.uk/manufacturing/heavy-castings-site-close-after-17544723 (accessed August 19, 2022).
[373] ISGEC | Sand Castings | Steel Casting | Stainless Steel Castings | Valve Casting 1970. http://www.isgec.com/steel-castings/ba-steel-castings-manufacturing.php (accessed August 19, 2022).
[374] Casting Directory. Cast Metals Federation 1970. https://www.castmetalsfederation.com/cmf-members/foundry-search (accessed August 19, 2022).
[375] Confederation of British Metal Forming. CBM 1970. https://thecbm.co.uk/our-members/search-our-members/ (accessed August 19, 2022).
[376] Machining & Capacity Guide | Somers Forge 1970. https://www.somersforge.com/capabilities/machining-and-capacity-guide/ (accessed August 19, 2022).
[377] Bespoke Fabrication | Machining & Fabrication 1970. http://oldham-eng.com/bespoke-fabrication/ (accessed August 19, 2022).
[378] Shakespeare Cast Products n.d. https://www.shakespearecp.com/ (accessed August 19, 2022).
[379] Specialised castings 1970. http://ww1.specialisedcastings.co.uk/ (accessed August 19, 2022).
[380] boroadmin. Boro Foundry Ltd. BORO Foundry Limited 1970. https://borofoundry.co.uk/foundry (accessed August 19, 2022).
[381] Capabilities | Westley Group 1970. https://www.westleygroup.co.uk/capabilities/ (accessed August 19, 2022).

[382] HDowns - Capacity 1970. http://www.hdowns.co.uk/castings/capacities.php (accessed August 19, 2022).
[383] H.I. Quality Steel Castings Ltd 1970. https://www.hiqsc.co.uk/ (accessed August 19, 2022).
[384] Open Die Ring Forging | Scot Forge n.d. https://www.scotforge.com/Products/Rings (accessed November 13, 2019).
[385] Lee S-M, Lee W-J. Finite-Element Analysis on Thermomechanical Behavior of a Marine Propeller Casting in the Sand-Casting Process. Journal of Materials Engineering and Performance 2005;14:388–94. https://doi.org/10.1361/10599490523931.
[386] Static Castings | Fondinox n.d. http://www.fondinox.it/en/static-castings/ (accessed November 13, 2019).
[387] Cast Steel Products. Smelter Castings n.d. https://caststeelproducts.com/DesktopModules/PTI_ProjectsViewingTool/images/Projects/139/6997-7.jpg (accessed November 13, 2019).
[388] Council NR. New Materials for Next-Generation Commercial Transports. 1996. https://doi.org/10.17226/5070.
[389] KUKA Linear Units and Positioners - KUKA AG - PDF Catalogs | Technical Documentation | Brochure n.d. http://pdf.directindustry.com/pdf/kuka-ag/kuka-linear-units-positioners/17587-752108.html (accessed April 26, 2019).
[390] Woy, U. Project AS411-AMRC-RP-120227A-01.doc. Nuclear AMRC; 2012.
[391] Woy, U. BAM SAT Checklist.docx 2016.
[392] Woy, U. NAMRC BAM-CoR01_03.docx 2018.
[393] Woy, U. Bespoke monitoring system features - observation checklist.pdf 2018.
[394] Fault-Listing-Manual.pdf 2021. http://www.wtech.com.tw/public/download/manual/kuka/Fault-Listing-Manual.pdf (accessed July 29, 2022).
[395] MSC Software Corporation. Marc 2019 Documentation Volume A: Theory and User Information 2019.
[396] Goldak J, Chakravarti A, Bibby M. A new finite element model for welding heat sources. Metallurgical Transactions B 1984;15:299–305. https://doi.org/10/ckb25g.
[397] Goldak JA, Akhlaghi M. Computational Welding Mechanics. Springer Science & Business Media; 2006.
[398] Lindgren L-E, Lundbäck A, Fisk M, Pederson R, Andersson J. Simulation of additive manufacturing using coupled constitutive and microstructure models. Additive Manufacturing 2016;12:144–58. https://doi.org/10.1016/j.addma.2016.05.005.
[399] Lindgren L-E. 2 - Understanding welding stress and distortion using computational welding mechanics. In: Michaleris P, editor. Minimization of Welding Distortion and Buckling, Woodhead Publishing; 2011, p. 22–78. https://doi.org/10.1533/9780857092908.1.22.
[400] Ding J, Colegrove P, Mehnen J, Ganguly S, Sequeira Almeida PM, Wang F, et al. Thermo-mechanical analysis of Wire and Arc Additive Layer Manufacturing process on large multi-layer parts. Computational Materials Science 2011;50:3315–22. https://doi.org/10.1016/j.commatsci.2011.06.023.
[401] Almeida DF, Martins RF, Cardoso JB. Numerical simulation of residual stresses induced by TIG butt-welding of thin plates made of AISI 316L stainless steel. Procedia Structural Integrity 2017;5:633–9. https://doi.org/10.1016/j.prostr.2017.07.032.
[402] Montevecchi F, Venturini G, Scippa A, Campatelli G. Finite Element Modelling of Wire-arc-additive-manufacturing Process. Procedia CIRP 2016;55:109–14. https://doi.org/10.1016/j.procir.2016.08.024.
[403] MSC Software Corporation. Marc 2019 Documentation Volume A: Theory and User Information 2019.
[404] Montevecchi F, Venturini G, Grossi N, Scippa A, Campatelli G. Finite Element mesh coarsening for effective distortion prediction in Wire Arc Additive Manufacturing. Additive Manufacturing 2017;18:145–55. https://doi.org/10/ggd6sx.
[405] Stenbacka N, Choquet I, Hurtig K. Review of arc efficiency values for gas tungsten arc welding. IIW Commission IV-XII-SG212, Intermediate Meeting, BAM, Berlin, Germany, 18-20 April, 2012, 2012, p. 1–21.
[406] FUERSCHBACH PW, KNOROVSKY GA. A study of melting efficiency in plasma arc and gas tungsten arc welding : a method for selecting optimal weld schedules to minimize net heat input is derived frm calorimetric measuremts. Weld j 1991;70:287–97.
[407] Lundback A. CAD Support for heat input in a FE model. BOOK-INSTITUTE OF MATERIALS 2002;784:1113–22.
[408] Lindgren L-E, Lundbäck A, Fisk M, Pederson R, Andersson J. Simulation of additive manufacturing using coupled constitutive and microstructure models. Additive Manufacturing 2016;12:144–58. https://doi.org/10/f3rr3z.
[409] Söderberg M. Coupled models related to manufacturing simulations. PhD Thesis. Lule\aa tekniska universitet, 2014.
[410] MSC Software Corporation. Marc 2019 Documentation Volume B: Element Library 2019.
[411] MSC Software Corporation. Marc 2019 Documentation Volume B: Element Library 2019.
[412] Lindgren L-E. Finite element modeling and simulation of welding. Part 2: Improved material modeling. Journal of Thermal Stresses 2001;24:195–231. https://doi.org/10/fpr349.
[413] MSC Software Corporation. Marc 2019 Documentation Volume E: Demonstration Problems 2019.

[414] Joshi S, Hildebrand J, Aloraier AS, Rabczuk T. Characterization of material properties and heat source parameters in welding simulation of two overlapping beads on a substrate plate. Computational Materials Science 2013;69:559–65. https://doi.org/10/f4n54c.
[415] Kinovea reference manual — Kinovea 0.9.5 documentation 2004. https://www.kinovea.org/help/en/ (accessed August 16, 2022).
[416] Heigel JC. Thermo-Mechanical Model Development and Experimental Validation for Directed Energy Deposition Additive Manufacturing Processes. The Pennsylvania State University, 2015.
[417] Heigel JC, Michaleris P, Reutzel EW. Thermo-mechanical model development and validation of directed energy deposition additive manufacturing of Ti–6Al–4V. Additive Manufacturing 2015;5:9–19. https://doi.org/10/ggcqv9.
[418] Boivineau M, Cagran C, Doytier D, Eyraud V, Nadal M-H, Wilthan B, et al. Thermophysical Properties of Solid and Liquid Ti-6Al-4V (TA6V) Alloy. Int J Thermophys 2006;27:507–29. https://doi.org/10/b2fwt2.
[419] Murgau CC, Pederson R, Lindgren LE. A model for Ti–6Al–4V microstructure evolution for arbitrary temperature changes. Modelling Simul Mater Sci Eng 2012;20:055006. https://doi.org/10/f23pjs.
[420] Charles Murgau C, Lundbäck A, Åkerfeldt P, Pederson R. Temperature and Microstructure Evolution in Gas Tungsten Arc Welding Wire Feed Additive Manufacturing of Ti-6Al-4V. Materials 2019;12:3534. https://doi.org/10/gh8hzj.
[421] Fisk M, Lundbäck A, Andersson J, Lindgren L-E. Finite element analysis using a dislocation density based flow stress model coupled with model for precipitate evolution. International Symposium on Superalloy 718 and Derivatives, Pittsburgh, Pennsylvania (2014), John Wiley & Sons; 2014, p. 155–68. https://doi.org/10/gjw38p.
[422] Sente Software - History of JMatPro® 1999. https://www.sentesoftware.co.uk/history-of-jmatpro (accessed August 17, 2022).
[423] Neikter M, Akerfeldt P, Pederson R, Antti M-L. Microstructure characterisation of Ti-6Al-4V from different additive manufacturing processes. IOP Conf Ser: Mater Sci Eng 2017;258:012007. https://doi.org/10/gcjjs6.
[424] Kofstad P. High-temperature oxidation of titanium. Journal of the Less Common Metals 1967;12:449–64. https://doi.org/10.1016/0022-5088(67)90017-3.
[425] Bermingham MJ, Thomson-Larkins J, St John DH, Dargusch MS. Sensitivity of Ti-6Al-4V components to oxidation during out of chamber Wire + Arc Additive Manufacturing. Journal of Materials Processing Technology 2018;258:29–37. https://doi.org/10.1016/j.jmatprotec.2018.03.014.
[426] Casadebaigt A, Hugues J, Monceau D. High temperature oxidation and embrittlement at 500–600 °C of Ti-6Al-4V alloy fabricated by Laser and Electron Beam Melting. Corrosion Science 2020;175:108875. https://doi.org/10.1016/j.corsci.2020.108875.
[427] Dong E, Wei Y, Cai Q, Lei C, Shi J. High-Temperature Oxidation Kinetics and Behavior of Ti–6Al–4V Alloy. Oxidation of Metals 2017;88. https://doi.org/10.1007/s11085-017-9770-0.
[428] WordItOut n.d. https://worditout.com/ (accessed January 28, 2024).